NUREG/CR-2530
SAND82-0218

Review of the Grand Gulf Hydrogen Igniter System

Prepared by J. C. Cummings, A. L. Camp, M. P. Sherman,
M. J. Wester, D. Tomasko, R. K. Byers, B. W. Burnham

Sandia National Laboratories

Prepared for
U.S. Nuclear Regulatory
Commission

GPO Printed copy price $8.50

NUREG/CR-2530
SAND82-0218
R2

Review of the Grand Gulf Hydrogen Igniter System

Manuscript Completed: February 1983
Date Published: March 1983

Prepared by
J. C. Cummings, A. L. Camp, M. P. Sherman,
M. J. Wester, D. Tomasko, R. K. Byers, B. W. Burnham

Sandia National Laboratories
Albuquerque, NM 87185

Prepared for
Office of Nuclear Reactor Regulation
Office of Nuclear Regulatory Research
U.S. Nuclear Regulatory Commission
Washington, D.C. 20555
NRC FINs A1308, A1246

Abstract

The Mississippi Power and Light Company has proposed instaliation of a Hydrogen Igniter System (HIS) at the Grand Gulf Nuclear Station (BWR Mark III) to burn hydrogen generated during accidents more severe than the design-basis accidents. Sandia National Laboratories, under a contract with the US Nuclear Regulatory Commission, has performed a technical evaluation of the adequacy of the proposed HIS to meet the threat posed by hydrogen combustion. Areas considered in this review include: HIS design and testing; location and distribution of igniters; containment pressure and temperature response calculations; detonations; containment atmosphere mixing mechanisms; actuation criteria for the HIS; and the spectrum of hydrogen-generating accidents.

Acknowledgments

A number of individuals provided help, assistance, support, and review. Without their assistance this report could not have been produced.

Lawrence D. Buxton and Michael L. Corradini were involved early in the project with the RALOC and MARCH computer codes.

Susan Dingman and Peter Prassinos were instrumental in providing assistance with the HECTR and MARCH codes when difficulties arose well into the project.

Marshall Berman provided leadership to the project and painstakingly reviewed several drafts of this report. His high standards of excellence and commitment of time are deeply appreciated by the authors.

We are forever indebted to Pat Rosario, Jan Frey, and Carol Henry. Without their dedicated efforts in typing the manuscript, we never would have produced the first draft of this document on schedule. Finally, we would like to thank E. W. Shepherd and the Publication Services Division for the high quality of the format of this document.

Contents

Review of the Grand Gulf Hydrogen Igniter System

1.0 Summary

1.1 Introduction

As a result of several investigations of the accident at the Three Mile Island Nuclear Plant (TMI-2) in March of 1979, the US Nuclear Regulatory Commission (NRC) has required that boiling water reactor (BWR) nuclear plants employing the Mark III design be equipped with additional systems to control large quantities of hydrogen. In this regard, the Mississippi Power and Light Company (MP&L) has proposed installation of the Hydrogen Igniter System (HIS) at the Grand Gulf Nuclear Station to burn the hydrogen generated during accidents more severe than the design-basis accidents. The NRC must now evaluate the effectiveness and reliability of the proposed HIS as part of the Grand Gulf licensing activities.

In August of 1981, Sandia National Laboratories (SNL) agreed to assist the NRC by making a technical evaluation of the adequacy of the HIS to meet the threat posed by hydrogen combustion at the Grand Gulf Nuclear Station. The technical goals of our evaluation of the design and testing of the HIS were:

1. To assess the adequacy of the location and distribution of igniters,
2. To perform independent calculations of the containment atmosphere pressure and temperature response to hydrogen combustion and compare these to the calculations performed by the applicant (MP&L has used the CLASIX-3 computer code exclusively),
3. To determine the likelihood (qualitative assessment) and consequences of detonations (in terms of calculating impulsive loads, not in terms of estimating structural failure),
4. To examine and estimate containment (including wetwell) atmosphere mixing,
5. To assess the adequacy of the actuation criteria for the HIS, and
6. To assess the adequacy and completeness of the spectrum of accidents considered in the applicant's evaluation.

As necessary, we were to provide recommendations to the NRC for corrective action or design changes.

1.2 Preliminary (Task 1) Report

At the end of August 1981, we submitted a Task 1 Report to the NRC. This report summarized our preliminary evaluation, discussed our technical approach for the Task 2 (draft report) evaluation, and requested additional information in a number of areas. Our preliminary evaluation was based primarily on the following items:

1. Review of the MP&L document *Preliminary Evaluation of Additional Hydrogen Control Measures for the Grand Gulf Nuclear Station* (April 9, 1981)
2. Review of the MP&L document *Final Report on the Grand Gulf Nuclear Station Hydrogen Igniter System* (June 19, 1981)
3. A tour (and associated photographic records) of the Grand Gulf Nuclear Station on August 6, 1981 by J. C. Cummings, M. P. Sherman, and A. L. Camp of SNL
4. Discussions (and associated SNL notes) with S. Hobbs and J. Richardson, MP&L, on August 6, 1981
5. MARCH computer code calculations of accident scenarios in the Grand Gulf plant
6. Engineering judgments made by the Sandia staff during review of the above five items

In our Task 1 Report, we indicated that our evaluation of the adequacy of the HIS would depend

heavily on the value of containment failure pressure or "ultimate capacity of the containment." An NRC analysis indicated that 56 psig (71 psia, 4.8 atm) would be an acceptable value. MP&L has reported calculated values from 47 to 67 psig for the ultimate capacity of the containment. Unfortunately, this uncertainty band overlaps with the expected uncertainty in hydrogen-burn pressure associated with the transition from incomplete to complete combustion. For example, the NRC estimate of failure pressure could be exceeded if a *single, complete, adiabatic, isochoric burn* were to take place with 8% to 9% hydrogen distributed homogeneously in the containment air.* Our preliminary conclusion, therefore, was that the uncertainties of the HIS performance overlap with the uncertainties of the calculated failure pressure. Consequently, we stated that more accurate and detailed analyses would be required before an assessment of the HIS adequacy could be made. Our goal was to reduce the uncertainty of the estimates of HIS performance during various accident scenarios, but we noted that uncertainties would still remain even after we had completed this evaluation. We also recommended that the NRC obtain independent estimates of containment failure pressure for Grand Gulf.

The request for additional information that was included in our Task 1 Report is included at the end of this report as Appendix A. As part of that request, we recommended a significant change to the compartment model used by MP&L in their CLASIX-3 calculations and a number of additional CLASIX-3 calculations to examine variations in several key parameters (hydrogen source term, flame speed, etc). We also requested answers to specific questions that we felt were important in conducting our evaluation of the design and testing of the Grand Gulf HIS.

1.3 Final (Task 2) Report Summary

Our technical approach has involved the use of several computer codes combined with the engineering judgment of the SNL staff. The Sandia code HECTR (Hydrogen Event: Containment Transient Response) and the MARCH code (written by Battelle Columbus Laboratory) were used extensively as counterparts to CLASIX-3 to calculate the containment atmosphere pressure and temperature response to hydrogen combustion. The German code RALOC was used to investigate mixing effectiveness by calculating the spatial and temporal behavior of the hydrogen concentration (preburn conditions only). The Sandia code CSQ was used to calculate the impulsive loads that would accompany a local detonation.

In addition to the items listed in Section 1.2, we have reviewed other documents as part of our Task 2 evaluation (most of these were not received until late December 1981):

1. *Report on the Grand Gulf Nuclear Station Hydrogen Ignition System*, MP&L (August 31, 1981)
2. Letter and attachments from L. F. Dale, MP&L, to H. R. Denton, USNRC (September 11, 1981)
3. *The CLASIX Computer Program for the Analysis of Reactor Plant Containment Response to Hydrogen Release and Deflagration*, Off-Shore Power Systems Rept No. 36A31, nonproprietary version (October 1981)
4. *CLASIX-3 Containment Response Sensitivity Analysis for the Mississippi Power & Light Grand Gulf Nuclear Station*, Off-Shore Power Systems Rept No. 37A15 (December, 1981)
5. Letter and attachments from L. F. Dale, MP&L, to H. R. Denton, USNRC (December 21, 1981)

In summarizing the results of our Task 2 assessment, we must repeat several statements that were made in the preliminary (Task 1) report. First, we have used the NRC value of 56 psig for the containment failure pressure. If this value were to increase or decrease by 5 to 10 psi, it could have a significant effect on our evaluation and recommendations. Second, after several months of intensive study and hundreds of computer calculations, we are still left with uncertainties about the adequacy of the HIS. None of the available computer codes (MARCH, CLASIX-3, or HECTR) is sophisticated enough at present to allow us to predict peak pressures with high precision, and all the codes are very sensitive to certain input parameters and models of phenomena that are simply not known very well.

It is also important to note that we have not analyzed in any significant detail a number of phenomena associated with hydrogen combustion. These include accelerated flames, missile generation, spatial and temporal nonhomogeneities in gas mixtures, multiple and sequential ignitions, and equipment failures. Theoretical models and computer codes are not presently available as calculational tools to analyze these phenomena. In addition, experimental data are

*The exact hydrogen concentration required to attain 56 psig depends on the preburn pressure (e.g., the addition of the drywell non-condensable gases to the containment atmosphere can increase the initial pressure by 19%).

sparse, especially under nuclear plant accident conditions (very large geometrical scales, three-dimensional obstacles and flame paths, concentration gradients in the gas mixture, etc).

The net result of our evaluation, including uncertainties, can be stated as follows. In our judgment, the currently proposed HIS is "marginally adequate" to meet the threat posed by hydrogen releases within the containment building. By marginally adequate, we mean the following: In order to calculate the combustion behavior of hydrogen inside the Grand Gulf containment, we must specify a number of parameters for the simple models presently in our computer codes. If each of these parameters is at the optimistic end of its "best-estimate" range, the computer codes predict combustion-generated pressures well below the specified value for failure. If each of these parameters is at the pessimistic end of its best-estimate range, the computer codes predict pressures in excess of the assumed failure value. Midrange values for these parameters will generally result in calculated pressures which are high, but below the specified failure pressure.

Later in this report, we make recommendations for changes to the proposed HIS design which we feel would improve its ability to meet the hydrogen threat (Chapter 6.0). Several "advanced concepts" that we believe might be desirable alternatives or adjuncts to an igniter system for BWR Mark III plants are discussed in another report.[11]

Several things cause us to judge the HIS to be marginally adequate. There are significant uncertainties in the hydrogen release rate, the degree and rate of mixing within the wetwell/containment, and the ignition and propagation behavior of burns. In addition, for some accident scenarios the containment spray system is not available. These items tend to dominate the results of our calculations, and consequently, reliable conclusions are difficult to draw. We do know that if conservative upper bounds or assumptions are made regarding these key items, our calculations indicate the generation of pressures in excess of the assumed failure value.

Hydrogen release rates for accidents in nuclear plants cannot be predicted with confidence at present. This is true for low-pressure accidents in either a PWR or a BWR. Low-pressure (large-break) accidents tend not to produce significant hydrogen prior to total core uncovery due to high steam flow rates which maintain the core temperature below that required for significant metal-water reaction. On the other hand, high-pressure (e.g., small-break) accidents tend to have considerably lower steam flow rates, which results in higher core temperatures and significant hydrogen generation prior to complete core uncovery. Our present understanding of core behavior during loss-of-coolant accidents (LOCAs) is quite limited, primarily due to a lack of knowledge and data concerning core-slump phenomena. MARCH calculations for TPE* and S_1** BWR accidents indicate that little or no hydrogen would be produced before complete uncovery of the core. Consequently, the bulk of the hydrogen generation and release is predicted to occur when the core slumps into the vessel lower plenum.

The processes governing production of hydrogen during a degraded-core accident are not well known, and in some respects, are expected to be indeterminate. The hydrogen generation rate will depend on the rate of coolant injection from the Emergency Core Cooling System (ECCS) and the time that the injection begins. The degraded-core models in MARCH can predict very high to very low hydrogen yields, because the predictions are dominated by input assumptions. Until better data and models are produced, we must either accept the (perhaps artificial) conservative upper bound or select another (equally arbitrary) model.

MP&L used the MARCH code predictions up to the point of core slump (when the rate increases enormously) and then assumed a constant rate equal to the largest previous value. Since the hydrogen release rate is such an important parameter, we recommend further study of the MP&L approach to assess its validity.

The degree and speed of mixing within the wetwell/containment region are very difficult to estimate. Based on engineering judgment, we believe that if containment sprays are operating, the upper dome region will be well mixed. If they are not operating, the degree of mixing will be uncertain. Independent of the question of spray operation are the degree and rate of mixing in the annular region. The computer codes MARCH, CLASIX-3, and HECTR essentially account for only pressure-driven flow between idealized compartments. These codes do not realistically model the postburn flow and mixing, or natural convective mixing. Consequently, when the codes predict a large number of burns in one region and no burns elsewhere, or oxygen depletion in one region, or a volume filled with hydrogen existing stably below a volume filled

*Accident that is initiated by a transient event, followed by failure of a safety/relief valve to reclose and failure of emergency core cooling.

**Small pipe (with an equivalent diameter of ~2 to 6 in.) break and failure of emergency core cooling.

with air, we think the models are too crude to provide refined answers.

The ignition and propagation of burns in the containment are obviously phenomena that must be correctly modelled in order to calculate realistic pressure and temperature transients. The computer codes treat these phenomena very simplistically. Consequently, we are forced to specify values for ignition criteria, propagation criteria, combustion completeness, and flame speed. The values we select can have tremendous leverage on the calculations. The combustion processes that would actually occur in containment for our postulated accident scenarios are probably much different than the idealized models. Spatial and temporal gradients in hydrogen, oxygen, and steam concentrations, coupled with discrete igniter locations, would tend to produce a very complex series of local burns which might result in smaller loads than our calculated "compartment" burns. It is well beyond our present capability to model such behavior.

Finally, the issue of whether or not containment sprays operate is very important. It is beyond the scope of this report to determine the quantitative likelihood or probability of spray availability. We can, however, observe the effect of spray availability on our calculations. We conclude that spray operation is very important to plant safety for the accident scenarios (hydrogen release rates in particular) examined in our study. The benefits of containment sprays are threefold: the peak pressure of a single burn will be reduced by spray evaporation if the burn duration is sufficiently long; the baseline pressure for multiple burns will be reduced if the time between burns is sufficently long; and the thermal environment to which plant equipment will be exposed will be less severe.

Calculations of the containment atmosphere pressure and temperature response to hydrogen combustion are a very important part of this HIS assessment. But due to the uncertainties discussed above, total reliance on the code calculations is unwarranted. At present, engineering judgment may be as important to the assessment as calculations even though it might appear to be more subjective. A good example of this is the CLASIX-3 sensitivity study of containment sprays. The CLASIX-3 calculations indicate that burns without sprays result in lower peak pressures than burns with full spray operation. This result is exactly opposite to our intuition, and in our opinion, is an artifact of the compartment model and input assumptions. Our engineering judgment dictates that, if possible, the sprays should be initiated before significant hydrogen production occurs and remain on until the accident is brought under control.

Comparisons between the various computer codes is difficult because we know little of the calculational models within CLASIX-3 and even MARCH. We have attempted to carry out calculations with MARCH and HECTR that are nearly identical to several CLASIX-3 cases. Unfortunately, we invariably end up comparing "apples" to "oranges." HECTR has no drywell compartment model; MARCH has a drywell, but only zero-flow-resistance connections to and from it. Since it is not an input for MARCH calculations, the MARCH hydrogen release rate is not the same as that used in HECTR and CLASIX-3. Despite these and other differences, the three codes predict the same general kind of wetwell/containment behavior. (As acknowledged in the CLASIX-3 sensitivity study, the calculational results are sensitive to input parameters for the baseline compartment configuration—our "B" configuration.) Specific differences in calculated pressures and temperatures from the three codes can probably be attributed to differences in modelling and input assumptions for heat and mass transfer. We have some concern regarding the CLASIX-3 calculational models for flow through the drywell vacuum breakers and flow into the drywell through the suppression pool. The CLASIX-3 treatment of heat transfer to and evaporation of the spray droplets is another area of concern.

Regarding detonations inside the Grand Gulf containment building, two conditions must be satisifed simultaneously: a detonable mixture must exist, and an ignition source or mechanism must exist. In our judgment, the likelihood of forming detonable mixtures is small, especially for regions of significant extent. We also currently believe that the likelihood of detonation occurring, either by direct initiation or by transition from deflagration (flame acceleration), is very small. However, it is our belief that some degree of flame acceleration, upward through the wetwell obstacles, is highly likely. The degree of acceleration will depend on the effectiveness of the HIS in burning very lean mixtures and on the spatial concentration gradients of hydrogen and air.

Details of our calculations and assessments are contained in the chapters that follow. Chapter 2.0 discusses the HECTR calculations while Chapter 3.0 covers the MARCH calculations. Where possible, we have made comparisons to CLASIX-3 calculations. Chapter 4.0 presents RALOC code calculations of hydrogen mixing for a number of scenarios. Chapter 5.0 discusses a CSQ code calculation of the effects of a localized detonation as well as the likelihood of detonations or detonation-like phenomena. In Chapter 6.0, we present our assessment results and recommendations.

1.4 Reference

[1.1]M. Berman, *Light Water Reactor Safety Research Program Quarterly Report, April-September 1981*, Sandia National Laboratories, SAND82-0006, NUREG/CR-2481, February 1982.

2.0 HECTR Calculations for the Grand Gulf Nuclear Station

2.1 Description of the HECTR Computer Program

In order to model hydrogen burns in nuclear power plant containment buildings, we have developed a computer code called HECTR (Hydrogen Event: Containment Transient Response). HECTR can be used to analyze as many as ten separate containment compartments (at present HECTR does not have a drywell compartment model). It includes models for hydrogen burns, radiative and convective heat transfer, heat transfer to sprays, and wall heat conduction.

Flows between compartments are pressure driven, and the compartment interconnections are modelled as orifices. Gases are instantaneously mixed within each compartment. Steam and hydrogen source terms are specified by the user.

The hydrogen burn model in HECTR allows combustion to be initiated in a compartment whenever a specified hydrogen concentration is exceeded, provided that the compartment is not inerted due to a shortage of oxygen or an excess of steam. Typical values used to determine whether or not a gas mixture is inert are oxygen $< 5\%$ and/or steam $> 55\%$.

The compartment burn time is calculated by dividing a characteristic compartment length by the flame speed. The flame speed, v, is determined in most cases from the following experimental correlation:

$$v = 59.2X + 1.792 \text{ m/s} \qquad (2.1)$$

where X is the hydrogen mole fraction present at the beginning of the burn (v is held constant during the burn). The above correlation was derived from turbulent flame experiments in the Sandia VGES 16 ft tank. (Note that this was an essentially open, clean-walled vessel; hence, flame acceleration due to obstacles did not occur. See Figure 2.1 and Reference 2.1 for more details.) Other values of the flame speed can be specified, if desired. Combustion is carried out either to a given completeness (user specified) during the calculated burn time or until the compartment runs out of oxygen.

The burn can propagate into adjacent compartments after a specified time delay if the propagation criteria are met in those compartments. These criteria are based upon the hydrogen concentration, and typical values are $> 4.1\%$ hydrogen by volume for upward propagation, $> 6\%$ for horizontal propagation, and $> 9\%$ for downward propagation.[2.2]

The radiative heat transfer model breaks up the emission from steam into seven spectral bands and calculates an emissivity for each band. The wall surfaces are assumed to be gray and have constant emissivities.

Convective heat transfer is modelled for both vertical slabs and horizontal water pool surfaces. The vertical slab model allows for free or forced convection, either with or without condensation. The pool model assumes laminar flow over a horizontal flat plate.

The spray model treats both condensation on and evaporation from spray drops. The spray drops are assumed to fall through a homogeneous atmosphere, none of whose properties changes during the fall time of the drop. Heat and mass transfer rates are determined from the size and temperature of the drops when they reach the bottom of the compartment. A distribution of droplets including up to ten different drop sizes can be modelled.

Walls are treated either as slabs, using standard finite-difference techniques, or as lumped masses. The heat flux to each wall surface is the sum of the radiative and convective heat fluxes. Up to 30 different wall surfaces can be analyzed.

Each of the various models in HECTR is discussed in more detail in Appendix B.

2.1.1 Summary and Conclusions

A wide variety of cases were run using HECTR, including cases to examine compartmentalization, flame speed, completeness of combustion, propagation limits, sprays and the hydrogen source term. Based upon the HECTR analysis and a study of the CLASIX-3 analysis presented in Reference 2.3, we have reached the conclusions discussed below.

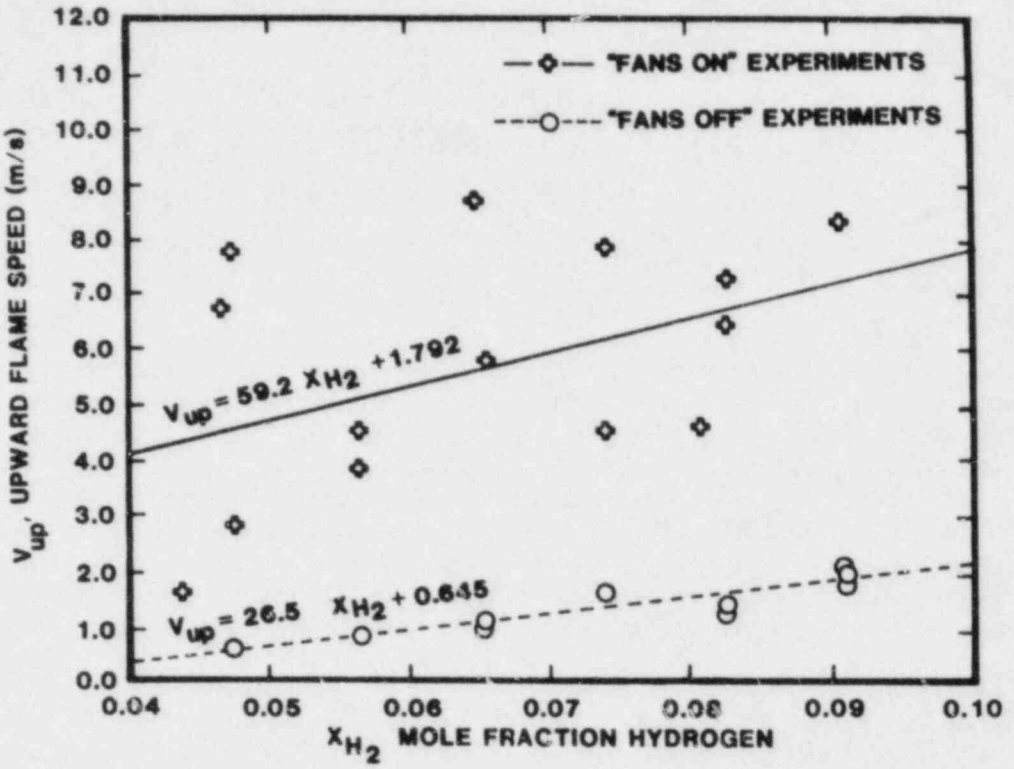

Figure 2.1. Experimental Flame Speed (From Ref 2.1)

In most cases the HECTR analysis predicts peak pressures that are much higher than those predicted by the CLASIX-3 analysis.* The CLASIX-3 analysis divided the containment into two compartments: the wetwell region just above the suppression pool and the rest of the containment, including the dome. The CLASIX-3 analysis generally predicts a large number of burns in the wetwell resulting in small pressure rises and no burns in the dome. HECTR generally predicts at least one burn in the dome resulting in high pressures, due to the large volume of the dome relative to the wetwell. The reason that burns are predicted in the dome is that HECTR predicts inerting in the wetwell due to oxygen depletion at an earlier time than CLASIX-3 does. Once the wetwell inerts, hydrogen is transferred from the wetwell to the dome at a higher rate, and burns in the dome occur soon afterward. Both CLASIX-3 and HECTR show that, after a burn in the wetwell, oxygen is drawn back into the wetwell from the dome as the wetwell cools down. HECTR predicts a slightly lower rate of cooling in the wetwell, and thus, inerting occurs a few burns earlier than in the CLASIX-3 analysis. This difference in cooling rate could be due to assumptions regarding passive heat sinks, heat transfer models, or the treatment of containment sprays. Because a small difference in the models or input assumptions can have such a dramatic impact on the results, the problem is "ill-conditioned." Despite the differences in the results, we feel that the behavior of CLASIX-3 and HECTR is similar. Both codes predict eventual wetwell inerting, just at different times; and, as will be discussed later, some of the CLASIX-3 cases were close to ignition in the dome at the end of the run. Differences in the heat transfer models appear to be small.

A significant uncertainty in the analysis involves mixing of hydrogen and oxygen in the containment, and neither HECTR nor CLASIX-3 properly addresses this issue. Both codes include pressure-driven mass transfer, but not convection or diffusion. Therefore, both codes underestimate the rate of mixing between compartments. In contrast, the rate of mixing within a compartment is over-estimated, since it is assumed to occur instantaneously.

Based upon experimental data discussed in the next section, we feel that the flame speed used in the CLASIX-3 analysis is a factor of three or more low. The lower flame speeds result in more time for heat transfer during a burn, particularly if the sprays are

*Including the drywell compartment volume might reduce the pressures calculated with HECTR.

on, and correspondingly lower temperatures and pressures. The difference in peak pressure using the CLASIX-3 flame speed as opposed to the HECTR flame speed can be 5% to 15% depending upon the input assumptions. Flame speeds higher than those used in HECTR (due, for example, to flame acceleration) could result in an additional increase of 2% to 8% in peak pressure.

When varying other burn parameters we found that incomplete combustion results in decreased pressure rises; however, the benefit is not always as large as expected due to the fact that burns are more numerous and closer together in time. Additionally, we found that burns propagating from the wetwell into hydrogen concentrations of 4% to 6% in the dome will probably not produce pressures in excess of the assumed failure pressure. Burns propagating into 8% to 10% hydrogen concentrations in the dome or burns originating in the dome might produce pressures that could threaten containment.

Containment sprays almost always result in a significant reduction in temperature and pressure during a burn. Sprays may have a slight negative effect early in the accident if they enter the containment at a higher temperature than the containment atmosphere and result in a small elevation in pressure. However, this effect is small, if in fact it is real, and we would recommend that the sprays be turned on as early as possible in the accident and remain on until all danger of a hydrogen burn has passed.

Additional efforts should be undertaken to better define or bound the hydrogen source term. Very slow release rates allow more time for mixing and make global burns more likely. Very fast release rates result in rapid inerting in the wetwell and also a significant addition of hydrogen to a burn in progress.

As expected, we found that relatively small changes in initial pressure can produce significant changes in observed peak pressure. This occurs because, for any given hydrogen concentration, the ratio of peak pressure to initial pressure is almost constant for an adiabatic burn. Therefore, a 10% change in initial pressure results in about a 10% change in the peak pressure. Because the results are fairly sensitive to assumptions regarding the initial conditions, one should use caution when examining the quantitative results.

Finally, we observed that hydrogen burns may occur well after hydrogen production has stopped due to condensation of steam and the corresponding increases of the hydrogen and oxygen mole fractions. Several of the HECTR cases and some of the CLASIX-3 cases produced final conditions indicating that such an occurrence was likely.

2.2 Grand Gulf Analysis

2.2.1 Case Descriptions and HECTR Inputs

Forty-four separate cases were run using HECTR. Six cases were run for comparison with the CLASIX-3 cases presented in Reference 2.3, and the remaining 38 cases were selected to address what we felt were important questions regarding the CLASIX-3 analysis. The factors that needed more evaluation included

1. Compartmentalization
2. Flame speed
3. Completeness of combustion
4. Propagation limits
5. The hydrogen source term

In our Task 1 Report, we stated that the way the containment was compartmentalized would be very important, particularly in the way that mixing would be affected. Both CLASIX-3 and HECTR have pressure-driven mass transfer between compartments and instantaneous mixing within compartments. There is considerable uncertainty as to how mixing should be modelled. Because of this uncertainty, we felt it was prudent to examine five different compartment configurations, shown in Figures 2.2 to 2.4 and designated as A, B, C, D, and E.

Configuration A treats the containment as one large compartment and allows us to evaluate the effects of global burns. Configurations B and C add a second compartment in the annular region surrounding the drywell. Configuration B was used in most of the CLASIX-3 cases and divides the compartments at the 135 ft level, while configuration C puts the entire annular region into compartment 2. The region below the 135 ft level is open, while the region between the 135 ft level and the 209 ft level contains large amounts of equipment and structures. Configuration D divides the containment into three compartments with divisions occurring at the 135 ft level and the 209 ft level. Configuration E divides the containment into five compartments, with four of the compartments located in the annular region surrounding the drywell. Compartments 1, 2, and 5 are relatively open, while compartments 3 and 4 contain large amounts of equipment and structures.

The flame speed of 1.83 m/s used in the CLASIX-3 analysis appears to be significantly low. This speed may be appropriate for a flame in a quiescent atmosphere (Figure 2.1), but is probably not appropriate for the environment expected in a reactor containment. Higher flame speeds result in less time for heat transfer, and subsequently, higher pressure.

The flame speed used in most HECTR cases was determined from Eq (2.1).

The next area of concern involves the completeness of combustion. CLASIX-3 cases 3, 5, and 6 from Reference 2.3 had ignition occurring at 8% hydrogen with a burn completeness of 85%. We did not feel that there was sufficient evidence available to conclude that combustion would be incomplete in all cases, and therefore, conservatively assumed 100% combustion for most of the HECTR cases.

Another question involves propagation limits. In all of the CLASIX-3 runs, the propagation limits were set equal to the ignition limits. In CLASIX-3 case 2, for example, ignition occurs in the wetwell region with 10% hydrogen present, but propagation into the dome region does not occur even when the hydrogen concentration in the dome is above 8%. This is clearly unrealistic. For most of the HECTR cases, we have set upward propagation limits at 4.1% hydrogen and downward propagation limits at 9.0% hydrogen.[2.2] Using realistic propagation limits generally causes upward-propagating burns to occur, which limit the buildup of hydrogen in upper compartments.

The final area of concern involves the hydrogen source term. The CLASIX-3 source term in Reference 2.3 comes from a MARCH[2.4] calculation for a degraded-core accident modified by an arbitrary extrapolation to a specified quantity of hydrogen (consistent with 75% metal-water reaction excluding the channel boxes). There is a great deal of controversy surrounding the MARCH hydrogen source term. Therefore, we felt it was prudent to make some HECTR calculations with alternative release rate histories (Figure 2.5). These runs considered the possibility of a very rapid release of hydrogen, although we have no estimates of the probabilities of such release rates. Detailed descriptions of five of the CLASIX-3 cases and the 44 HECTR cases are presented in Tables 2.1 to 2.6. In all cases, the hydrogen is assumed to enter the containment through the suppression pool.

Inputs to HECTR are described in Tables 2.7 to 2.14. The CLASIX-3 hydrogen source terms from Reference 2.3 are presented in Table 2.7. The time, for all cases, is referenced to 3295 s into the accident, which corresponds to the time when significant hydrogen production begins.

One problem was encountered in interpreting Reference 2.3. We assumed that the hydrogen source term was constant over a time interval, while in fact, CLASIX-3 uses linear interpolation between data points. This results in a difference of ~ 8% in the total amount of hydrogen released (the HECTR source term results in less hydrogen released). Case B-1 was altered to use a source term more in agreement with the CLASIX-3 source term (Figure 2.6).

Compartment volumes and surface areas were estimated based upon available drawings, or in some cases were taken from the CLASIX-3 inputs. One difference between the input parameters for HECTR and those for CLASIX-3 is that the upper pool was assumed to remain in place during the HECTR analysis, while during the CLASIX-3 analysis, a portion of the upper pool was drained into the suppression pool. Additionally, in the HECTR analysis, the suppression pool was kept at a constant temperature of 358.15 K (185°F), and the hydrogen was assumed to enter the containment at that temperature. In all cases, the containment atmosphere was initially assumed to be air saturated with water vapor at 299.82 K (80°F). These values were obtained from Reference 2.3.

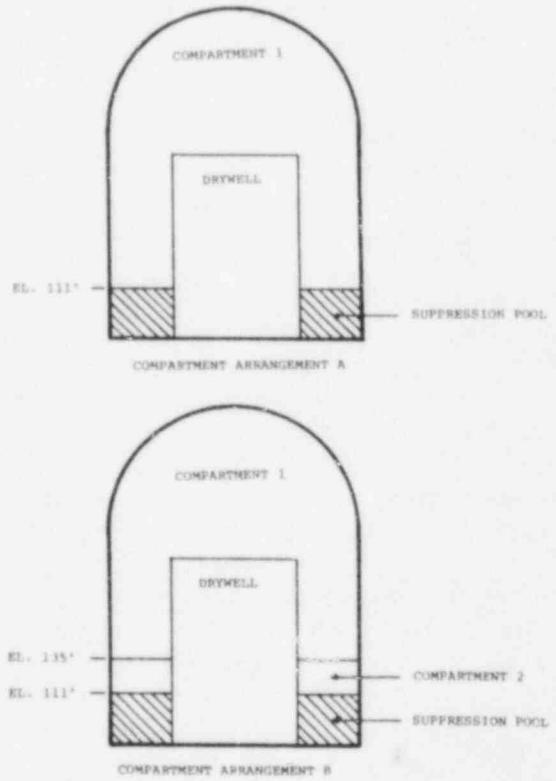

Figure 2.2. Compartment Configurations A and B

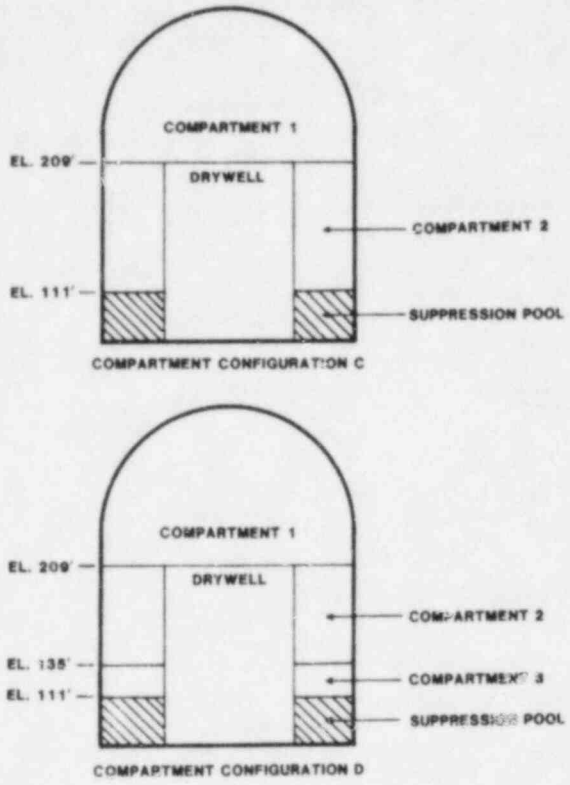

Figure 2.3. Compartment Configurations C and D

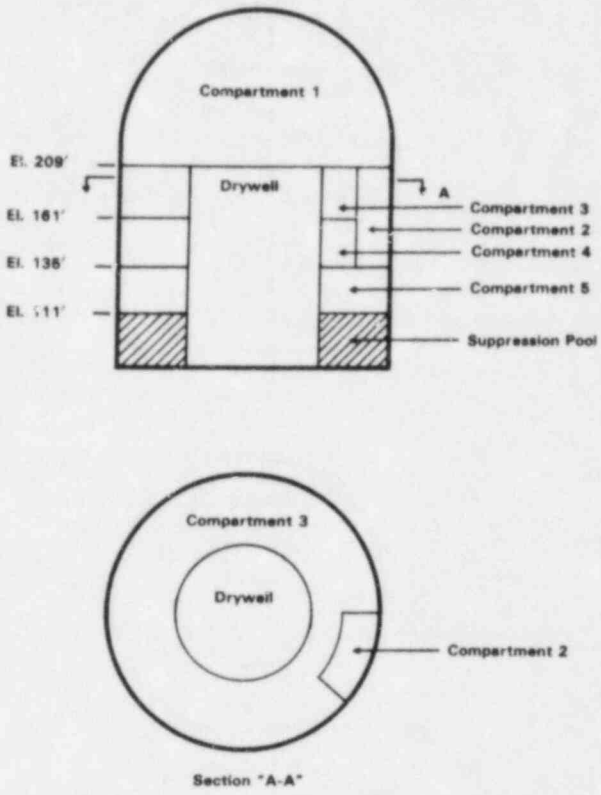

Figure 2.4. Compartment Configuration E

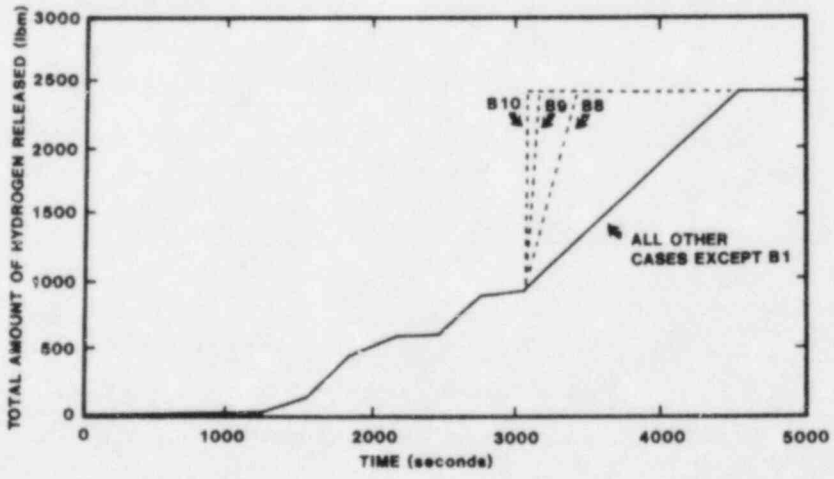

Figure 2.5. Hydrogen Release Into Containment for HECTR Cases B8, B9, B10, and All Others (Except Case B1)

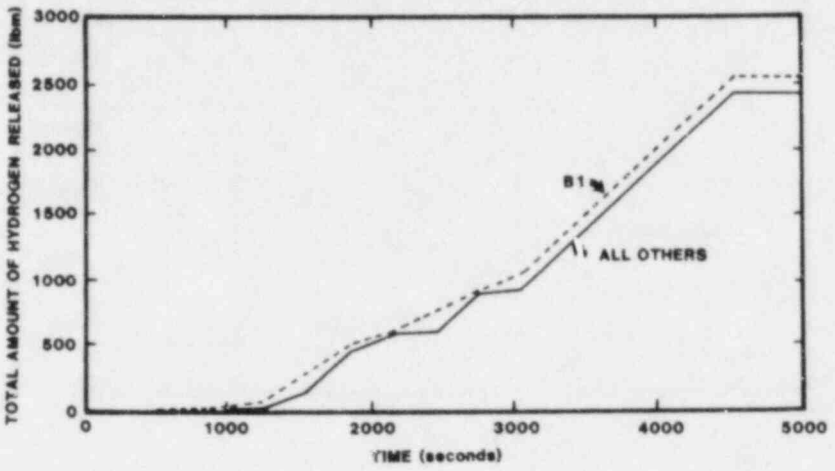

Figure 2.6. Hydrogen Release Into Containment for HECTR Case B1 (Approximately the CLASIX-3 Release History) and All Others (Except B8, B9, and B10)

Table 2.1. CLASIX-3 Case Descriptions[a]

Case Number	Compartment Configuration	Ignition Limit %H_2	Propagation Limits %H_2	Combustion Completeness %	Flame Speed (m/s)	Temp at 3295 Seconds (K)[b]	Pressure at 3295 Seconds (atm)[b]	Spray[c]
1	F[d]	10	10	100	1.8288	299.82	1.157	Auto
2	F	10	10	100	1.8288	299.82	1.0	Auto
3	F	8	8	85	1.8288	299.82	1.0	Auto
5[e]	F	8	8	85	1.8288	299.82	1.0	Off
6	F	8	8	85	1.8288	299.82	1.0	Off

[a]These descriptions were taken from Reference 2.3

[b]3295 seconds is the time when hydrogen production becomes significant. This corresponds to time = 0 in the HECTR cases. Conditions at this time are taken from the plots in Reference 2.3

[c]For Auto, the sprays were turned on after the first burn and remained on for the rest of the run

[d]Similar to configuration B, Fig 2.2, except that the drywell is included as an additional compartment

[e]Ignition was prevented in the wetwell but a burn could propagate into the wetwell with 1% H_2 in it and there burn to 100% completion

Table 2.2. HECTR Case Descriptions for CLASIX-3 Comparison

Case Number	Compartment Configuration	Ignition Limit %H_2	Propagation Limits %H_2	Combustion Completeness %	Flame Speed (m/s)	Initial Temp (K)	Initial Pressure (atm)	Spray*
B-1	B	10	10	100	1.8288	299.82	1.157	Auto
B-2	B	10	10	100	1.8288	299.82	1.0	Auto
B-2'	B	10	10	100	1.8288	299.82	1.0	Auto
B-3	B	8	8	85	1.8288	299.82	1.0	Auto
A-1	A	8	8	85	1.8288	299.82	1.0	Off
B-4	B	8	8	85	1.8288	299.82	1.0	Off

*Sprays: Off —off during entire run
Auto —turned on after temperature or pressure setpoints exceeded and left on for the rest of the run

Table 2.3. Single Compartment (Configuration A) HECTR Case Description

Case Number	Compartment Configuration	Ignition Limit %H_2	Propagation Limits %H_2	Combustion Completeness %	Flame[a] Speed (m/s)	Initial Temp (K)	Initial Pressure (atm)	Spray[b]
A-2	A	8	--	100	F(% H_2)	299.82	1.0	Off
A-3	A	8	--	100	F(% H_2)	299.82	1.0	On
A-4	A	8	--	100	F(% H_2)	299.82	1.0	Auto
A-5	A	8	--	100	F(% H_2)	299.82	1.157	Auto
A-6	A	10	--	100	F(% H_2)	299.82	1.0	Off
A-7	A	10	--	100	F(% H_2)	299.82	1.0	On
A-8	A	10	--	100	F(% H_2)	299.82	1.0	Auto
A-9	A	10	--	100	F(% H_2)	299.82	1.157	Auto
A-10	A	9	--	100	F(% H_2)	299.82	1.0	On
A-11	A	7	--	100	F(% H_2)	299.82	1.0	On
A-12	A	9	--	100	F(% H_2)	299.82	1.0	On

[a]Flame speed is calculated from $V = 59.2\ X_{H_2} + 1.792$ m/s where X_{H_2} is the initial hydrogen mole fraction

[b]Sprays: Off—off during entire run
On—on during entire run
Auto—turned on after temperature or pressure setpoints exceeded and left on for the rest of the run

Table 2.4. Additional Multicompartment HECTR Case Descriptions

Case Number	Compartment Configuration	Ignition Limit %H_2	Propagation Limits[a] %H_2	Combustion Completeness %	Flame Speed[b] (m/s)	Initial Temp (K)	Initial Pressure (atm)	Spray[c]
B-5	B	8	G(% H_2)	100	F(% H_2)	299.82	1.0	Auto
B-6	B	10	G(% H_2)	100	F(% H_2)	299.82	1.0	On
B-6'	B	10	G(% H_2)	100	F(% H_2)	299.82	1.0	On
B-7	B	10	G(% H_2)	100	F(% H_2)	299.82	1.0	Auto
C-1	C	8	G(% H_2)	100	F(% H_2)	299.82	1.0	Auto
C-2	C	10	G(% H_2)	100	F(% H_2)	299.82	1.0	On
C-3	C	10	G(% H_2)	100	F(% H_2)	299.82	1.0	Auto
C-4	C	8	G(% H_2)	100	F(% H_2)	299.82	1.0	Off
D-1	D	8	G(% H_2)	100	F(% H_2)	299.82	1.0	Auto
D-2	D	10	G(% H_2)	100	F(% H_2)	299.82	1.0	Auto
D-3	D	8	G(% H_2)	100	F(% H_2)	299.82	1.0	Off
E-1	E	10	G(% H_2)	100	F(% H_2)	299.82	1.0	Auto

[a]Propagation limits: Upward — 4.1%
Horizontal — 6.0%
Downward — 9.0%

[b]Flame speed is calculated from $V = 59.2\ X_{H_2} + 1.792$ m/s where X_{H_2} is the initial hydrogen mole fraction

[c]Sprays: Off — off during entire run
On — on during entire run
Auto — turned on after temperature or pressure setpoints exceeded and left on for the rest of the run

Table 2.5. Single-Compartment Flame Speed Sensitivity Case Descriptions

Case Number	Compartment Configuration	Ignition Limit %H_2	Propagation[a] Limits %H_2	Combustion Completeness %	Flame Speed (m/s)	Initial Temp (K)	Initial Pressure (atm)	Spray[b]
A-13	A	10	G(% H_2)	100	42.37	299.82	1.0	Off
A-14	A	10	G(% H_2)	100	8.47	299.82	1.0	Off
A-15	A	10	G(% H_2)	100	4.24	299.82	1.0	Off
A-16	A	10	G(% H_2)	100	1.69	299.82	1.0	Off
A-17	A	10	G(% H_2)	100	0.67	299.82	1.0	Off
A-18	A	10	G(% H_2)	100	0.42	299.82	1.0	Off
A-19	A	10	G(% H_2)	100	42.37	299.82	1.0	On
A-20	A	10	G(% H_2)	100	8.47	299.82	1.0	On
A-21	A	10	G(% H_2)	100	4.24	299.82	1.0	On
A-22	A	10	G(% H_2)	100	1.69	299.82	1.0	On
A-23	A	10	G(% H_2)	100	0.67	299.82	1.0	On
A-24	A	10	G(% H_2)	100	0.42	299.82	1.0	On

[a]Propagation limits: Upward — 4.1%
Horizontal — 6.0%
Downward — 9.0%

[b]Sprays: Off — off during entire run
On — on during entire run

Table 2.6. Source Term Sensitivity Case Descriptions

Case Number	Compartment Configuration	Ignition Limit %H_2	Propagation[a] Limits %H_2	Combustion Completeness %	Flame[b] Speed (m/s)	Initial Temp (K)	Initial Pressure (atm)	Spray[c]	Maximum H_2[d] Release Rate (Moles/s)
B-8	B	8	G(% H_2)	100	F(% H_2)	299.82	1.0	Auto	938.4
B-9	B	8	G(% H_2)	100	F(% H_2)	299.82	1.0	Auto	3753.6
B-10	B	8	G(% H_2)	100	F(% H_2)	299.82	1.0	Auto	15014.4

[a]Propagation limits: Upward — 4.1%
Horizontal — 6.0%
Downward — 9.0%

[b]Flame speed is calculated from $V = 59.2\ X_{H_2} + 1.792$ m/s where X_{H_2} is the initial hydrogen mole fraction

[c]Sprays: Auto—sprays turned on after temperature or pressure setpoints exceeded and left on for the rest of the run

[d]Maximum H_2 release rate for all other cases is 234.6 moles/s

Table 2.7. Hydrogen Source Terms Used in HECTR Calculations

Case B1		Case B8		Case B9		Case B10		All Other Cases	
Time (s)	Release Rate (Moles/s)	Time (s)	Release Rate (Moles/s)	Time (s)	Release Rate (Moles/s)	Time (s)	Release Rate (Moles/s)	Time (s)	Release Rate (Moles/s)
0	.8671	0	.1351	0	.1351	0	.1351	0	.1351
306	1.802	306	1.599	306	1.599	306	1.599	306	1.599
336	6.397	336	2.004	336	2.004	336	2.004	336	2.004
606	10.87	606	10.79	606	10.79	606	10.79	606	10.79
906	41.36	906	10.95	906	10.95	906	10.95	906	10.95
1246	153.2	1246	71.76	1246	71.76	1246	71.76	1246	71.76
1563	172.6	1563	234.6	1563	234.6	1563	234.6	1563	234.6
1863	63.03	1863	110.5	1863	110.5	1863	110.5	1863	110.5
2163	122.4	2163	15.56	2163	15.56	2163	15.56	2163	15.56
2463	120.9	2463	229.2	2463	229.2	2463	229.2	2463	229.2
2763	105.3	2763	12.52	2763	12.52	2763	12.52	2763	12.52
3063	216.4	3063	198.1	3063	198.1	3063	198.1	3063	198.1
3064	234.6	3064	938.4	3064	3753.6	3064	15014.4	3064	234.6
4512	0	3426	0	3155	0	3087	0	4512	0
4525		4000		4000		4000		4525	

Table 2.8. Compartment Volumes

Compartment Configuration	Compartment Volume (m^3)				
	1	2	3	4	5
A	37886	—	—	—	—
B	33545	4341	—	—	—
C	23683	14203	—	—	—
D	23683	9862	4341	—	—
E	23683	1654	4480	3278	4341

Table 2.9. Compartment Flame Propagation Lengths

Compartment Configuration	Compartment Flame Propagation Length (m)				
	1	2	3	4	5
A	25.4	—	—	—	—
B	21.9	3.7	—	—	—
C	19.0	11.1	—	—	—
D	19.0	11.1	3.7	—	—
E	19.0	11.1	14.3	7.9	7.3

Table 2.10. Interconnection Areas and Flow Coefficients

Compartment Configuration or Connections	Interconnection Area (m^2)	Flow Coefficient
Two-Compartment Models		
B	206.8	1.2
C	226.4	1.2
Three-Compartment Model (D)		
1 – 2	226.4	1.2
2 – 3	206.8	1.2
Five-Compartment Model (E)		
1 – 2	74.3	0.75
1 – 3	152.1	1.5
2 – 3	135.64	1.5
2 – 4	157.0	1.5
2 – 5	62.4	0.75
3 – 4	228.8	1.5
4 – 5	144.4	1.5

Table 2.11. Spray Data for All Cases

Data	Measurement
Inlet Temperature	330.37 K
Flow Rate (One Spray Train)	11300 gpm
Fall Height*	19.5 m
Number of Drop Sizes	2
Frequency of First Drop Size	0.95
Frequency of Second Drop Size	0.05
Diameter of First Drop	309 microns
Diameter of Second Drop	810 microns
Containment Temperature Setpoint**	358.15 K
Containment Pressure Setpoint**	1.6124 atm
Time Delay for Spray Actuation	120 s

*For case B2', in which the spray was allowed to carry over into the wetwell, the wetwell fall height was assumed to be 7.315 m, and 10% of the spray was assumed to carry over from compartment 1 into the wetwell.
**Sprays on Auto are turned on when either of these setpoints is exceeded in any compartment and remain on throughout the rest of the run.

Table 2.12. Surface Descriptions

Surface Number	Surface	Area (m^2)	Material
1.	Concrete Floor	297	Concrete
2.	Steel Pool Walls	128	Steel
3.	Upper Pool	396	Water
4.	Crane	1188	Steel
5.	Dome	3291	Steel
6.	Wetwell Wall	393	Steel
7.	Grating at 209' Level	575	Steel
8.	Grating at 185' Level	358	Steel
9.	Equipment	3027	Steel
10.	Concrete	2103	Concrete
11.	Wetwell Wall	950	Steel
12.	Drywell Wall	202	Concrete
13.	Grating at 161' Level	745	Steel
14.	Equipment	1334	Steel
15.	Concrete	396	Concrete
16.	Wetwell Wall	702	Steel
17.	Drywell Wall	487	Concrete
18.	Grating at 135' Level	792	Steel
19.	Concrete	308	Concrete
20.	Grating at 121' Level	335	Steel
21.	Suppression Pool	619	Water
22.	Wetwell Wall	832	Steel
23.	Drywell Wall	557	Concrete

Table 2.13. Location of Surfaces

Compartment Configuration	Surface from Table 2.12 Contained in Compartment				
	1	2	3	4	5
A	all	--	--	--	--
B	1-17	18-23	--	--	--
C	1-5	6-23	--	--	--
D	1-5	6-17	18-23	--	--
E	1-5	6	7-12	13-17	18-23

Table 2.14. Wall Properties All Cases

	Steel	Concrete	Water
Thermal Conductivity W/m-K	43.27	1.385	---
Thermal Diffusivity m^2/s	1.17×10^{-5}	5.5×10^{-7}	---
Specific Heat J/kg-K	460.5	879.	---
Emissivity	0.7*	0.9	0.94

*Assumes all steel surfaces are painted

2.2.2 Results

Results for the five CLASIX-3 cases are summarized in Table 2.15. Results for the 44 HECTR cases are summarized in Tables 2.16 to 2.21. The number of burns in each compartment is presented along with the final gas compositions and the maximum temperature and pressure encountered during the run. Each of the HECTR cases is discussed briefly below, and seven cases (B2′, A6, A8, B5, C3, D2, and E1) have been selected for presentation in more detail. For many two-or-more-compartment cases only a single pressure plot has been presented. These can be considered to be effectively the containment pressure plots since the pressures in individual compartments follow each other closely. In the following discussions, the containment failure pressure is assumed to be 4.8 atm[2,3] (all pressures are absolute).

Cases B1, B2, and B2′—HECTR case B1 was meant to model CLASIX-3 case 1, and HECTR cases B2 and B2′ were meant to model CLASIX-3 case 2. In CLASIX-3 cases 1 and 2, large numbers of burns occurred in compartment 2 (wetwell), and no burns occurred in the dome. In the HECTR runs, oxygen inerting in the wetwell occurs earlier than in the CLASIX-3 runs, leading to more hydrogen transferred to compartment 1 (containment). The result is that HECTR cases B1, B2 and B2′, contrary to CLASIX-3, predict a burn in compartment 1 and a peak pressure in excess of the 4.8 atm failure pressure.

The only difference between HECTR cases B2 and B2′ is that in case B2′ the sprays were allowed to fall from compartment 1 into the wetwell. Case B2′ was added to see if the treatment of sprays in the wetwell was responsible for the differences between HECTR cases B1 and B2 and CLASIX-3 cases 1 and 2. The results were that in case B2′, wetwell inerting was delayed with respect to case B2, but the end results were similar. Pressure plots for cases B1 and B2 are shown in Figures 2.7 and 2.8, and case B2′ is presented in detail in Figures 2.9 to 2.20. Figure 2.19 shows oxygen inerting at approximately 3600 s and Figures 2.14 and 2.20 show large increases in the hydrogen mole fraction after this time. Note that when ignition finally occurs in compartment 1, oxygen is pushed back into compartment 2 and a burn occurs there also. The wetwell temperature plot for HECTR case B2 is presented in Figure 2.21 for comparison with case B2′ (Figure 2.15).

Despite the fact that the CLASIX-3 case 1 and 2 results and the HECTR cases B1, B2, and B2′ results appear to be very different, we feel that the codes are behaving similarly. Close examination of CLASIX-3 case 2 reveals that the wetwell is inert ($X_{O_2} = 0.049 < 0.05$) near the end of the run (Table 2.15). In the HECTR cases, wetwell inerting occurred just soon enough to get a compartment 1 burn before the end of the run, and in CLASIX-3 case 2, wetwell inerting occurred just late enough not to get a compartment 1 burn. Note that there was 8.5% hydrogen in compartment 1 at the end of CLASIX-3 case 2.

Cases B3, A1, and B4—HECTR cases B3, A1, and B4 (Figures 2.22, 2.23, and 2.24) were meant to model CLASIX-3 cases 3, 5, and 6. Each of these runs involved ignition at an 8% hydrogen concentration and combustion that was 85% complete. HECTR cases B3 and B4 involved compartment configuration B, while case A1 involved compartment configuration A. CLASIX-3 cases 3 and 6 predicted a large number of wetwell burns and no burns in the dome, while the corresponding HECTR cases B3 and B4 predicted eventual inerting in the wetwell followed by a burn in the dome. However, containment failure was not predicted in either case B3 or B4, although case B4 predicted pressures within 0.2 atm of the assumed failure pressure. HECTR case A1 and CLASIX-3 case 5 produced similar results, with HECTR predicting a higher pressure, but not one close to failure.

Cases A2 Through A12—Cases A2 through A12 were run to examine the effects of global burns under a variety of conditions. As discussed earlier, combustion is assumed to be 100% complete and the flame speed (6.5 m/s for 8% burn and 7.7 m/s for 10% burn) is about a factor of 4 higher than that used in CLASIX-3.

Cases A2 and A6 examine the effects of having no containment sprays. As expected, high pressures are achieved. A pressure plot for case A2 is shown in Figure 2.25. Case A6, with a maximum pressure well in excess of the failure pressure, is presented in detail in Figures 2.26 to 2.31.

Cases A3, A7, A10, A11, and A12 (Figures 2.32 through 2.36) were run with the sprays on from the beginning of the accident, and significant reductions in maximum pressures are observed, although in case A7 the maximum pressure is very close to failure. These cases also show the effect of varying the ignition point from 6% hydrogen to 10% hydrogen. Case A10, which ignites hydrogen at 6%, has a peak pressure of 3.2 atm, and case A7, which ignites hydrogen at 10%, has a peak pressure of 4.8 atm.

In cases A4 and A8, the sprays come on shortly after the first burn, and the results are similar to the

results of cases A3 and A7. A pressure plot for case A4 is shown in Figure 2.37, and case A8 is presented in detail in Figures 2.38 through 2.43. It should be pointed out that in case A6, the first burn did not fail containment, so the main difference between the results of case A6 and case A8 is the difference in pressure rise after the second and third burns. The reason that cases A3 and A7 resulted in higher pressures than cases A4 and A8 is that the sprays contributed to heating up the containment slightly before the first burn. This was due to our choice of spray temperature which was taken from Reference 2.3.

Cases A5 and A9 (Figures 2.44 and 2.45) show the effect of a slightly elevated pressure at the start of the run. Marked increases in maximum pressure over cases A4 and A8 are observed, with case A9 well above the failure pressure. These elevated initial pressures would be characteristic of a drywell break, in which air is pushed from the drywell into the containment. It should be noted that reverse flow, from the containment into the drywell (through the suppression pool), would afford some measure of pressure relief during a burn.

Cases B5, B6, B6′ and B7—Cases B5, B6, B6′ and B7 (Figures 2.46 through 2.60) all use compartment configuration B, which is very similar to that used in the CLASIX-3 analysis. However, we have assumed complete combustion and higher flame speeds. Additionally, the propagation limits discussed earlier were in effect.

In case B6, a global burn was predicted, but the pressure rise was small due to the fact that the hydrogen concentration in compartment 1 was not far above the 4.1% upward propagation limit when the burn occurred. Cases B5 and B7 resulted in containment failure due to the fact that compartment 2 eventually inerted, resulting in compartment 1 burns with hydrogen concentrations at the ignition limits rather than at the propagation limits.

Most of the cases were arbitrarily stopped shortly after the hydrogen source went to zero. However, it was noted that in some of the cases (particularly A2, A3, A4, and B6) the hydrogen concentration in the dome region at the end of the run was very close to the ignition point. This was also true of CLASIX-3 cases 3 and 6 and, to a lesser extent, CLASIX-3 cases 1 and 2. In all of these cases, there is a significant amount of steam present at the end of the run. It is to be expected that, as the containment cools down, the steam will condense, thus raising the hydrogen mole fraction and resulting in a burn at a later time. Case B6′ is an exact duplicate of case B6, except that a longer run time is used, and demonstrates this point. In case B6′, a compartment 1 burn that fails containment occurs about 2 min after the hydrogen source becomes zero.

Cases C1 Through C4—Cases C1 through C4 (Figures 2.61 through 2.75) involve compartment configuration C. In each of these cases, upper compartment burns occur; however, they occur just above the propagation limits, and the pressure rises do not result in containment failure.

Cases D1 Through D3—Cases D1 through D3 (Figures 2.76 through 2.89) represent the three-compartment model. In each case, most of the burns occur in compartment 3 (wetwell). Compartment 3 eventually inerts, leading to burns in compartment 2 and one burn propagating into compartment 1 (dome). The predicted peak pressures do not threaten containment.

Case E1—Case E1 represents the five-compartment model and is presented in Figures 2.90 through 2.109. There are several burns observed in compartment 5 (wetwell) before it finally inerts due to oxygen depletion. After compartment 5 inerts, most of the burns occur in compartment 2. The burns occur in compartment 2 rather than in compartment 4 due to a lower flow coefficient between compartments 5 and 2 than between compartments 5 and 4. This results in hydrogen moving preferentially into compartment 2. Two burns are observed in compartment 1 (dome); however, they occur at hydrogen concentrations just above the propagation limits and do not result in containment failure.

Cases A13 Through A24—Cases A13 through A24 (Figures 2.110 through 2.121) show the effects of varying the flame speed. The flame speeds used result in burn times ranging from 0.01 to 1.0 min. Cases A13 to A18 assumed no sprays, and the differences in pressure rise were small except for very long burn times. Cases A19 through A24 assumed the sprays were on, and the differences in pressure rise were much more pronounced. This was to be expected because the sprays are usually the dominant heat transfer mechanisms.

Cases B8 Through B10—Cases B8 through B10 (Figures 2.122 through 2.124) show the effects of injecting hydrogen very rapidly into the wetwell. In each case, the results are similar. Once the hydrogen starts coming in rapidly, the wetwell inerts after one or two burns. The hydrogen is released so fast that there is no time to cool down and draw oxygen back into the wetwell from the dome between burns. Soon after the wetwell inerts, a burn in the dome follows, resulting in very high pressures (even with sprays on). Usually this burn in the dome pushes oxygen back into the wetwell, causing a burn there also.

Table 2.15. Results for CLASIX-3 Runs[a]

Case Number	Number of Burns		Final Mole Fractions								Maximum Temperature (K)[b]	Maximum Pressure (atm)[b]
			Compartment 1 (Containment)				Compartment 2 (Wetwell)					
	Comp. 1	Comp. 2	N_2	O_2	H_2	H_2O	N_2	O_2	H_2	H_2O		
1	0	18	.64	.135	.075	.15	.58	.11	.05	.26	1085.4	1.755
2	0	43	.64	.055	.085	.22	.59	.049	.111	.25	1072.6	1.504
3	0	58	.66	.052	.078	.21	.615	.045	.11	.23	845.4	1.456
5	4	4	.655	.035	.03	.28	.64	.04	.055	.265	1379.3	3.361
6	0	68	.63	.05	.075	.245	.603	.049	.112	.236	1130.4	1.701

[a]These results were taken from Reference 2.3

[b]Maximum of the wetwell and containment values

Table 2.16. Results of HECTR Runs for CLASIX-3 Comparison

Case Number	Number of Burns		Final Mole Fractions								Maximum Temperature (K)	Maximum Pressure (atm)
			Compartment 1				Compartment 2					
	Comp. 1	Comp. 2	N_2	O_2	H_2	H_2O	N_2	O_2	H_2	H_2O		
B - 1	1	21	.4890	.0462	.0112	.4535	.3759	.0306	.2871	.3064	1298	5.600
B - 2	1	24	.5715	.0468	.0192	.3625	.3424	.0185	.3273	.3118	1323	4.845
B - 2'	1	21	.4201	.0291	.0060	.5448	.3601	.0144	.2110	.4145	1263	5.042
B - 3	1	32	.7013	.0778	.0571	.1638	.2749	.0210	.4770	.2271	1298	3.830
A - 1	4	--	.6315	.0403	.0330	.2951	--	--	--	--	1053	4.090
B - 4	1	30	.6759	.0766	.0409	.2067	.2635	.0180	.5073	.2112	1315	4.630

Table 2.17. Results for Single-Compartment HECTR Cases

Case Number	Number of Burns		Final Mole Fractions								Maximum Temperature (K)	Maximum Pressure (atm)
			Compartment 1				Compartment 2					
	Comp. 1	Comp. 2	N_2	O_2	H_2	H_2O	N_2	O_2	H_2	H_2O		
A - 2	3	--	.6231	.0591	.0712	.2466	--	--	--	--	1178	4.414
A - 3	3	--	.7056	.0630	.0727	.1586	--	--	--	--	968	3.982
A - 4	3	--	.6953	.0652	.0781	.1614	--	--	--	--	1122	3.902
A - 5	3	--	.6773	.0651	.0358	.2218	--	--	--	--	1126	4.514
A - 6	3	--	.6362	.0266	.0052	.3319	--	--	--	--	1353	5.278
A - 7	3	--	.5057	.0208	.0034	.4701	--	--	--	--	1156	4.774
A - 8	3	--	.5306	.0245	.0089	.4360	--	--	--	--	1304	4.647
A - 9	2	--	.6894	.0849	.0737	.1520	--	--	--	--	1308	5.326
A - 10	5	--	.5887	.0265	.0086	.3763	--	--	--	--	767	3.177
A - 11	4	--	.6396	.0375	.0269	.2960	--	--	--	--	866	3.599
A - 12	3	--	.6240	.0389	.0308	.3063	--	--	--	--	1067	4.441

Table 2.18. Results for Additional HECTR Two-Compartment Cases

Case Number	Number of Burns		Final Mole Fractions								Maximum Temperature (K)	Maximum Pressure (atm)
			Compartment 1				Compartment 2					
	Comp. 1	Comp. 2	N_2	O_2	H_2	H_2O	N_2	O_2	H_2	H_2O		
B - 5	1	30	.6944	.0672	.0434	.1950	.3304	.0292	.4137	.2267	1305	4.877
B - 6	1	18	.6710	.1145	.0968	.1177	.1051	.0136	.7872	.0940	1305	2.467
B - 6'	2	19	.7557	.0510	.0410	.1523	.6517	.0424	.0727	.2331	1410	5.693
B - 7	2	21	.5100	.0332	.0043	.4526	.4566	.0263	.2684	.2487	1384	5.502
C - 1	1	9	.7451	.1003	.0278	.1267	.4675	.0308	.2601	.2416	1088	2.694
C - 2	1	7	.7293	.1029	.0411	.1268	.4878	.0307	.2430	.2384	1212	2.898
C - 3	1	7	.7277	.1046	.0417	.1260	.4828	.0317	.2512	.2343	1211	2.858
C - 4	1	9	.6786	.0883	.0263	.2069	.5145	.0300	.1832	.2723	1111	3.310

Table 2.19. Results for HECTR Three- and Four-Compartment Cases

Case	Compartment	Number of Burns	Final Mole Fraction				Maximum Temperature (K)	Maximum Pressure (atm)
			N_2	O_2	H_2	H_2O		
D - 1	1	1	0.7333	0.0921	0.0078	0.1668	1195	2.630
	2	8	0.5468	0.0458	0.1394	0.2630		
	3	17	0.2365	0.0205	0.6006	0.1423		
D - 2	1	1	0.7431	0.1071	0.0168	0.1330	1310	2.800
	2	6	0.5179	0.0400	0.1568	0.2853		
	3	13	0.1957	0.0195	0.6611	0.1237		
D - 3	1	1	0.6918	0.0854	0.0092	0.2136	1207	3.270
	2	8	0.6377	0.0314	0.0293	0.3017		
	3	19	0.3258	0.0274	0.4781	0.1688		
E - 1	1	2	0.7185	0.0774	0.0466	0.1574	1477	2.579
	2	24	0.5069	0.0496	0.2669	0.1766		
	3	1	0.7113	0.0901	0.0371	0.1615		
	4	6	0.6941	0.0932	0.0519	0.1608		
	5	18	0.2377	0.0221	0.5906	0.1496		

Table 2.20. Results of Flame Speed Sensitivity Analysis

Case Number*	Flame Speed (m/s)	Maximum Temperature (K)	Maximum Pressure (atm)
A - 13	42.37	1322	4.652
A - 14	8.47	1301	4.574
A - 15	4.24	1274	4.482
A - 16	1.69	1207	4.253
A - 17	0.67	1084	3.828
A - 18	0.42	1004	3.555
A - 19	42.37	1287	5.106
A - 20	8.47	1167	4.838
A - 21	4.24	1043	4.555
A - 22	1.69	756	3.766
A - 23	0.67	456	2.658
A - 24	0.42	405	2.394

*These runs were stopped after the first burn.

Table 2.21. Results of H_2 Source Term Sensitivity Analysis

Case Number	Number of Burns		Final Mole Fractions								Maximum Temperature (K)	Maximum Pressure (atm)
			Compartment 1				Compartment 2					
	Comp. 1	Comp. 2	N_2	O_2	H_2	H_2O	N_2	O_2	H_2	H_2O		
B - 8	1	22	.6930	.0748	.0740	.1582	.4194	.0430	.2887	.2490	1362	5.438
B - 9	1	21	.7020	.0723	.0768	.1489	.4658	.0451	.2194	.2697	1345	5.762
B - 10	2	21	.7455	.0417	.0251	.1876	.5373	.0324	.0775	.3529	1342	5.271

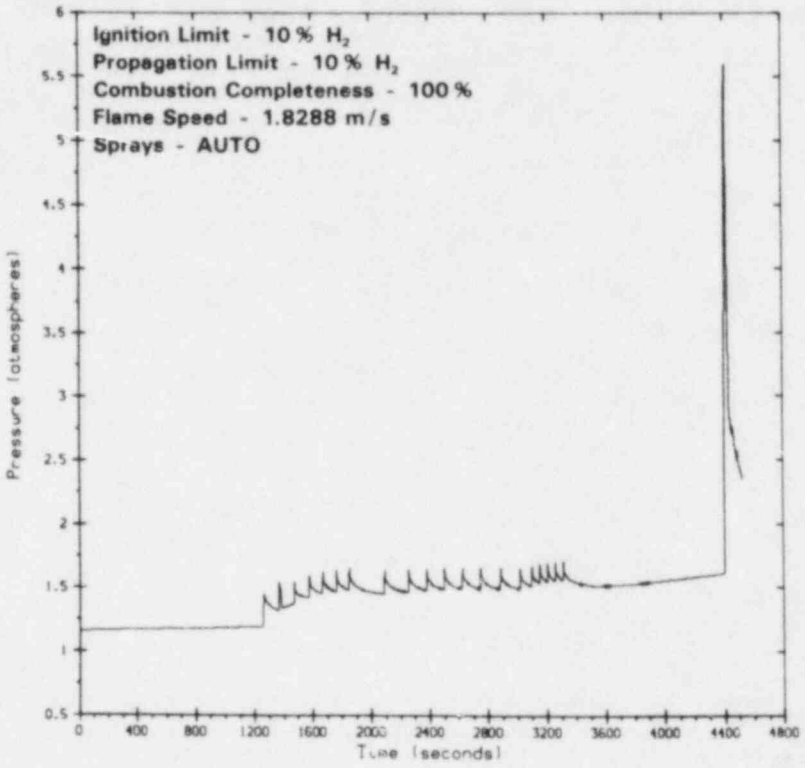

Figure 2.7. Case B1, Compartment 1 Pressure

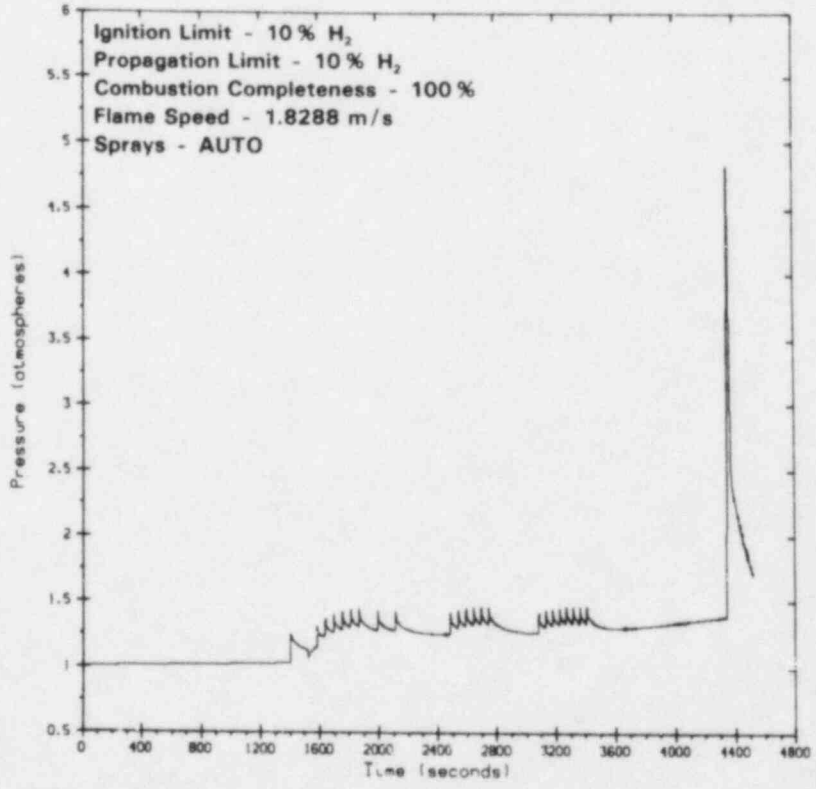

Figure 2.8. Case B2, Compartment 1 Pressure

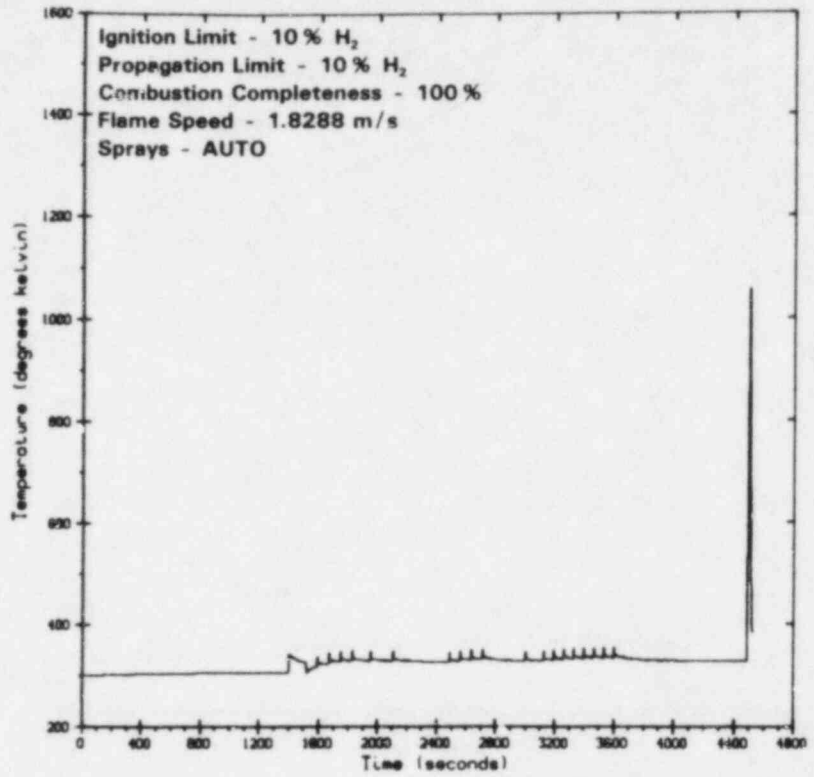

Figure 2.9. Case B2′, Compartment 1 Temperature

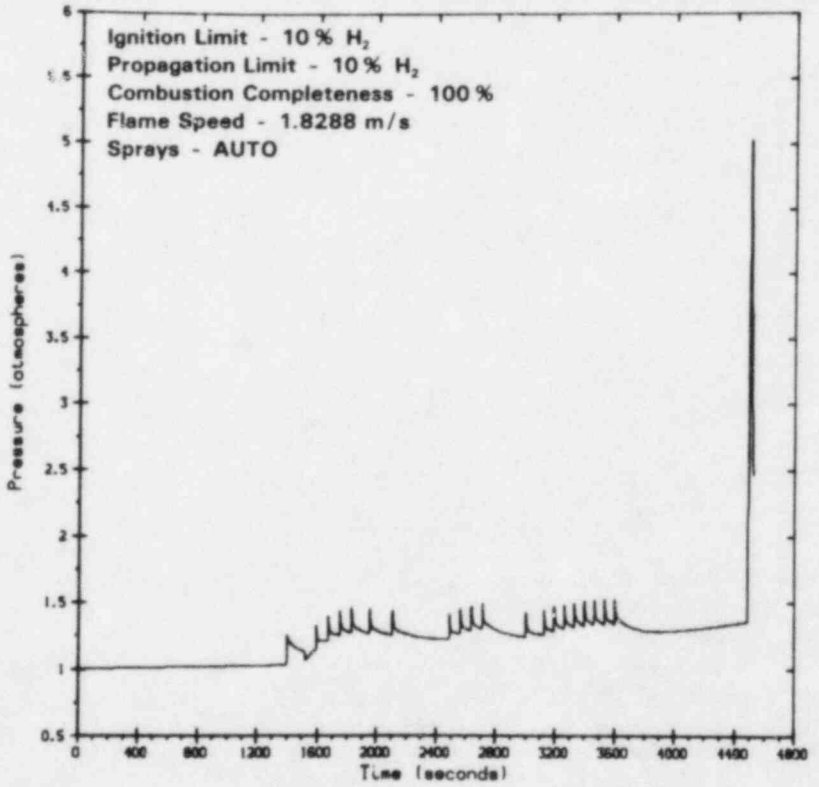

Figure 2.10. Case B2′, Compartment 1 Pressure

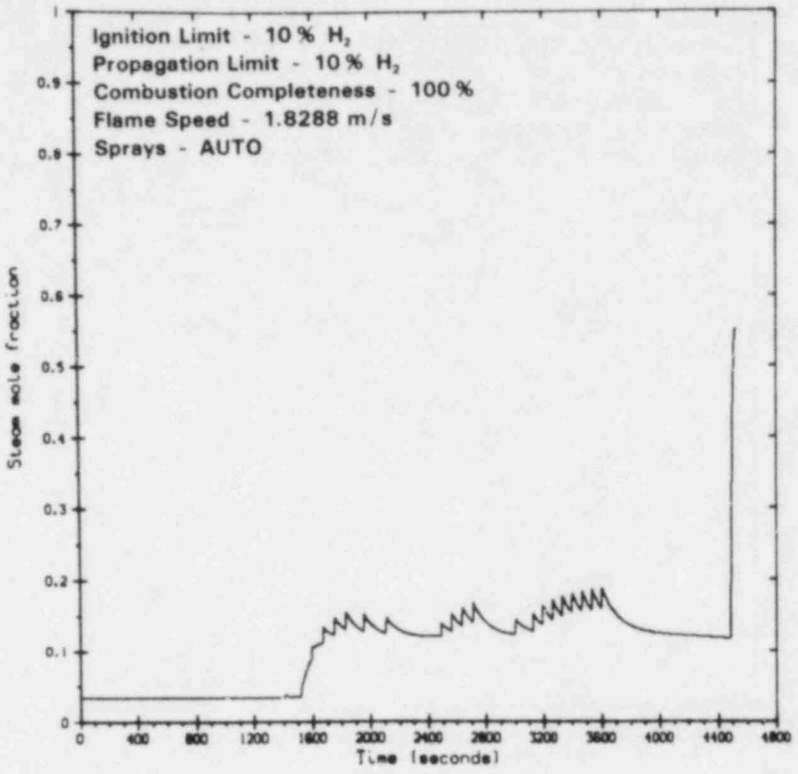

Figure 2.11. Case B2′, Compartment 1 Steam Mole Fraction

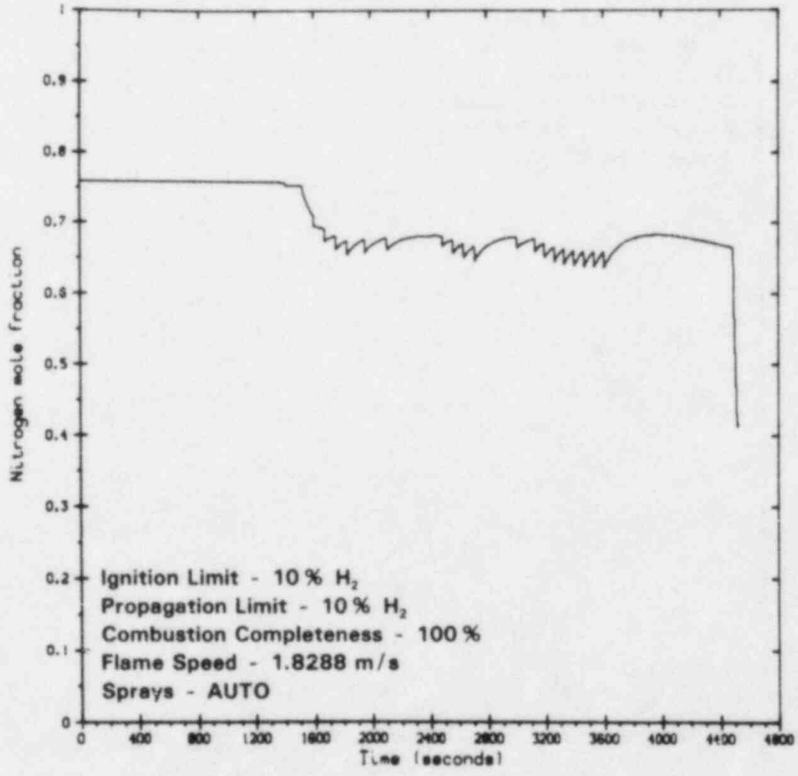

Figure 2.12. Case B2′, Compartment 1 Nitrogen Mole Fraction

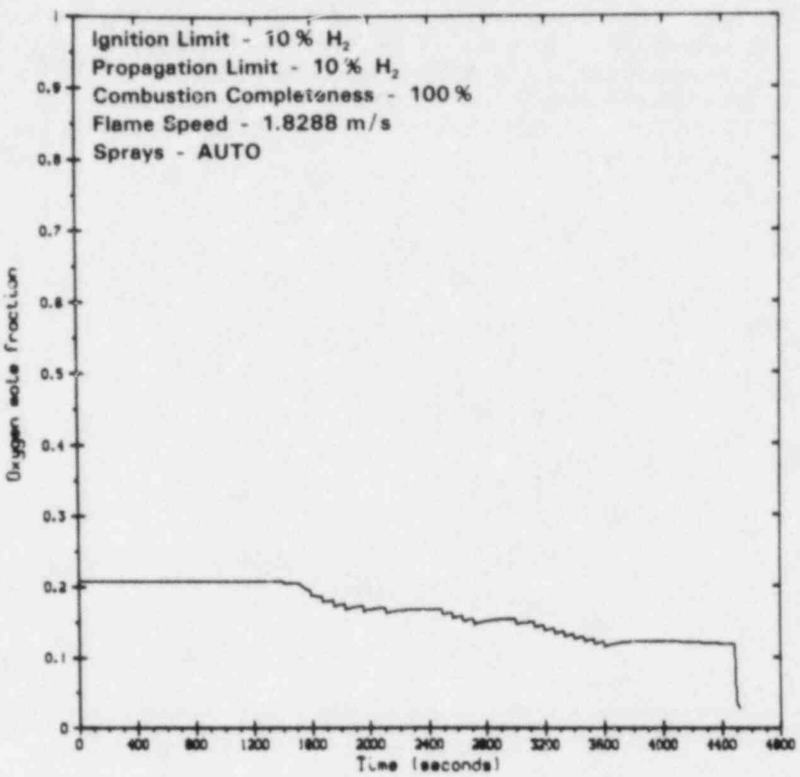

Figure 2.13. Case B2′, Compartment 1 Oxygen Mole Fraction

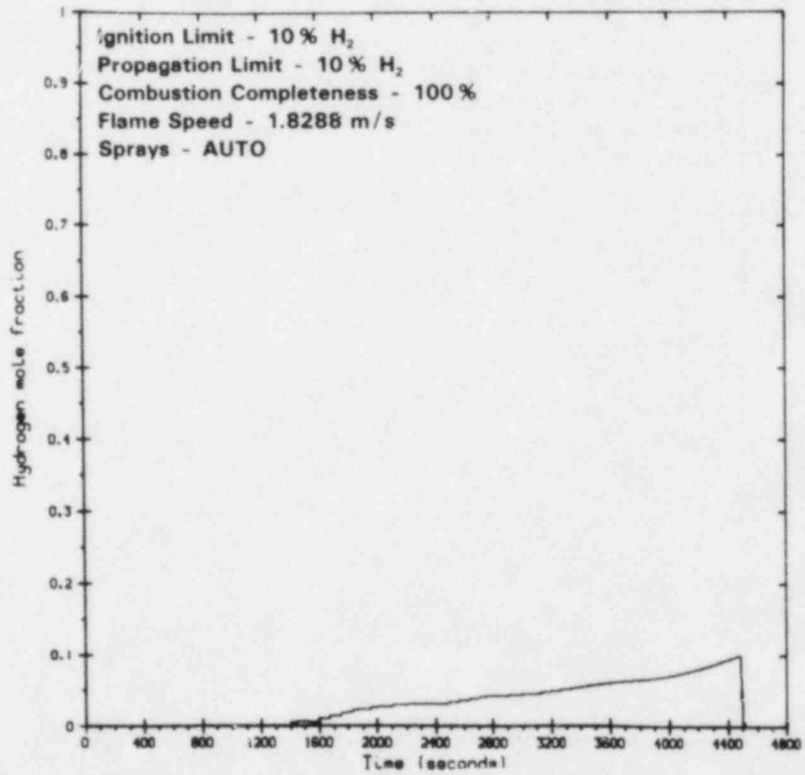

Figure 2.14. Case B2′, Compartment 1 Hydrogen Mole Fraction

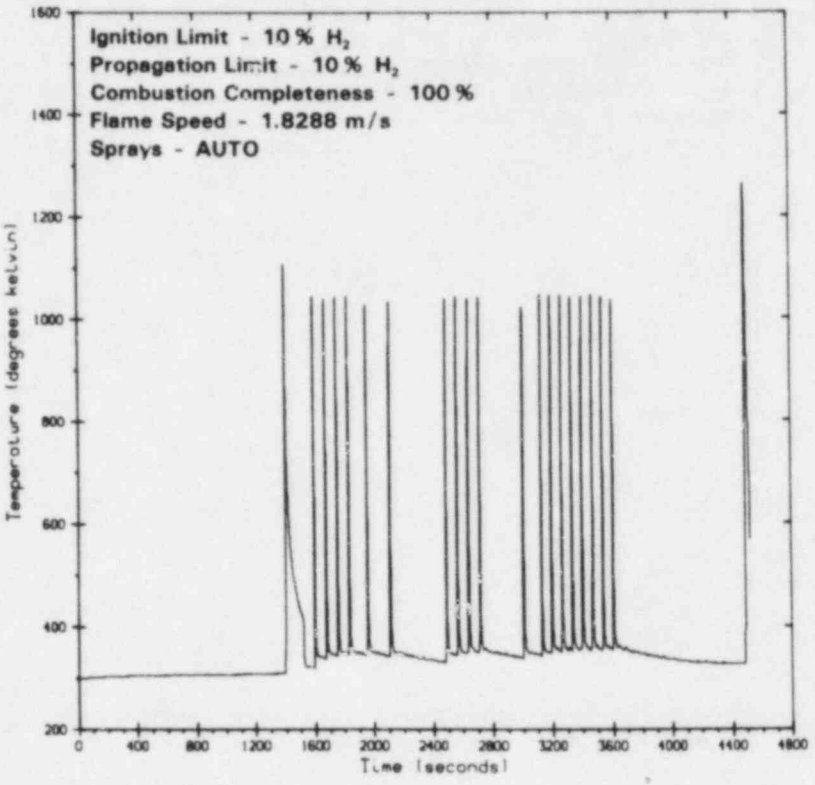

Figure 2.15. Case B2′, Compartment 2 Temperature

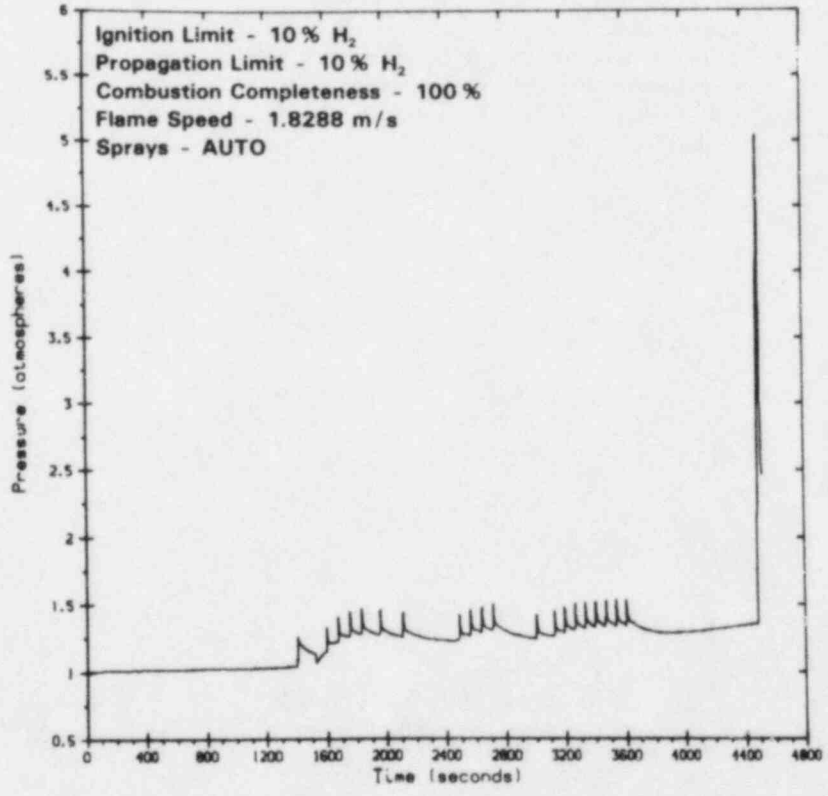

Figure 2.16. Case B2′, Compartment 2 Pressure

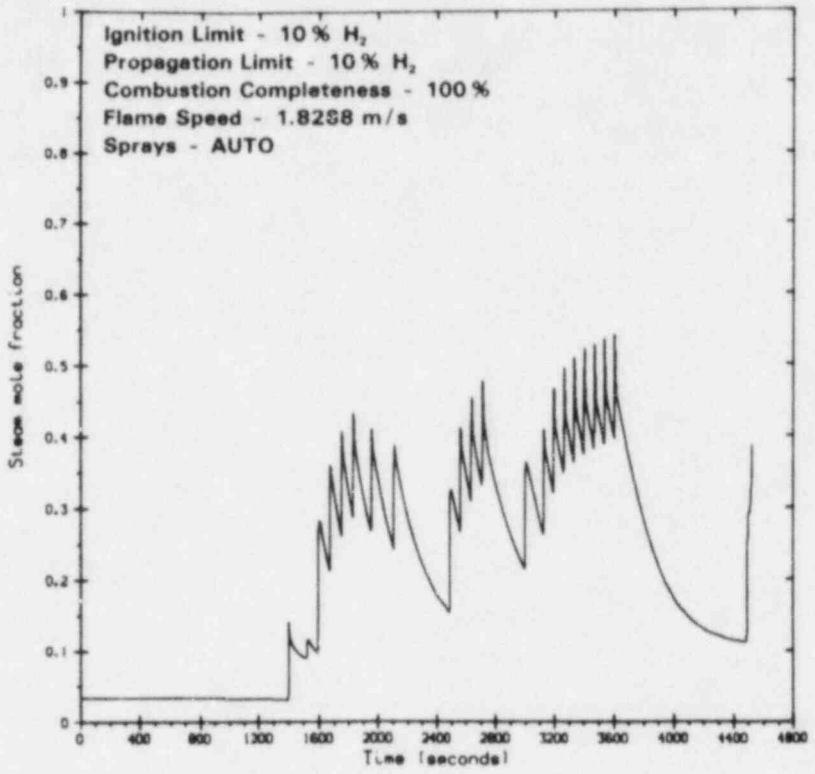

Figure 2.17. Case B2′, Compartment 2 Steam Mole Fraction

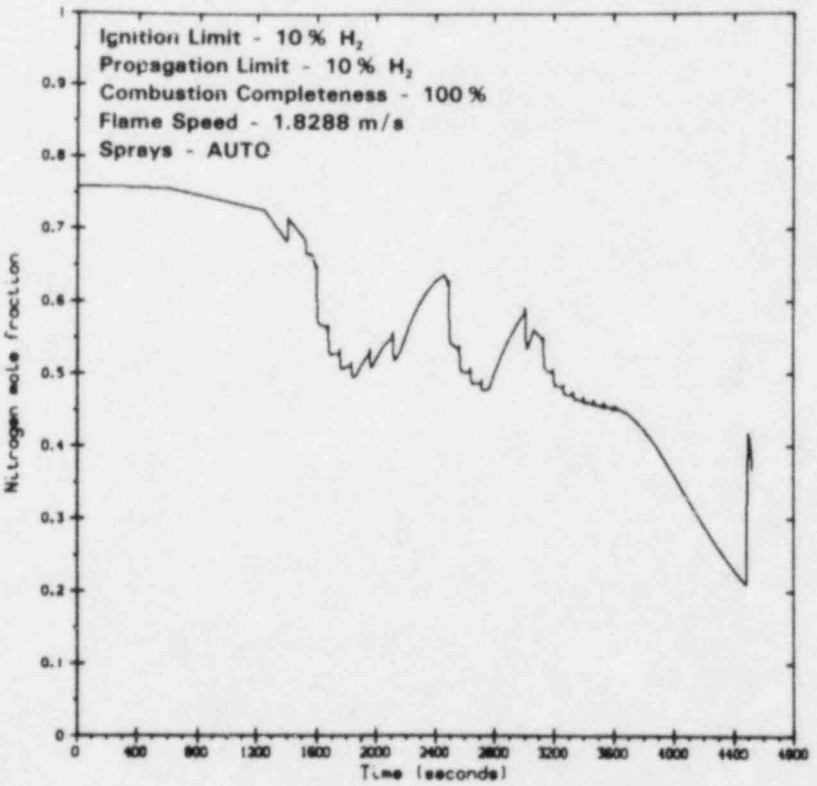

Figure 2.18. Case B2′, Compartment 2 Nitrogen Mole Fraction

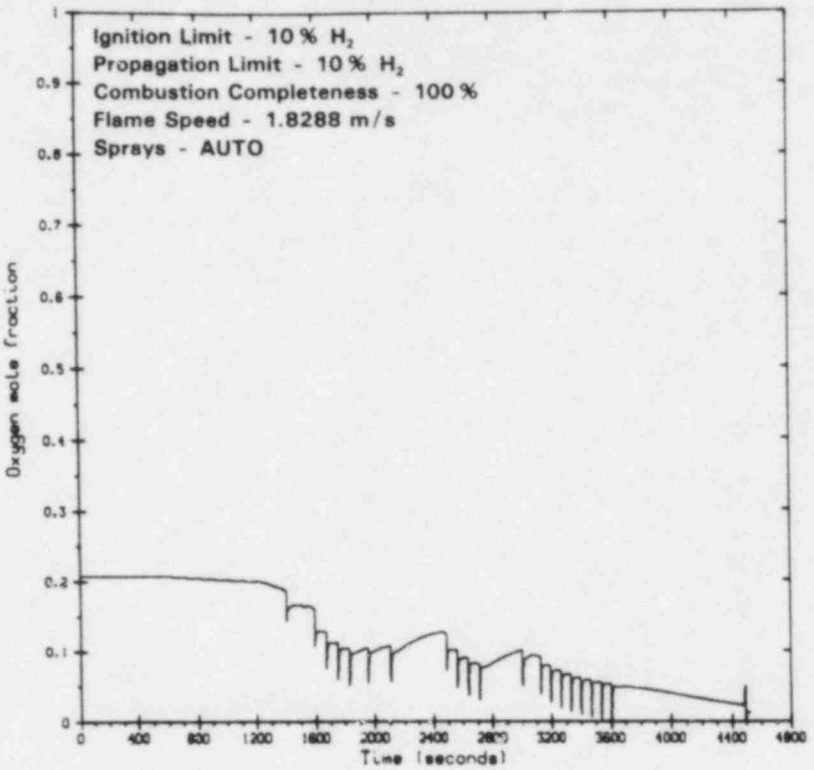

Figure 2.19. Case B2′, Compartment 2 Oxygen Mole Fraction

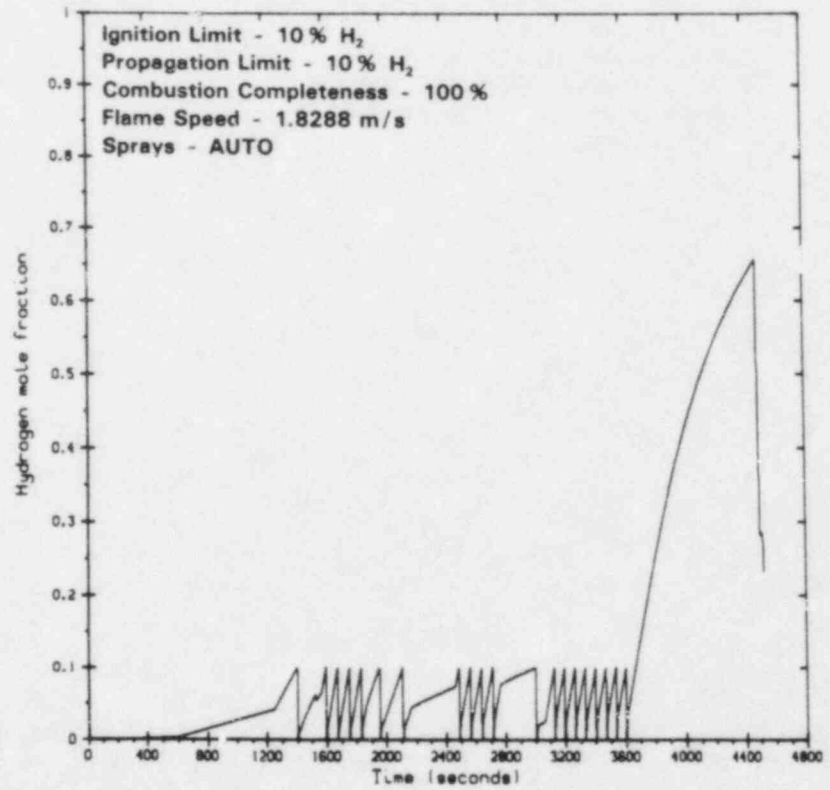

Figure 2.20. Case B2′, Compartment 2 Hydrogen Mole Fraction

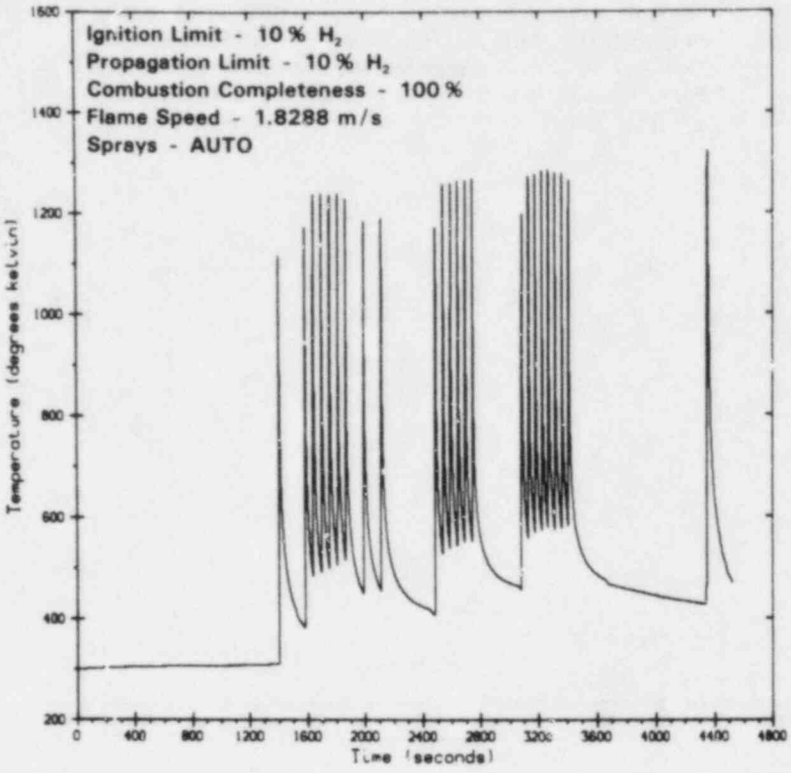

Figure 2.21. Case B2, Compartment 2 Temperature

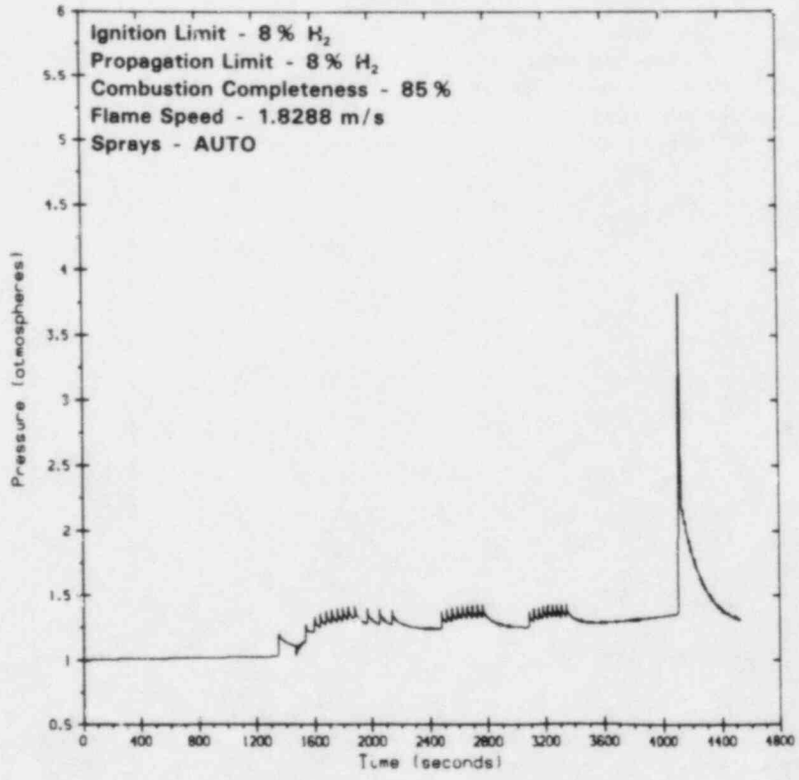

Figure 2.22. Case B3, Compartment 1 Pressure

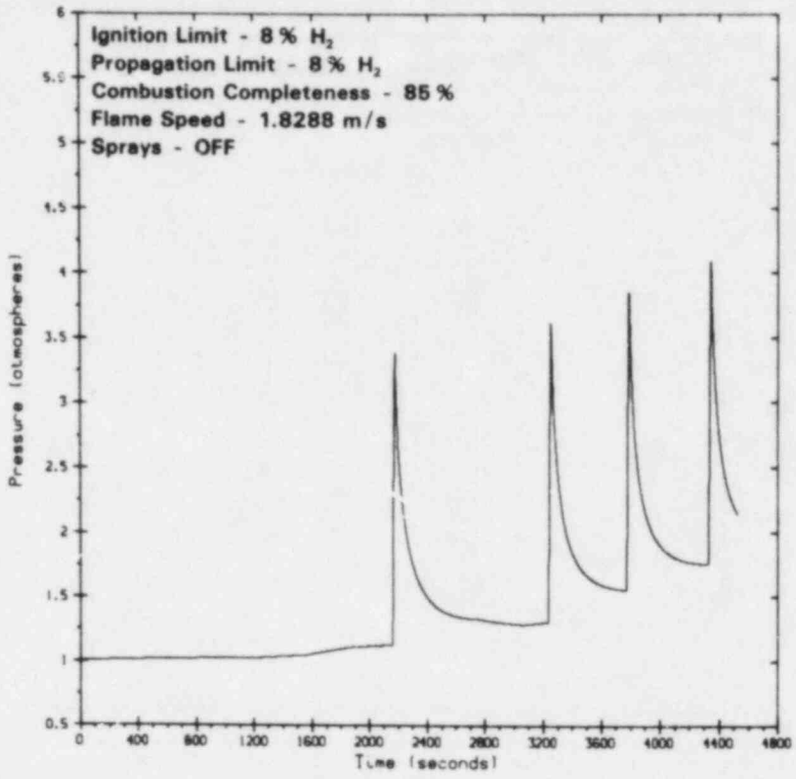

Figure 2.23. Case A1, Compartment 1 Pressure

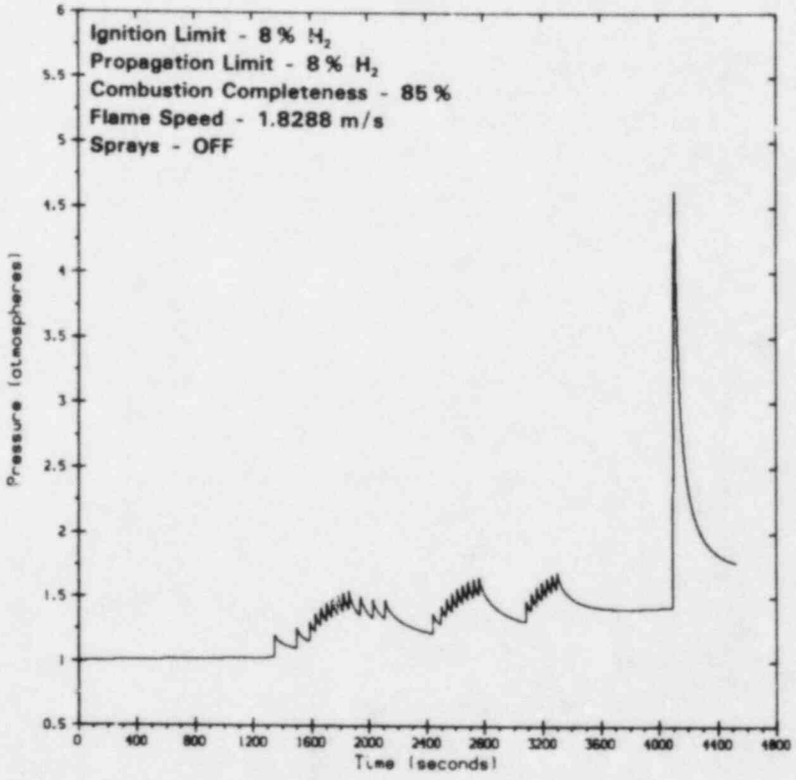

Figure 2.24. Case B4, Compartment 1 Pressure

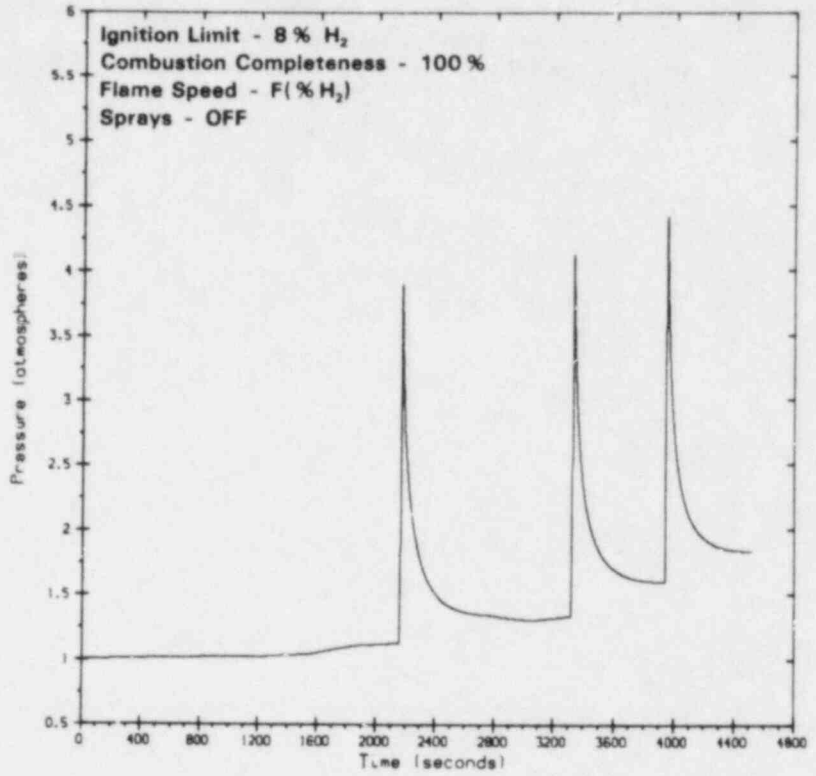

Figure 2.25. Case A2, Compartment 1 Pressure

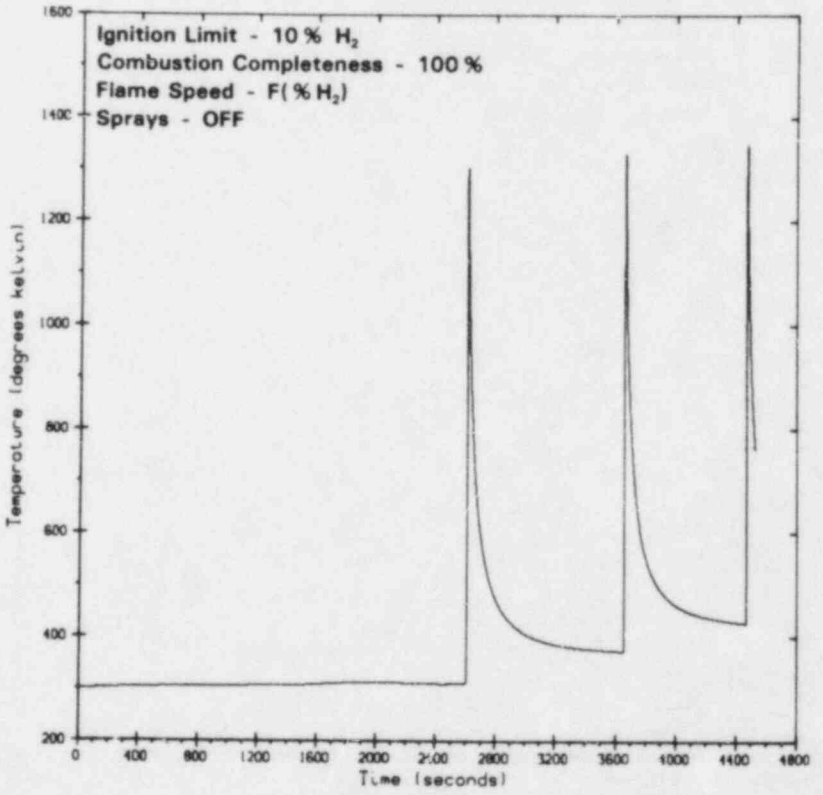

Figure 2.26. Case A6, Compartment 1 Temperature

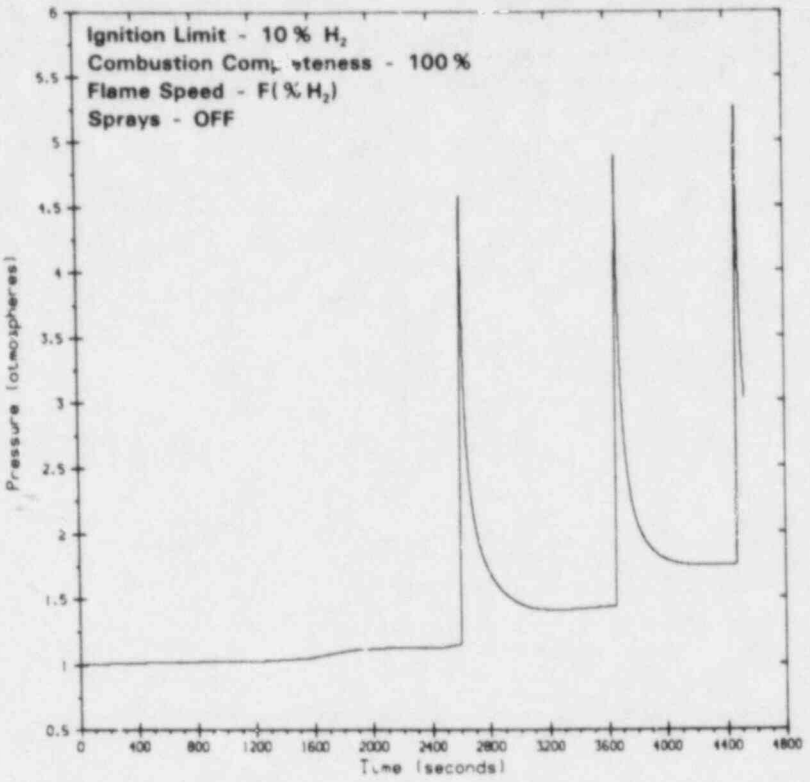

Figure 2.27. Case A6, Compartment 1 Pressure

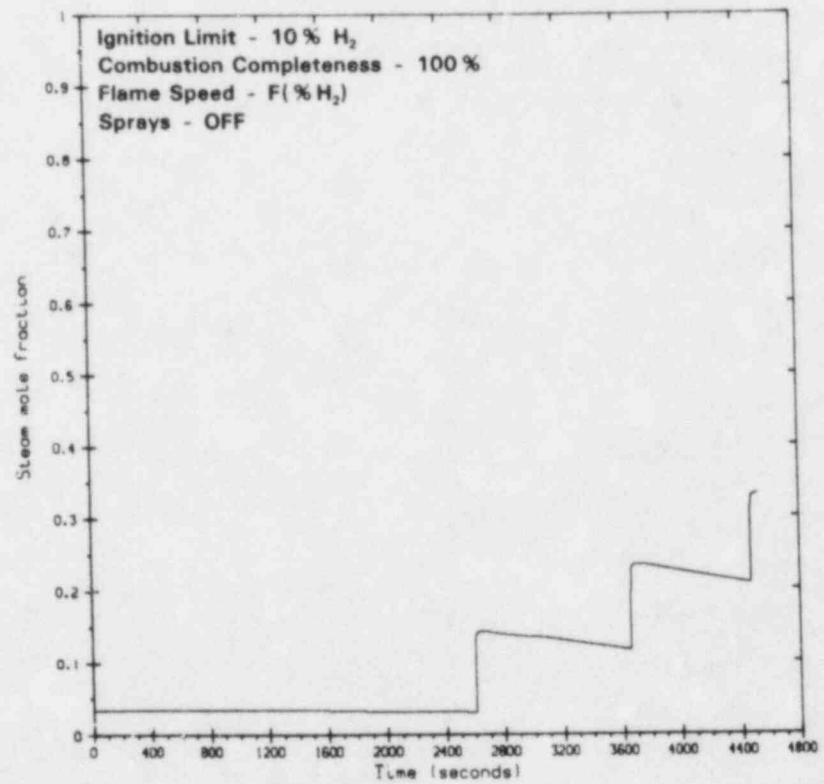

Figure 2.28. Case A6, Compartment 1 Steam Mole Fraction

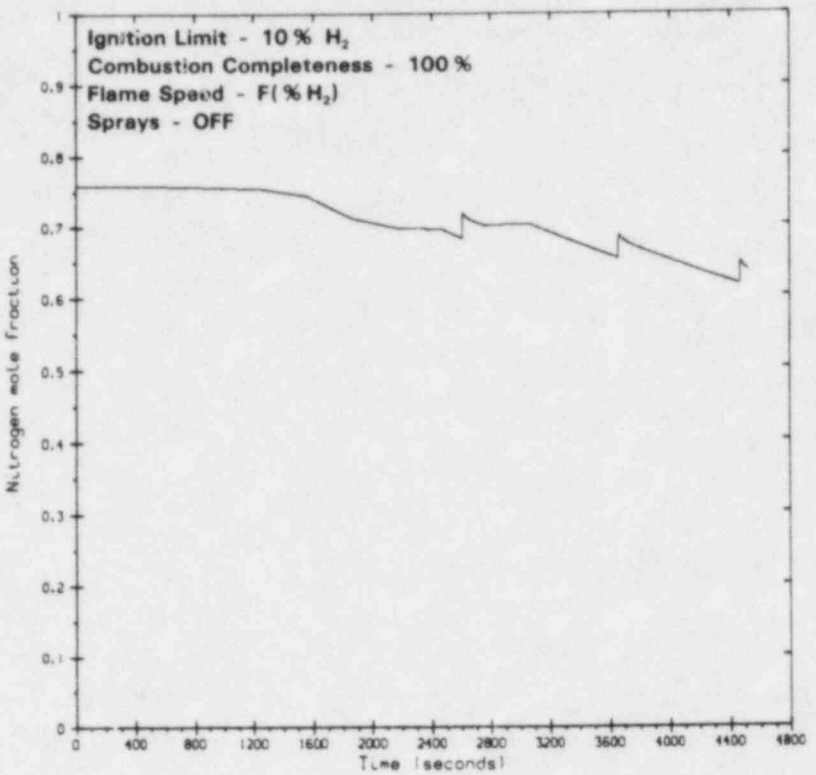

Figure 2.29. Case A6, Compartment 1 Nitrogen Mole Fraction

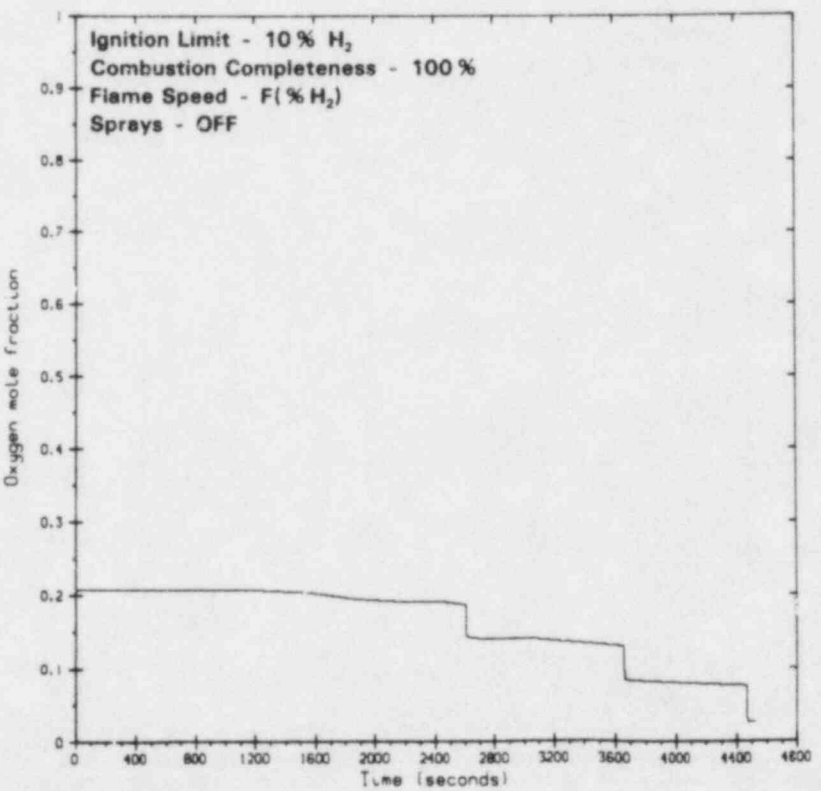

Figure 2.30. Case A6, Compartment 1 Oxygen Mole Fraction

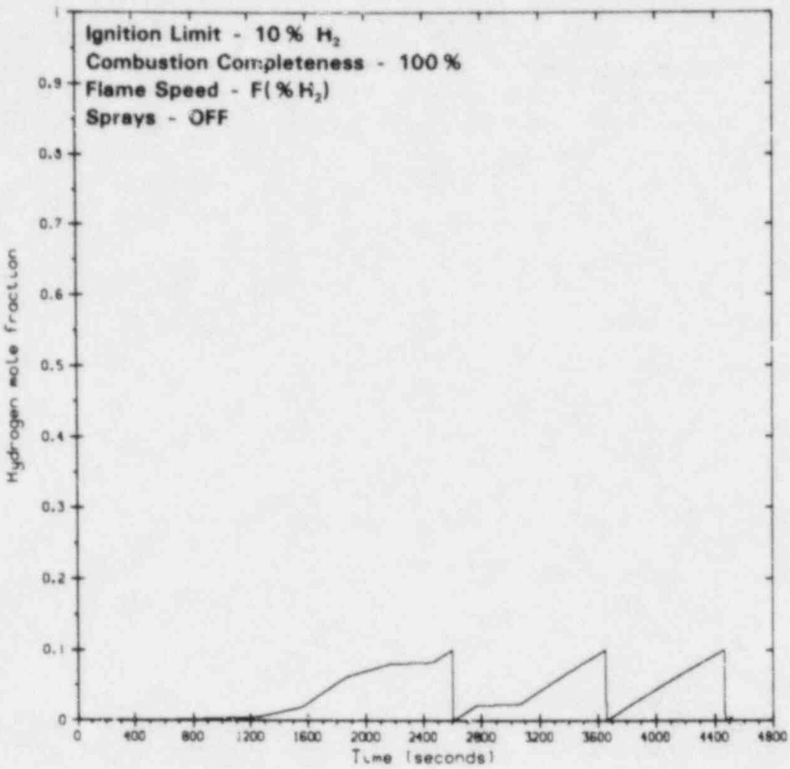

Figure 2.31. Case A6, Compartment 1 Hydrogen Mole Fraction

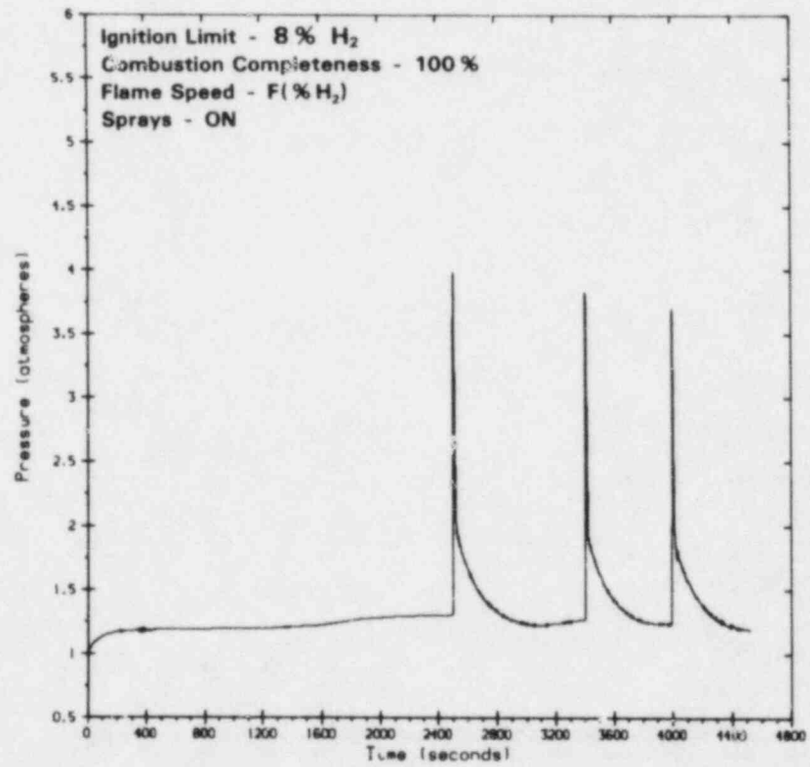

Figure 2.32. Case A3, Compartment 1 Pressure

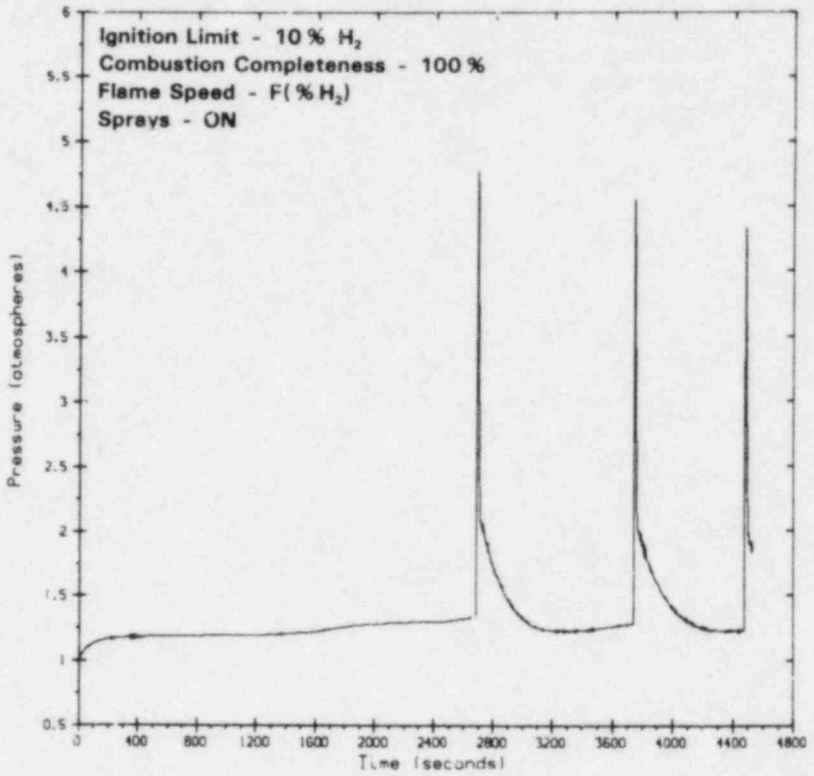

Figure 2.33. Case A7, Compartment 1 Pressure

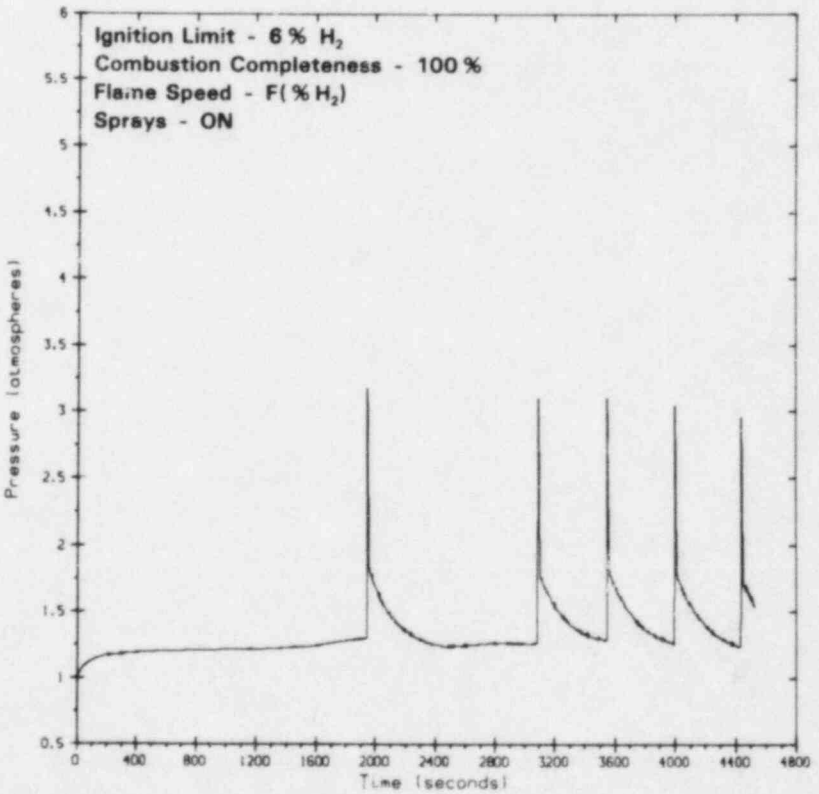

Figure 2.34. Case A10, Compartment 1 Pressure

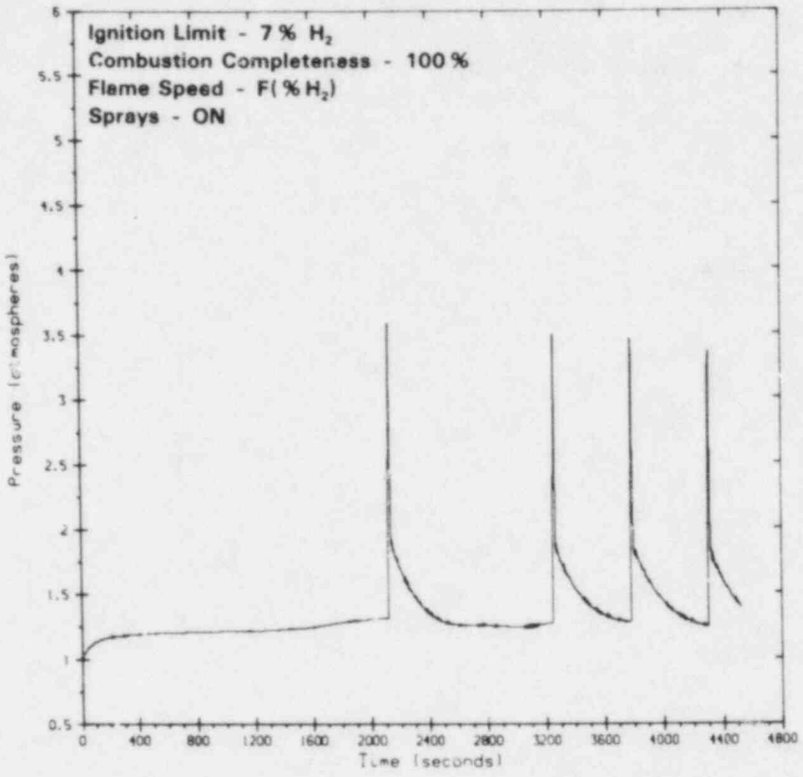

Figure 2.35. Case A11, Compartment 1 Pressure

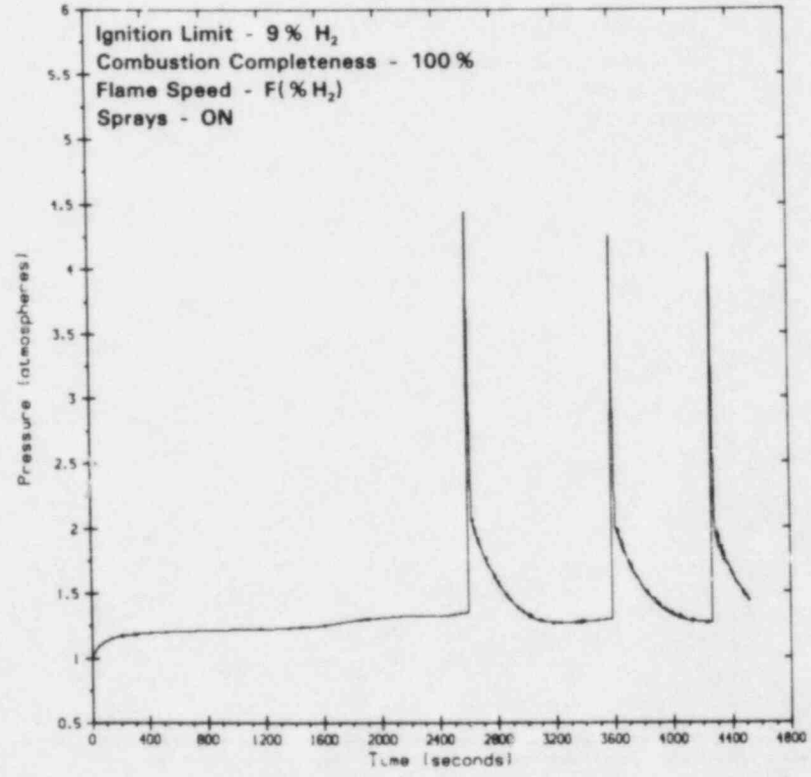

Figure 2.36. Case A12, Compartment 1 Pressure

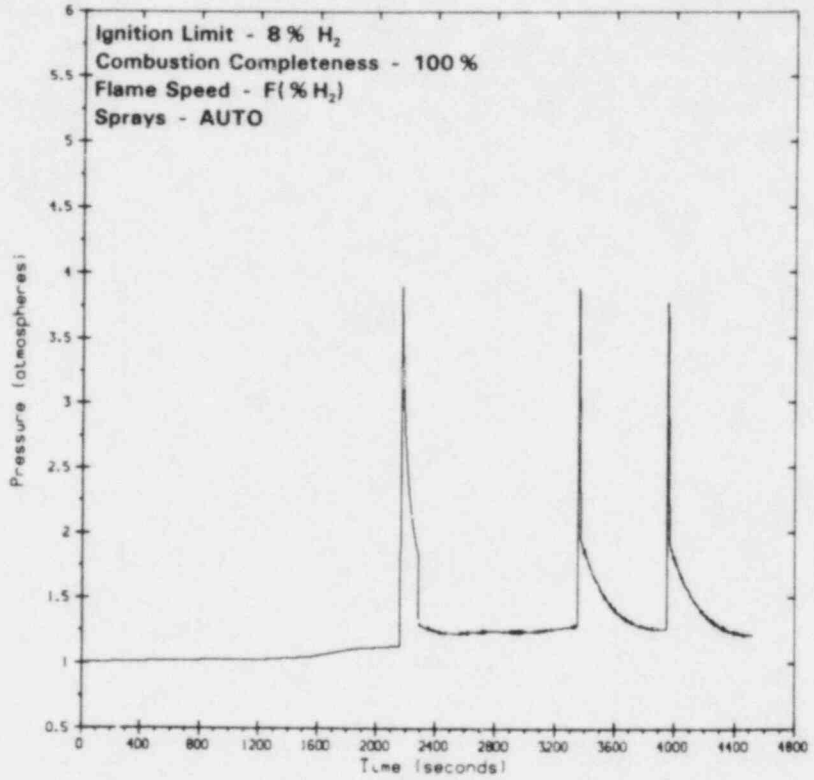

Figure 2.37. Case A4, Compartment 1 Pressure

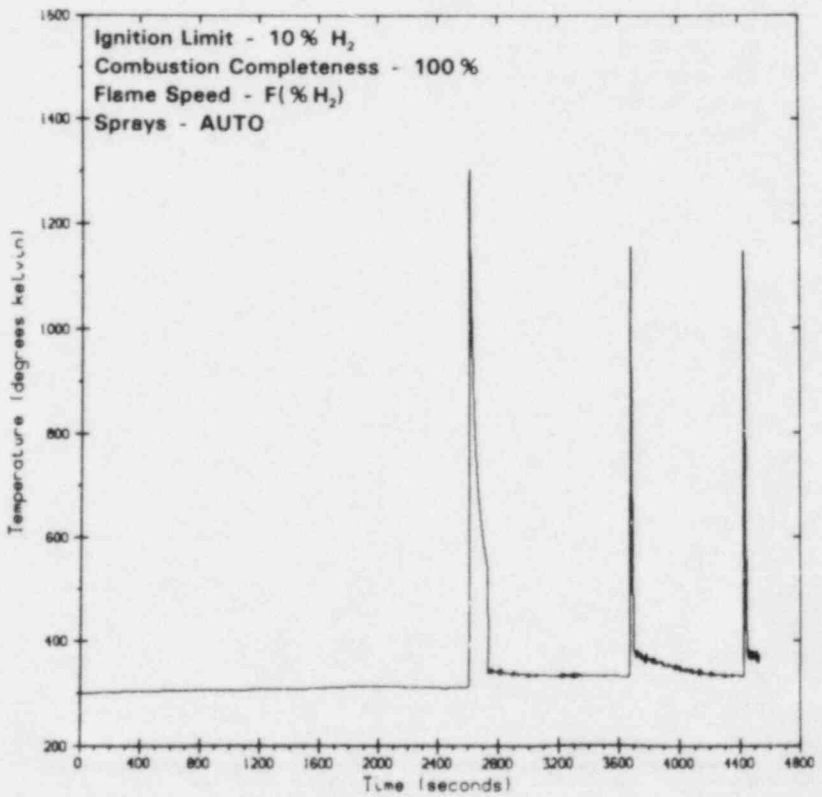

Figure 2.38. Case A8, Compartment 1 Temperature

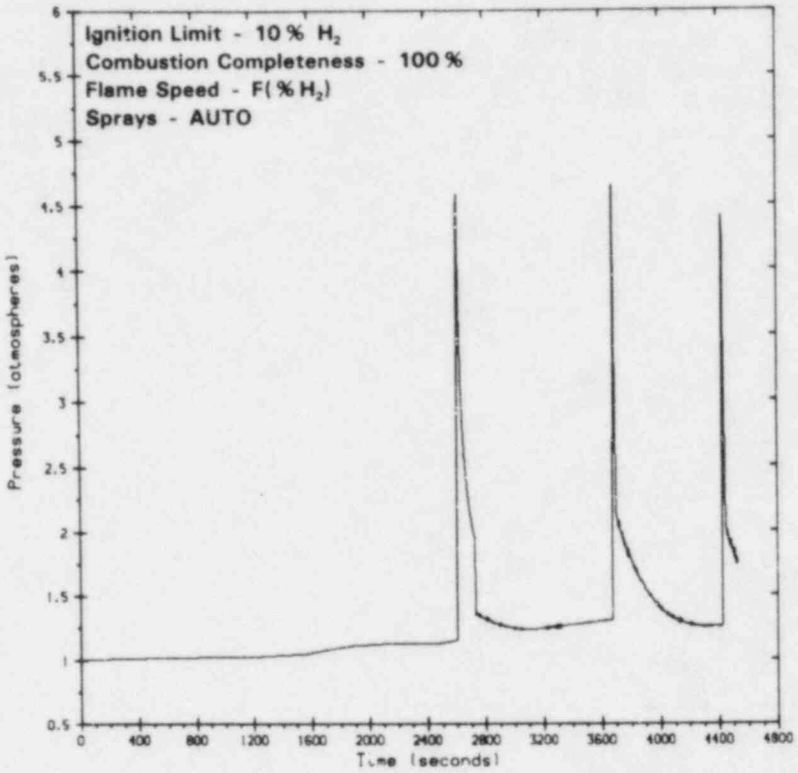

Figure 2.39. Case A8, Compartment 1 Pressure

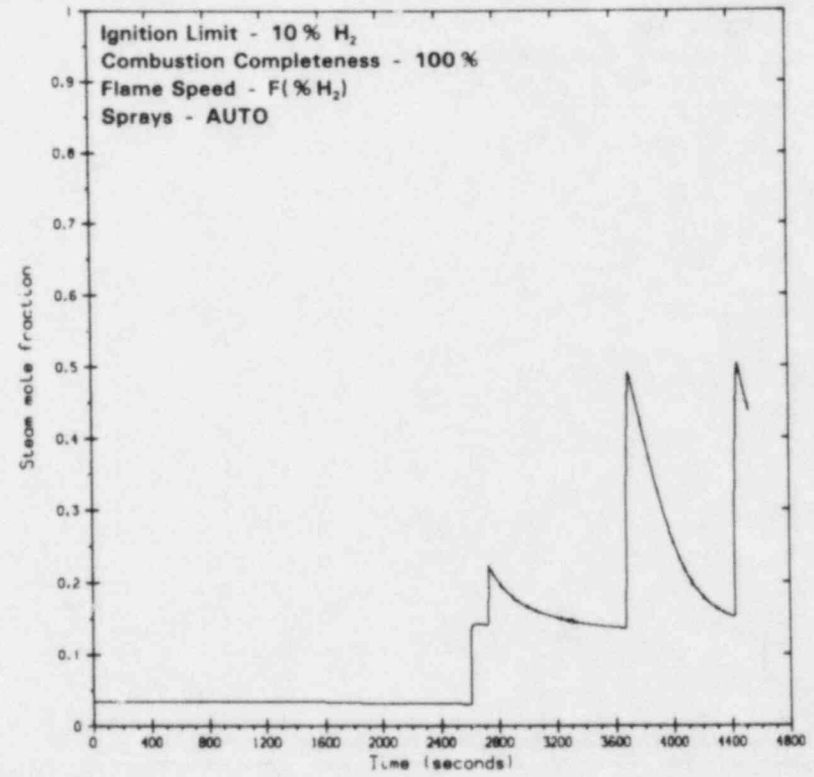

Figure 2.40. Case A8, Compartment 1 Steam Mole Fraction

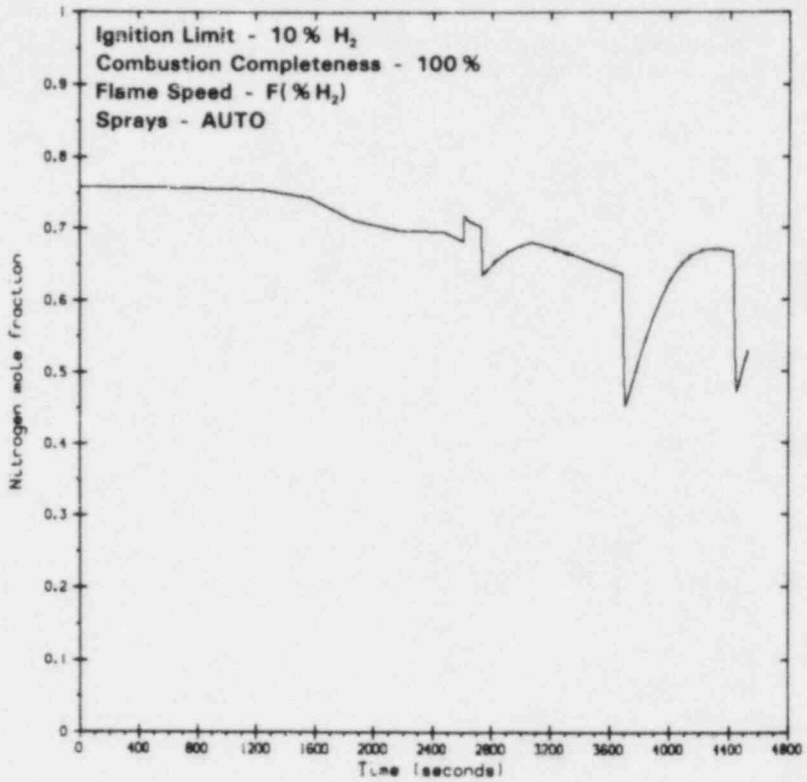

Figure 2.41. Case A8, Compartment 1 Nitrogen Mole Fraction

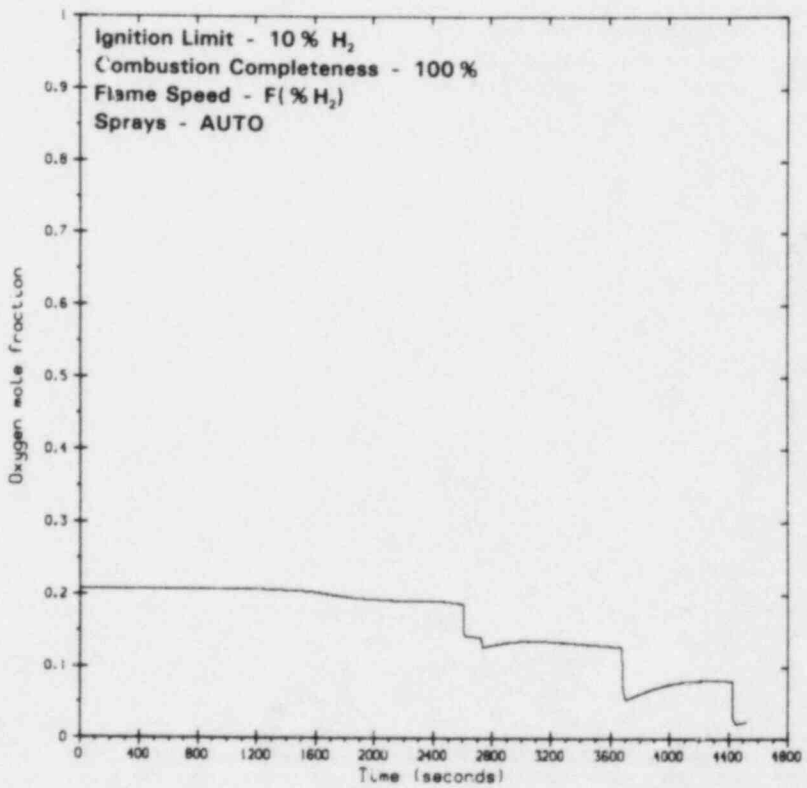

Figure 2.42. Case A8, Compartment 1 Oxygen Mole Fraction

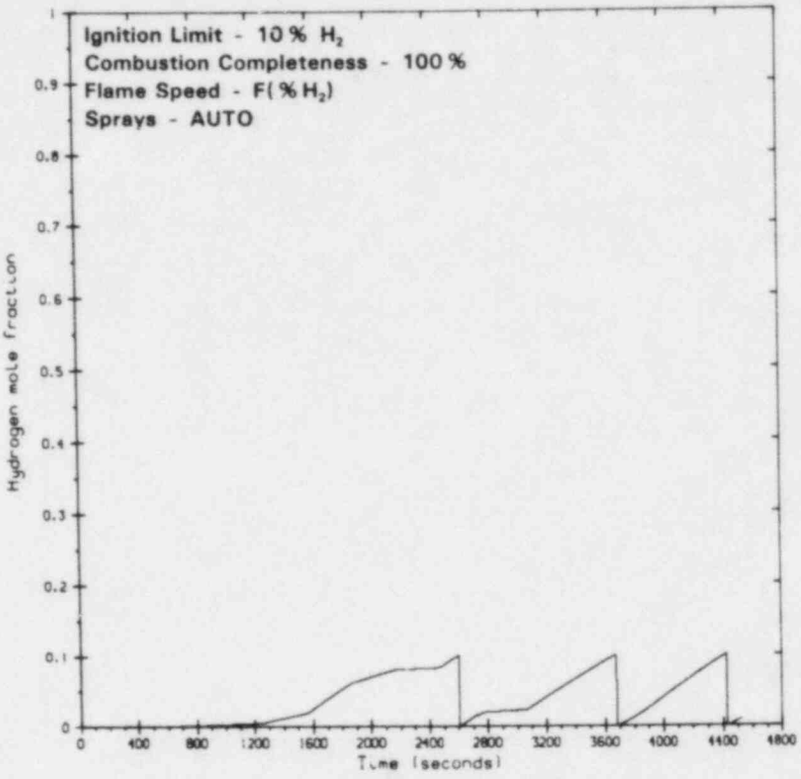

Figure 2.43. Case A8, Compartment 1 Hydrogen Mole Fraction

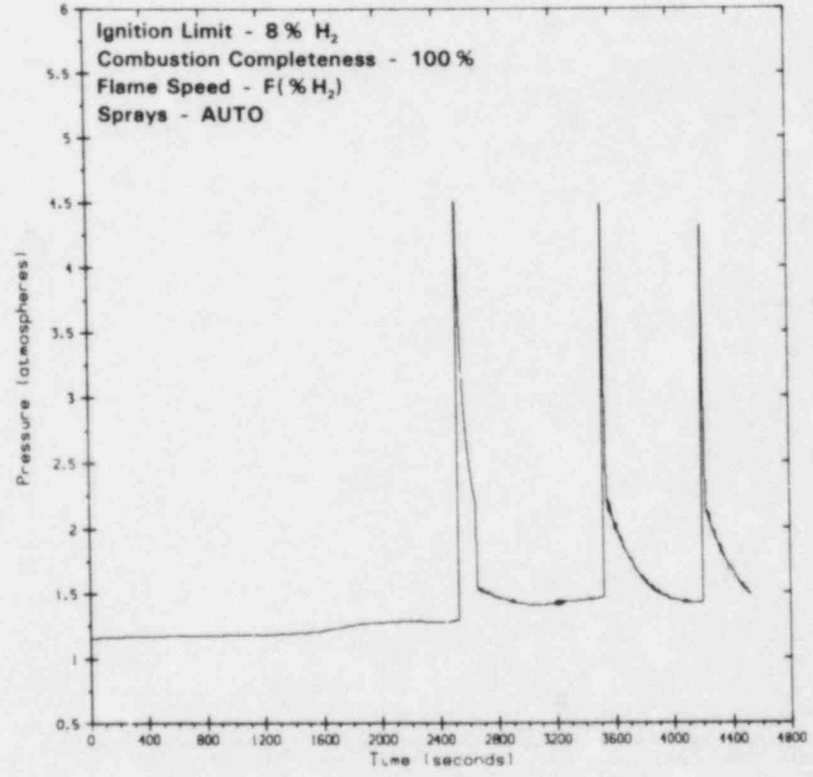

Figure 2.44. Case A5, Compartment 1 Pressure

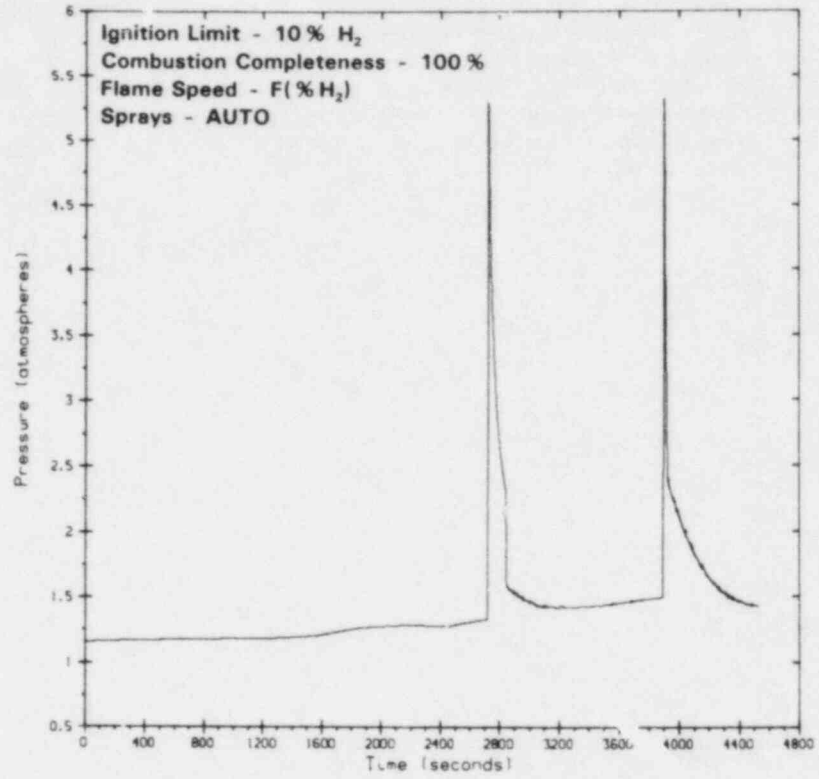

Figure 2.45. Case A9, Compartment 1 Pressure

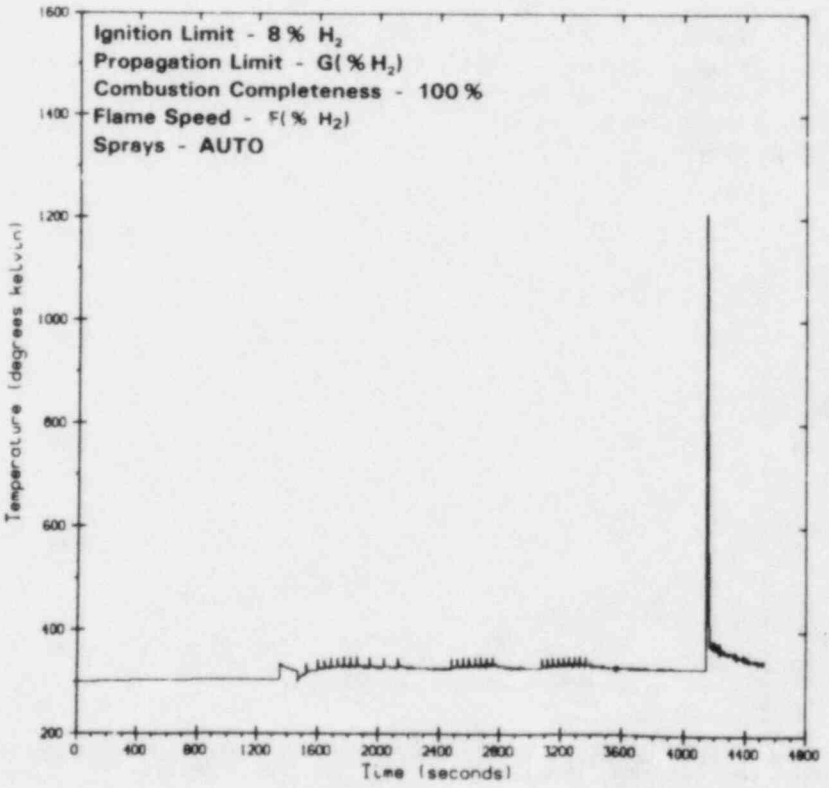

Figure 2.46. Case B5, Compartment 1 Temperature

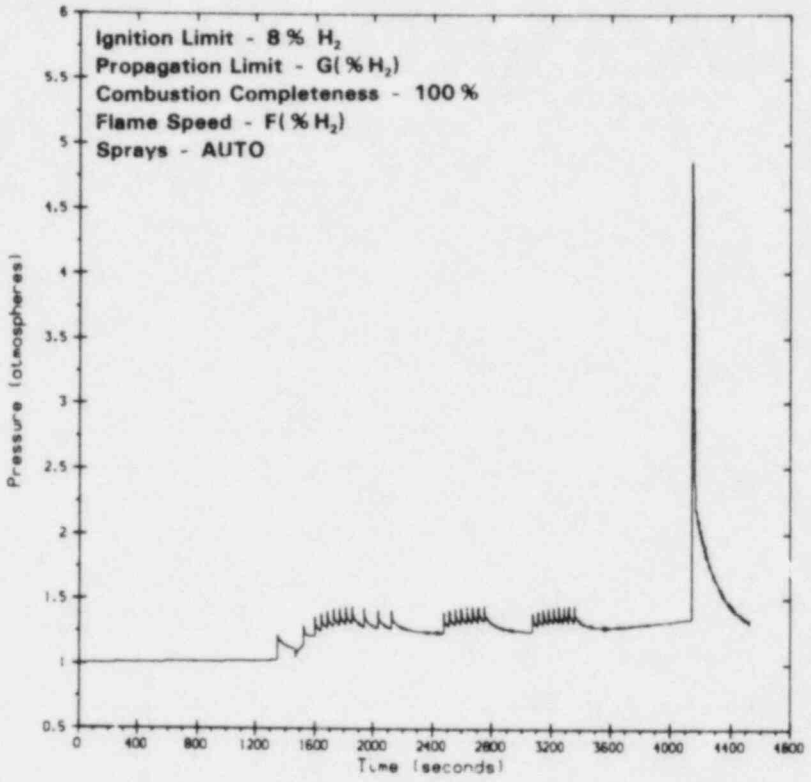

Figure 2.47. Case B5, Compartment 1 Pressure

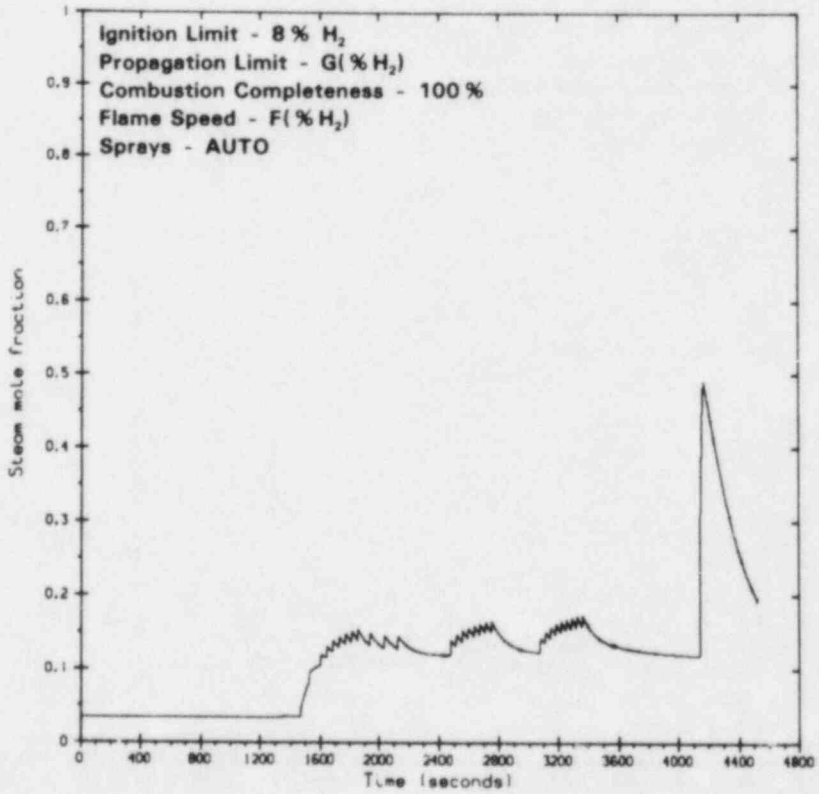

Figure 2.48. Case B5, Compartment 1 Steam Mole Fraction

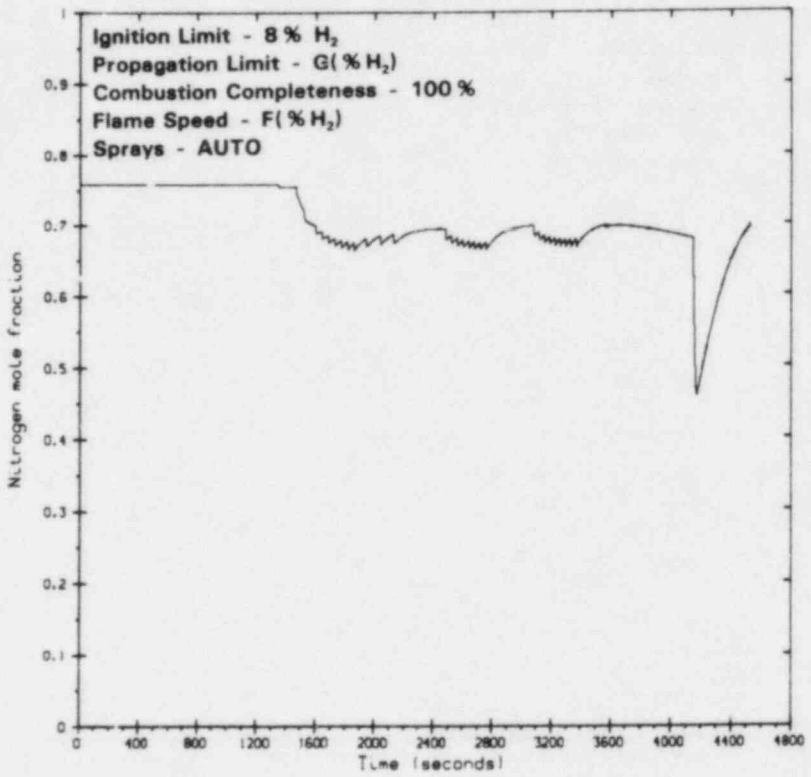

Figure 2.49. Case B5, Compartment 1 Nitrogen Mole Fraction

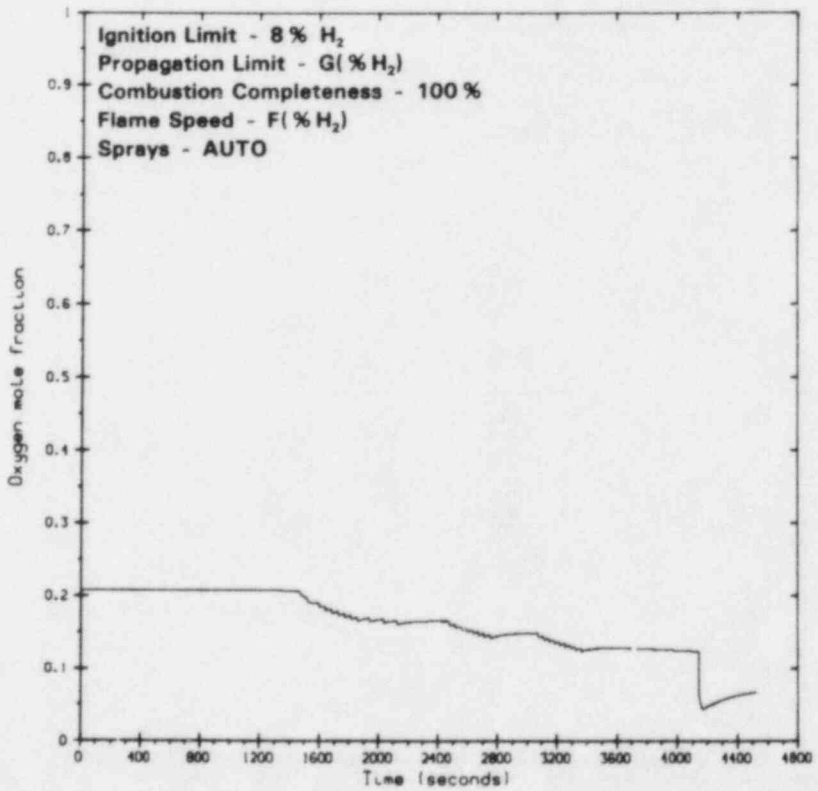

Figure 2.50. Case B5, Compartment 1 Oxygen Mole Fraction

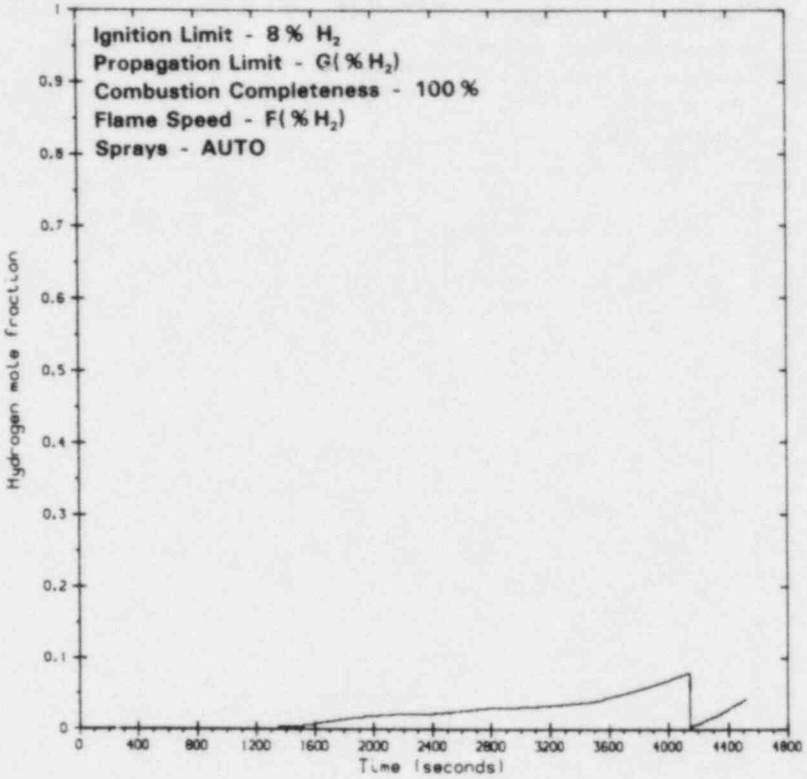

Figure 2.51. Case B5, Compartment 1 Hydrogen Mole Fraction

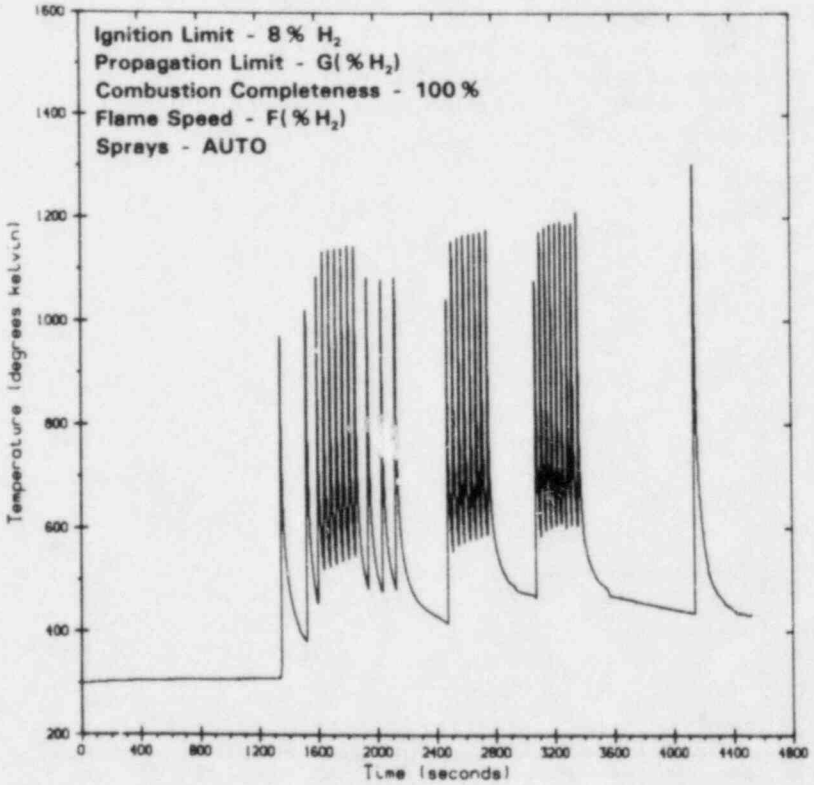

Figure 2.52. Case B5, Compartment 2 Temperature

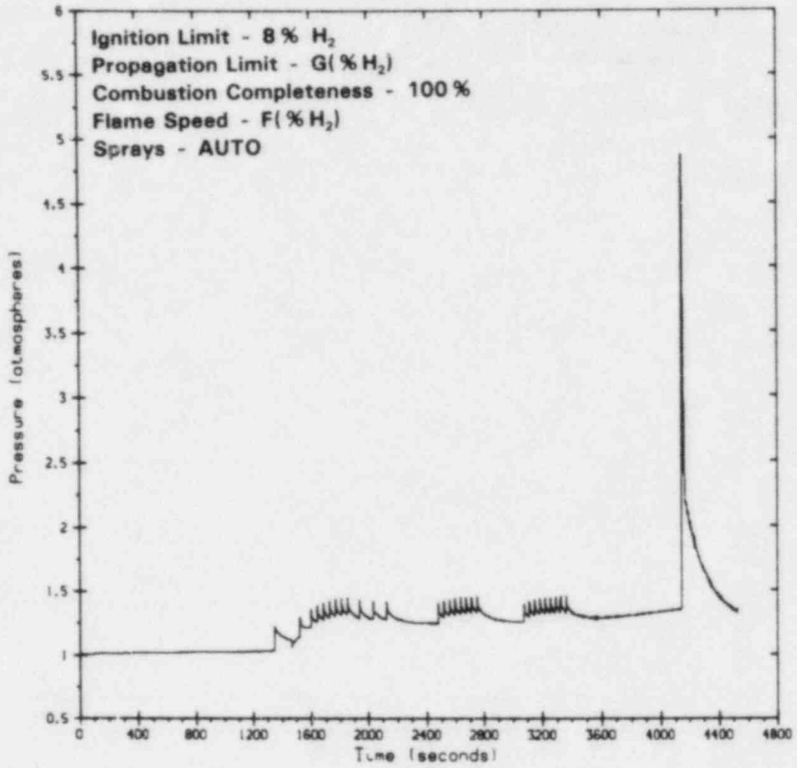

Figure 2.53. Case B5, Compartment 2 Pressure

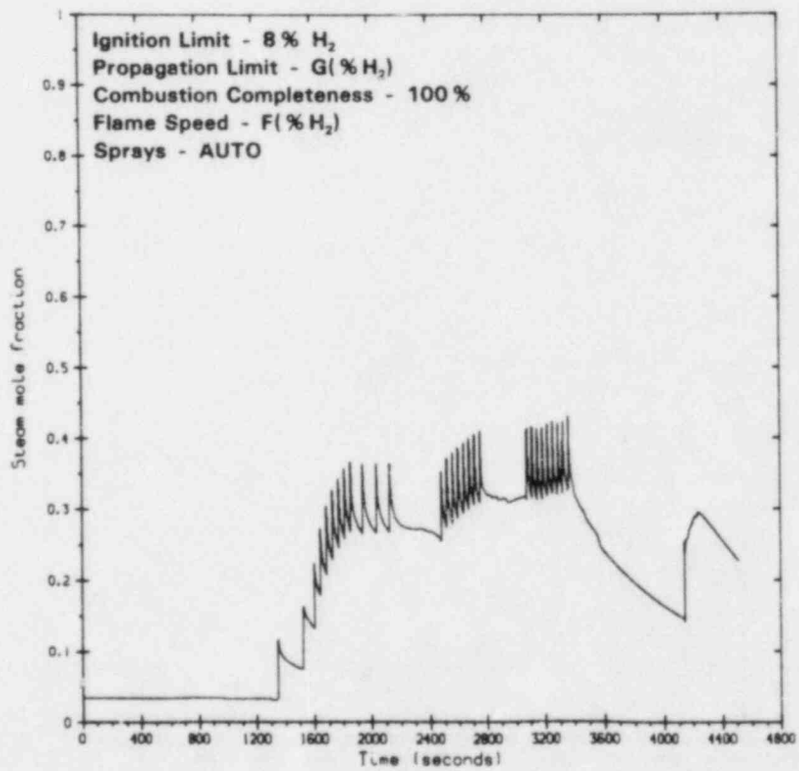

Figure 2.54. Case B5, Compartment 2 Steam Mole Fraction

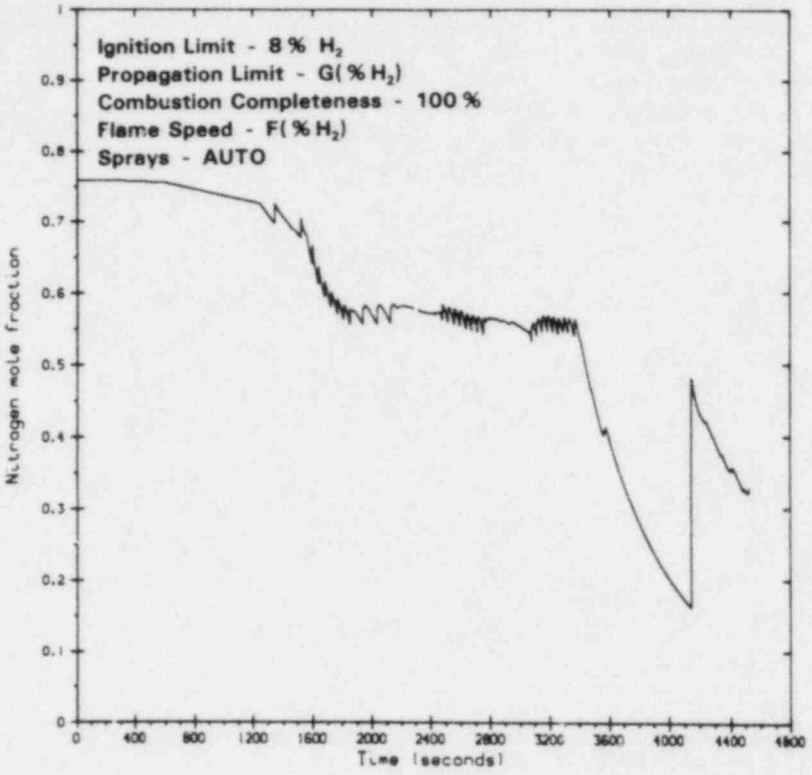

Figure 2.55. Case B5, Compartment 2 Nitrogen Mole Fraction

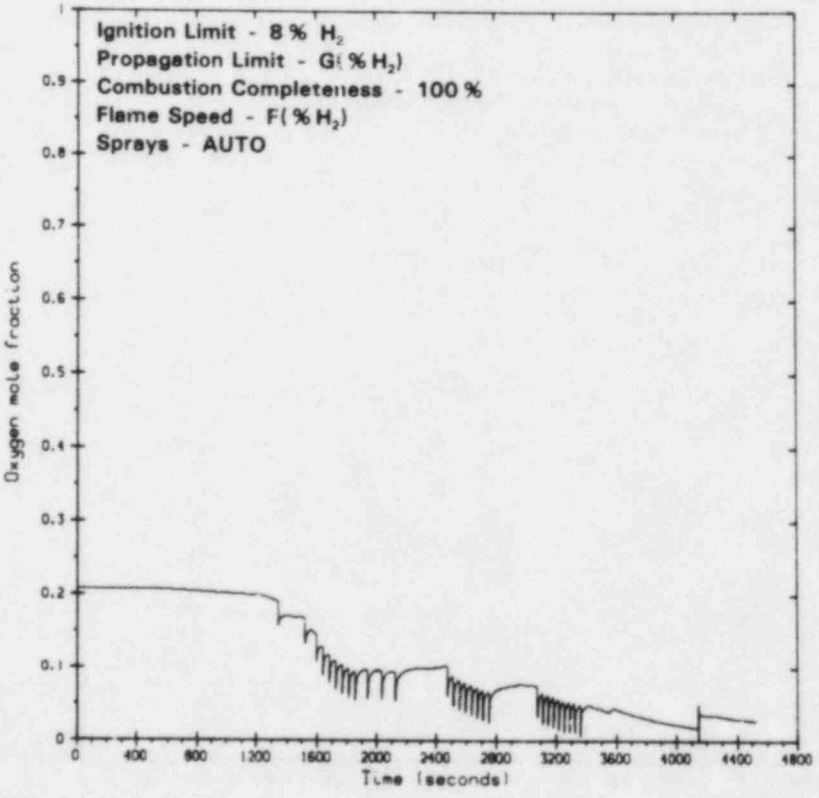

Figure 2.56. Case B5, Compartment 2 Oxygen Mole Fraction

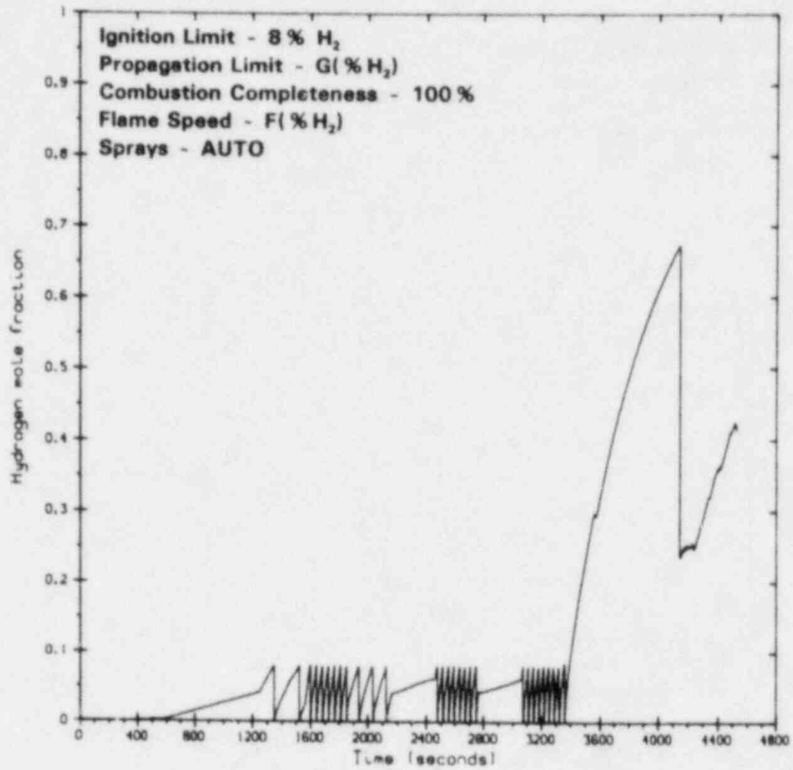

Figure 2.57. Case B5, Compartment 2 Hydrogen Mole Fraction

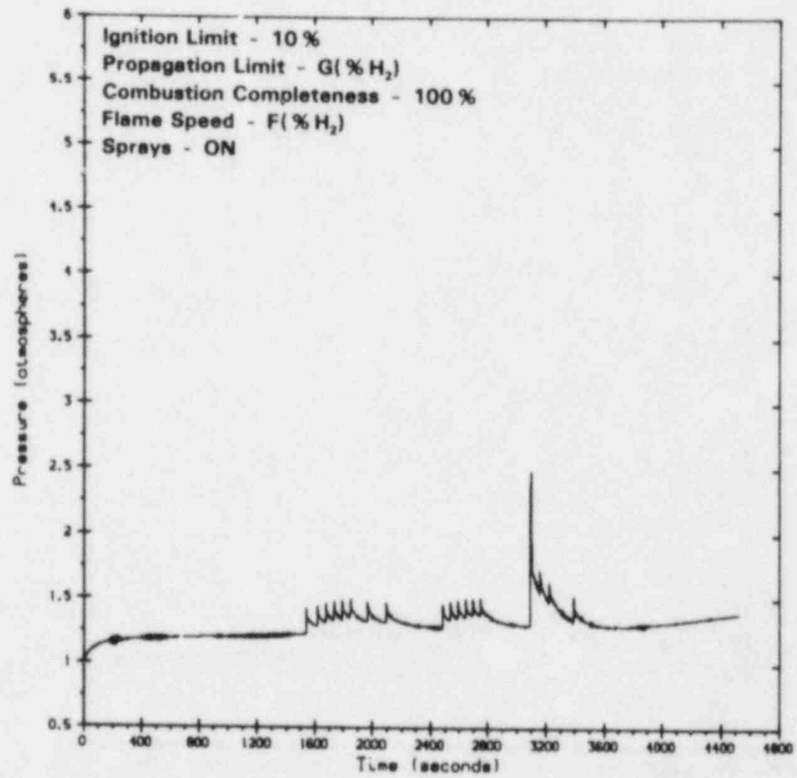

Figure 2.58. Case B6, Compartment 1 Pressure

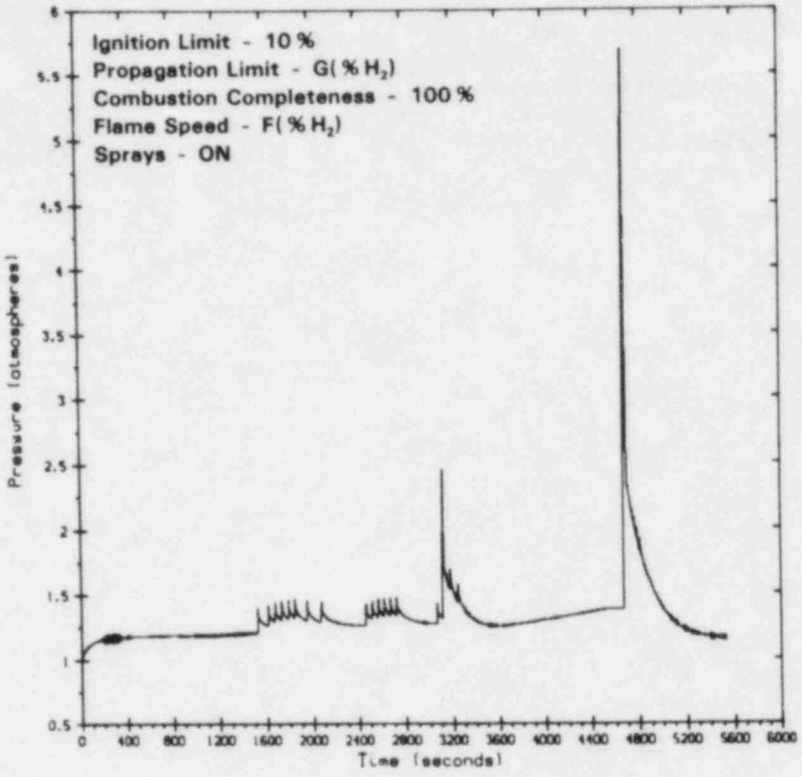

Figure 2.59. Case B6′, Compartment 2 Pressure

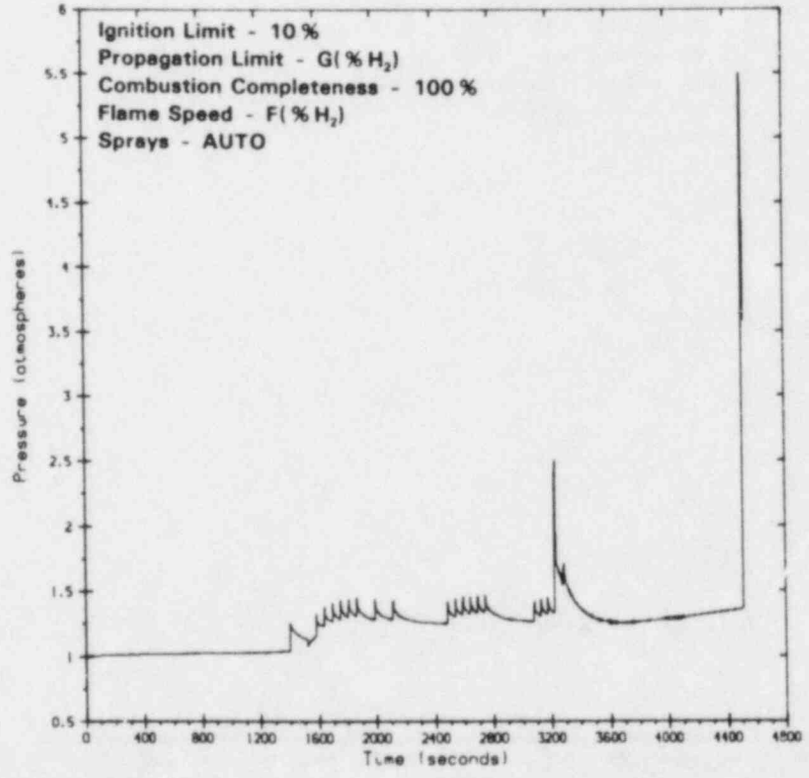

Figure 2.60. Case B7, Compartment 2 Pressure

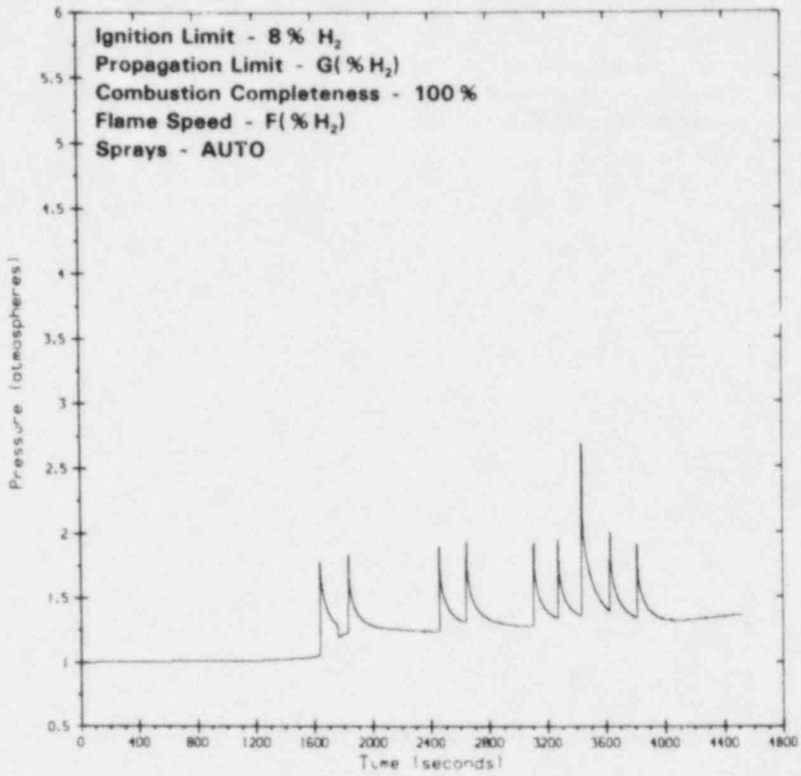

Figure 2.61. Case C1, Compartment 1 Pressure

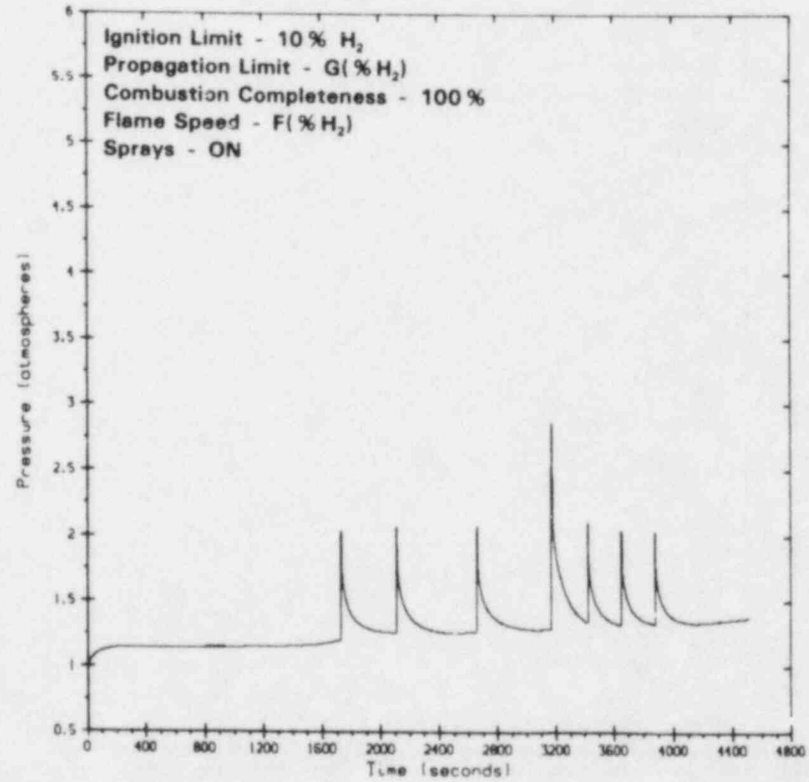

Figure 2.62. Case C2, Compartment 1 Pressure

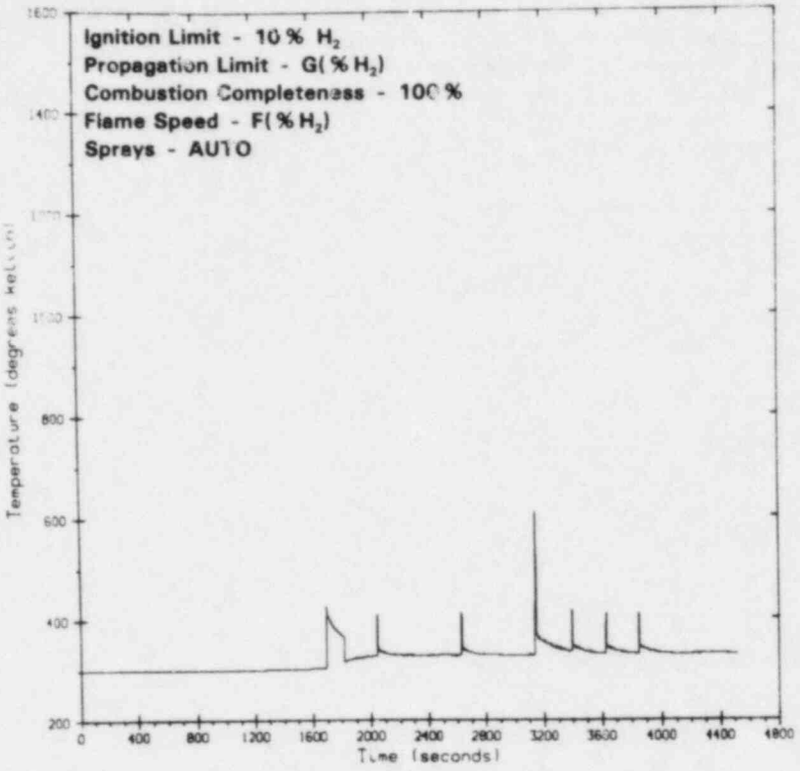

Figure 2.63. Case C3, Compartment 1 Temperature

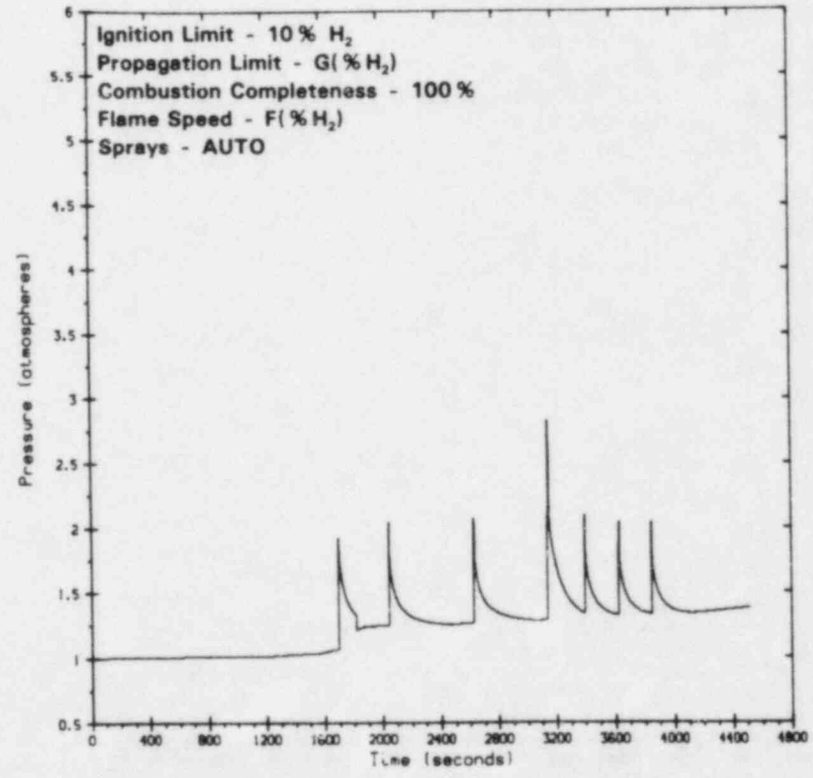

Figure 2.64. Case C3, Compartment 1 Pressure

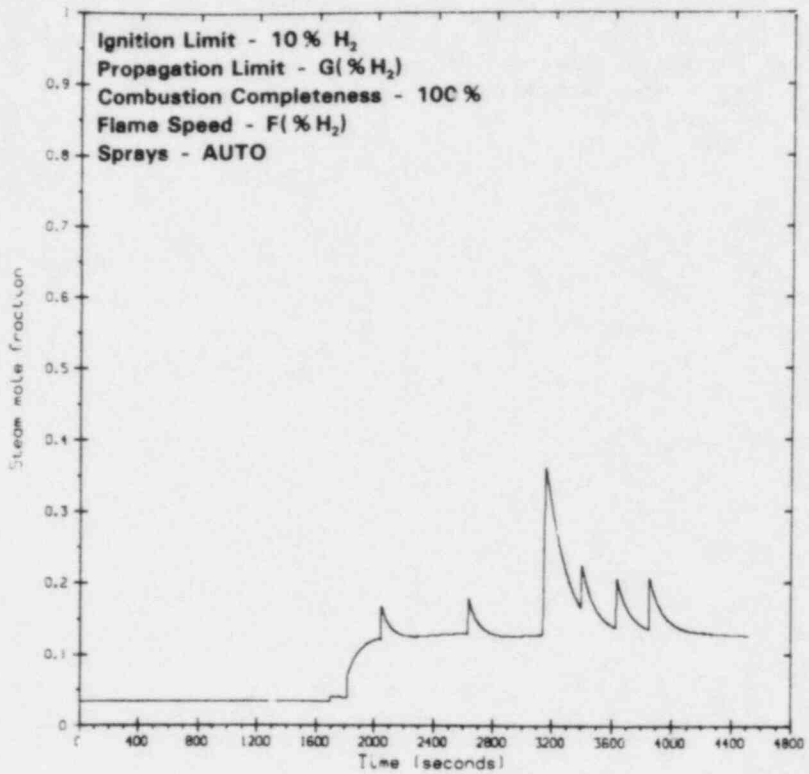

Figure 2.65. Case C3, Compartment 1 Steam Mole Fraction

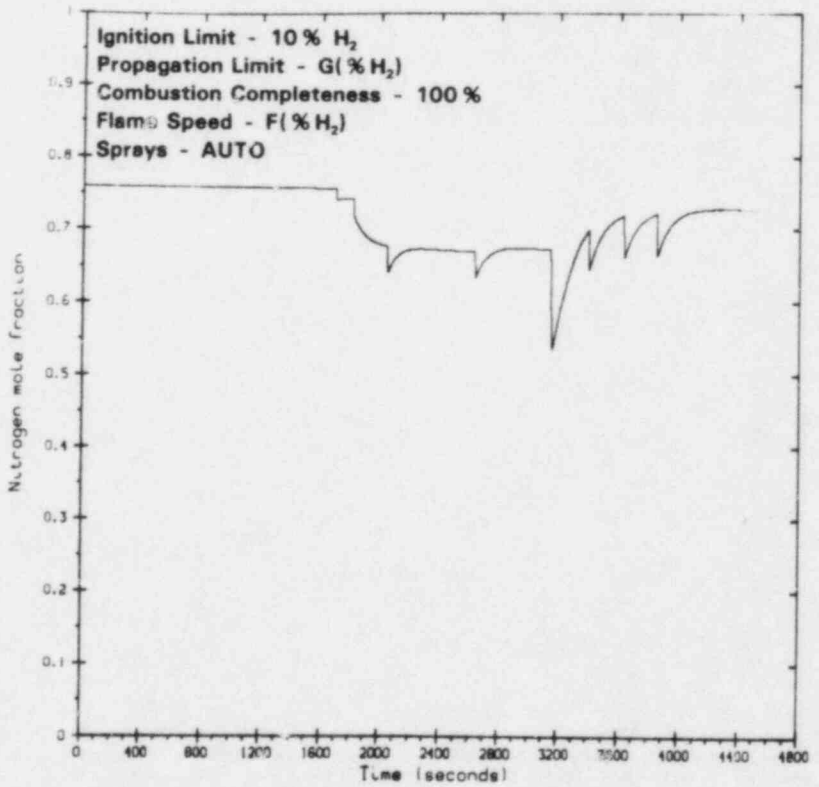

Figure 2.66. Case C3, Compartment 1 Nitrogen Mole Fraction

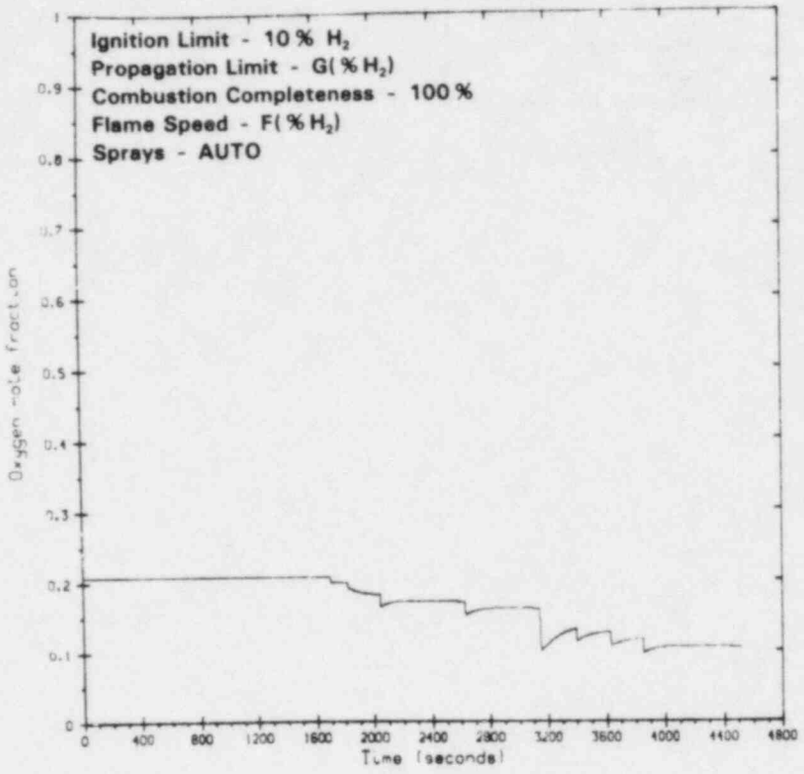

Figure 2.67. Case C3, Compartment 1 Oxygen Mole Fraction

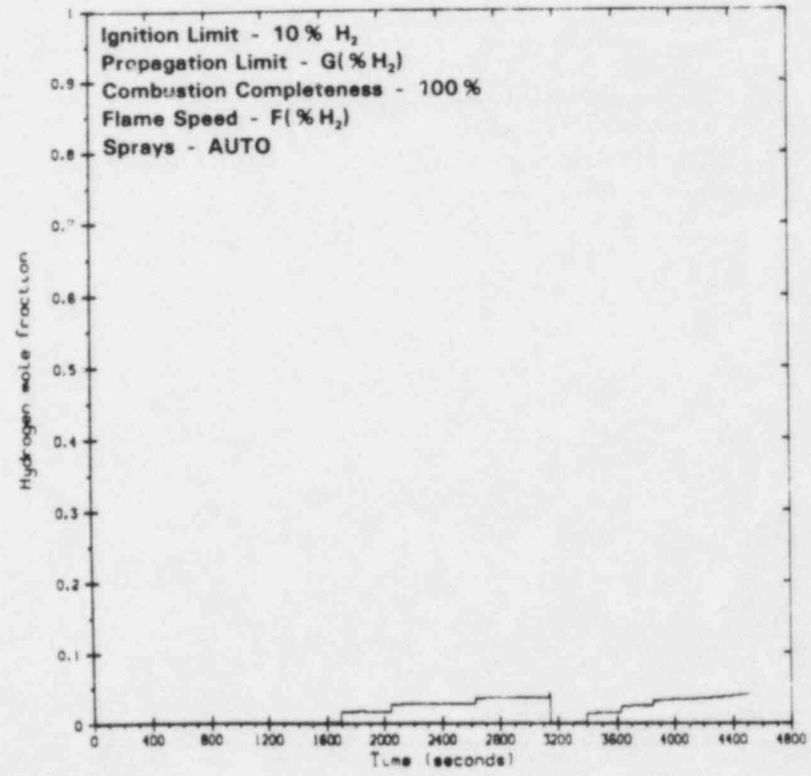

Figure 2.68. Case C3, Compartment 1 Hydrogen Mole Fraction

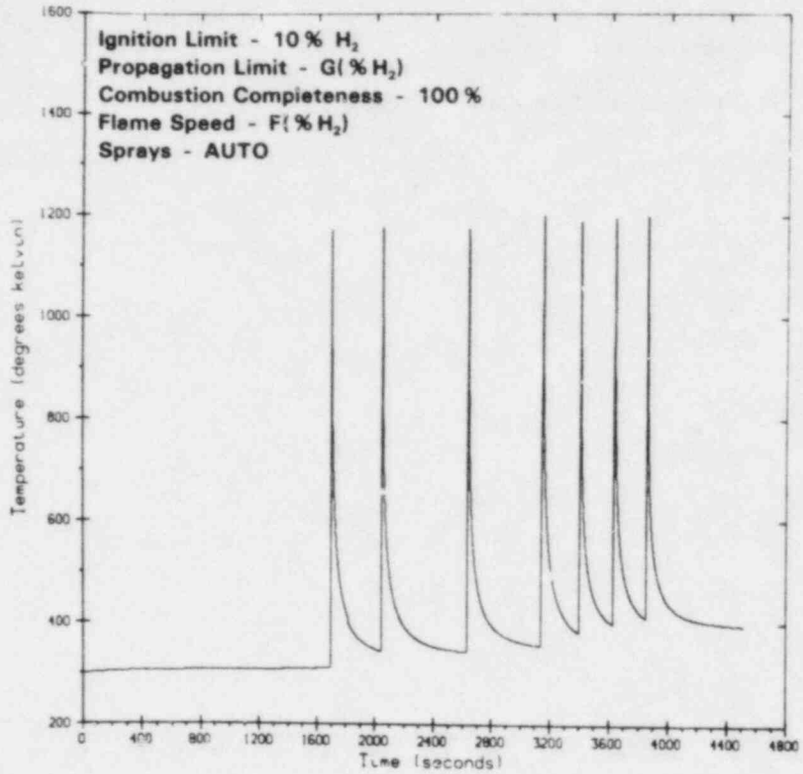

Figure 2.69. Case C3, Compartment 2 Temperature

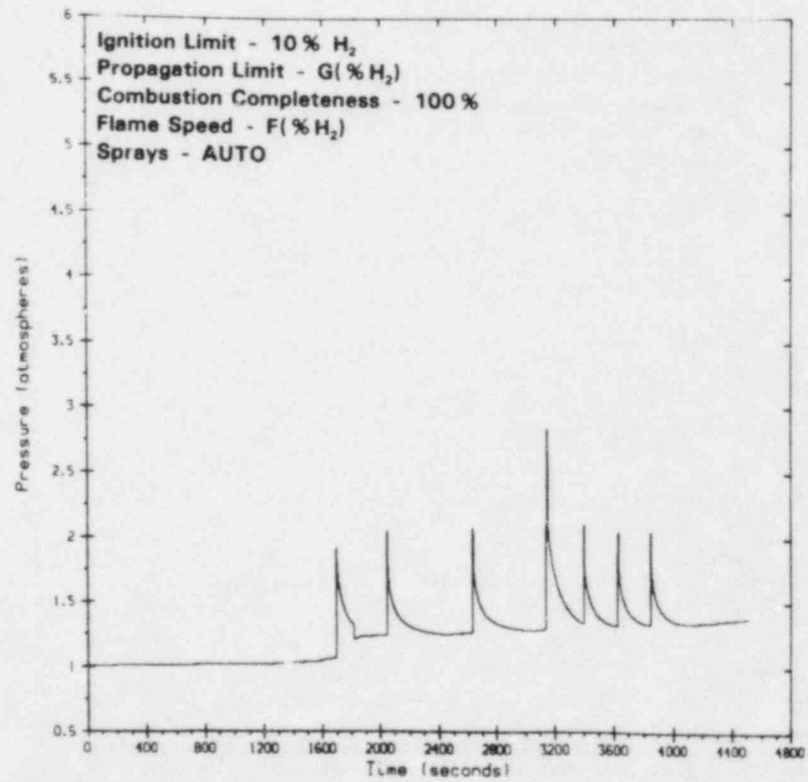

Figure 2.70. Case C3, Compartment 2 Pressure

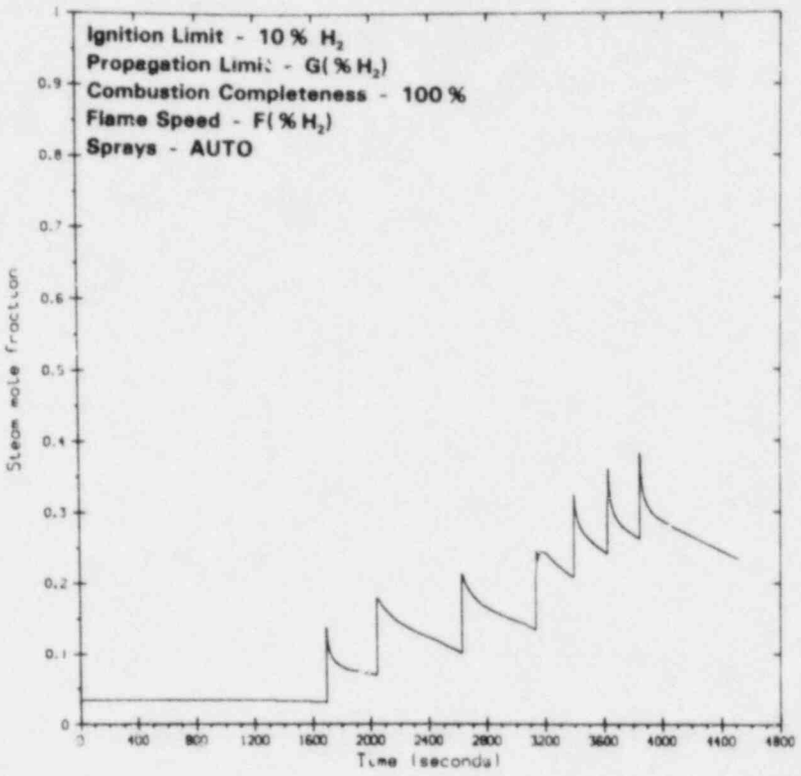

Figure 2.71. Case C3, Compartment 2 Steam Mole Fraction

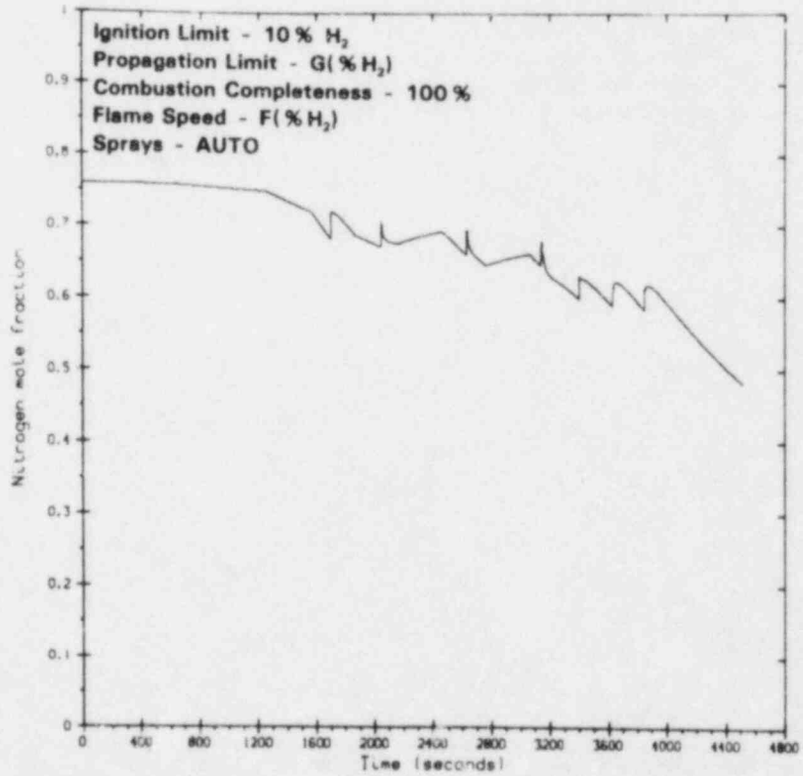

Figure 2.72. Case C3, Compartment 2 Nitrogen Mole Fraction

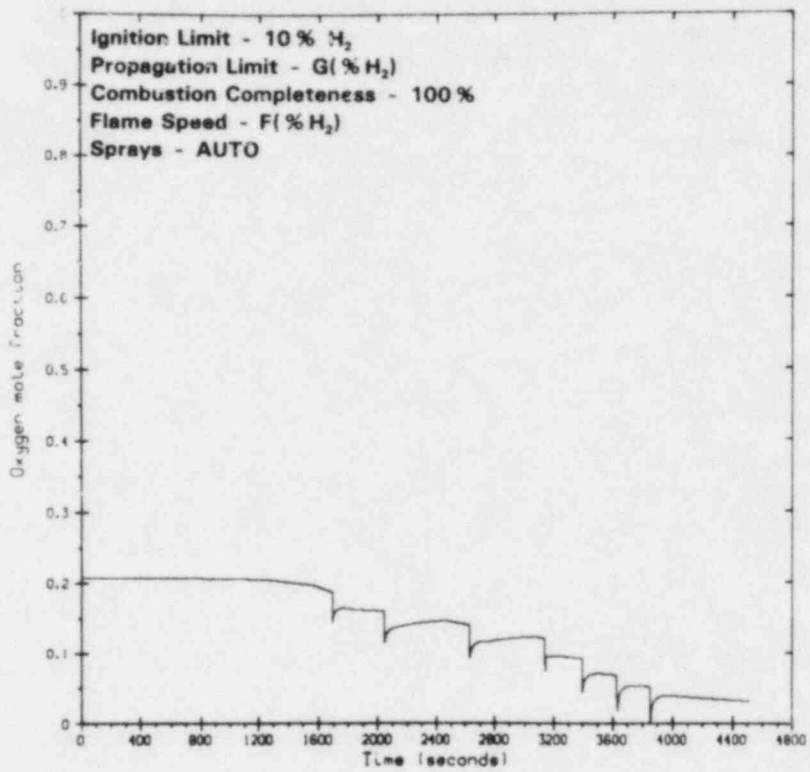

Figure 2.73. Case C3, Compartment 2 Oxygen Mole Fraction

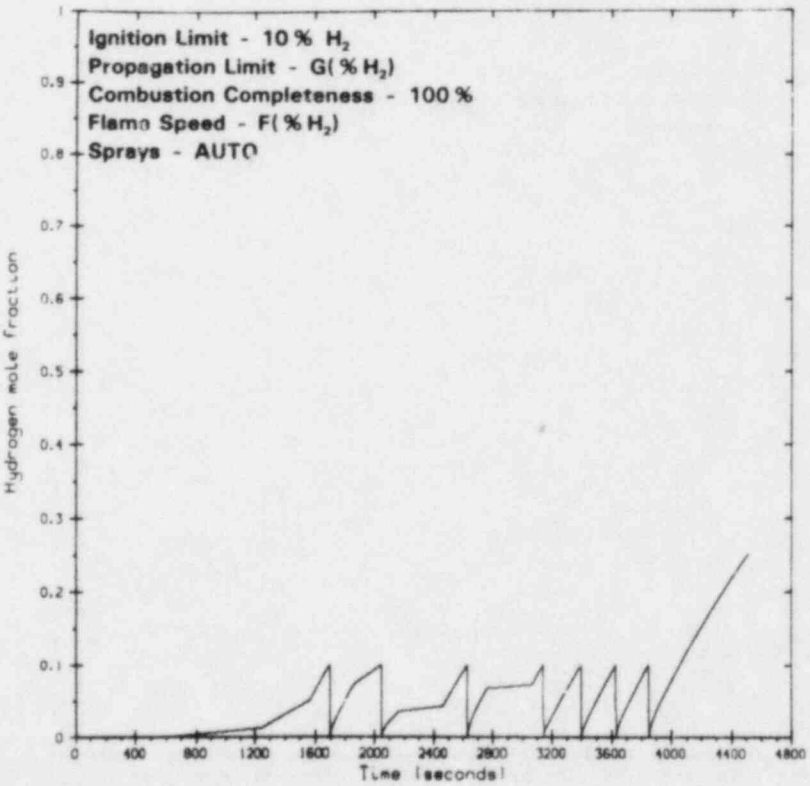

Figure 2.74. Case C3, Compartment 2 Hydrogen Mole Fraction

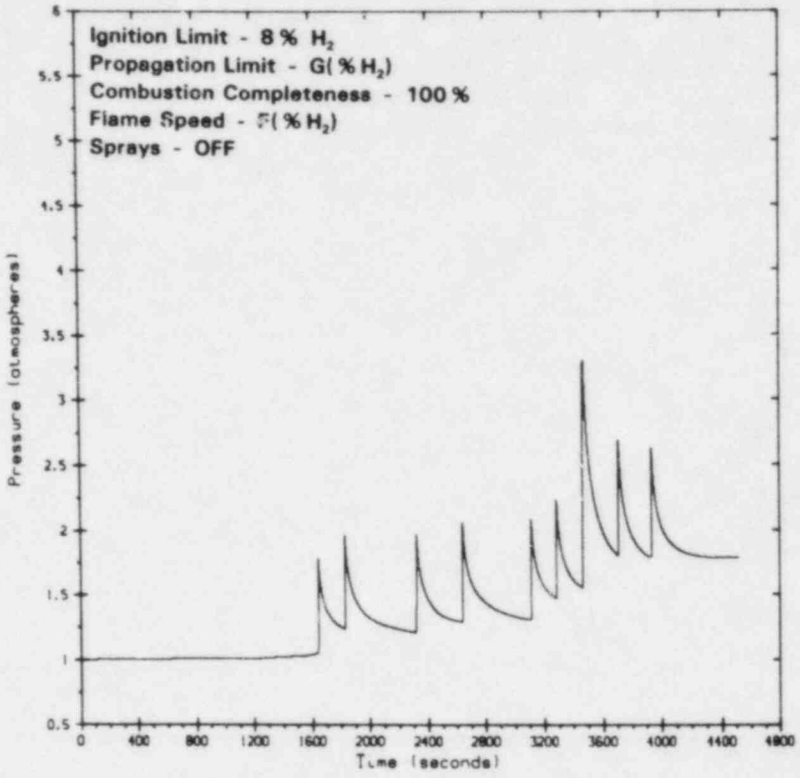

Figure 2.75. Case C4, Compartment 1 Pressure

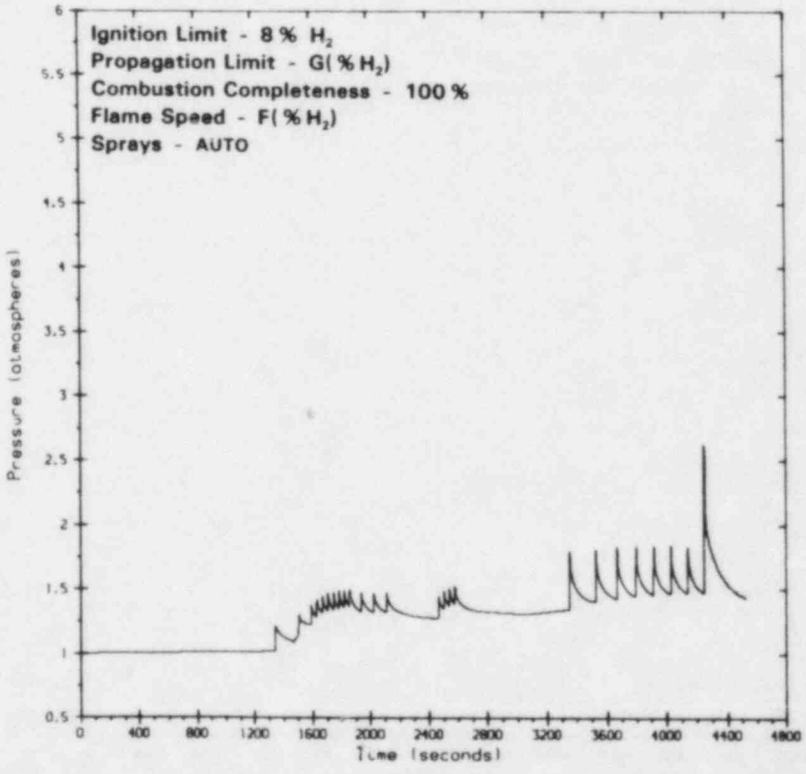

Figure 2.76. Case D1. Compartment 1 Pressure

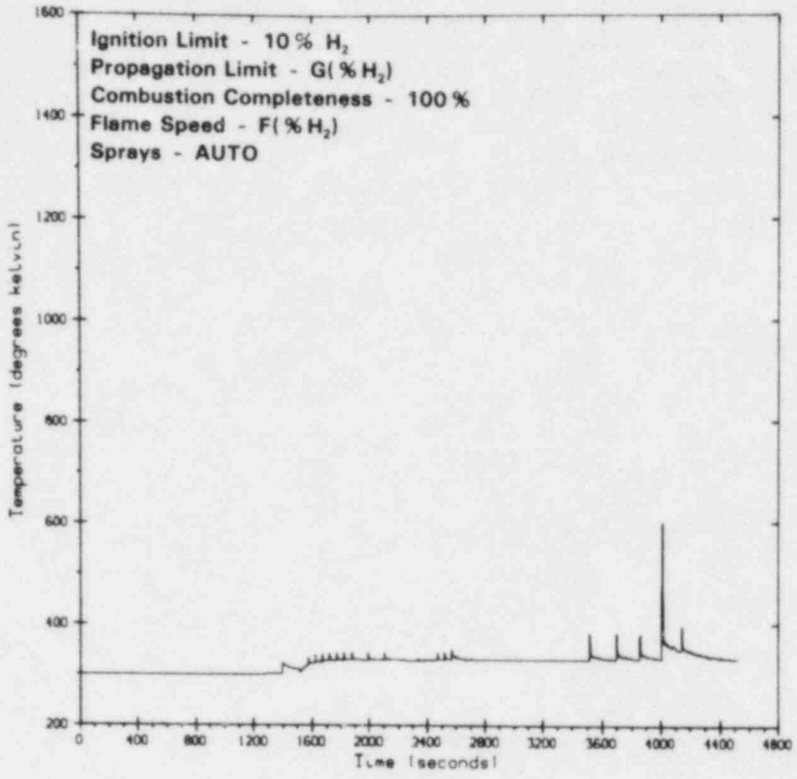

Figure 2.77. Case D2, Compartment 1 Temperature

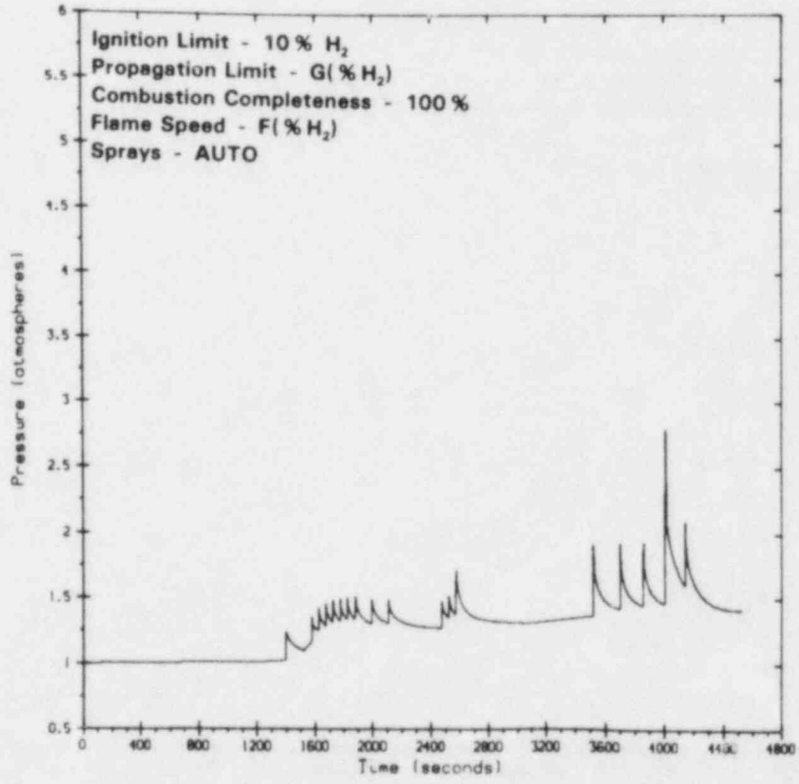

Figure 2.78. Case D2, Compartment 1 Pressure

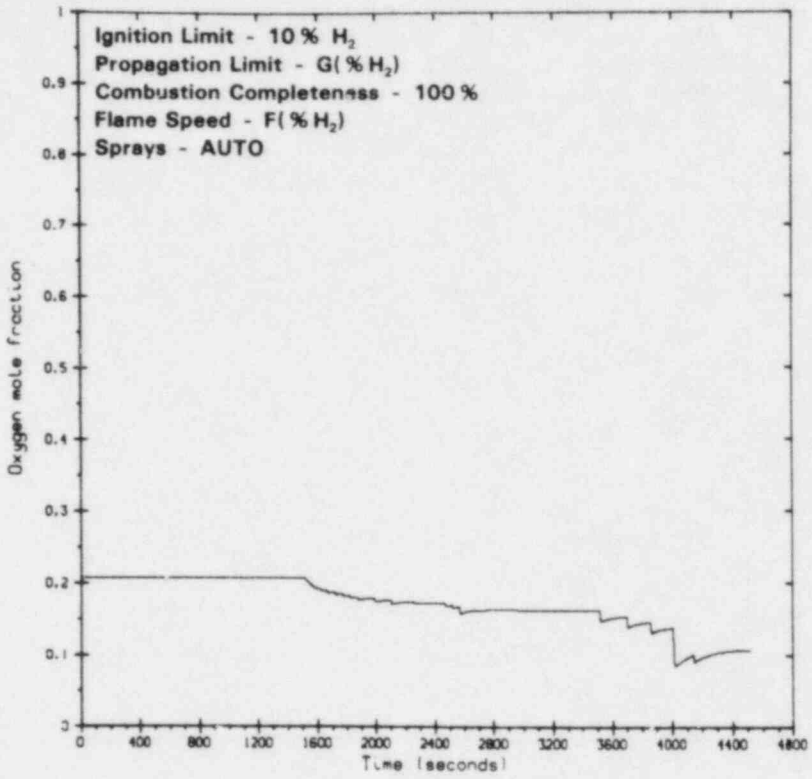

Figure 2.79. Case D2, Compartment 1 Oxygen Mole Fraction

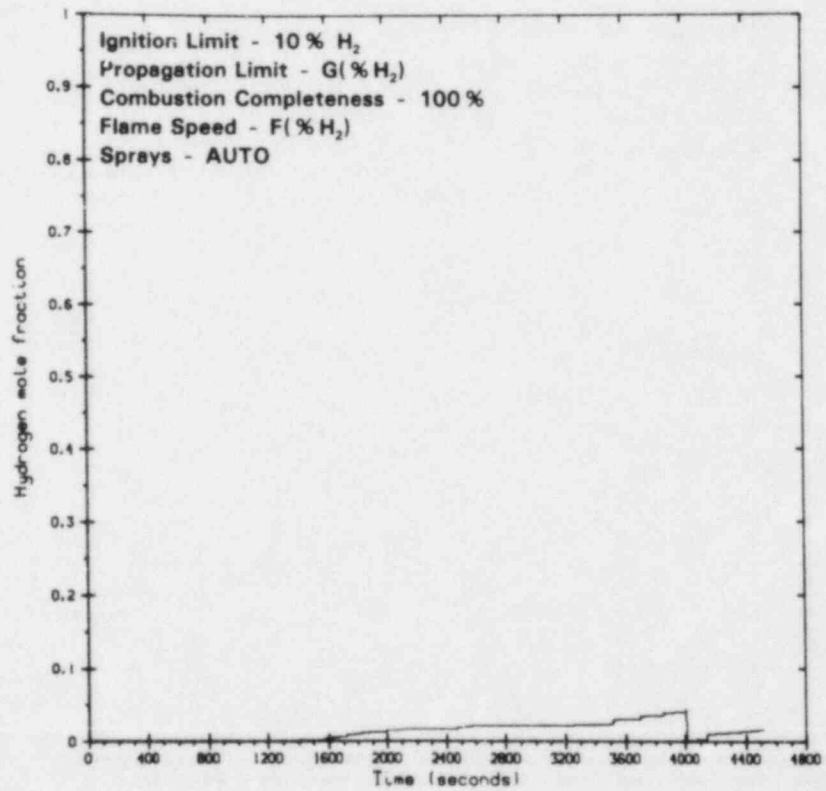

Figure 2.80. Case D2, Compartment 1 Hydrogen Mole Fraction

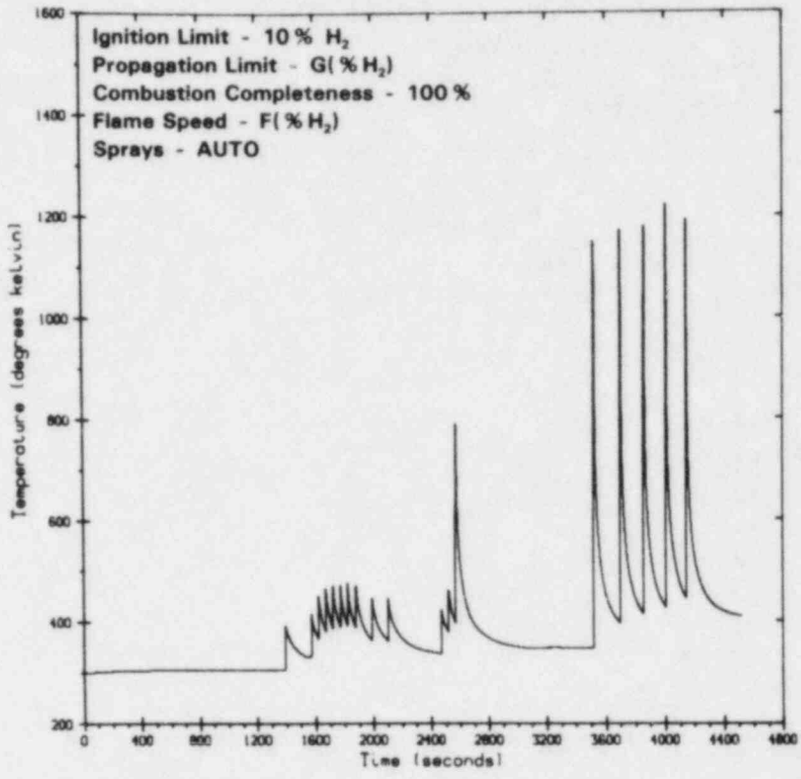

Figure 2.81. Case D2, Compartment 2 Temperature

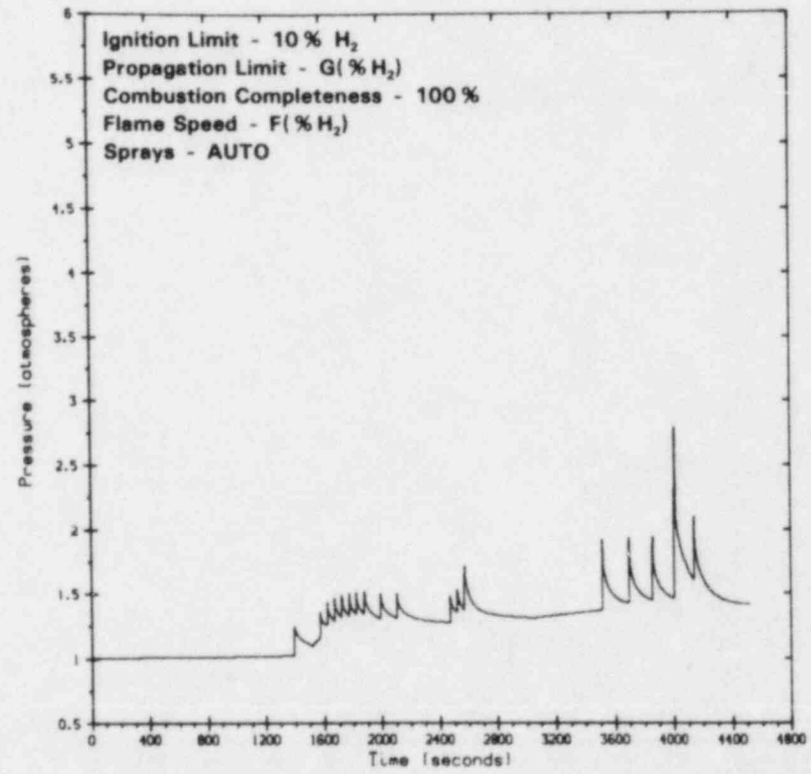

Figure 2.82. Case D2, Compartment 2 Pressure

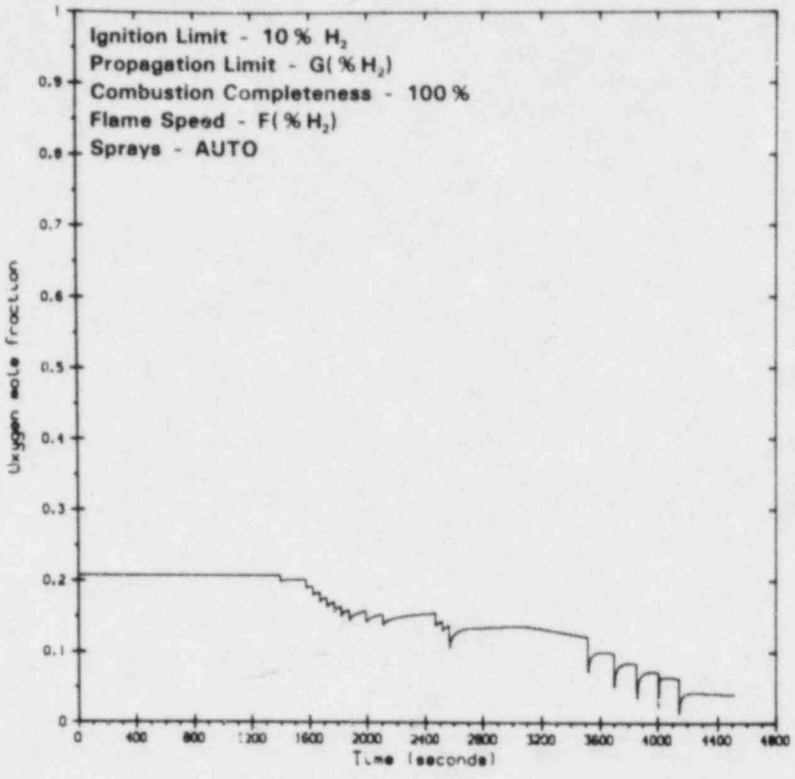

Figure 2.83. Case D2, Compartment 2 Oxygen Mole Fraction

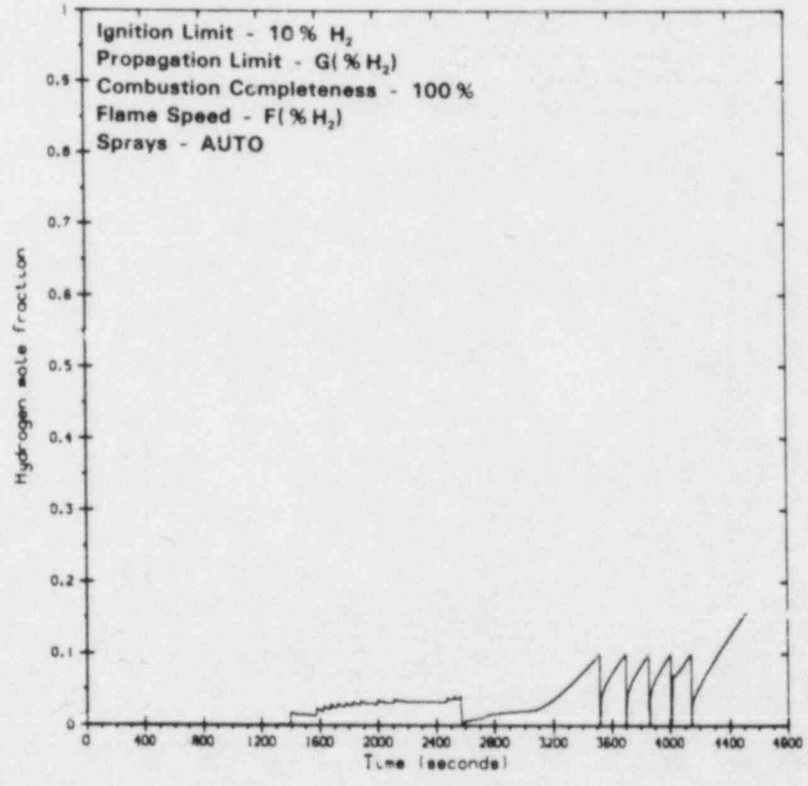

Figure 2.84. Case D2, Compartment 2 Hydrogen Mole Fraction

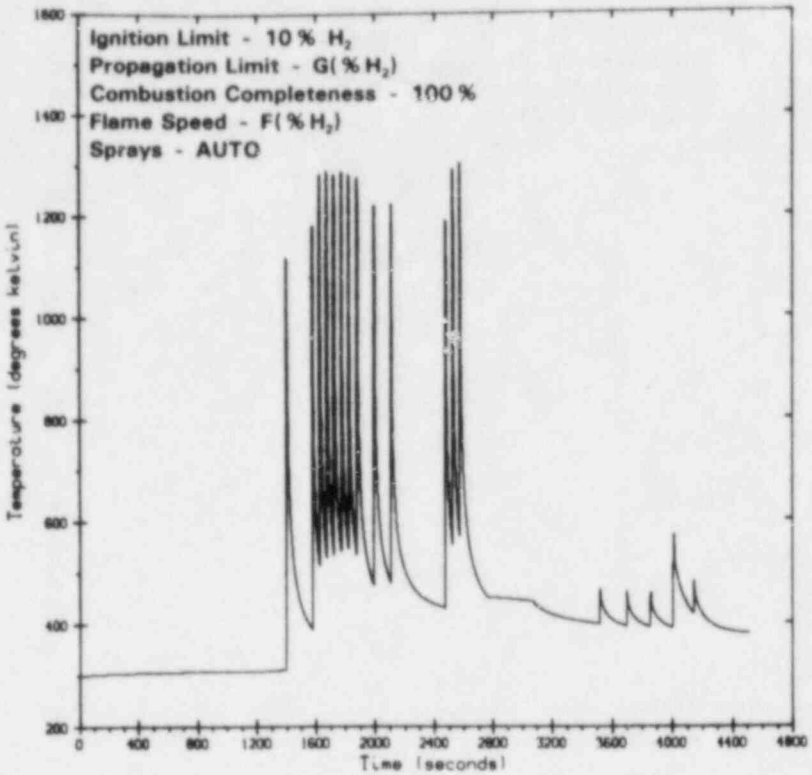

Figure 2.85. Case D2, Compartment 3 Temperature

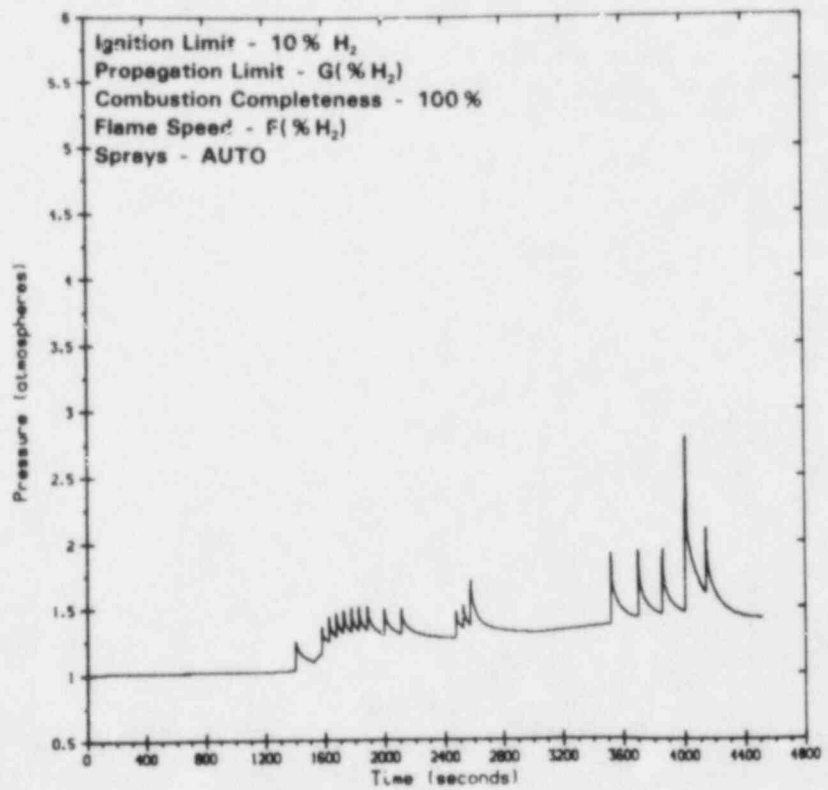

Figure 2.86. Case D2, Compartment 3 Pressure

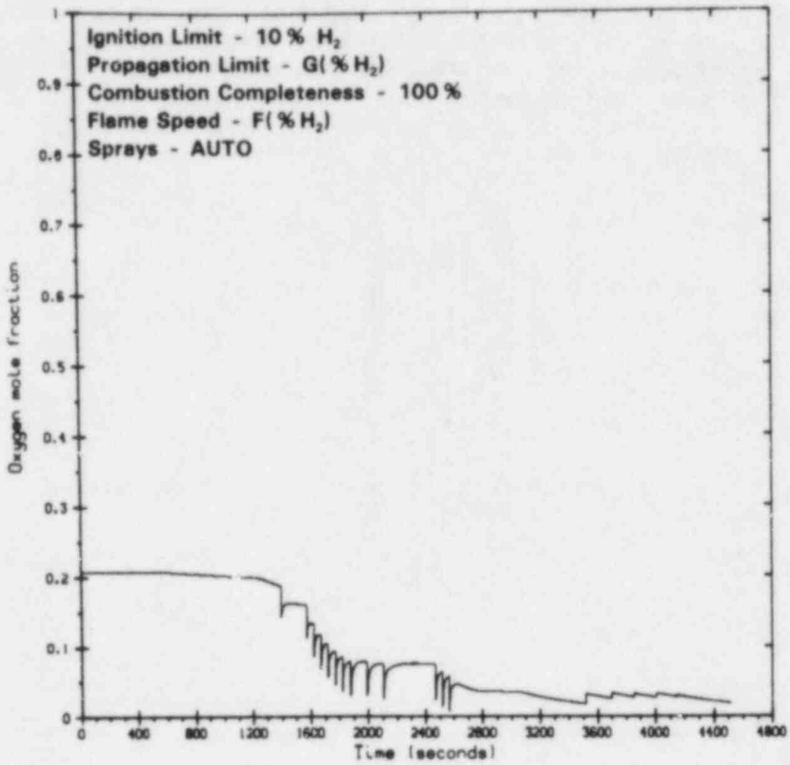

Figure 2.87. Case D2, Compartment 3 Oxygen Mole Fraction

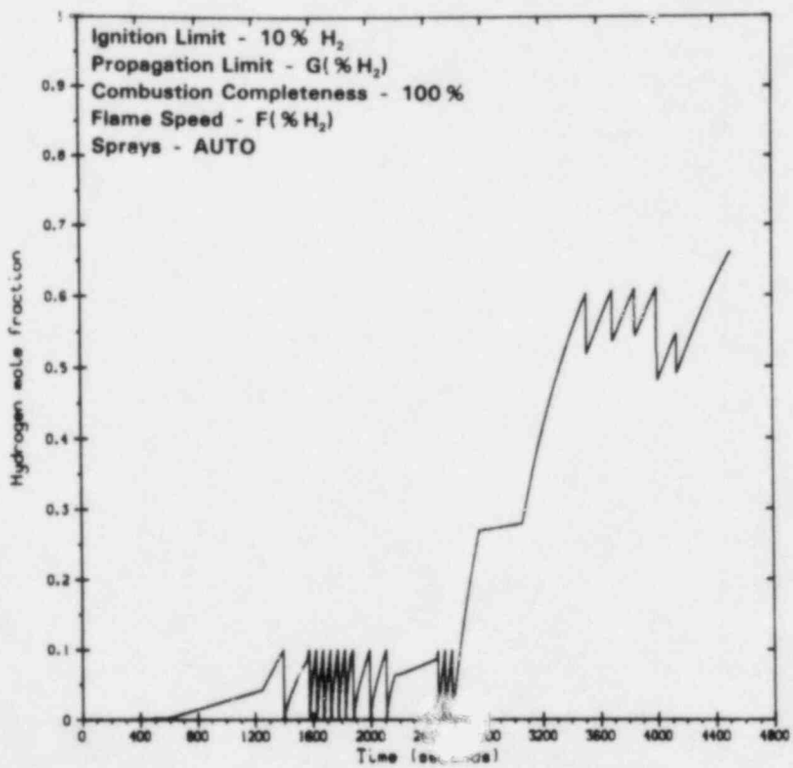

Figure 2.88. Case D2, Compartment 3 Hydrogen Mole Fraction

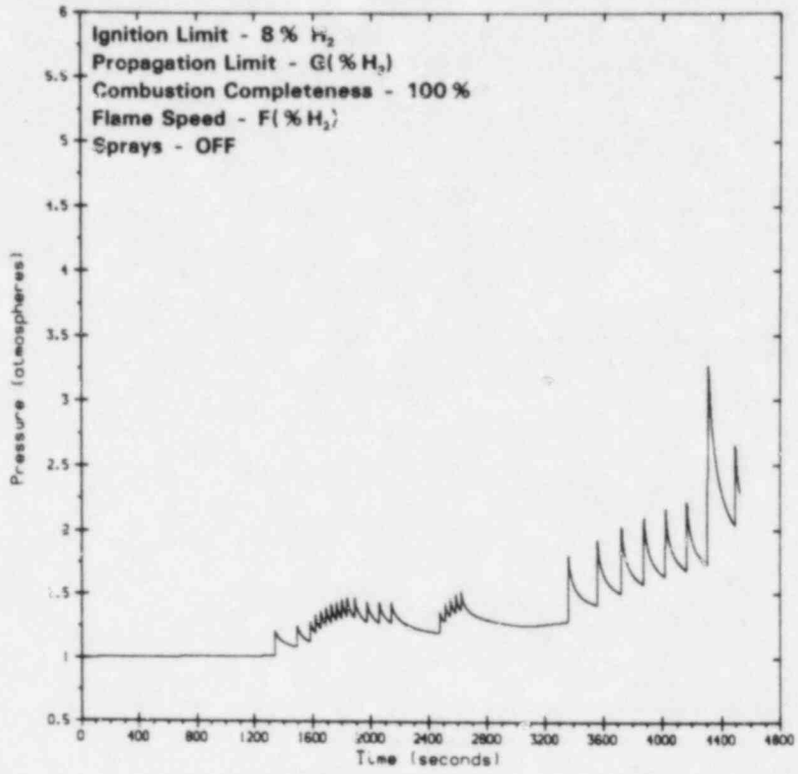

Figure 2.89. Case D3, Compartment 1 Pressure

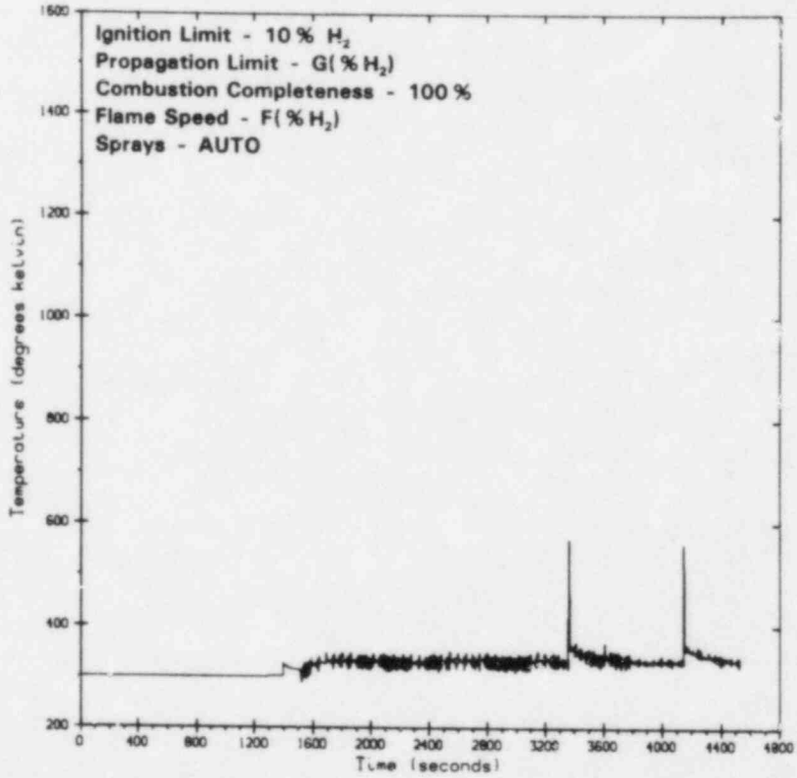

Figure 2.90. Case E1, Compartment 1 Temperature

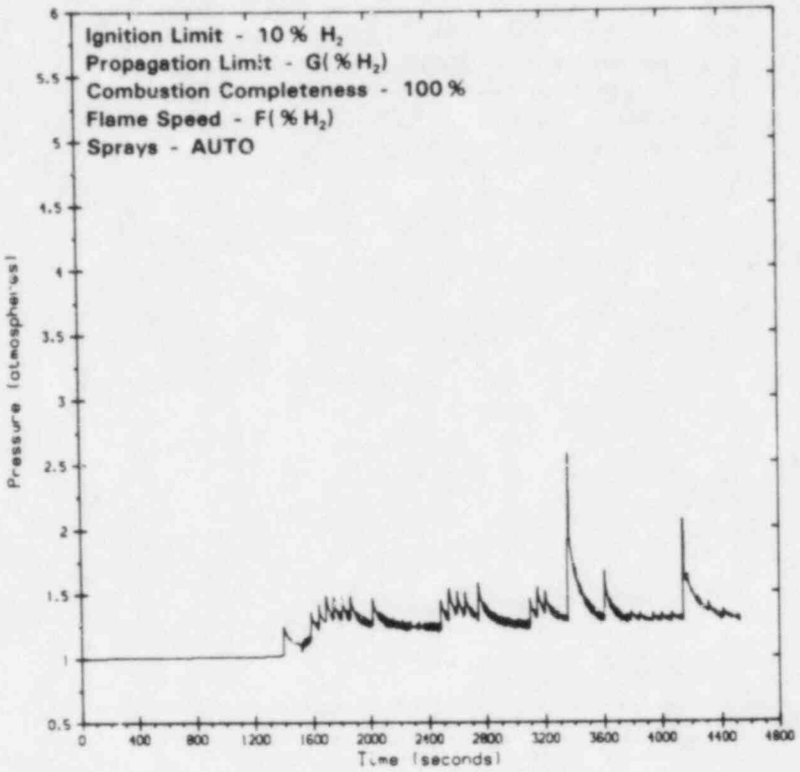

Figure 2.91. Case E1, Compartment 1 Pressure

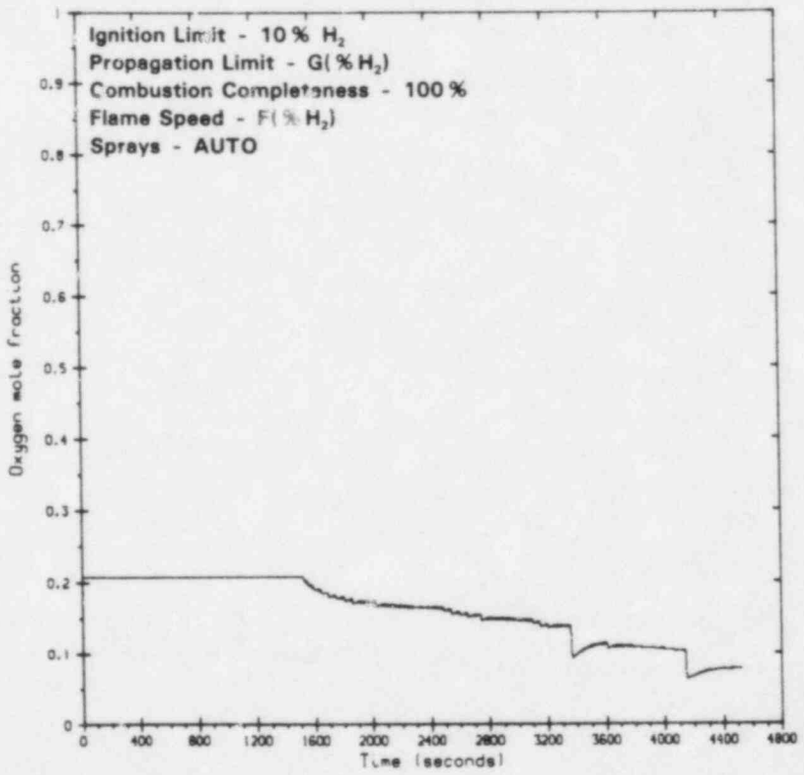

Figure 2.92. Case E1, Compartment 1 Oxygen Mole Fraction

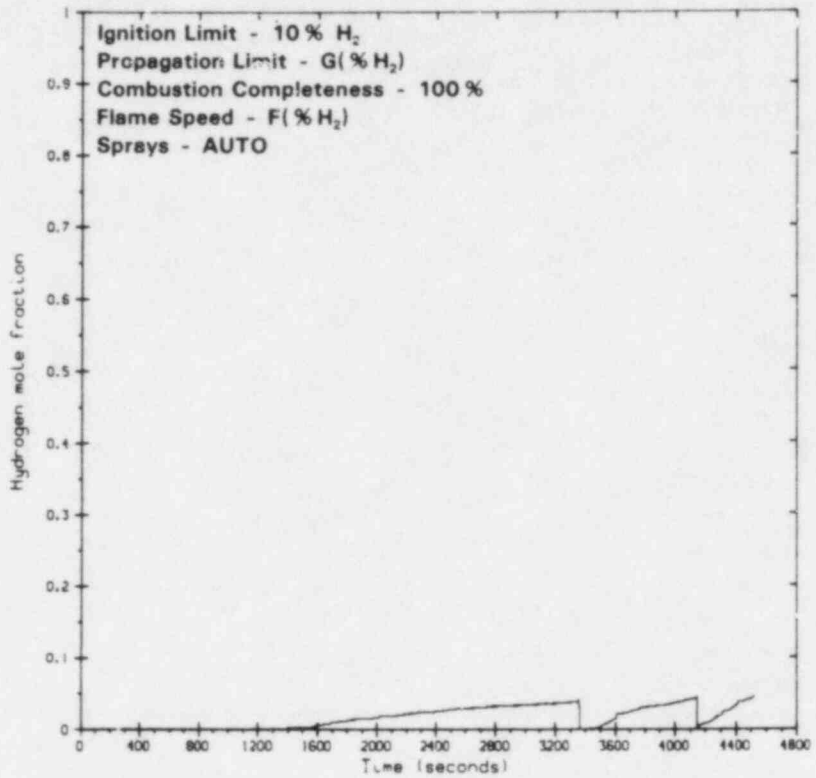

Figure 2.93. Case E1, Compartment 1 Hydrogen Mole Fraction

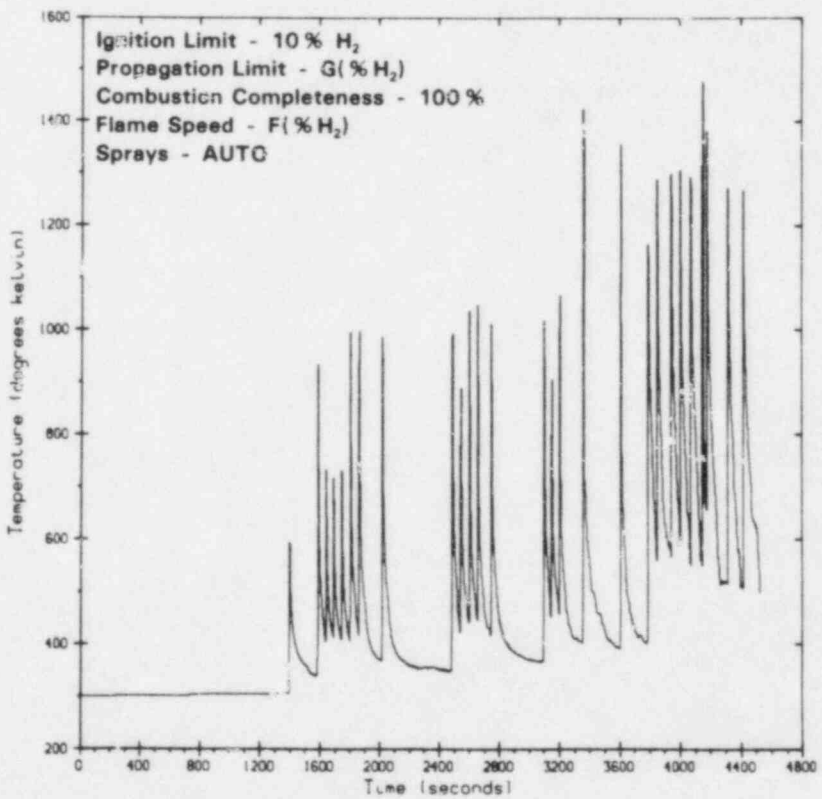

Figure 2.94. Case E1, Compartment 2 Temperature

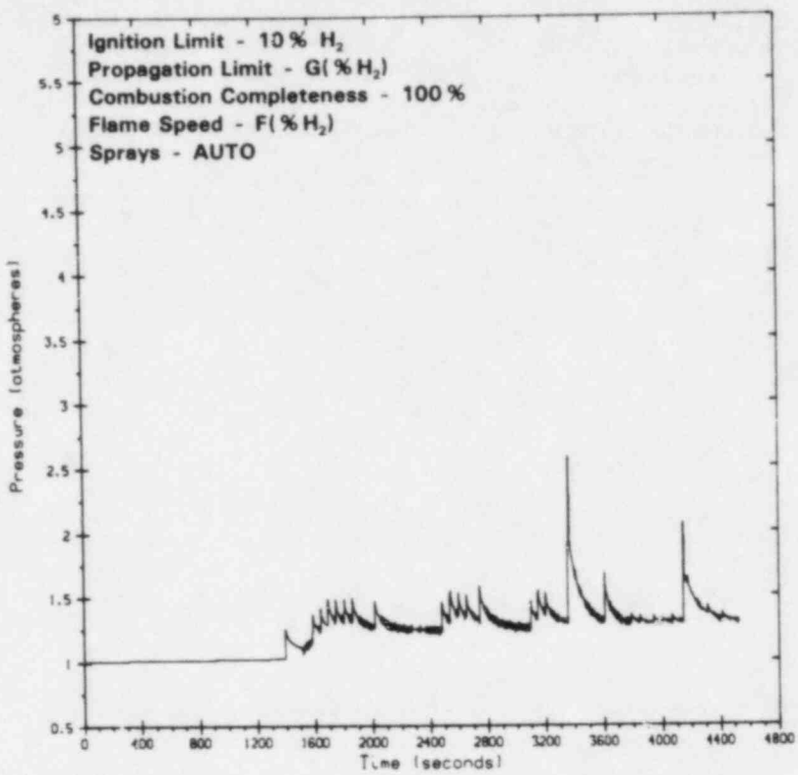

Figure 2.95. Case E1, Compartment 2 Pressure

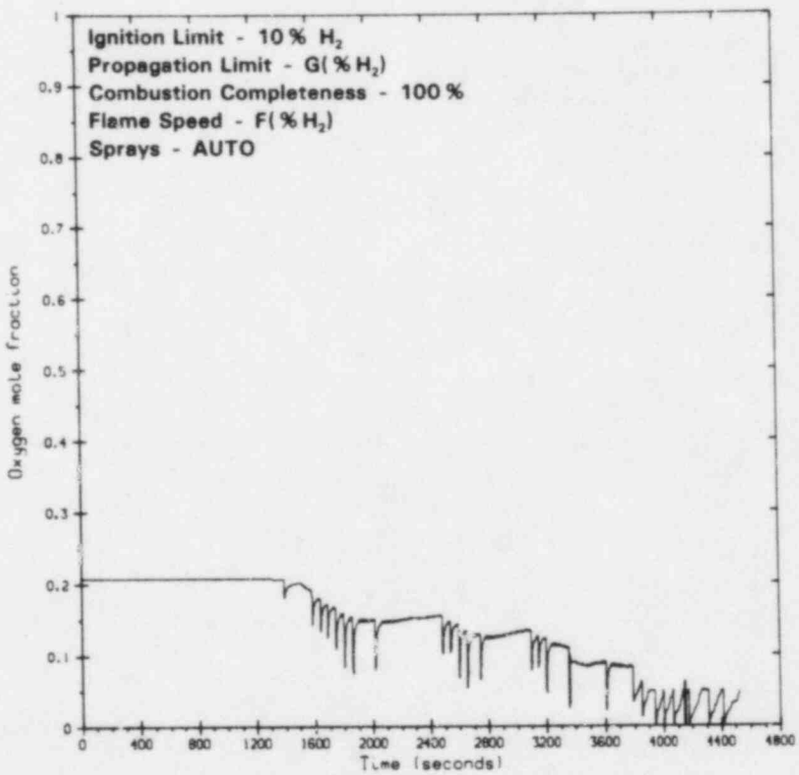

Figure 2.96. Case E1, Compartment 2 Oxygen Mole Fraction

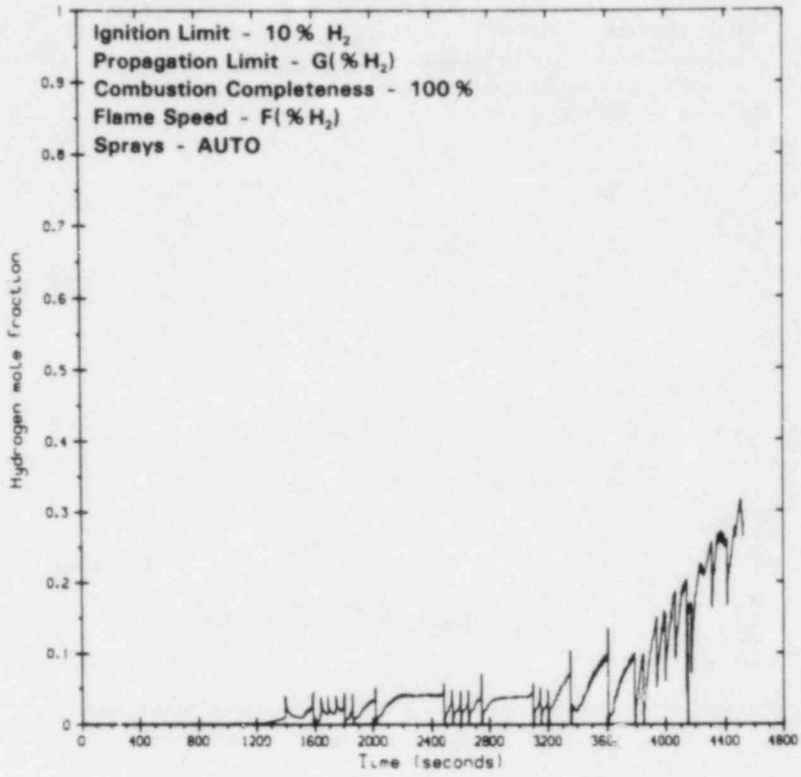

Figure 2.97. Case E1, Compartment 2 Hydrogen Mole Fraction

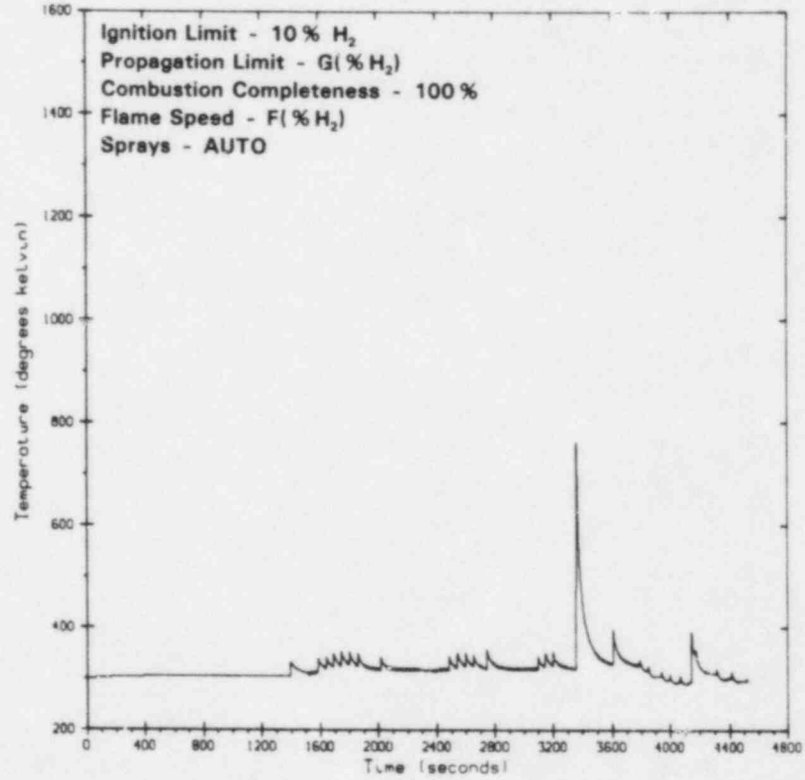

Figure 2.98. Case E1, Compartment 3 Temperature

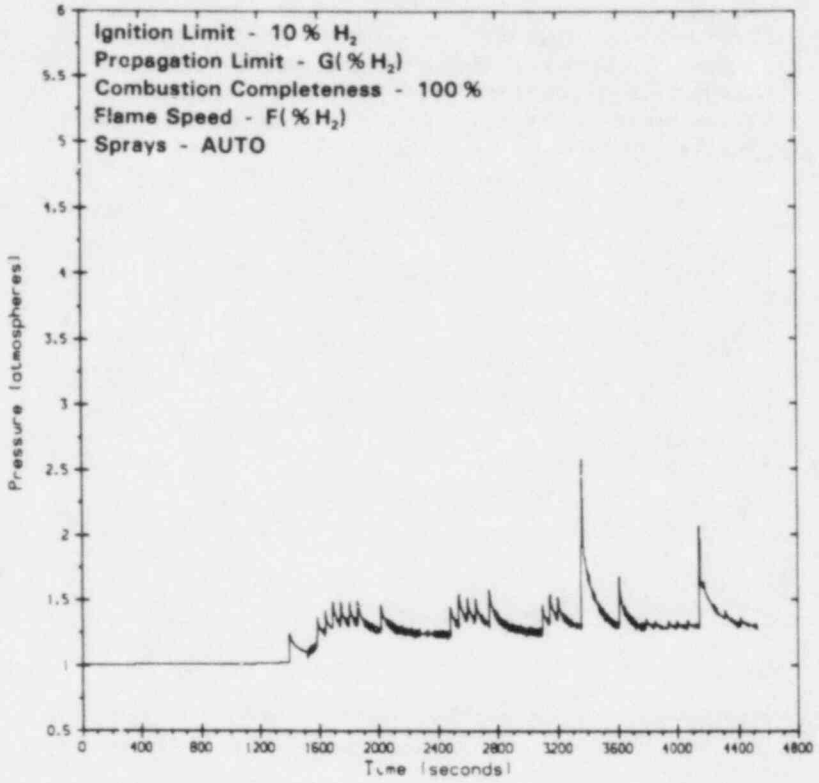

Figure 2.99. Case E1, Compartment 3 Pressure

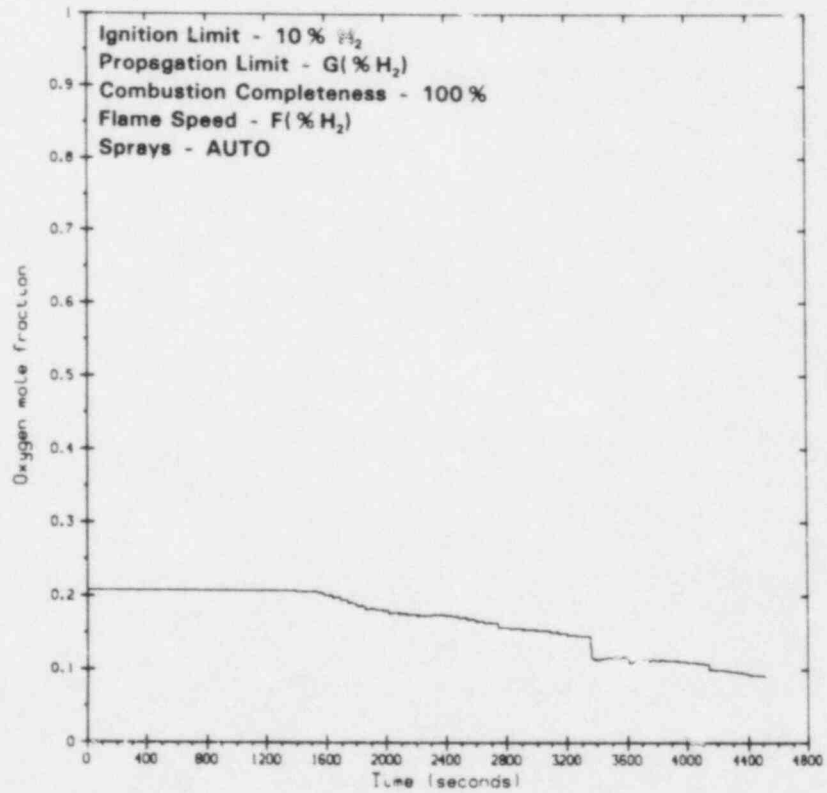

Figure 2.100. Case E1, Compartment 3 Oxygen Mole Fraction

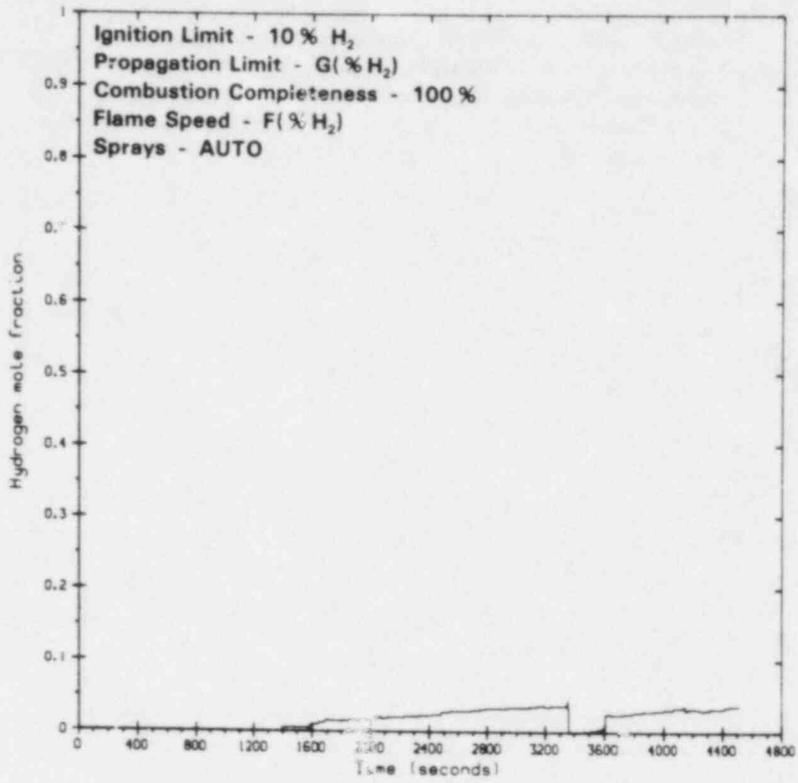

Figure 2.101. Case E1, Compartment 3 Hydrogen Mole Fraction

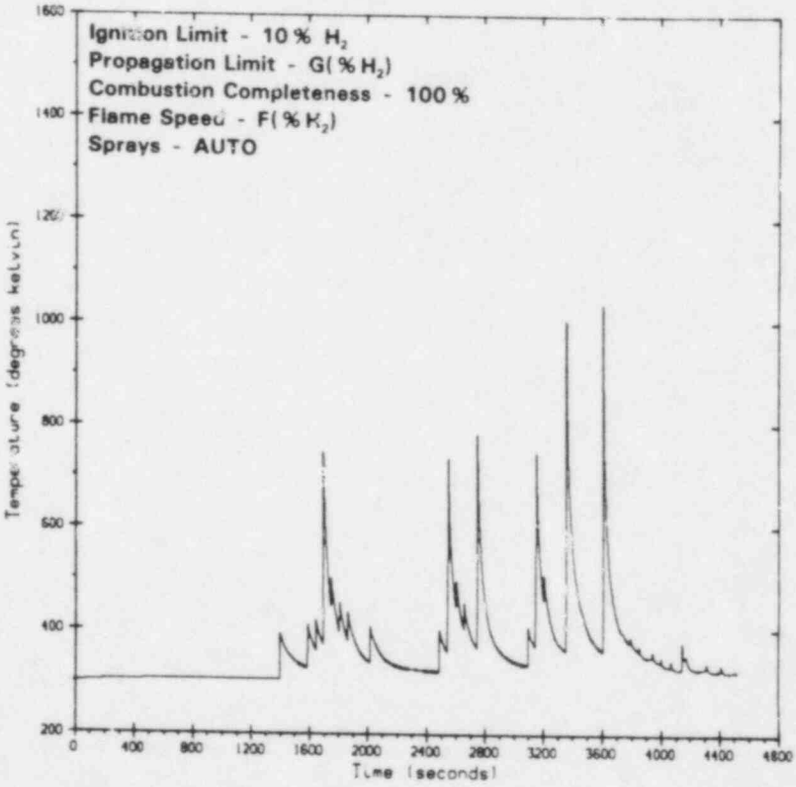

Figure 2.102. Case E1, Compartment 4 Temperature

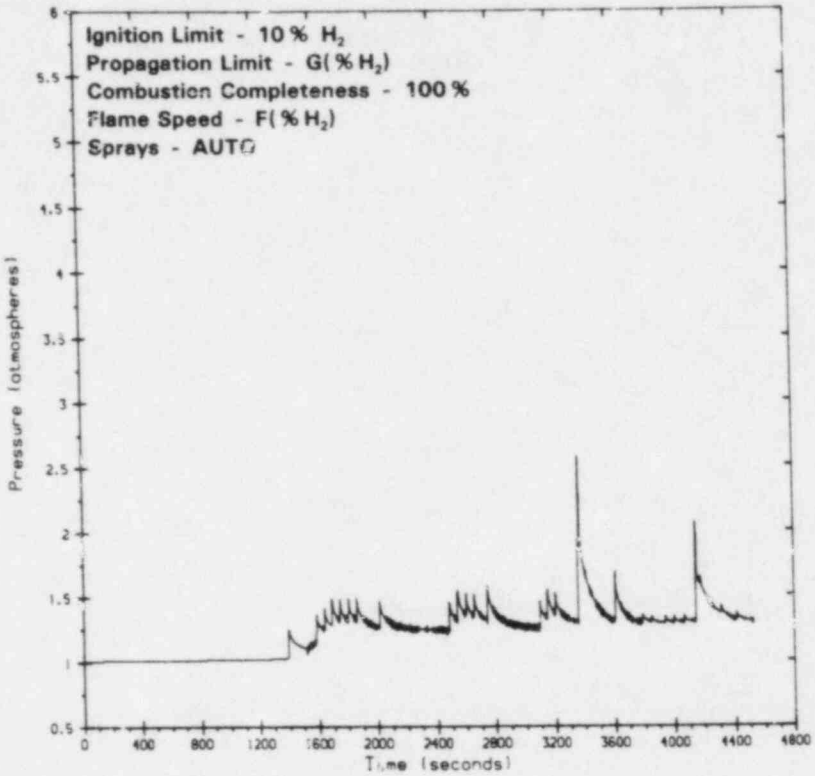

Figure 2.103. Case E1, Compartment 4 Pressure

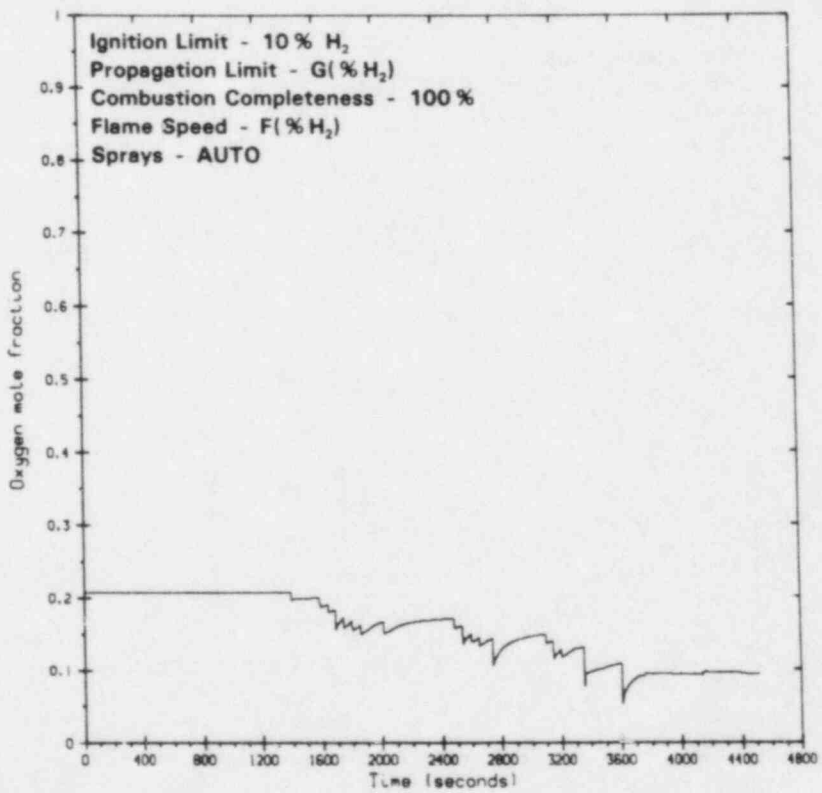

Figure 2.104. Case E1, Compartment 4 Oxygen Mole Fraction

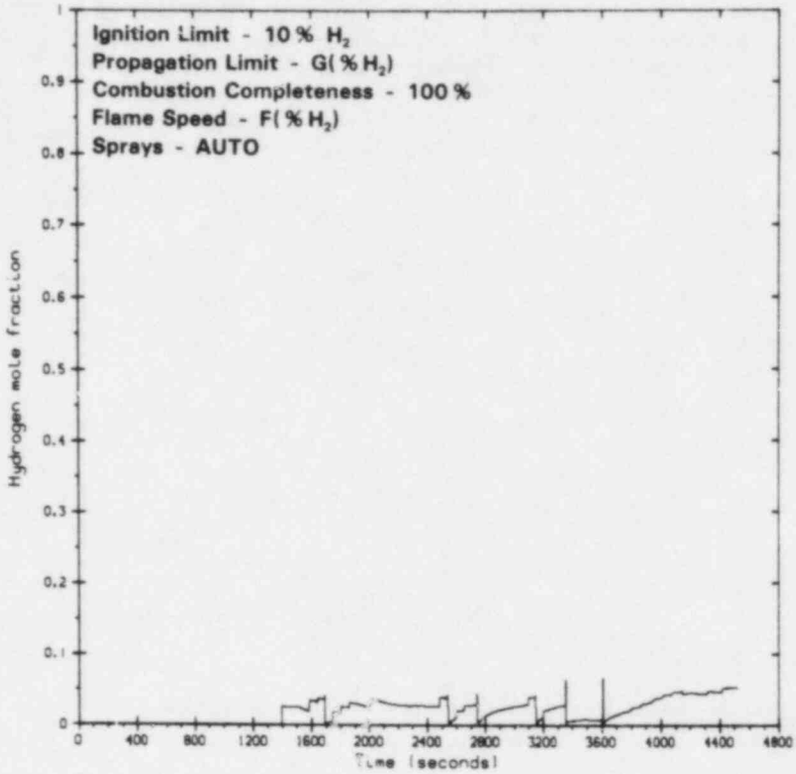

Figure 2.105. Case E1, Compartment 4 Hydrogen Mole Fraction

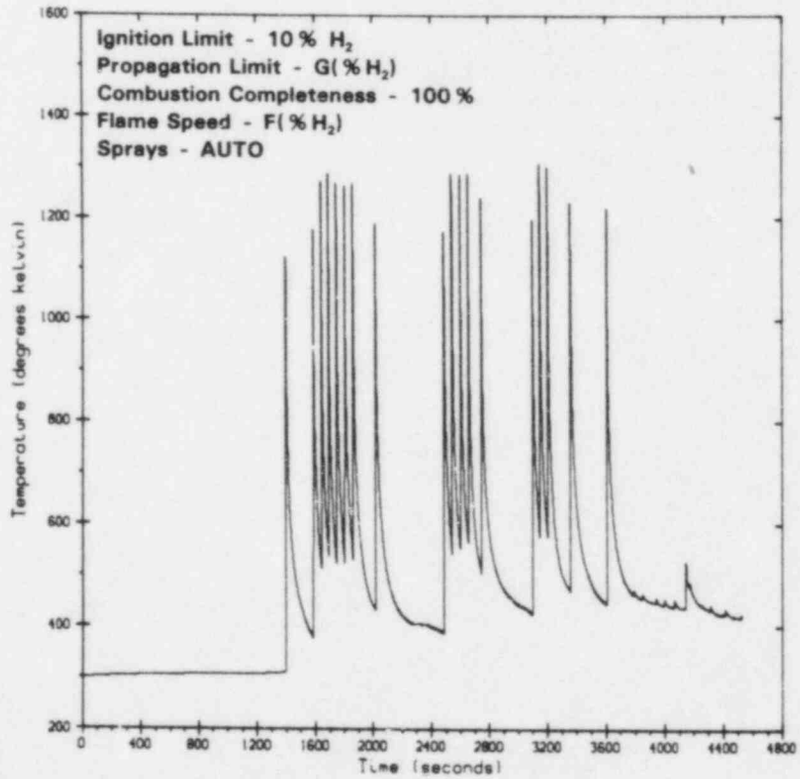

Figure 2.106. Case E1, Compartment 5 Temperature

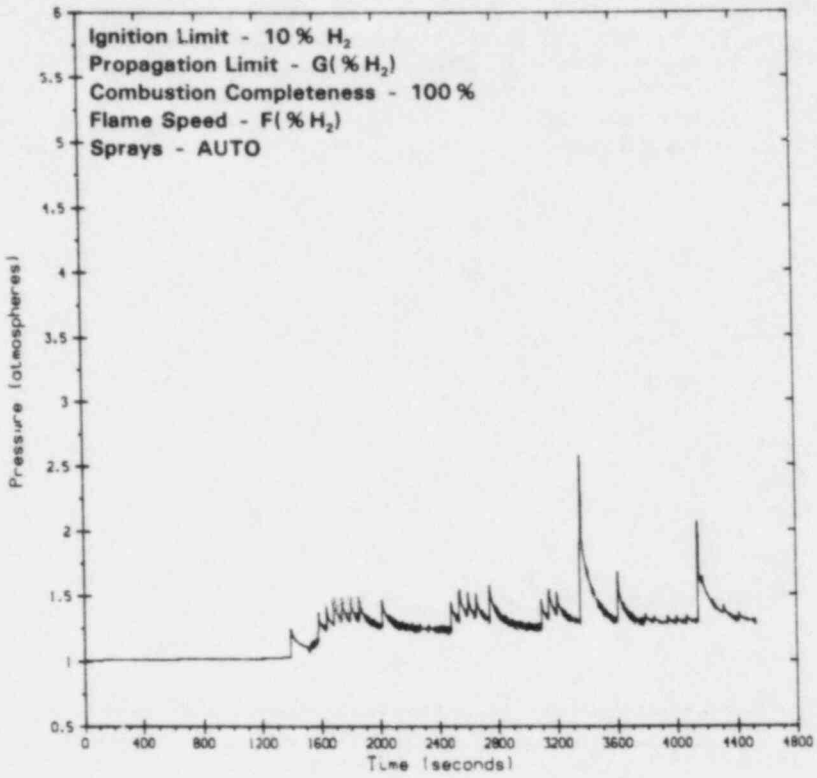

Figure 2.107. Case E1, Compartment 5 Pressure

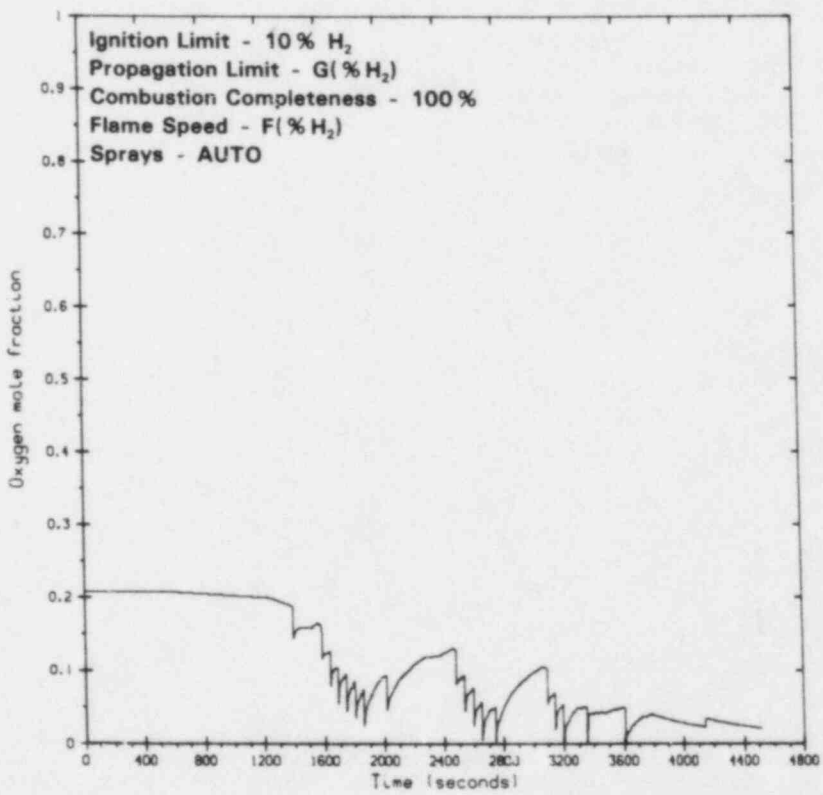

Figure 2.108. Case E1, Compartment 5 Oxygen Mole Fraction

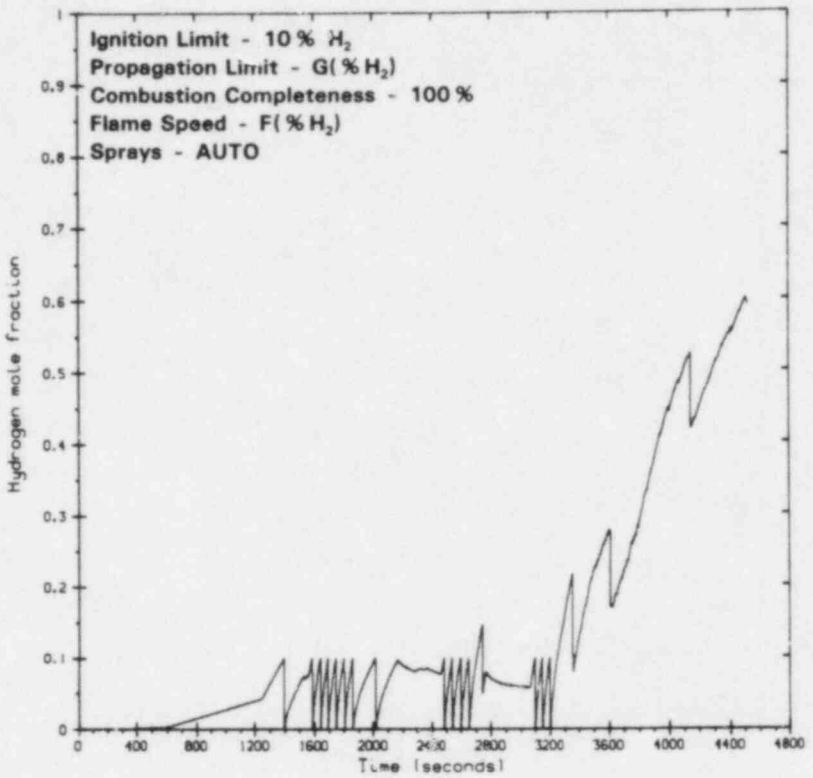

Figure 2.109. Case E1, Compartment 5 Hydrogen Mole Fraction

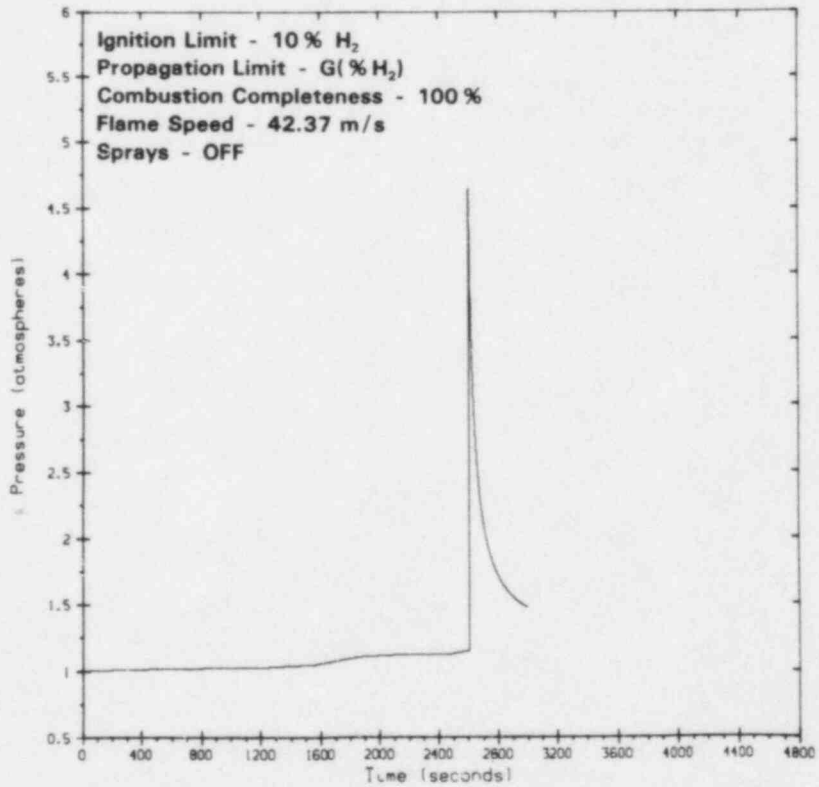

Figure 2.110. Case A13, Compartment 1 Pressure

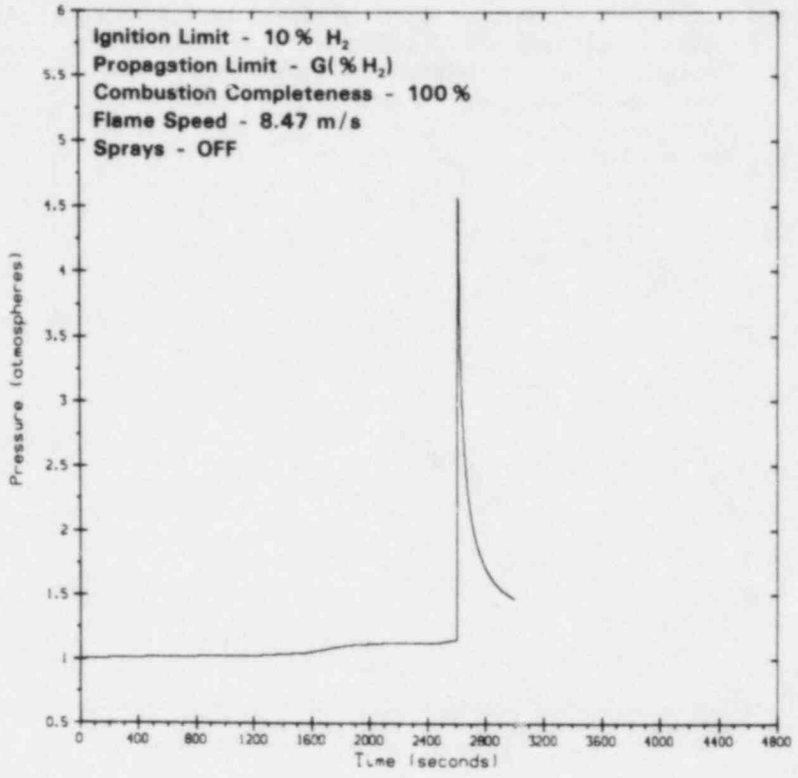

Figure 2.111. Case A14, Compartment 1 Pressure

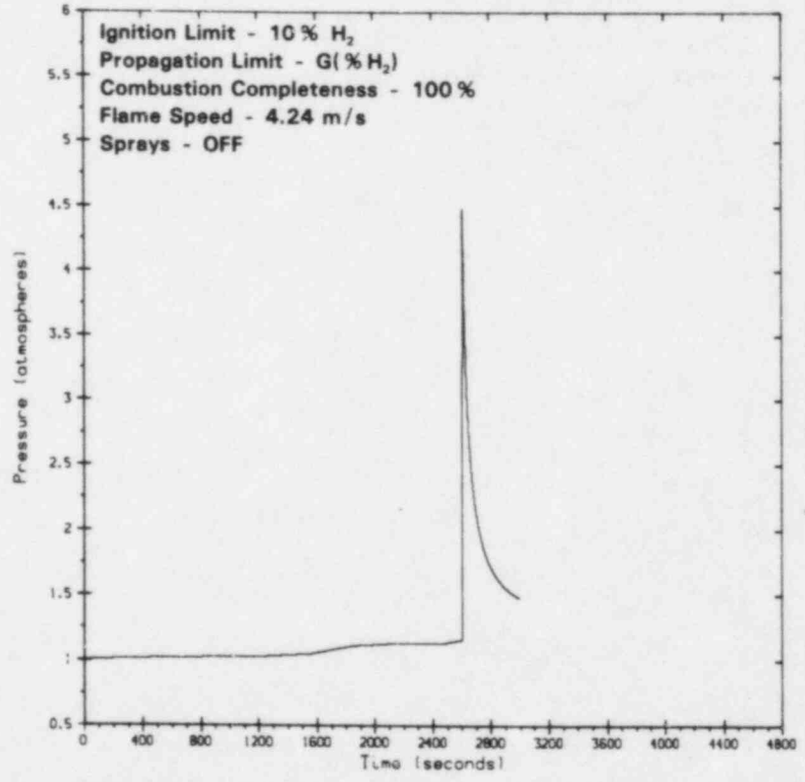

Figure 2.112. Case A15, Compartment 1 Pressure

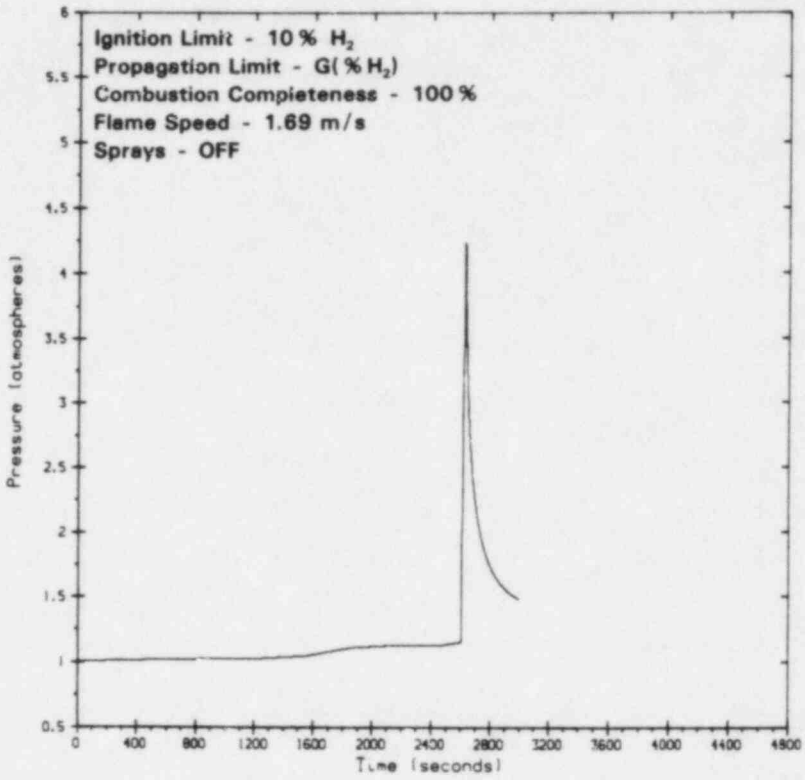

Figure 2.113. Case A16, Compartment 1 Pressure

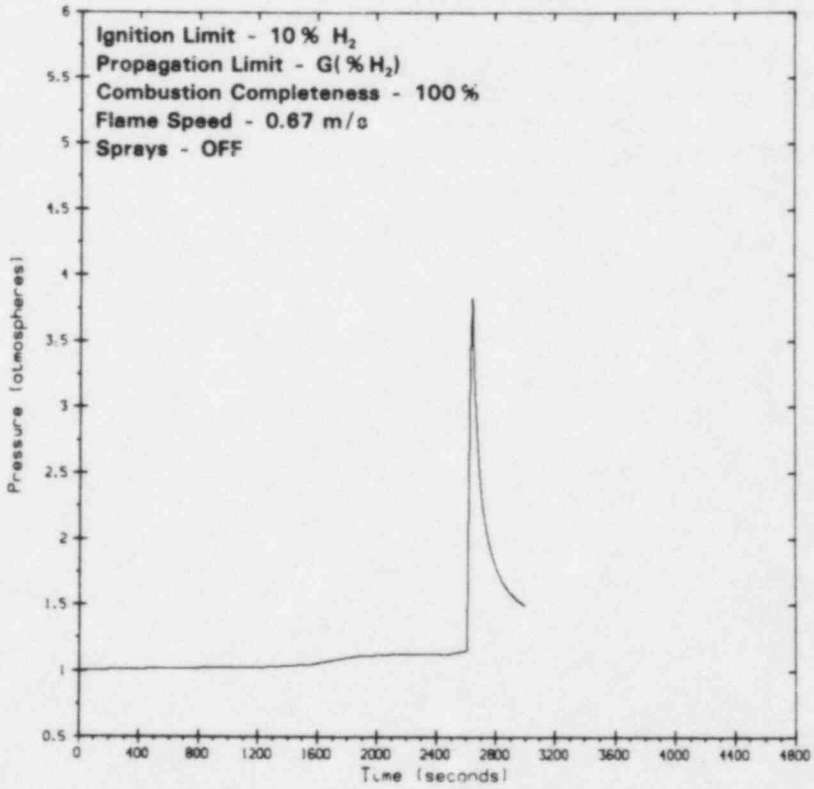

Figure 2.114. Case A17, Compartment 1 Pressure

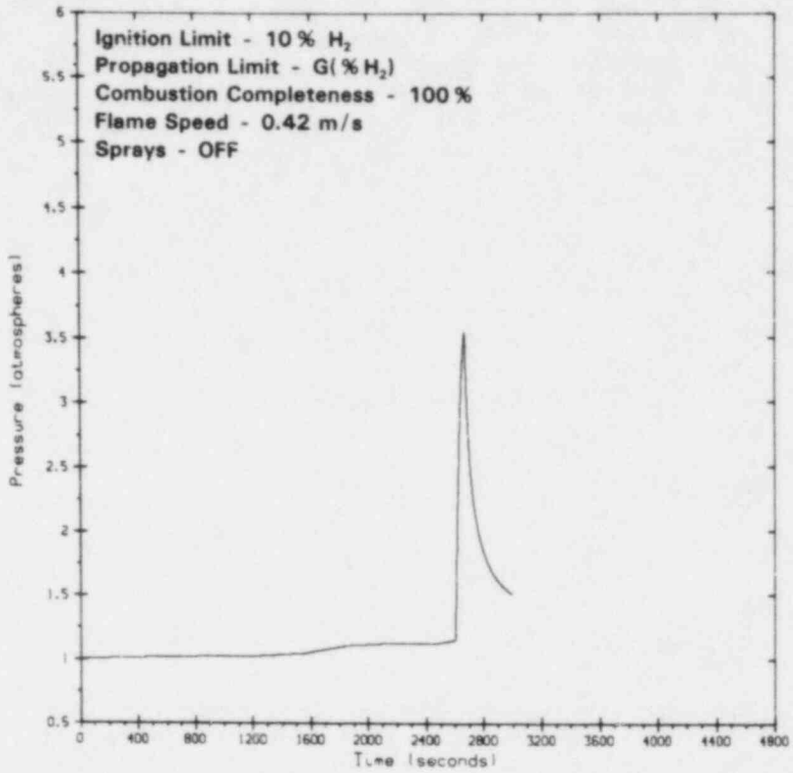

Figure 2.115. Case A18, Compartment 1 Pressure

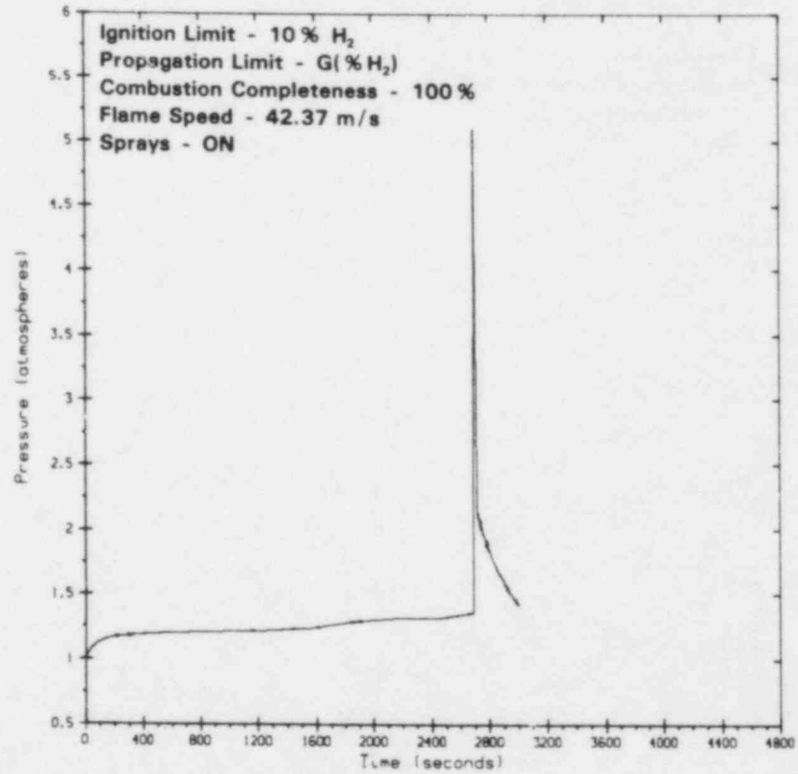

Figure 2.116. Case A19, Compartment 1 Pressure

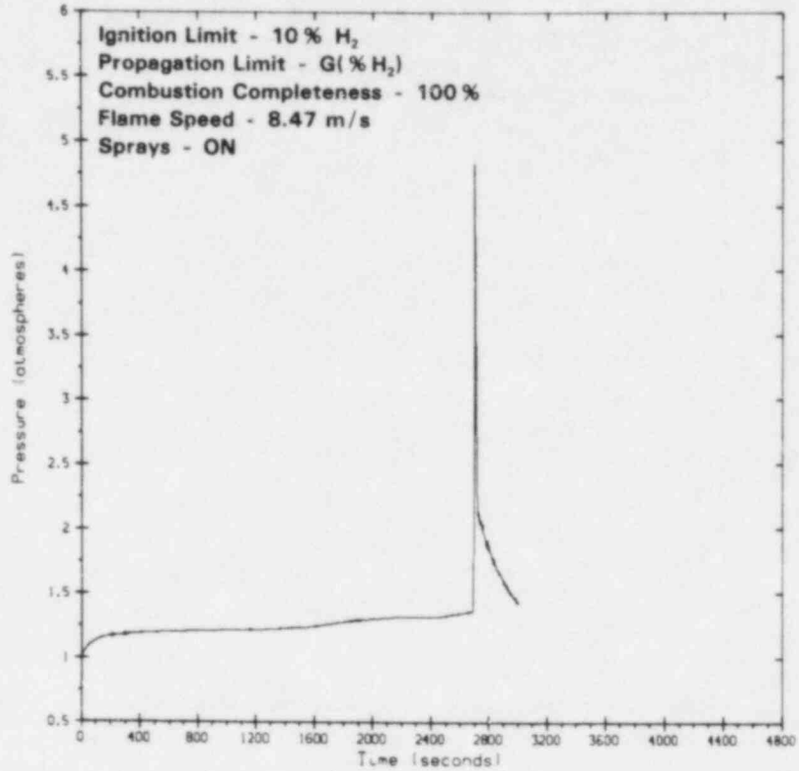

Figure 2.117. Case A20, Compartment 1 Pressure

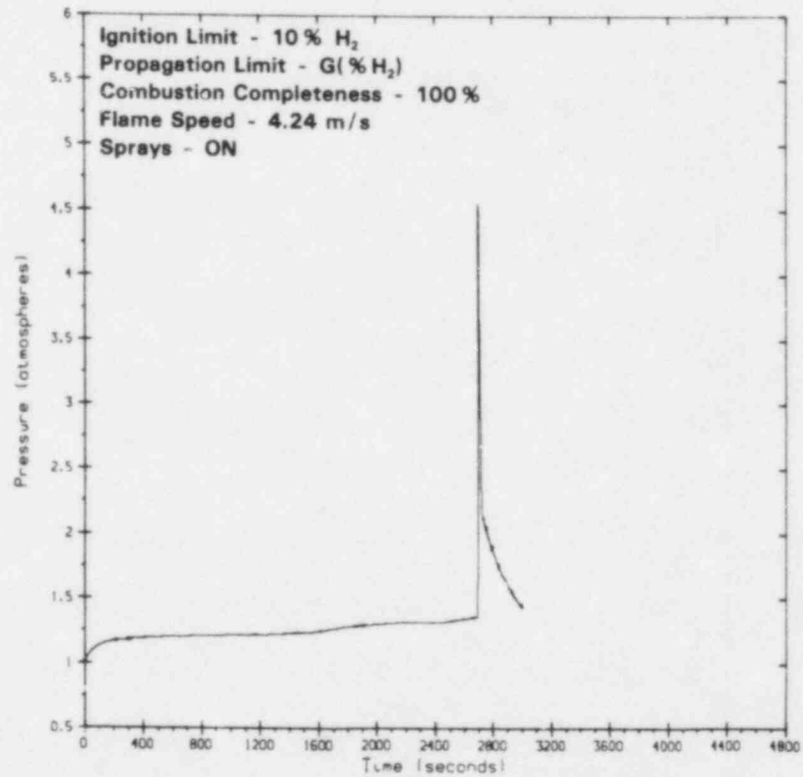

Figure 2.118. Case A21, Compartment 1 Pressure

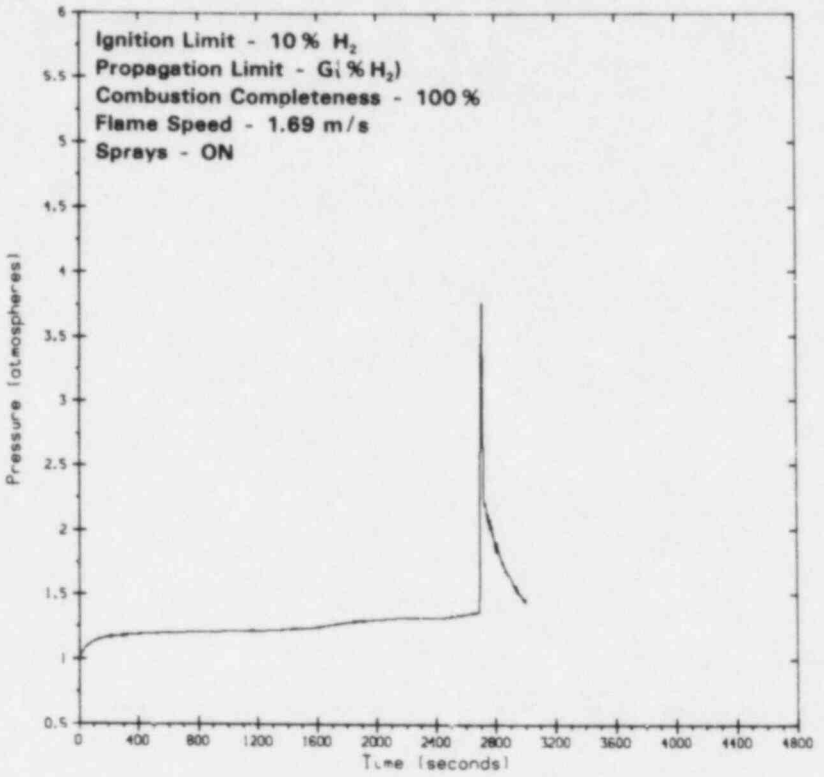

Figure 2.119. Case A22, Compartment 1 Pressure

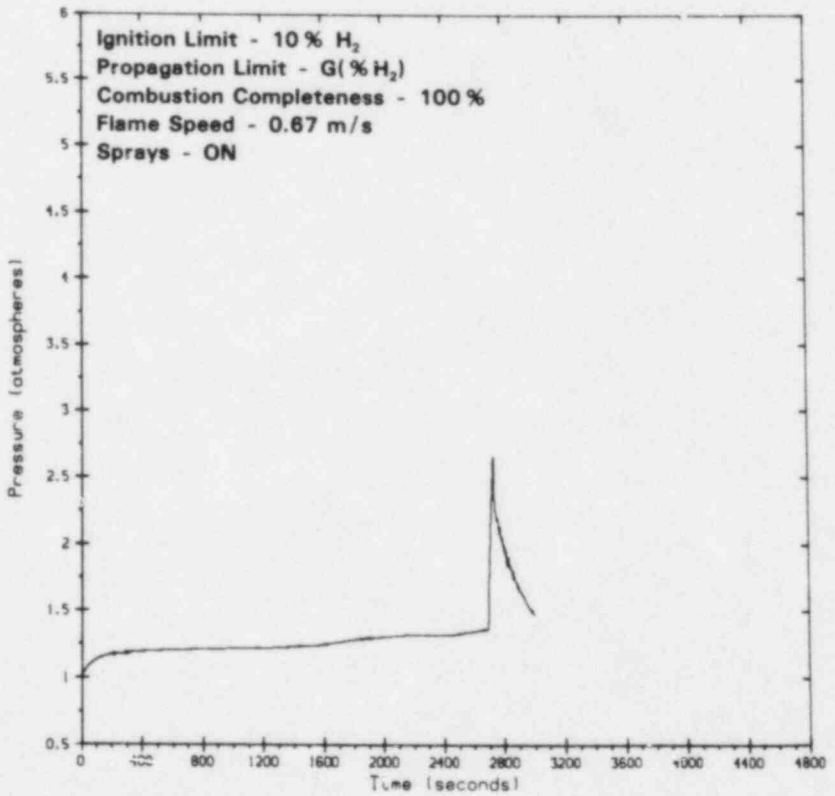

Figure 2.120. Case A23, Compartment 1 Pressure

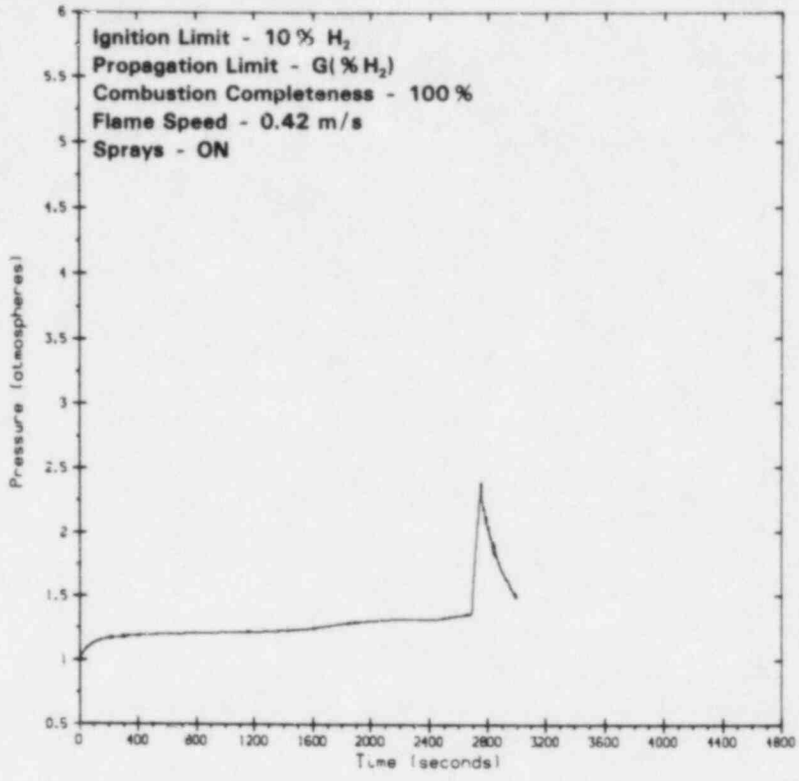

Figure 2.121. Case A24, Compartment 1 Pressure

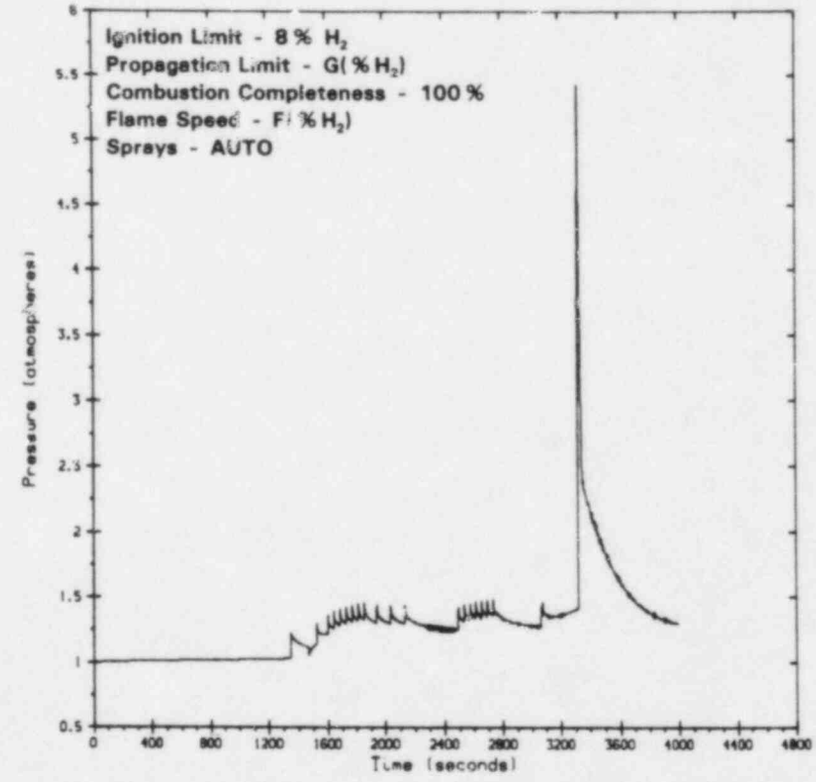

Figure 2.122. Case B8, Compartment 1 Pressure

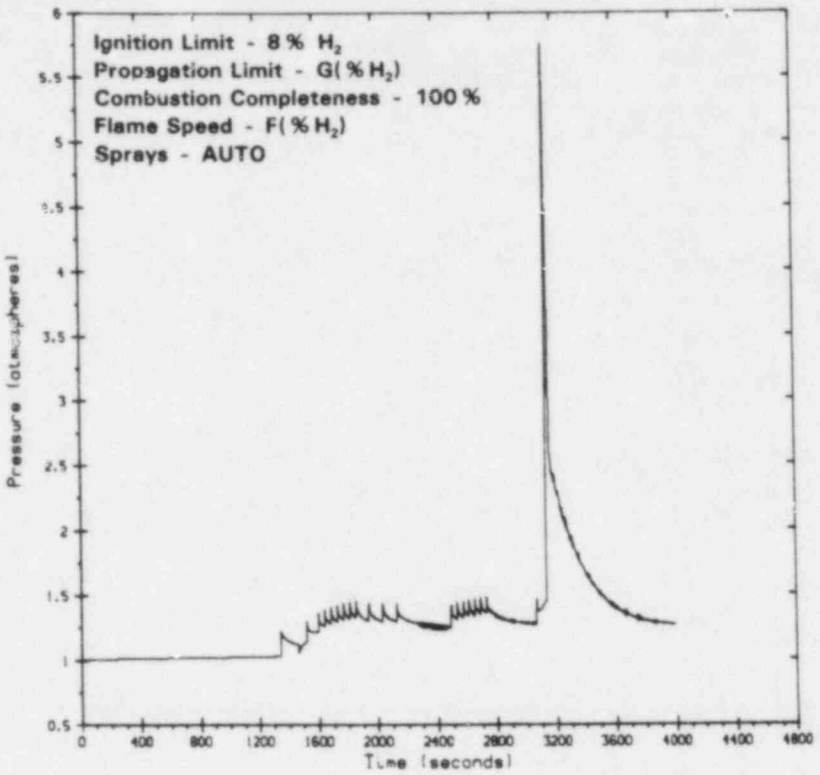

Figure 2.123. Case B9, Compartment 1 Pressure

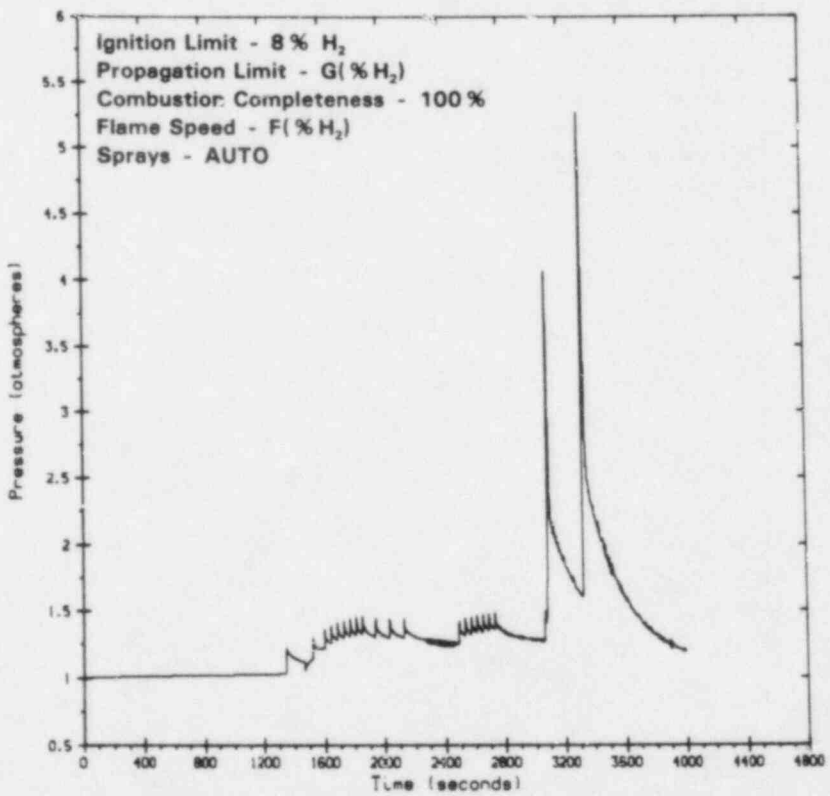

Figure 2.124. Case B10, Compartment 1 Pressure

2.2.3 Analysis

In Section 2.2.1, we identified several areas of concern regarding the CLASIX-3 analysis. These concerns, along with some additional considerations, are addressed below.

Compartmentalization and Mixing—The 44 HECTR cases show clearly that high pressures can result if global burns occur. Whether or not global burns occur depends on how rapidly hydrogen and oxygen are mixed within containment. There are three mechanisms to consider when addressing mixing. They are

1. Pressure-driven mass transfer
2. Diffusion
3. Convection

HECTR, and apparently CLASIX-3, ignore diffusion and convection. Thus, in both cases, the mixing rate *between* compartments is underestimated; mixing *within* a compartment, however, is instantaneous.

The two-compartment HECTR cases tend to show that the wetwell region eventually inerts due to a lack of oxygen, and burns occur in the dome region soon afterward. This inerting in the wetwell may not be realistic. After a burn in the wetwell, the temperature there may be higher than the temperature in the dome, and significant convective mixing might result. However, the same convective mixing mechanisms that will bring oxygen into the wetwell between burns will also move hydrogen into the dome region. Therefore, the analyses may also underestimate the amount of hydrogen that escapes from the wetwell region unburned.

As far as compartmentalization is concerned, the one-compartment cases would be typical of very rapid mixing, and the three- and five-compartment models would be typical of slower mixing. For both CLASIX-3 and HECTR, the transport and mixing of hydrogen are controlled more by arbitrary modelling assumptions than by physics. HECTR will be modified to calculate convection in the near future. A more detailed analysis of mixing is presented in Chapter 4.0 of this report.

Flame Speed—The CLASIX-3 flame speed of 1.83 m/s results in burns that last about 12 s in the dome region. In 12 s a significant amount of heat transfer can occur, particularly if the sprays are on. Our opinion is that the CLASIX-3 flame speed may be too low and, therefore, the predicted pressure rises may be lower than can be realistically expected.

Figure 2.125 presents the results of cases A13 through A24 in a different format to illustrate the effect of burn time on the pressure rise. The burnout time in Figure 2.125 is equal to the flame propagation length divided by the flame speed. The flame speeds used in most of the other HECTR cases are about a factor of 3 or 4 higher than the flame speed of 1.83 m/s used in HECTR cases A1 and B1 through B4, and in the CLASIX-3 cases. As described previously in section 2.1.3, these speeds are based upon experimental data. It should be pointed out that even the higher speeds do not take into account the possibility of flame acceleration due to the presence of obstacles in the annular region above the suppression pool. Therefore, even the higher speeds may not be conservative. Increasing the flame speed above the values used in HECTR will result in an increase in the pressure rise. The pressure increases observed are already a significant fraction (greater than 90% in most cases) of the adiabatic pressure rise and the net increase would be ~10% or less, which may be important for some cases.

Completeness of Combustion—Incomplete combustion results in lower pressure rises than complete combustion; however, the pressure rises are not always as much lower as one would expect. For example, the only differences between HECTR cases A1 and A2 are flame speed and completeness of combustion. Surprisingly, case A1, with a lower flame speed and incomplete (85%) combustion, has a peak pressure close (93%) to that of case A2. The reason is that case A1 has one more burn than case A2. Therefore, while the pressure rise for any single burn is larger for Case A2, the cumulative results are similar. Whether or not this will hold true in other cases will depend upon the time between burns and the pressure and temperature decrease between burns (cases A1 and A2 had no sprays). Typically, incomplete combustion results in more burns that occur closer together in time and, therefore, tend to be more additive. Complete combustion results in fewer burns with larger pressure rises accompanying each burn.

Propagation Limits—In cases B5 through B7, C1 through C4, D1 through D3, and E1, burns were allowed to propagate from one compartment to another with a lower hydrogen concentration. It was noted previously that in some of the CLASIX-3 cases, significant hydrogen concentrations were present in the dome while burns were occurring in the wetwell. The effects of including propagation vary. In some cases (B5, B6, and B7) the end result is still eventual wetwell inerting, followed by a burn in the dome at the ignition limits. However, in other cases (C1 through C3, D1 through D3, and E1) the only burns in the dome occurred just above the 4.1% upward propagation limit and resulted in relatively small pressure rises.

Burning at high concentrations in the wetwell and propagating into concentrations of 4% to 6% hydrogen in the dome would cause few problems. However, propagating upward into 8% to 10% hydrogen would produce results similar to the results for cases A2 through A12 (one compartment model). Clearly, the key question once again is mixing, and neither HECTR nor CLASIX-3 adequately addresses this.

Hydrogen Source Term—The hydrogen source term used in the HECTR analysis came from Reference 2.3, as discussed earlier. This source term was apparently produced from a combination of MARCH[2.4] results and hand calculations. Cases B8 through B10 were run to examine the effects of very rapid hydrogen injection. There appear to be two major effects of rapid injection. First, the wetwell inerts very rapidly because there is less time between burns to bring oxygen back in. This effect results in burns in the dome region soon afterward. Second, a significant amount of hydrogen enters the containment during a burn, thus making an 8% burn look more like a 9% to 10% burn.

In contrast to very rapid hydrogen injection, slow injection would result in a long time between burns and little hydrogen injection during the burn. However it should be noted that slow injection rates result in more time available for mixing, making global burns more likely. A much better understanding of the phenomenology of hydrogen production is needed before definitive statements can be made about this issue.

Containment Sprays—Containment sprays produce significant reductions in peak pressures. The degree of reduction depends upon the burn time (time available for heat transfer; see Figure 2.125). The only time that sprays have a minor negative effect is when they are turned on before the first burn and cause a slight increase in pressure (due to the spray temperature exceeding the gas temperature) before the first burn. However, this slight increase will be more than offset by heat transfer for slow burns, and in any case, it is clearly better to turn the sprays on too early than to turn them on too late.

The effect of adding sprays in the wetwell (case B2′) was to delay inerting there. This effect appears to be due to increased cooling in the wetwell, which leads to a lower pressure and more mass transfer from the oxygen-rich dome region back into the wetwell.

Initial Conditions—For an adiabatic hydrogen burn, the ratio of final pressure to initial pressure is approximately constant for any particular hydrogen mole fraction. Thus, a 10% change in initial pressure yields a 10% change in final pressure. While the burns in the HECTR analysis are not adiabatic, the basic idea still holds. Comparing cases A8 and A9, for example, we find that a 0.157 atm difference in initial pressure results in a 0.679 atm difference in peak pressure. In both cases, the peak pressure occurred at the end of the first burn, and the ratio of peak pressure to initial pressure was about the same.

Elevated initial pressures may result from drywell air being pushed into containment and/or heating up of the containment atmosphere during the accident. Because relatively small increases in initial pressure can have such a significant impact on peak pressure, caution should be used when evaluating the quantitative results produced by any of the analysis codes.

Long-Term Considerations—It was noted that, in several cases, the hydrogen concentrations were close to the ignition point at the end of the run. As demonstrated in case B6′, burns may occur at later times due to removal of steam from the atmosphere and the associated rise in hydrogen mole fraction. Additionally, due to inerting, some of the cases show very high hydrogen concentrations (40% to 80%) in the wetwell region at the end of the run. It cannot be expected that this hydrogen would remain in the wetwell. Rather, it will eventually mix with the containment atmosphere and additional burns could result.

2.3 References

[2.1] M. Berman, *Light Water Reactor Safety Research Program Semiannual Report, April-September 1981*, Sandia National Laboratories, NUREG/CR-2481, SAND82-0006, February 1982.

[2.2] M. P. Sherman et al, *The Behavior of Hydrogen During Accidents in Light Water Reactors*, Sandia National Laboratories, NUREG/CR-1561, SAND80-1495, August 1980.

[2.3] *Report on the Grand Gulf Nuclear Station Hydrogen Ignition System*, Mississippi Power & Light Company, August 31, 1981.

[2.4] R. O. Wooton and H. I. Avci, *March (Meltdown Accident Response Characteristics) Code Description and Users Manual*, Battelle Columbus Laboratories, BMI-2064, NUREG/CR-1711, October 1980.

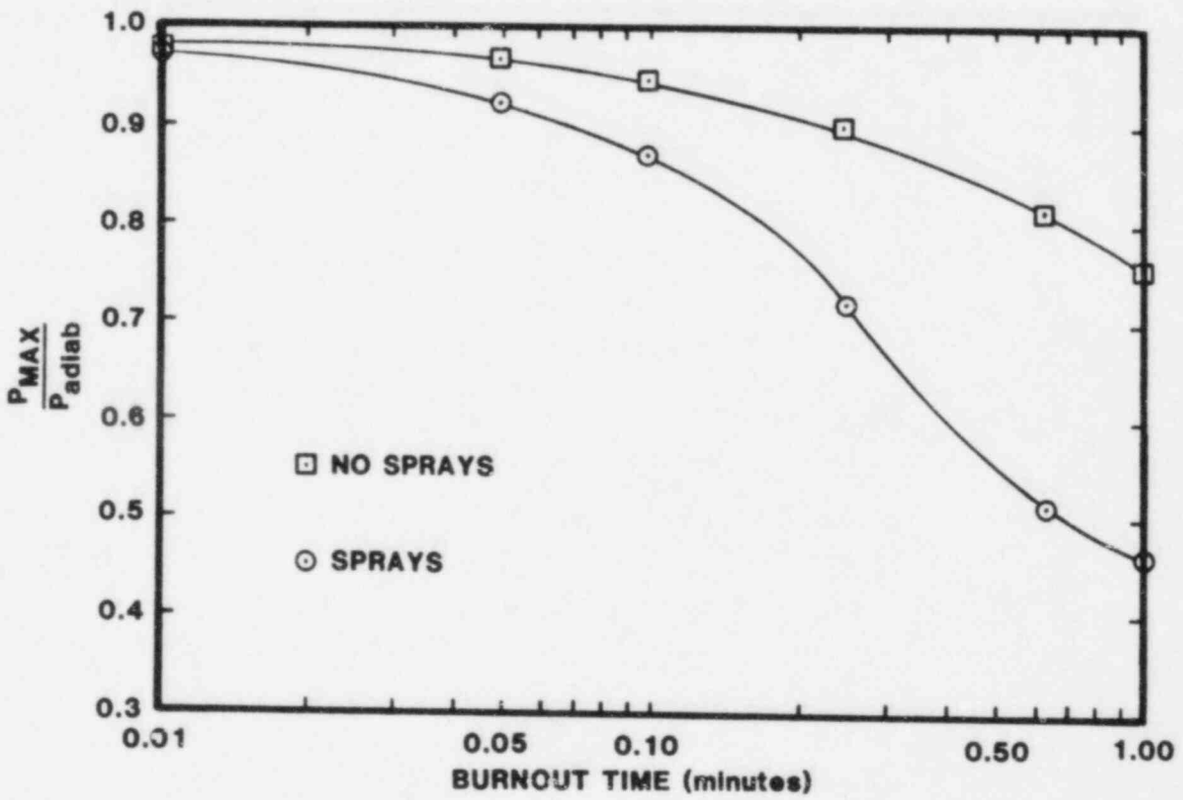

Figure 2.125. Effect of Burnout Time on Peak Pressure

3.0 Grand Gulf Accident Calculations Using the MARCH Code

3.1 Summary and Conclusions

The actual number, timing, location, and peak pressures that would be associated with hydrogen burns during a reactor accident depend on the local concentrations of the gases and the mixing processes which produced those concentrations (prior burns, natural and forced convection, H_2 injection rates, etc). The MARCH, HECTR, and CLASIX-3 computer codes, however, introduce an artificial mixing of the containment atmosphere. The gas entering a compartment is assumed instantly mixed with the contents of the compartment, and hence each compartment atmosphere is homogeneous. Real mixing processes such as natural or forced convection are not considered.* The results of combustion, as predicted by these codes, therefore depend strongly on the compartment model used. The number and arrangement of compartments is arbitrary. The most "realistic" model will be the one that best approximates the real mixing behavior in containment. We will first discuss some general conclusions from our work and then discuss the results obtained from the individual compartment model studies.

If containment sprays are inactive, both MARCH and HECTR predict a relatively small decrease in peak pressure as the burn duration is increased. Since MARCH does not include radiation heat transfer from the hot steam after a hydrogen burn (the most important heat transfer mechanism in HECTR when sprays are inactive), the agreement is surprising. Longer burn time corresponds to slower flame speed. Experimental work at SNL would predict more rapid flame speeds, typically 8 m/s, than those used in the CLASIX-3 calculations, 2 m/s.[3.1] With containment sprays operating, MARCH and HECTR are not in good agreement. MARCH predicted much greater reductions in peak pressure due to hydrogen burns than did HECTR for the same initial conditions and same burn times. The results are shown in Figure 3.1.

For multicompartment models, MARCH predicted a series of burns in the wetwell, the compartment into which hydrogen was introduced from the suppression pool. The inerting of the wetwell by oxygen depletion occurred in all cases and led to the buildup of large hydrogen mole fractions in the wetwell and combustible mole fractions in the upper compartments. In all cases considered but one, burns occurred in the upper containment and led to significant pressure peaks. Most of the cases predicted pressure peaks below the NRC estimate of containment failure pressure, 71 psia (4.8 atm), but some were higher. The results emphasize the importance of those failure estimates to conclusions drawn from this work.

The compartment models we used are shown in Figures 2.2 through 2.4. Configuration A considers the entire wetwell/containment as one volume. Results from this simple compartmentalization will be realistic if the time for mixing is shorter than the time between burns and also shorter than a characteristic time for hydrogen release (since the mixture will then be nearly homogeneous). Configuration B divides this volume into two compartments: a small wetwell volume (from the top of the suppression pool to the 135 ft elevation) and a much larger upper containment. Configuration C also divides the volume into two compartments with the division being at the 209 ft elevation (the top being the open volume under the containment dome). Configuration D divides the volume into three compartments: a wetwell up to 135 ft, an intermediate annular region up to 209 ft, and an upper containment. Configuration E′ differs from configuration E used in the HECTR analysis since MARCH cannot analyze parallel flow paths. Configuration E′ divides the volume into four compartments, similar to configuration D except for one more division at the 165 ft elevation. The more compartments used in the model, the slower the calculated mixing. Without more knowledge of the mixing process, it is not clear which model gives the most realistic results.

Our MARCH results using configuration A agree fairly well with results obtained with HECTR. The number of burns predicted by the two codes for various cases either is the same or differs by one. The peak pressures predicted without sprays are very high and the two codes agree well. With sprays, the peak pressures are lower, MARCH giving lower results than HECTR. Given the known differences in models and

*MP&L did consider a small amount of forced convection in one CLASIX-3 sensitivity case.

inputs, the agreement between MARCH and HECTR is probably fortuitous.

The majority of the CLASIX-3 results were obtained using configuration B. We have found the exact history of the accident to be very sensitive to the input assumptions used with this configuration. In particular, the number of wetwell burns is highly variable. However, in all MARCH and HECTR calculations upper containment burns were predicted. This is in contrast to the CLASIX-3 calculations in which upper containment burns were not predicted for most cases. Depending on the assumptions made, the peak pressures for the MARCH and HECTR calculations range from moderately high to above the estimated failure pressure for the containment. Sprays help reduce the peak pressures.

For configuration C, in one MARCH calculation with a connected drywell there was no upper containment burn. For all other runs, one or more upper containment burns were predicted. The peak pressures were moderately high. The agreement between MARCH and HECTR for configuration C is fairly good.

In configuration D, we predict gradual inerting of the lower sections of the wetwell/containment and burning higher in the containment. The peak pressures are moderately high. MARCH and HECTR are in fairly good agreement.

The results for configuration E′ are similar to configuration D. The E′ configuration used in MARCH is sufficiently different from the E configuration used in HECTR to preclude direct comparison.

For configurations B through E′, high pressures correspond to burns in the upper containment. In nearly all cases, we get upper containment burns, and hence the peak pressures are high. For upper containment burns, the peak pressure depends on the assumed volume of the upper compartment, the assumed hydrogen mole fraction required for ignition, and the amount of heat tranferred from the gas during the burn.

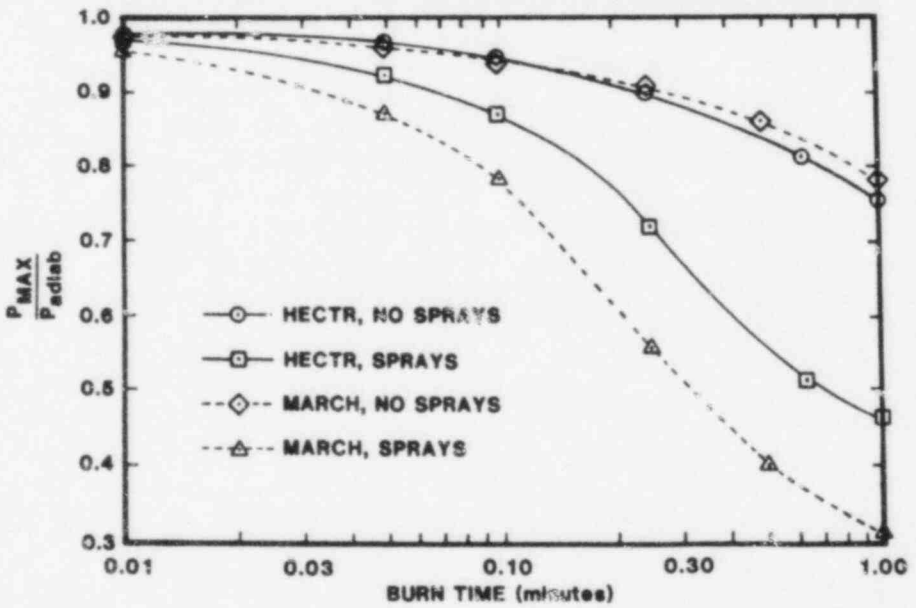

Figure 3.1 Effect of Hydrogen Combustion Burn Time on the Predicted Single Compartment Peak Pressure by HECTR and MARCH Codes

3.2 Introduction

The MARCH computer code is a simple, widely used computer program for modelling a wide variety of nuclear reactor accident scenarios.[3.2] Because computer run time is short, studies involving many runs are feasible and inexpensive. Reservations have been expressed by some MARCH users about the accuracy of the results. A recent study showed that MARCH contains numerous limitations and some errors.[3.3] Nevertheless, MARCH continues to play an important role in reactor accident analysis. Both CLASIX-3 and HECTR use the output of a comparable MARCH run to determine the conditions in the reactor coolant system, and in particular the hydrogen and steam generation rates. Both codes replace the MARCH

containment-response subroutines with better ones. In this section we give a brief introduction to the features of the MARCH program. A more detailed discussion can be found in Appendix C.

All three computer codes (MARCH, HECTR, and CLASIX-3) treat the wetwell/containment volume as if it were composed of one or more discrete compartments. In each compartment the gases are assumed to be uniformly mixed. The compartments are connected by user-specified, one-way, zero-flow-resistance connections. Usually, one interconnects compartments with two such connections, one for flow in each direction. In MARCH, flows between interconnected compartments are created so that the pressure in each compartment is equalized. If the required flows transport too great an energy, more than one time step may be required to equalize pressure between compartments. This happens briefly only at times such as hydrogen burns. MARCH cannot simulate connections with finite flow resistance, nor can it analyze parallel flow paths through the various compartments.

For the cases considered in sections 3.3 to 3.7, MARCH was run with a connection from the drywell to the wetwell, but with no connection back to the drywell. These cases were run with steam and hydrogen from the reactor coolant system directly injected into the suppression pool and hence out to the wetwell/containment. (This simulates a TPE accident, a transient followed by a stuck-open relief valve and failure of emergency core cooling.) With these assumptions, the temperature, pressure, and gas compositions of the drywell stayed fixed. In particular, no hydrogen entered the drywell. The drywell was effectively isolated, and we have ignored it in sections 3.3 to 3.7. The drywell was isolated so that MARCH calculations could be compared to HECTR calculations, HECTR having no drywell compartment at this time. For comparison, cases were considered in section 3.8 with a connection to the drywell from the wetwell or from higher up in the containment to simulate flow from the vacuum breakers. With flow possible to and from the drywell, MARCH tends to equalize pressures between the drywell and the rest of containment. Hydrogen can enter the drywell, so that drywell burns are possible. Accidents involving a break in the reactor coolant system inside the drywell, a small (intermediate) break LOCA similar to an S_2 (S_1) accident, can be so modelled (instead of modelling the reactor steam and hydrogen as entering directly into the suppression pool and the original air in the drywell as being pushed out into the wetwell; this approach was used for HECTR cases B-1, A-5, and A-9).

A major problem in comparing MARCH calculations to HECTR calculations is that HECTR uses a more sophisticated criterion for flame propagation from compartment to compartment. In MARCH, HECTR, or CLASIX-3 one can require each compartment to meet the conditions for ignition in order to have combustion. Additionally, in HECTR and CLASIX-3, one can also allow a flame to propagate from one compartment to an adjacent one if the hydrogen mole fraction in the second compartment is above some specified propagation limit, a number usually lower than the ignition limit. In MARCH, however, one can only use an option in which the flame propagates from one compartment to an adjacent compartment if the hydrogen mole fraction in the second compartment is above a user-specified minimum value for combustion to exist. If one specifies complete combustion (i.e., a zero burnout value) in any compartment which has initiation of a flame, then MARCH will propagate a flame into all connected compartments containing any hydrogen and completely consume all the hydrogen if there is sufficient oxygen present. It will do this in compartments containing very small fractions of hydrogen, below the flammability limit. The MARCH option is much less flexible than those available in HECTR or CLASIX-3.

MARCH contains provision for heat transfer (including condensation) from the containment gases to passive heat sinks, walls, gratings, etc. It also models containment sprays, with cooling of the containment gases resulting from water drop vaporization. From the rapid temperature drops in our multicompartment models, it is clear that MARCH simulates water spray cooling in all compartments, but it is not clear how it distributes the sprays between compartments. This point is discussed in more detail in Appendix C. MARCH does not consider radiative heat transfer in the containment, an important omission, since radiation heat transfer from hot steam is the main heat transfer mechanism after a hydrogen burn if containment sprays are not operable.

Both HECTR and CLASIX-3 calculations were performed with approximately the same hydrogen release rate input, HECTR using an approximation of the CLASIX-3 rates. Our MARCH calculations were carried out using a different model for the reactor core. Because of the interaction of the reactor coolant system and the containment response in MARCH, the same model for the reactor core produced slightly different hydrogen release rates for the various cases considered by MARCH. However, these differences were negligible compared to the differences between the hydrogen release rates predicted by MARCH and

those used in HECTR and CLASIX-3. We produced about 4000 lb (1800 kg) of hydrogen by the end of the accident as compared to 2605 lb (1185 kg) used in the CLASIX-3 study (Figure 3.2). The combustion of about 3312 lb (1505 kg) of hydrogen is required to burn up all the oxygen in containment, including the drywell. The amount of hydrogen that must be burned to just inert containment by oxygen depletion will be lower: about 2484 lb (1130 kg) for the containment including drywell and 2160 lb (982 kg) for the containment excluding drywell.

MARCH normally uses a value of 0.065 oxygen mole fraction as the inerting limit. We have altered the MARCH code to change this to 0.050, in agreement with HECTR and CLASIX-3. In section 3.4 we present some results using the 0.065 limit and compare them to those using the 0.050 limit. We have also introduced into the MARCH code the possibility of steam inerting. Our MARCH code version will inert compartments if the steam mole fraction goes above 0.56, in agreement with HECTR. This did not occur in our calculations, except in the drywell for periods after a break into the drywell compartment from the reactor coolant system.

Section 3.3 discusses results obtained using the configuration A compartment model; section 3.4 discusses results obtained using the configuration B compartment model, etc. Diagrams of the various configurations can be found in section 2.2.1, Figures 2.2, 2-3, and 2.4. Briefly, configuration A consists of a single compartment of the wetwell/containment. Configuration B, the one used for most of the CLASIX-3 studies, consists of a small wetwell and a large upper containment, the division being at the 135 ft elevation. Configuration C also divides the wetwell/containment into two compartments, but puts the division at the top of the annular region (the 209 ft elevation). Configuration D divides the volume into three compartments: a small wetwell, the intermediate annular region, and the upper containment above the 209 ft elevation. Configuration E′ differs somewhat from configuration E used in the HECTR calculations. It divides the volume into four compartments: a wetwell, a lower annular region, an upper annular region, and the upper containment (the divisions occurring at elevations of 135, 165, and 209 ft).

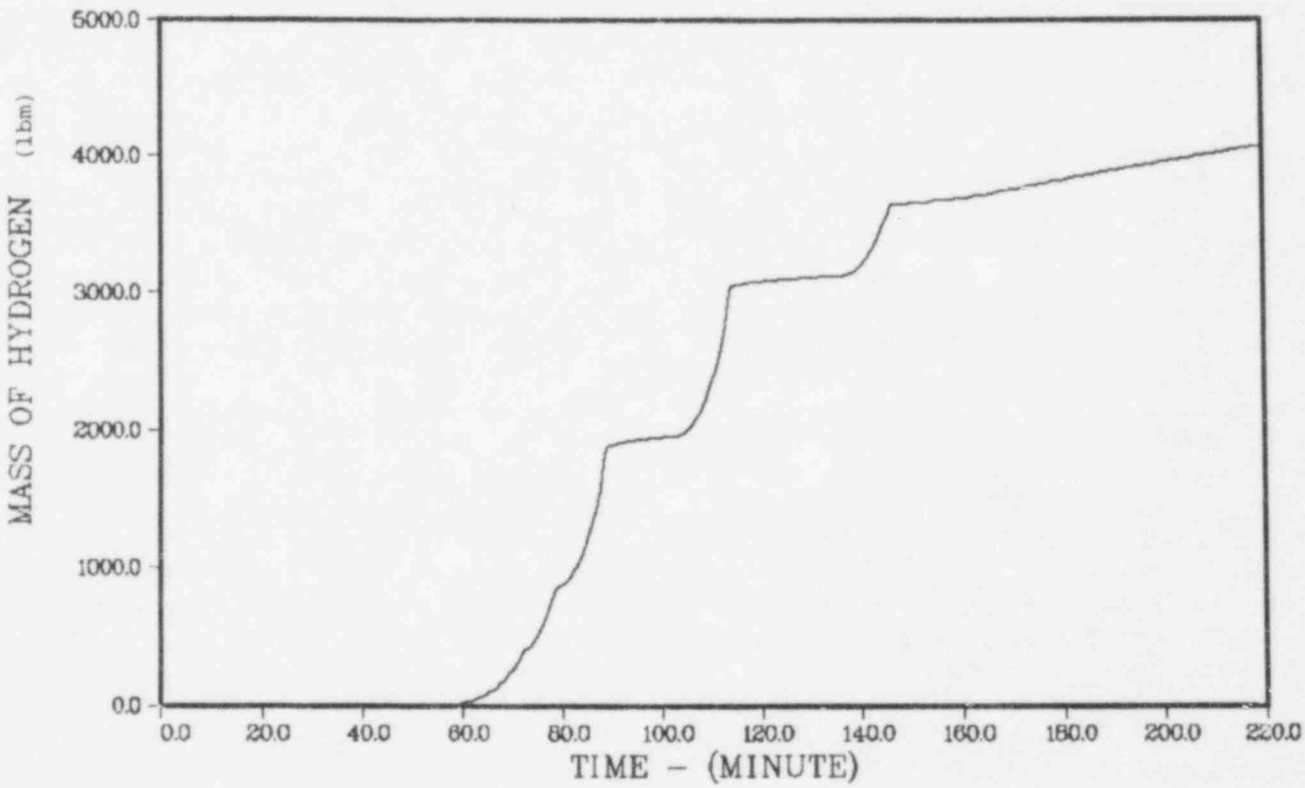

Figure 3.2. Hydrogen Release Into Containment, lb, for Case A-1 Without Burns. Approximately true for all MARCH cases

Three containment spray options are considered in the cases to follow:

- No sprays
- All sprays on very early in the accident and remain on
- "Auto," all sprays on after the first hydrogen burn and remain on

Apparently, the automatic option is the one planned for use at Grand Gulf.

The time to burn up hydrogen in a compartment is based on the expected flame speed and the compartment size. Some MARCH calculations were carried out using a burn time corresponding to the flame speed considered in the CLASIX-3 study, 6 ft/s. Most of the MARCH calculations were carried out using burn times corresponding to higher flame speeds, in agreement with some experimental work on hydrogen combustion at SNL.[3.1] In agreement with HECTR and CLASIX-3, we have used values from 0.08 to 0.10 for the hydrogen mole fraction required for ignition. The lower limit of hydrogen mole fraction for hydrogen burns (the extinguishment limit) has been set at either 15% of the ignition limit or zero. In each of the following sections a table is presented with the case descriptions and results.

3.3 Analysis of MARCH Calculations for Configuration A

In configuration A, the containment is divided into two compartments: the drywell, and a wetwell consisting of all the free volume between the suppression pool and the top of the containment dome. As stated in section 3.2, the drywell is isolated in the model used in this section and hence ignored. The effect of the drywell will be considered in section 3.8. Since here we consider only one compartment, all hydrogen burns are global burns. The use of configuration A causes MARCH to instantly mix any hydrogen or steam entering the wetwell uniformly throughout the volume. Configuration A then represents the limiting case of very rapid mixing. If the time for mixing is shorter than the time between burns and shorter than the characteristic time for release of hydrogen to the wetwell, the atmosphere will tend to be nearly homogeneous, and configuration A will tend to more accurately model the situation than the more complex multicompartment models. There is some evidence that mixing due to natural convection can be relatively rapid (order of minutes), and this mixing would be increased if sprays were activated and other forced convection were present. This is discussed in Chapter 4.0.

The case descriptions and summary of results for the configuration A computer runs can be found in Table 3.1. The graphical results for case A-1 can be found in Figures 3.3 through 3.7. For the other configuration A runs, only graphs of pressure vs time are given (Figures 3.8 through 3.15). The cases correspond as closely as possible to the corresponding ones used in Chapter 2.0

In case A-1 there were no containment sprays. The burn time corresponded to the flame speed used in the CLASIX-3 analysis, 6 ft/s. The ignition limit used was 0.08 hydrogen mole fraction. The extinction limit for combustion was 0.012, corresponding to an 85% burn completion. Figure 3.5 seems to indicate a minimum hydrogen mole fraction higher than 0.012. This is probably due to the introduction of hydrogen during the burn, which is not consumed. The amount of hydrogen generated is shown in Figure 3.2 and in Appendix C. MARCH predicted three burns. The highest pressure was 60 psia (4.1 atm). This value is high, but below the estimated containment failure pressure of 71 psia (4.8 atm). After the last burn, MARCH predicted the containment was inerted due to oxygen depletion. The oxygen mole fraction varied somewhat as steam condensed, but MARCH predicted it to be about 0.045, below the inerting limit of 0.050. For case A-1, HECTR predicted four burns, a peak pressure of 60 psia (4.1 atm), and a final oxygen mole fraction of 0.040. Both codes agree on the most important result, a peak pressure of 60 psia (4.1 atm).

The data in Figures 3.3 and 3.4 show that the temperature and pressure peaks associated with the burns have almost fully decayed by the time subsequent burns occur. Hence the initial conditions for the subsequent burns are not sensitive to the rate of heat transfer from the previous burns for this case. We investigated the effect of heat transfer, in the form of different burn times, on the peak pressure of a hydrogen burn for configuration A in Appendix C. We found that without sprays activated MARCH and HECTR predicted nearly the same small reduction in peak pressure due to heat transfer for reasonable burn times. This was surprising, since MARCH does not include radiation heat transfer from the hot steam. Evidently, MARCH compensates by having a higher convective heat transfer loss. With sprays activated, the two computer codes give different results, as will be discussed in the following cases that have sprays activated.

Case A-2 differs from case A-1 only in that the burn time is reduced, corresponding to our estimates of faster flame speeds, 8 m/s. The results were as expected (Figure 3.8). MARCH predicted three burns, with a maximum pressure of 65 psia (4.4 atm), slightly higher than the 60 psia (4.1 atm) of case A-1. The reduced burn time reduces the heat transfer during the burn and gives results closer to the adiabatic, isochoric combustion pressure. HECTR also predicted three burns and a peak pressure of 65 psia (4.4 atm). Note that the predicted peak pressure is close to the estimated containment failure pressure of 71 psia (4.8 atm). MARCH predicted that the containment was inerted by oxygen depletion after the third burn, while HECTR predicted the final oxygen mole fraction was 0.07, which is above the inerting limit.

Case A-3 differs from case A-2 only in that sprays are turned on early in the accident (long before the first burn) and stay on. The results shown in Figure 3.9 indicate MARCH predicted four burns. Each of the burns has a lower peak than those of cases A-1 and A-2, and the pressure peak decays much more rapidly due to the cooling of the gases by the containment sprays. The peak pressure was 48 psia (3.3 atm) on the first burn. After the last burn, the containment was inerted by oxygen depletion. HECTR predicted three burns, a peak pressure of 59 psia (4.0 atm), and sufficient oxygen remaining after the last burn for a fourth burn. Case A-3 is the first case discussed with sprays. It shows that both MARCH and HECTR predict reductions in peak pressure due to the presence of sprays, but MARCH predicts a greater reduction. This point is discussed in Appendix C.

Case A-4 differs from case A-3 only in that the sprays are turned on after the first burn. As a result, the pressure peak associated with the first burn, 62 psia (4.2 atm), is far larger than the highest pressure associated with the next two burns, 44 psia (3.0 atm). HECTR also predicted three burns, but with a peak pressure of 57 psia (3.9 atm). The slight increase in peak pressure because of the presence of sprays* before the first burn in HECTR is discussed in section 2.2.3 and Appendix B. For all the cases considered, MARCH predicted a benefit in turning the sprays on before the first burn. Both codes predicted that the containment had oxygen mole fractions near the inerting limit after the last burn, and that hence there was the possibility of one further burn.

Case A-5 models an accident involving a break in the reactor coolant system inside the drywell. This is modelled by assuming the air in the drywell is pushed out into the wetwell, raising the pressure to 17 psia. The adequacy of this assumption is addressed in section 3.8 which discribes the situation where the break flow is allowed to be directed into the drywell and the drywell is interconnected with the wetwell. Aside from the use of the higher initial pressure, the input for case A-5 is identical to case A-4. MARCH predicted four burns. The peak pressure of 76 psia (5.2 atm) occurred during the first burn, before the sprays were turned on. This is above the estimated containment failure pressure. The containment was predicted to be nearly depleted of oxygen after the last burn. HECTR predicted only three burns, but with sufficient oxygen remaining to have a fourth. The peak pressure predicted by HECTR was 66 psia (4.5 atm), with nearly equal values for the first and second burns. Again notice that MARCH predicts greater peak pressure reduction when sprays are activated than does HECTR.

Cases A-1 through A-5 used an ignition criterion of hydrogen mole fraction equal to 0.08. Cases A-6 to A-9 used a more conservative criterion of 0.10. For comparable situations one expects this to give higher peak pressures, and this was so.

Case A-6 can be compared to case A-2 since neither has sprays in operation. For case A-6, MARCH predicted only two burns, but with the oxygen mole fraction after the second burn just below the inerting limit; HECTR predicted three burns and very little oxygen left after the last burn. The peak pressure predicted by MARCH was 80 psia (5.4 atm), and that predicted by HECTR was 78 psia (5.3 atm). Both values are higher than the estimated containment failure pressure. A homogeneous 10% hydrogen burn without spray may fail containment.

In case A-7 (as in case A-3) sprays are in operation early in the accident. Both MARCH and HECTR predicted four burns with subsequent inerting by oxygen depletion. The two codes differ in that MARCH predicted a peak pressure of 56 psia (3.8 atm) and HECTR predicted 70 psia (4.8 atm). Again, MARCH predicts a greater reduction in peak pressure due to spray cooling of the containment gases than does HECTR. Both programs indicate an increase of about 10 psia (0.7 atm) in peak pressure over case A-3.

In case A-8 (as in case A-4) the sprays come on after the first burn. As expected, the peak pressure caused by the first burn is the highest. MARCH

*The spray temperature in HECTR is specified to be 135°F while the initial air temperature is specified to be 80°F. This mismatch artificially causes the preburn air pressure to be higher when sprays are initiated early. MARCH considers the energy additions to the containment sprays and hence has a change in spray temperature.

predicted three burns for case A-8 and a peak pressure of 74 psia (5.0 atm). HECTR predicted three burns and a peak pressure of 68 psia (4.6 atm). Both codes predicted inerting due to oxygen depletion after the third burn. These pressures are near the containment failure pressure. Again, the results of cases A-6, A-7, and A-8 indicate the value of turning on the sprays early in the accident.

Case A-9, like case A-5, starts with a pressure of 17 psia (1.16 atm) in the containment, and sprays are turned on after the first burn. For case A-9 MARCH predicted three burns followed by oxygen depletion, while HECTR predicted two burns, with sufficient oxygen for a third. The peak pressure predicted by MARCH was 78 psia (5.3 atm) for the first burn, and 78 psia (5.3 atm) was also predicted by HECTR.

Table 3.1. Configuration A – Case Descriptions and Results

Case No.	Initial Pressure psia	Hydrogen Mole Fraction For Ignition	Hydrogen Mole Fraction For Extinguishment	Containment Sprays	Burn Time Seconds	No. of Burns	Peak Pressure Psia (atm)
A-1	14.7	0.08	0.012	Off	38	3	60 (4.1)
A-2	14.7	0.08	0.00	Off	8	3	65 (4.4)
A-3	14.7	0.08	0.00	On	8	4	48 (3.3)
A-4	14.7	0.08	0.00	Auto	8	3	62 (4.2)
A-5	17.0	0.08	0.00	Auto	8	4	76 (5.2)
A-6	14.7	0.10	0.00	Off	8	2	80 (5.4)
A-7	14.7	0.10	0.00	On	8	3	56 (3.8)
A-8	14.7	0.10	0.00	Auto	8	3	74 (5.0)
A-9	17.0	0.10	0.00	Auto	8	3	78 (5.3)

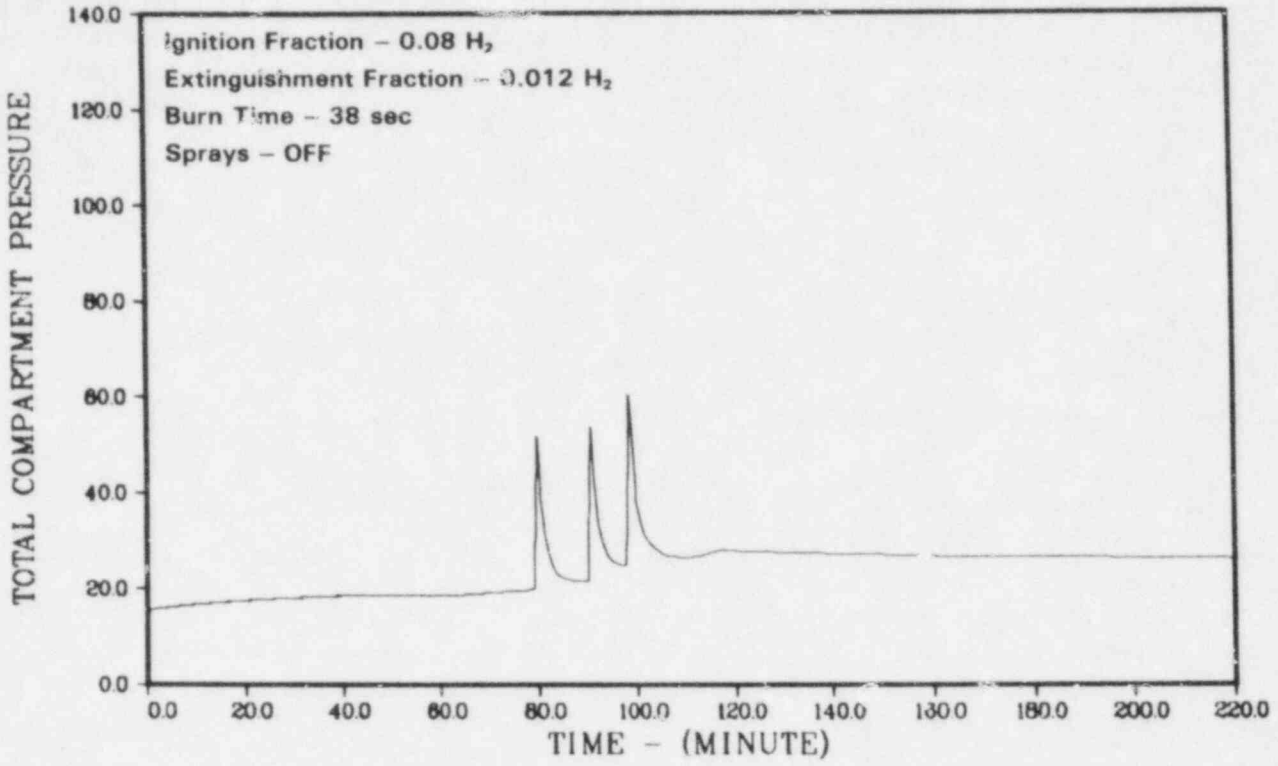

Figure 3.3. Case A-1, Pressure in Containment, psia

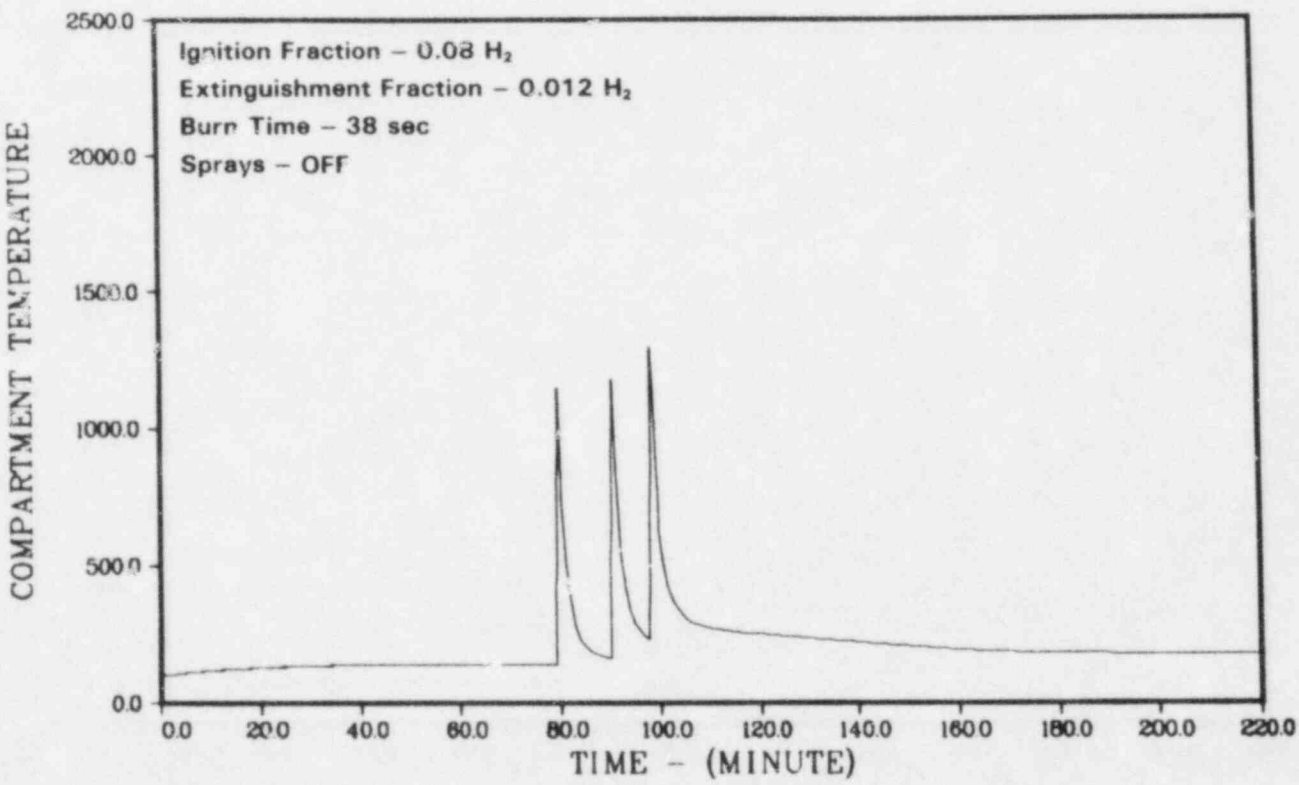

Figure 3.4. Case A-1, Temperature in Containment, °F

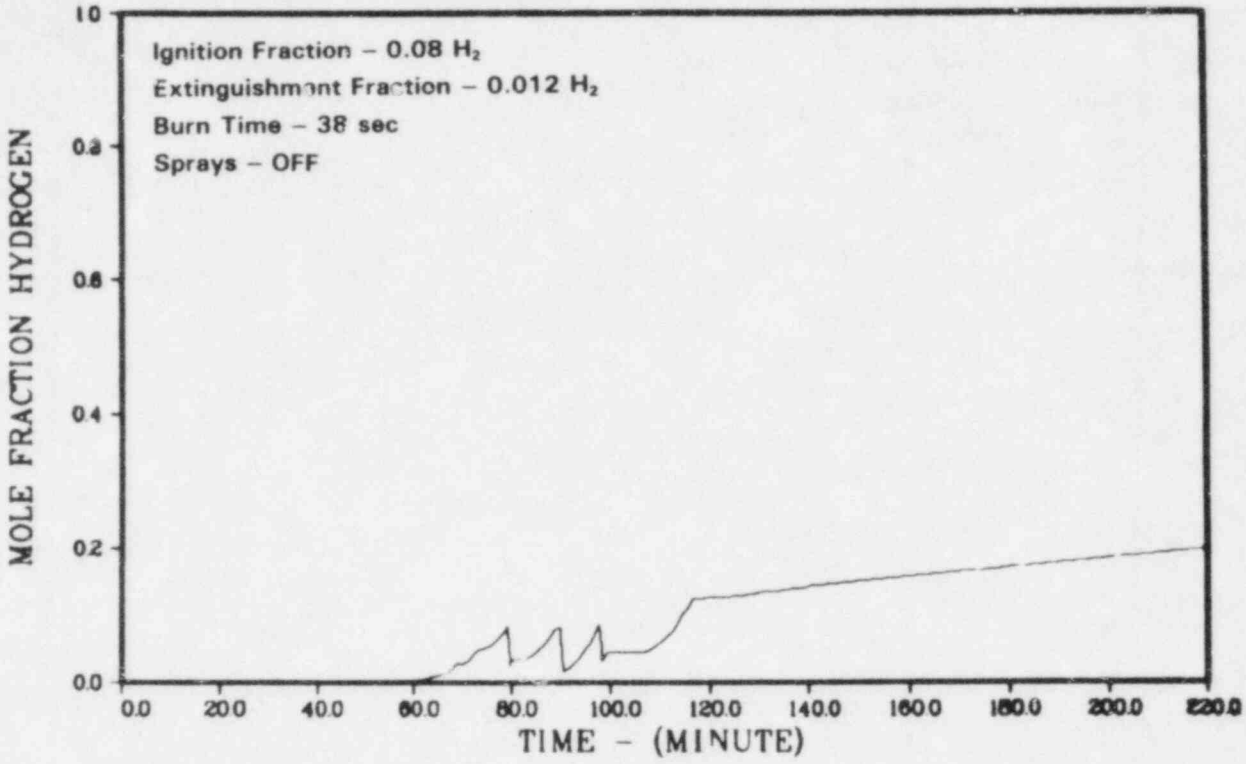

Figure 3.5. Case A-1, Hydrogen Mole Fraction in Containment

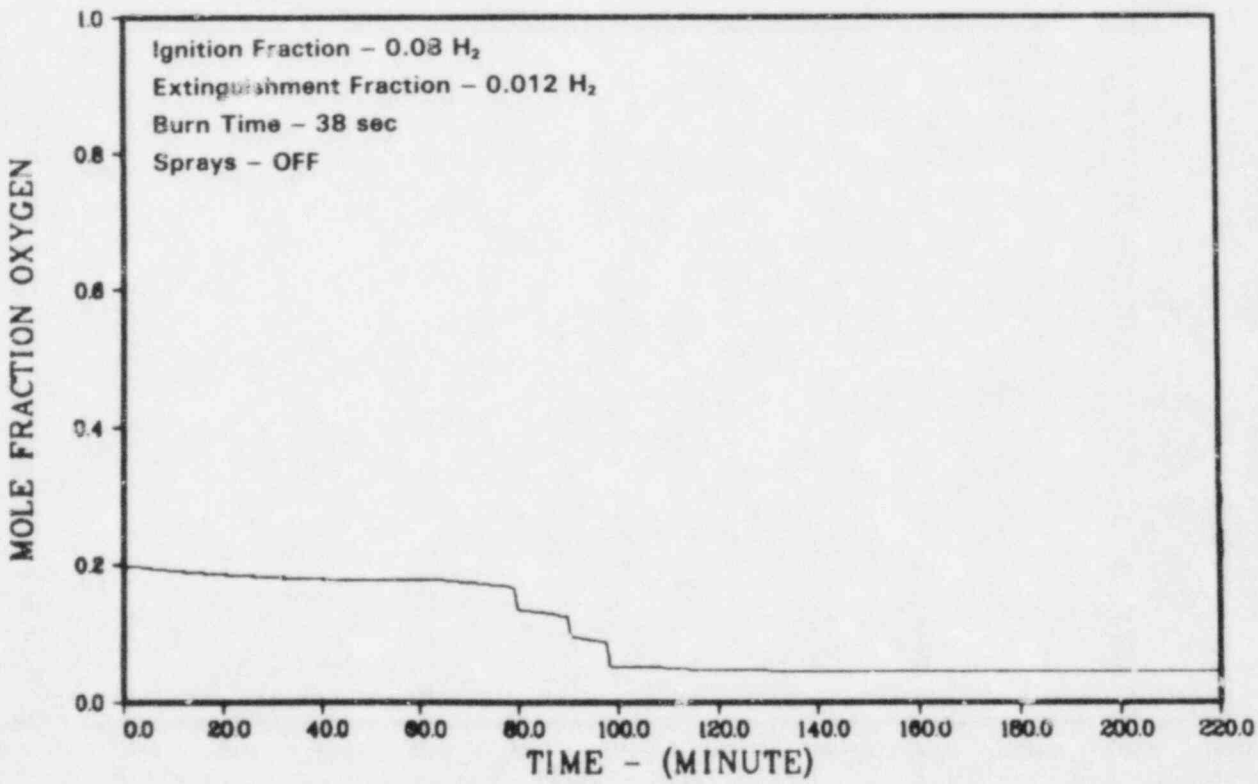

Figure 3.6. Case A-1, Oxygen Mole Fraction in Containment

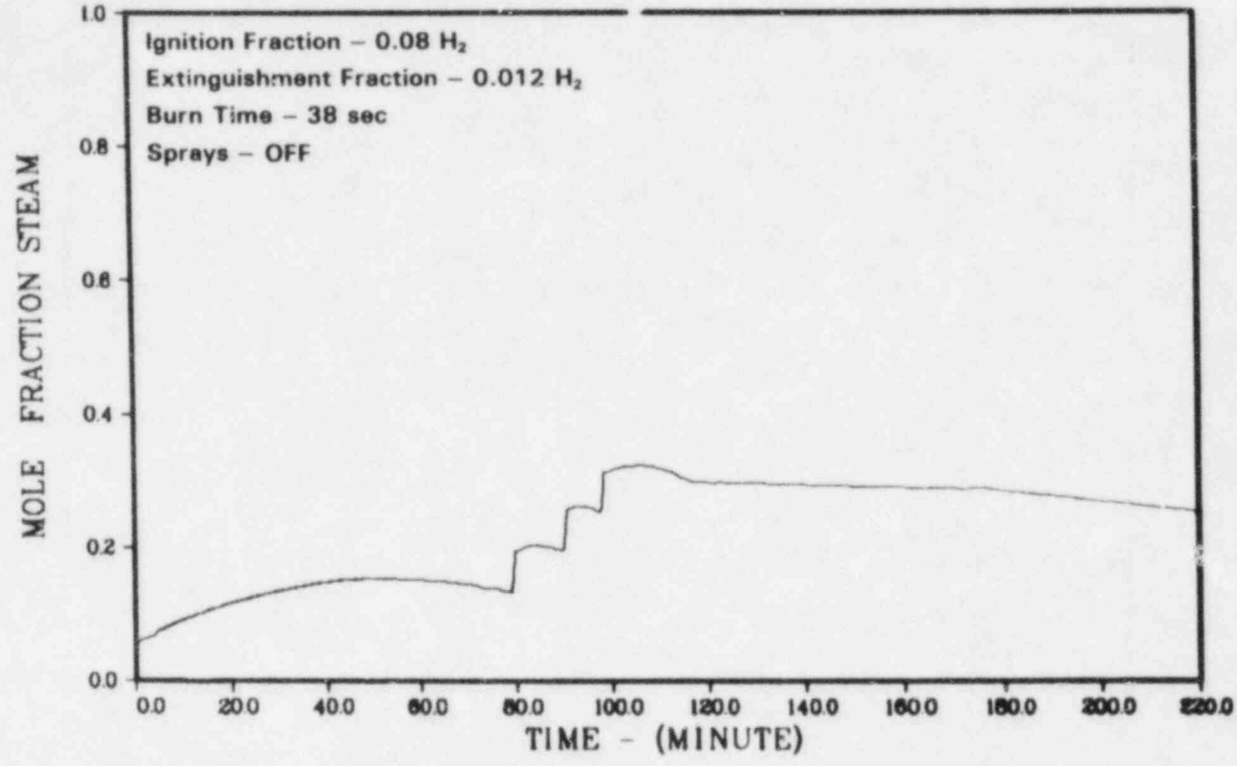

Figure 3.7. Case A-1, Steam Mole Fraction in Containment

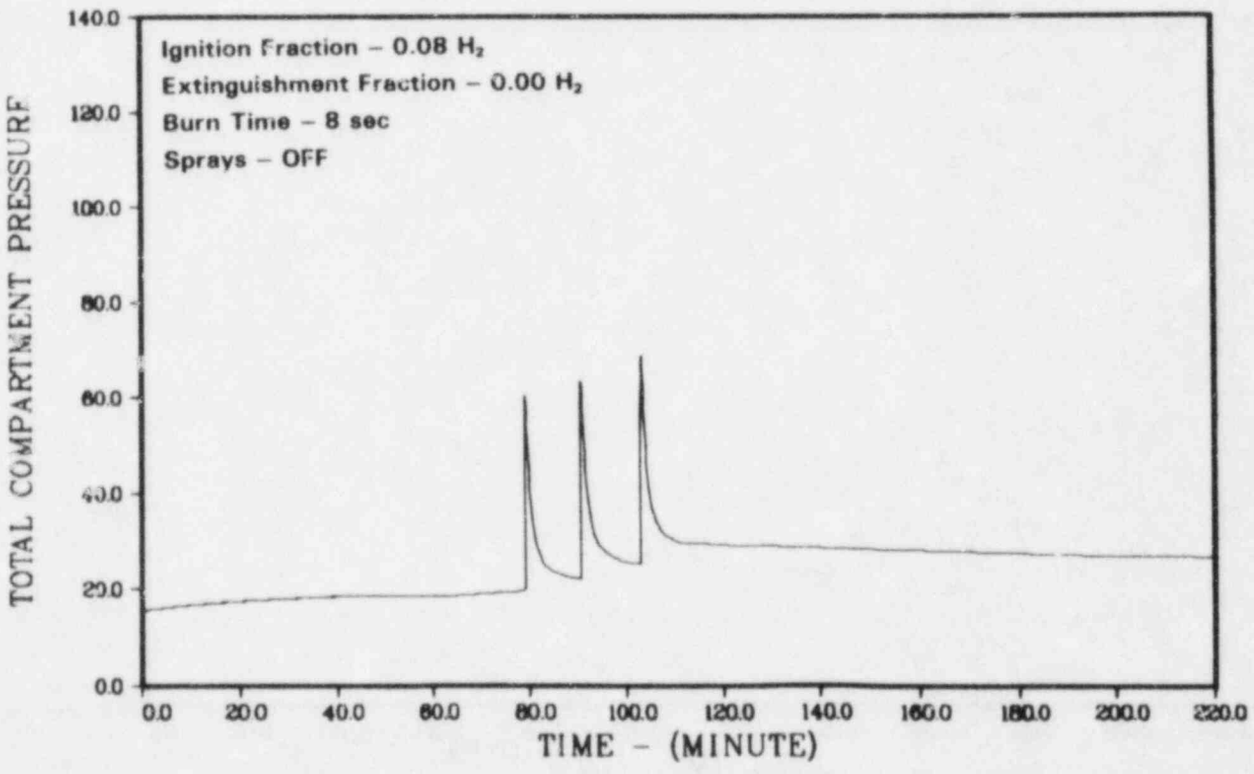

Figure 3.8. Case A-2, Pressure in Containment, psia

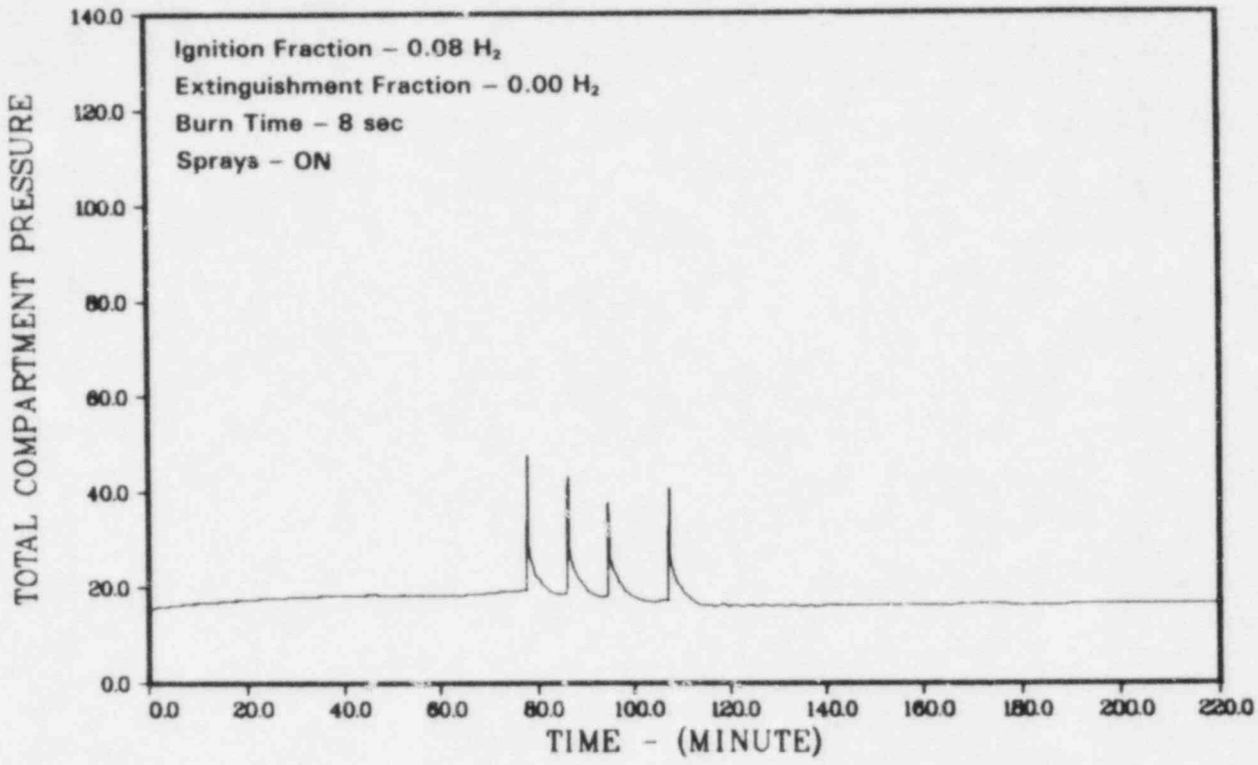

Figure 3.9. Case A-3, Pressure in Containment, psia

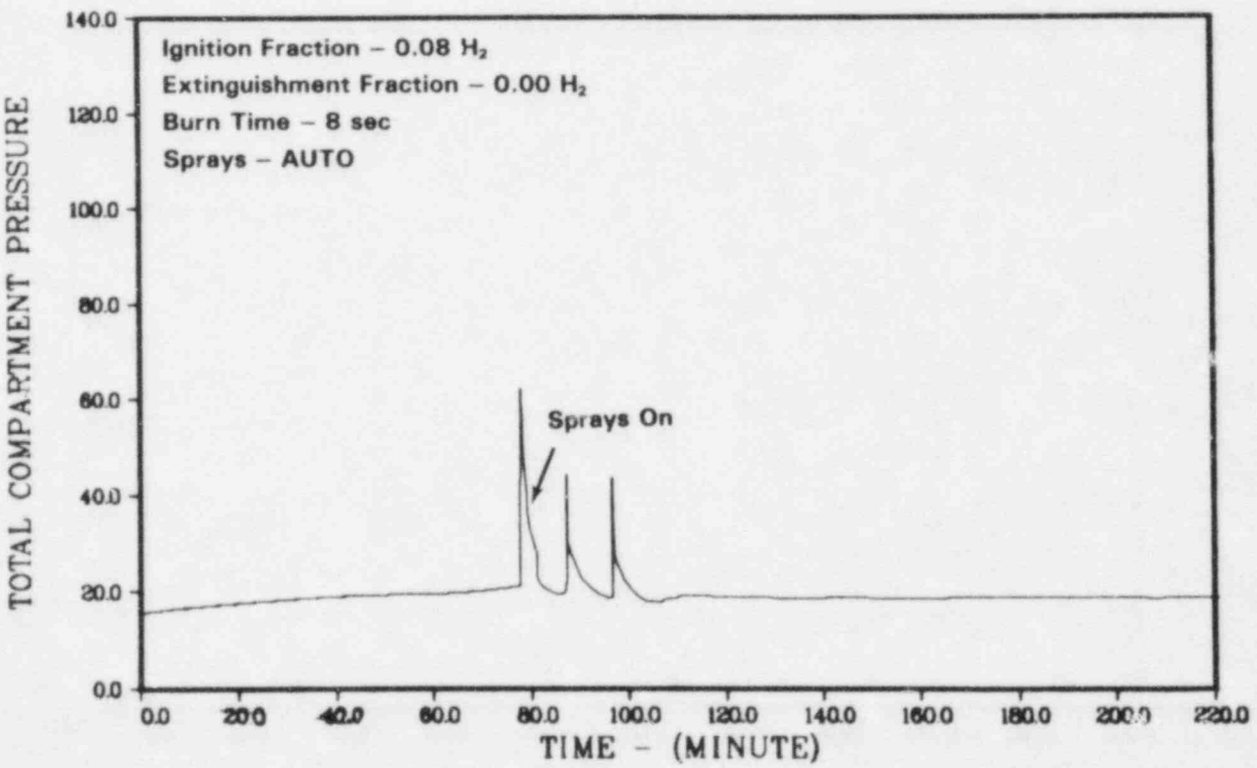

Figure 3.10. Case A-4, Pressure in Containment, psia

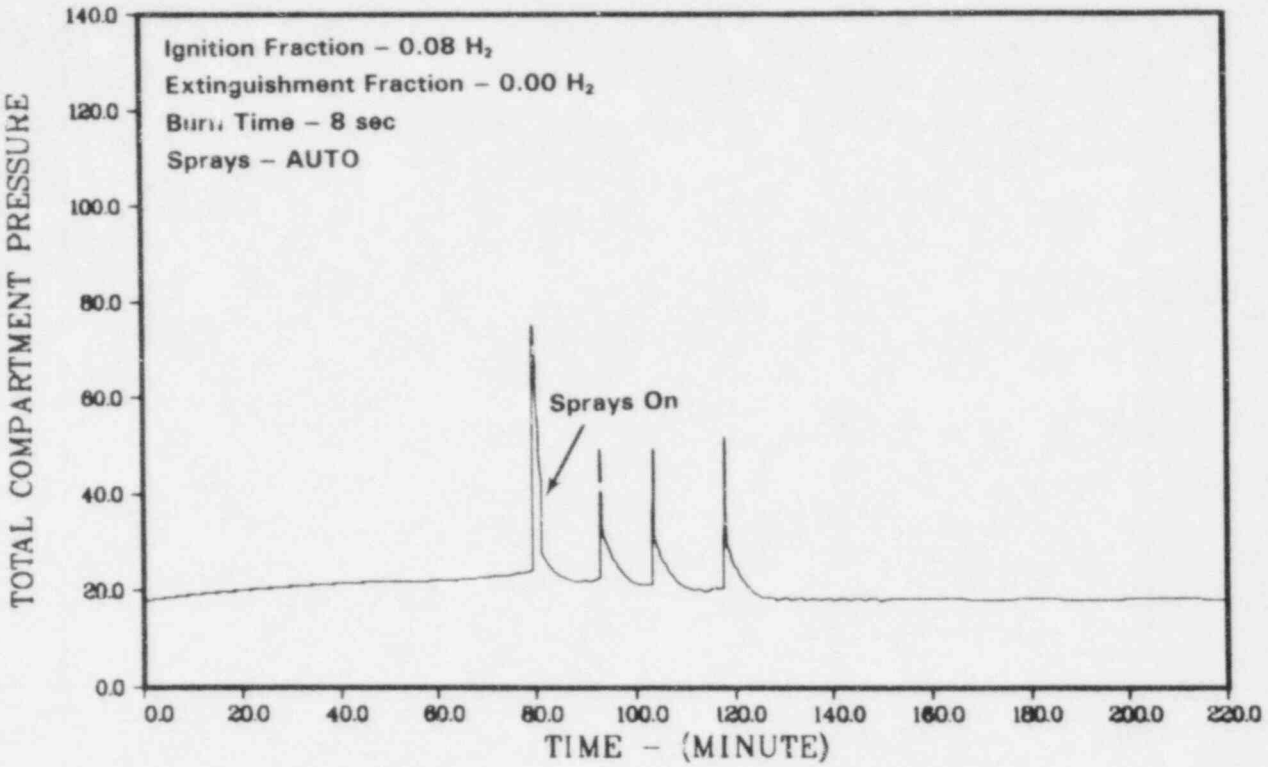

Figure 3.11. Case A-5, Pressure in Containment, psia

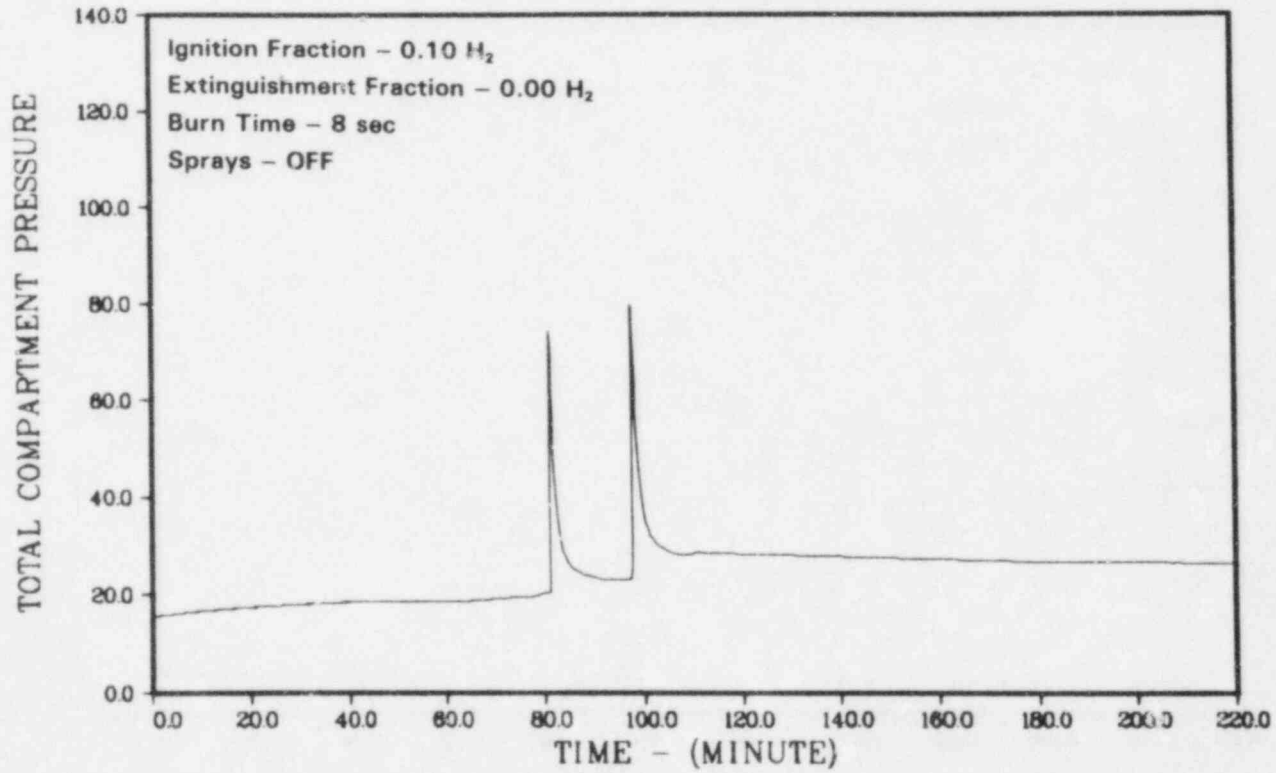

Figure 3.12. Case A-6, Pressure in Containment, psia

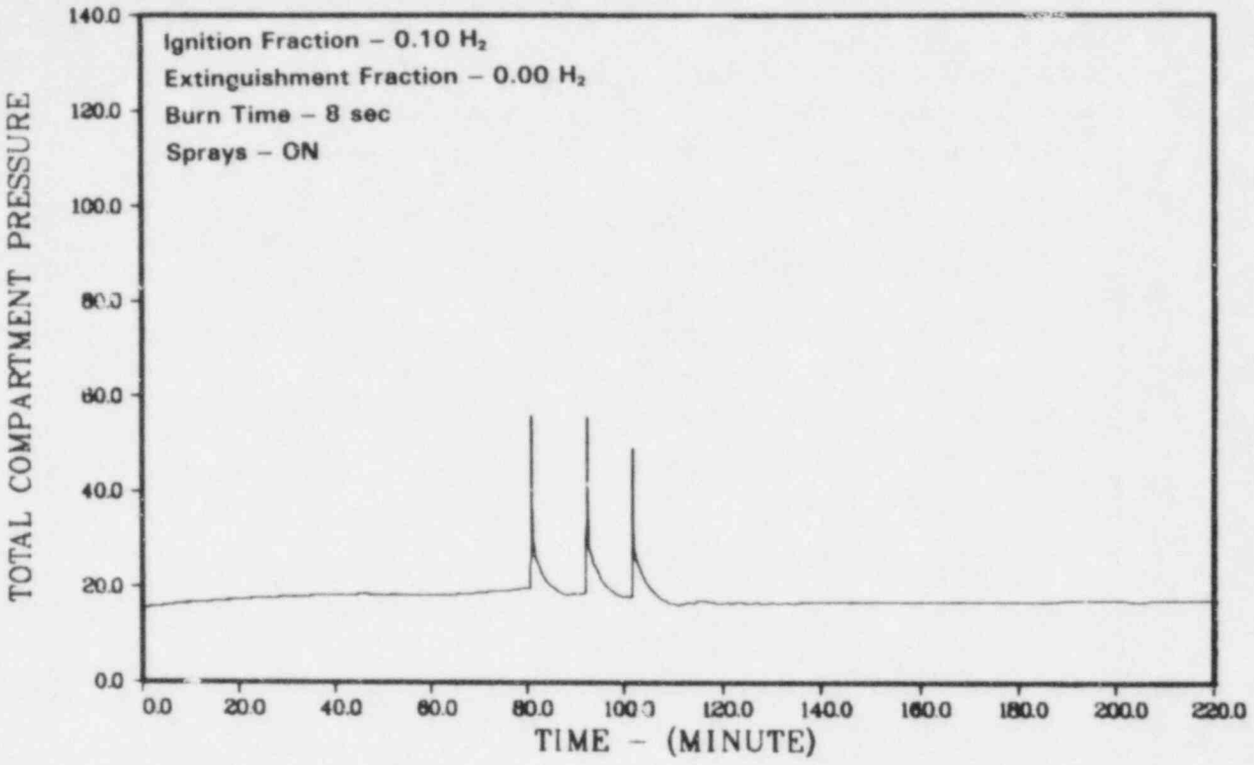

Figure 3.13. Case A-7, Pressure in Containment, psia

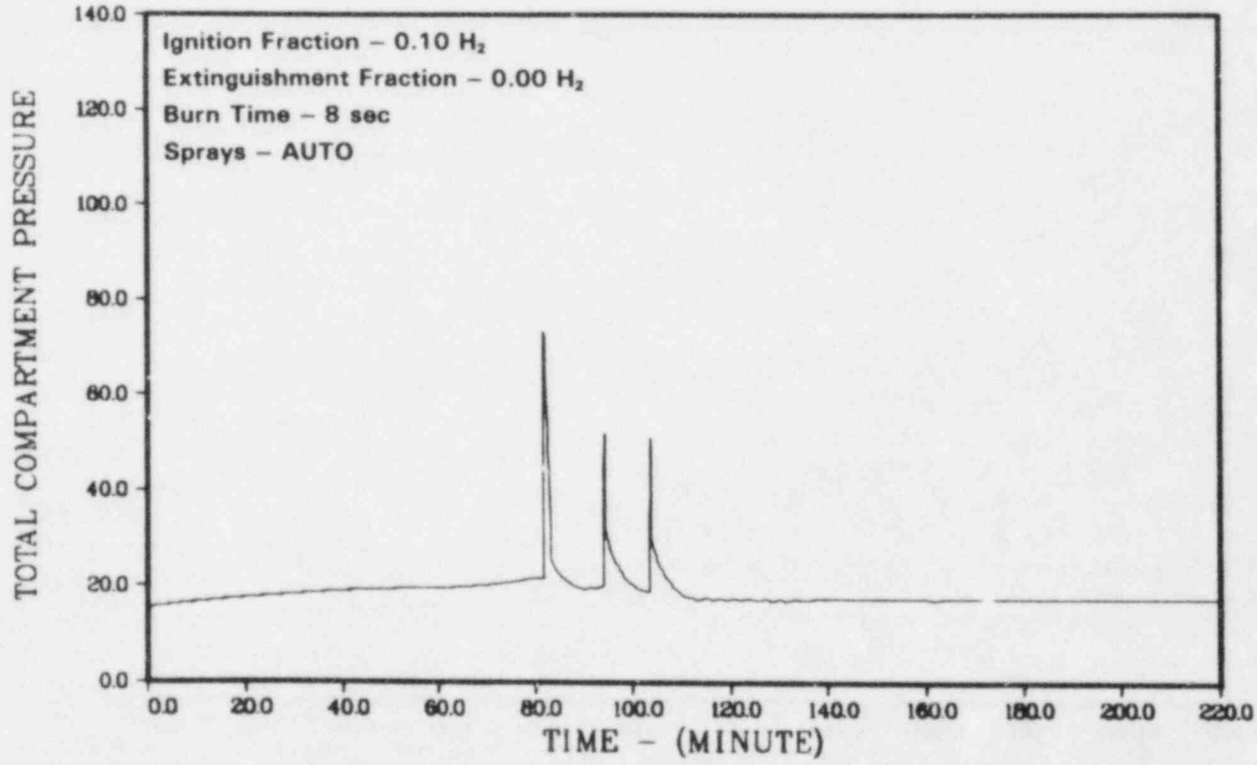

Figure 3.14. Case A-8, Pressure in Containment, psia

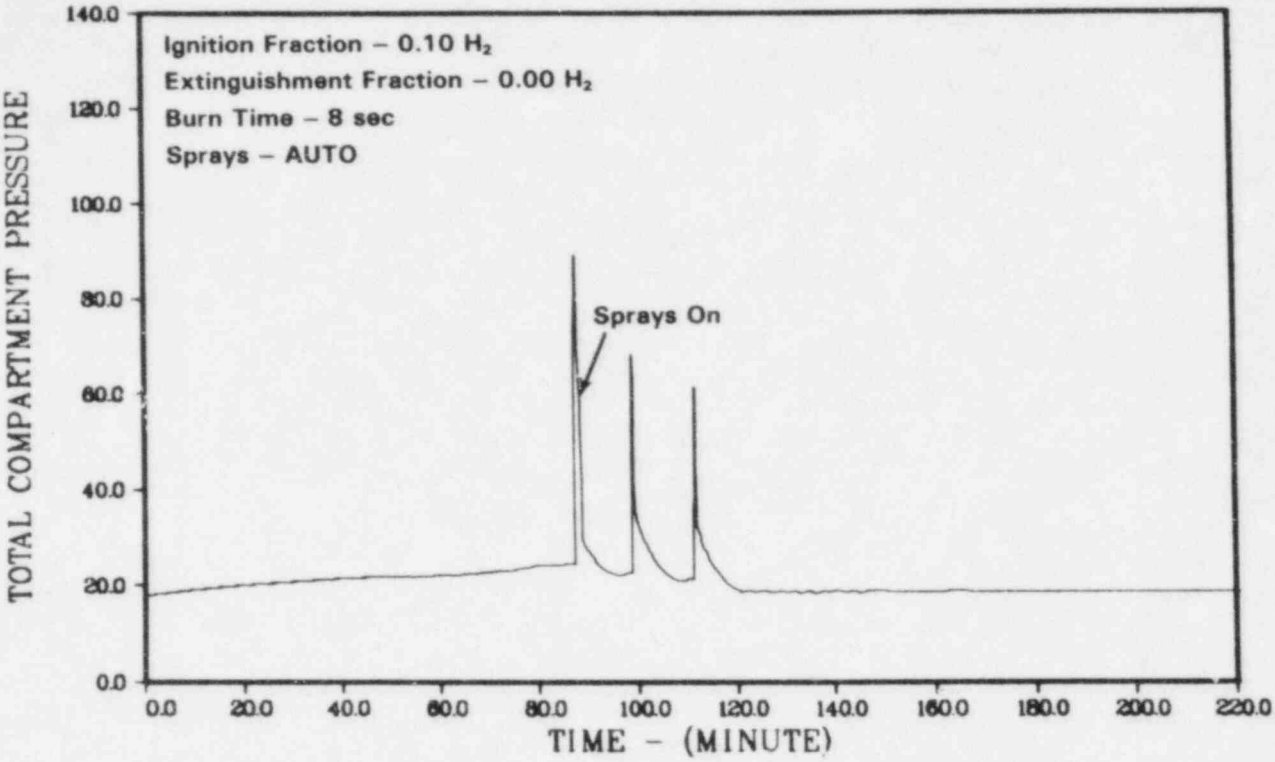

Figure 3.15. Case A-9, Pressure in Containment, psia

3.4 Analysis of MARCH Calculations for Configuration B

In configuration B, the containment is divided into three volumes: the drywell, a small wetwell (the volume between the suppression pool and the 135 ft elevation), and a very large upper containment volume. This configuration is the same as that used in the majority of the CLASIX-3 calculations. As discussed in Appendix C, this appears to be the first time MARCH has been used in BWR calculations with models having more than two compartments. Uncertainties exist on how MARCH treats certain phenomena in such multicompartment BWR models, particularly the containment sprays. As mentioned previously, for these MARCH calculations there is no connection from the wetwell or upper containment to the drywell; hence the drywell is isolated. We will consider only the behavior of the wetwell and the upper containment volume. The effect of the drywell is considered in section 3.8.

Wetwell burns involve the combustion of such small masses of hydrogen that the resultant total pressure rise in containment is small. Combustion in the upper containment, because of the large volume involved, is nearly a global burn. Consequently, only upper containment burns can cause pressure peaks large enough to fail containment from simple deflagrations. Because of inerting of the wetwell due to oxygen depletion, very high mole fractions of hydrogen can accumulate in the wetwell. The potential for local detonations exists if this hydrogen mixes with sufficient oxygen. Detonations are discussed in Chapter 5.0.

The typical sequence of events for configuration B predicted by MARCH is as follows:

1. Numerous wetwell burns
2. Inerting of the wetwell by oxygen depletion
3. Buildup of the hydrogen mole fraction to high values in the wetwell and to combustible amounts in the upper containment
4. Burns in the upper containment, wetwell, or both
5. Wetwell is again inerted by oxygen depletion; the upper containment is either oxygen depleted or has insufficient hydrogen for ignition

For all the cases considered using configuration B, MARCH and HECTR predicted one or more upper containment burns, and hence significant pressure peaks. For several of the comparable cases, CLASIX-3 did not predict any upper containment burns, and hence it predicted only small pressure peaks. The number of wetwell burns, the occurrence and duration

of wetwell inerting, and the number of upper containment burns differ somewhat among MARCH, HECTR, and CLASIX-3. Part of the reason for the differences is that the configuration B model is "ill-conditioned;" i.e., small changes in the input values or differences in the assumptions used in the codes can give rise to considerably different results.

Our configuration B runs were initially carried out using the normal MARCH value of 0.065 oxygen mole fraction for inerting. This was later altered to 0.050 to agree with HECTR and CLASIX-3. In the following discussion of configuration B cases we will first describe results obtained using the 0.050 value. We will then compare those results to the ones obtained using the 0.065 value. The results are often quite different, giving additional confirmation of our statement that the configuration B model is ill-conditioned.

The case descriptions and a partial summary of the results of the MARCH configuration B calculations (for both the 0.050 and 0.065 oxygen inerting limits) are given in Table 3.2. The results of case B-1 are shown in Figures 3.16 through 3.24 using the 0.050 limit. The pressure history for case B-1 with the 0.065 oxygen inerting limit is shown in Figure 3.25. Pressure histories for cases B-2 to B-7 with the 0.050 limit are shown in Figures 3.26 through 3.31.

Case B-1 modelled one of the cases considered in the CLASIX-3 analysis. The break into the drywell and expulsion of air into the wetwell was simulated by using a wetwell/containment pressure of 17 psia (1.16 atm). Sprays came on after the first burn. Combustion occurred only in compartments that met the ignition criterion, hydrogen mole fraction equal to 0.10. The results are shown in Figures 3.16 through 3.24. Figure 3.25 shows the pressure for case B-1 with the 0.065 oxygen inerting criteria.

For case B-1, with the 0.05 oxygen inerting criterion MARCH predicted 15 wetwell burns, a period of wetwell inerting due to oxygen depletion, another wetwell burn, a further period of wetwell inerting, and then a burn in both the upper containment and wetwell. The peak pressure due to the last burn was 65 psia (4.4 atm). After the last burn, the containment was inert due to oxygen depletion, the mole fraction of oxygen being 0.045 in the upper containment and 0.043 in the wetwell.

By comparison, when the oxygen inerting limit of 0.065 was used for case B-1, MARCH predicted nine wetwell burns, a period of wetwell inerting, and then an upper containment burn followed in seconds by a final wetwell burn. The peak pressure was 70 psia (4.8 atm). After the last burn the containment was inert due to oxygen depletion, but the oxygen mole fraction was above 0.05.

Figures 3.17 and 3.20 show simultaneous spikes of temperature and steam in the wetwell late in the accident. These spikes are not hydrogen burns. We have investigated the possibility that they are due to the release of either hot hydrogen or steam from the reactor coolant system. We have not been able to explain them. R. O. Wooton of Battelle Columbus Laboratory implied that MARCH may be having computational difficulties at this point since the reactor coolant pressure is close to the containment pressure.

HECTR predicted 22 wetwell burns and, late in the accident, 1 large upper containment burn with a peak pressure of 82 psia (5.6 atm). CLASIX-3 predicted no upper containment burns, and hence a low peak pressure. In later work with CLASIX-3, an upper containment burn was "forced" when the mole fraction of hydrogen ended up just below the ignition limit. Of course these results are closer to those of MARCH than the earlier CLASIX-3 results. Case B-1 is typical of all the B configuration cases. MARCH and HECTR predict upper containment burns and high peak pressures, while CLASIX-3 generally does not predict upper containment burns. The peak pressure predicted for case B-1 is close to or above the predicted failure pressure for the containment, 71 psia (4.8 atm).

Case B-2 is similar to case B-1 except the initial pressure was 14.7 psia (1.0 atm). The pressure history predicted by MARCH is shown in Figure 3.26. MARCH predicted 13 wetwell burns, a period of wetwell inerting, two more wetwell burns, an upper containment burn and a final wetwell burn, for a total of 16 wetwell burns and 1 upper containment burn. The peak pressure was 52 psia (3.5 atm). After the last burn the oxygen mole fractions in the upper containment and wetwell were just below the inerting limit of 0.050. When case B-2 was run using the oxygen inerting limit of 0.065, MARCH predicted seven wetwell burns, a period of wetwell inerting, an upper containment burn, a wetwell burn, and a final upper containment burn. The peak pressure was 63 psia (4.3 atm). For case B-2, HECTR predicted 23 wetwell burns, a period of wetwell inerting, and a final burn starting in the upper containment and propagating to the wetwell. The peak pressure predicted was 71 psia (4.8 atm). HECTR and the two MARCH runs for case B-2 show that the number of burns in the wetwell is very sensitive to the assumptions made, but all three calculations predict one or two upper compartment burns with peak pressures in the range 52 to 71 psia (3.5 to 4.8 atm). By comparison, CLASIX-3 predicted 43 wetwell burns and no upper containment burns. Consequently, the peak pressure predicted by CLASIX-3 was low, 22.5 psia (1.5 atm).

Case B-3 differs from case B-2 only in that the hydrogen mole fraction was reduced to 0.08 for ignition and was raised to 0.012 for extinguishment. MARCH predicted 14 wetwell burns, a period of wetwell inerting, a rapid sequence of wetwell/upper-containment/wetwell burns, and finally two more upper containment burns. The peak pressure was 42 psia (2.9 atm). After the last burn the containment was oxygen-depleted. The corresponding MARCH run using the 0.065 oxygen inerting limit predicted 11 wetwell burns, a period of oxygen inerting, a wetwell burn, a nearly simultaneous upper containment and wetwell burn, and a final upper containment burn. The peak pressure predicted was 44 psia (3.0 atm). HECTR predicted 31 wetwell burns, a period of wetwell inerting, and an upper containment burn propagating into the wetwell. The peak pressure predicted was 56 psia (3.8 atm). As in case B-2, CLASIX-3 predicted many wetwell burns (58) and no upper containment burns. The pattern is clear. While HECTR generally has at least one upper containment burn, and CLASIX-3 predicts no upper containment burns, MARCH most easily inerts the wetwell and has the most upper containment burns. The fact that the MARCH runs include more hydrogen generated may explain this pattern.

Case B-4 is similar to case B-3 except that there were no sprays and the combustion completeness was assumed to be unity. Without sprays, MARCH predicted 24 wetwell burns in a 20-min time period. The pressure rise for each burn was about 4 psi (0.3 atm) and the pressure did not have time to fall back completely to the initial pressure before the next burn. The peak pressure for the series of wetwell burns was 27 psia (1.8 atm). After the 24 wetwell burns, the wetwell was inert due to oxygen depletion. The hydrogen concentration increased in both the wetwell and upper containment. MARCH then predicted two upper containment burns with a peak pressure of 56 psia (3.8 atm). After the last burn, the containment was inert due to oxygen depletion. When case B-4 was run using the 0.065 oxygen inerting limit, the results were altered. MARCH predicted 14 wetwell burns with a peak pressure of 28 psia (1.9 atm), and 3 upper containment burns with a peak pressure of 65 psia (4.4 atm). After the last burn the oxygen mole fraction in the containment was very low.

For case B-4, HECTR predicted 30 wetwell burns and 1 upper containment burn, with a peak pressure of 68 psia (4.6 atm). After the last burn, there was still enough oxygen in the upper containment for another burn. Comparing the results of the two MARCH runs with the HECTR run for case B-4, it is clear that the number of burns varies greatly. However, both of the codes predict one or more upper containment burns with peak pressures between 56 and 68 psia (3.8 and 4.6 atm). These pressures are high, but they are below the predicted failure pressure.

Case B-5 is the first of the MARCH cases in which we allowed flame propagation from one compartment to all others which contain more than the minimum amount of hydrogen required for flame extinguishment. Since these MARCH runs are to try to duplicate those HECTR runs having complete combustion, we took the hydrogen mole fraction for extinguishment to be sufficiently low, 0.002, as to be essentially zero. By using a small positive number, we force MARCH to avoid burning negligible amounts of hydrogen in a compartment and hence help clarify the output with respect to which compartments burned significant amounts of hydrogen. The hydrogen mole fraction for ignition was taken as 0.08 and the flame speed as 8 m/s, and the sprays came on after the first burn.

For case B-5, MARCH predicted 11 burns mainly in the wetwell, a period of wetwell inerting due to oxygen depletion, a combined wetwell and upper compartment burn, a wetwell burn, a second period of wetwell inerting, and finally a burn mainly in the upper containment. The peak pressure predicted was 60 psia (4.1 atm). After the last burn both the wetwell and upper containment were inert due to oxygen depletion. When the 0.065 oxygen mole fraction limit for inerting was used, MARCH predicted nine burns mainly in the wetwell, a period of wetwell inerting due to oxygen depletion, a combined wetwell and upper containment burn, and finally a burn that was mainly in the upper containment. The peak pressure for the last two burns was nearly identical, 56 psia (3.8 atm).

For case B-5, HECTR predicted 15 wetwell burns, a wetwell burn propagating into the upper containment, 2 more wetwell burns, and then an upper containment burn propagating down into the wetwell. If case B-5 had been carried out further in time, HECTR might have predicted another large burn. The peak pressure predicted was 72 psia (4.9 atm).

A comparison of the various results for case B-5 shows that the exact number of burns varies greatly with the input and code. All the runs indicate upper containment burns and high pressures. MARCH predicted lower peak pressures than HECTR, 60 and 56 psia vs 72 psia. This is believed to be primarily due to MARCH's over-estimate of the cooling effect of containment sprays.

Case B-6 differs from case B-5 only in that the hydrogen mole fraction for ignition was raised to 0.10 and the sprays were turned on early in the accident. MARCH predicted 13 burns mainly in the wetwell and 1 burn in the upper containment. The peak

pressure predicted was 63 psia (4.3 atm). After the last burn, the oxygen mole fraction in both upper containment and the wetwell was 0.04. When the 0.065 oxygen mole fraction limit for inerting was used, MARCH predicted eight burns mainly in the wetwell, a period of wetwell inerting due to oxygen depletion, a large burn in both compartments, a second period of wetwell inerting, and a final upper containment burn. The peak pressure predicted was 66 psia (4.5 atm).

For case B-6′, HECTR predicted 17 wetwell burns, 1 wetwell burn propagating into the upper containment, and 1 upper containment burn propagating into the wetwell. The peak pressure predicted was 84 psia (5.7 atm). Just as in case B-5, the number of burns predicted by the two MARCH calculations and the HECTR calculation differ, all calculations predict upper containment burns, and the peak pressures predicted by HECTR are above those predicted by MARCH. All the peak pressures predicted are high and near the estimated failure pressure of containment.

Case B-7 differs from case B-6 only in that the sprays are turned on after the first wetwell burn. MARCH predicted 12 burns mainly in the wetwell, a period of wetwell inerting due to oxygen depletion, and then 2 burns in both the upper containment and wetwell. The peak pressure predicted was 62 psia (4.2 atm) during the first of the two global burns. After the last burn there was very little oxygen left in containment. When the 0.065 oxygen mole fraction inerting limit was used, MARCH predicted eight burns mainly in the wetwell, a period of wetwell inerting, and two upper containment/wetwell burns. The peak pressure was predicted during the last burn, 61 psia (4.2 atm).

For case B-7, HECTR predicted 18 wetwell burns, a period of wetwell inerting, a wetwell burn propagating into the upper containment, another wetwell burn, and a final upper containment burn propagating into the wetwell. The peak pressure predicted was 81 psia (5.5 atm). One expects case B-7 to give nearly identical results to case B-6. The results are very similar, but the exact number of burns differ. The peak pressure predicted by HECTR is significantly different, but MARCH predicted nearly the same pressures in both B-6 and B-7.

Table 3.2. Configuration B Case Description and Results

Case No.	Initial Pressure (psia)	Hydrogen Mole Fraction for Ignition	Hydrogen Mole Fraction for Extinguishment	Burn Time, Seconds	Flame Propagation	Sprays	Number of Significant Upper Containment Burns	Peak Pressure (psia)	Oxygen Mole Fraction Required to Inert
B-1	17	0.10	0.0	4.8	No	Auto	1	65	.05
							1	70	.065
B-2	14.7	0.10	0.0	4.8	No	Auto	1	52	.05
							2	63	.065
B-3	14.7	0.08	0.012	4.8	No	Auto	2	42	.05
							2	44	.065
B-4	14.7	0.08	0.002	4.8	No	Off	2	56	.05
							3	65	.065
B-5	14.7	0.08	0.002	2.0	Yes	Auto	2	60	.05
							2	56	.065
B-6	14.7	0.10	0.002	2.0	Yes	On	1	66	.05
							2	66	.065
B-7	14.7	0.10	0.002	2.0	Yes	Auto	2	62	.05
							2	61	.065

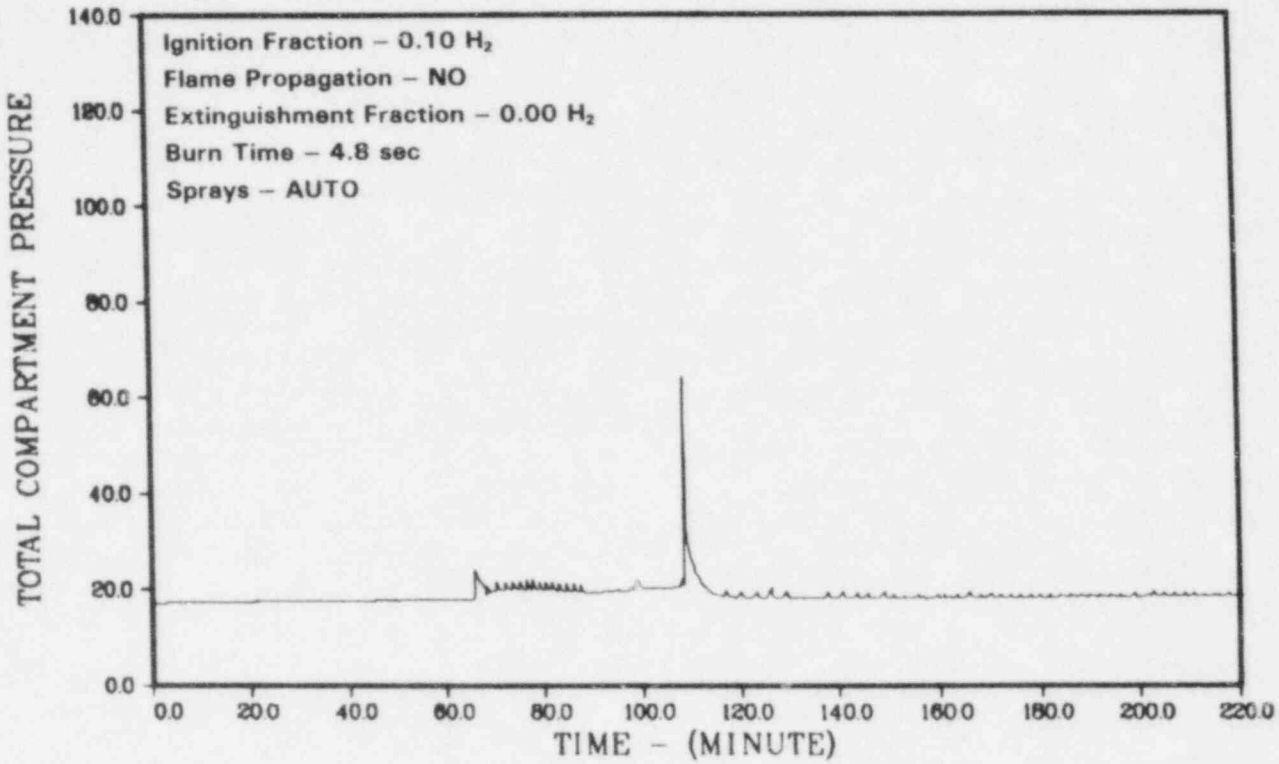

Figure 3.16. Case B-1, Pressure in Containment, psia

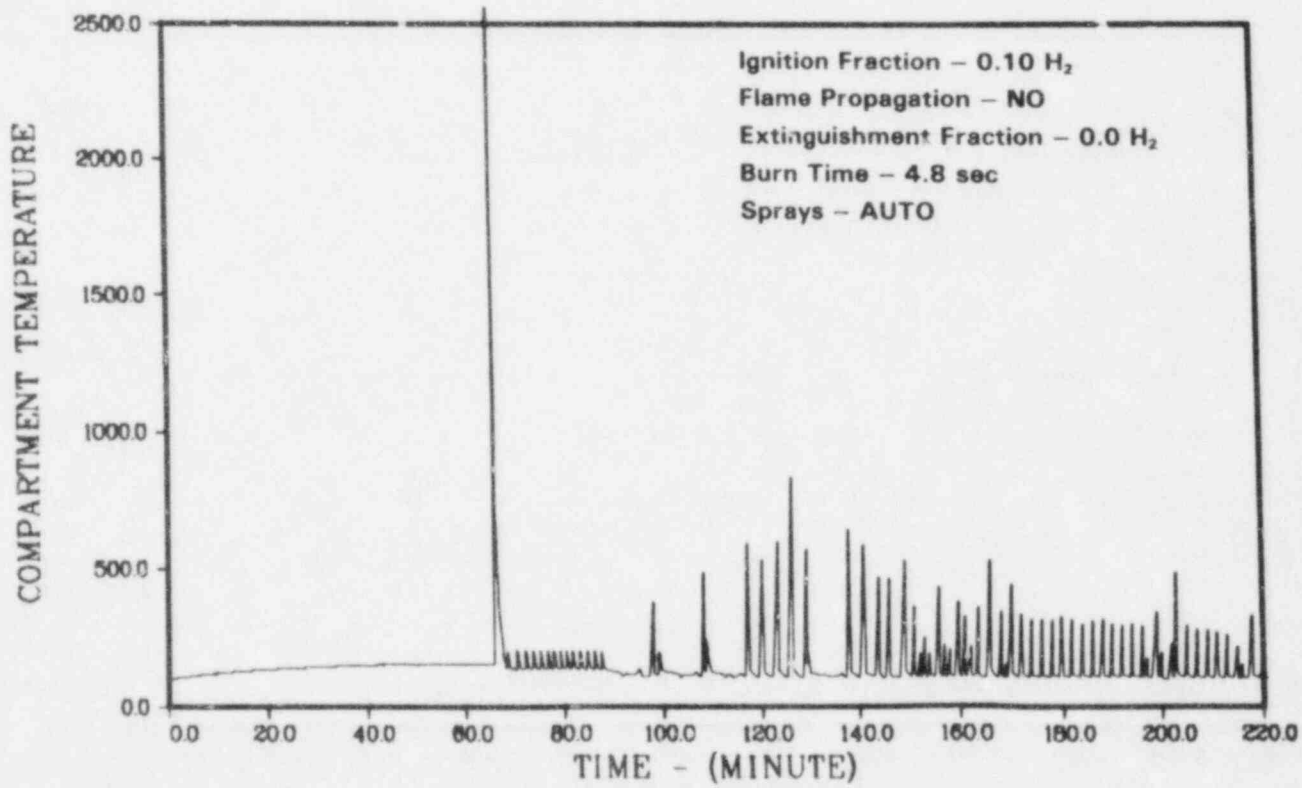

Figure 3.17. Case B-1, Temperature in Wetwell, °F

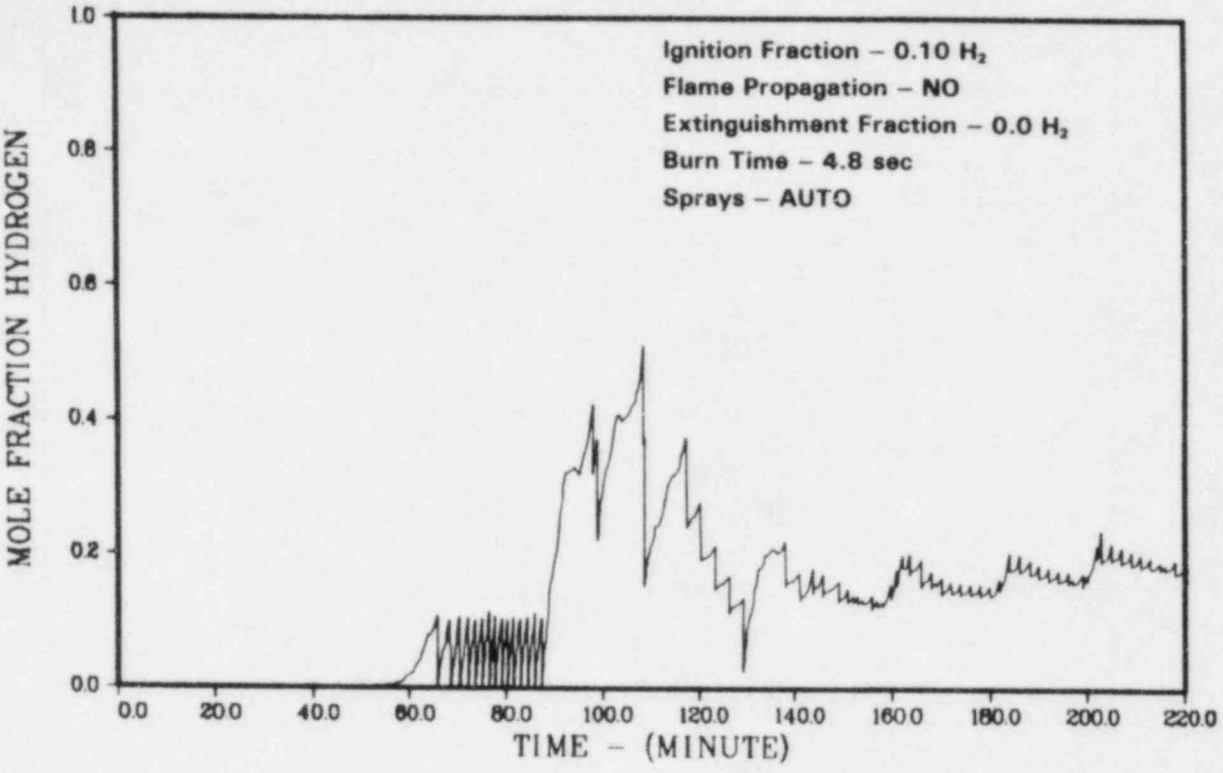

Figure 3.18. Case B-1, Hydrogen Mole Fraction in Wetwell

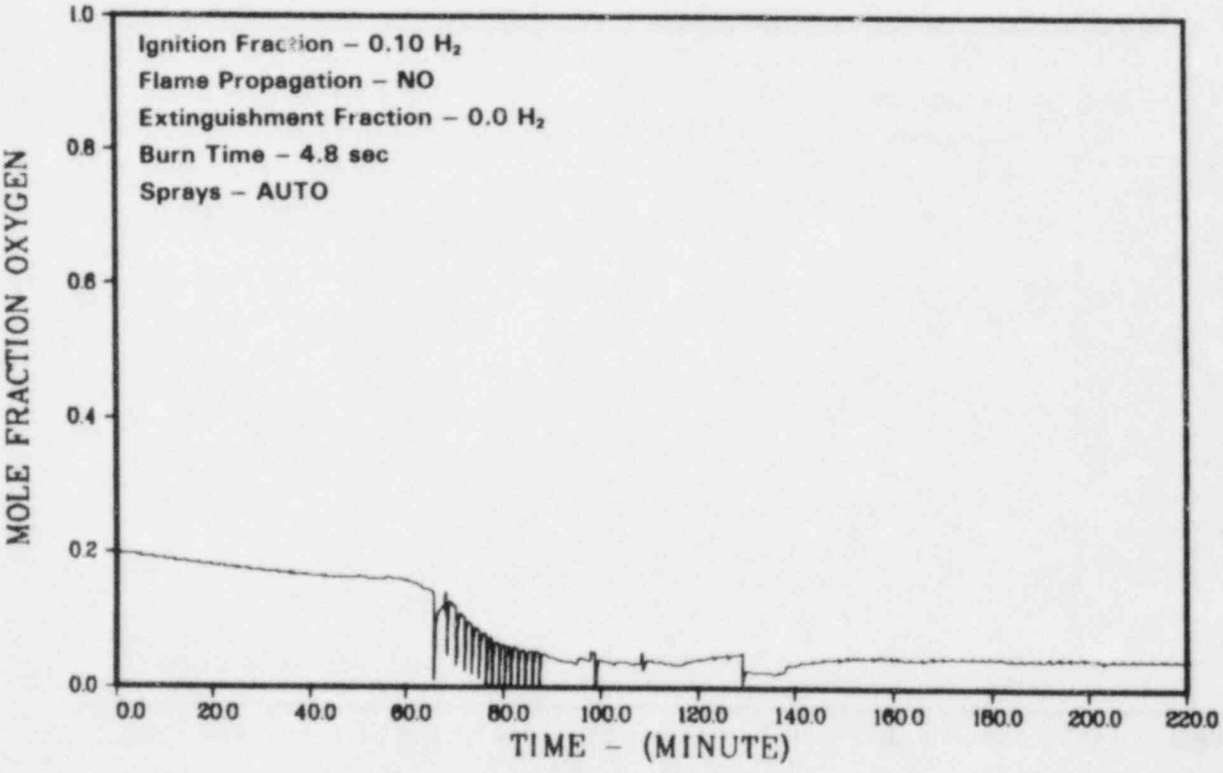

Figure 3.19. Case B-1, Oxygen Mole Fraction in Wetwell

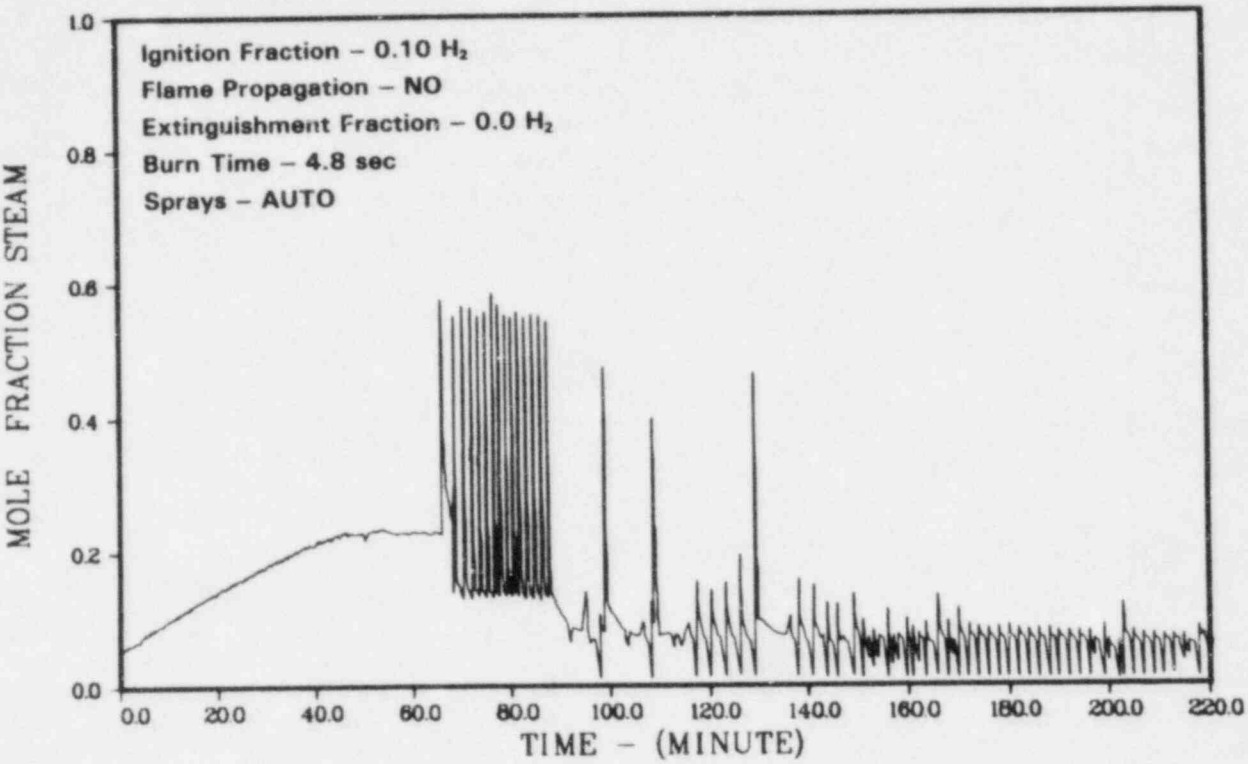

Figure 3.20. Case B-1, Steam Mole Fraction in Wetwell

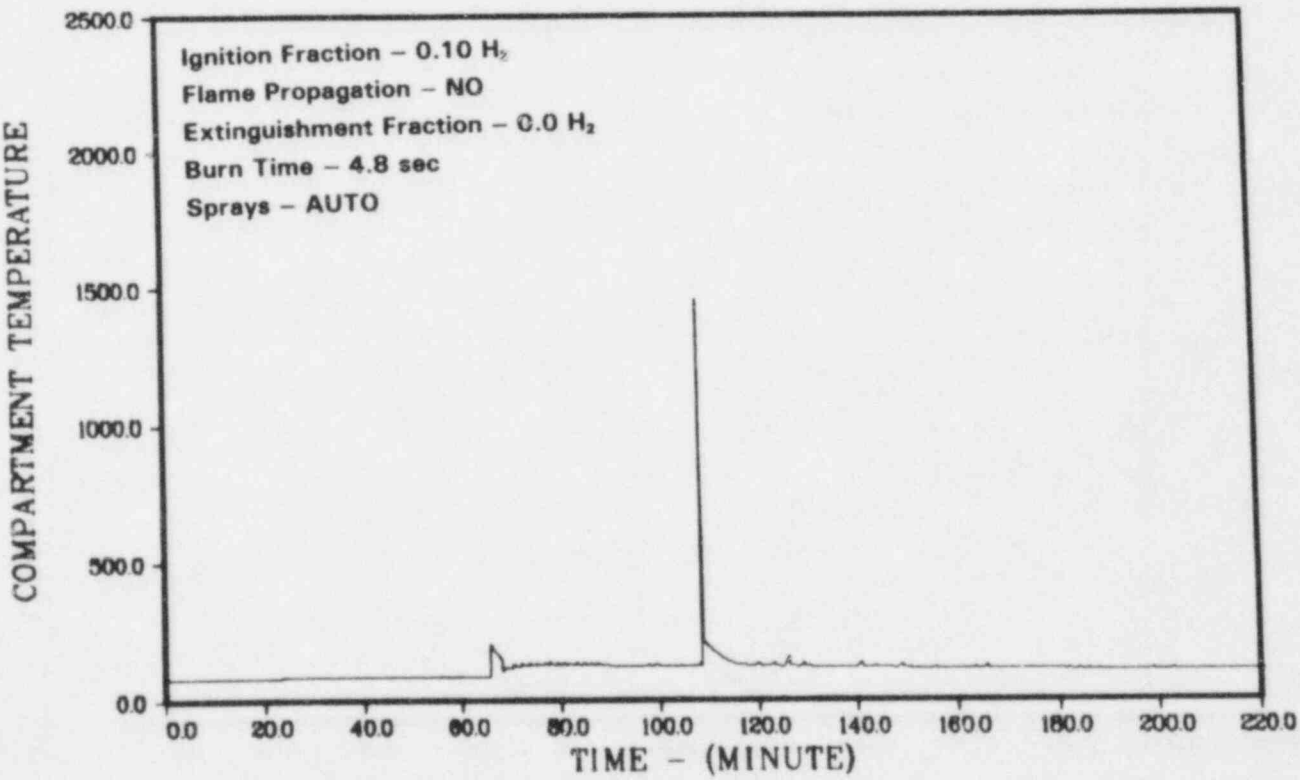

Figure 3.21. Case B-1, Temperature in Upper Containment, °F

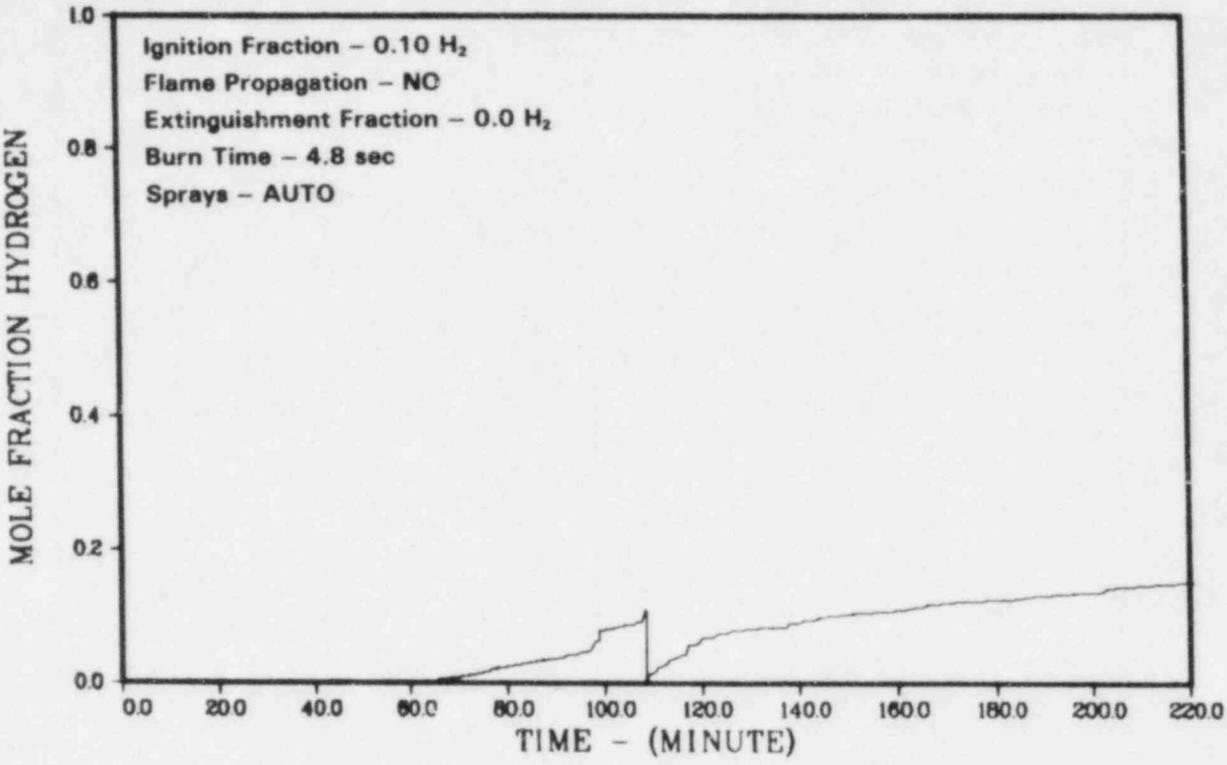

Figure 3.22. Case B-1, Hydrogen Mole Fraction in Upper Containment

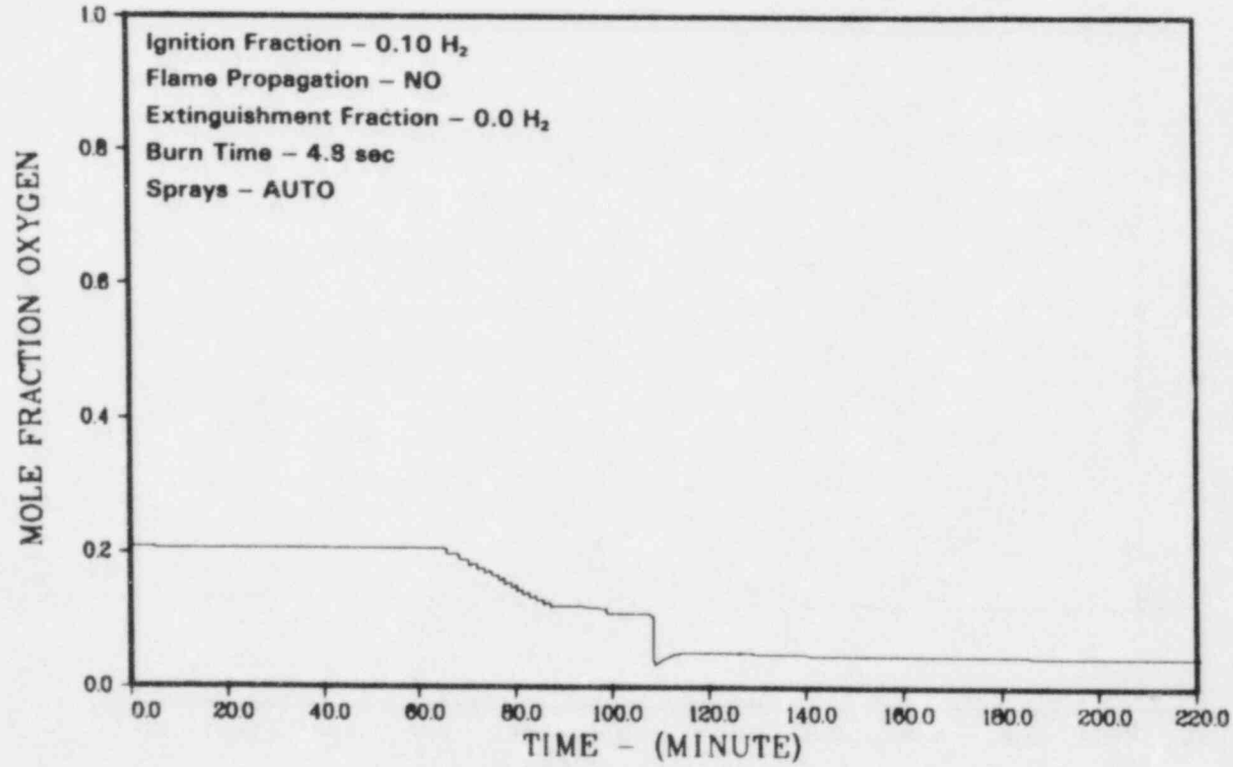

Figure 3.23. Case B-1, Oxygen Mole Fraction in Upper Containment

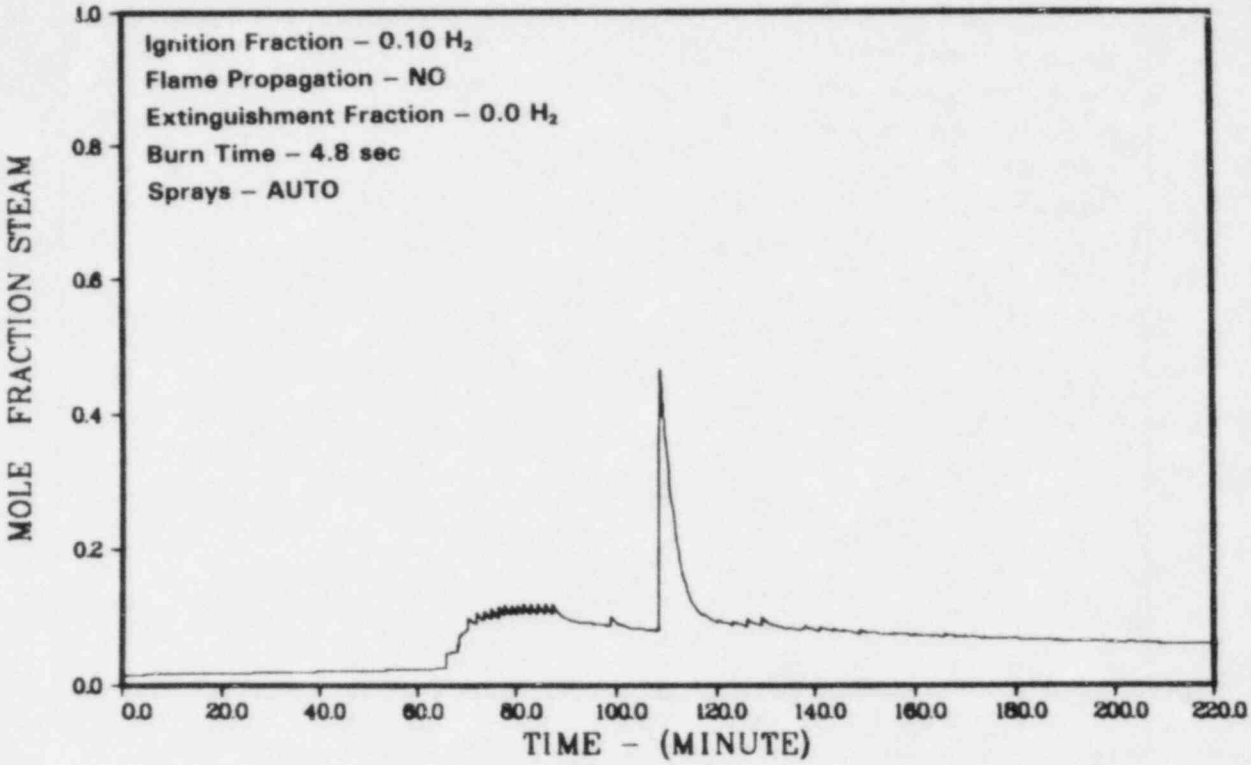

Figure 3.24. Case B-1, Steam Mole Fraction in Upper Containment

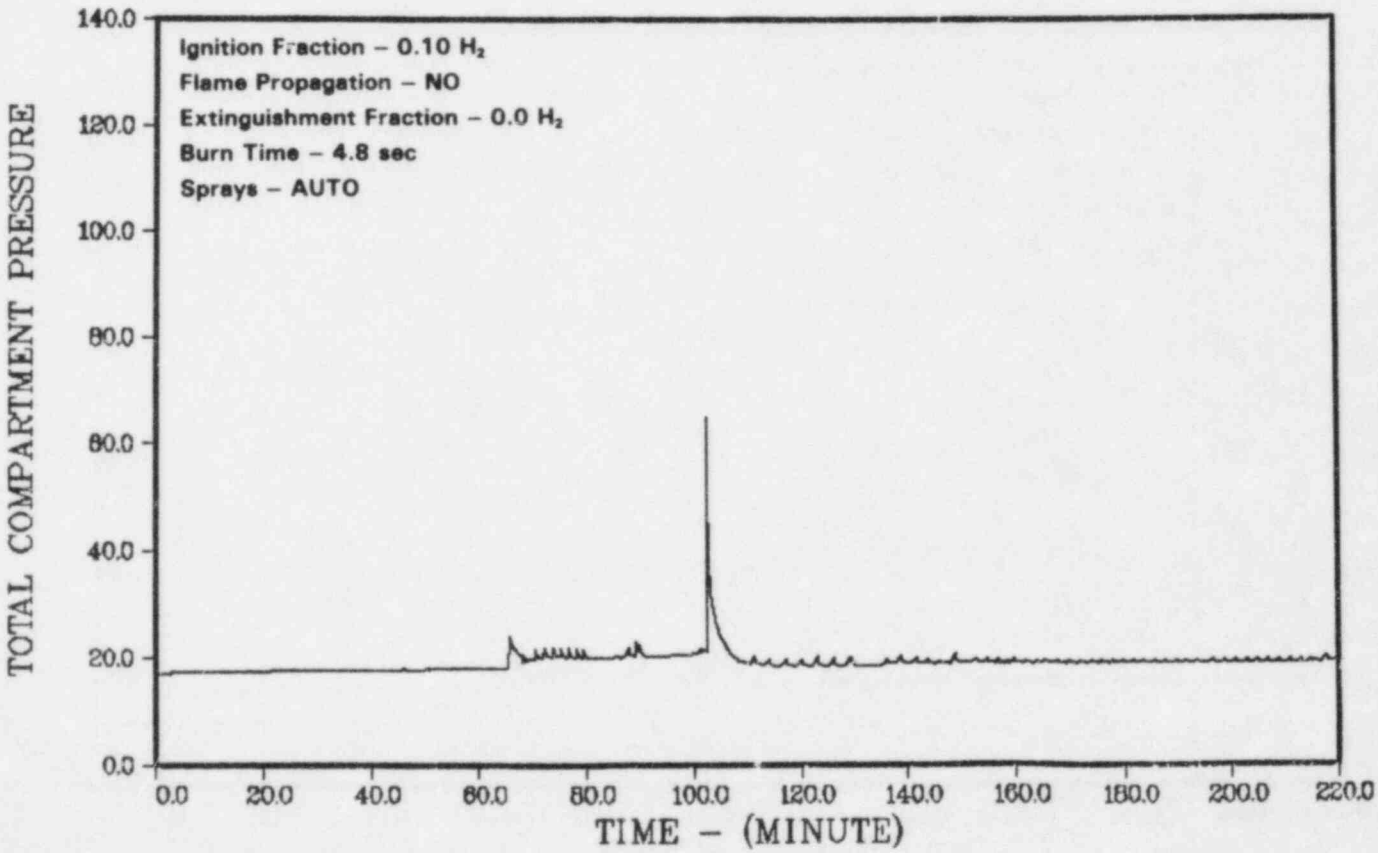

Figure 3.25. Case B-1 (6.5% Oxygen Inerting Limit), Pressure in Containment, psia

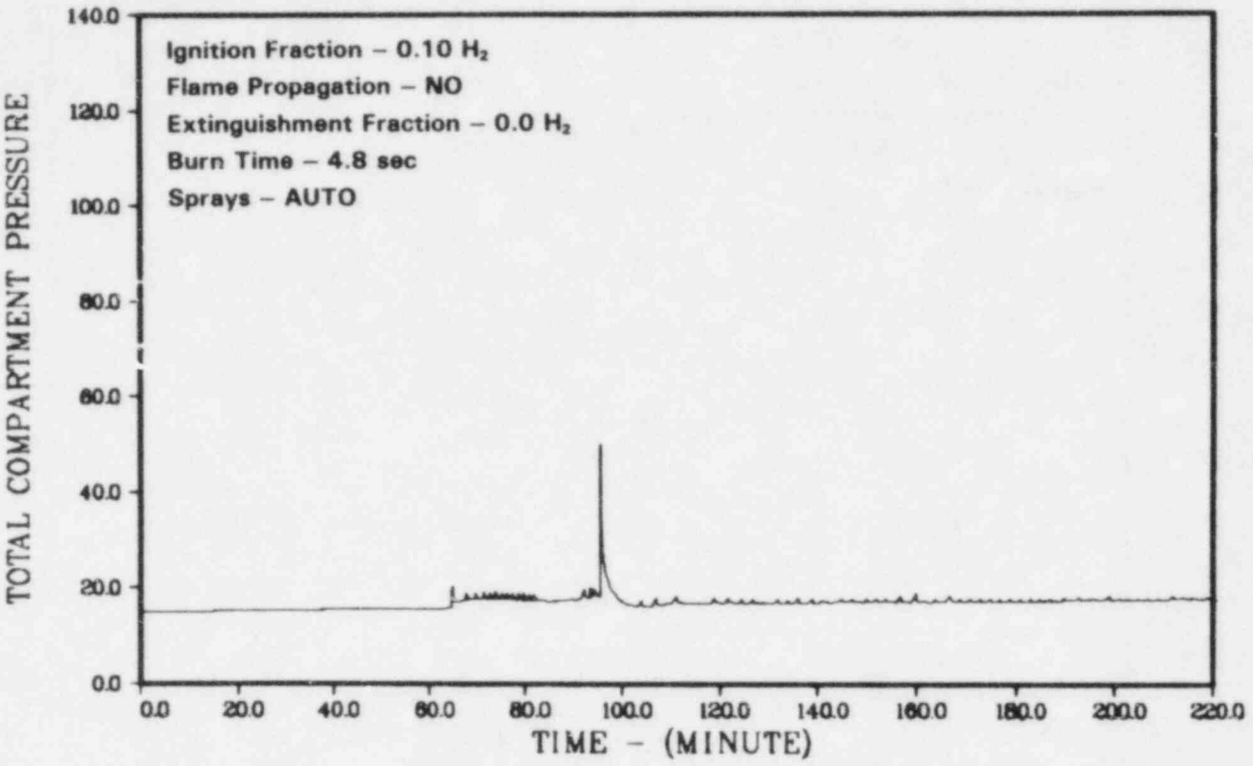

Figure 3.26. Case B-2, Pressure in Containment, psia

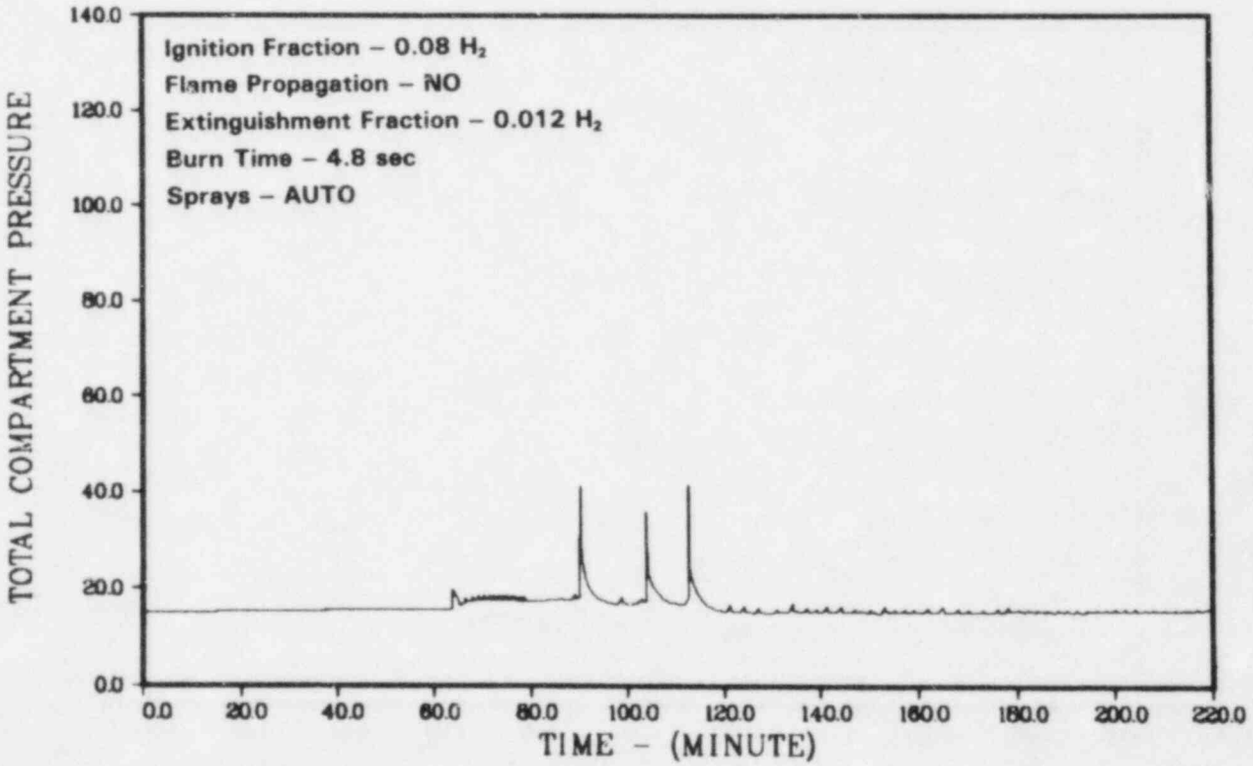

Figure 3.27. Case B-3, Pressure in Containment, psia

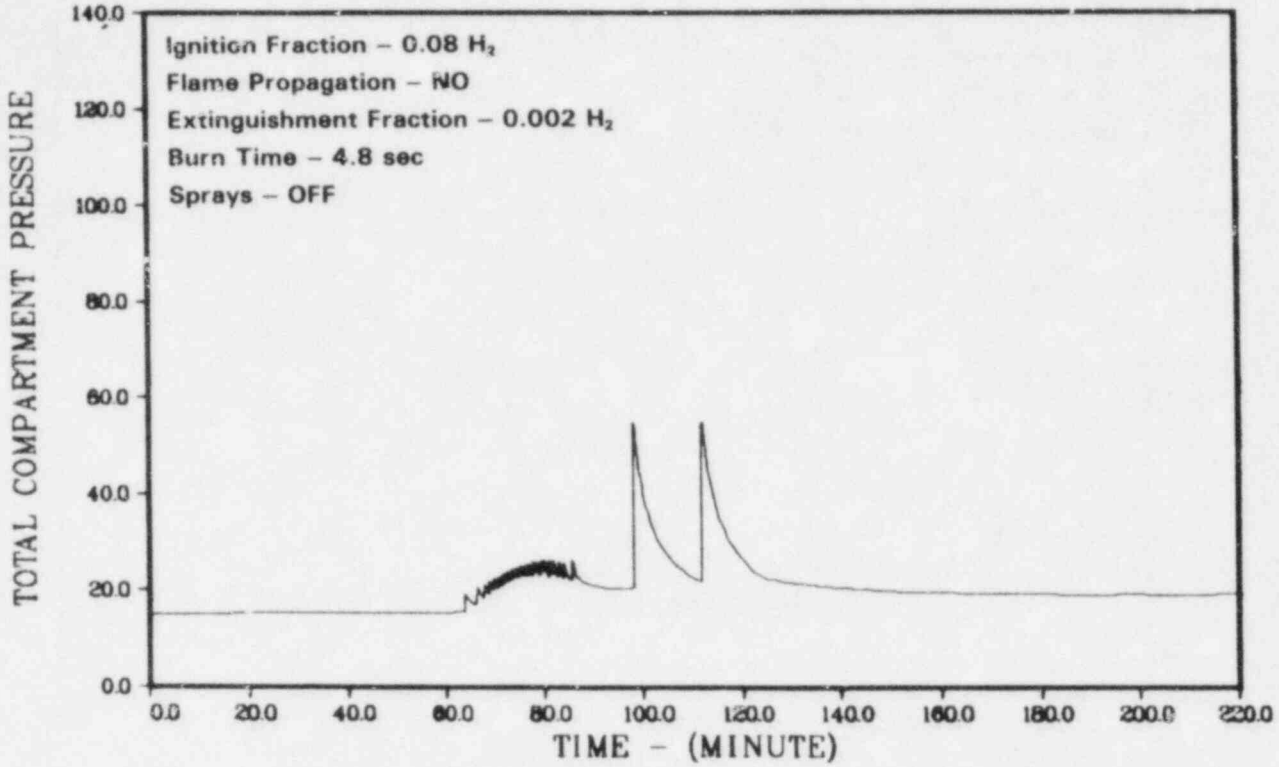

Figure 3.28. Case B-4, Pressure in Containment, psia

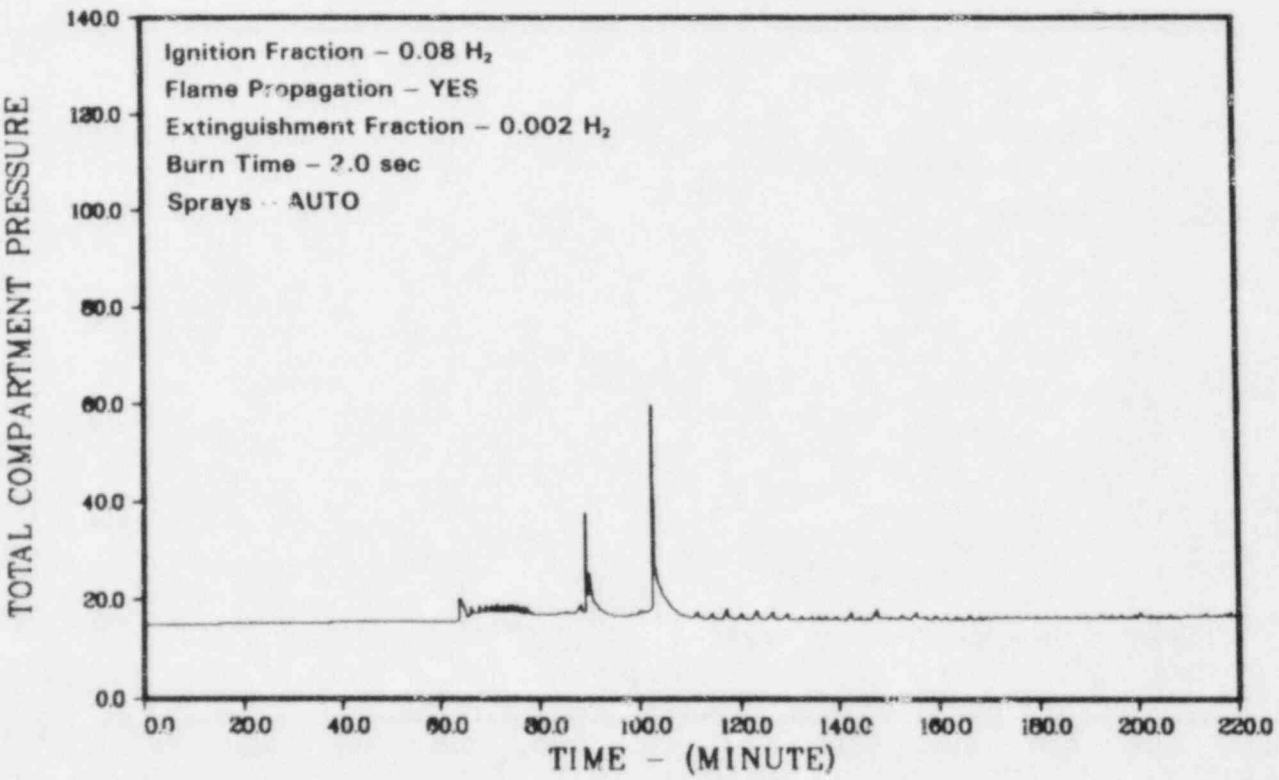

Figure 3.29. Case B-5, Pressure in Containment, psia

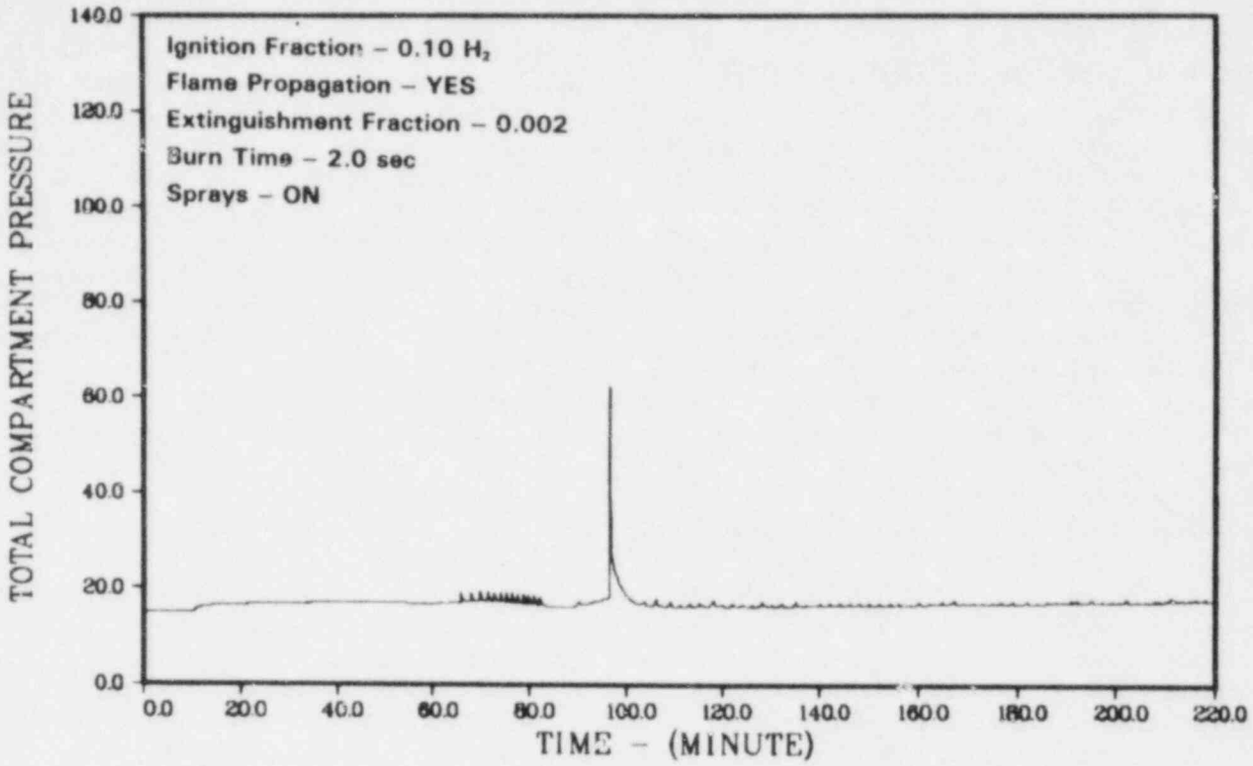

Figure 3.30. Case B-6, Pressure in Containment, psia

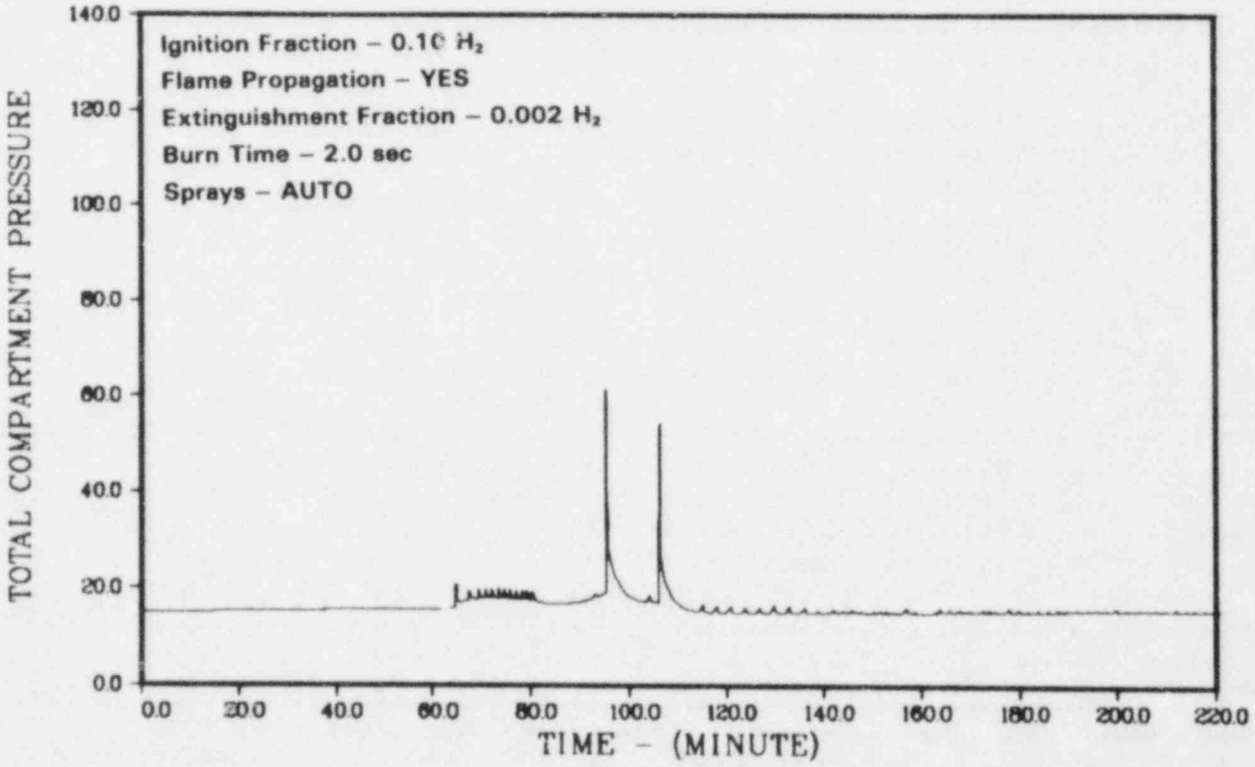

Figure 3.31. Case B-7, Pressure in Containment, psia

3.5 Analysis of MARCH Calculations for Configuration C

Configuration C consists of three volumes: the drywell, a large wetwell (the volume from the suppression pool to the 209-ft elevation), and the still larger upper containment volume. The ratio of wetwell to upper containment volume is 0.600 compared to 0.129 for configuration B. For configuration C, wetwell burns give rise to moderate pressure peaks (larger than wetwell burns in configuration B) and upper-containment burns give rise to somewhat higher peak pressures (smaller than upper containment burns in configuration B). For the cases considered in this section, there was no connection from the wetwell back to the drywell, as stated in section 3.2. Consequently, we ignore the drywell in this section. The effect of the drywell is considered in section 3.8. One upper containment burn occurred in all of the cases considered in this section, but none in the case considered in section 3.8.

The case descriptions and a partial summary of results for the configuration C calculations are in Table 3.3. Graphical results for case C-1 are shown in Figures 3.32 through 3.40. The pressure histories of cases C-2 to C-4 are shown in Figures 3.41 through 3.43.

The qualitative behavior of the four cases considered for configuration C is as follows:

1. Several wetwell burns with moderate pressure peaks
2. Wetwell inerting due to oxygen depletion
3. A buildup of hydrogen mole fraction to high values in the wetwell and combustible values in the upper containment
4. One upper containment or combined wetwell/upper-containment burn
5. Inerting of the wetwell by oxygen depletion. Insufficient hydrogen in the upper containment for a second burn, but sufficient oxygen

For case C-1, MARCH predicted six wetwell burns, a period of wetwell inerting, and then a combined wetwell/upper-containment burn. Since the sprays came on after the first burn, MARCH predicted that the first burn generated a higher peak pressure than the next five wetwell burns, 33 psia (2.2 atm). The peak pressure due to the combined wetwell/upper-containment burn was 45 psia (3.1 atm). After the last burn, the concentration of hydrogen and oxygen in the upper containment approached that required to ignite another burn. The wetwell contained a high mole fraction of hydrogen, but was inerted due to oxygen depletion.

For case C-1 HECTR predicted six wetwell burns, a seventh burn starting in the wetwell and propagating into the upper containment, and then two more wetwell burns. The peak pressure was 40 psia (2.7 atm). After the last burn the upper compartment contained sufficient oxygen for a second burn, but insufficient hydrogen for ignition. The wetwell contained a high mole fraction of hydrogen, but was inerted due to oxygen depletion. A comparison of the MARCH and HECTR results for case C-1 shows many similarities. The predicted peak pressures are reasonably close. However, the number of wetwell burns differs.

In case C-2 the hydrogen ignition limit was raised to 0.10 and the sprays were turned on early in the accident. MARCH predicted five wetwell burns, all with peak pressures of about 28 psia (1.9 atm). After the five wetwell burns, the wetwell was inerted due to oxygen depletion, and late in the accident MARCH predicted a burn mainly in the upper containment with a peak pressure of 48 psia (3.3 atm). After the last burn, the entire containment was oxygen depleted.

HECTR predicted three wetwell burns, one wetwell burn propagating into the upper containment, and then three more wetwell burns. At the end of the HECTR calculation the upper compartment had an oxygen mole fraction of 0.10 but a hydrogen mole fraction of only 0.028. The two codes are in reasonable agreement about the peak pressure (both have one burn in the upper containment), but disagree on the number of wetwell burns. The peak pressure is high but below the estimated failure pressure of containment.

In case C-3, the sprays came on after the first burn, but otherwise the case is identical to C-2. In this case MARCH predicted five wetwell burns, a long period in which the wetwell was oxygen depleted, and then a combined wetwell and upper containment burn. The peak pressure of the first wetwell burn, before the sprays were operated, was 38 psia (2.6 atm), and the peak pressure after the last burn was 47 psia (3.2 atm). After the last burn, the wetwell and upper containment were oxygen depleted.

For case C-3, HECTR predicted three wetwell burns, a wetwell burn propagating into the upper containment, and then three more wetwell burns. The peak pressure predicted was 42 psia (2.0 atm). After the last burn, the upper containment was not predicted to be oxygen depleted.

In case C-4, the sprays were off. As a result, the peak pressures and temperatures were higher and their decay after the burns was much slower. MARCH predicted four wetwell burns, with gradually increasing peak pressures up to 50 psia (3.4 atm), and a final

upper containment and wetwell burn with a peak pressure of 70 psia (4.8 atm). This is about equal to the estimated failure pressure for the containment. After the last burn, the upper containment was not oxygen depleted.

For case C-4 HECTR predicted six wetwell burns, a wetwell burn propagating into the upper containment, and then two more wetwell burns. The peak pressure predicted was 49 psia (3.3 atm).

In cases C-1, C-2, and C-3, MARCH predicted somewhat higher pressures than HECTR. However, in case C-4, without sprays, the MARCH prediction of 70 psia (4.8 atm) is much higher than the HECTR prediction due to the nature of the propagating burn in the HECTR calculation. The MARCH case C-4 peak pressure prediction is the only one that approaches the estimated containment failure pressure of 71 psia (4.8 atm).

Table 3.3. Configuration C Case Descriptions and Results

Case No.	Initial Pressure, psia	Hydrogen Mole Fraction for Ignition	Hydrogen Mole Fraction for Extinguishment	Flame Propagation	Comp. Burn Time, Sec.	Sprays	Peak Pressure, psia atm	No. of Significant Upper Containment Burns	No. of Significant Wetwell Burns
C-1	14.7	0.08	0.002	Yes	4	Auto	45 (3.1)	1	7
C-2	14.7	0.10	0.002	Yes	4	On	48 (3.3)	1	5
C-3	14.7	0.10	0.002	Yes	4	Auto	47 (3.2)	1	6
C-4	14.7	0.10	0.002	Yes	4	Off	70 (4.8)	1	5

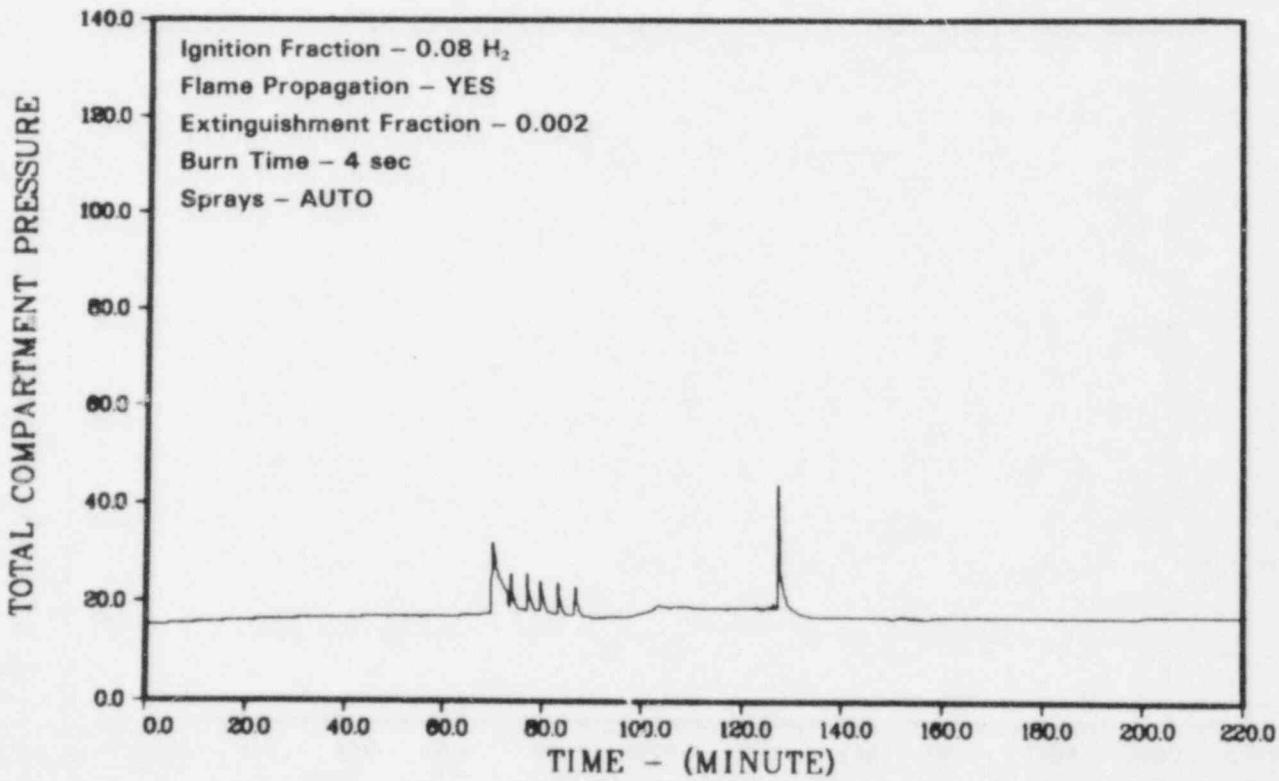

Figure 3.32. Case C-1, Pressure in Containment, psia

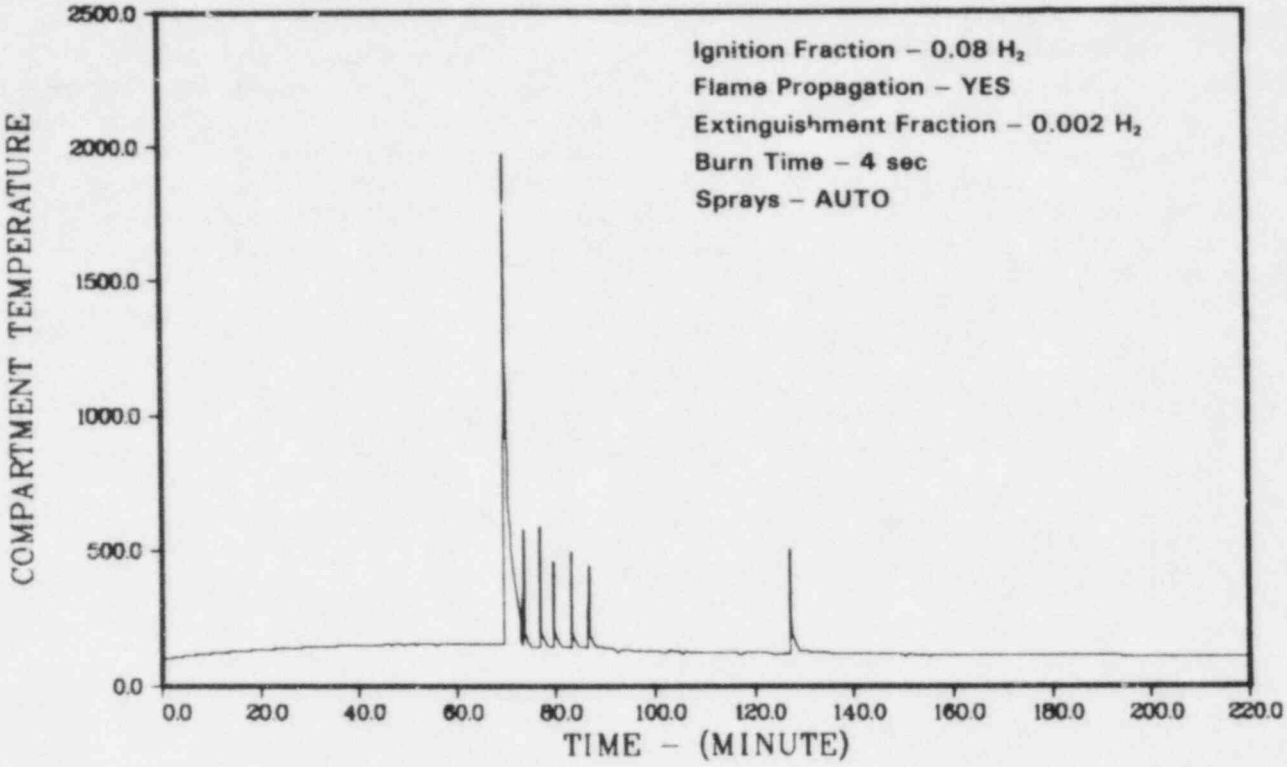

Figure 3.33. Case C-1, Temperature in Wetwell, °F

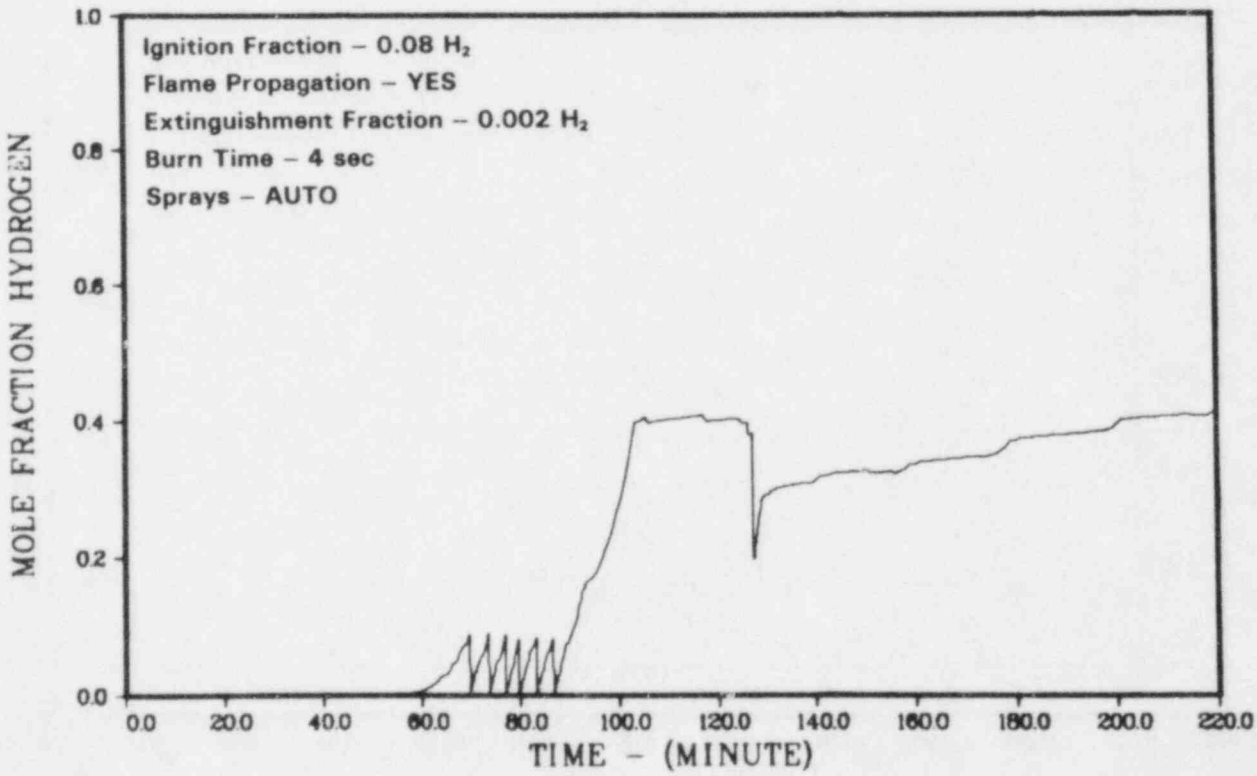

Figure 3.34. Case C-1, Hydrogen Mole Fraction in Wetwell

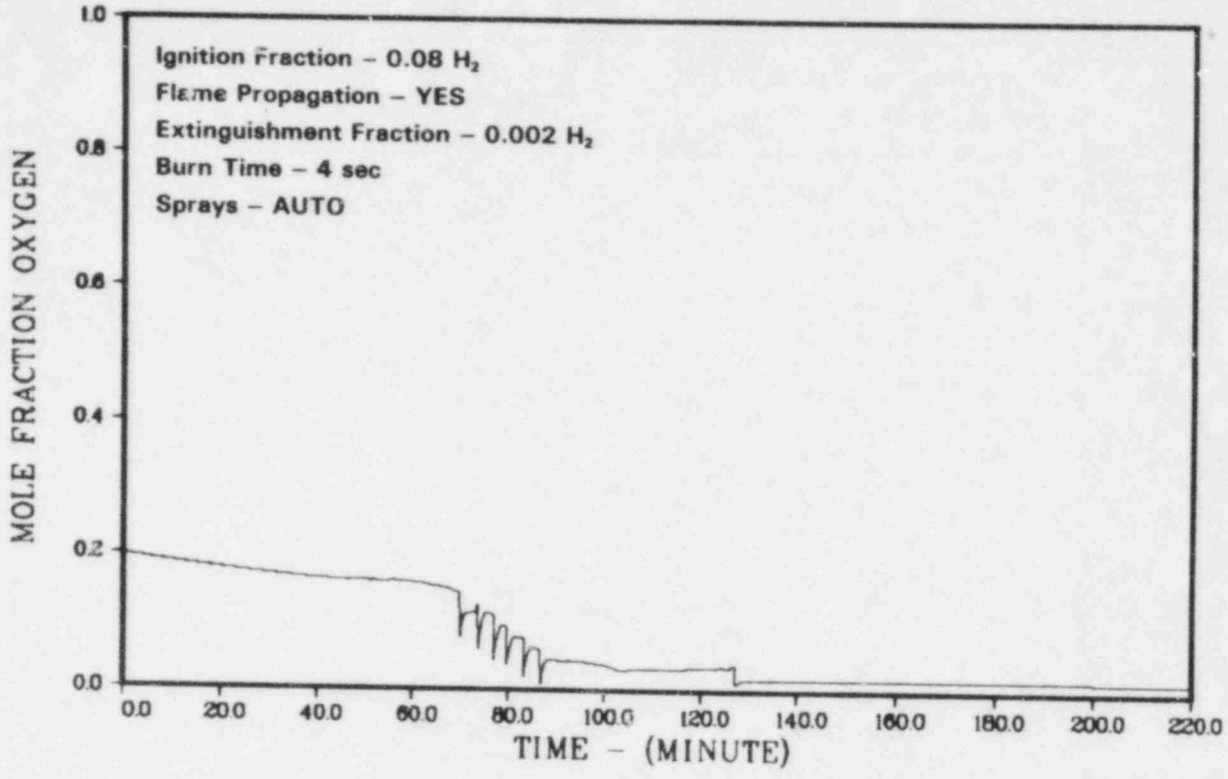

Figure 3.35. Case C-1, Oxygen Mole Fraction in Wetwell

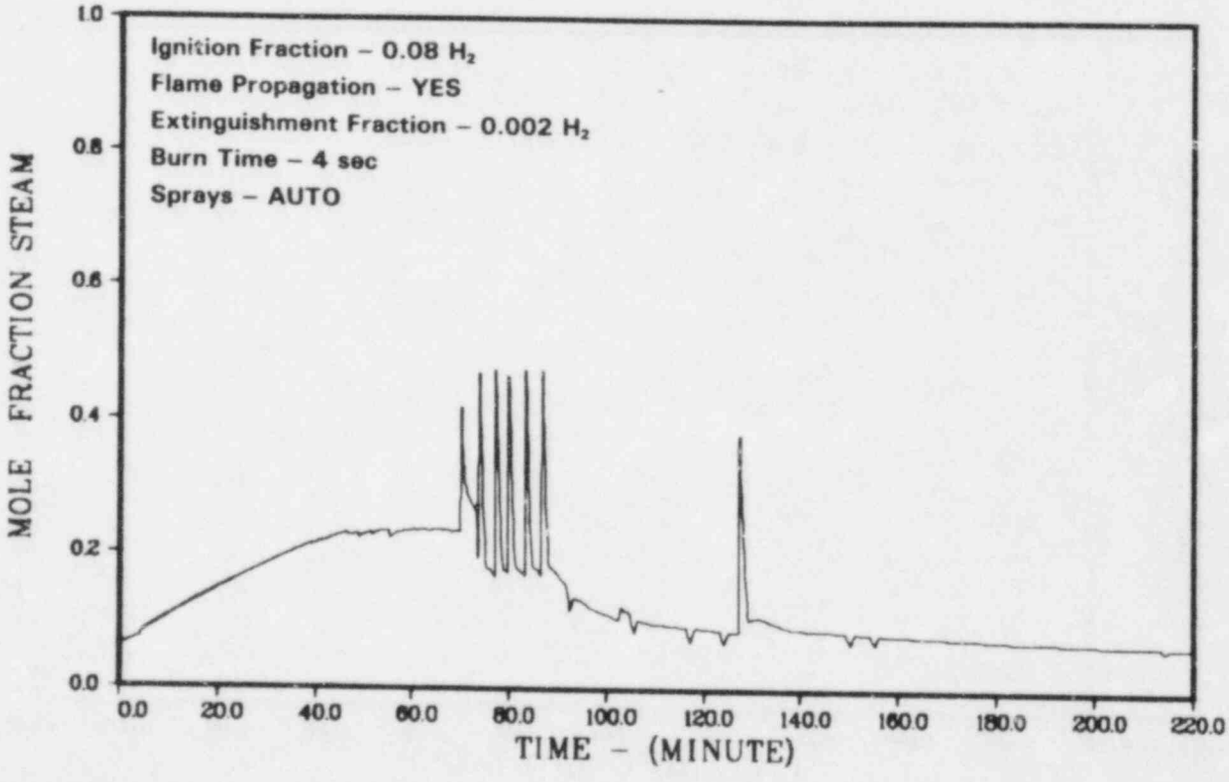

Figure 3.36. Case C-1, Steam Mole Fraction in Wetwell

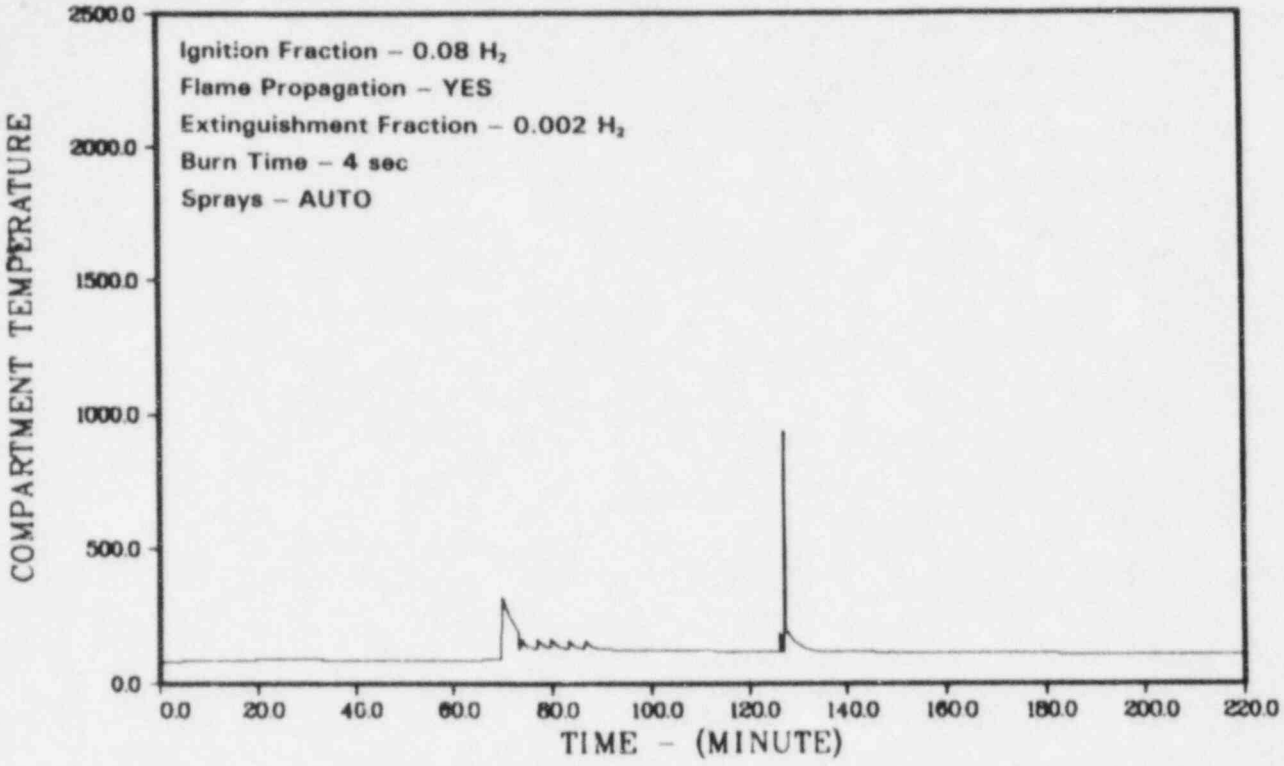

Figure 3.37. Case C-1, Temperature in Upper Containment, °F

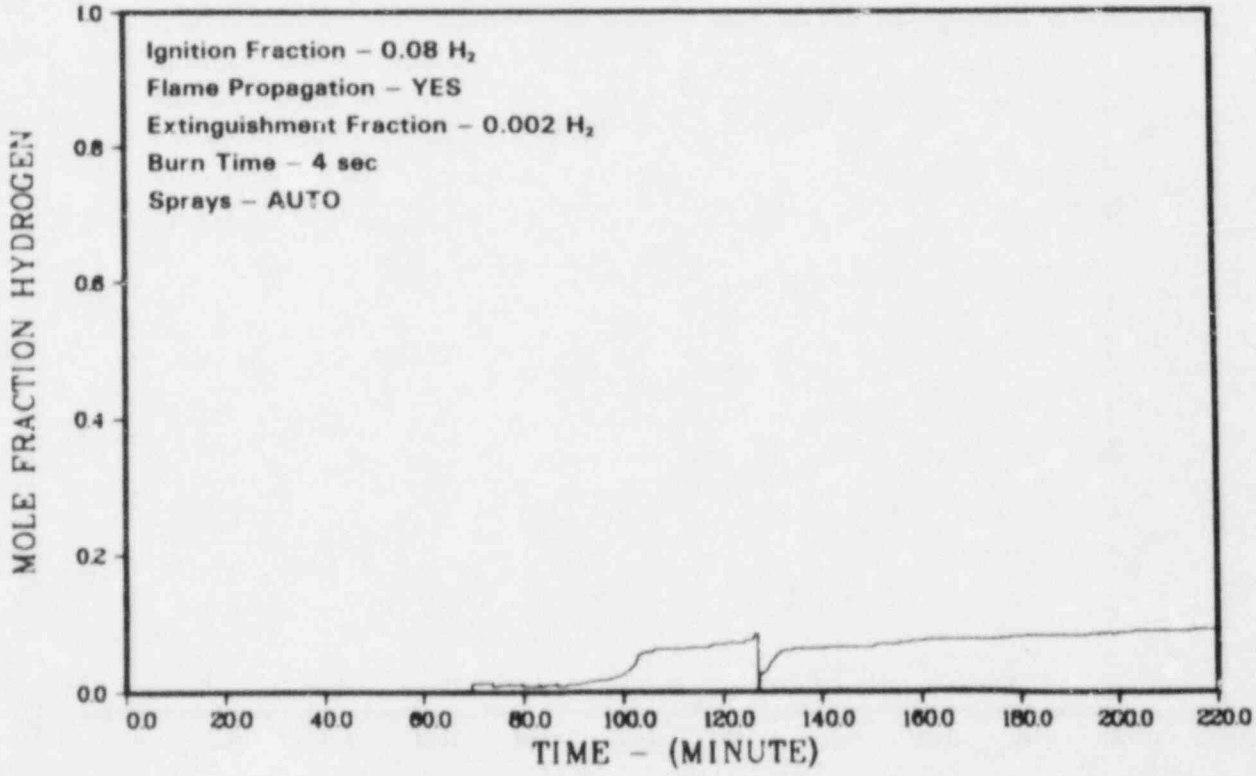

Figure 3.38. Case C-1, Hydrogen Mole Fraction in Upper Containment

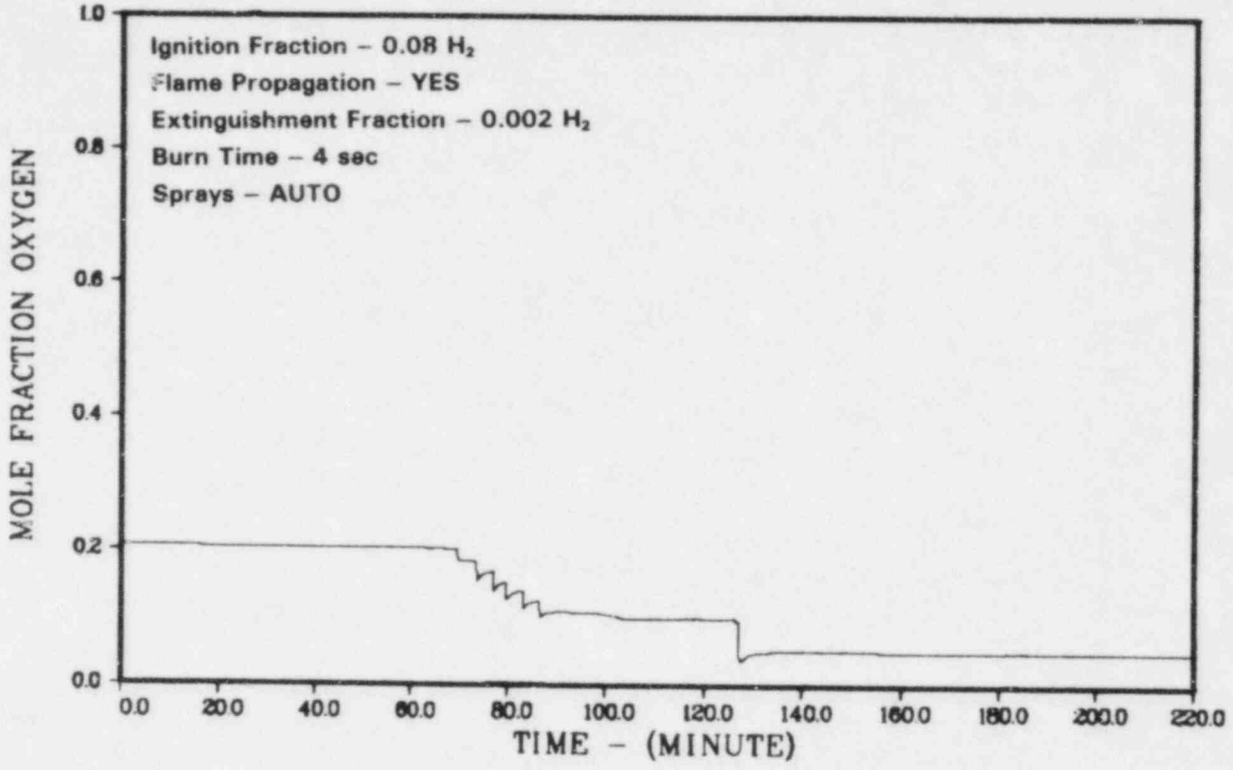

Figure 3.39. Case C-1, Oxygen Mole Fraction in Upper Containment

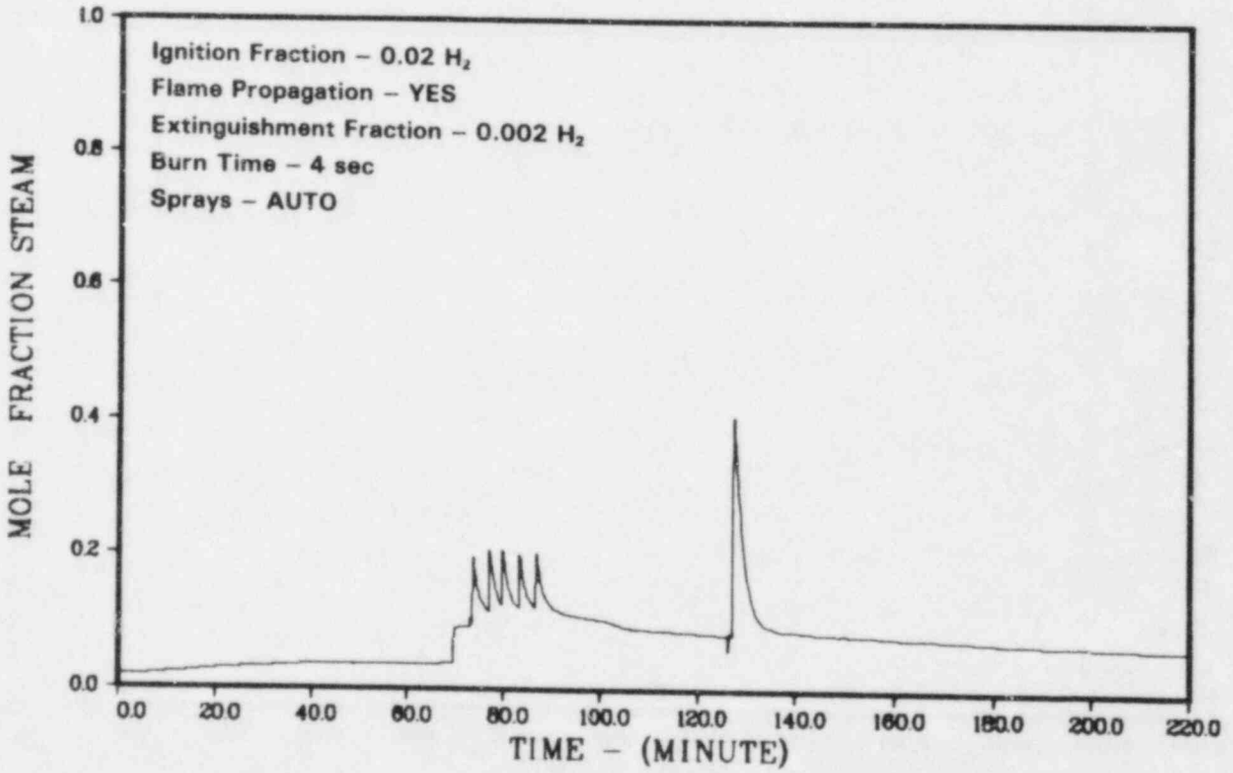

Figure 3.40. Case C-1, Steam Mole Fraction in Upper Containment

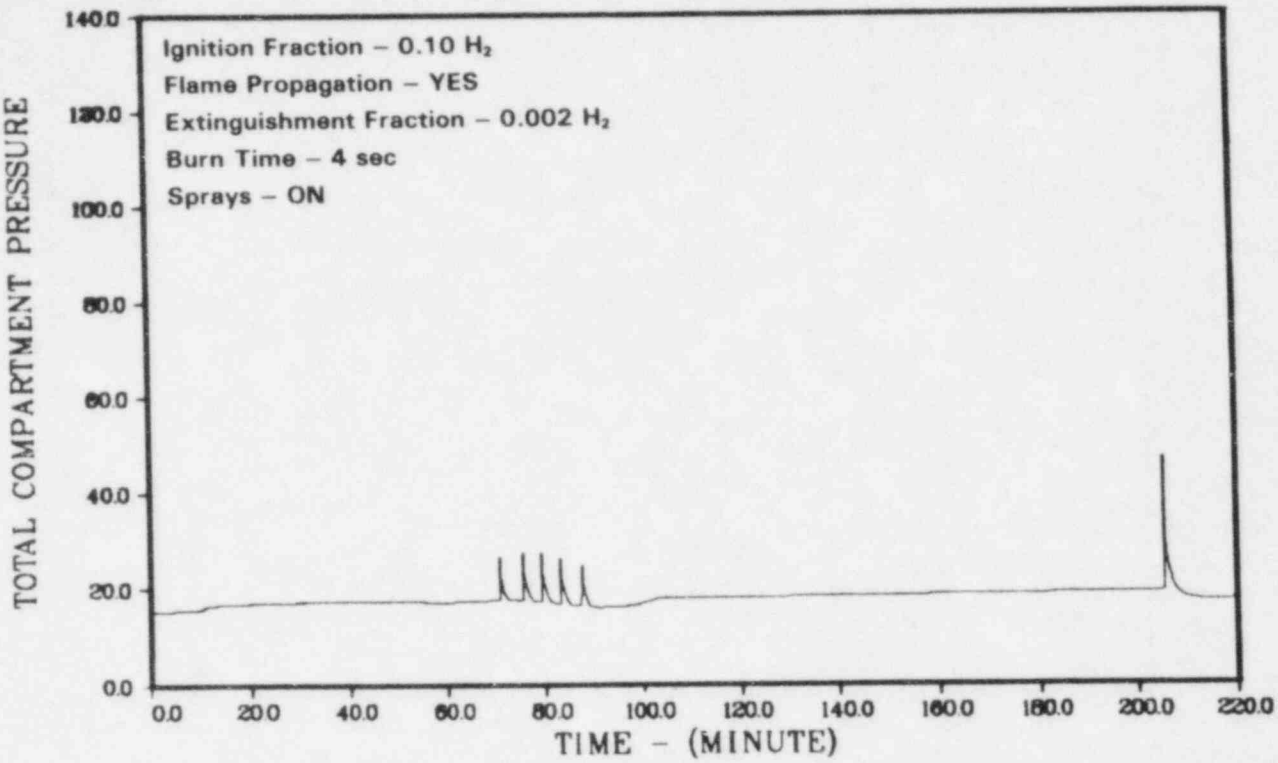

Figure 3.41. Case C-2, Pressure in Containment, psia

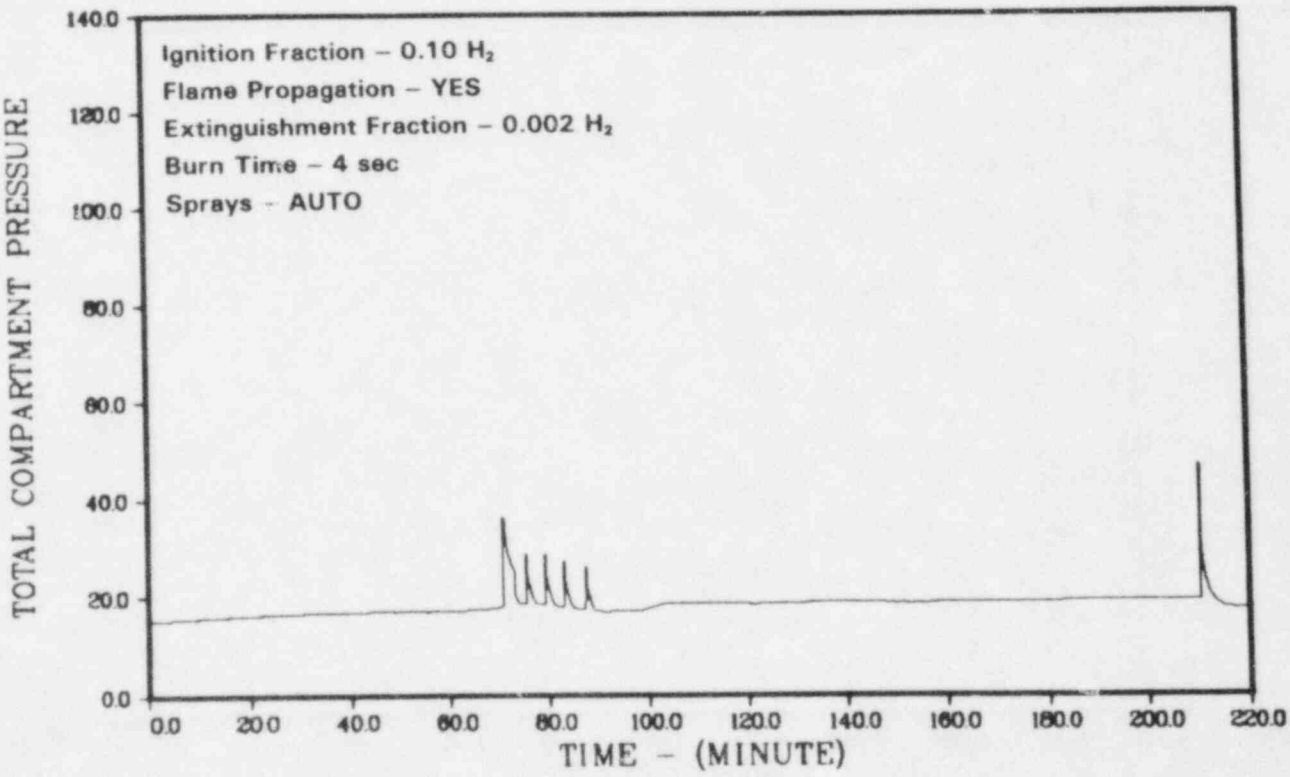

Figure 3.42. Case C-3, Pressure in Containment, psia

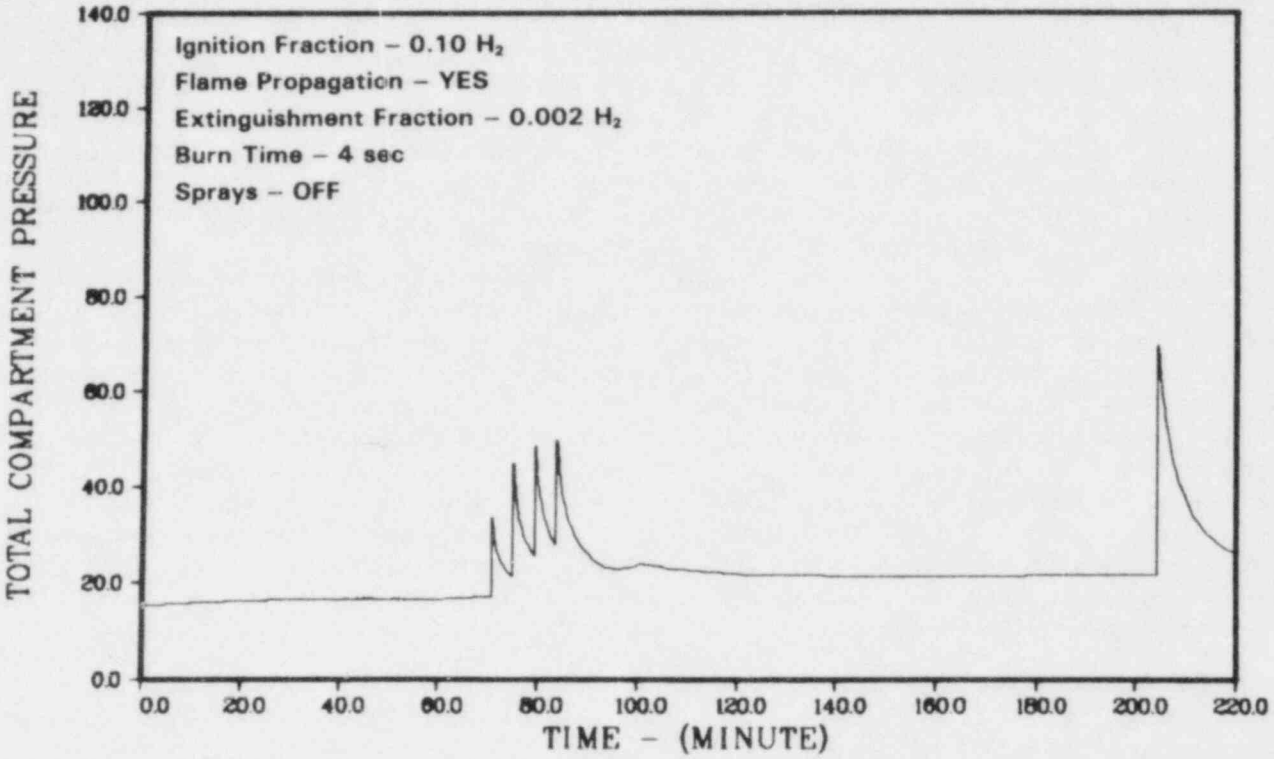

Figure 3.43. Case C-4, Pressure in Containment, psia

3.6 Analysis of MARCH Calculations for Configuration D

Configuration D consists of a drywell and three compartments: a wetwell volume up to the 135 ft elevation, an intermediate annular volume up to the 209 ft elevation, and an upper containment volume. In this section the drywell was not interconnected to the rest of the containment; hence it was isolated and ignored. The effect of the drywell is considered in section 3.8.

The case descriptions and a partial summary of results for configuration D are in Table 3.4. Graphical results for case D-1 are shown in Figures 3.44 through 3.56. Pressure histories for cases D-2 and D-3 are shown in Figures 3.57 and 3.58.

The general pattern of results can be summarized as follows:

1. Numerous wetwell burns
2. Inerting of the wetwell due to oxygen depletion
3. Buildup of hydrogen mole fractions in all compartments
4. Burns in the intermediate annular volume
5. Possible inerting of the intermediate annular volume
6. One burn mainly in the upper containment

Case D-1 used a hydrogen mole fraction of 0.08 for ignition and had sprays after the first burn. Of our cases, it most closely matches the one configuration D case calculated with CLASIX-3. MARCH predicted seven burns mainly in the wetwell, a period of wetwell inerting due to oxygen depletion, four burns mainly in the intermediate annular region, and finally a burn mainly in the upper containment with a peak pressure of 61 psia (4.2 atm). For case D-1, HECTR predicted 17 wetwell burns, a period of wetwell inerting, 7 burns in the intermediate annular region, and a final burn starting in the intermediate annular region and propagating into the upper containment. The predicted peak pressure was 39 psia (2.7 atm). Although the general pattern of burns is similar in HECTR and MARCH, the number of burns and the peak pressure differ greatly. CLASIX-3 predicted no upper containment burn and consequently low peak pressure (27 psia, 1.8 atm).

Case D-2 differs from case D-1 only in that the hydrogen mole fraction for ignition was increased to 0.10. MARCH predicted eight burns mainly in the wetwell, a period of wetwell inerting, three burns mainly in the intermediate annular region, and a final burn in all three compartments with a peak pressure of 46 psia (3.1 atm). This result is surprising, since one

expects a larger peak pressure in case D-2 than D-1, but the reverse was found. The mole fraction for the last burn of hydrogen in the upper containment was lower for case D-2 than for D-1, and therefore the peak pressure was lower.

For case D-2, HECTR predicted 12 wetwell burns, a wetwell burn propagating into the intermediate annular region, 3 burns in the intermediate annular region, a burn starting in the intermediate annular region and propagating into the upper containment, and a final burn in the intermediate annular region. The peak pressure predicted was 41 psia (2.8 atm).

Case D-3 involved a hydrogen ignition mole fraction of 0.08 and no sprays. MARCH predicted nine wetwell burns, wetwell inerting, three burns mainly in the intermediate annular region, and inerting of the intermediate annular region. At the end of the calculation, the oxygen mole fraction in the upper containment volume was far above the inerting limit, and the hydrogen mole fraction, 0.062, was approaching the ignition limit. However, MARCH did not predict an upper-containment burn. The peak pressure, 41 psia (2.8 atm), was generated by the first of the three intermediate annular region burns.

For case D-3, HECTR predicted 19 wetwell burns, a period of wetwell inerting, 7 burns in the intermediate annular region, and a final burn in the intermediate annular region propagating into the upper containment. The peak pressure predicted was 48 psia (3.3 atm).

The results obtained for the configuration D cases show a variation in peak pressure, number of burns, etc, that indicate that the compartment model is ill-conditioned. Small variations in the input give considerably different results. Using MARCH, case D-1, which one would expect to generate the lowest peak pressure, generates the highest peak pressure; case D-3, which one would expect to generate the highest peak pressure, generates the lowest. The HECTR-predicted peak pressures do agree with the expectation of having D-1 the lowest and D-3 the highest.

Table 3.4. Configuration D – Case Descriptions and Results

Case No.	Initial Pressure psia	Hydrogen Mole Fraction for Ignition	Hydrogen Mole Fraction for Extinguishment	Burn Time, sec	Flame Propagation	Sprays	Peak Pressure, psia (atm)	Number of Significant Upper Containment Burns	Number of Significant Annular Region Burns
D-1	14.7	0.08	0.002	2	Yes	Auto	61 (4.2)	1	4
D-2	14.7	0.10	0. 002	2	Yes	Auto	46 (3.1)	1	4
D-3	14.7	0.08	0.002	2	Yes	No	41 (2.8)	0	3

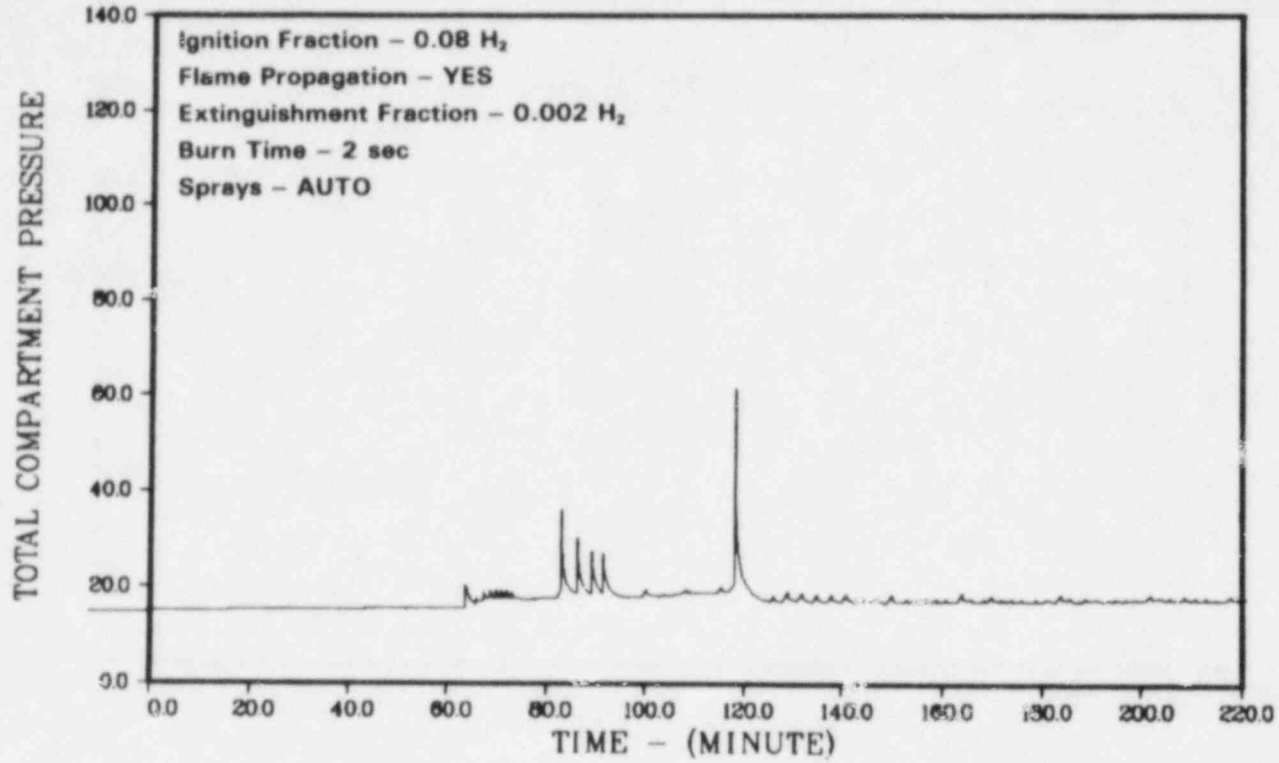

Figure 3.44. Case D-1, Pressure in Containment, psia

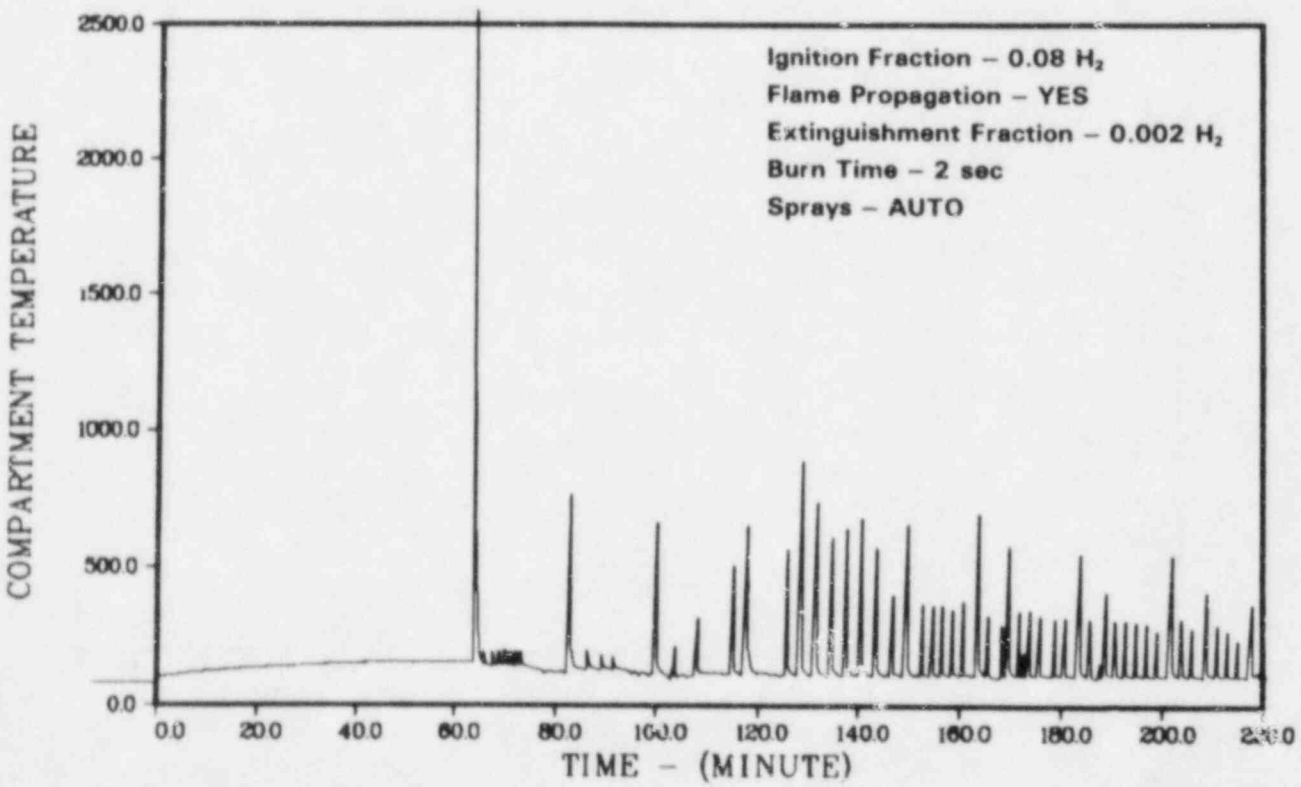

Figure 3.45. Case D-1, Temperature in Wetwell, °F

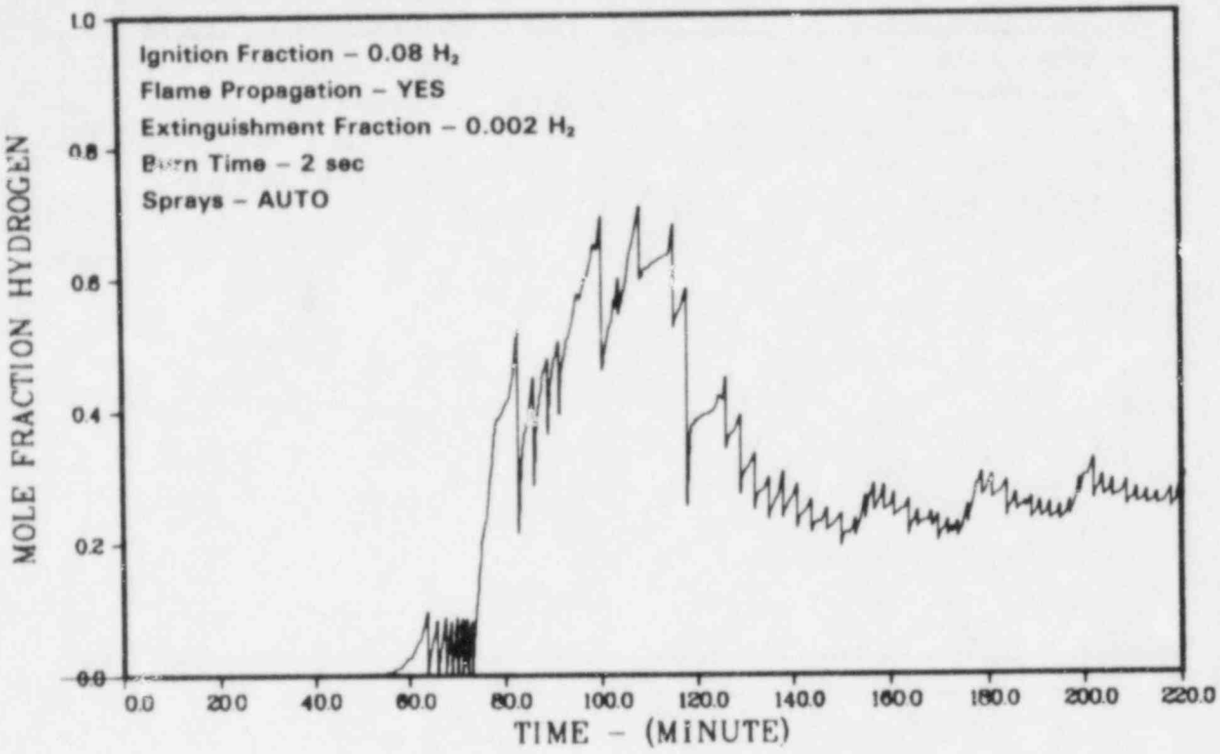

Figure 3.46. Case D-1, Hydrogen Mole Fraction in Wetwell

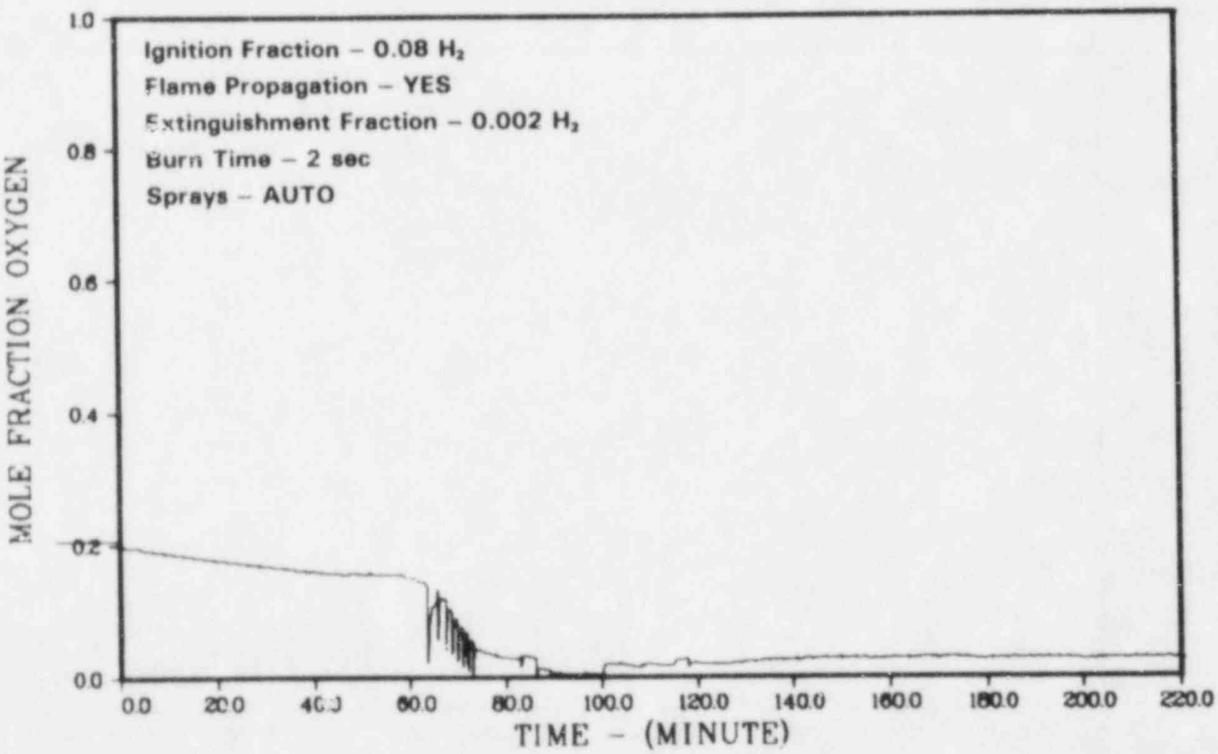

Figure 3.47. Case D-1, Oxygen Mole Fraction in Wetwell

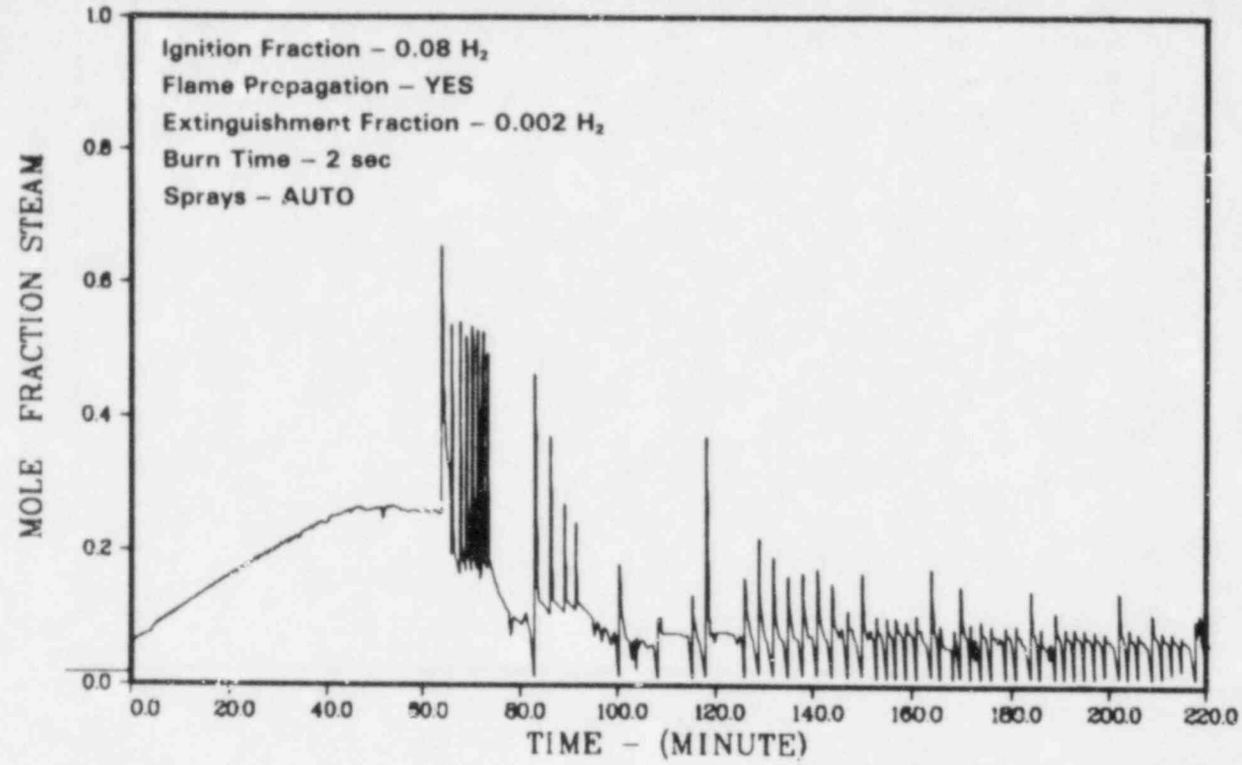

Figure 3.48. Case D-1, Steam Mole Fraction in Wetwell

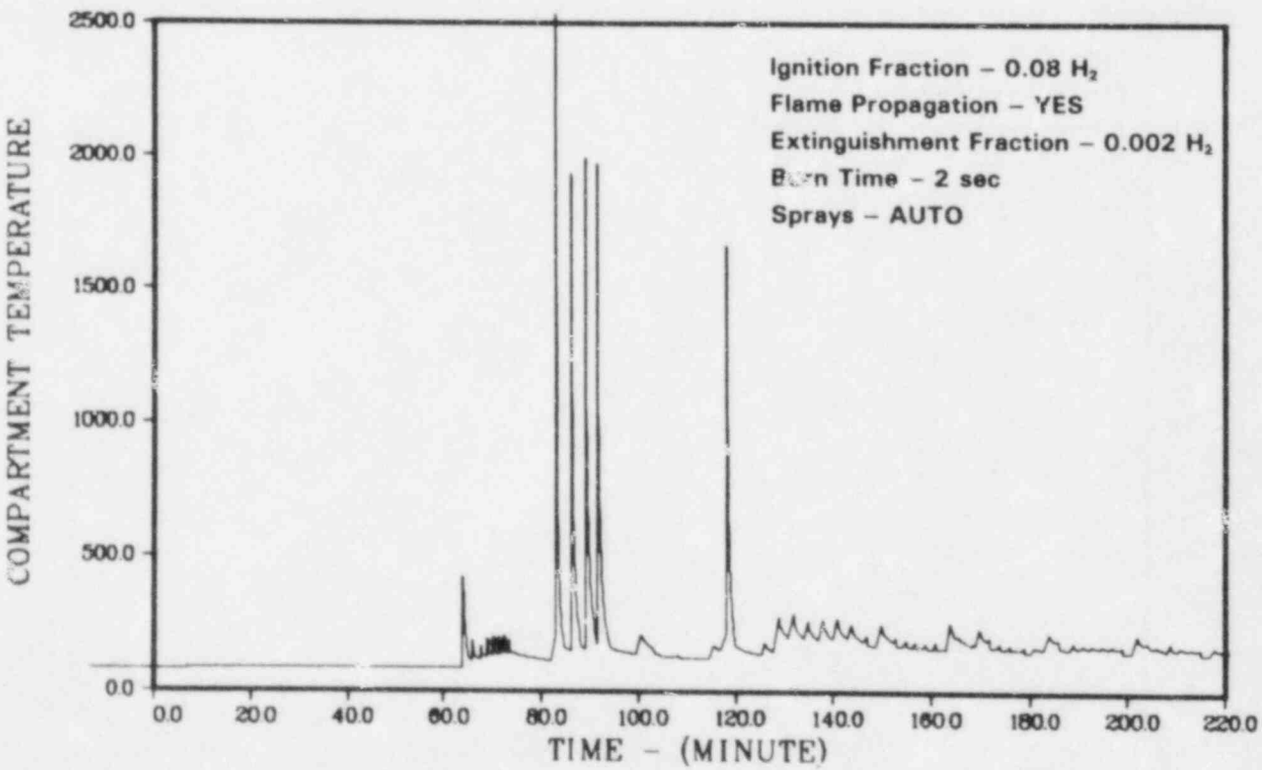

Figure 3.49. Case D-1, Temperature in Intermediate Annular Region, °F

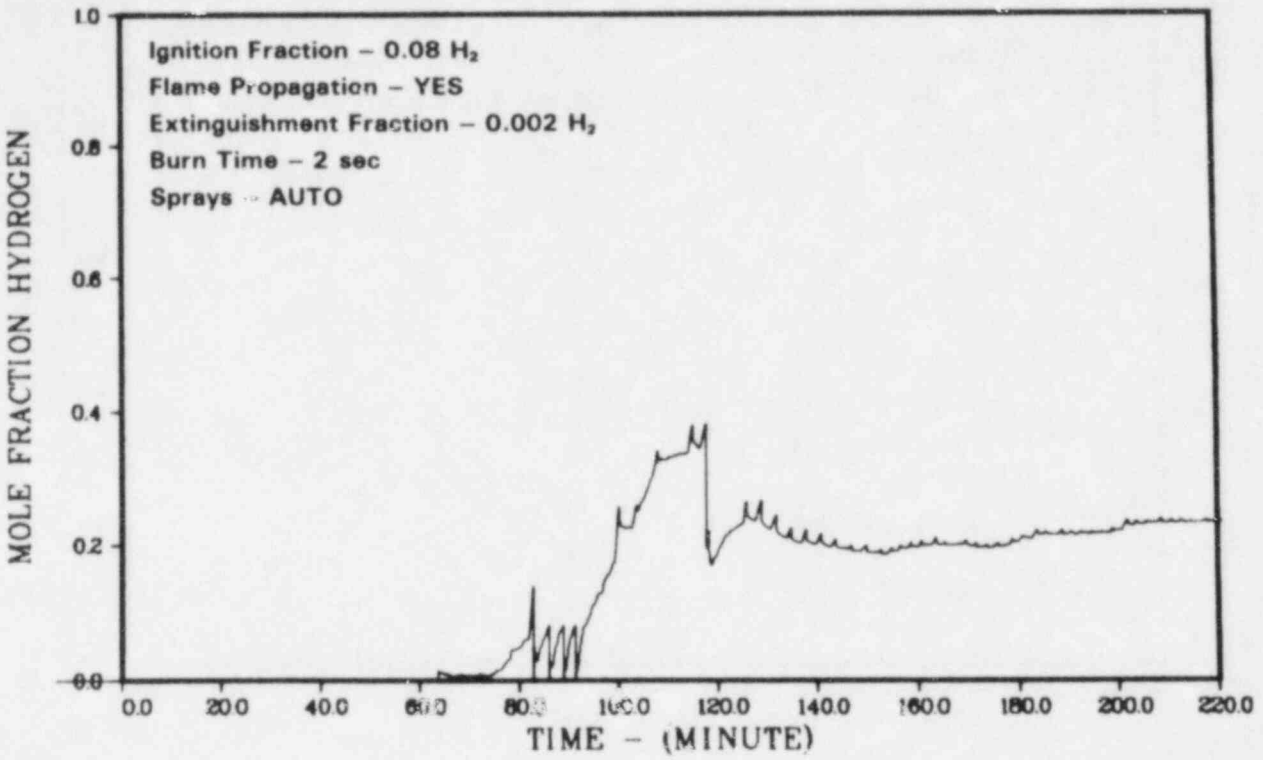

Figure 3.50. Case D-1, Hydrogen Mole Fraction in Intermediate Annular Region

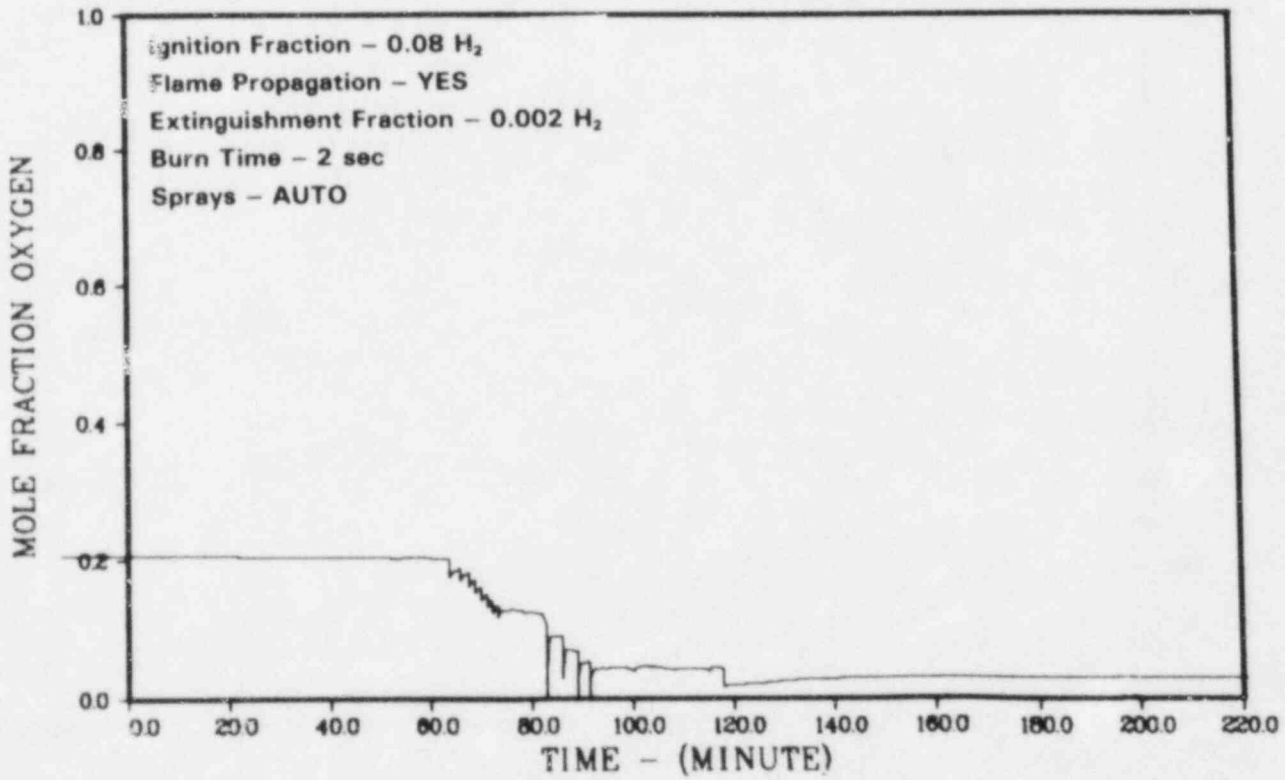

Figure 3.51. Case D-1, Oxygen Mole Fraction in Intermediate Annular Region

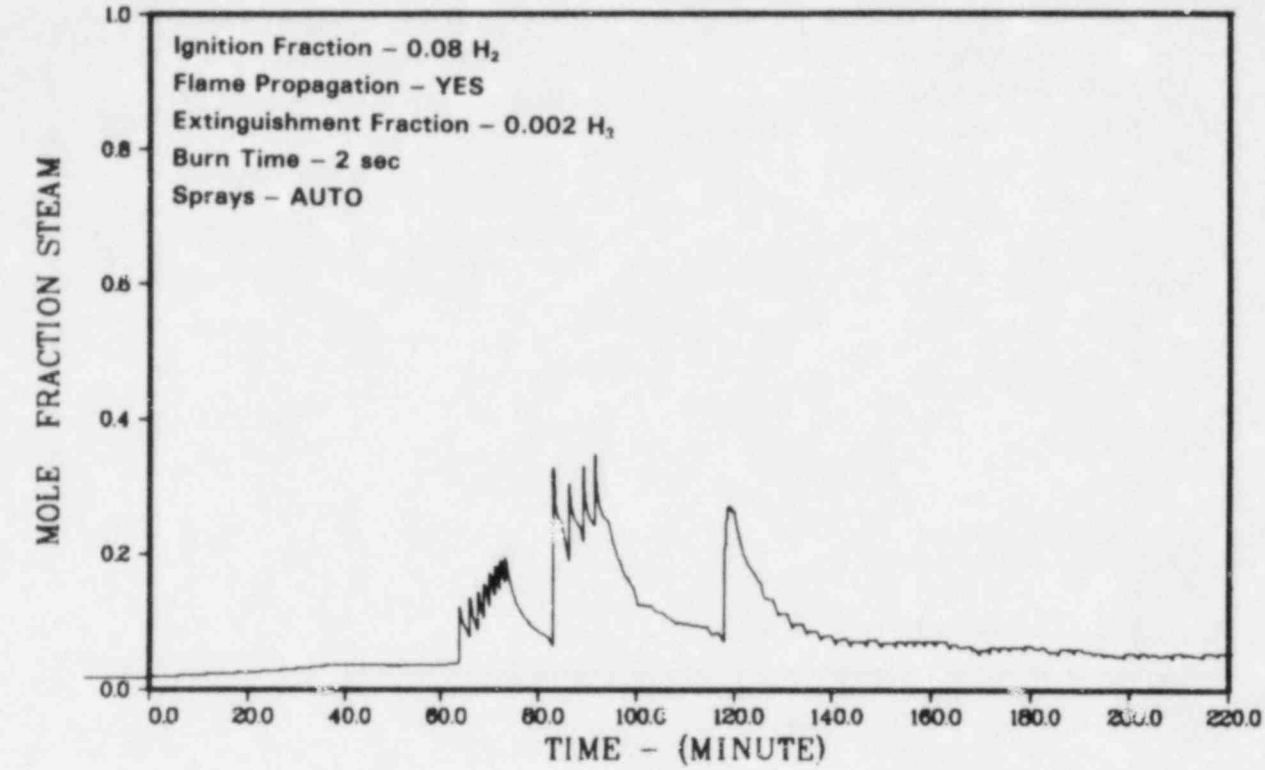

Figure 3.52. Case D-1, Steam Mole Fraction in Intermediate Annular Region

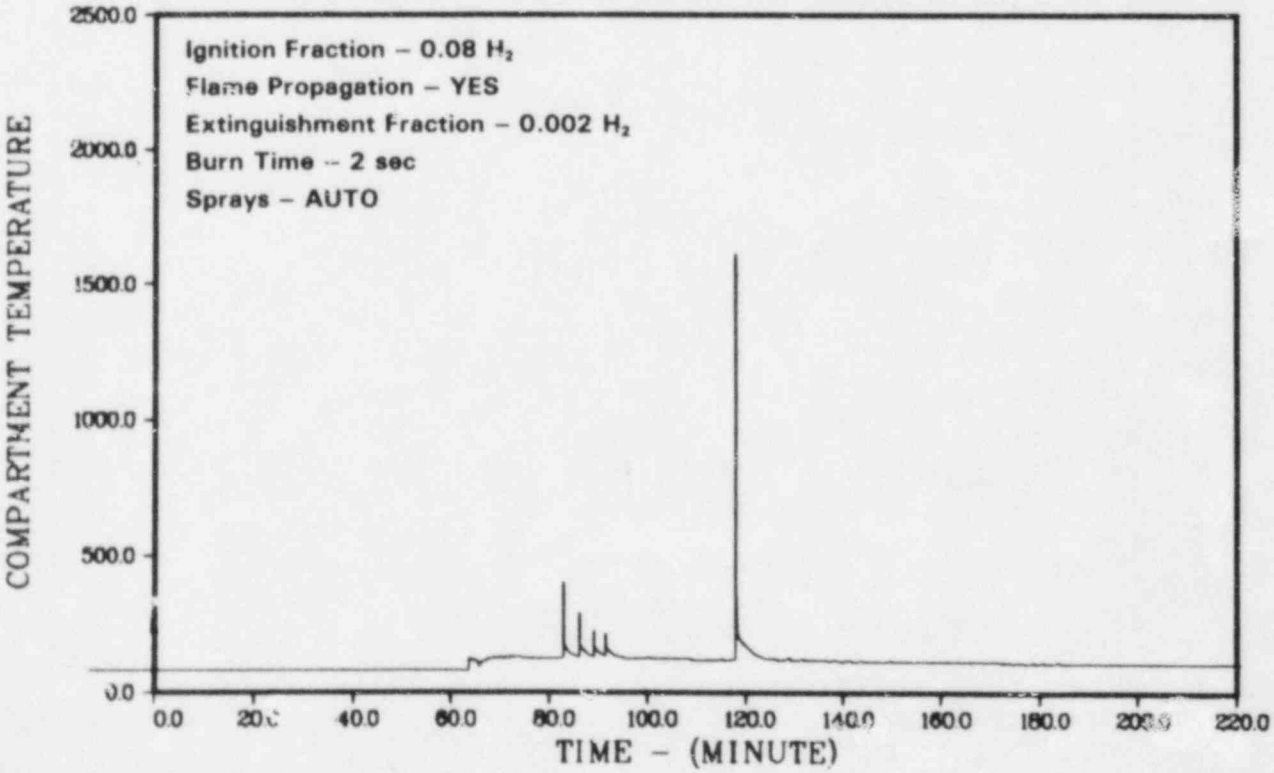

Figure 3.53. Case D-1, Temperature in Upper Containment, °F

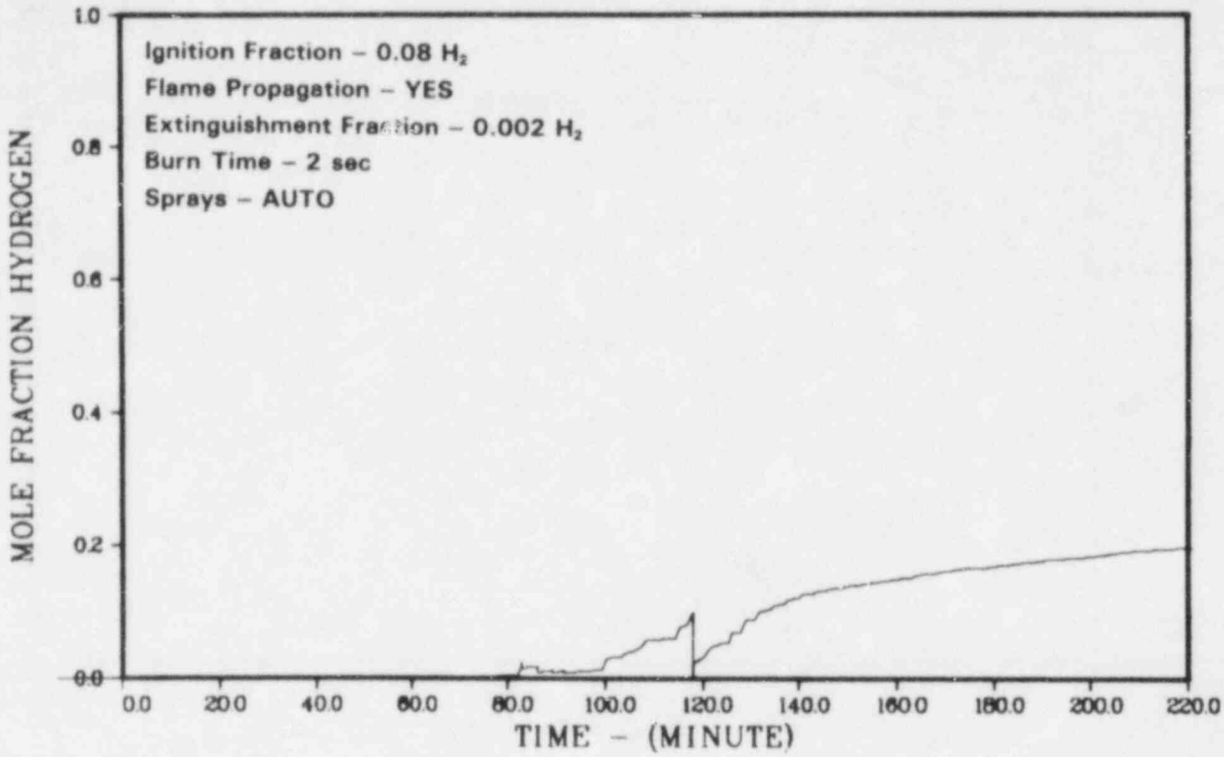

Figure 3.54. Case D-1, Hydrogen Mole Fraction in Upper Containment

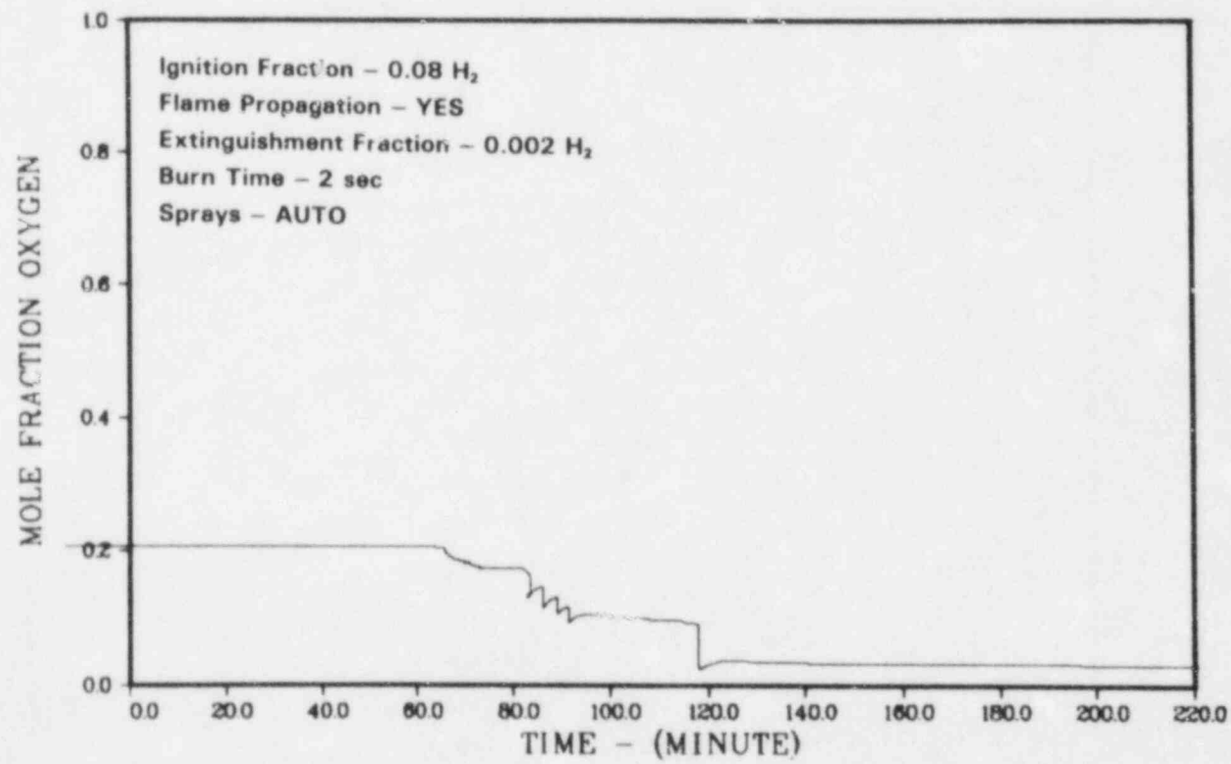

Figure 3.55. Case D-1, Oxygen Mole Fraction in Upper Containment

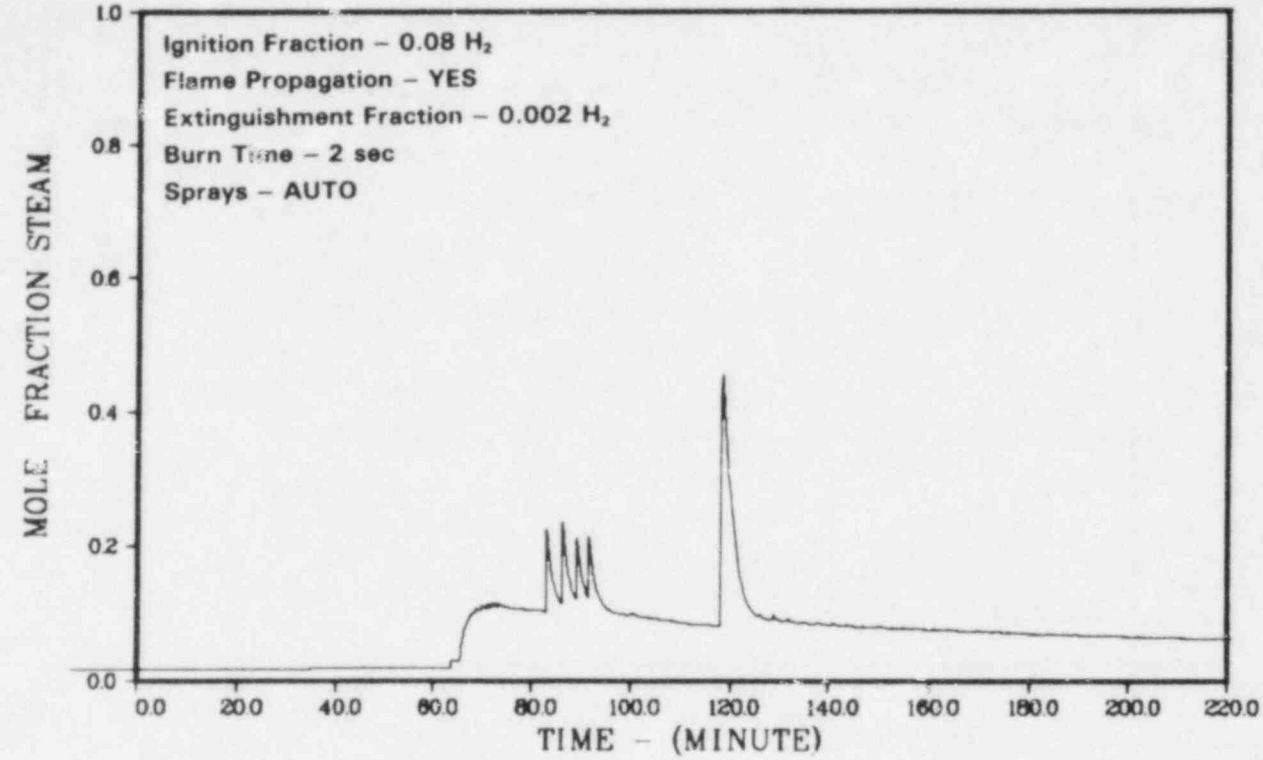

Figure 3.56. Case D-1, Steam Mole Fraction in Upper Containment

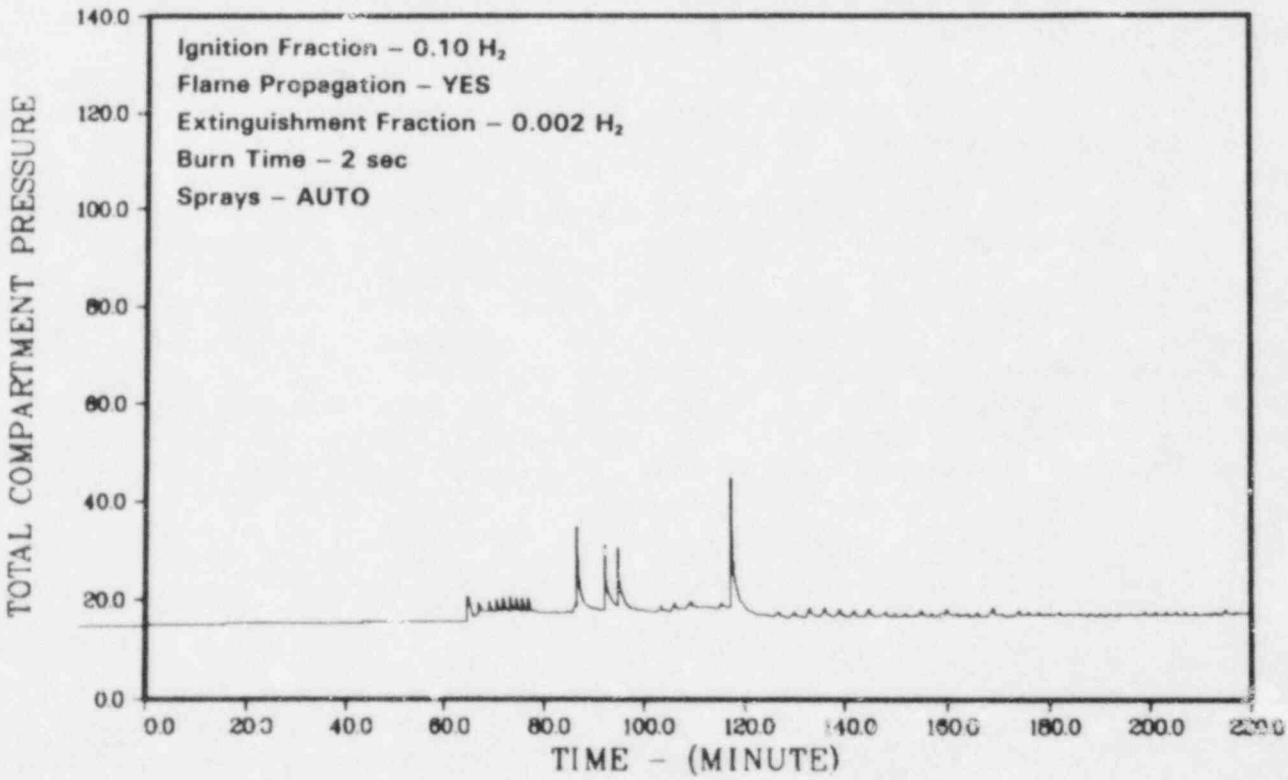

Figure 3.57. Case D-2, Pressure in Containment, psia

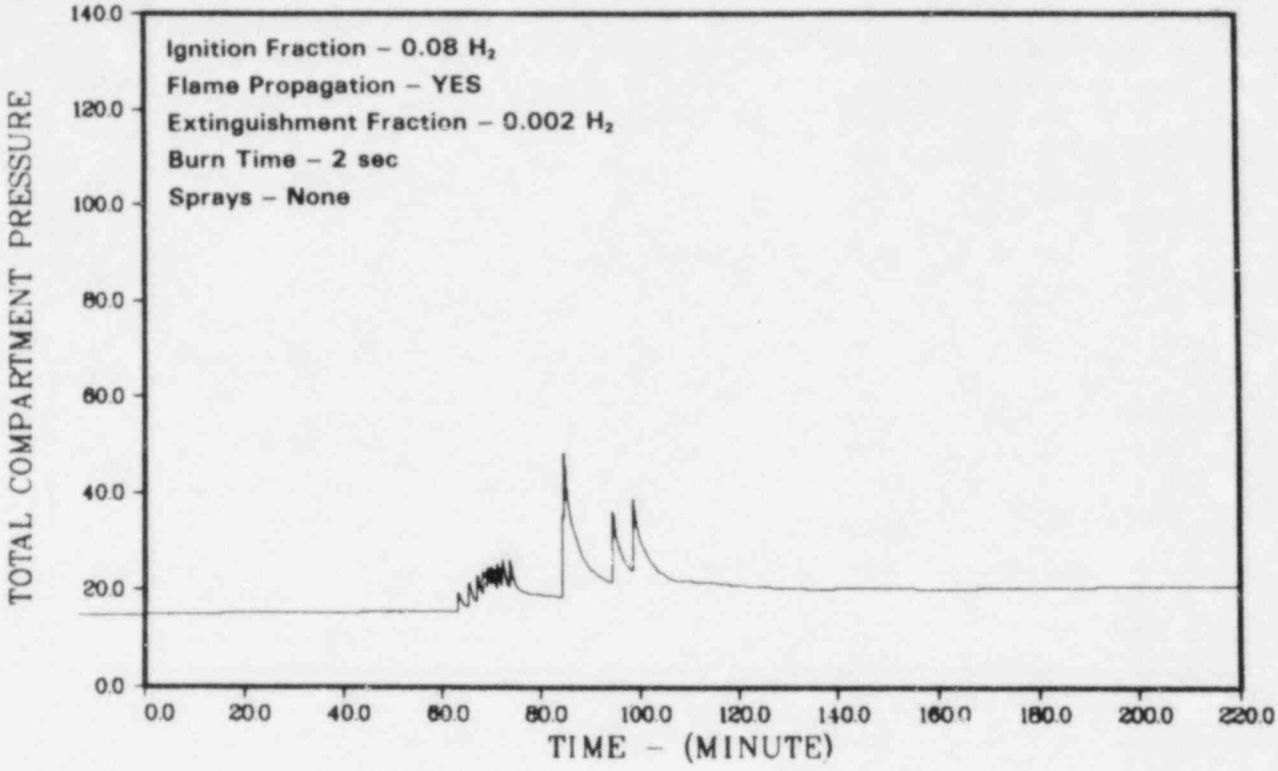

Figure 3.58. Case D-3, Pressure in Containment, psia

3.7 Analysis of MARCH Calculations for Configuration E′

The configuration E used in the HECTR analysis involved parallel flow paths from the bottom of the wetwell to the upper containment. Since MARCH cannot treat parallel flow paths we have modified the compartment configuration from E to E′. Configuration E′ consists of five compartments: a drywell, a wetwell, a lower annular region (from the 135 ft elevation to 165 ft elevation), an upper annular region (from the 165 ft elevation to the 209 ft elevation), and an upper containment volume. Examination of the HECTR configuration E results shows that the pie-shaped sector volume, eliminated in going from configuration E to E′, is of great importance to the calculations. Consequently, we do not have a HECTR result to compare to the result of this section. As in the previous sections, there was no flow path from the wetwell to the drywell. The drywell is therefore isolated and we will not discuss it.

In order to handle multiple compartments, we found it necessary to make changes in the MARCH code. For example, the plot subroutine had to be modified to give us graphs. In carrying out the following calculations, the MARCH code stopped the run about 105 min into the accident, instead of going out the full 220 min as in all other cases.

The behavior expected for configuration E′ was multiple wetwell burns, inerting of the wetwell, burns in the lower annular region, inerting of that region, burns in the upper annular region, inerting of that

region, and finally burning in the upper containment. This is roughly the behavior that was found, but MARCH did not predict an upper containment burn during the first 165 min of the accident.

In case E'-1 the hydrogen mole fraction for ignition was 0.10 and sprays came on after the first two wetwell burns. The initial pressure was 14.7 psia and initial temperature was 80°F. The mole fraction for extinguishment was 0.002 hydrogen, burn time was 2 s and flame propagation was allowed into all compartments with more than 0.002 H_2. Graphical results are shown in Figures 3.59 through 3.75. MARCH predicted seven burns mainly in the wetwell, after which the wetwell stayed inerted due to oxygen depletion. The next four burns took place mainly in the lower annular region, which was then inerted due to oxygen depletion. The final three burns took place in the upper annular region, which was then inerted due to oxygen depletion. At 165 min into the accident the lower three containment compartments were inerted due to oxygen depletion, but the upper containment still had a considerable amount of oxygen. The wetwell and lower annular region had very high mole fractions of hydrogen, the upper annular region had a mole fraction of hydrogen approaching 0.20, but the upper containment still had very little hydrogen. It is not clear if there would have eventually been an upper containment burn if the MARCH calculation had continued. The peak pressure predicted without an upper containment burn was low, 35 psia (2.4 atm).

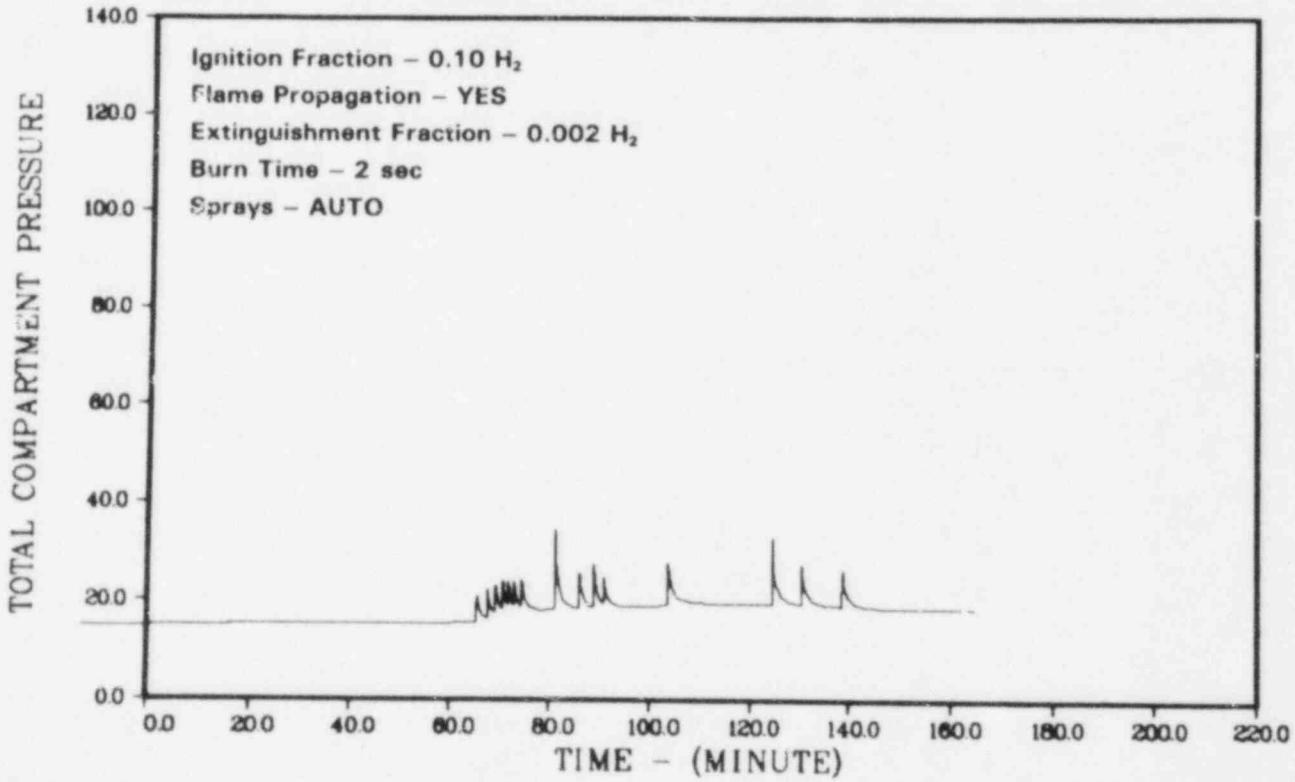

Figure 3.59. Case E', Pressure in Containment, psia

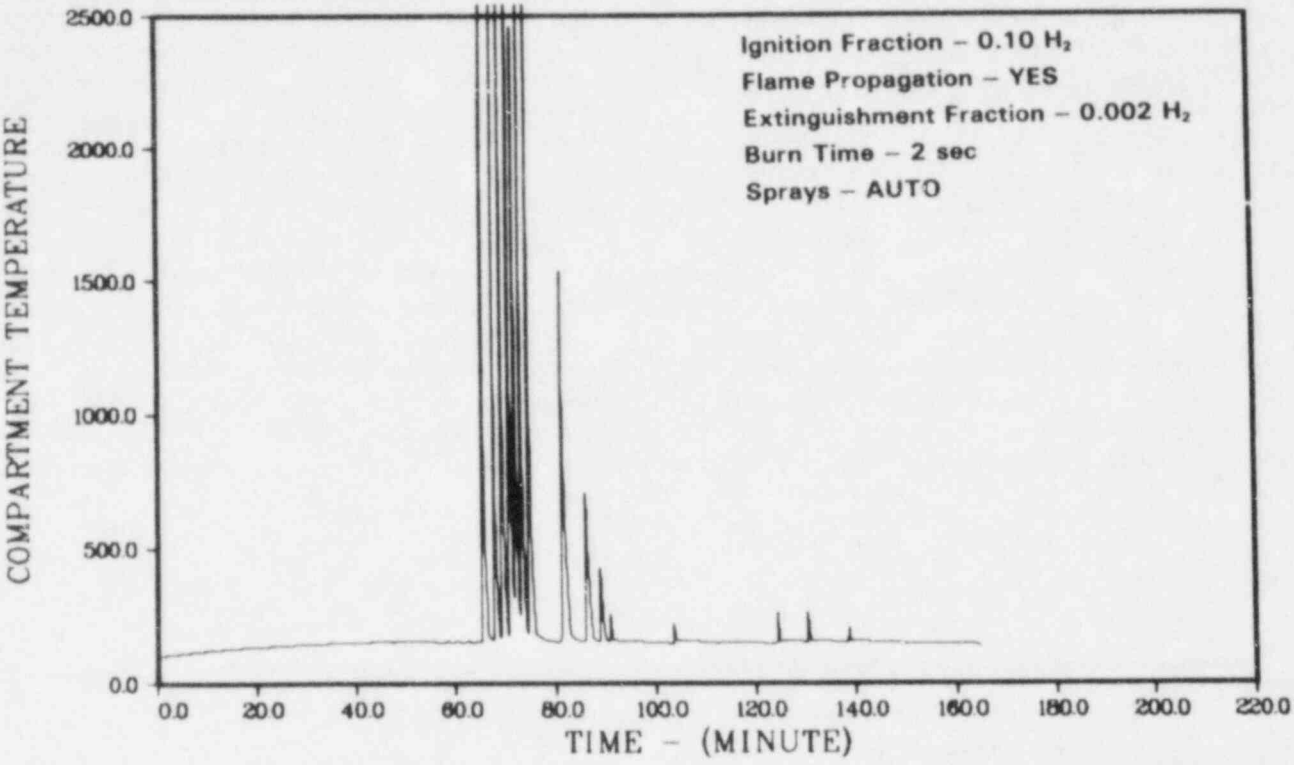

Figure 3.60. Case E', Temperature in Wetwell, °F

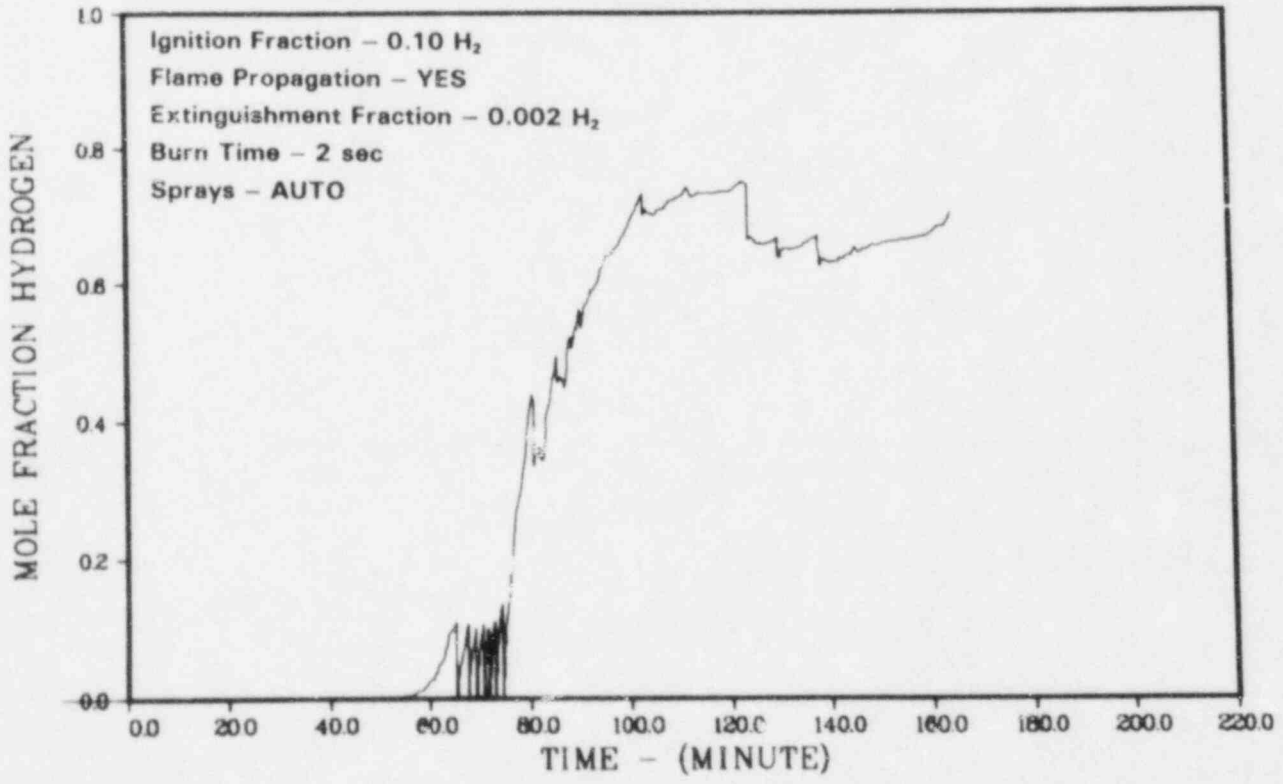

Figure 3.61. Case E', Hydrogen Mole Fraction in Wetwell

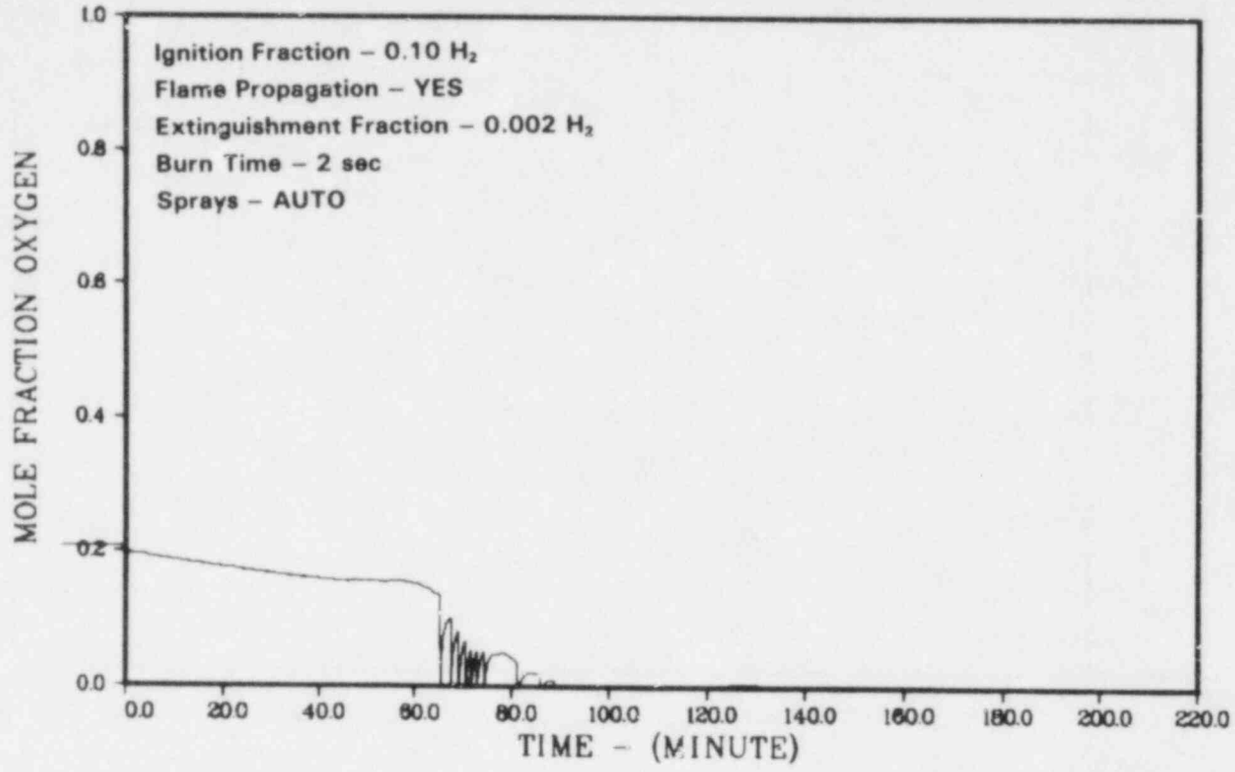

Figure 3.62. Case E', Oxygen Mole Fraction in Wetwell

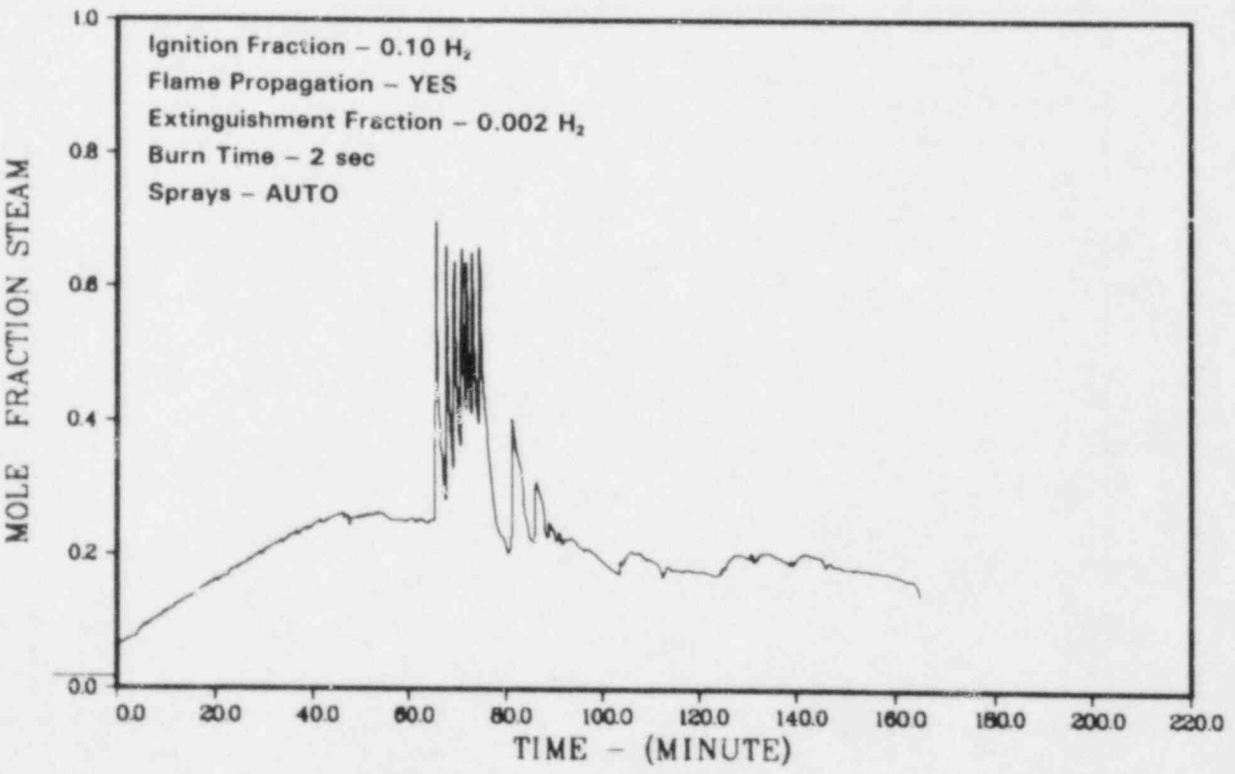

Figure 3.63. Case E', Steam Mole Fraction in Wetwell

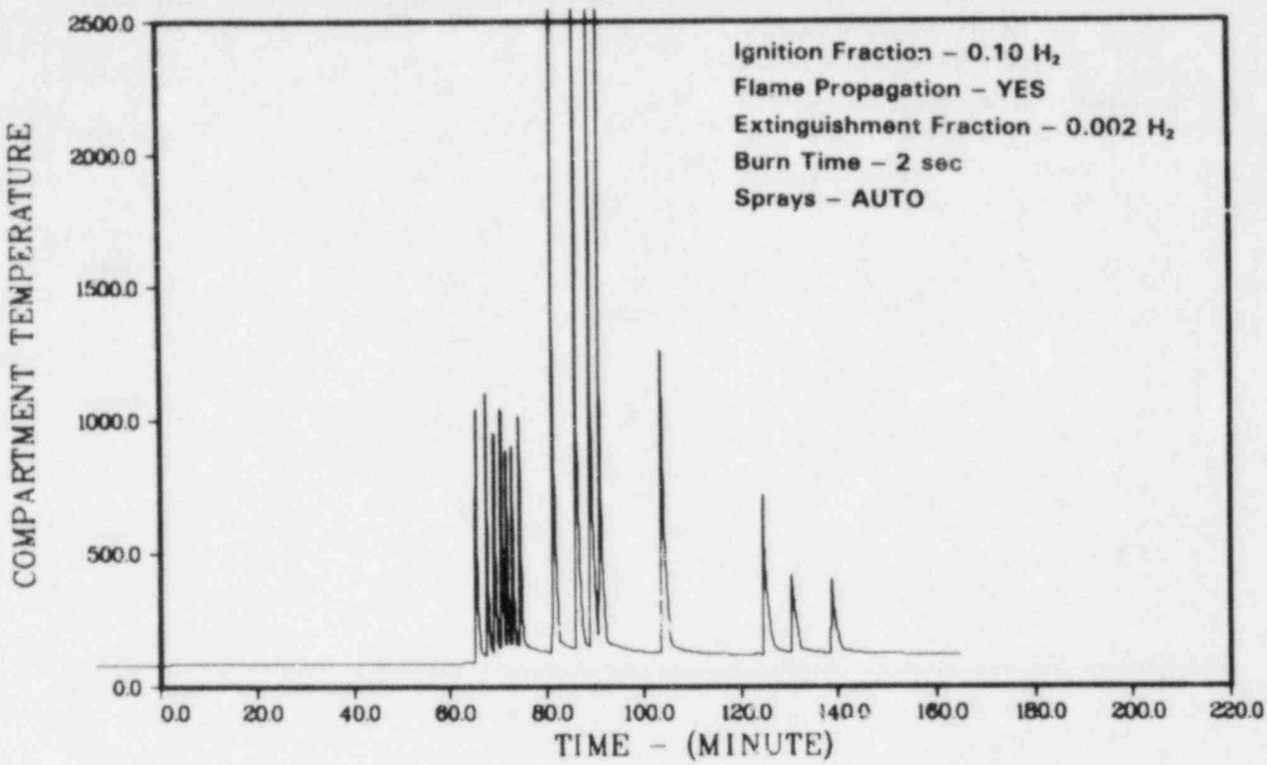

Figure 3.64. Case E′, Temperature in Lower Annular Region, °F

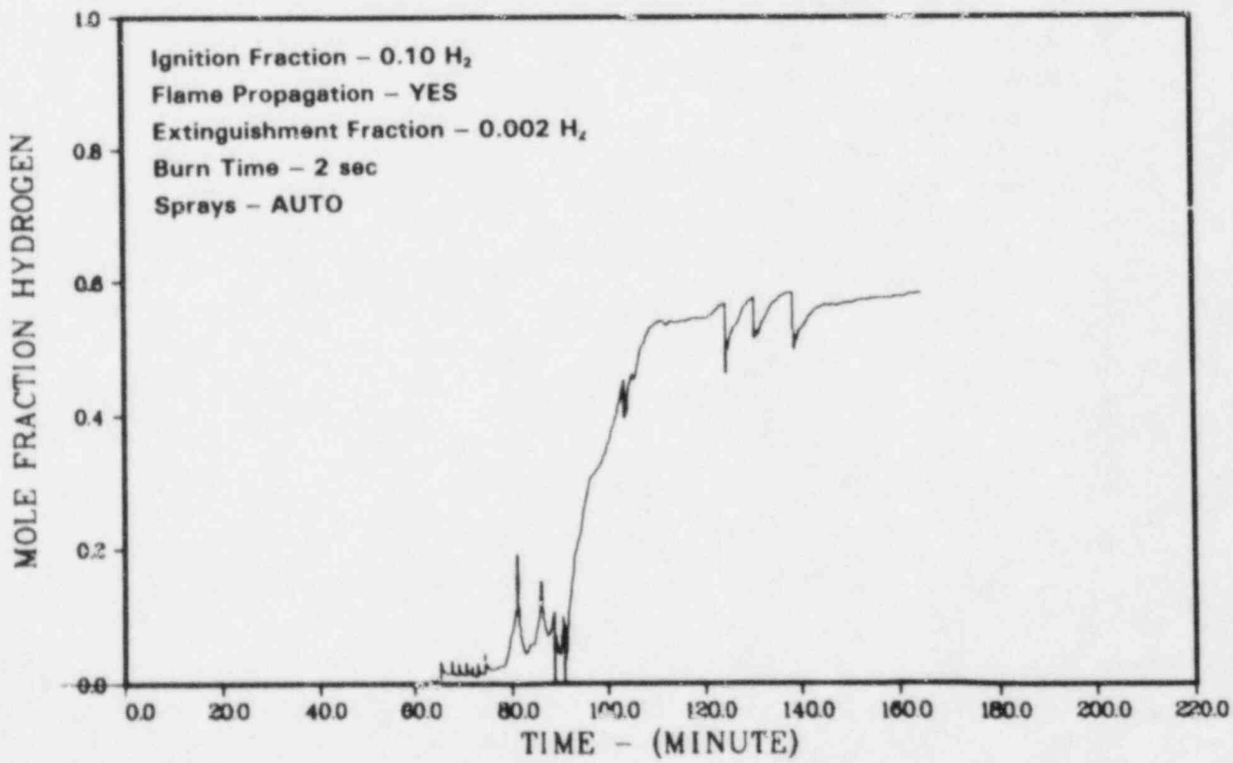

Figure 3.65. Case E′, Hydrogen Mole Fraction in Lower Annular Region

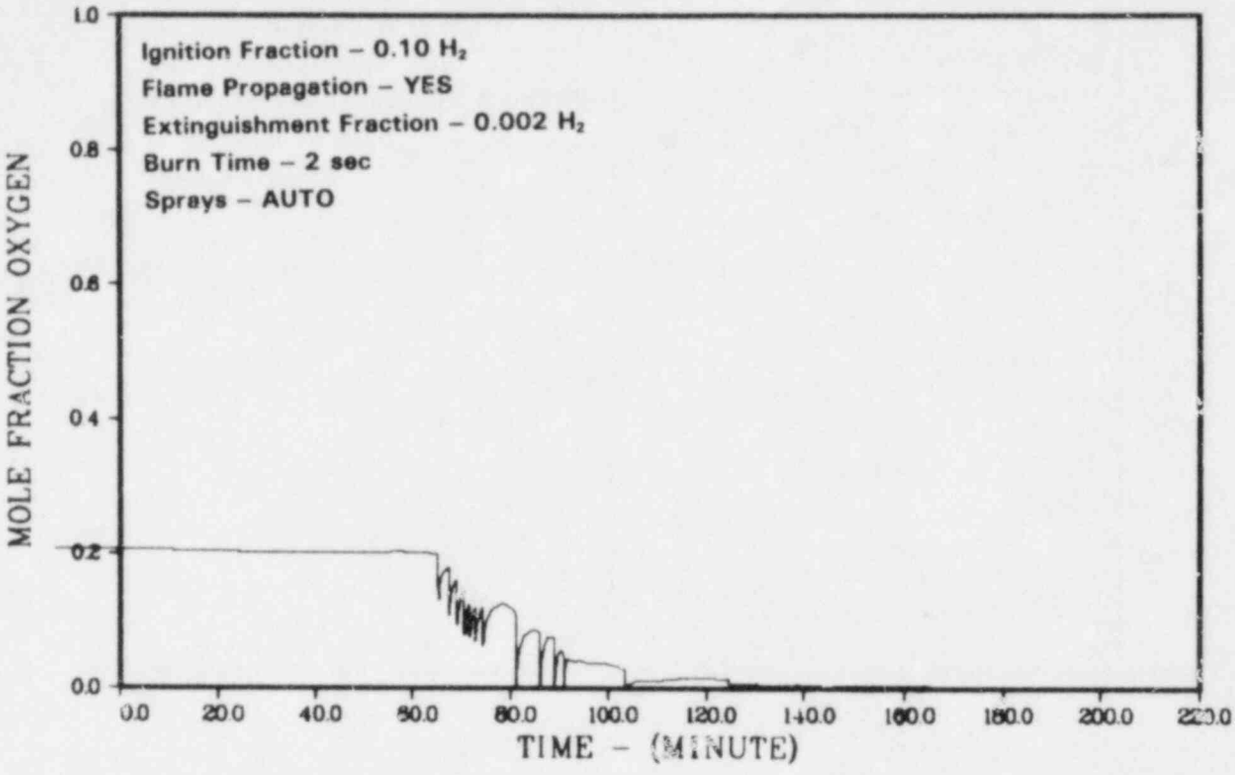

Figure 3.66. Case E', Oxygen Mole Fraction in Lower Annular Region

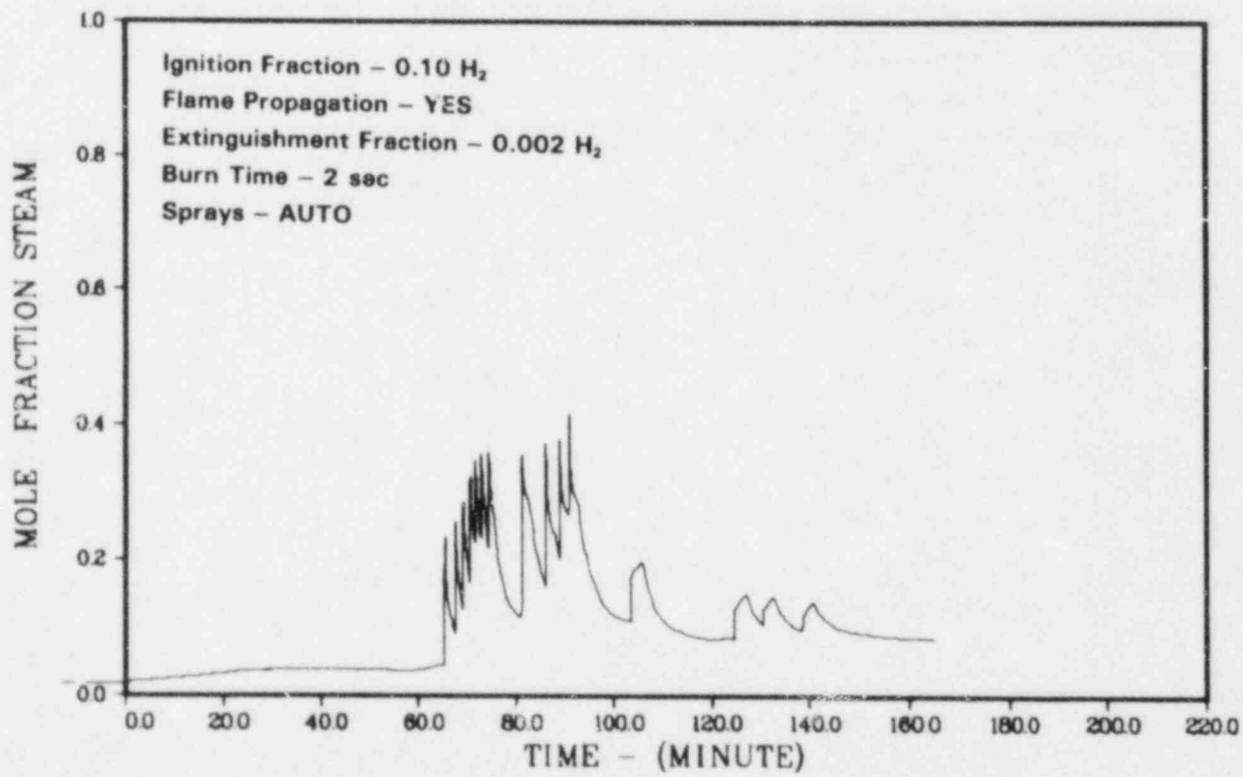

Figure 3.67. Case E', Steam Mole Fraction in Lower Annular Region

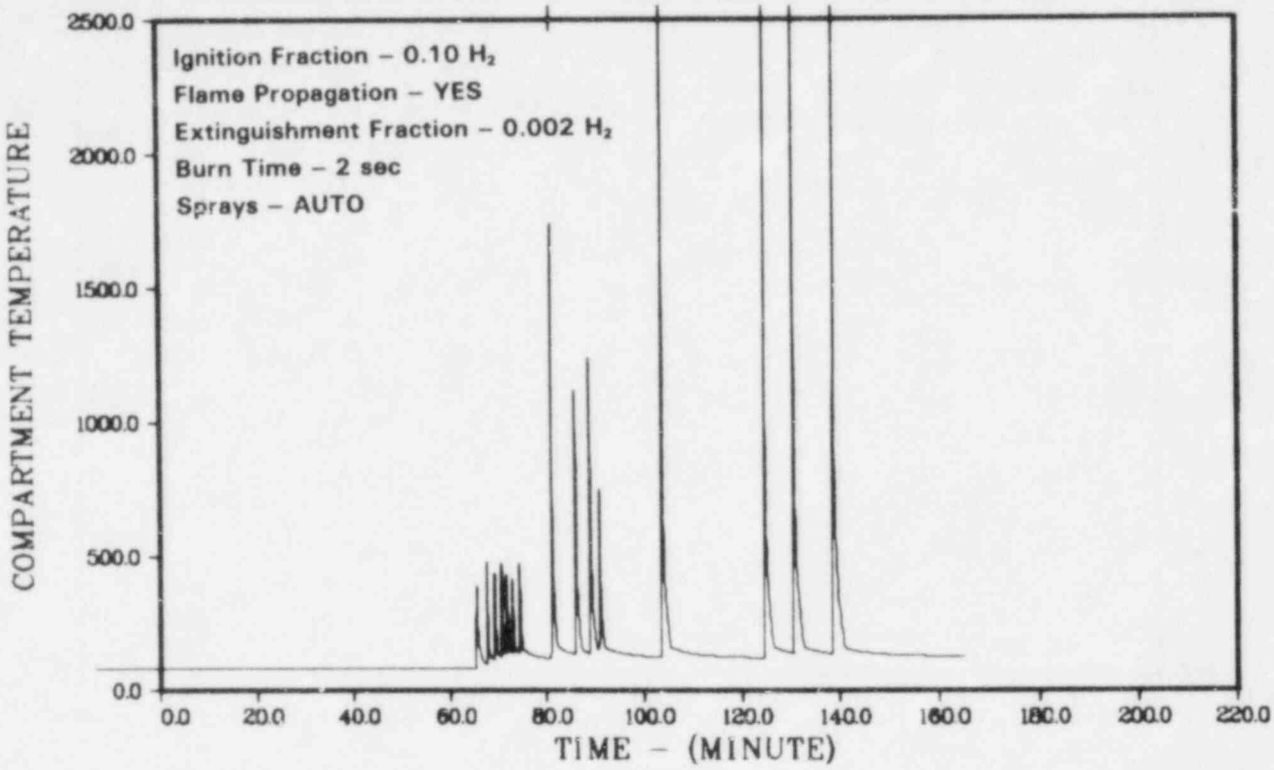

Figure 3.68. Case E', Temperature in Upper Annuiar Region. °F

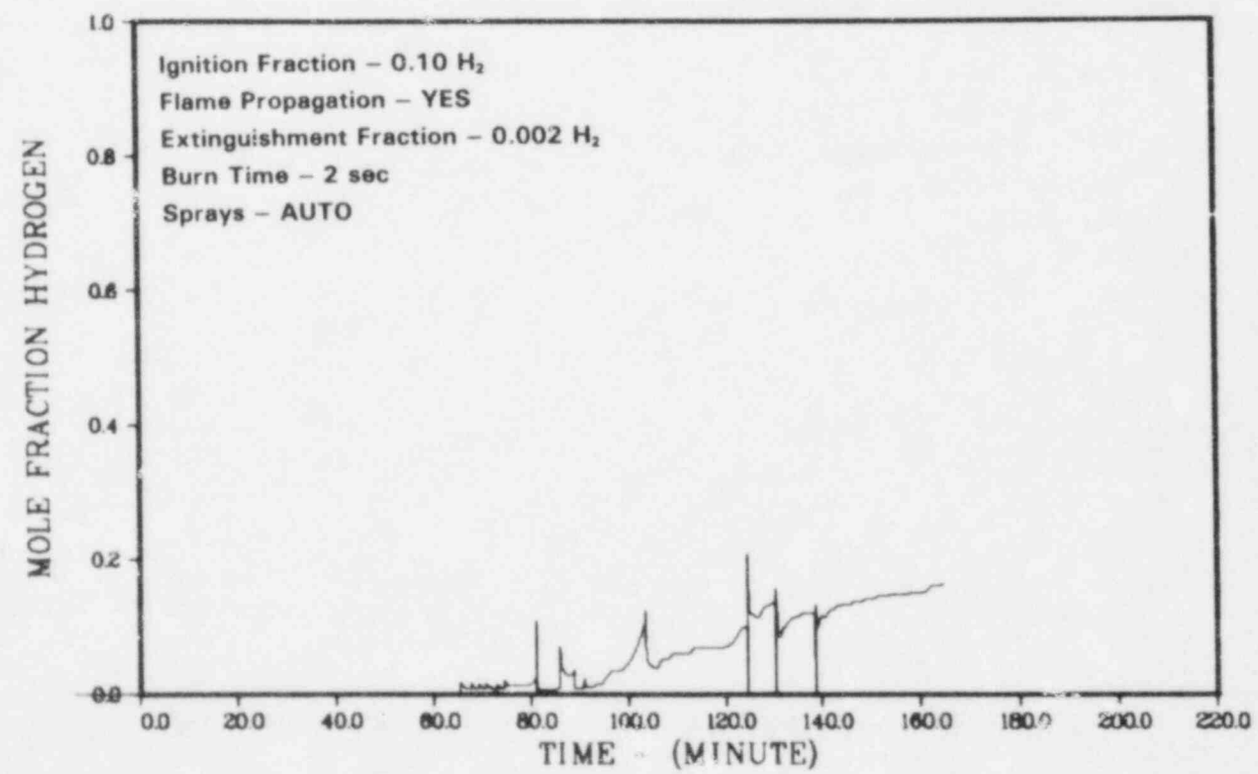

Figure 3.69. Case E', Hydrogen Mole Fraction in Upper Annular Region

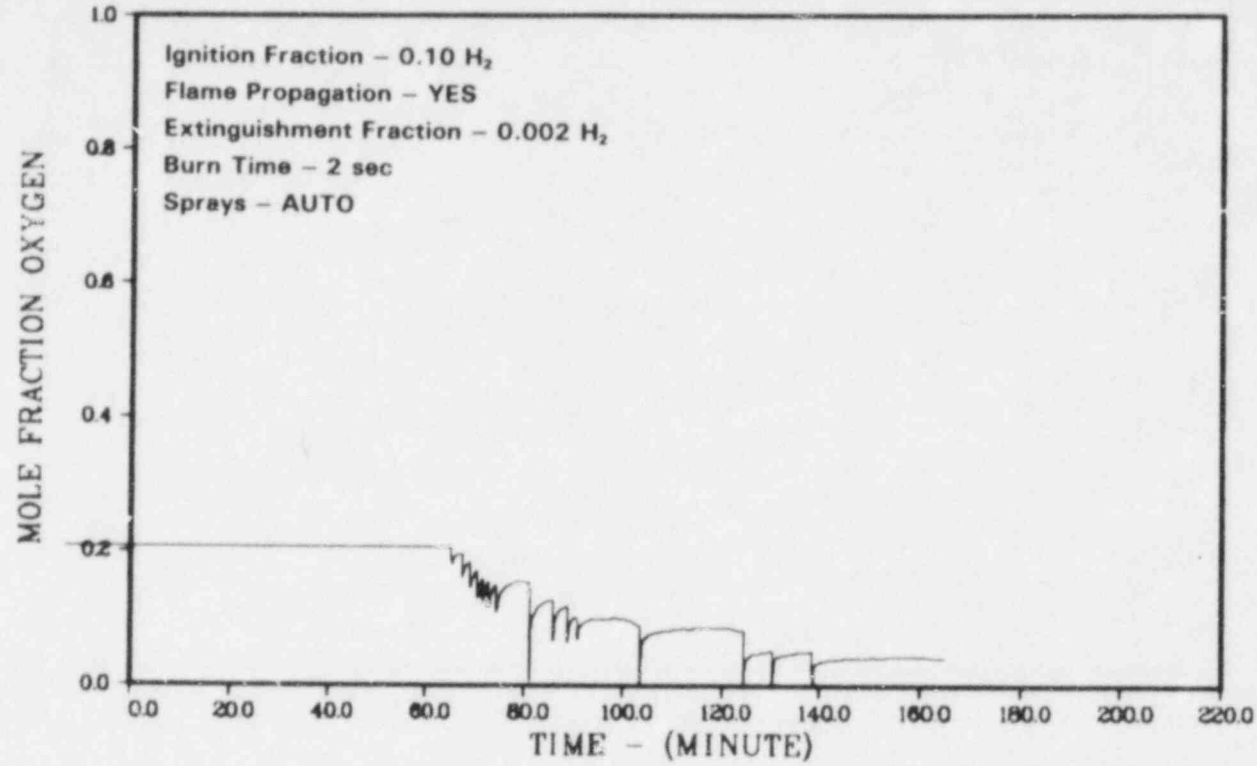

Figure 3.70. Case E', Oxygen Mole Fraction in Upper Annular Region

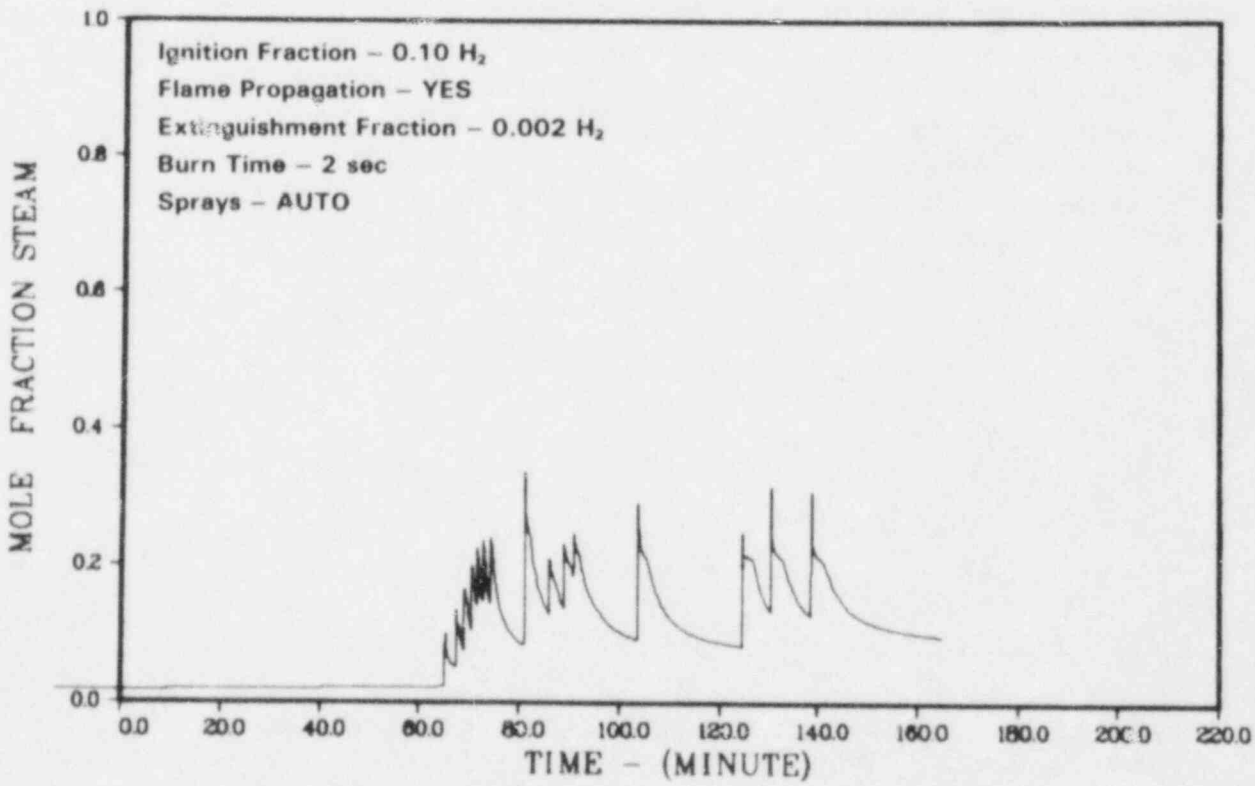

Figure 3.71. Case E', Steam Mole Fraction in Upper Annular Region

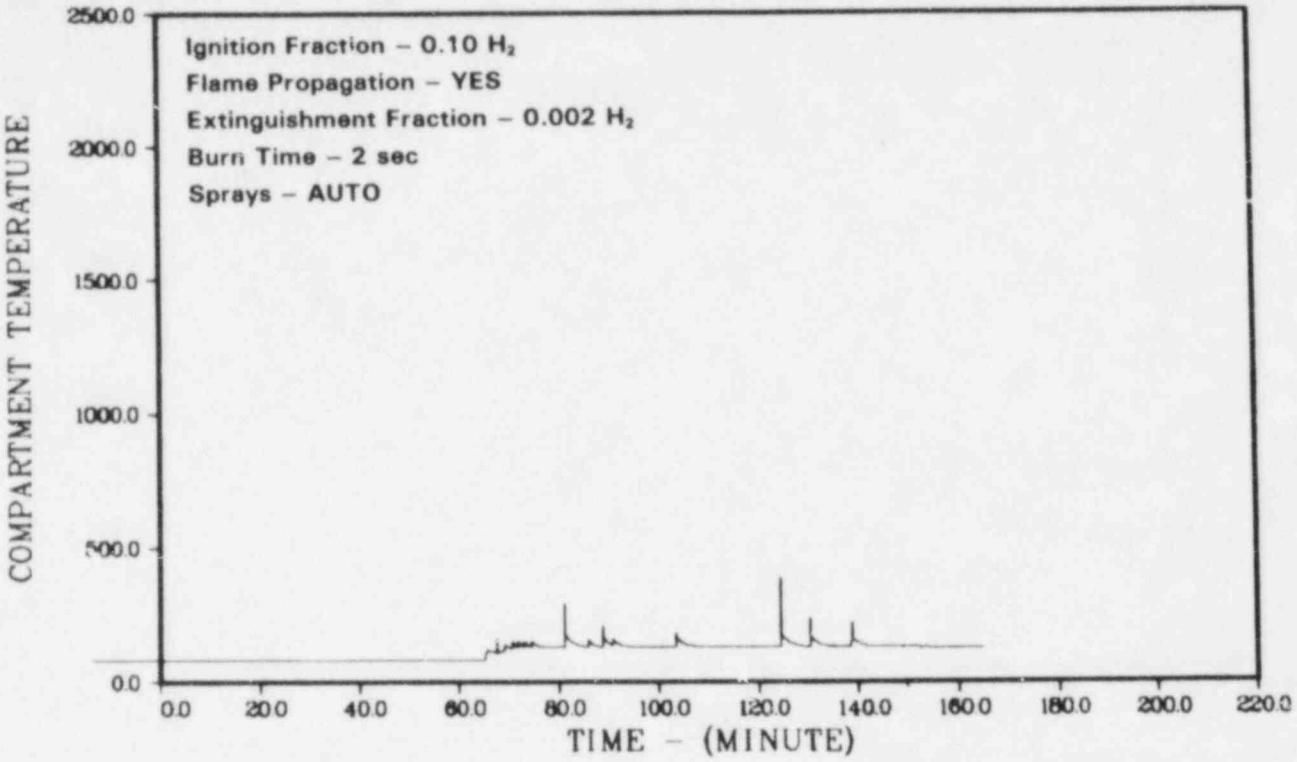

Figure 3.72. Case E', Temperature in Upper Containment

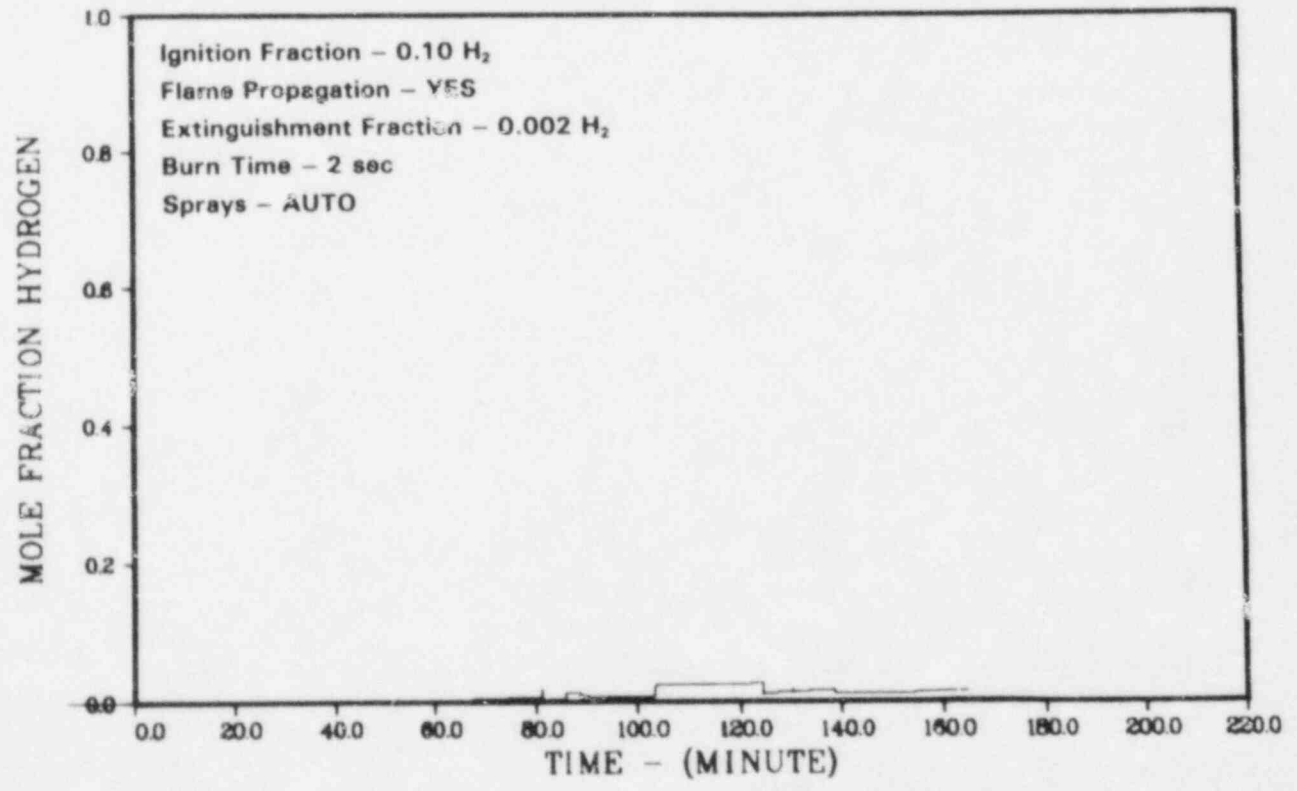

Figure 3.73. Case E', Hydrogen Mole Fraction in Upper Containment

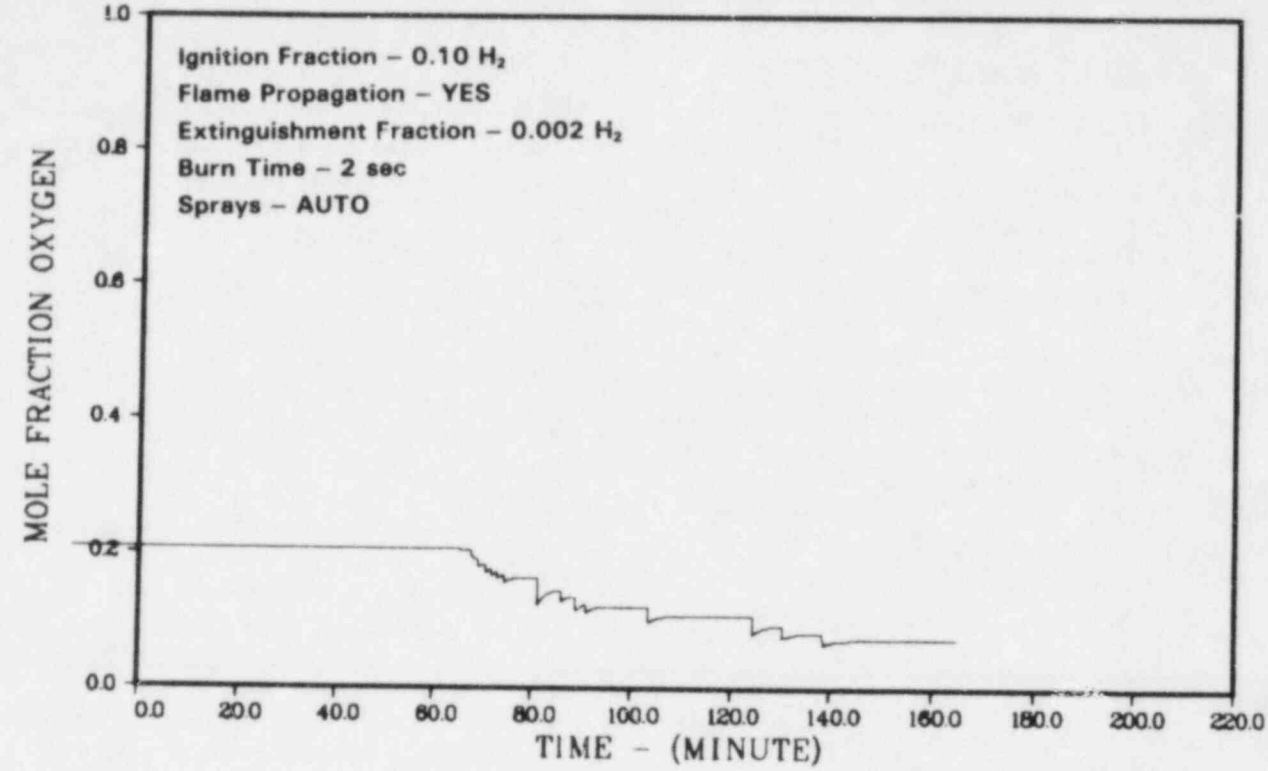

Figure 3.74. Case E′, Oxygen Mole Fraction in Upper Containment

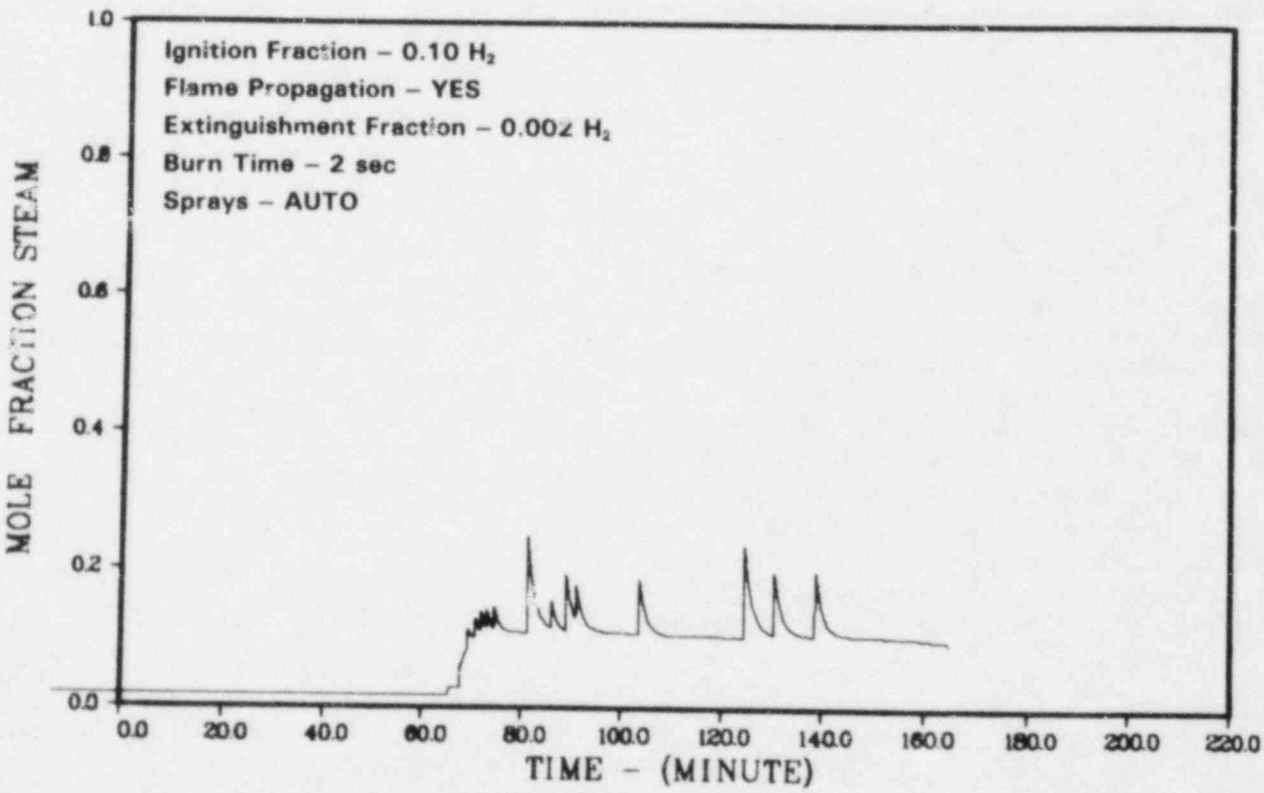

Figure 3.75. Case E′, Steam Mole Fraction in Upper Containment

3.8 The Effect of Connections to the Drywell from the Wetwell/Containment

In the MARCH calculations discussed in sections 3.3 to 3.7, a connection was used from the drywell to the wetwell, but no connection was used back to the drywell. Our models isolated the drywell so that comparisons could be made with the results of the HECTR code. In this section, we include the effects of the drywell by adding a zero-flow-resistance connection from either the wetwell or a region corresponding to the entrance of the vacuum breakers. In Appendix C, we mention that flow back to the drywell may occur when the suppression pool is forced down below the level of the drywell vents, and that this flow may be much more important than that through the vacuum breakers. CLASIX-3 uses a finite-flow-resistance connection to model the vacuum breaker flow,* and apparently also considers flow back to the drywell through the suppression pool.

For the TPE accidents, all that was changed in this section from the corresponding cases in the previous section was the addition of a connection to the drywell. For the accidents modelling breaks from the reactor coolant system into the drywell, additional changes were made in the code to send the steam and hydrogen from the reactor system into the drywell rather than the suppression pool and to set the initial pressure in all compartments to 14.7 psia (1.0 atm). The TPE accidents that are reconsidered in this section are cases A-6, A-7, B-2, B-6, B-7, C-2, and D-2; the drywell break accidents that are reconsidered are A-5, A-9, and B-1.

For configurations A and C, there is no distinction between a connection through the vacuum breakers and one through the suppression pool. For configuration B, the vacuum breaker entrance is in the upper containment. For configuration D, the vacuum breaker entrance is in the intermediate annular region.

Case A-7 considered an ignition criterion of 0.10 hydrogen mole fraction and no containment sprays; case A-9 is identical except containment sprays are on. The results are shown in Table 3.5 and Figures 3.76 and 3.77 (also in Figures 3.12 and 3.13). For both cases in which there was a connection to the drywell, some hydrogen did enter. Because of the flame propagation option used, this hydrogen was burned, but in no case was the burn mole fraction of hydrogen high enough for a burn to be called significant. In case A-6 without a connection to the drywell, the final state of the wetwell was close to igniting a third burn. The results shown in Table 3.5 indicate that the effect of the drywell is to lower the peak pressure (for the TPE accident using configuration A), but by less than 10 psia (0.7 atm).

Cases A-5 and A-9 model LOCAs with a break inside the drywell. Graphical results for case A-5 are shown in Figures 3.78 through 3.86, and the pressure history for case A-9 is shown in Figure 3.87. The results for the two cases with and without a connection to the drywell are shown in Table 3.6. For these two cases, air is driven from the drywell early in the accident. The drywell is therefore inerted due to oxygen depletion. The procedure of assuming an initial pressure of 17 psia in the wetwell and neglecting the drywell is reasonable for the two cases shown in Table 3.6. The peak pressures with the connected drywell are a little lower than without the drywell.

For configuration B, one has a choice of connecting the wetwell back to the drywell, simulating backflow through the suppression pool, or connecting the upper containment back to the drywell, simulating flow through the vacuum breakers. We have carried out runs with both options (Figures 3.88, 3.89; also Figure 3.26). The results for case B-2 are shown in Table 3.7. It is clear that for configuration B the number of wetwell burns is as highly sensitive to the assumptions made about the drywell connections as it is to other input assumptions. The variation in the peak pressure between the cases is significant. The use of a connection from the upper containment to the drywell (the choice used in CLASIX-3) gave the lowest peak pressure and avoided a drywell burn.

With the flame propagation option used in case B-6, the burns extend through all connected compartments. The results for case B-6 are shown in Table 3.8 (Figures 3.90, 3.91; also Figure 3.30). We indicate the number of burns with significant combustion of hydrogen in the compartment. These results indicate no consistent pattern of peak pressure vs drywell connection except that the model with the upper containment to drywell connection produced the lowest peak pressures, and the wetwell to drywell connection led to a drywell burn.

Case B-7 differs from B-6 only in that the sprays were turned on after the first burn instead of early in the accident. The results for this case are shown in Table 3.9 and Figures 3.92 and 3.93 (also Figure 3.31). The results agree in pattern with those of case B-6.

*We believe that the CLASIX-3 calculation of flow through the vacuum breakers (1.09-ft^2 total flow area) may be too large. Details of that calculation are not available at present.

Case B-1 also considered a LOCA break inside the drywell, as in cases A-5 and A-9, but employed the configuration B compartment model. The results are shown in Table 3.10 and Figure 3.94 (also Figures 3.16 through 3.24). In this case, the addition of a drywell gave a significant reduction in peak pressure, contrary to the cases considered with a break in the drywell for configuration A.

In configuration C, the vacuum breakers are in the large wetwell volume, so for MARCH it does not matter if one assumes flow through the suppression pool or the vacuum breakers. The results for case C-2 with a wetwell-to-drywell connection are unique. Graphical results are shown in Figures 3.95 through 3.107. This MARCH calculation is the only one in which there was no upper containment burn (except possibly for case E'-1). MARCH predicted six wetwell burns. At the end of the run, the upper containment had mole fractions of 0.082 for hydrogen and 0.084 for oxygen. The mole fractions in the wetwell were 0.487 for hydrogen and 0.029 for oxygen. Clearly, if the atmosphere were allowed to mix, or a bit more hydrogen were produced, or the ignition limit for hydrogen mole fraction were reduced, there would be an upper-containment burn. Without an upper-containment burn, the peak pressure was low, 27 psia (1.8 atm). The results are compared in Table 3.11 to the case without a drywell connection (Figures 3.95 through 3.107; also Figure 3.41).

Using configuration D, one has two choices:

- Making a connection from the wetwell to the drywell, simulating flow through the suppression pool
- Making a connection from the intermediate annular volume to the drywell, simulating flow through the vacuum breakers.

We have carried out a case D-2 calculation with a connection from the wetwell to the drywell and then from the intermediate annular region to the drywell. The pressure histories are shown in Figures 3.108 and 3.109. The results are shown in Table 3.12. The addition of a connection from the wetwell to the drywell resulted in a somewhat lower peak pressure and one drywell burn. The addition of a connection from the intermediate annular region to the drywell led to a slight increase in peak pressure and also one drywell burn.

3.9 References

[3.1] M. Berman, ed, *Light Water Reactor Safety Research Program Semiannual Report, April-September 1981*, NUREG/CR-2481, SAND82-0006, February 1982.

[3.2] R. O. Wooton and H. I. Avci, *MARCH (Meltdown Accident Response Characteristics Code Description and User's Manual*, Battelle Columbus Laboratories, NUREG/CR-1711, BMI-2064 R3 October 1980.

[3.3] J. B. Rivard et al, *Interim Technical Assessment of the MARCH Code*, Sandia National Laboratories, NUREG/CR-2285, SAND81-1672 R3, November 1981.

Table 3.5. Effect of Connections to the Drywell on Cases A-6 and A-7

	Case A-6		Case A-7	
	No Connection	Connection	No Connection	Connection
Peak Pressure (psia)	80	71	56	51
(atm)	5.4	4.8	3.8	3.5
No. of Significant Burns in Wetwell	2	3	3	3
No. of Significant Burns in Drywell	0	0	0	0

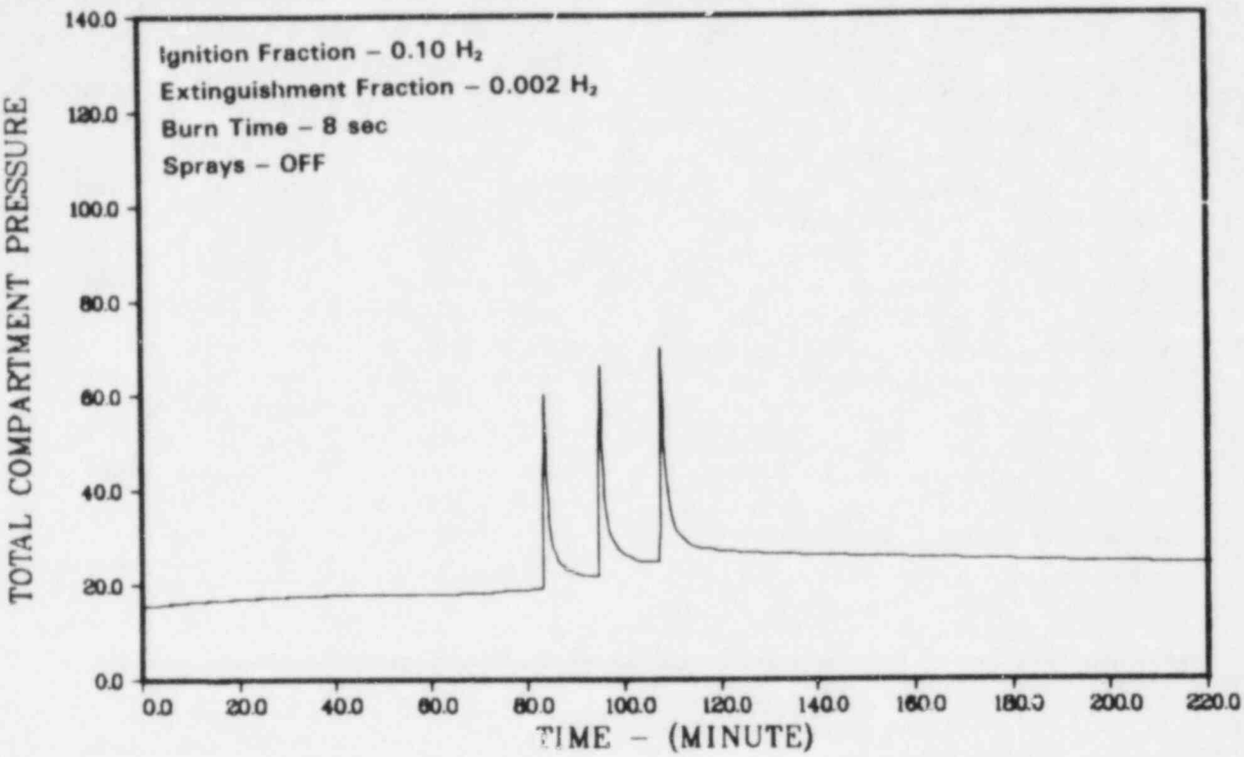

Figure 3.76. Case A-6 (With Containment to Drywell Connection), Pressure in Containment, psia

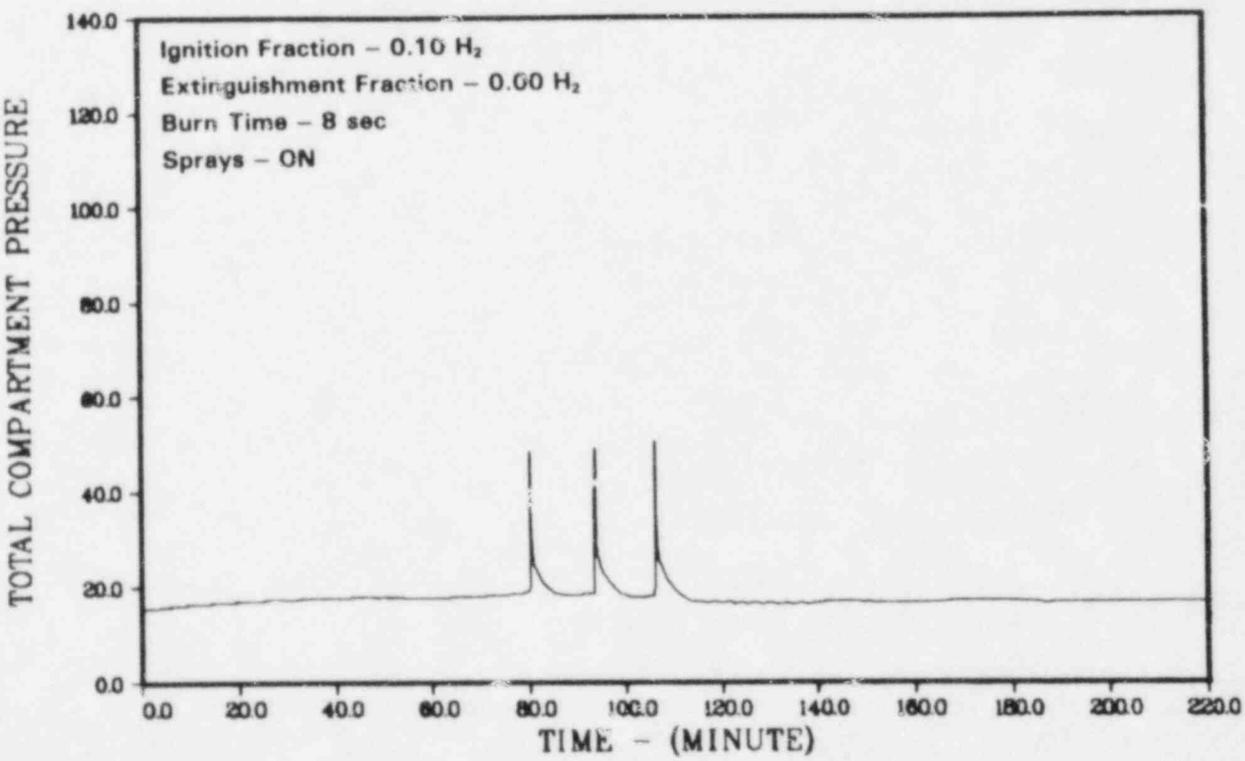

Figure 3.77. Case A-7 (With Containment to Drywell Connection), Pressure in Containment, psia

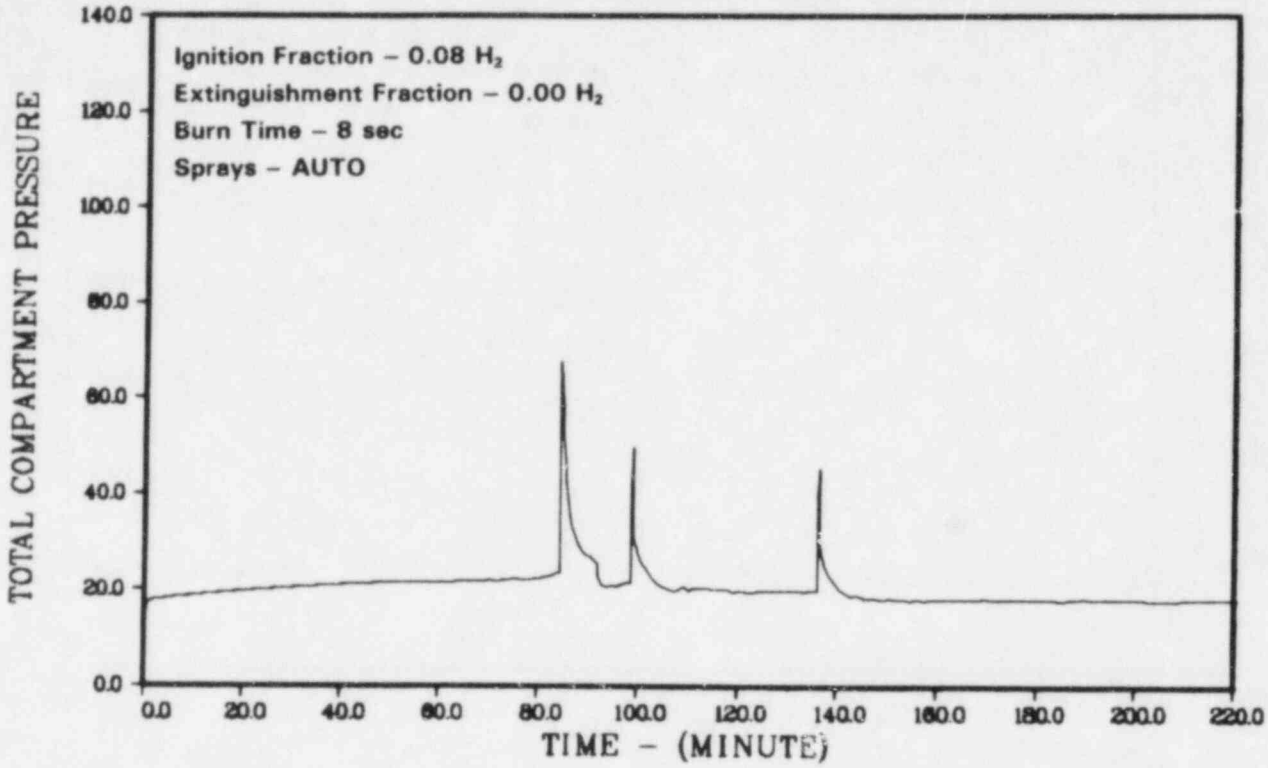

Figure 3.78. Case A-5, Pressure in Containment, psia

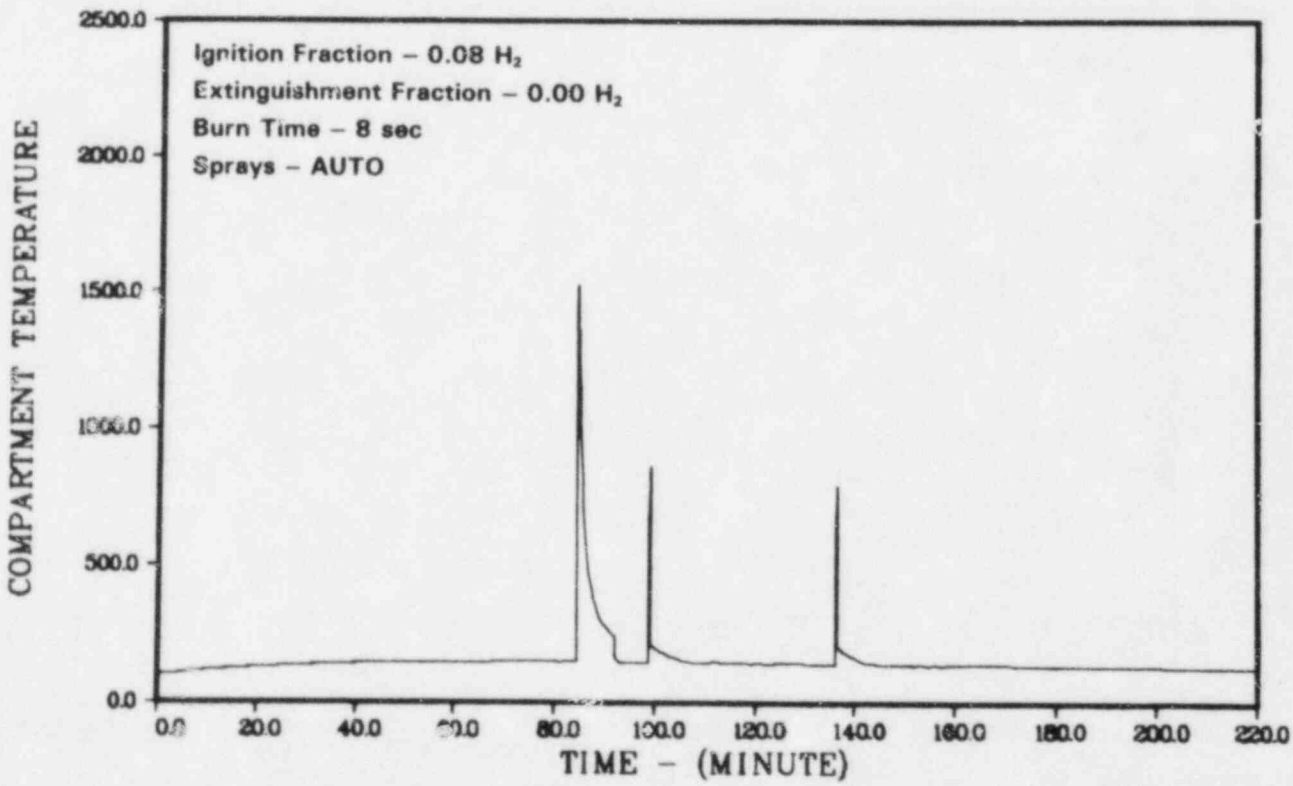

Figure 3.79. Case A-5, Temperature in Containment, °F

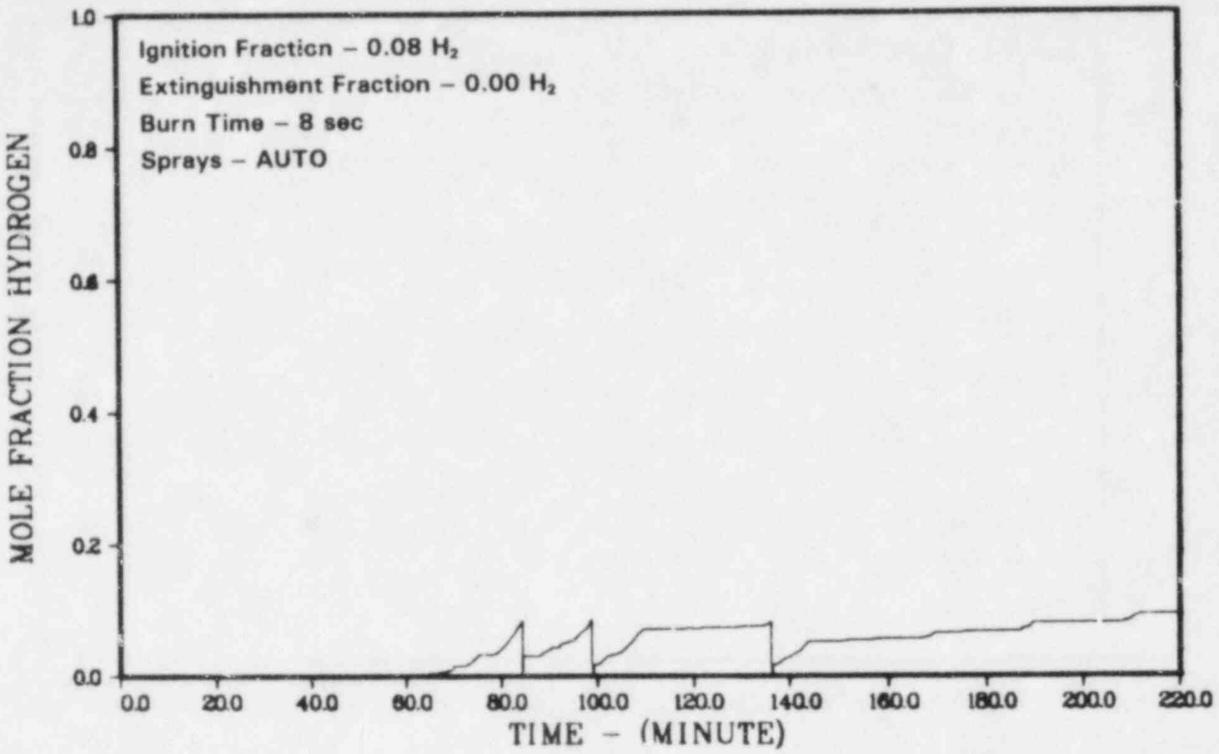

Figure 3.80. Case A-5, Hydrogen Mole Fraction in Containment

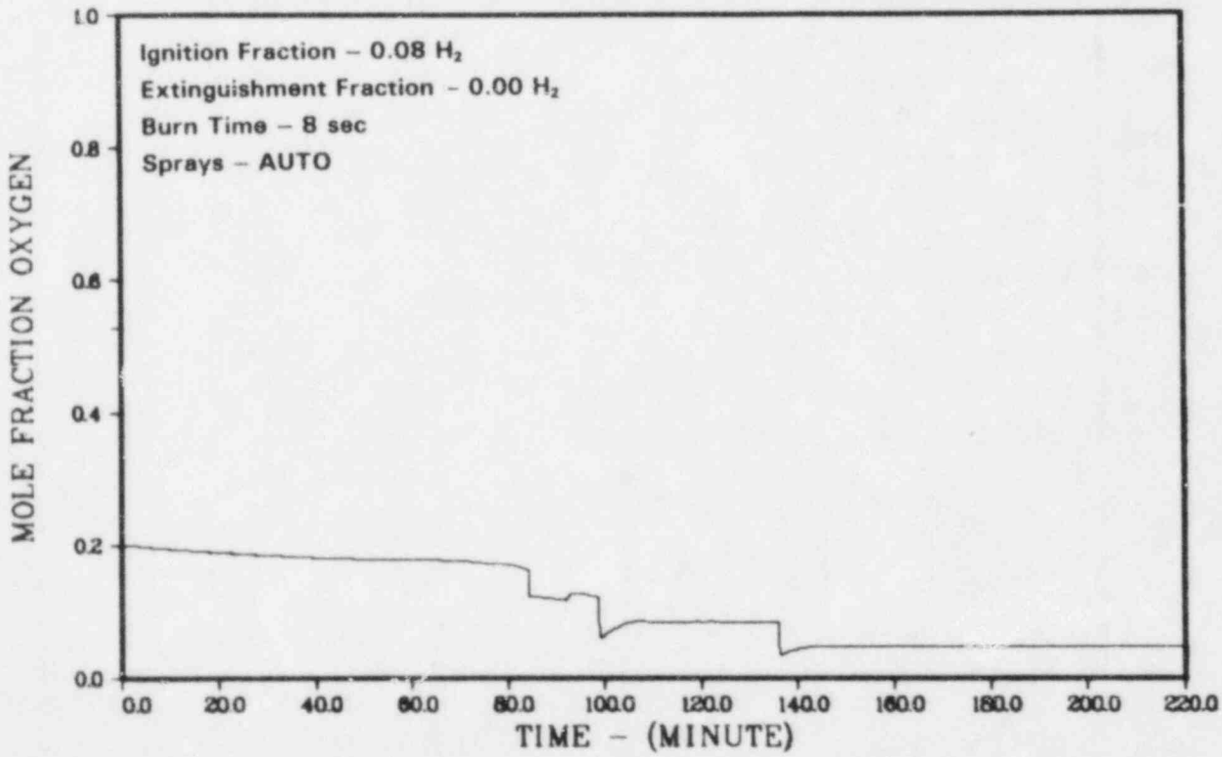

Figure 3.81. Case A-5, Oxygen Mole Fraction in Containment

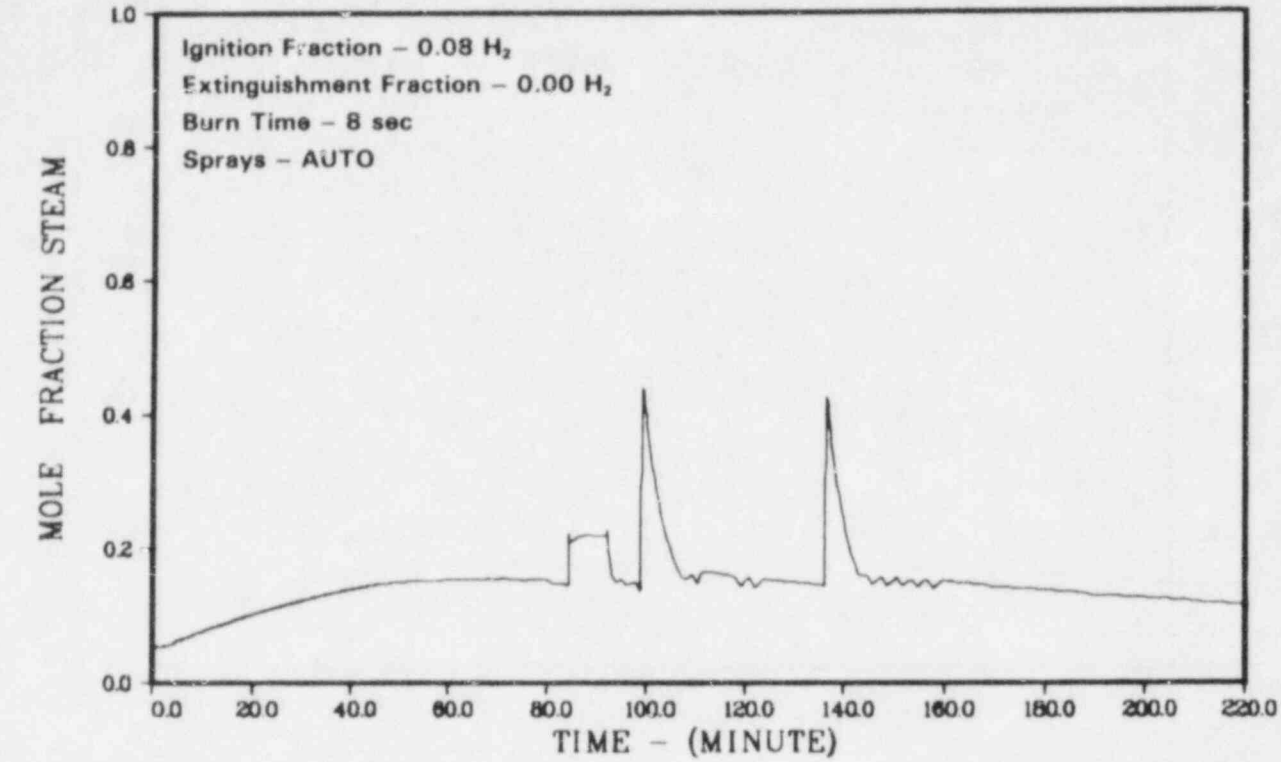

Figure 3.82. Case A-5, Steam Mole Fraction in Containment

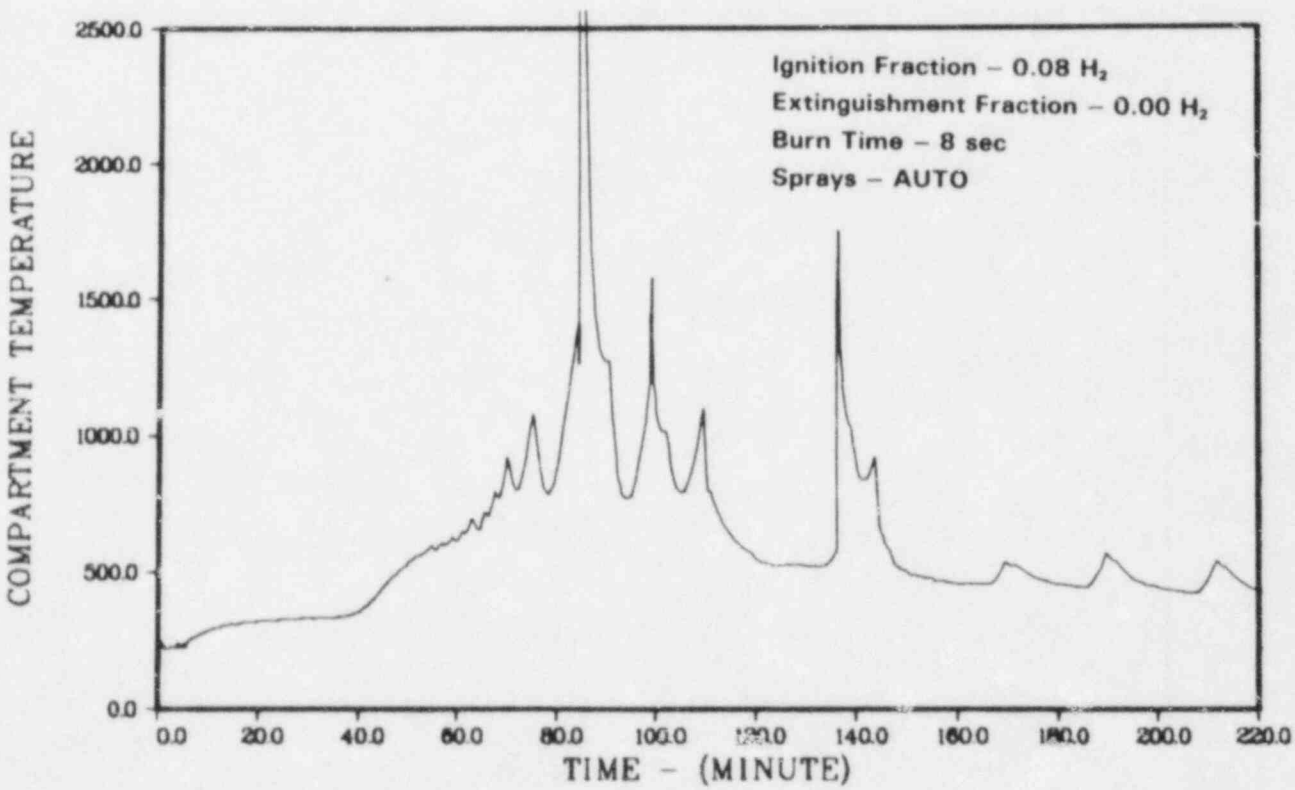

Figure 3.83. Case A-5, Temperature in Drywell, °F

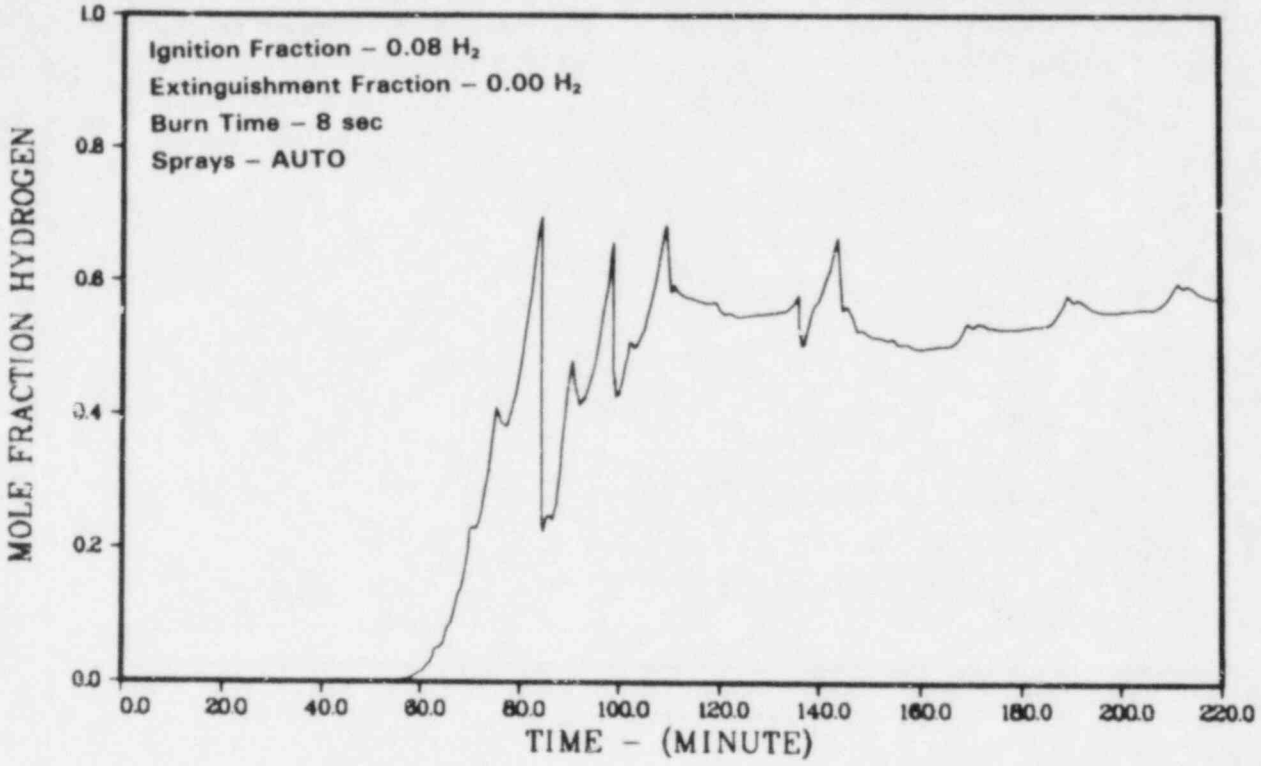

Figure 3.84. Case A-5, Hydrogen Mole Fraction in Drywell

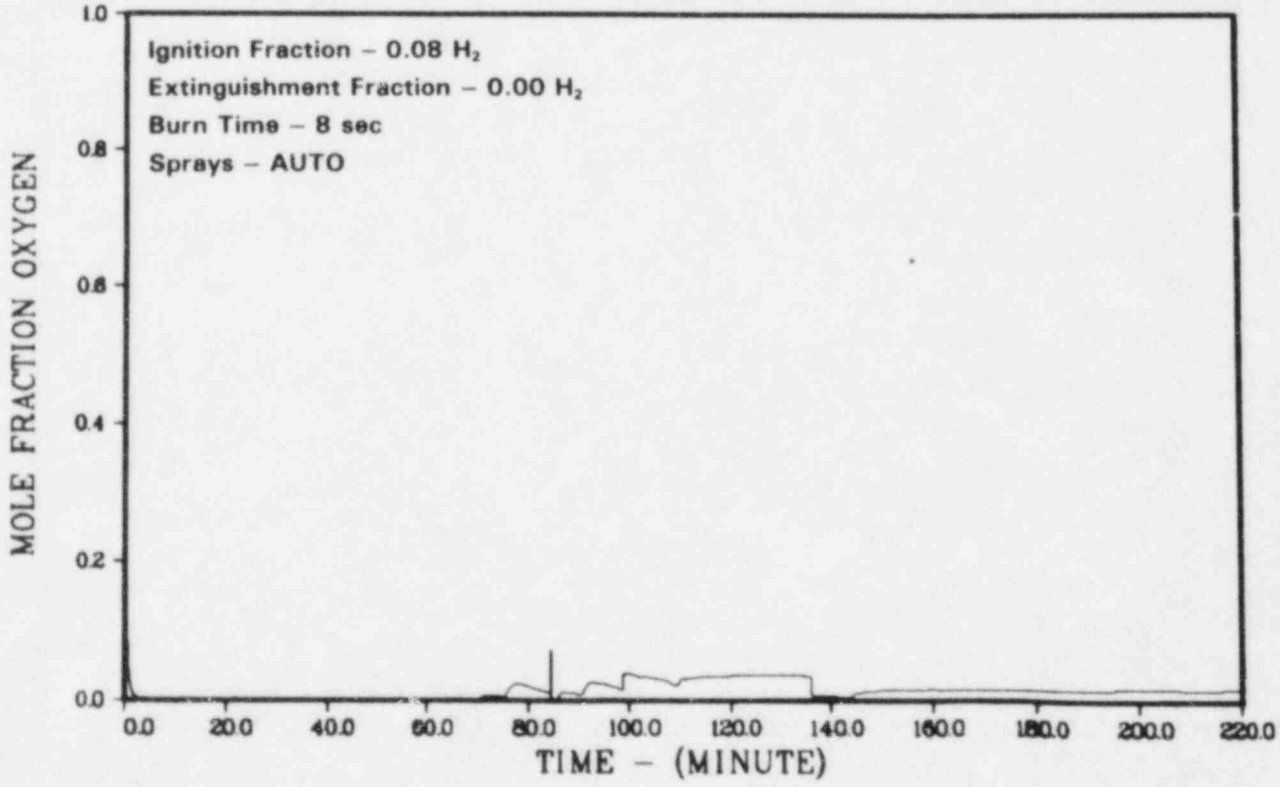

Figure 3.85. Case A-5, Oxygen Mole Fraction in Drywell

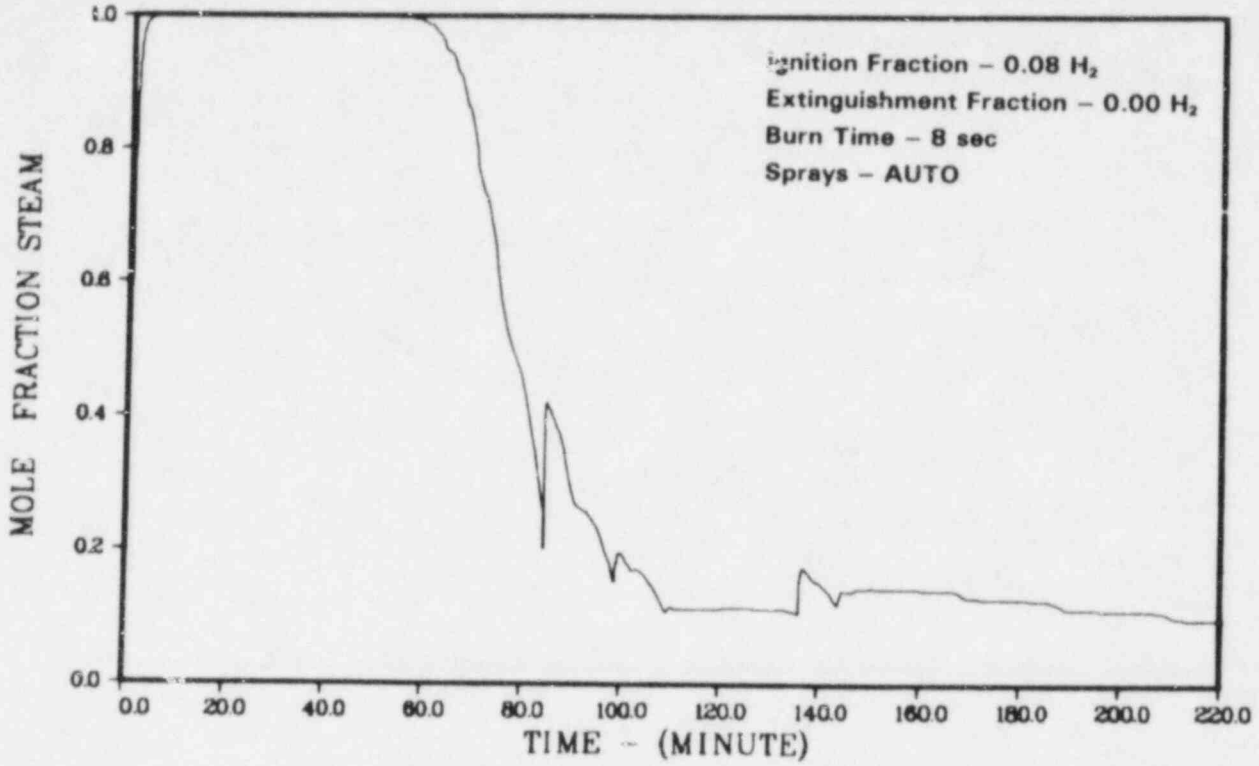

Figure 3.86. Case A-5, Steam Mole Fraction in Drywell

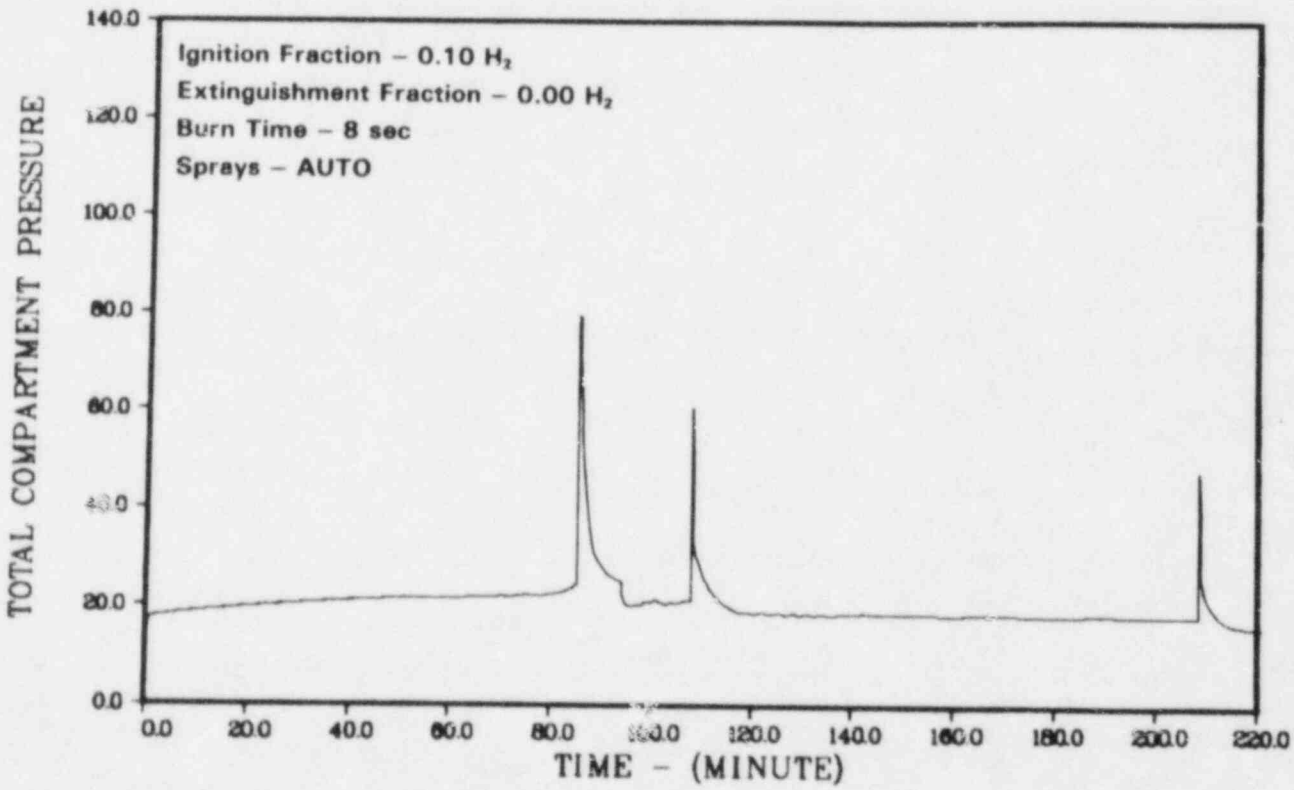

Figure 3.87. Case A-9, Pressure in Containment, psia

Table 3.6. Effect of Connections to the Drywell on Cases A-5 and A-9

	Case A-6		Case A-7	
	No Connection	Connection	No Connection	Connection
Peak Pressure (psia)	76	69	78	75
(atm)	5.2	4.7	5.3	5.1
No. of Significant Burns in Wetwell	4	3	3	3
No. of Significant Burns in Drywell	0	0	0	0

Table 3.7. Effect of Drywell Connections on the Results of Case B-2

	No Connection to Drywell	Wetwell to Drywell Connection	Upper Containment to Drywell Connection
No. of Upper Containment Burns	1	1	1
Peak Pressure (psia)	52	44	40
(atm)	3.5	3.0	2.7
No. of Wetwell Burns	16	20	21
No. of Drywell Burns	0	1	0

Table 3.8. Effect of Drywell Connections on the Results of Case B-6

	No Connection to Drywell	Wetwell to Drywell Connection	Upper Containment to Drywell Connection
No. of Upper Containment Burns	1	1	2
Peak Pressure (psia)	63	66	60
(atm)	4.3	4.5	4.1
No. of Significant Burns in Drywell	0	1	0
	0	1	0
No. of Significant Burns in Wetwell	13	15	18

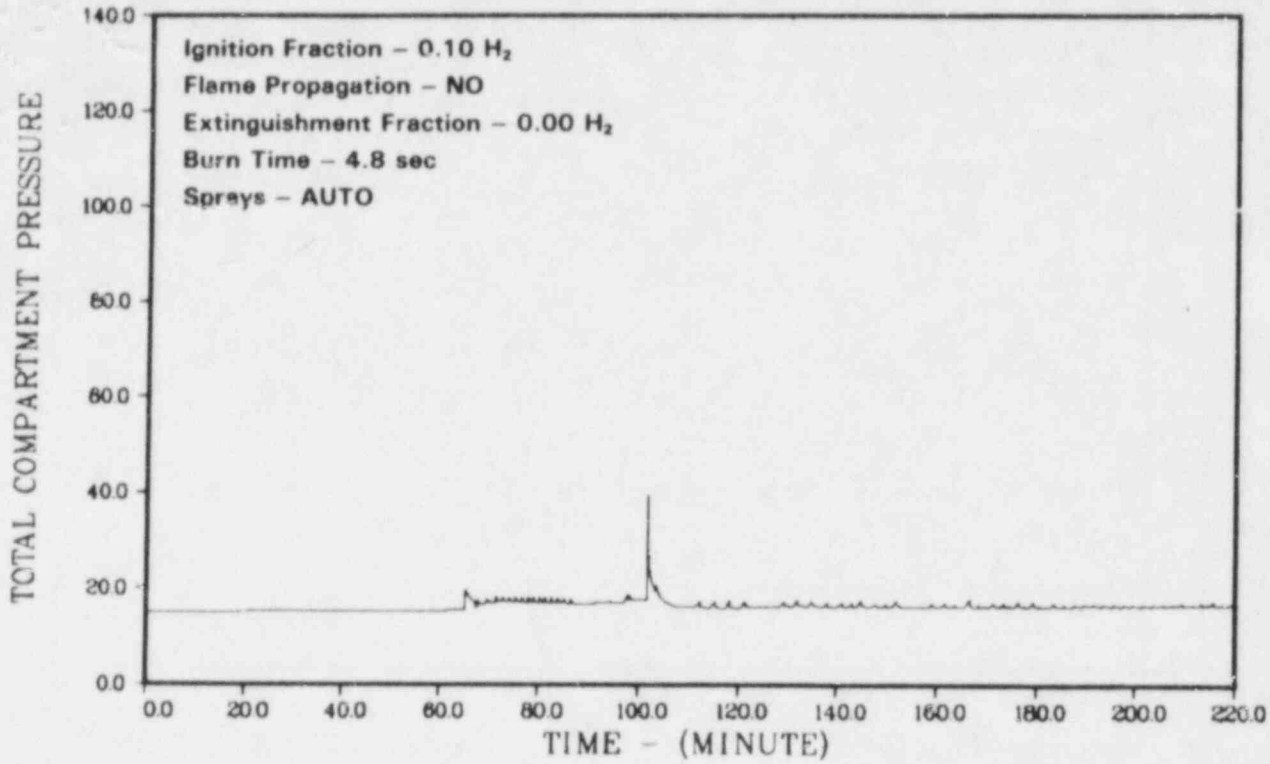

Figure 3.88. Case B-2 (With Containment to Drywell Connection), Pressure in Upper Containment, psia

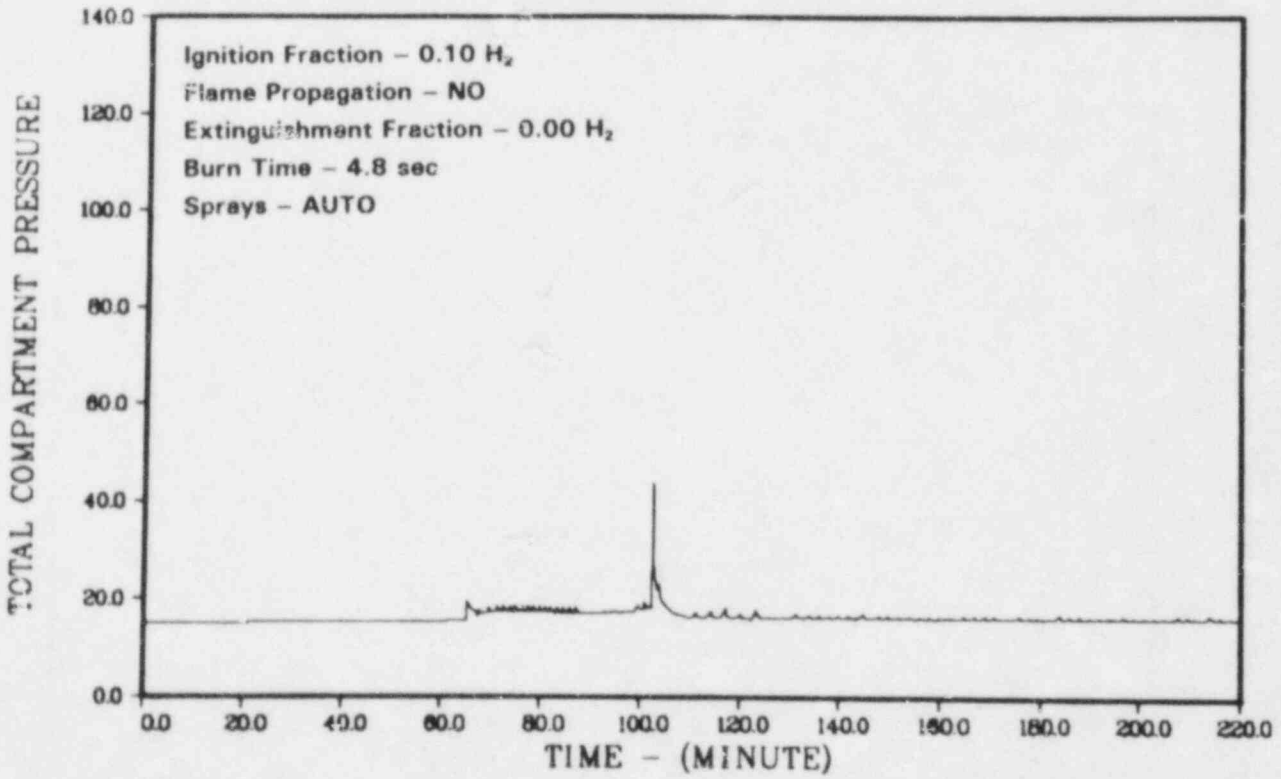

Figure 3.89. Case B-2 (With Wetwell to Drywell Connection), Pressure in Upper Containment, psia

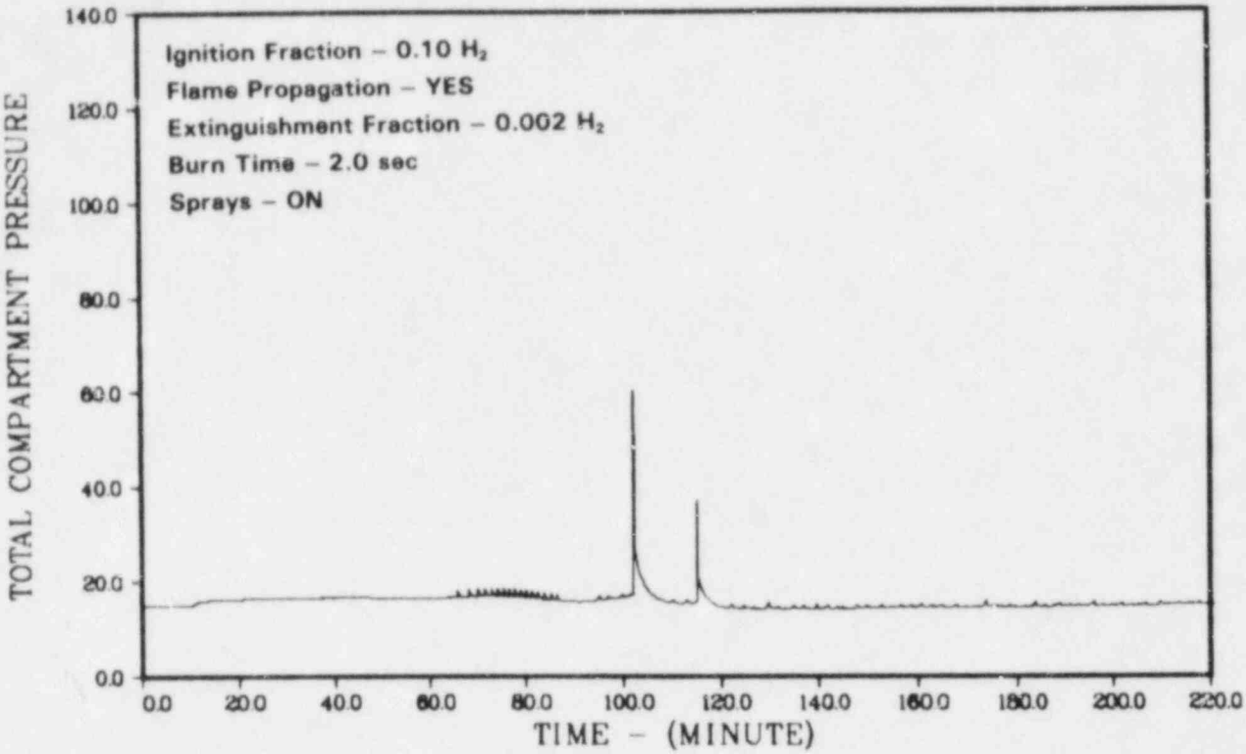

Figure 3.90. Case B-6 (With Containment to Drywell Connection), Pressure in Upper Containment, psia

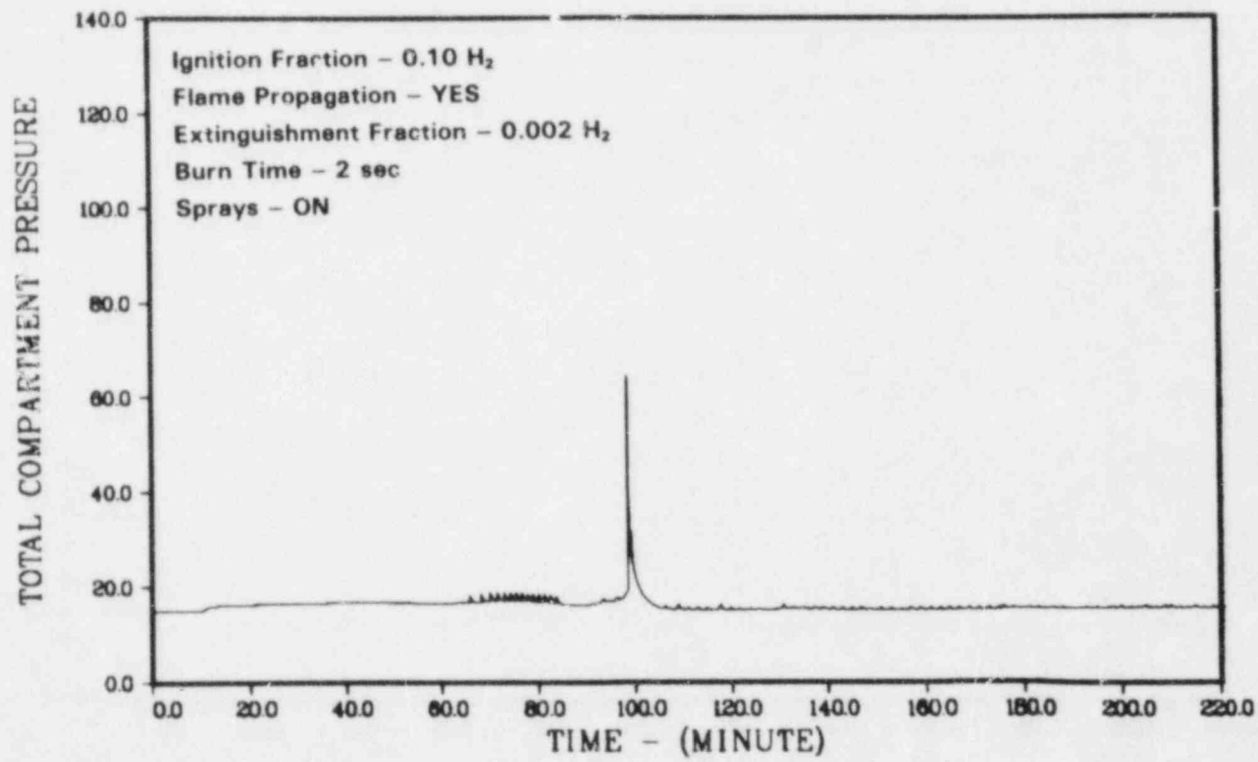

Figure 3.91. Case B-6 (With Wetwell to Drywell Connection), Pressure in Upper Containment, psia

Table 3.9. Effect of Drywell Connections on the Results of Case B-7

	Connection to Drywell	Wetwell to Drywell Connection	Upper Containment to Drywell Connection
No. of Significant Upper Containment Burns	2	1	2
Peak Pressure			
(psia)	62	71	60
(atm)	4.2	4.8	4.1
No. of Significant Drywell Burns	0	1	0
No. of Significant Wetwell Burns	14	15	16

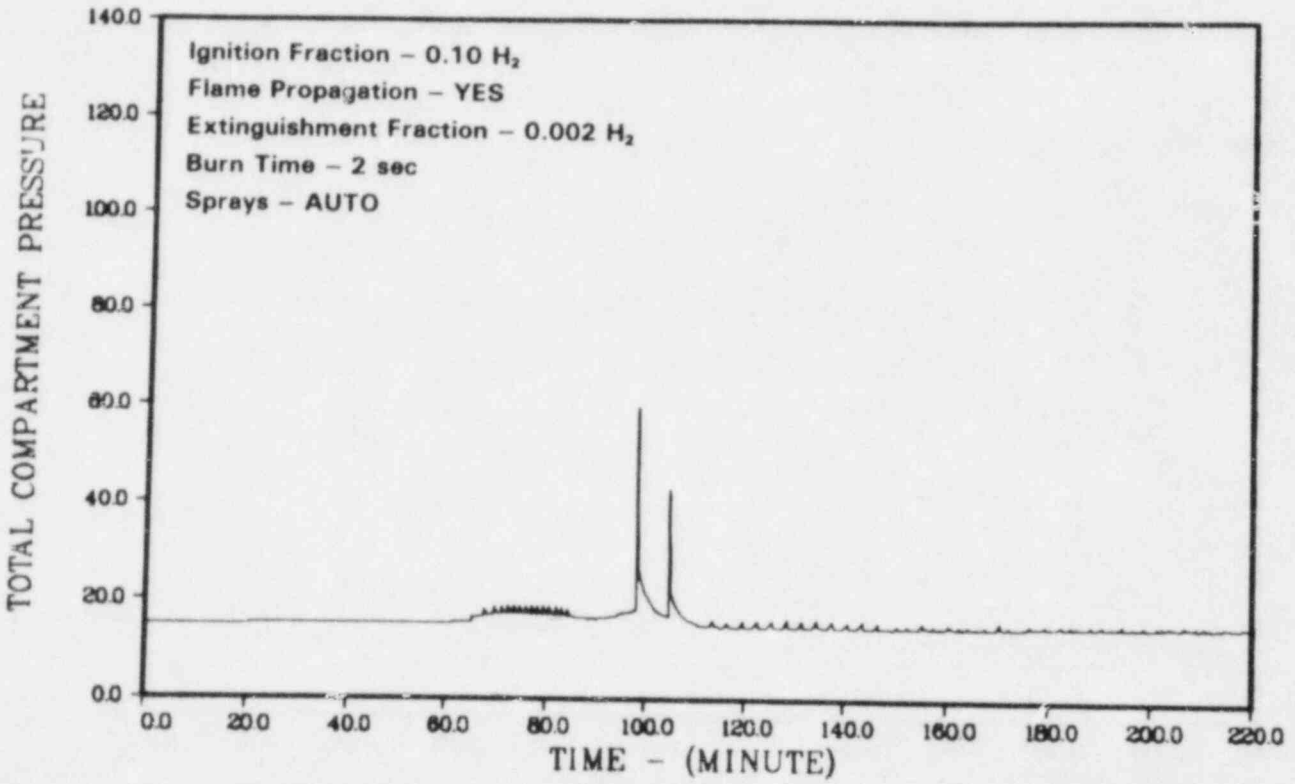

Figure 3.92. Case B-7 (With Containment to Drywell Connection), Pressure in Upper Containment, psia

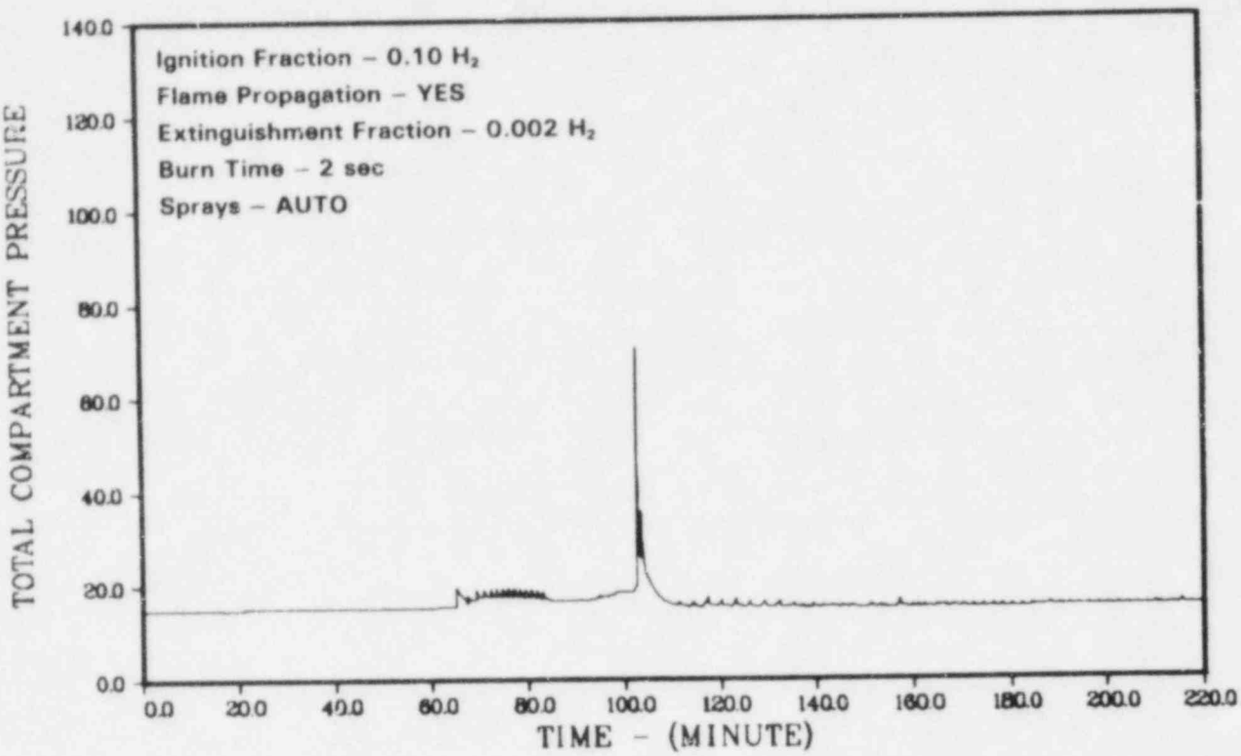

Figure 3.93. Case B-7 (With Wetwell to Drywell Connection), Pressure in Upper Containment, psia

Table 3.10. Effect of Wetwell to Drywell Connection on Case B-1

	No Connection to Drywell	Wetwell to Drywell Connection
Peak Pressures (psia)	65	52
(atm)	4.4	3.5
No. of Wetwell Burns Before First Wetwell Inerting	15	14
No. Upper Containment Burns	1	1
No. Drywell Burns	0	0
Total No. Of Wetwell Burns	16	19

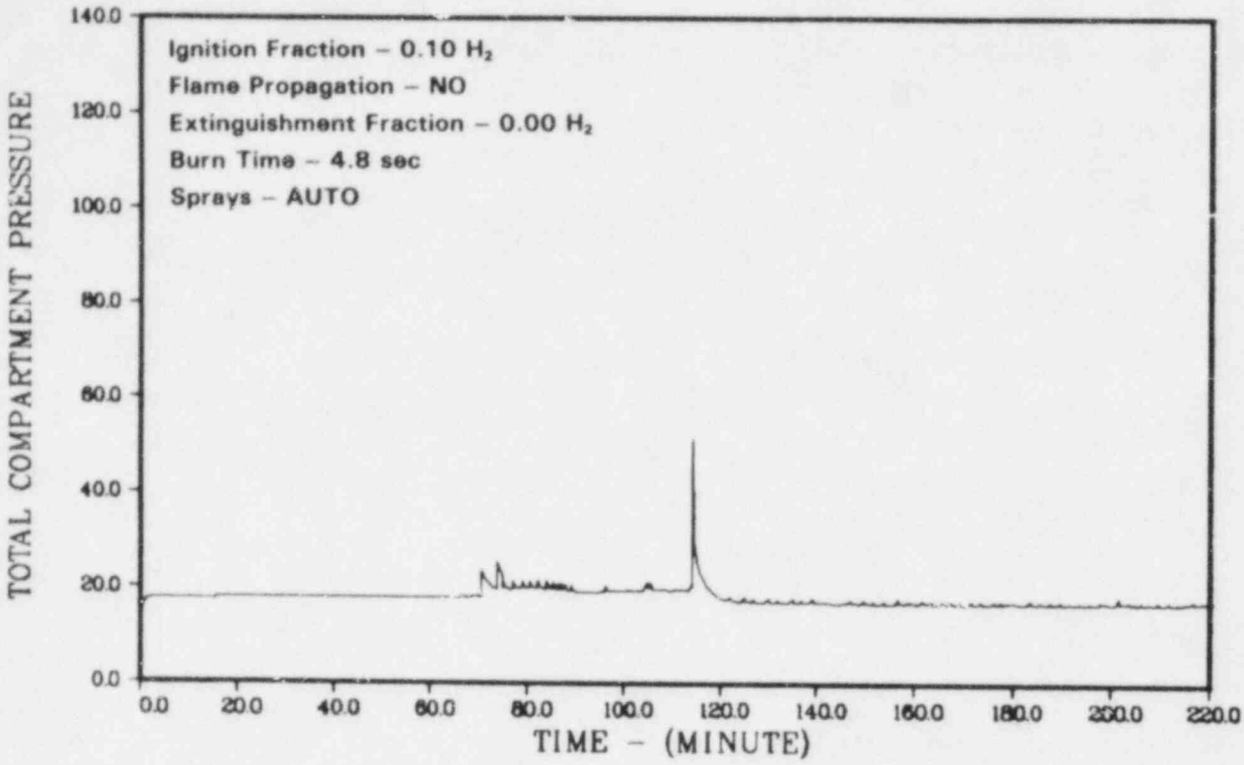

Figure 3.94. Case B-1, Pressure in Upper Containment, psia

Table 3.11. Effect of Wetwell to Drywell Connection on Case C-2

	No Connection to Drywell	Wetwell to Drywell Connection
No. of Significant Upper Containment Burns	1	0
Peak Pressure		
(psia)	48	27
(atm)	3.3	1.8
No. of Significant Wetwell Burns	8	6
No. of Significant Drywell Burns	0	0

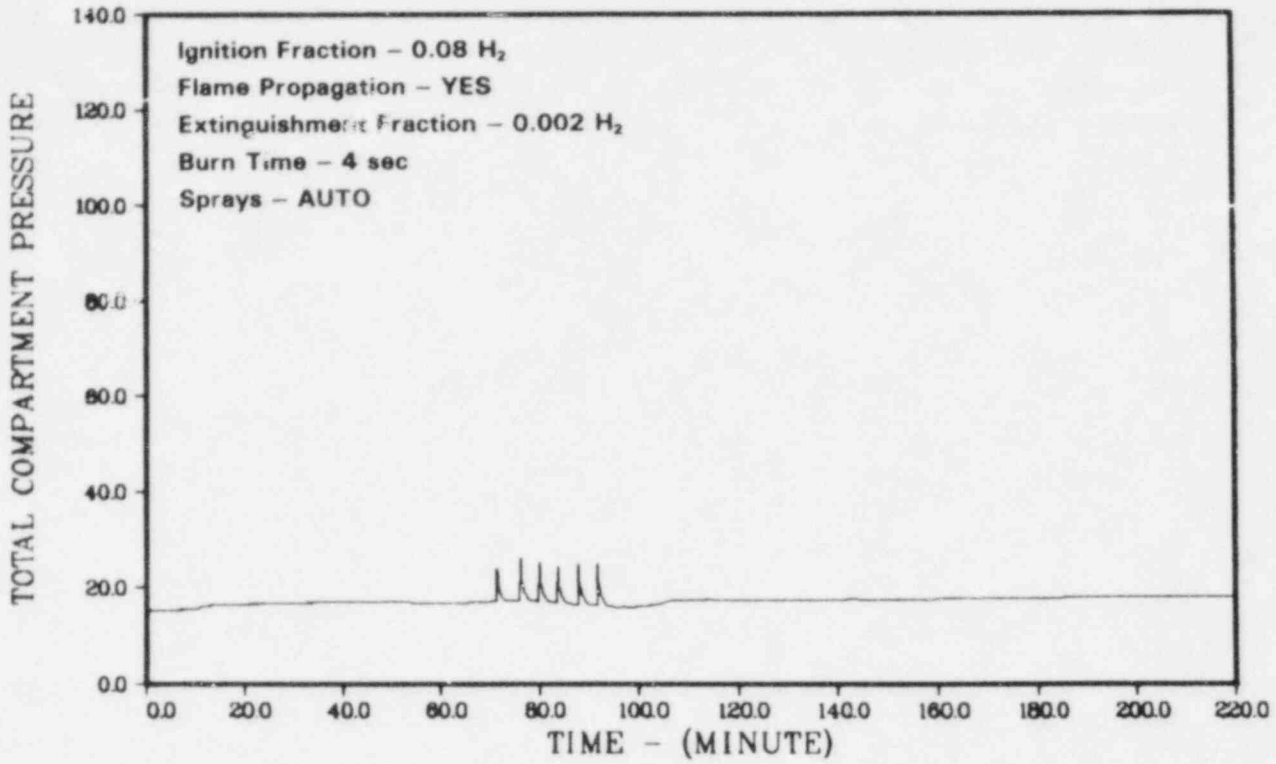

Figure 3.95. Case C-2 (With Wetwell to Drywell Connection), Pressure in Upper Containment, psia

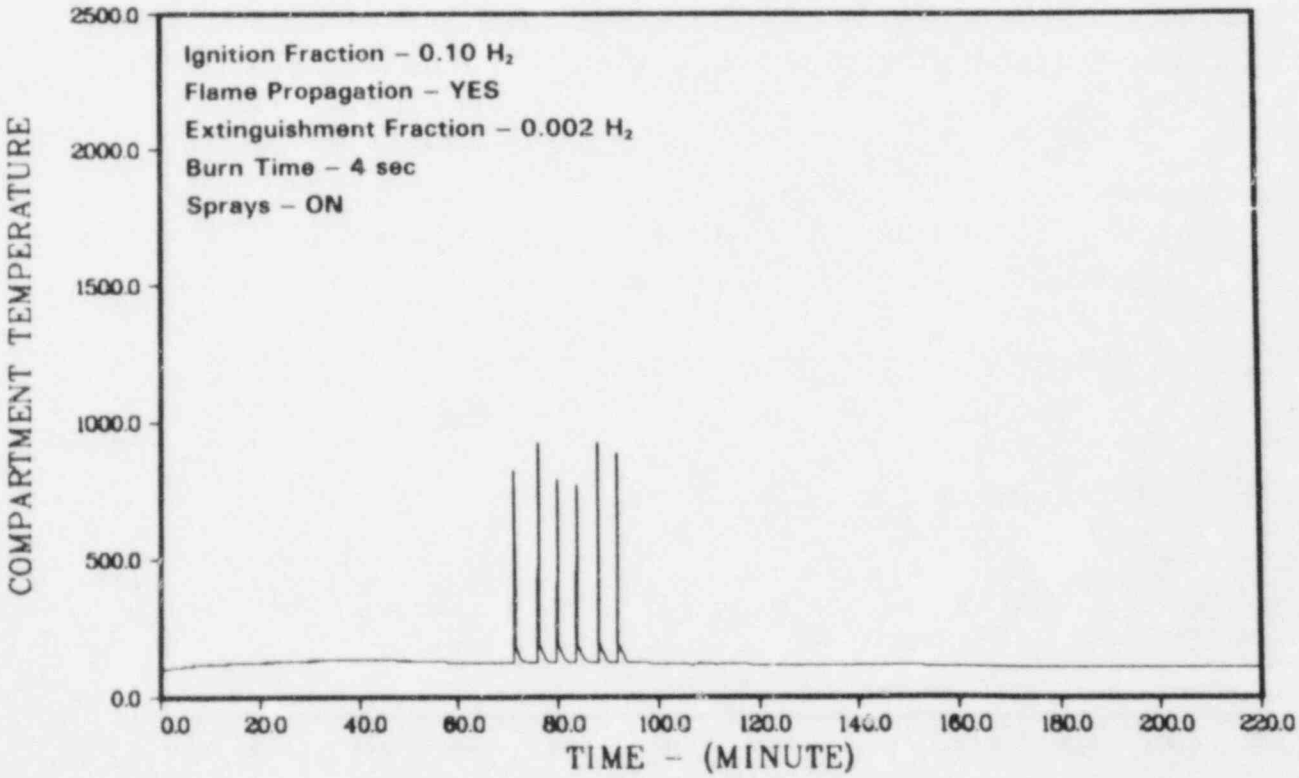

Figure 3.96. Case C-2 (With Wetwell to Drywell Connection), Temperature in Wetwell, °F

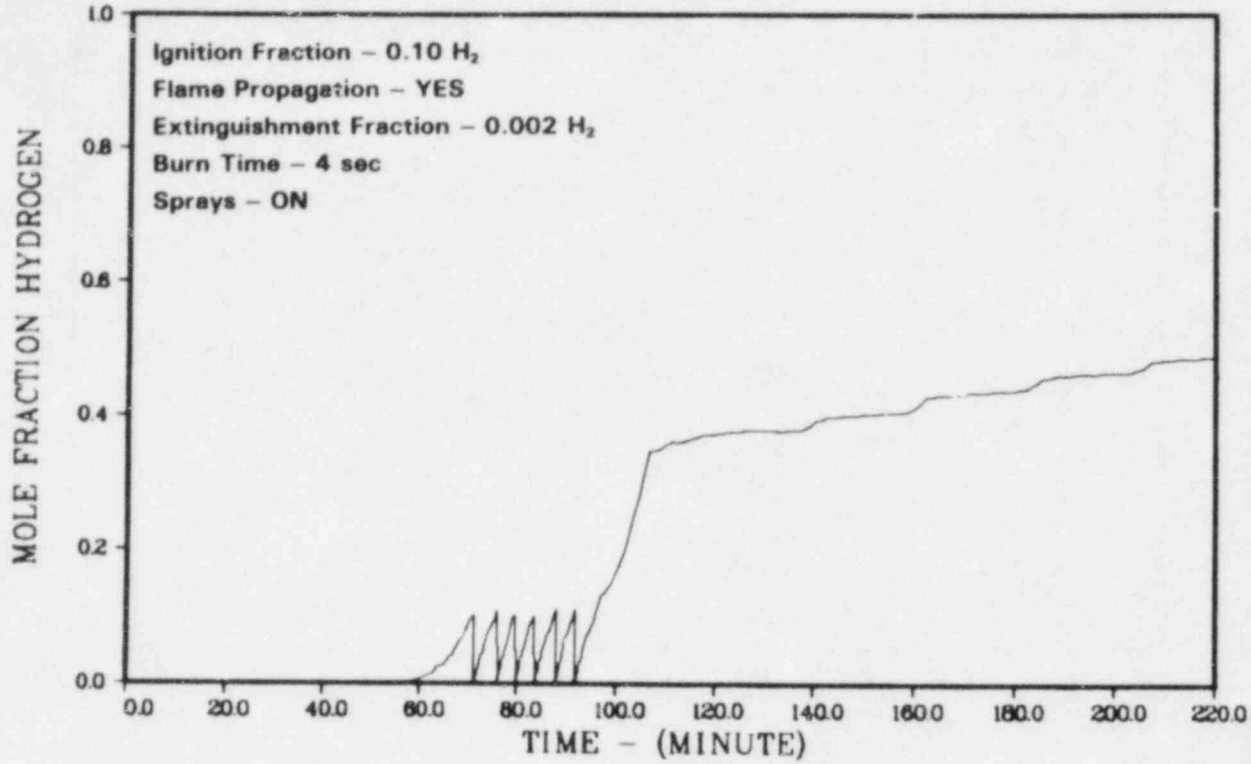

Figure 3.97. Case C-2 (With Wetwell to Drywell Connection), Hydrogen Mole Fraction in Wetwell

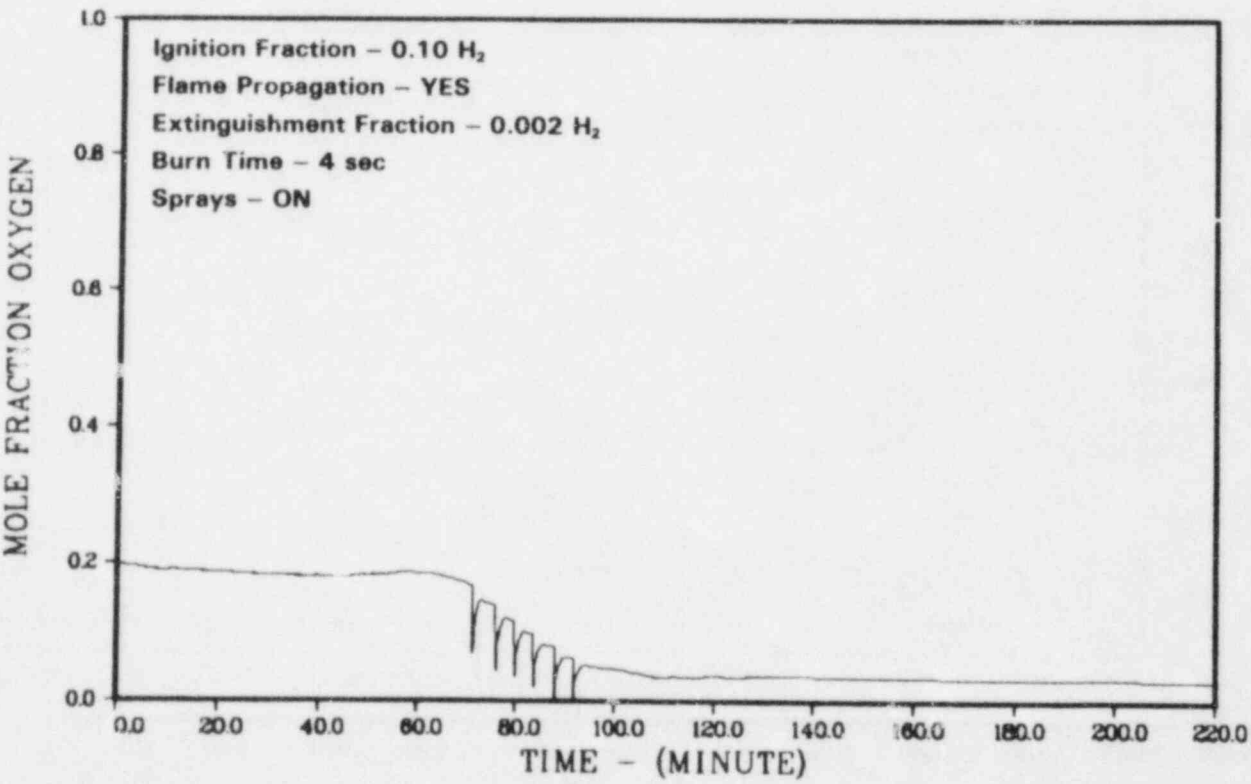

Figure 3.98. Case C-2 (With Wetwell to Drywell Connection), Oxygen Mole Fraction in Wetwell

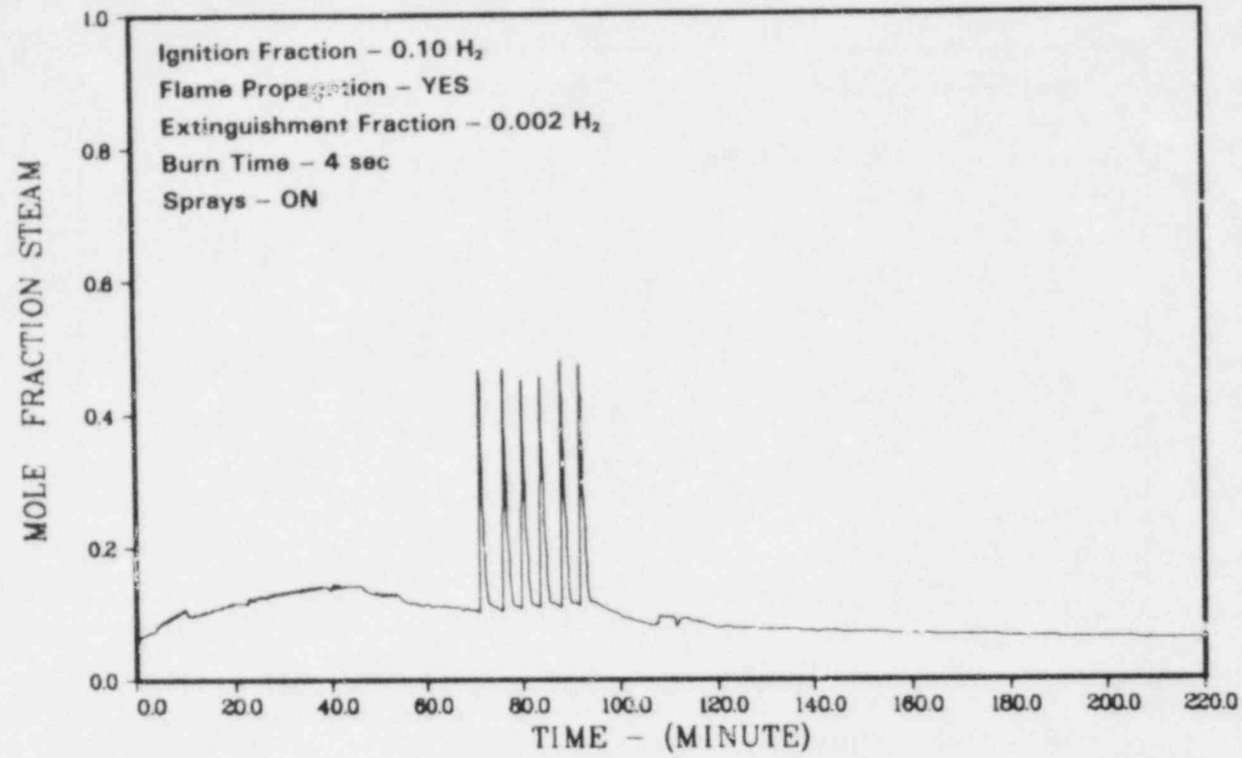

Figure 3.99. Case C-2 (With Wetwell to Drywell Connection), Steam Mole Fraction in Wetwell

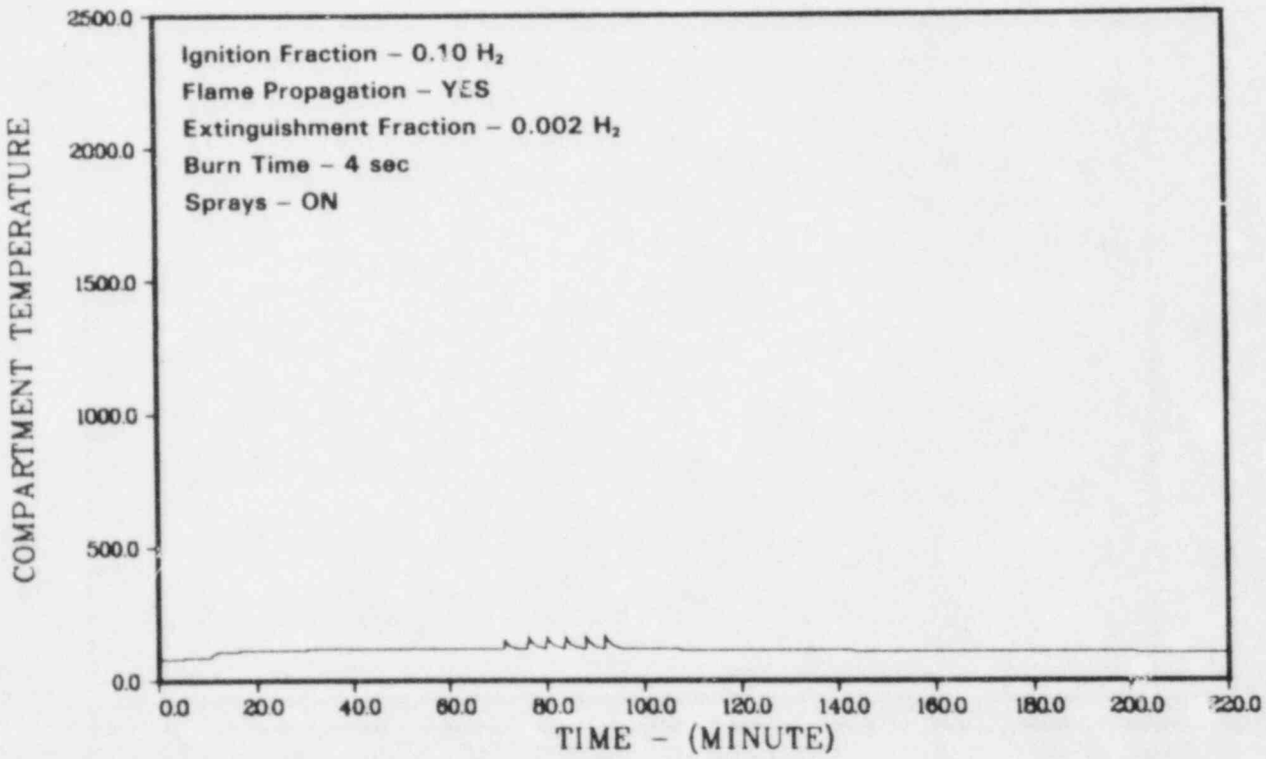

Figure 3.100 Case C-2 (With Wetwell to Drywell Connection), Temperature in Upper Containment, °F

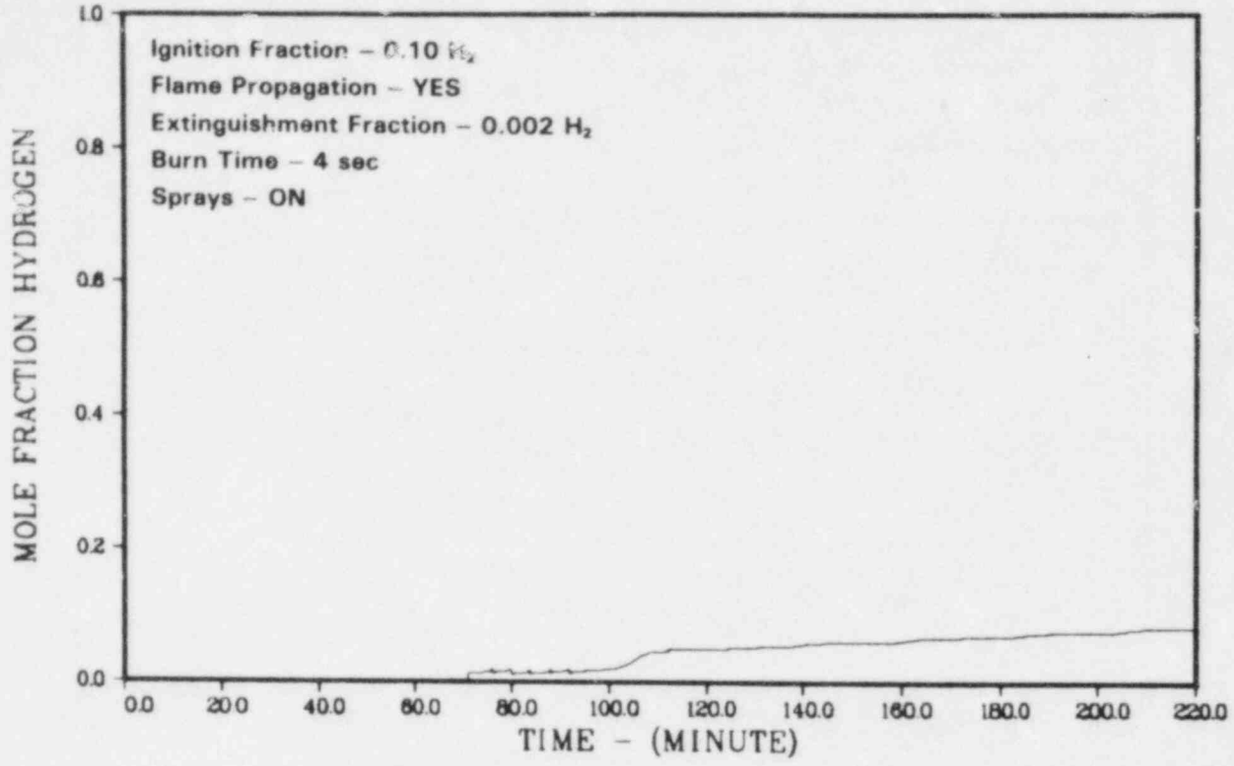

Figure 3.101. Case C-2 (With Wetwell to Drywell Connection), Hydrogen Mole Fraction in Upper Containment

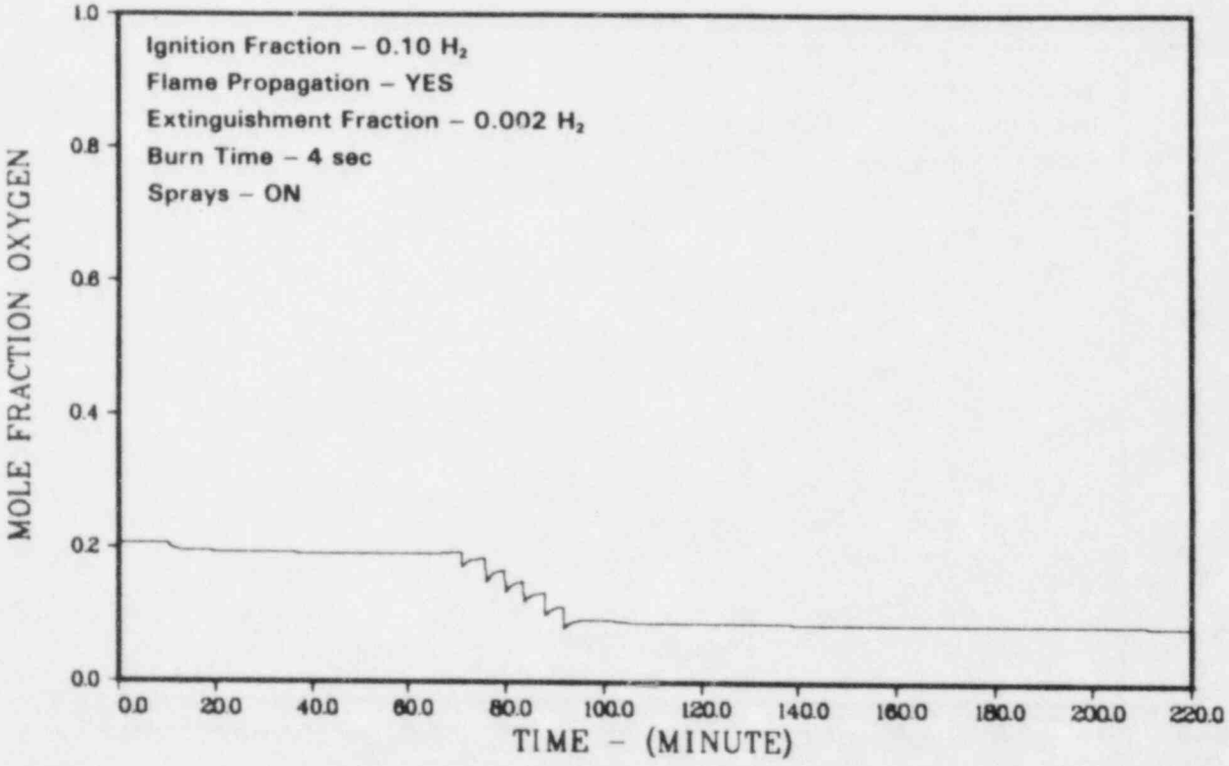

Figure 3.102. Case C-2 (With Wetwell to Drywell Connection), Oxygen Mole Fraction in Upper Containment

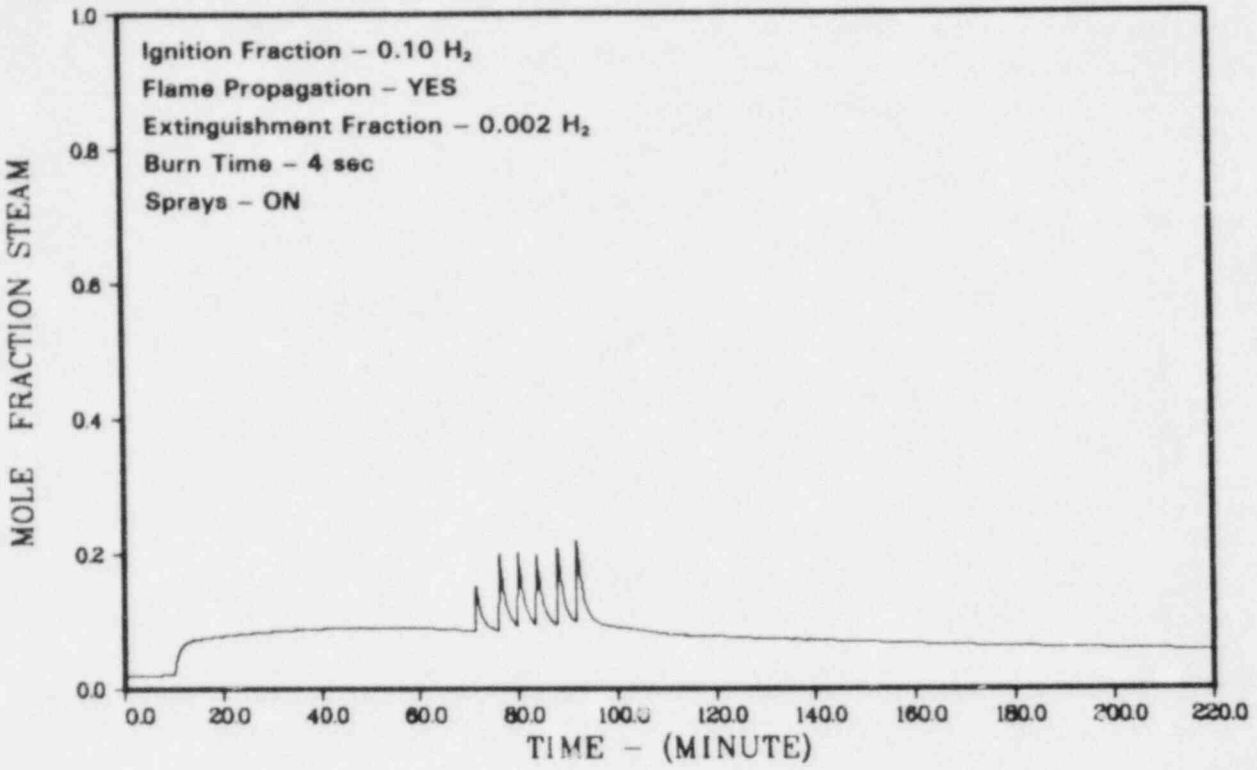

Figure 3.103. Case C-2 (With Wetwell to Drywell Connection), Steam Mole Fraction in Upper Containment

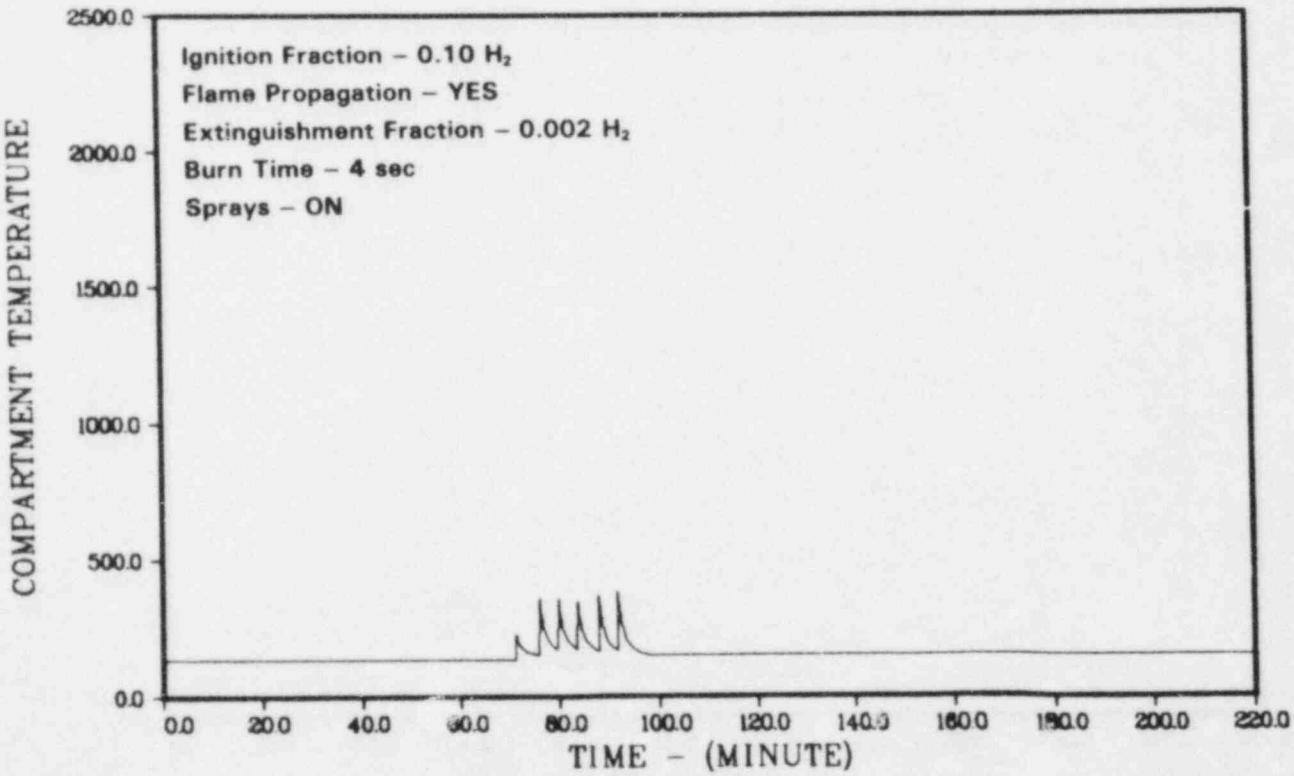

Figure 3.104. Case C-2 (With Wetwell to Drywell Connection), Temperature in Drywell, °F

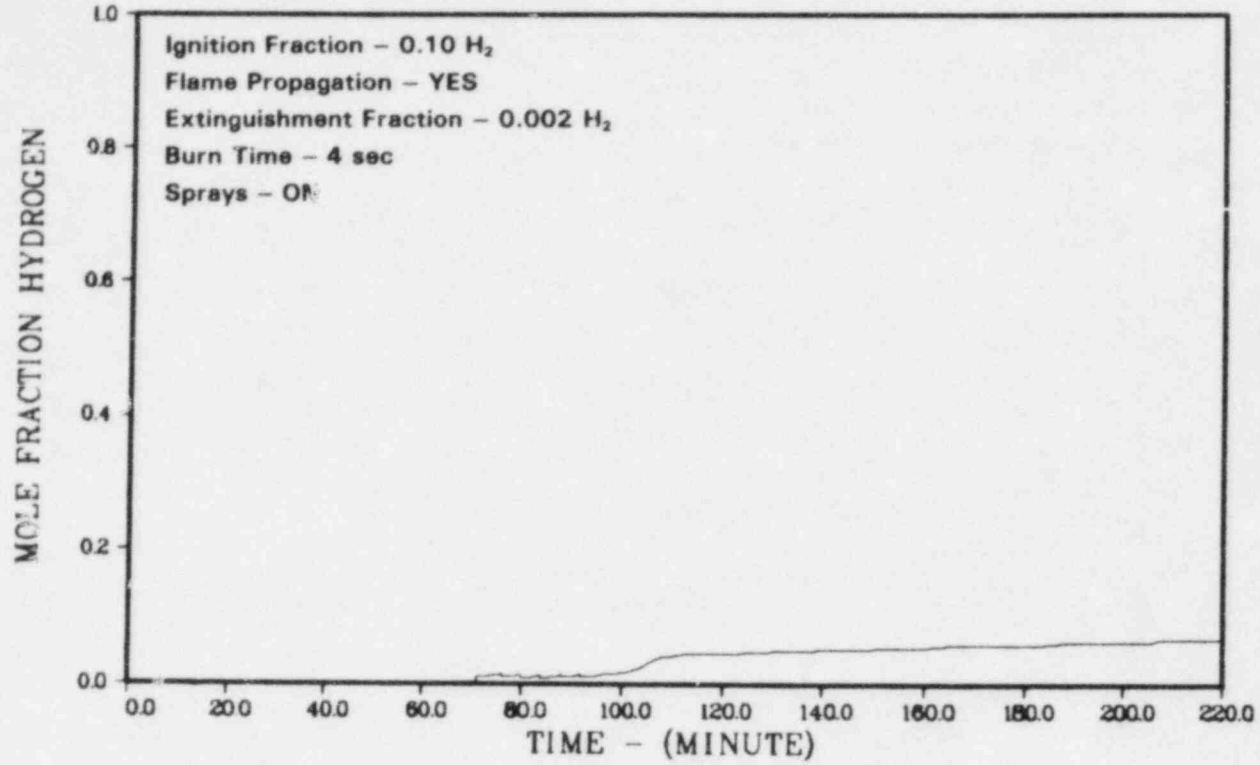

Figure 3.105. Case C-2 (With Wetwell to Drywell Connection), Hydrogen Mole Fraction in Drywell

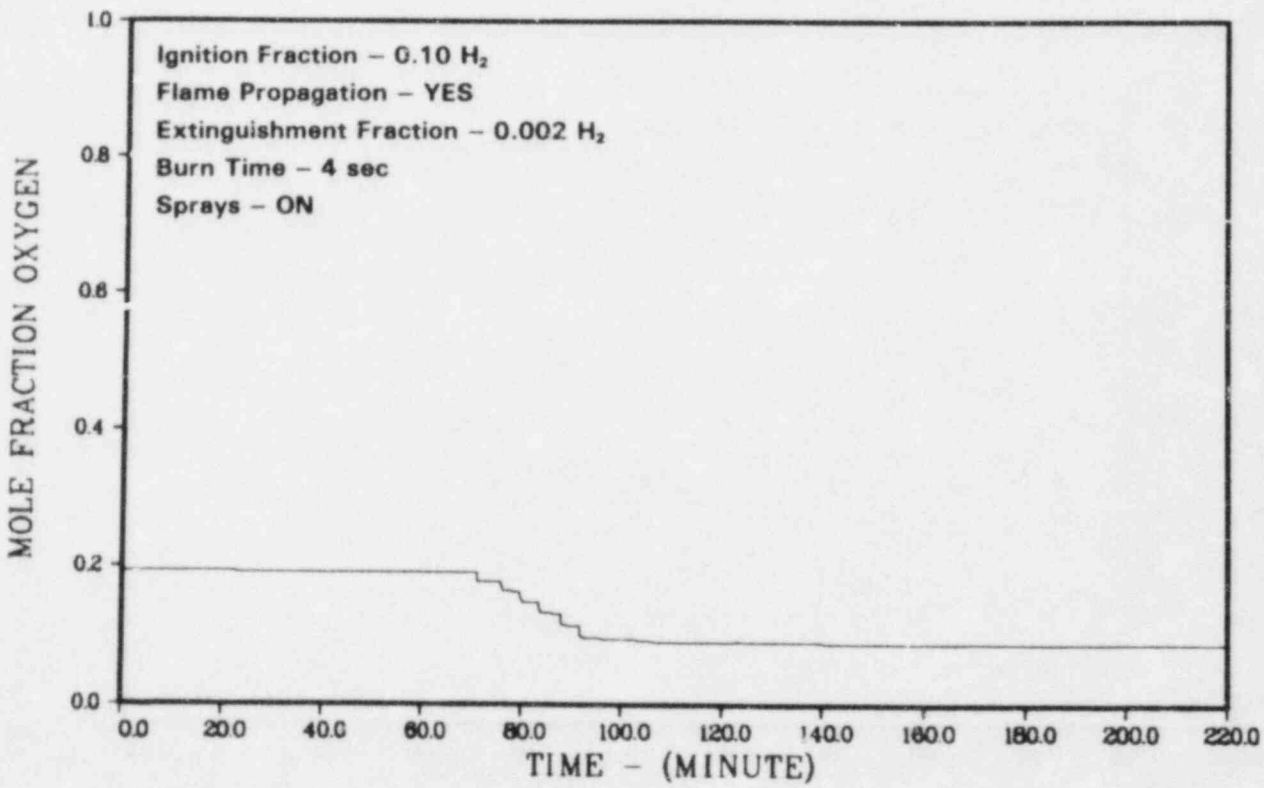

Figure 3.106. Case C-2 (With Wetwell to Drywell Connection), Oxygen Mole Fraction in Drywell

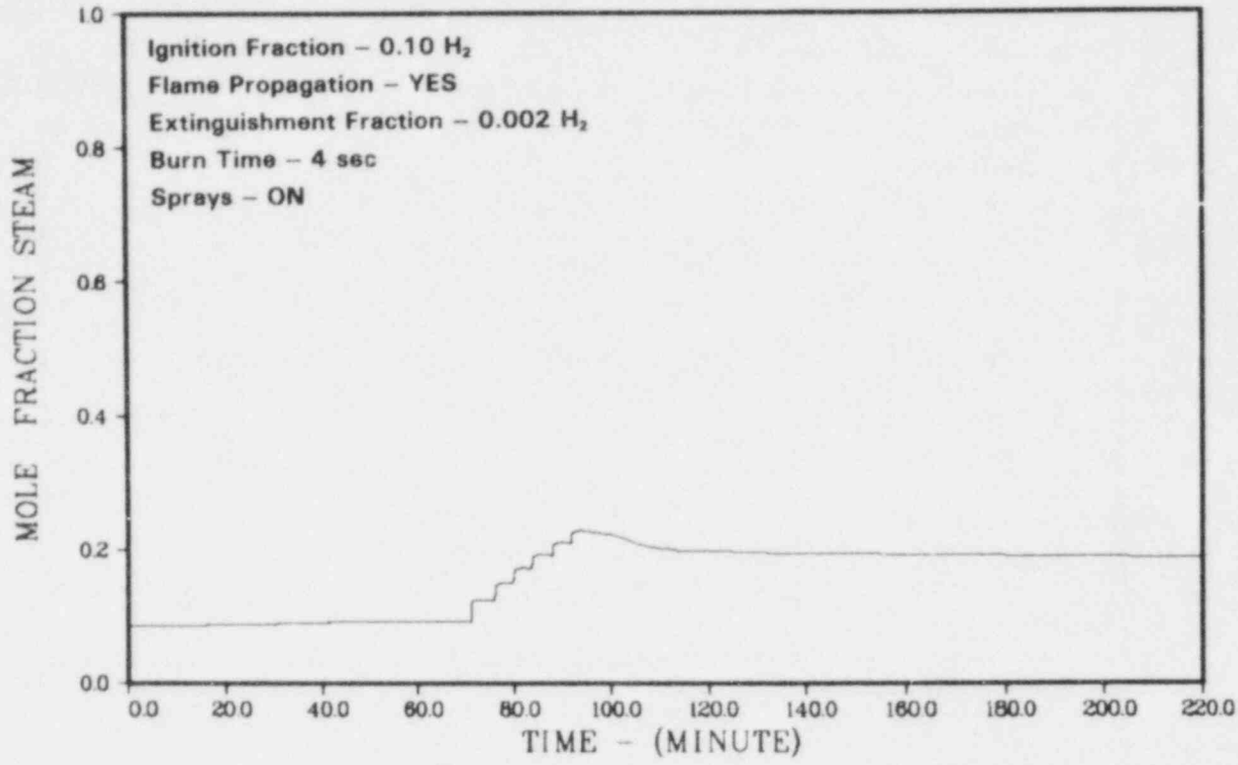

Figure 3.107. Case C-2 (With Wetwell to Drywell Connection), Steam Mole Fraction in Drywell

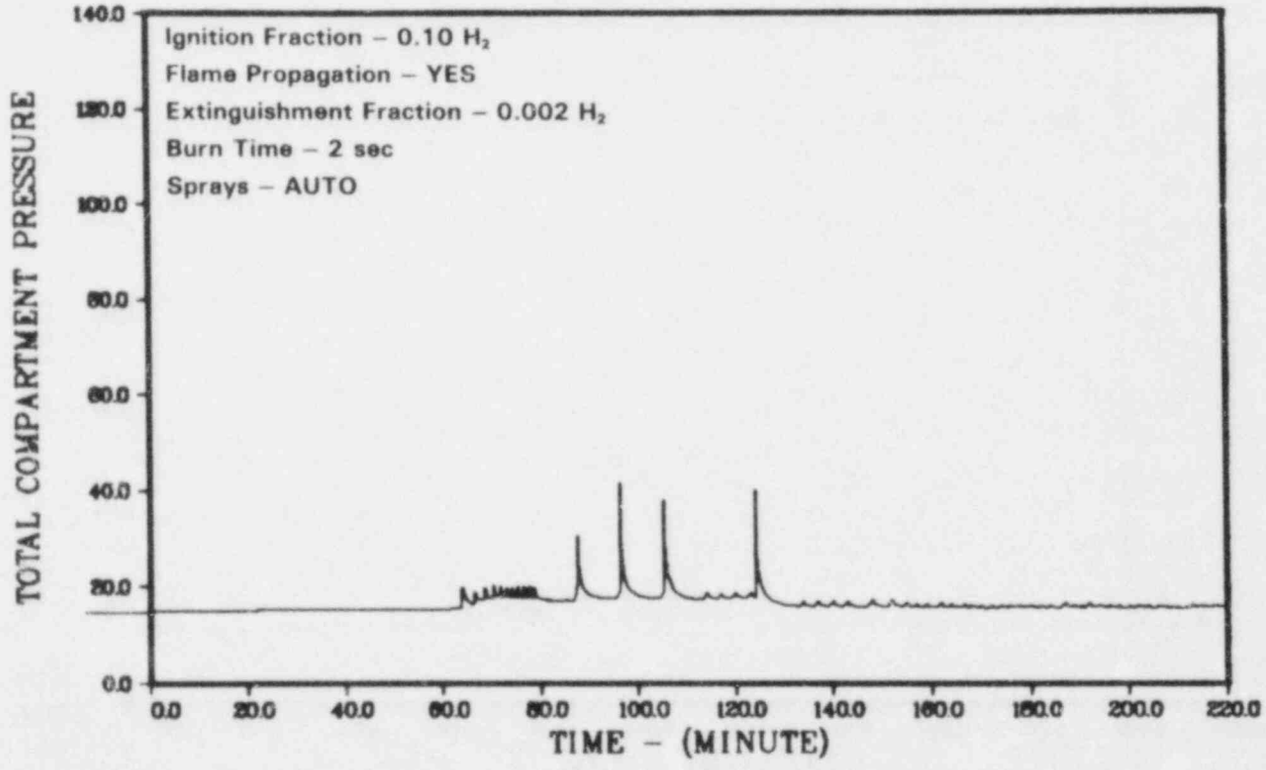

Figure 3.108. Case D-2 (Wetwell to Drywell Connection), Containment Pressure, psia

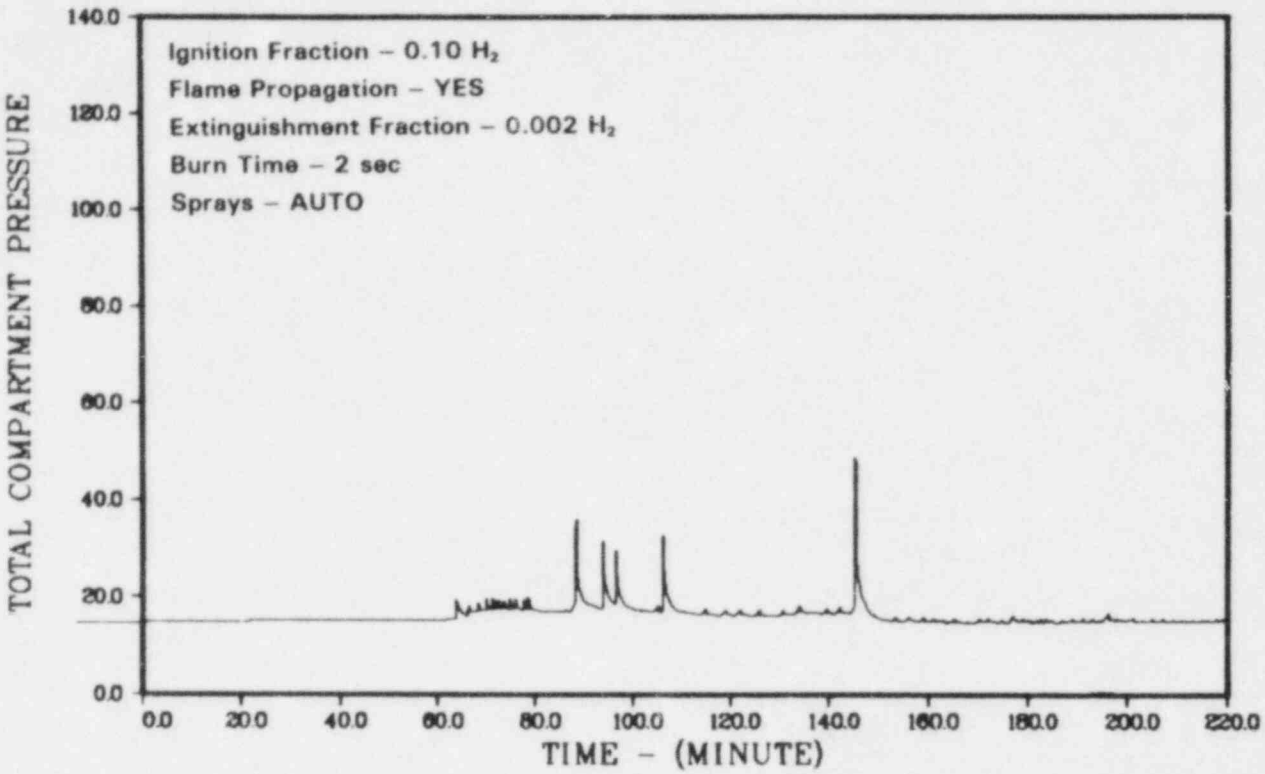

Figure 3.109. Case D-2 (Intermediate Annular Region Connection to Drywell), Containment Pressure, psia

Table 3.12. Effect of Wetwell to Drywell Connection on Case D-2

	No Connection to Drywell	Wetwell to Drywell Connection	Intermediate Annular Region to Drywell Connection
Peak Pressure (psia)	46	41	50
(atm)	3.1	2.8	3.4
No. of Significant Burns in Upper Containment	1	1	1
No. of Significant Burns in Intermedidate Annular Volume	3	4	4
No. of Significant Burns in Wetwell	9	12	11
No. of Significant Burns in Drywell	0	1	1

4.0 RALOC Hydrogen Transport Calculations for the Grand Gulf Nuciear Station

4.1 Summary

Hydrogen transport calculations made with the computer code RALOC[4.1] are discussed in this chapter. The objective of these calculations was to provide an estimate of the volumetric hydrogen concentration in the upper compartments of the Grand Gulf containment building when the bottom compartment achieves a reliable combustible hydrogen level at the igniters (assumed to be approximately 8% to 10%). A sensitivity study, rather than a best-estimate technique, was used to attain this objective. This was done for two reasons: First, there are large uncertainties associated with the hydrogen release models following a LOCA; second, the RALOC code itself has had only limited assessment to date.[4.2] It must be noted that all RALOC calculations involve precombustion conditions—no mixing *during* or *after* combustion was considered.

Two groups of parameters were varied in this study. The first group contains parameters which test the reliability of the code. These are the maximum time step allowed during the implicit integration of the differential equations, and the number of zones and connections used to model the Grand Gulf containment (nodalization). The second group consists of physical parameters which are either uncertain in the hydrogen source description or are known to affect the transport of hydrogen in a containment. They are the amount and rate of hydrogen injection, the hydrogen injection temperature, and the initial temperature distribution present in the containment building.

Although the quantitative results of our sensitivity studies varied a little, the qualitative results were the same. During the injection period, nonhomogeneities existed in the hydrogen volumetric concentrations. Increasing the rate of hydrogen injection, or inverting the temperature distribution (higher temperature at the top of the containment than at the bottom) produced larger asymmetries. (Temperature inversions appear to be possible if containment sprays are inoperable, especially if burns have occurred previously.) When the bottom compartment reached the assumed lower combustion limit of 8%, the upper containment levels had a hydrogen concentration between 3% and 6%, depending on the rate of hydrogen injection and the degree of resolution used in the RALOC nodalization. Once the bottom compartment reached 8%, an additional 5 min were typically required to bring the upper compartment to the same value. As expected, the hydrogen transport was dominated by convection.

For initially isothermal conditions, the hydrogen concentration becomes uniform (independent of vertical and azimuthal location) within 15 to 20 min after the end of injection. Inverting the initial temperature distribution in the containment produced nonhomogeneous hydrogen concentrations as late as 10 000 s (2.8 h) into the calculation (there was a lower hydrogen concentration at the top than at the bottom). Homogenization of the hydrogen concentration was inhibited by a thermal barrier produced by the temperature distribution.

The concentration of hydrogen achieved at the end of the calculation (10 000 s) is clearly a function of the total hydrogen injected. Injecting 500 lb of hydrogen produced volumetric concentrations on the order of 30%. Injecting less hydrogen produced lower final concentrations, as expected.

4.2 Introduction

Predicting the volumetric concentrations of hydrogen in individual compartments of a nuclear power plant following a degraded-core accident is extremely important for reactor-safety calculations. Knowledge of these concentrations could be crucial to the design of possible hydrogen mitigation schemes.

Sandia has recently obtained the computer code "RALOC-MOD1 with 1980 updates" in order to perform hydrogen transport calculations for severe accidents. The code was obtained from GRS (Gesellschaft für Reaktorsicherheit) under an NRC-BMI (Bundesministerium des Innern) agreement consistent with the existing NRC-BMFT (Bundesministerium für Forschung und Technologie) agreement.

Using RALOC, calculations were performed to analyze the transport of hydrogen in the Grand Gulf Nuclear Station following a hypothetical degraded-core accident. In particular, we wanted to determine the upper-containment volumetric hydrogen concentrations when the bottom compartment concentration

was near some lower combustion limit for hydrogen igniters. The calculations were performed using a sensitivity approach in which parameters relevant to the calculation were varied over a wide range to determine their overall relative importance. Qualitative conclusions can be drawn from this study, but no precise quantitative results should be deduced.

The following sections will discuss the RALOC computer code, the RALOC models for Grand Gulf, hydrogen source models used for the transport calculations, two RALOC code-reliability calculations, and the sensitivity studies performed for the physical parameters.

4.3 RALOC

RALOC is a computer code developed by H. Jahn of GRS under the sponsorship of BMI.[4.1] RALOC was designed to calculate time histories of local gas concentrations in subdivided containments. In particular, RALOC was developed to determine the distribution of radiolytically-produced hydrogen in a nuclear plant following a LOCA. Hydrogen concentrations calculated with RALOC represent mole percentages. For ideal gases, the mole percentage is equivalent to the volumetric percentage.

In solving the hydrogen transport problem, RALOC uses lumped-parameter control volumes connected by flow junctions. Within a given zone, up to five constituents can be treated assuming thermodynamic equilibrium and saturated steam. Possible constituents are liquid water, steam, hydrogen, air, nitrogen, and helium. Junction gas flow is driven by both convection and diffusion and is opposed by resistance between the zones. Differential equation integration is explicit during the problem startup and fully implicit after the calculation has stabilized.

Other code options include fans/recombiners, optional heat transfer to constant-temperature heat sinks, and optional heat transfer to and from variable-temperature heat sinks with one heat slab allowed per control volume. In addition, the user can specify one zone as a hydrogen : air source and can specify a coolant path for transport of recirculation coolant water with dissolved gases.

To date, RALOC has had limited assessment. Qualitatively, good agreement has been obtained with the experimental data of Battelle-Frankfurt (multiroom geometries with various initial temperature distributions and hydrogen injection rates).[4.2, 4.3] Additional verification of RALOC will be performed as more experimental data become available.

Currently, RALOC is being modified by SNL to simulate the EPRI/HEDL tests now being performed (hydrogen, helium-steam injection into a multiroom geometry).[4.4]

4.4 RALOC Grand Gulf Models

Figure 4.1 shows a diagram of the Grand Gulf Nuclear Station containment building. Figures 4.2 and 4.3 show coarse- and fine-zone RALOC models for the Grand Gulf containment building. Zone numbers are shown in large type and connection numbers in small type, and the arrows indicate the initial gas flow directions assigned (negative flows are in a direction opposite to the initial assigned direction). Altitudes of the zone centers are given in meters to the left of each diagram. Volumes and flow areas for these nodalizations were based on values calculated by M. P. Sherman.[4.5] Cells 8 and 17 were used as hydrogen sources in the coarse- and fine-nodalization models, respectively. These sources simulate injection of hydrogen into the annular region of the containment building between 110 and 135 ft, just above the suppression pool. Zones 1 through 3 of Figure 4.2 represent the dome and regions above an elevation of 209 ft. Zone 5 represents a pie-shaped shaft at azimuth 225° extending from 135 to 208 ft. Zones 4 and 6 model the annular regions between 135 and 209 ft, and zone 8 models the entire annular region from 110 to 135 ft elevation. Zone volumes are given in Tables 4.1 and 4.2 for the coarse- and fine-zone models, respectively.

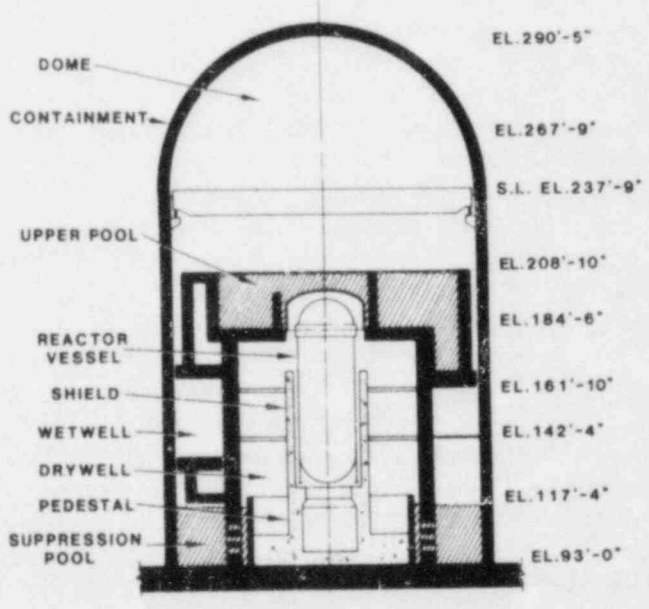

Figure 4.1 Simplified Diagram of the Grand Gulf Nuclear Station

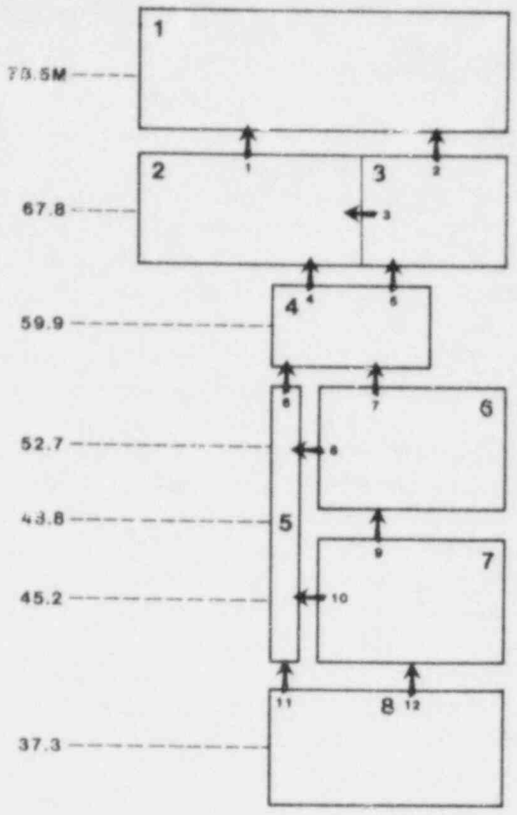

Figure 4.2 RALOC Coarse-Zone Model for the Grand Gulf Containment Building

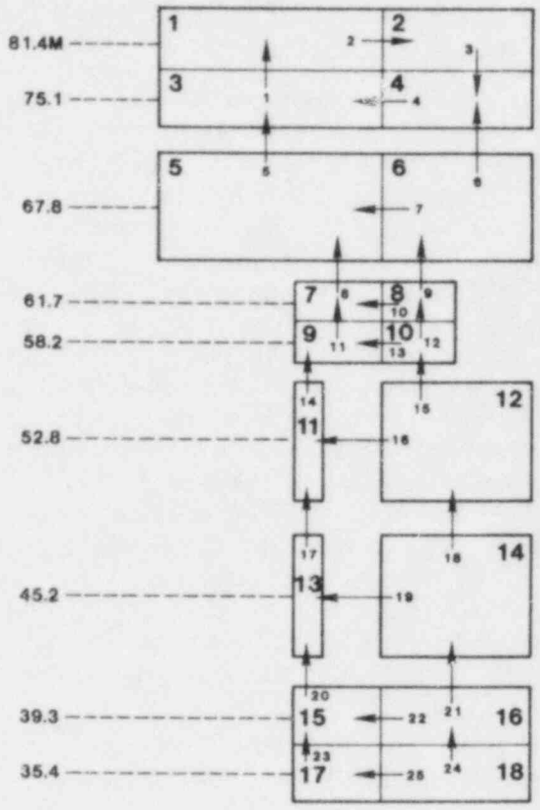

Figure 4.3 RALOC Fine-Zone Model for the Grand Gulf Containment Building

Table 4.1. Volumes for RALOC Coarse-Zone Grand Gulf Model

Zone Number	Volume (m^3)
1	1.414×10^4
2	5.876×10^3
3	3.701×10^3
4	2.808×10^3
5	1.133×10^3
6	3.987×10^3
7	3.728×10^3
8	4.341×10^3

Table 4.2. Volumes for RALOC Fine-Zone Grand Gulf Model

Zone Number	Volume (m^3)
1	4.335×10^3
2	2.735×10^3
3	4.335×10^3
4	2.735×10^3
5	5.876×10^3
6	3.701×10^3
7	6.489×10^2
8	7.543×10^2
9	7.543×10^2
10	7.543×10^2
11	5.408×10^2
12	3.987×10^3
13	5.852×10^2
14	3.728×10^3
15	5.726×10^2
16	1.595×10^3
17	3.792×10^2
18	1.225×10^3

4.5 Grand Gulf Hydrogen Source Models

Due to the uncertainties in the release of hydrogen following a core melt, four different time-dependent sources were used in this study. These are shown in Figure 4.4. Sources A, B, and C were used to investigate the effects of the rate and temperature of the hydrogen injection. Source A injects hydrogen twice as fast as B and four times as fast as C. Approximately 1500 lb of hydrogen (800 m^3) and 400 m^3 of air were injected with each of these sources. Curve D of Figure 4.4 shows a hydrogen source for Grand Gulf based on calculations performed with the computer code MARCH.[4,6] The release of hydrogen in curve D is assumed to be slow for the first 45 min after the accident, and then rapid for the next 15 min. The release rate for curve D resulted in a total injection of 5000 lb of hydrogen (total injection = 22 000 m^3 H_2 and 11 000 m^3 air). This model was used primarily to investigate effects caused by variations in the initial containment temperature distribution. Injection of the hydrogen took place in the annular region immediately above the suppression pool (RALOC does not have a suppression pool model).

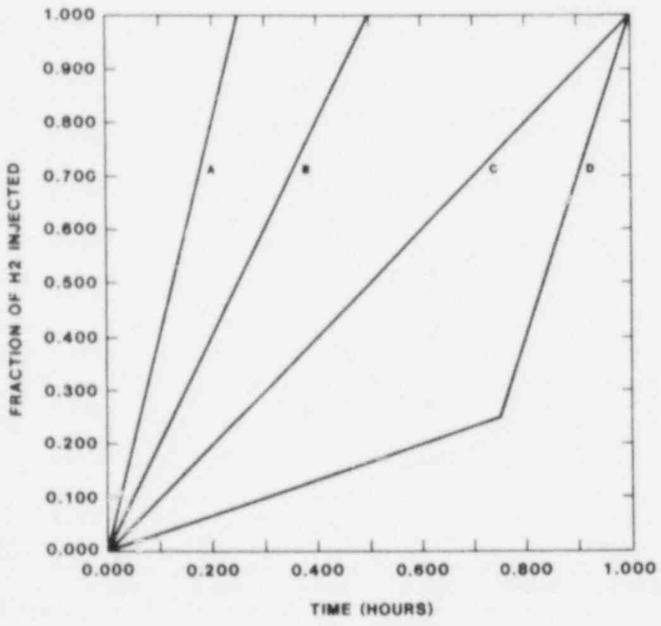

Figure 4.4 Hydrogen Source Models Used in the RALOC Grand Gulf Transport Calculations. Total injected hydrogen was approximately 1500 lb for cases A, B, and C. Case D injected 5000 lb.

4.6 Results of a Typical RALOC Calculation

RALOC results obtained with the coarse nodalization shown in Figure 4.2 and the model B hydrogen injection source shown in Figure 4.4 are given in Figures 4.5 through 4.8. Isothermal initial conditions were assumed in this calculation (60°C). Figure 4.5 shows the time histories of the hydrogen volumetric concentrations for all zones in the calculation. Hydrogen injection began at 200 s and ended 1800 s later. A uniform concentration of hydrogen was predicted approximately 1000 s after the end of injection (~14.6% in all zones). When the bottom compartment (zone 8) reached a hydrogen concentration of 8%, zones 1 and 2 (upper containment) had concentrations of approximately 3%. Discontinuities in the slope of the hydrogen time histories were the result of the edit frequency used in plotting the results (400 s).

Mass flows for connections 1 and 2 are shown in Figures 4.6 and 4.7. The mass flow in Figure 4.6 is negative; negative flows correspond to flows in a direction opposite to the initial direction assigned (arrow of Figure 4.2). The mass flow curves of Figures 4.6 and 4.7 are approximate mirror images of each other because most of the gas convects through zone 1. After hydrogen injection stopped (2000 s), the mass flows decreased and nearly reached zero flow at 10 000 s into the calculation.

Two convection loops were calculated for the Grand Gulf containment building by RALOC. These loops are shown in Figure 4.8. An upper convective loop consists of zones 1 through 4, while zones 4 through 8 participate in a lower loop. Zone 4 is a member of both loops and transfers hydrogen from the lower elevations to the upper containment.

4.7 Code Reliability Calculations

Two RALOC code reliability calculations were performed in this study. These calculations were done because the code had been recently acquired and we had not had much experience in using it, and because the code had only limited previous assessment. The first calculation varied the maximum allowable time step during the implicit integration in order to test the stability of the solution. The second calculation tested the ability of the code to asymptotically approach a converged solution when the nodalization was made finer.

4.7.1 Effect of Maximum Allowable Time Step

Figure 4.9 shows a comparison between two calculations differing only in the maximum allowable time step used during the implicit portion of the calculation (50 s vs 200 s). Decreasing the time step did not significantly affect the calculation.

4.7.2 Effect of Nodalization

One of the attributes of a good computer code is that the calculated results approach an asymptotic limit as the degree of resolution is increased. A calculation was performed to determine if the RALOC solution would change appreciably if the number of zones and connections in the Grand Gulf model were increased. To accomplish this objective, the coarse nodalization of Figure 4.2 was modified to the fine nodalization shown in Figure 4.3. Zones which were tall (zone 5 of Figure 4.2) were split vertically into two zones to reduce any gravitational effects (properties in RALOC are evaluated at cell centers). Also, zones which had a high degree of activity or importance (zones 1, 4, and 8 of Figure 4.2) were subdivided to provide smoother convective transport. To reduce computational time, the remaining coarse zones were not changed (zones 2, 3, 6, and 7 of Figure 4.2).

Comparisons between the fine-zone and coarse-zone calculations using the isothermal source model D of Figure 4.4 (60°C) are shown in Figures 4.10 and 4.11. As hoped, the RALOC calculations appear to be fairly insensitive to the degree of discretization used in the nodalization.

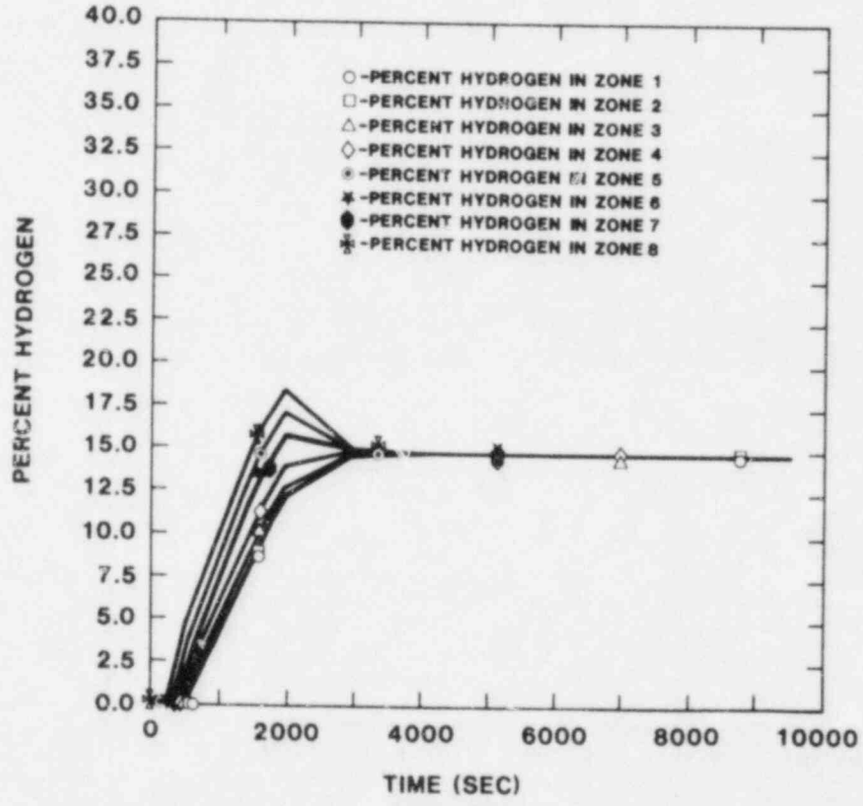

Figure 4.5 RALOC Grand Gulf Hydrogen Transport Prediction for Source Model B and Coarse Nodalization

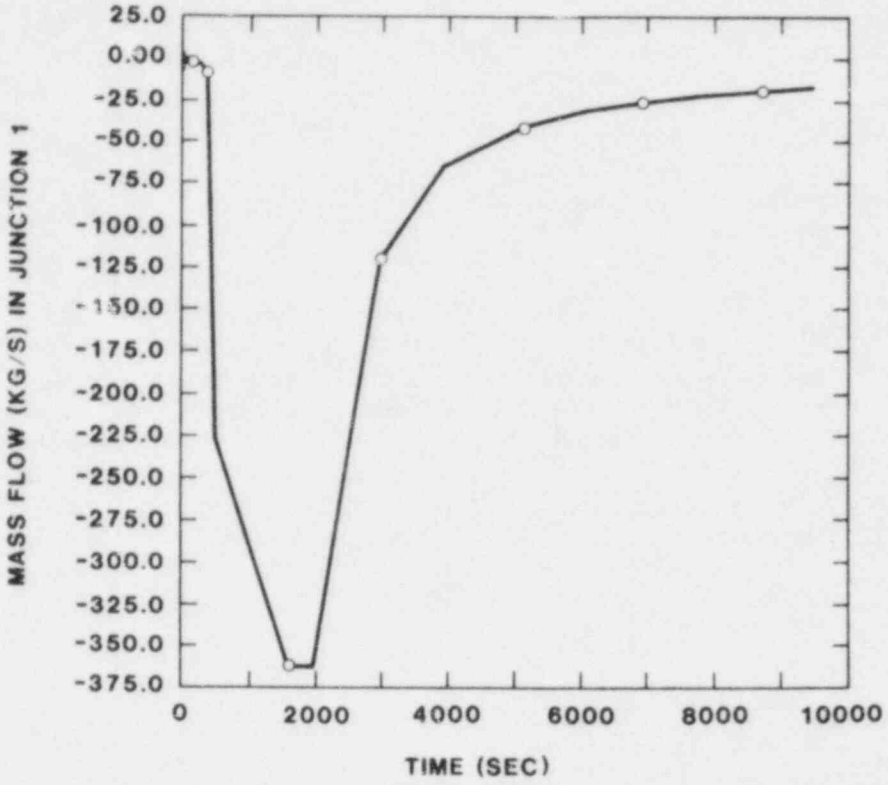

Figure 4.6 RALOC Mass Flow Prediction for Connection 1 (source model B and coarse nodalization)

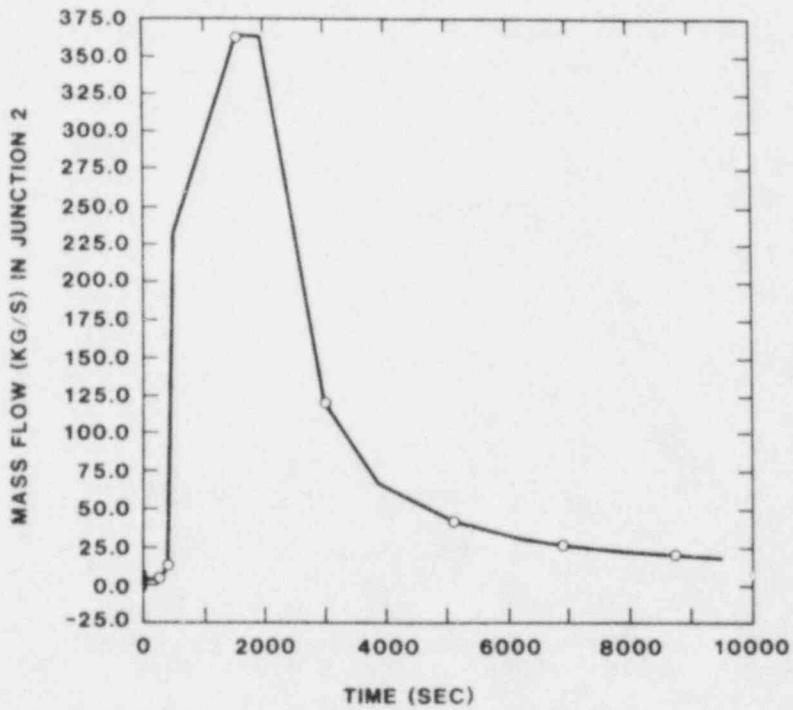

Figure 4.7 RALOC Mass Flow Prediction for Connection 2 (source model B and coarse nodalization)

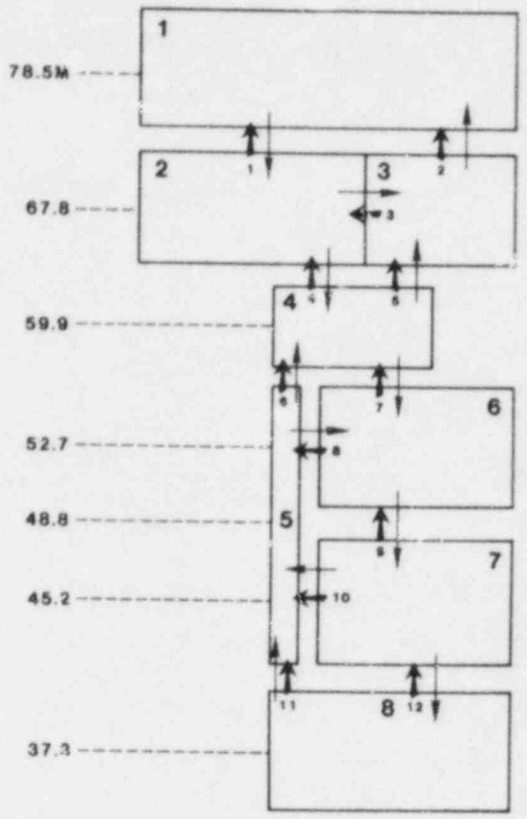

Figure 4.8 RALOC Calculated Convection Loops for Grand Gulf Containment. Small arrows indicate flow direction. Large arrows represent the initial gas direction assigned.

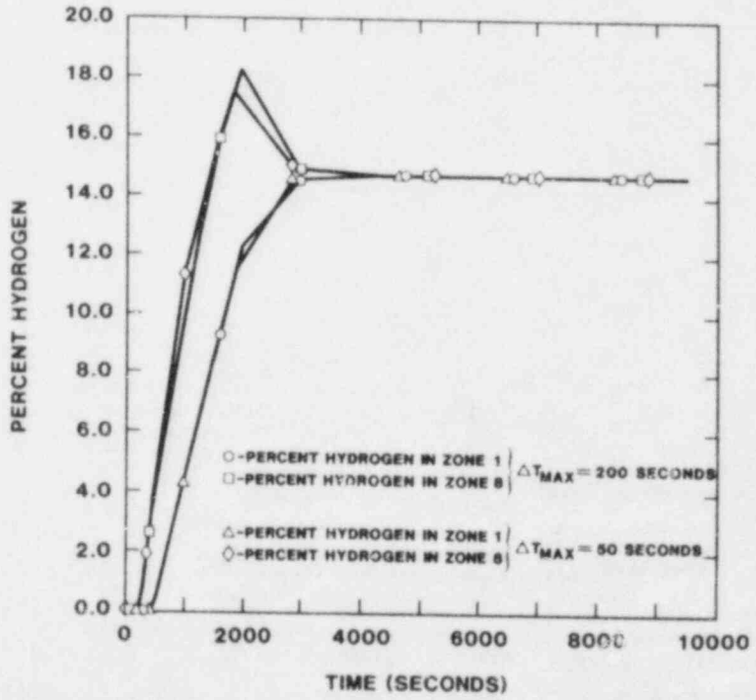

Figure 4.9 Effect of Maximum Allowable Time Step on the RALOC Calculation (source model B and coarse nodalization)

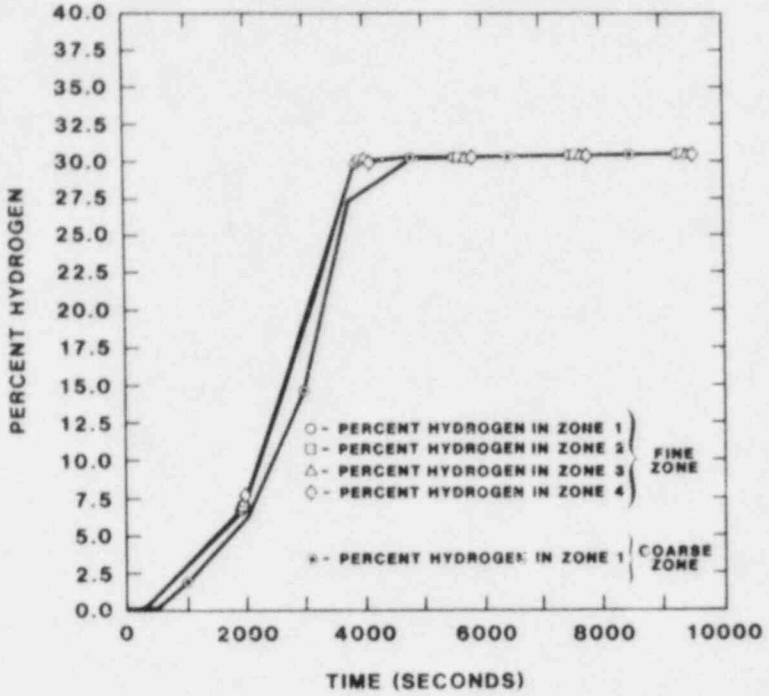

Figure 4.10 Comparison of RALOC Fine- and Coarse-Zone Results for the Top of the Grand Gulf Containment

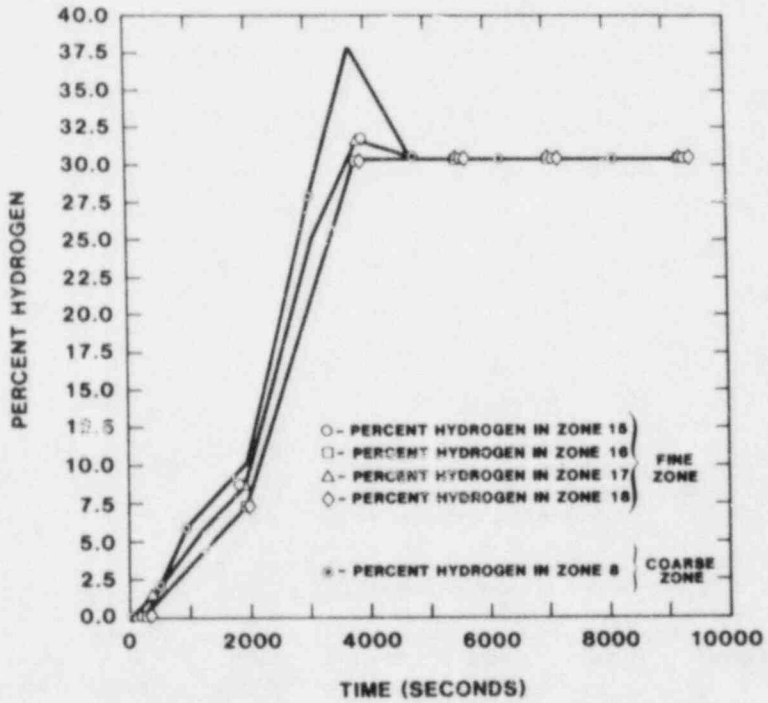

Figure 4.11 Comparison of RALOC Fine- and Coarse-Zone Results for the Bottom of the Grand Gulf Containment

4.8 Physical Parameter Sensitivity Studies

The previous section demonstrated that the RALOC calculations are numerically well behaved. The solutions obtained are reasonably independent of the maximum time step specified by the user and of the degree of resolution used in the model nodalization. This section discusses the effects of physical parameters on the RALOC calculations. These parameters are associated with the time-dependent release of hydrogen following an accident, and the intial conditions present at the start of hydrogen injection into the containment.

4.8.1 Hydrogen Injection Rates

Figure 4.12 shows a comparison between RALOC calculations using source models A and B of Figure 4.4. Increasing the hydrogen injection rate increases the spatial nonhomogeneity of the hydrogen. Faster rates of injection allow less time to mix. Decreasing the injection rate decreases the hydrogen asymmetry by extending the mixing time (Figure 4.13 comparison of source models B and C). Differences in the final concentration values of Figures 4.12 and 4.13 were caused by small differences in the total amount of hydrogen injected (source A injected 85 lb more hydrogen than source B, while source C injected 25 lb less).

Figure 4.14 compares the hydrogen concentrations at various altitudes when the bottom compartment reaches 8%. Larger hydrogen injection rates produce greater volumetric differences in the local hydrogen concentrations.

4.8.2 Hydrogen Injection Temperature

In the event of a degraded-core accident in Grand Gulf, the temperature of the hydrogen injected into the suppression pool will be hotter than the water temperature. M. L. Corradini has indicated that the temperature of the hydrogen exiting the suppression pool will be nearly the same as the water temperature (or perhaps somewhat higher).[4.7] To test the effect of a higher hydrogen temperature, the injection temperature was increased from 60° to 300°C and a comparison was made with the base-case calculation (source model B, 60°C isothermal, and coarse nodalization). This comparison is shown in Figure 4.15. The effect of a higher hydrogen injection temperature on the RALOC calculation is negligible.

4.8.3 Initial Containment Temperature Distribution

Battelle-Frankfurt experimental data demonstrate that the initial temperature distribution in a containment can significantly affect the hydrogen volumetric concentrations. To investigate this effect for the Grand Gulf calculations, concrete slabs were added to the fine nodalization model of Figure 4.3 as time-dependent heat sources. Two initial temperature distributions were assigned to the heat slabs and the gas initially present in the containment. Both distributions were linear with elevation and started at 60°C. The first temperature distribution assumed that the temperature in the containment decreased linearly with elevation (20°C hotter at the bottom than at the top of the containment), while the second profile assumed an inverted distribution; i.e., the temperature was assumed to increase linearly with elevation (20°C cooler at the bottom than at the top of the containment).

Figure 4.16 shows a comparison between an isothermal containment and the decreasing temperature model. The results are based on source model D of Figure 4.4. Differences in the hydrogen concentration during the injection period were insignificant. Final hydrogen concentrations were somewhat higher for the decreasing temperature model. This occurred because the convecting gases cooled the containment and condensed some additional steam.

Figure 4.17 shows a comparison made between the isothermal base case and the inverted temperature model. During the injection period, a significant difference is seen between the hydrogen concentrations in the top compartment. The higher temperatures present in the top of the containment produced a thermal barrier which inhibited the convection of hydrogen. Final concentrations for the inverted temperature model were lower than for the isothermal case. Convecting gases warmed the containment and created more steam. Increasing the temperature difference between the top and bottom of the containment from 20° to 50°C results in even more pronounced hydrogen asymmetries (Figures 4.18 and 4.19). Again, the higher overall containment temperature produced lower end-of-calculation hydrogen concentrations due to an increased production of steam.

Figure 4.20 compares the hydrogen concentrations at various elevations when the bottom compartment reaches 8%. A decreasing temperature distribution has little effect on the hydrogen volumetric

concentrations. Inverting the temperature distribution significantly affects the concentrations, especially in the uppermost compartments. Middle elevations (less than 209 ft) were not as affected by the inverted temperature profile and actually showed a slight increase in mixing.

In the absence of containment sprays, our RALOC calculations clearly demonstrate the importance of an inverted temperature distribution. Asymmetries caused by the temperature inversion are greatest during the injection period. These asymmetries can significantly affect the design of possible mitigation schemes.

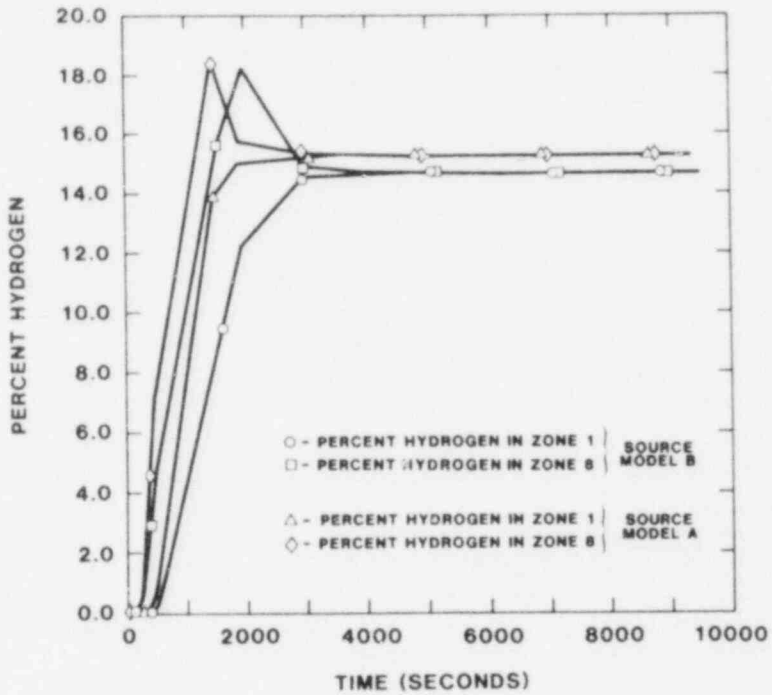

Figure 4.12 Effect of Hydrogen Injection Rate on the RALOC Calculations. Source A versus source B.

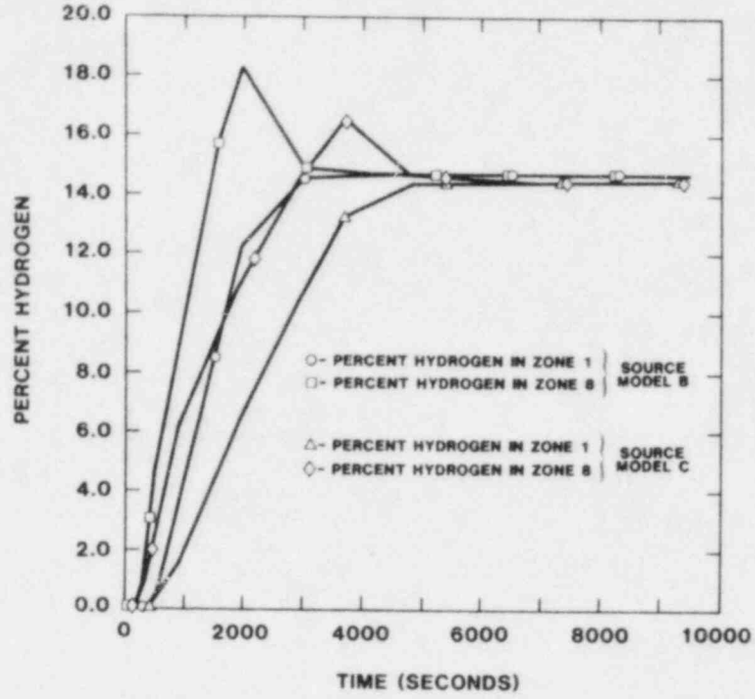

Figure 4.13 Effect of Hydrogen Injection Rate on the RALOC Calculations. Source C versus B.

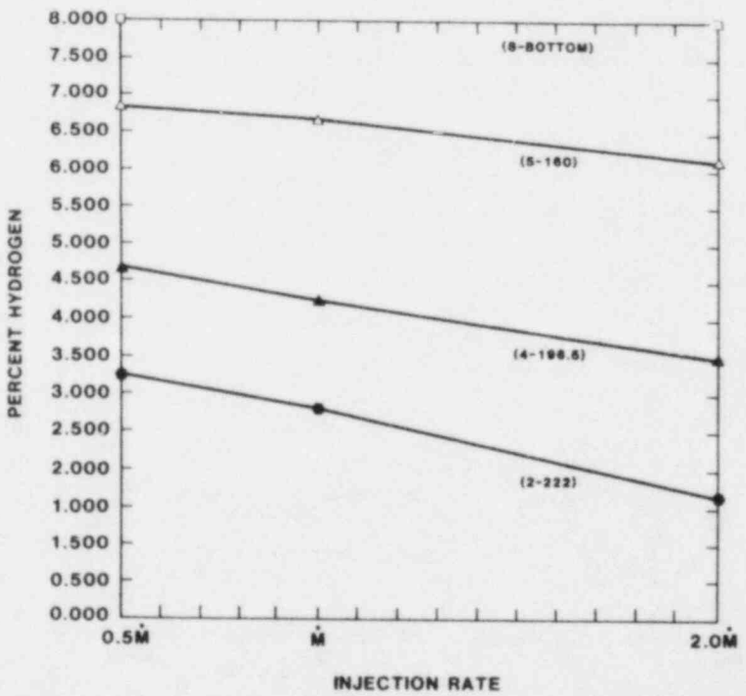

Figure 4.14 Percent of Hydrogen in a Zone When Zone 8 has 8% as a Function of the Rate of Hydrogen Injection. Numbers in parentheses are zone number and elevation of the zone in feet.

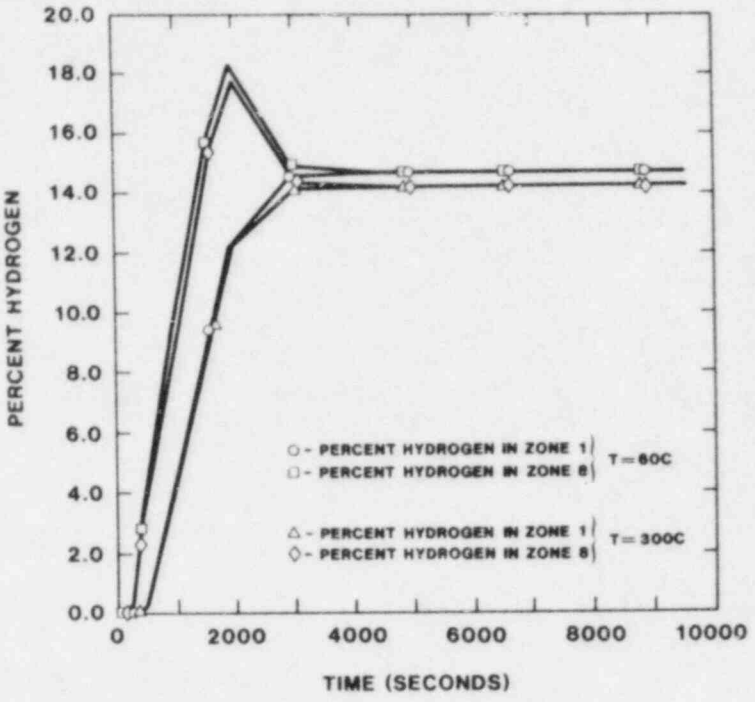

Figure 4.15 Effect of Hydrogen Injection Temperature on the RALOC Calculation

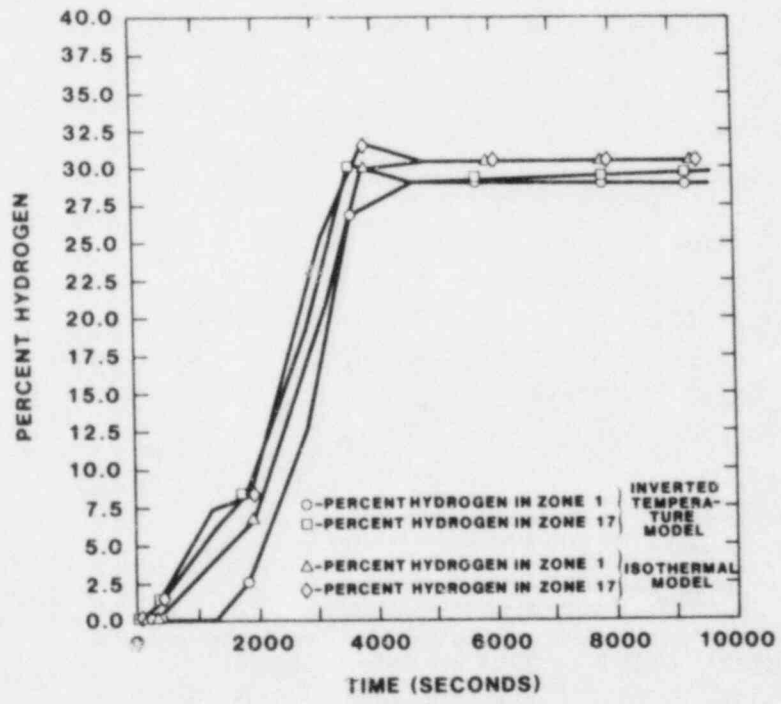

Figure 4.16 Comparison of Isothermal Base Case With a Decreasing Temperature Model. Results are shown for the top and bottom of the Grand Gulf containment.

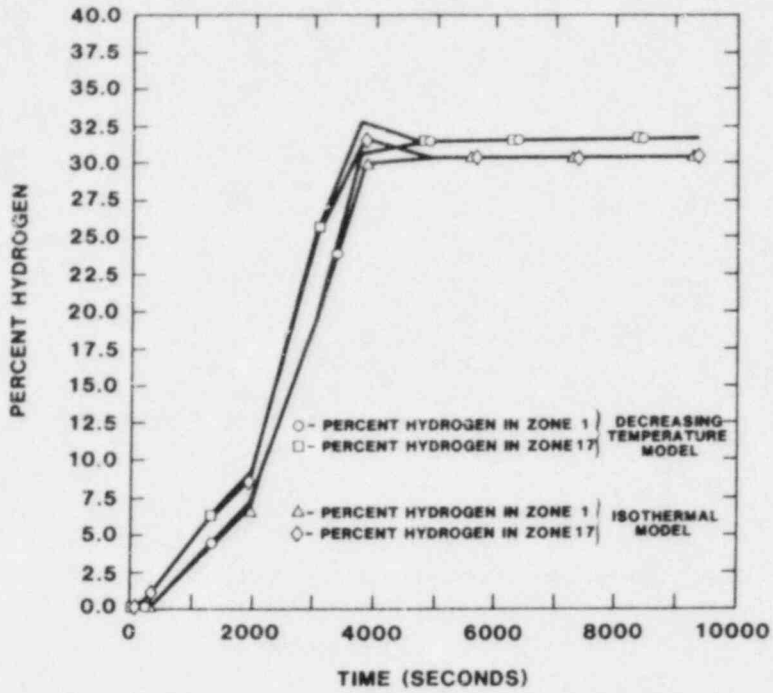

Figure 4.17 Comparison of Isothermal Base Case With an Inverted Temperature Model. Results are shown for the top and bottom of the Grand Gulf containment.

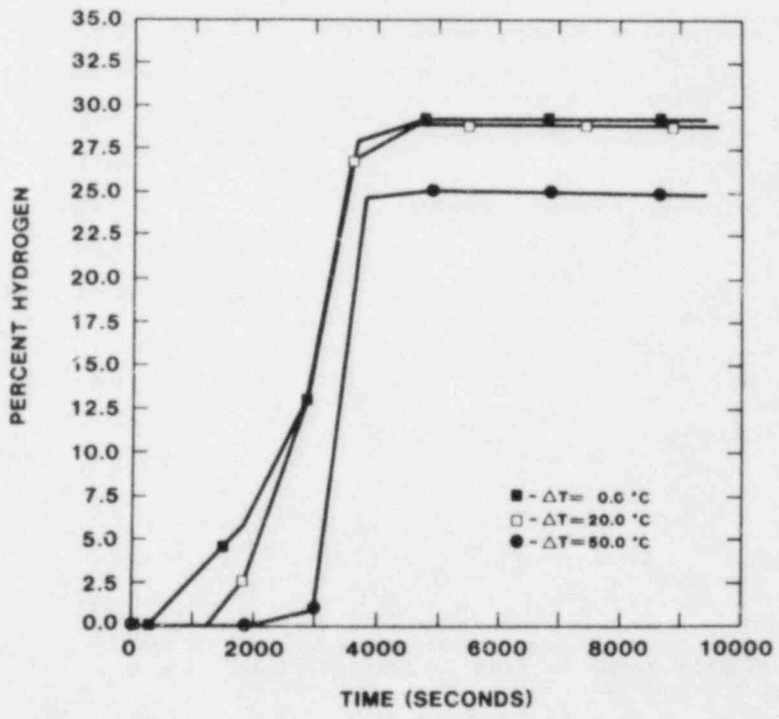

Figure 4.18 RALOC Comparison for Hydrogen Concentrations in the Top of the Grand Gulf Containment (Zone 1) as a Function of Time and Magnitude of the Initial Temperature Inversion (0.0°C, 20.0°C, and 50.0°C)

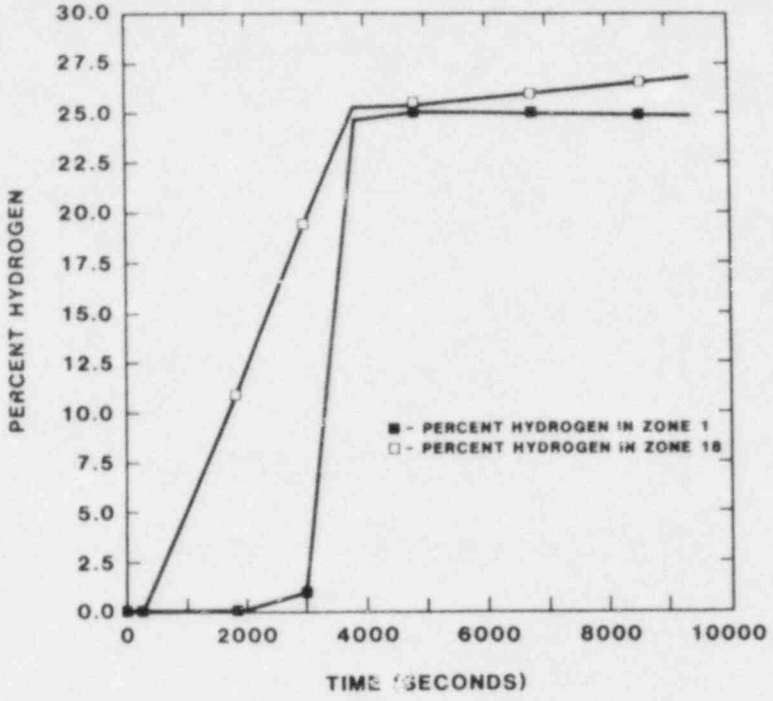

Figure 4.19 RALOC Comparison of the Hydrogen Concentration Between the Top and the Bottom of the Grand Gulf Containment for the Initial Temperature Inversion of 50°C

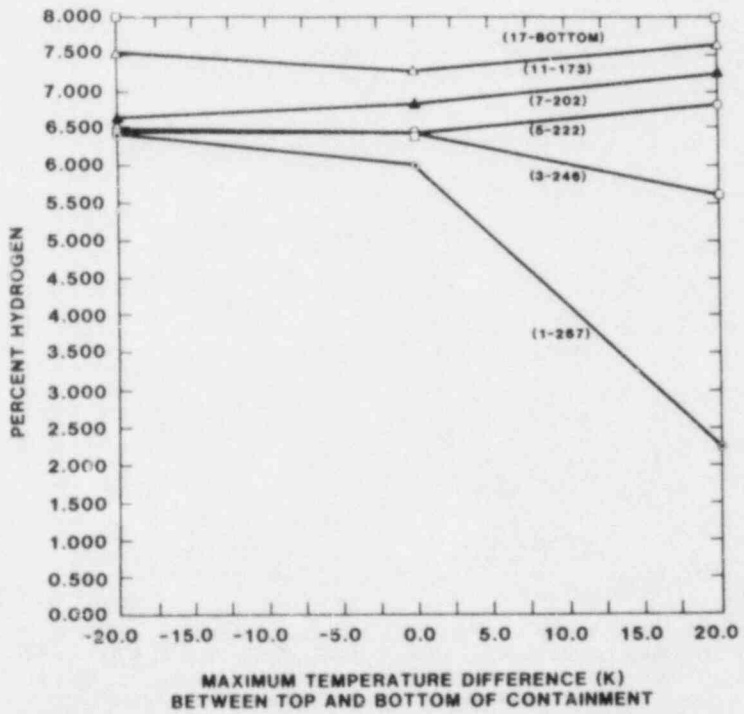

Figure 4.20 Percent of Hydrogen in a Zone When Zone 17 has 8% as a Function of the Initial Temperature Distribution. Numbers in parentheses are the zone number and the elevation of the zone in feet. (Fine nodalization).

4.9 Conclusions

The following conclusions are based on the sensitivity studies that we performed with RALOC. However, until additional assessment calculations have been completed, these calculations should be regarded as tentative.

1. The concentration of hydrogen in the upper compartments of the Grand Gulf containment are probably combustible (~6%) when the bottom compartment concentration reaches 8% for isothermal initial conditions.
2. Increasing the hydrogen injection rate increases the degree of nonhomogeneity in the hydrogen concentrations due to reduced mixing time.
3. An initial temperature distribution which is hotter at the top of containment than at the bottom increases hydrogen asymmetry during injection and long-term stratified concentrations (10 000 s) by establishing a thermal barrier to convection.
4. A temperature profile which is colder at the top than at the bottom produces nearly the same results as isothermal conditions. Mixing is not significantly enhanced.
5. Hydrogen injection temperatures greater than the temperature of the suppression pool do not significantly affect the mixing calculations.
6. Nearly steady-state solutions are achieved approximately 20 min after the end of hydrogen injection.
7. The upper containment compartment reaches 8% hydrogen concentration approximately 5 min after the bottom has reached 8%.

4.10 References

[41]H. Jahn, "RALOC-MOD1 with 1980 Updates," undocumented revision of proprietary RALOC-MOD1, *RALOC-MOD1 - A Computer Program for the Determination of Local Gas Concentrations in Subdivided Vessels (Particulary: H_2 Distribution in PWR Full Pressure Containments Following a Loss-of-Coolant Accident*, NRC Translation 654, GRS-A-263 (January 1979), Contract No. 82260, Gesellschaft für Reaktorsicherheit, Federal Republic of Germany.

[42]H. Jahn, *Status Report on the Hydrogen Distribution Following a Coolant Loss Accident*, NRC Translation 796, GRS-A-333 (August 1979), Gesellschaft für Reaktorsicherheit, Federal Republic of Germany.

[43]G. Langer, R. Jenior, and H. G. Wentlandt, *Experimental Investigation of the Hydrogen Distribution in the Containment of a Light Water Reactor Following a Coolant Loss Accident*, NRC Translation 801, BF-F-63.363-3 (October 1980), Battelle Institute e.v. Frankfurt, Federal Republic of Germany.

[44]G. R. Bloom, L. D. Muhlestein, and A. K. Postma, "Hydrogen Mixing in Containment Atmosphere," Proprietary paper presented at the EPRI Hydrogen Project Review and Workshop (October 5, 1981), Palo Alto, CA.

[45]M. P. Sherman, Sandia National Laboratories, Private communication (September 1981).

[46]B. W. Burnham, Sandia National Laboratories, Private communication (September 1981).

[47]M. L. Corradini, University of Wisconsin, Private communication (September 1981).

5.0 Dynamic Combustions and Impulsive Loading

5.1 Introduction

In this section we will discuss qualitatively the likelihood of a detonation occurring in a mixture of hydrogen and air at the Grand Gulf Nuclear Station. We begin by listing the conditions which seem to be necessary, but not always sufficient, to cause a detonation in hydrogen : air mixtures. Then we discuss the forms of combustion that can produce impulsive loads: detonations, quasi-detonations, transitions to detonation, and accelerated flames. Finally, we examine the Grand Gulf plant and various accident scenarios in order to make a qualitative estimate of the likelihood of detonations.

5.2 Necessary Conditions for Detonation

For a gaseous mixture containing hydrogen, oxygen, nitrogen, and steam, a detonation can propagate if the component gas concentrations fall within a given range (recently it has been shown that a concentration of 13.8% hydrogen in air is detonable). The fact that a mixture is detonable does not mean that it will detonate. In general, it is also necessary that at least one of the following initial conditions be satisfied:

- A "strong" ignition source exists
- A "weak" ignition source followed by either a long run-up distance, or an obstacle-filled run, exists

Geometries (boundary conditions) also play a very important role in the initiation and propagation of detonations. These conditions are given in a qualitative manner because quantitative criteria are not yet generally available, accepted, or applicable. If the mixture is detonable, the boundary conditions are right, and at least one of the above initial conditions is satisfied, detonation is possible but not a certainty.

5.3 Detonations, Quasi-Detonations, Transitions to Detonation, and Accelerated Flames

Classical or Chapman-Jouguet (C-J) detonations in hydrogen : air mixtures have been studied extensively in laboratory-scale devices. A more detailed discussion of C-J detonations and the impulsive pressures that they produce is given elsewhere.[5.1] Quasi-detonations and accelerated flames can also produce impulsive loads that significantly exceed the calculated deflagration pressures. This happens whenever the flame-front velocity is comparable to or greater than the speed of sound in the unburned gas ahead of the front so that strong shock waves are produced.

Quasi-detonations are defined here to be supersonic combustion waves that, for one reason or another, have not developed into full C-J detonations. An example would be a combustion that is initiated in an obstacle-filled tube using a detonable mixture, or a fully developed detonation that enters an obstacle-filled tube. Figure 5.1 illustrates this behavior. Researchers at McGill University[5.2] used a 5-cm-dia by 11-m-long detonation tube to produce the results shown in the figure. The first 3 m of the tube contained orifice-plate obstacles (area blockage ratio 0.6; distance between orifice plates ~5 cm). The ignition source was a glow wire ("weak" igniter). Flame speeds were measured as a function of distance from the igniter for hydrogen : air mixtures containing 20% to 30% hydrogen (by volume).

The data shown in Figure 5.1 illustrate four phenomena of interest to this discussion. For all mixtures, the flame accelerates to supersonic speeds by the time it has travelled 0.5 m from the igniter. The 30% hydrogen case is apparently unstable (with the 0.6 area-blockage orifice plates) because it can behave as either a quasi-detonation (flame speed ~1300 m/s) or an accelerated flame (flame speed ~850 m/s) while it travels through the obstacles. The quasi-detonation becomes a C-J detonation (~2000 m/s) shortly after it emerges from the obstacles, but the accelerated flames actually decelerate for 0.5 to 1.5 m before making a deflagration-to-detonation transition (DDT).

The net effects of flame acceleration can range from mild to strong depending on the degree of acceleration. For flame velocities, v, that are small compared to the sound speed ($v \ll 400$ m/s), the major effect of an increase in velocity is to decrease the heat losses; consequently, the combustion pressure more closely approaches the adiabatic value. When the

flame speed becomes comparable to or greater than the sound speed, significant shock waves are produced by the flame; consequently, impulsive pressure loads greatly exceeding the adiabatic, equilibrium pressure can occur. The damage potential of these dynamic loads depends on the specific structures that are exposed to them.

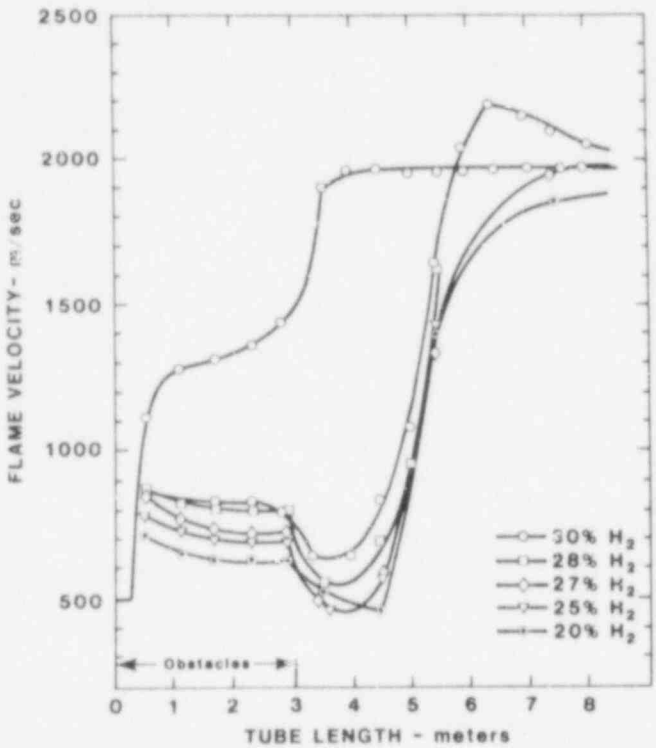

Figure 5.1 Flame speed as a function of distance from the igniter for various H_2 : air mixtures. The first 3m of the detonation tube contained orifice-plate obstacles with an area-blockage ratio equal to 0.6.

5.4 Local Detonation Calculation for Grand Gulf

Detonation of hydrogen : air mixtures will result in spatially varying dynamic loads on the containment structure. In order to obtain estimates of the magnitude and nature of such loads, the two-dimensional wave propagation code, CSQ,[5.3] was used for a calculation modelling a local detonation in the Grand Gulf containment. This computational tool has previously been applied to detonations in large, dry containments and ice condenser plants.[5.4, 5.5]

CSQ is a well-tested computer program which solves finite-difference analogs to the differential equations describing conservation of mass, momentum, and energy, together with equations of state for the materials in a given problem. Either Cartesian or cylindrical coordinates may be chosen; the latter option was used in the calculation described here. The numerical method used in the program includes an artificial viscous pressure, which smooths strong compression waves so that results agree well with steady shock wave solutions. This smoothing, and the finite spatial mesh size, result in peak and reflected pressures for a steady detonation wave (C-J wave) that are *lower* than the theoretical values. The "conservative" effect of the assumption of axial symmetry is thus counterbalanced, although the amount of this compensation is unknown. For the hydrogen : air detonation modelling, a method was used which converts unburned material to burned material at a constant rate whenever a threshold pressure is exceeded; the rate and threshold values are input constants. The containment building boundaries were treated as rigid and smooth, and pressure histories were maintained at various points on the boundaries.

In our CSQ calculation for the Grand Gulf containment we only modelled the containment dome region and the wetwell above the suppression pool water level. The NRC estimated static failure pressure (0.48 MPa) would be exceeded if a mixture well below 18% hydrogen (a previously quoted detonation limit) filled containment, and underwent an adiabatic, isochoric deflagration. Therefore, only detonations of localized hydrogen : air mixtures need to be considered—the remainder of the volume can be modelled as containing only air. A 20% hydrogen mixture in dry air was assumed to occupy the bottom of the wetwell to a height of 7.7 m, and was detonated at the approximate center of its interface with the air (Figure 5.2). The wetwell was given irregular boundaries in an effort to approximate the presence of equipment and flow obstacles. For the initial conditions chosen for the mixture (275 K, 0.12 MPa), the C-J pressure is about 1.6 MPa. Because of the factors mentioned previously, and because the calculation requires a propagation distance of ~20 m to establish a steady wave, the maximum detonation pressure attained was only about one-half the theoretical C-J value.

Pressure histories in the wetwell region exhibited high, very narrow peaks early in the calculation and many complicated interactions, as shown in Figure 5.3. Peak pressures caused by the shock propagating through the air remained fairly high as far up as the wetwell flow path entrance to the containment dome (Figures 5.4 and 5.5). As this shock wave emerges into the containment dome, the toroidal expansion of the wave results in lower loads on the boundary (Figure 5.6). Because of the uncertainties in modelling the boundaries of the wetwell region, we are unable to

assess the threat to containment posed by the calculated pressures, either by direct wall loading or by missile generation.

The load histories produced on the dome boundaries had peaks of much longer duration than those in the wetwell. The 0.48 MPa value was exceeded for several milliseconds on the central region of the dome to a radius of about 4.6 m (Figures 5.7 and 5.8). Without dynamic structural analyses, we can make no realistic estimate of the threat to the dome region from the predicted loads. However, a very rough idea of the possibility of structural damage may be gained by considering an impulsive failure criterion proposed by Mark.[5.6] The criterion considers spatially uniform loading of the structure, and determines an acceptable impulse value which is proportional to the product of the maximum acceptable pressure and one-quarter of the first fundamental period of the structure. We know of no formal estimates for the latter quantity, but the period is probably in the range of 40 to 60 ms. With this estimate, and a pressure of 0.48 MPa, the criterion gives acceptable specific impulses of 6.2 to 9.3 kPa-s; according to Mark, these values should be conservative for a reinforced concrete structure. Because our computed loads are not spatially uniform, we computed specific impulses for all 10- and 15-ms intervals, rather than just the first. The results are shown in Figures 5.9 and 5.10 for the top center of the dome. It may be seen from the figures that for this calculation and the estimated periods chosen, the predicted impulses are below the acceptable values. However, because the calculated loads are not spatially uniform, we are uncertain as to the real meaning of this comparison. In addition, variations in the amount and concentration of the hydrogen : air mixture, in detonation location, and in the modelling of the flow path between the wetwell and the upper compartment may all be expected to affect the numerical results.

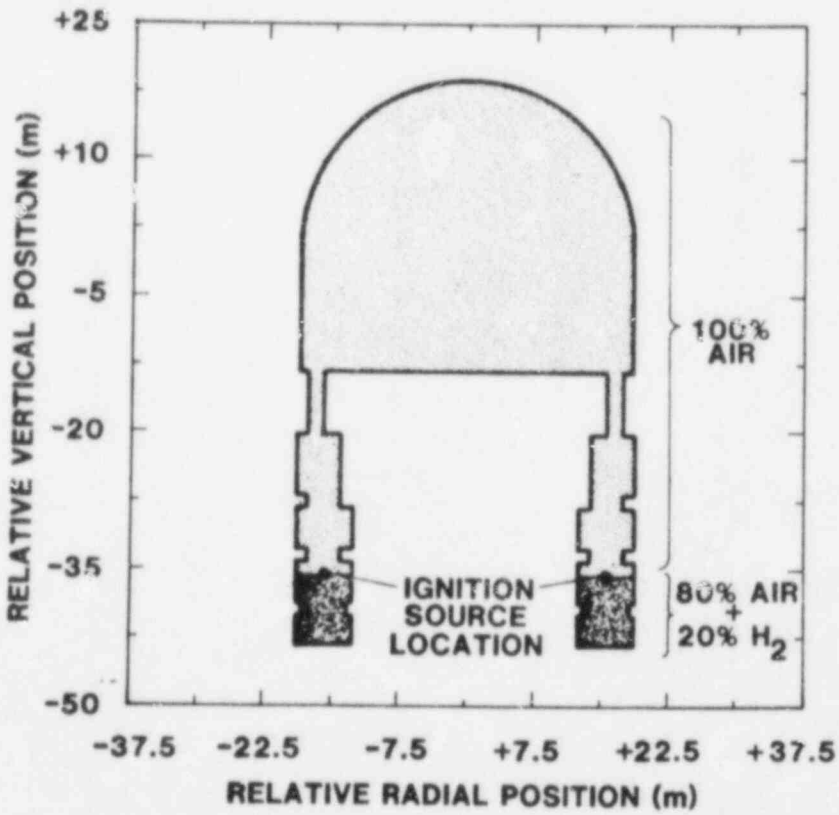

Figure 5.2 Grand Gulf Containment Model for CSQ Calculation (axisymmetric)

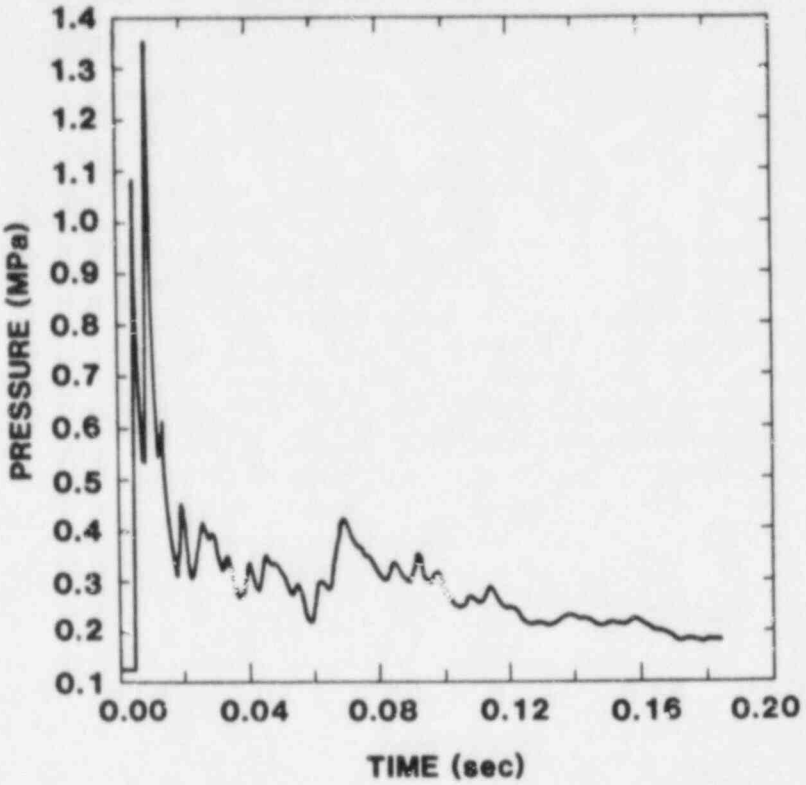

Figure 5.3 Pressure History on Outer Wall, Below Detonation Point (CSQ)

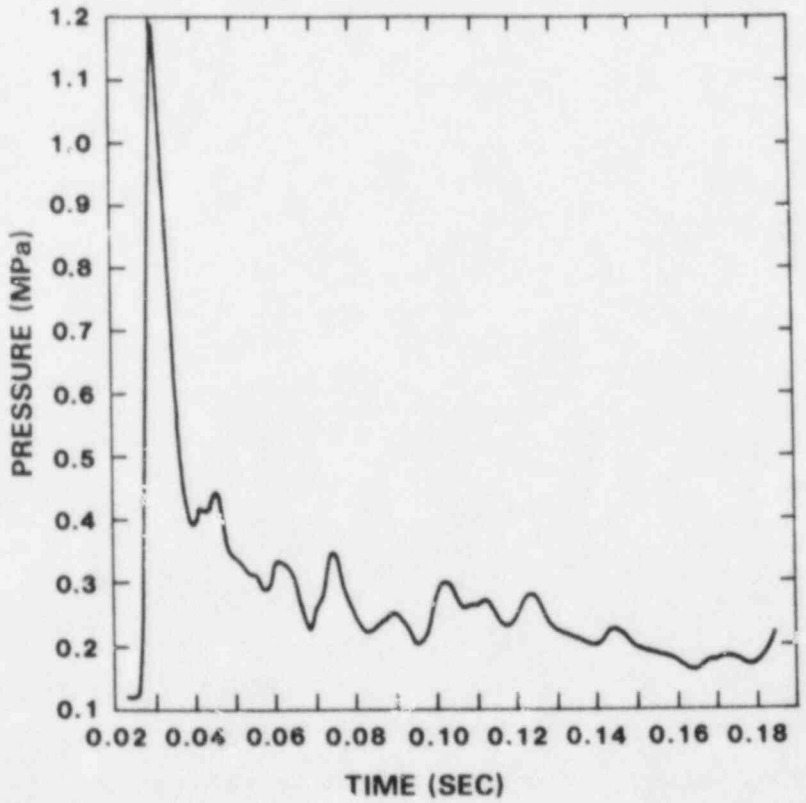

Figure 5.4 Pressure History at Outer Edge of the Wetwell Flow Path into the Containment Dome (CSQ)

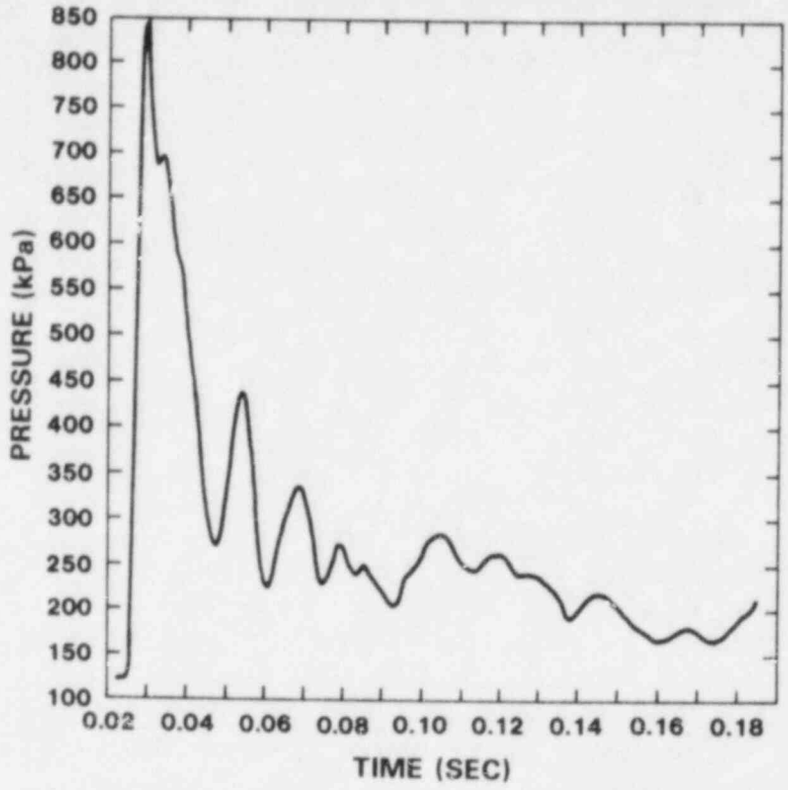

Figure 5.5 Pressure History at Inner Edge of the Wetwell Flow Path into the Containment Dome (CSQ)

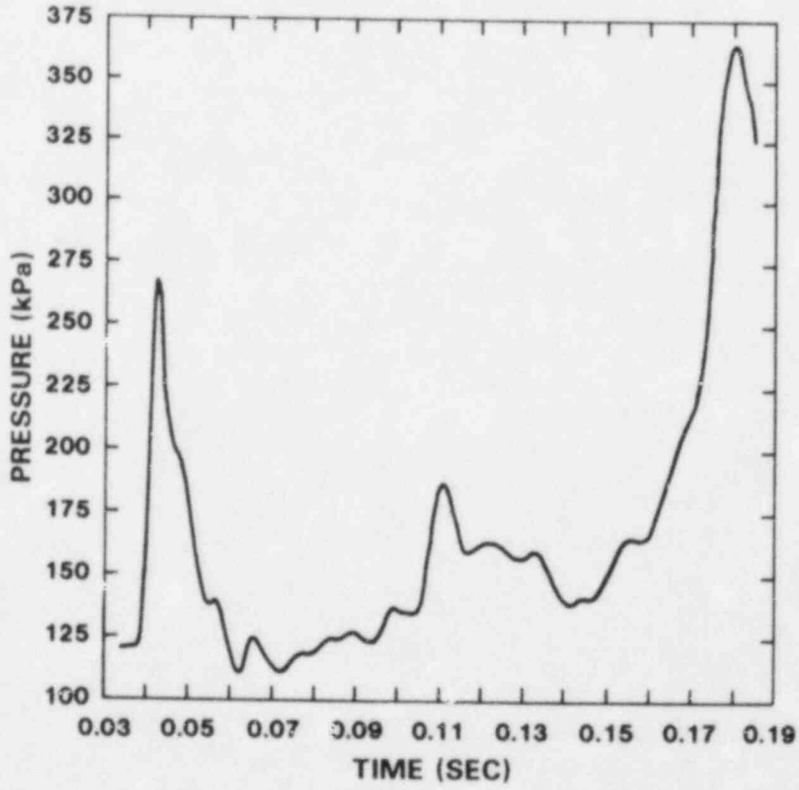

Figure 5.6 Pressure History at Lowest Point of the Containment Dome Wall (CSQ)

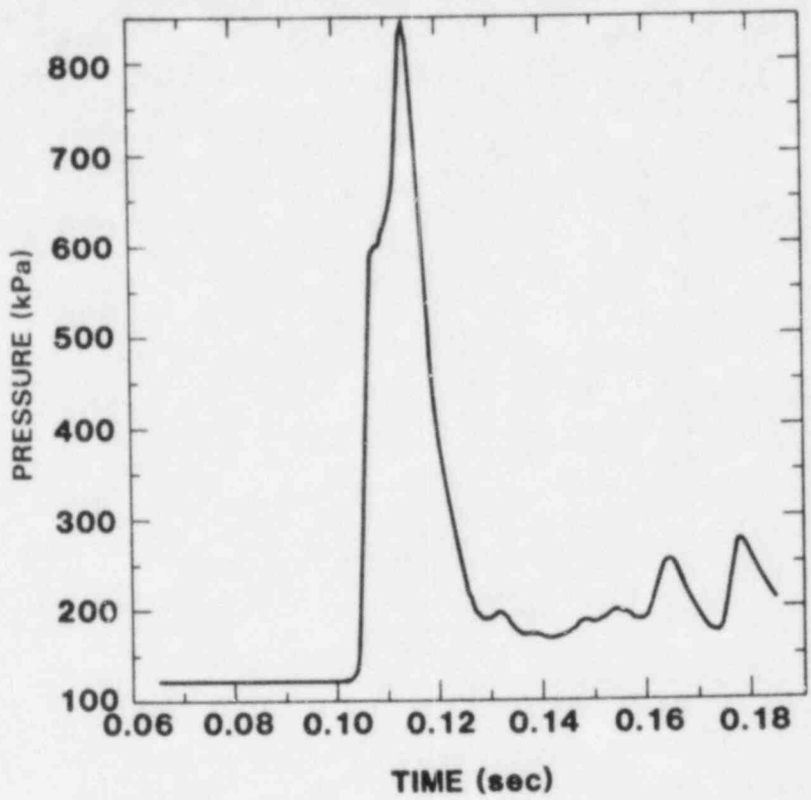

Figure 5.7 Pressure History at Dome Center (CSQ)

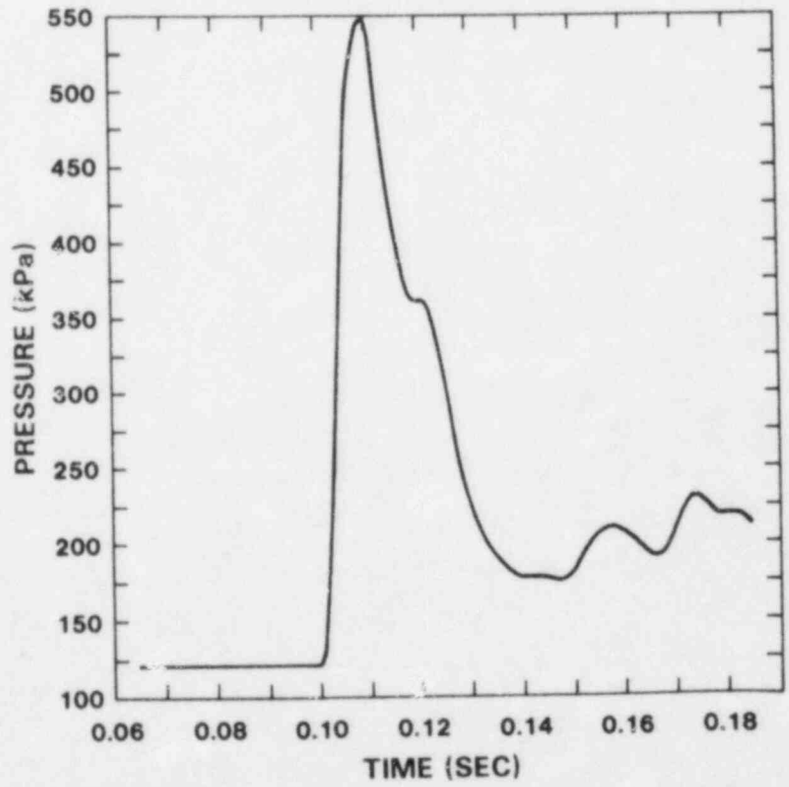

Figure 5.8 Pressure History on Dome 4.7 m From Center (CSQ)

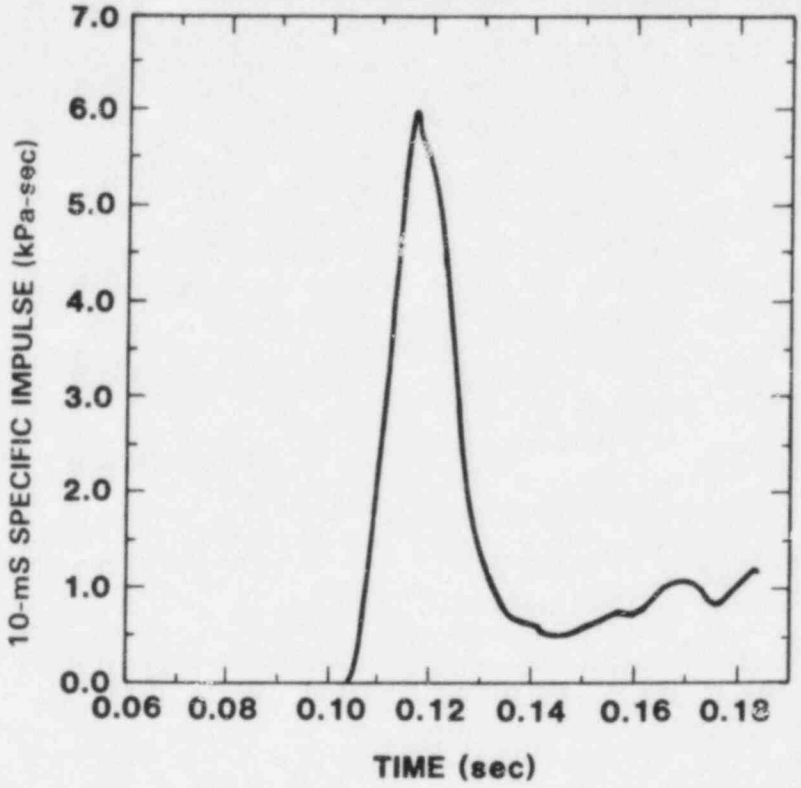

Figure 5.9 Specific Impulse at Dome Center for 10 ms intervals

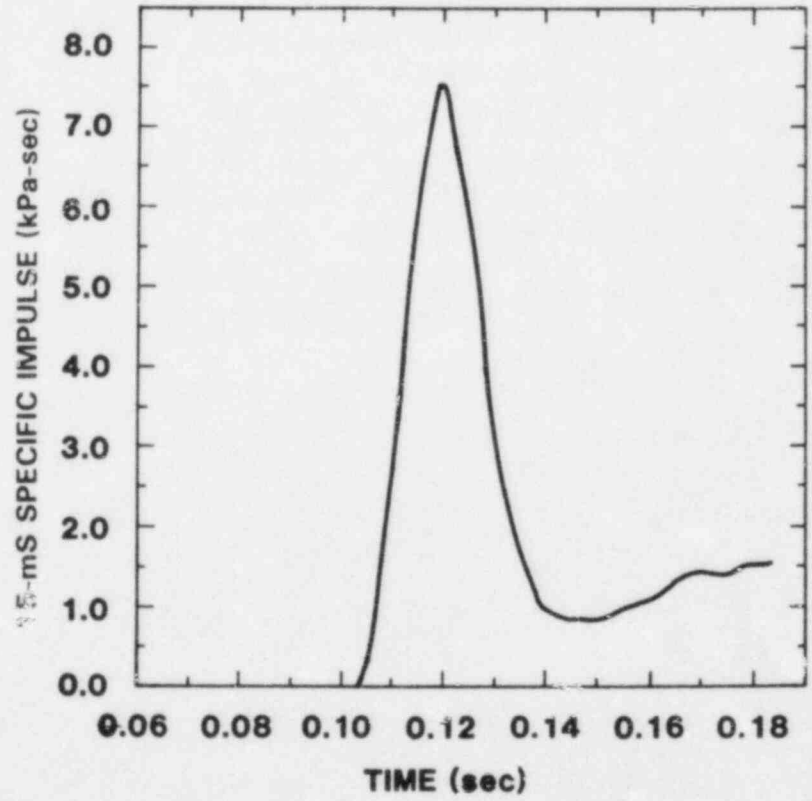

Figure 5.10 Specific Impulse at Dome Center for 15 ms Intervals

5.5 Likelihood of Detonation at the Grand Gulf Nuclear Station

It appears to us that several conditions could lead to the formation of detonable clouds of significant extent. In general, the igniters would have to be off for some time and other ignition sources (hot surfaces, switching sparks, motor sparks, etc) would also have to be temporarily off or ineffective. A sudden large increase in the hydrogen release rate or the movement of a large air mass into an oxygen-depleted, hydrogen-rich compartment (e.g., the drywell) might also lead to local regions of detonable proportions. The most likely regions for localized detonations appear to be the drywell and the bottom of the wetwell. Higher wetwell regions could become involved if steam inerting and/or oxygen depletion occurred due to previous combustion events.

Several complicating factors make it difficult to discuss the likelihood of forming a detonable mixture. Hydrogen, oxygen, and steam concentration gradients occur in the vertical (z), radial (r), and azimuthal (θ) directions. This would be true without combustion. With numerous combustion events occurring throughout the wetwell/containment region at various times, the picture is extremely complex. For each igniter we can envision a sequence of "pulsed" burns in which some hydrogen is locally combusted. A period of mixing follows each burn. In the region between the top of the suppression pool and the first wetwell igniters (z = 135 ft), the concentration of hydrogen may reach detonable proportions if the hydrogen release rate is high enough. A pulsed burn from z = 135 ft down to the top of the pool would remove all hydrogen (or oxygen) from the region and permit high hydrogen concentrations to form before the new mixture rose to the igniters. The spatial extent of such detonable mixtures would probably be limited.

In our judgment, given current information, the likelihood of a detonation occurring, as distinguished from the formation of detonable mixtures, is very small. The probability of a DDT occurring is also quite small. However, we feel that some degree of flame acceleration upward through the wetwell obstacles is almost a certainty. The degree of acceleration will depend significantly on the effectiveness of the igniters in burning very lean mixtures and on the spatial concentration gradients. Measurements in obstacle-filled tubes at McGill[5.7] indicate that flame acceleration mechanisms function with as little as 6% hydrogen present in air, and that high flame speeds can be achieved (>20 m/s for 8% H_2 and >150 m/s for 10% H_2, in the recent experiments).

5.6 References

[5.1] M. P. Sherman et al, *The Behavior of Hydrogen During Accidents in Light Water Reactors*, Sandia National Laboratories, SAND80-1495, NUREG/CR-1495, August 1980.

[5.2] Bimonthly Progress Letter (October and November, 1981), M. Berman (SNL) to J. T. Larkins (NRC), December 23, 1981.

[5.3] S. L. Thompson, *CSQII - An Eulerian Finite Difference Program for Two-Dimensional Material Response - Part I. Material Sections*, SAND77-1339, Sandia National Laboratories, Albuquerque, NM, January 1979.

[5.4] W. B. Murfin, *Report of the Zion/Indian Point Study: Volume I*, SAND80-0617/1 (NUREG/CR-1410), Sandia National Laboratories, Albuquerque, NM, August 1980.

[5.5] R. K. Byers, *CSQ Calculations of H_2 Detonations in the Zion and Sequoyah Nuclear Plants*, SAND81-2216. (NUREG/CR-2385), Sandia National Laboratories, Albuquerque, NM, to be published.

[5.6] J. C. Mark, Memorandum for ACRS Members, *Notes on Hydrogen Burn with Igniters*, December 4, 1980.

[5.7] M. Berman, *Light Water Reactor Safety Research Program Semiannual Report, April-September 1981*, Sandia National Laboratories, SAND82-0006, NUREG/CR-2481, February 1982.

6.0 Assessment Results and Recommendations

In this chapter we discuss the results of our assessment of the adequacy of the HIS to meet the threat posed by hydrogen combustion at the Grand Gulf Nuclear Station. Chapters 2.0 and 3.0 discussed our calculations of the containment atmosphere pressure and temperature response to hydrogen combustion. Comparisons to similar CLASIX-3 calculations are made in those chapters. Containment atmosphere mixing mechanisms are discussed in Chapters 2.0 through 4.0, with special emphasis in Chapter 4.0. The likelihood and consequences of detonations are discussed in Chapter 5.0 of this report.

The following sections of this chapter present our assessment of the adequacy of the HIS design, actuation criteria, and testing. The final section of this chapter discusses the adequacy of the accident spectrum considered in the MP&L evaluation.

6.1 Adequacy of the HIS Design

In our opinion the design of the HIS is basically sound (the deliberate ignition concept, however, is judged to be marginally adequate to meet the threat posed by hydrogen combustion). We do have a few suggestions that we feel would improve the Grand Gulf system in terms of reliability. The present design calls for a total of about 90 igniters distributed throughout the drywell and wetwell/containment. Redundancy is factored into the design by using two separate power distribution panels (Divisions I and II). Each panel uses two circuit breakers (approximately 23 igniters per breaker) to protect its igniters. The power system is attached to the station diesel generator in case of loss of offsite power.

The igniter distribution and location design is such that the igniters are no more than ~30 ft apart if all are operable (except vertically between elevations 209 and 262 ft in the containment dome, and near the bottom of the drywell); the igniters are no more than ~60 ft apart if only one Division is operable; all enclosed regions are served by at least one igniter from each Division. The drywell will be served by 18 igniters, 6 each at elevations 146, 161, and 179 ft. The wetwell distribution of igniters is such that 12 igniters are located near elevation 135 ft, 15 are located near elevation 160 ft, 8 are located near elevation 185 ft, and 19 are located near elevation 204 ft. In the containment dome there are 8 igniters at elevation 262 ft, 8 at elevation 285 ft 10 in., and 2 at elevation 295 ft.

In our judgment the HIS design could be improved in two ways: an increased number of circuit breakers (fewer igniters per breaker) and either a modified igniter support design or an increased number of igniters in the wetwell/containment region. We believe that if a short circuit at one igniter will deactivate 22 other igniters, the circuit breaker design is inadequate. In our opinion, no more than two igniters at any elevation should be protected by the same circuit breaker. This means that a total of 6 or 8 igniters can be protected by one breaker if those igniters are spatially distributed throughout the various regions. We strongly recommend that the drywell igniters be protected by their own circuit breakers, since our analysis of suppression pool motion during containment burns indicates that significant pool surge may occur inside the drywell.

The present design for igniter housing and support structure is such that it tends to limit the effectiveness of combustion ignition. In our opinion, the system will reliably ignite hydrogen : air mixtures in the ~10% hydrogen* range, but not necessarily in the 6% to 8% hydrogen* range. Since it is desirable to burn the hydrogen in containment at the lowest possible mole fraction, the igniters should be positioned so that they can burn out large volumes with upward propagation of flames. Hydrogen is unique in having a large difference between the upward and downward flame propagation limits, the upward propagation limit of 4.1% being much lower than the downward limit of 9% or the horizontal limit of 6%.

The design of the igniter housing incorporates a spray shield (horizontal plate with vertical sides) a few inches above the igniter. This shield tends to locally inhibit flame propagation. A much more serious problem, for all but those igniters located on the containment dome wall, is that most igniters are located within 2 ft of ceiling structures. Some of these ceilings are solid concrete, while others are metal gratings. The

*Average concentration in the region served by one igniter (~30 ft x 30 ft x 20 ft = 18 000 ft^3).

solid ceilings clearly inhibit the effectiveness of the igniters, and a similar inhibition of igniter effectiveness will occur if the grating area above igniters is covered with equipment. The main point here is not that the igniters will not work as proposed, but that *reliable* ignition of lean mixtures is questionable for the volume served by a single igniter.

We feel that the proper design of a support for an igniter in a specific location should incorporate consideration of the likely flame path. In general, it is desirable to have the igniter away from large solid surfaces, especially those above. If such an approach is not feasible at this time, we would recommend increasing the number of igniters, especially in the wetwell region (from elevation 135 to 209 ft). We also recommend that the igniters in the containment dome at elevation 285 ft 10 in. be symmetrically staggered in azimuthal position with respect to those at elevation 262 ft, so as to take advantage of the likely flame paths.

6.2 Adequacy of the Actuation Criteria

The stated actuation criteria[6.1] for the HIS is an indication that the primary-vessel water level has fallen to the top of active fuel. Our judgment is that actuation of the HIS at this point in an accident would provide sufficient time for the surface temperature of the igniters to reach an acceptable value for reliable ignition. It should be noted that we have not examined the availability or reliability, under accident conditions, of those systems involved in the primary-vessel water level measurement. We are somewhat concerned that the HIS actuation is done manually—apparently without an automatic backup system. Such an automatic activation system might be a desirable addition.

We suggest that MP&L consider incorporating hydrogen detector information into their procedures for containment spray activation and for HIS deactivation. We also recommend that the containment sprays be activated at the same time the HIS is activated or, at the latest, upon indication from the hydrogen detectors of perhaps 2% hydrogen concentration in containment. Our analyses indicate that the sprays are very important to the plant safety and should be maintained in operation throughout the accident.

6.3 Adequacy of the HIS Testing

In our judgment the operational inspection and testing program specified by MP&L for the HIS system[6.1] is reasonable and adequate (however, the frequency of the periodic testing was never defined). We assume that the station's diesel generators are also subjected to periodic testing. As discussed in section 6.1, we feel that the design of the HIS should be changed in several ways. The impact of these design changes to the operational testing program is beneficial. If fewer igniters are powered by one breaker, a change in the current drawn by that breaker is more easily detected and finding the cause of that change is simpler.

Testing of the system design with respect to igniter, transformer, or wiring failure under accident conditions is very important since one failure (short circuit) can shut off a number of igniters. The planned submergence test[6.1] is a step towards addressing this issue. We feel that it is desirable to test the igniter assembly under accident conditions for extended periods (several hours). These conditions would include hydrogen burn environments, high steam pressures, and water spray impingement.*

*Previous igniter tests at Fenwal may have addressed these issues partially.

6.4 Adequacy of the Spectrum of Accidents Considered in the Applicant's (MP&L) Evaluation

We consider the degraded-core accident spectrum considered by MP&L in their evaluation to be adequate for small-break LOCA and TPE. Basically, the hydrogen threat to a BWR Mark III plant manifests itself in one of two ways. The release path is either through a break in the drywell and then through the suppression pool, or it is directly into the suppression pool (from the pressure vessel safety relief valves). Due to the uncertainties in hydrogen generation and release rates,* we consider the MP&L approach for this parameter to be a reasonable approach, especially since the effect of increasing the rate was examined in their sensitivity study.[6.2]

*As discussed in a number of sections in this report, the hydrogen generation and release rates are uncertain. The release rate is such a dominant input parameter to our codes that we feel a separate study should address the issue for BWR plants.

There are several kinds of accidents not considered by MP&L or SNL that present a more severe challenge to the containment integrity. The possibility of significant hydrogen releases directly into the wetwell/containment without first traversing the suppression pool is apparently extremely unlikely.[6.1] Accidents involving loss of all offsite and emergency power are of course much more threatening but less likely. The inclusion of accidents involving the loss of the Residual Heat Removal (RHR) system may not be warranted because containment failure apparently occurs due to static over-pressurization before core degradation rather than due to hydrogen combustion.[6.3]

6.5 References

[6.1] Letter and attachments from L. F. Dale, MP&L, to H. R. Denton, USNRC (December 21, 1981).

[6.2] *CLASIX-3 Containment Response Sensitivity Analysis for the Mississippi Power & Light Grand Gulf Nuclear Station*, Off-Shore Power System Rept No. 37A15 (December, 1981).

[6.3] M. Berman, *Light Water Reactor Safety Research Program Semiannual Report, April-September 1981*, Sandia National Laboratories, SAND82-0006, NUREG/CR-2481, February 1982.

APPENDIX A

Excerpt From Task 1 Report

October 1, 1981

Request for Additional Information

We recommend that the applicant modify the compartmentalization model used in CLASIX-3. As a result of studying the applicant's final report (June 19, 1981), touring the Grand Gulf Nuclear Station, and studying the plant drawings at the end of this appendix, we feel that the wetwell/containment compartmentalization used in CLASIX-3 is inadequate.

The pressure rise caused by a hydrogen deflagration is mainly dependent on the initial pressure before the burn and on the number of moles of hydrogen consumed. If the hydrogen that enters the wetwell is mainly confined to the region between the top of the suppression pool and elevation 135 ft, if there is sufficient oxygen present, and if no steam inerting occurs, the ignition of even 10% hydrogen in that limited volume leads to a very small pressure rise (q.v., the CLASIX-3 results). On the other hand, if the mixing of hydrogen is rapid, so that the concentration of hydrogen is nearly uniform throughout the wetwell/containment region, or if the lower wetwell becomes inerted after several burns due to inadequate mixing downward of oxygen and/or the presence of too much steam, then an ignition can lead to the consumption of a large mass of hydrogen and a resultant large pressure increase.

In the CLASIX-3 code, mass is transported only because of pressure differences between compartments. Mass entering a compartment is assumed to be instantly mixed with the entire contents of that compartment. Mass transport due to natural convection and diffusion is not considered by the CLASIX-3 code. The two-compartment model of the wetwell/containment used by the applicant in the CLASIX-3 calculations consisted of a very small wetwell volume (152 000 ft^3) and a very large containment volume (1 250 000 ft^3). In view of the limitations of the CLASIX-3 code, we believe that the results obtained with this two-compartment model may underestimate the pressure rise due to hydrogen combustion.

Hydrogen will enter the wetwell/containment from the suppression pool. Because of the small wetwell volume and the neglect of natural convection, the hydrogen is largely confined to the wetwell and rapidly reaches the assumed concentration for ignition. The pressure rise associated with the combustion of this quantity of hydrogen is small because of the transport of gas from the wetwell to the much larger containment. Subsequent inerting in the wetwell, due to the depletion of oxygen or the generation of steam, is computationally prevented because fully mixed containment air is transported back into the wetwell (at an artificially high rate) when the post-combustion gases cool. Consequently, CLASIX-3 predicts a large number of burns confined to the wetwell region with associated small pressure increases. We believe that the net result of using the CLASIX-3 code with the present compartment model is an unrealistic calculation of the mixing and combustion processes.

In order to reduce the artificial mixing caused by the use of just two volumes for the wetwell/containment, we suggest developing a model with that region divided into five subvolumes. The five subvolumes are

1. Annular region from top of suppression pool to elevation 135 ft (150 000 ft^3).*
2. Partial annular region from elevations 135 to 161 ft (130 000 ft^3). This excludes the volume occupied by the steam tunnel and the section considered to be part of volume 5.
3. Free region between elevations 161 and 209 ft (170 000 ft^3). This complex region excludes the volume of the various pools, internal concrete walls, and the sector considered as volume 5.
4. Region above elevation 209 ft (840 000 ft^3). This region is open and free of obstructions except for the polar crane.

*The volumes indicated are based on our calculations and are accurate to no more than two significant figures.

5. Pie-shaped sector from elevations 135 to 209 ft (60 000 ft^3). This sector, near azimuth 225°, is free from obstructions since it is used in the movement of equipment from the equipment hatch.

A more detailed model would break the containment into even more volumes, separating the annuli azimuthally into additional sectors. The cruciform geometry between elevations 161 and 209 ft suggests this course.

In addition to modifying the compartment model used in CLASIX-3, we recommend that the applicant perform additional computations with variations in certain key parameters. We suggest that the sensitivity of the CLASIX-3 results to the following parameter variations be determined.

1. Hydrogen source term increased and decreased by a factor of 3. The present value represents a high production rate but a lower rate might actually pose a greater threat, especially if the hydrogen concentration for ignition and propagation are not made equal (see item 3 below). An increased source term could model a scenario such as that at TMI-2, where the production rate and release rate are decoupled (i.e., production can be relatively slow, but the hydrogen is trapped in the primary system for some time and then released rapidly).
2. Flame speed increased to 10 and 100 times the present value (1.8 m/s). In recent experiments at McGill University flame velocities in excess of 150 m/s were measured for a 10% concentration of hydrogen in air.* These experiments also indicated that the accelerating flame had not attained a maximum value of speed. For the computer model it may be desirable to make the flame speed a function of hydrogen concentration and compartment geometry (i.e., the flame would be expected to have a higher speed at higher concentration and in more cluttered compartments).
3. Hydrogen concentration criteria for combustion ignition and combustion propagation set at different values. We recommend an ignition criterion of 9% - 10% hydrogen and a propagation criterion of 4% - 5% hydrogen. A variation in assumed combustion completeness (from 1.0 at 9% to perhaps 0.1 at 4%) should accompany these changes. More sophisticated propagation and combustion-completeness criteria would include factors to account for propagation direction (upward, horizontal, and/or downward).
4. Burn propagation delay time (from one compartment to another) decreased to 0 sec. Since the compartments are intimately connected we feel that a zero delay time is realistic.
5. Containment spray carry-over fractions from the dome region into the wetwell (i.e., from above 209 ft to below 209 ft) in the range:
   $0.0 \leq$ droplets ≤ 0.20 decreasing as elevation decreases
   $0.33 \leq$ sheet flow ≤ 0.53 increasing as elevation decreases
   These values are based on our estimates of blocked areas at the 209 ft elevation.

A number of specific items need to be addressed before we can complete our evaluation of the Grand Gulf HIS. These items are listed below (following the topic of evaluation).

1. Testing of the HIS
   a. How will the system be tested? Specifically, what indicates that a particular igniter is or is not functioning properly?
   b. How often will the system be tested once the plant is operating normally?
   c. Are hydrogen detectors to be used as part of the HIS? If so, please specify the types of detectors, number, location of sampling ports, system response time, and testing format and frequency.
2. Location and distribution of igniters

   Please provide construction drawings for several "typical" igniter mounts in the wetwell and containment regions. Also provide a list of the approximate elevation coordinates for each igniter in these regions and the corresponding elevation coordinates of the nearest floor or ceiling.

*June/July Bimonthly Report to John Larkins (NRC) on the Hydrogen Program. M. Berman, ed, published August 1981.

3. Calculations to determine the containment atmosphere pressure and temperature response:

   a. Please check the list of CLASIX-3 input parameters given in the June 19, 1981 report and notify us if any errors exist.
   b. Justify the values of the following parameters and/or coefficients used in the CLASIX-3 calculations:

      (1) beam lengths
      (2) gas emissivity, absorptivity, heat capacity, heat conductivity, and viscosity
      (3) convective heat transfer rates and coefficients
      (4) wall thermal properties (emissivity, absorptivity, heat capacity, conductivity)
      (5) flow coefficients (define and justify values)
      (6) spray droplet fall time
      (7) heat sink surface areas (identify location)
      (8) upper pool surface thermal properties
      (9) painted surface thermal properties

   c. What is the form of the momentum equation used to link the control volumes?
   d. What model is used for heat transfer to and evaporation of the spray droplets?
   e. Why was the number-mean diameter (230 μm) used for the spray droplets instead of the mass-mean diameter (370 - 400 μm)?
   f. How are the various floor gratings treated thermally? Are they assumed to be a lumped mass? Are they assumed to be thermally isolated from the rest of the floor and/or walls?
   g. Are the presence of liquid layers on walls and condensation heat transfer treated consistently with radiative heat transfer to the walls?
   h. What fraction of the spray carryover (from containment to the wetwell) is assumed to remain as a spray and what fraction is assumed to be in liquid layers?
   i. What is the nominal elevation of the top of the suppression pool during an accident with and without sprays activated? What is the level of the upper pools under similar circumstances?
   j. How and under what conditions are the upper pools drained into the suppression pool?
   k. What is meant by "satisfactory" convergence of the CLASIX-3 solutions?
   l. Where have the sensitivity studies for CLASIX-3, mentioned in section C.3 of the June 19 final report, been published (list references)? Please provide copies.
   m. Please provide an estimate of free volume and surface areas (with appropriate thermal property estimates) as a function of elevation for the annular wetwell region for the following discrete elevation ranges: 110 - 135 ft, 135 - 161 ft, 161 - 209 ft.
   n. During normal operation, does the equipment "hatchway" (at azimuth angle 225°, radius 42 - 62 ft) have gratings in it? If so, at what elevations?

4. Containment atmosphere mixing mechanisms:

   a. Describe the flow rates of the ventilation system in the containment/wetwell regions.
   b. What are the elevations and radial positions of the spray rings?
   c. Which spray rings operate when a single RHR loop is operating and what is the flow rate under such conditions? Does the spray water contain additives?
   d. Describe any sprays, fans, or other systems that could move air in the annular wetwell region and estimate the velocities in the region due to these sources.

5. Actuation criteria:
   a. Under what conditions are the sprays activated?
   b. How long after the sprays are activated does the spray system attain full flow rate?
   c. When during an emergency situation would the HIS be activated?
   d. What role would hydrogen detectors play in actuating the HIS?
   e. What role, if any, would the hydrogen recombiners play with respect to the HIS?
6. Sprectrum of accidents considered in the applicant's evaluation:
   a. Are there any accident sequences that might lead to the introduction of hydrogen and steam *directly* into containment without having passed through the suppresion pool?
   b. Briefly explain the workings of the "drywell purge system" including "purge compressors" and "vacuum breakers." Estimate flowrates from this sytem during an accident.
   c. Briefly explain the workings of the "back up containment purge system."
   d. Justify the zirconium inventory in the reactor used to estimate hydrogen inventory from the metal-water reaction.
   e. Are there any accident sequences that might involve a localized injection of hydrogen into the suppression pool (e.g., a single stuck-open safety relief valve)?

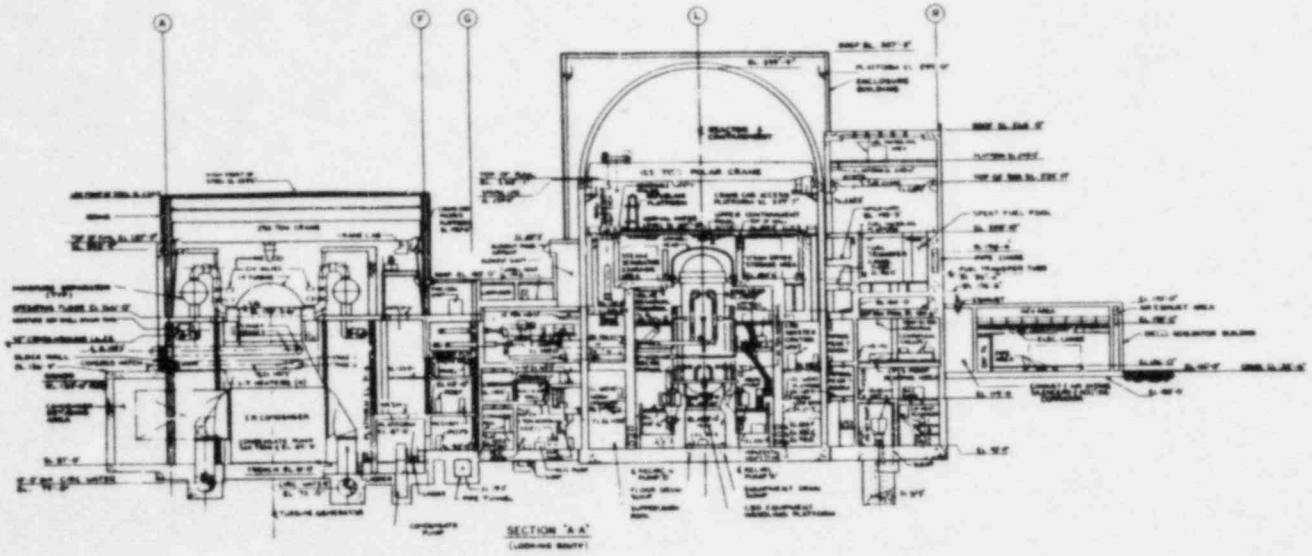

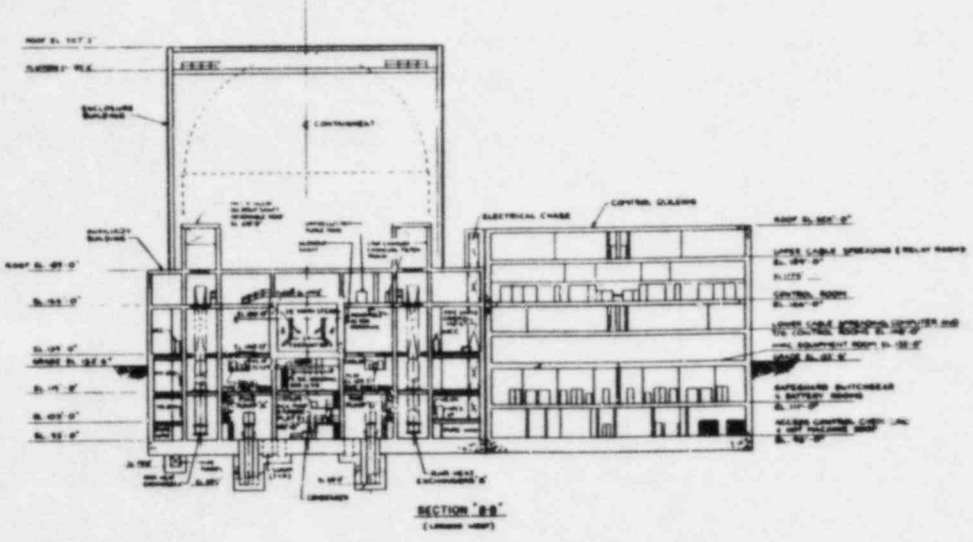

MISSISSIPPI POWER & LIGHT COMPANY
GRAND GULF NUCLEAR STATION
UNITS 1 & 2
FINAL SAFETY ANALYSIS REPORT

GENERAL ARRANGEMENT
SECTIONS "A-A" & "B-B"

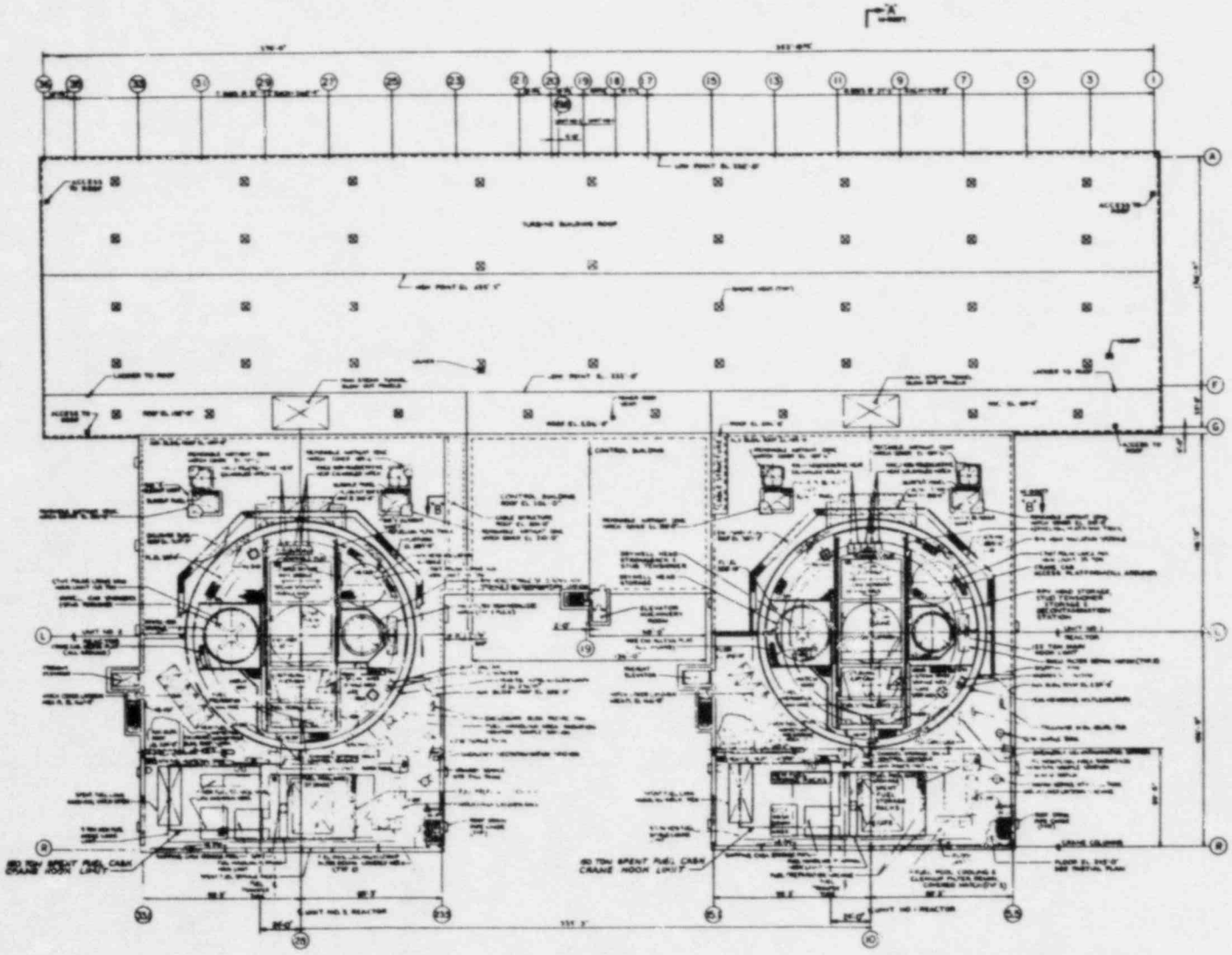

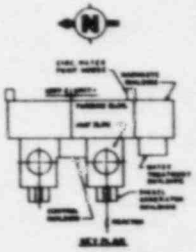

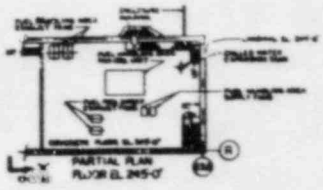

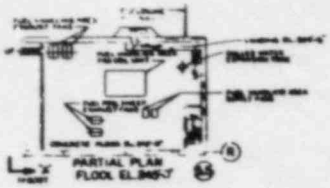

MISSISSIPPI POWER & LIGHT COMPANY
GRAND GULF NUCLEAR STATION
UNITS 1 & 2
FINAL SAFETY ANALYSIS REPORT

GENERAL ARRANGEMENT PLAN
AT EL. 208'-10"
UNITS 1 & 2

Amend. 25 8/78

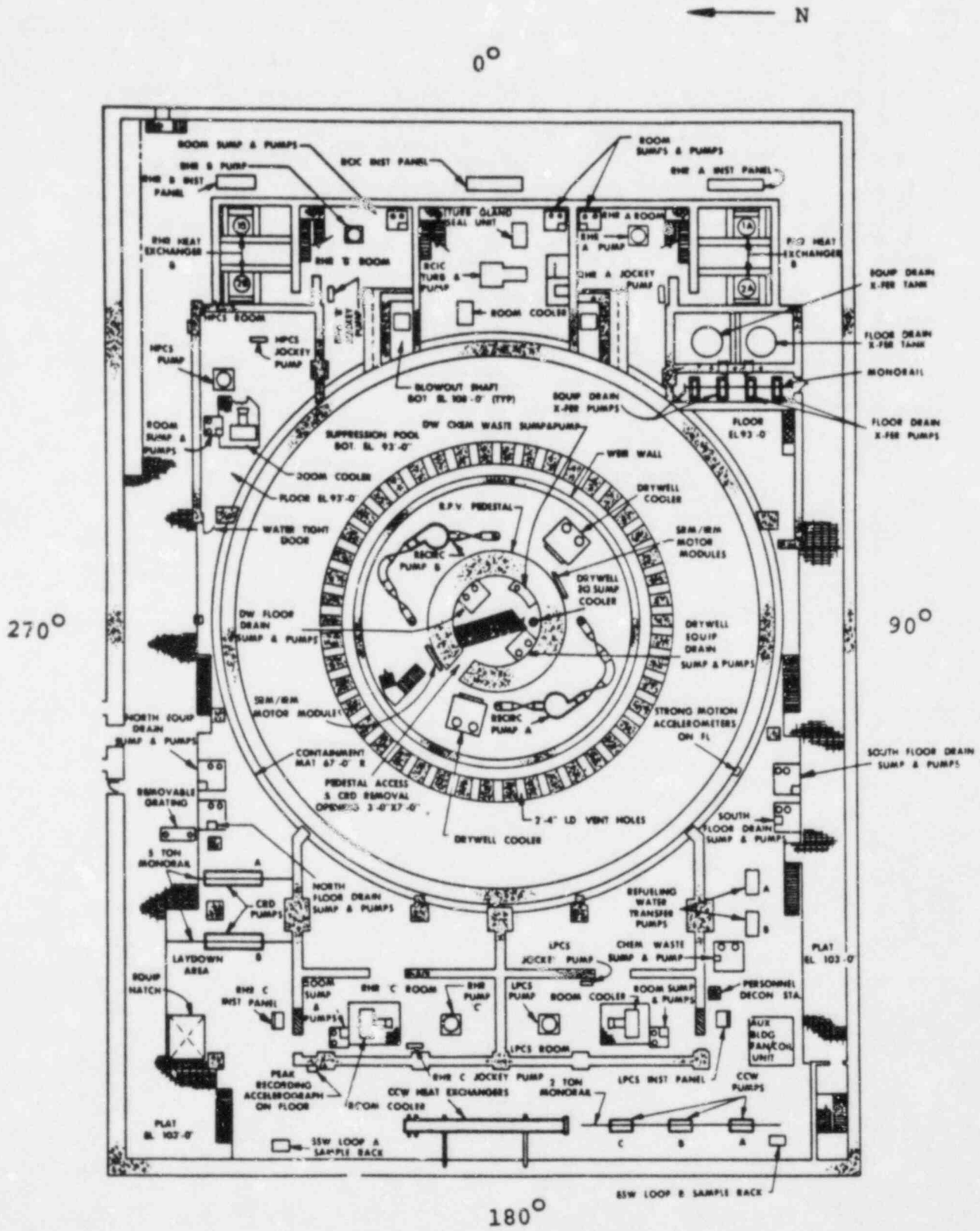

Bldg/Containment Elevation 93' 0'',100'9''

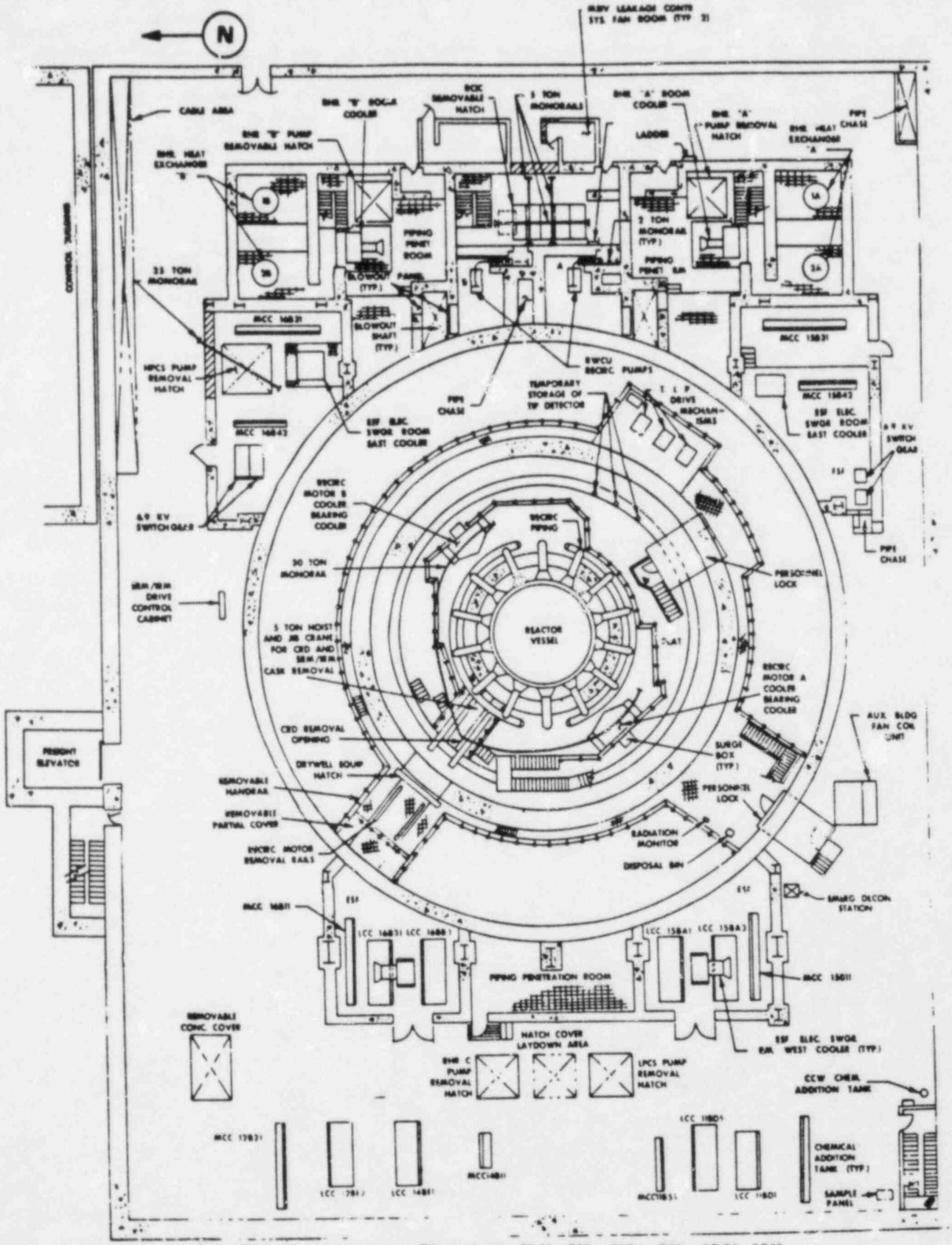

Aux Bldg/Containment, Elevations 114' 6", 119' 0", 120' 10"

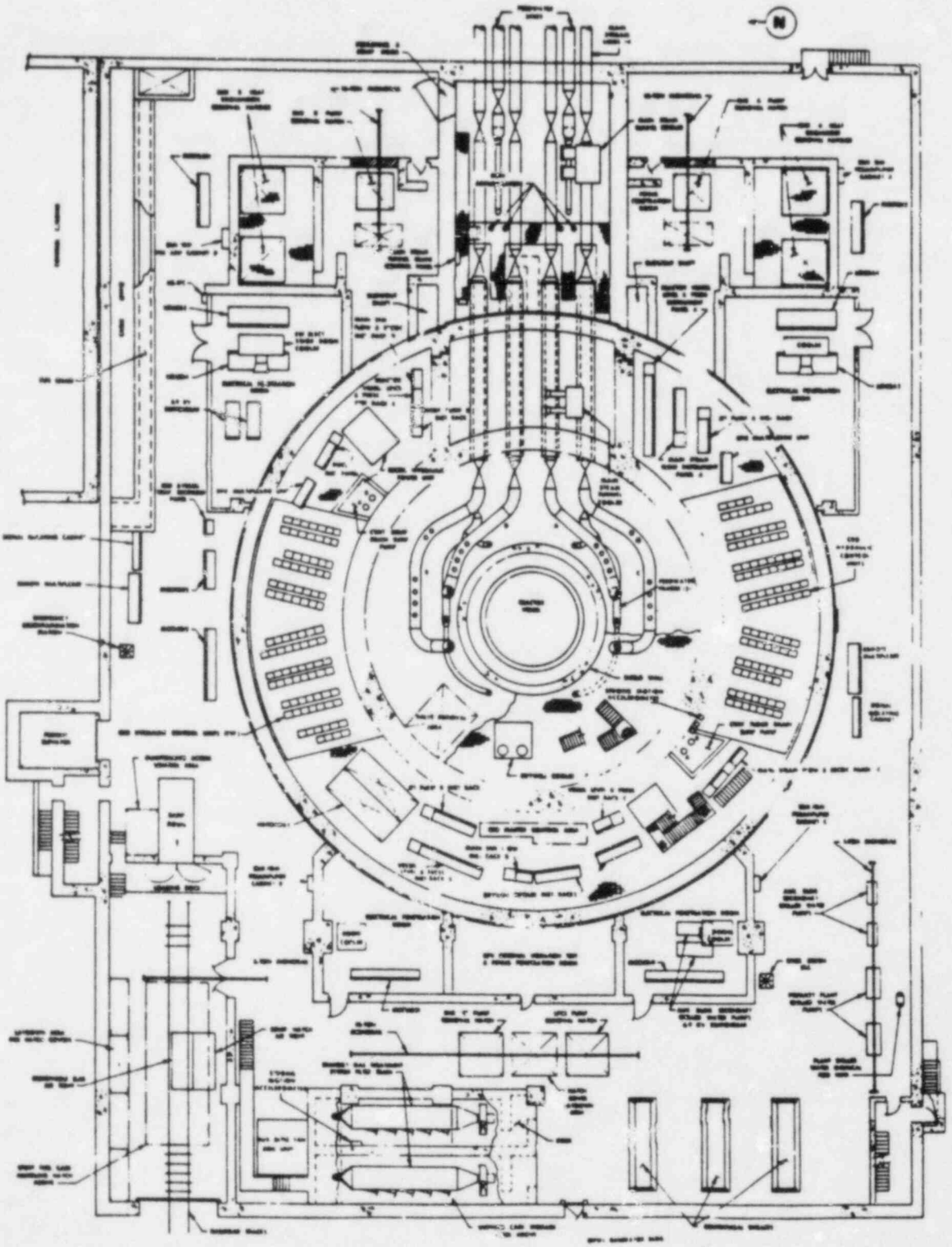

Aux Bldg/Containment 135'4", 139,0", 147'7"

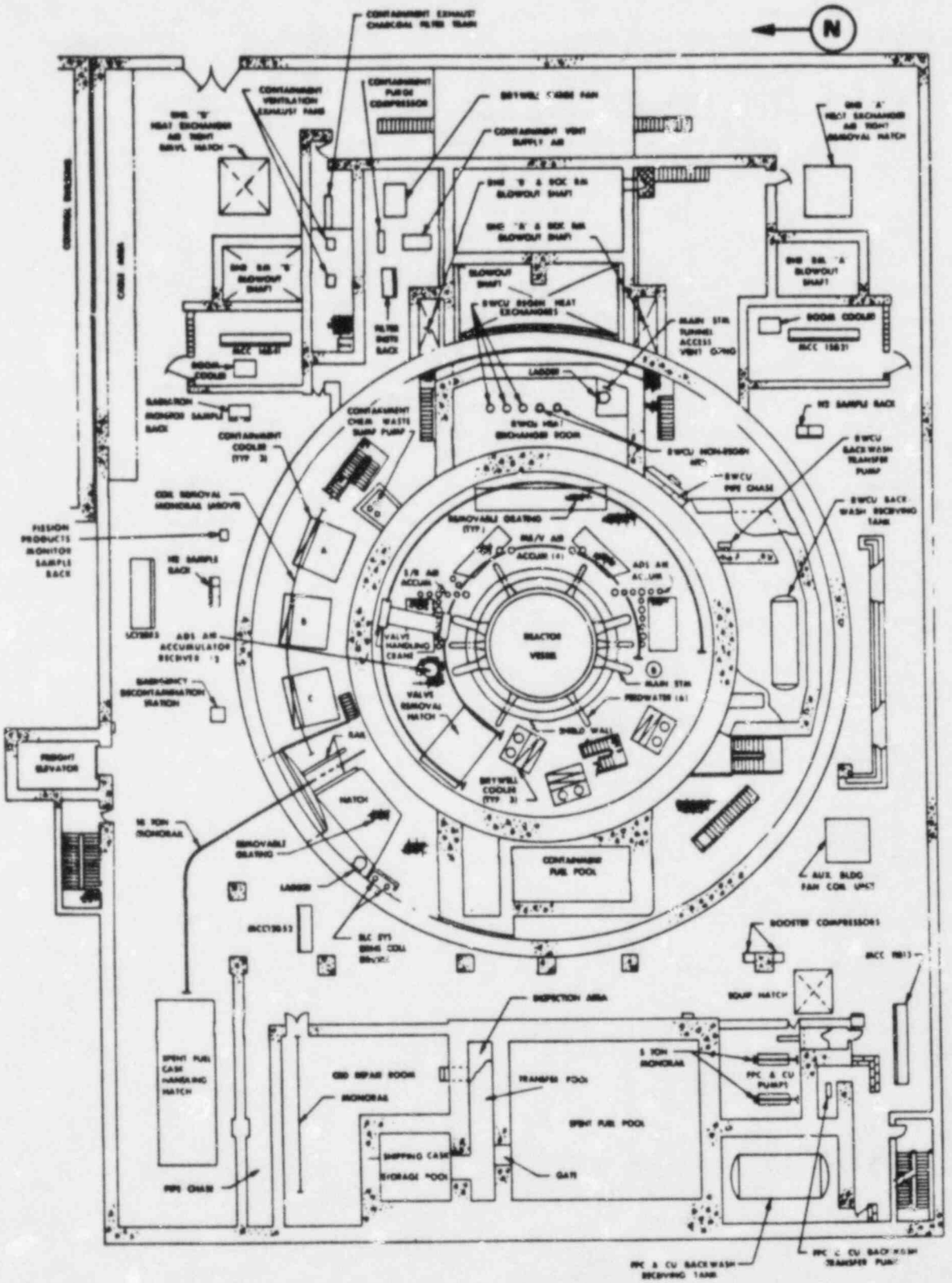

Aux Bldg/Containment Elevation , Elevation 161'10'' & 166'0''

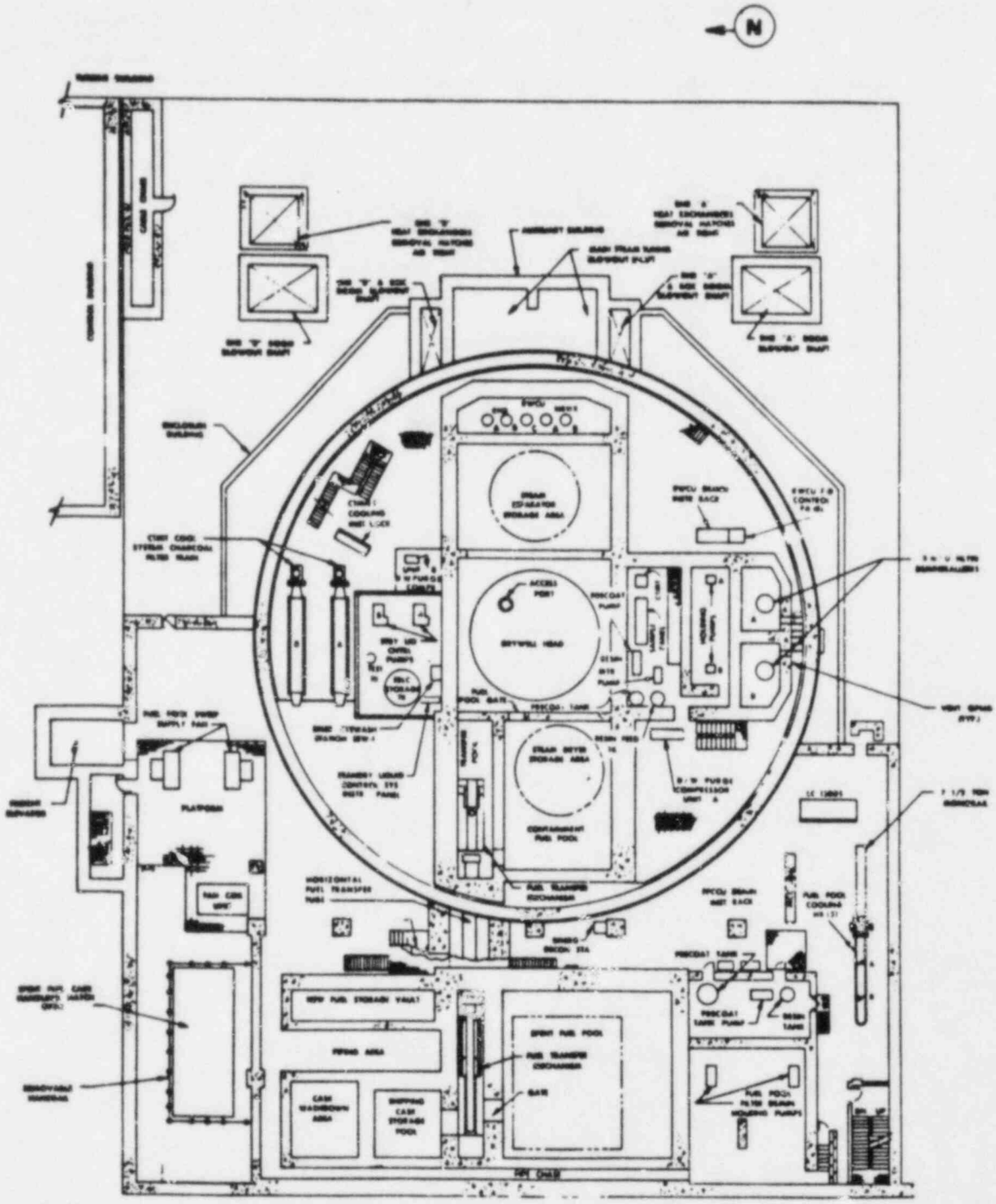

Bldg/Containment, Elevation 184'6" & 185'0"

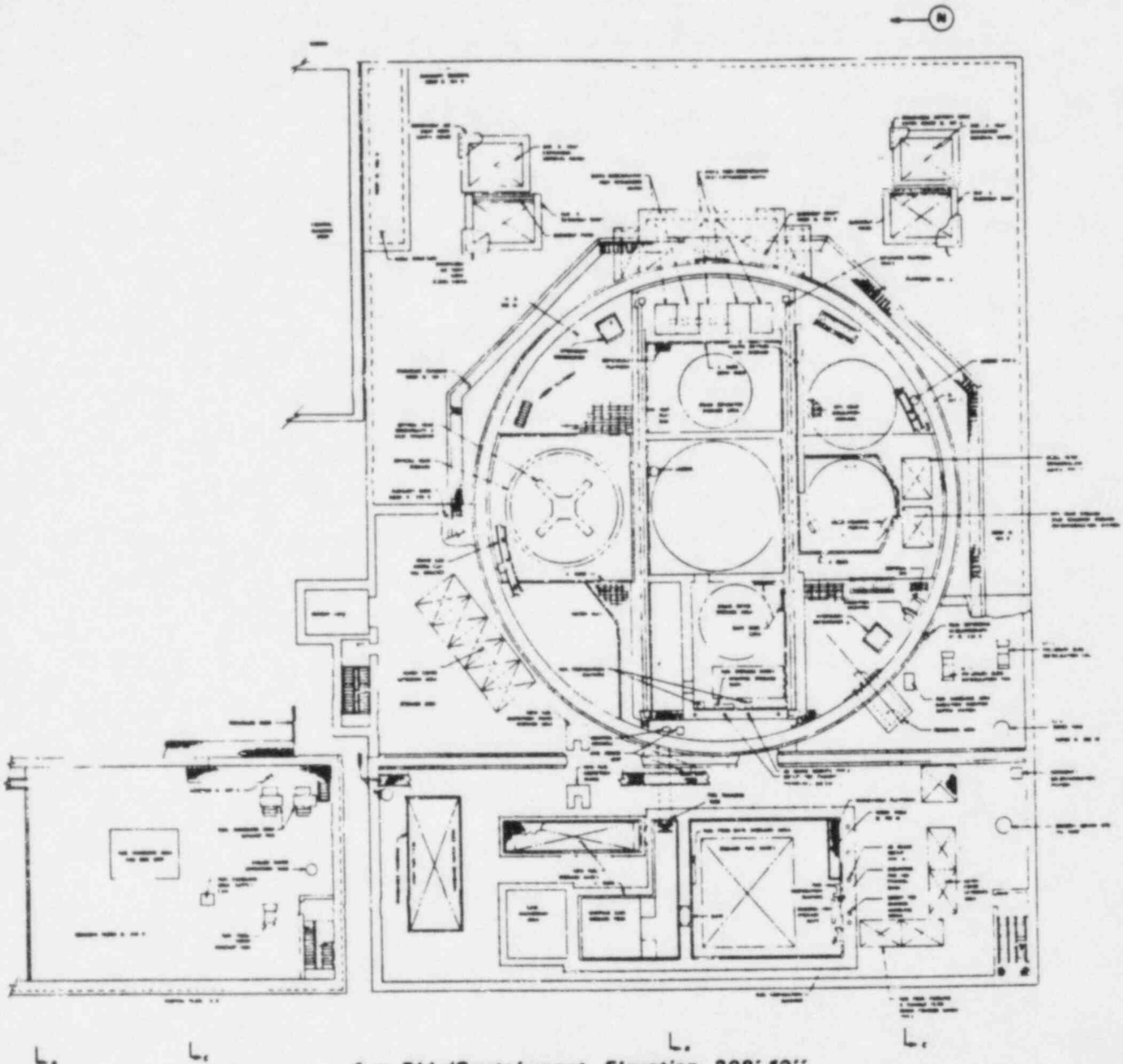

Aux Bldg/Containment, Elevation 208'-10"

APPENDIX B

HECTR Description

Each of the various models in HECTR is discussed in detail below except the hydrogen burn model which is discussed in section 2.1.

B.1 Multicompartment Mass and Energy Equations

The multicompartment model is a system of ordinary differential equations expressing mass and energy conservation. The dependent variables are the temperature and number of moles of hydrogen, nitrogen, oxygen, and water vapor in each compartment. Gas flow between compartments is caused by pressure differences and gravitational forces. The gases in each compartment are assumed to be ideal, homogeneous, and completely mixed at all times. Compartment interconnections are modelled as orifices with flow resistance.

Consider two compartments, i and k. The effective pressure difference between them is

$$\Delta P = P_i - P_k + \frac{g}{2}(Z_i - Z_k)(\rho_i + \rho_k) \qquad \text{(B1)}$$

where

P_i = pressure in compartment i
g = acceleration of gravity
Z_i = elevation of compartment i
ρ_i = gas density in compartment i

The gas flow velocity, v_{ik}, to compartment i from compartment k is then

$$v_{ik} = \begin{cases} -\sqrt{\dfrac{2\,\Delta P}{\rho_i K_{ik}}} & \text{if } \Delta P \geq 0 \\ \sqrt{-\dfrac{2\,\Delta P}{\rho_k K_{ki}}} & \text{if } \Delta P < 0 \end{cases} \qquad \text{(B2)}$$

K_{ik} is a coefficient defining the flow resistance encountered going from compartment i to compartment k.

The j^{th} species of gas ($1 \leq j \leq 4$) in the i^{th} compartment ($1 \leq i \leq 10$) will have its molar rate of change described by

$$\frac{\partial N_{ij}}{\partial t} = \sum_{k\ (v_{ik} < 0)} \frac{A_{ik} v_{ik}}{V_i} N_{ij} + \sum_{k\ (v_{ik} \geq 0)} \frac{A_{ik} v_{ik}}{V_k} N_{kj} + \left(\frac{\partial N_{ij}}{\partial t}\right)_{\text{chemical}} + \left(\frac{\partial N_{i,H_2O}}{\partial t}\right)_{\text{evaporation-condensation}} + \left(\frac{\partial N_{ij}}{\partial t}\right)_{\text{external source}} \qquad \text{(B3)}$$

where

N_{ij} = number of moles of gas species j present in compartment i

A_{ik} = interconnection area between compartments i and k

V_i = volume of compartment i

$\left(\dfrac{\partial N_{ij}}{\partial t}\right)_{\text{chemical}}$ = chemical molar rate of change due to combustion

$\left(\dfrac{\partial N_{i,H_2O}}{\partial t}\right)_{\text{evaporation-condensation}}$ = rate of change of water vapor due to evaporation or condensation on the wall surfaces and the spray droplet

$\left(\dfrac{\partial N_{ij}}{\partial t}\right)_{\text{external source}}$ = rate of addition of hydrogen or water vapor into compartment i from an external source

The conservation equation for energy in the i^{th} compartment is then

$$\left(\sum_{j=1}^{4} C_{v,ij}\, N_{ij}\right)\frac{\partial T_i}{\partial t} + \sum_{j=1}^{4} u_{ij}\frac{\partial N_{ij}}{\partial t} =$$

$$\sum_{j=1}^{4}\left[\sum_{k}\frac{A_{ik}\, v_{ik}}{V_i}\, N_{ij}\, h_{ij} + \sum_{k}\frac{A_{kj}\, v_{ik}}{V_k}\, N_{kj}\, h_{kj}\right]$$

$(v_{ik} < 0)$ $\qquad$ $(v_{ik} \geq 0)$

$$-\left(\frac{\partial Q}{\partial t}\right)_{radiation} - \left(\frac{\partial Q}{\partial t}\right)_{convection} - \left(\frac{\partial Q}{\partial t}\right)_{sprays}$$

$$+\left(\frac{\partial N_{i,H_2O}}{\partial t}\right)_{evaporation\text{-}condensation} h_{i,H_2O}$$

$$+\sum_{j=1}^{4}\left(\frac{\partial N_{ij}}{\partial t}\right)_{external\ source} h_j(T_{source}) \qquad \textbf{(B4)}$$

where

T_i = temperature in compartment i (K)

$C_{v,ij}$ = molar specific heat of the j^{th} gas in compartment i (J/mole-K)

u_{ij} = molar internal energy of the j^{th} gas in compartment i (J/mole)

h_{ij} = molar enthalpy of the j^{th} gas in compartment i (J/mole)

$h_j(T_{source})$ = molar enthalpy of the j^{th} gas evaluated at the source temperature (J/mole)

$\left(\frac{\partial Q}{\partial t}\right)_{radiation}$ = rate of radiative heat transfer out of the gas (watts)

$\left(\frac{\partial Q}{\partial t}\right)_{convection}$ = rate of convective heat transfer out of the gas (watts)

$\left(\frac{\partial Q}{\partial t}\right)_{sprays}$ = rate of heat transfer out of the gas to the spray droplets (watts)

Therefore, for each compartment there are four mass conservation equations and one energy conservation equation. For N compartments, a total of 5N differential equations are solved simultaneously.

B.2 Radiative Heat Transfer

In this analysis, the radiative spectrum is broken up into seven active regions and the emission from steam is considered in each spectral region. Regions in which the gas has no radiative bands, and in which wall emission is negligible, have no radiant heat transfer and are ignored. The bands are determined using an exponential wide-band molecular radiation model.[B.1] For each band, a gas emissivity is calculated which depends upon the temperature, pressure, mole fraction of steam, and beam length. For the rest of this discussion, the subscript i will refer to the i^{th} spectral band.

The rate of radiative heat transfer from the j^{th} surface per unit area, Q_j, will be the sum of the quantities calculated for each spectral band where

$$Q_{ji} = \frac{\epsilon_j}{1-\epsilon_j}\,(B_{ji} - J_{ji}) \quad , \qquad \textbf{(B5)}$$

where

ϵ_j = the emissivity of the j^{th} surface (assumed to be constant; hence the surfaces are considered to be gray bodies)

B_{ji} = the Planck blackbody flux emitted from the j^{th} surface per unit area

J_{ji} = the radiosity of the j^{th} surface (the rate of radiant heat flux leaving the surface per unit area)

The radiosities themselves are determined by solving a system of N simultaneous equations, where N is the total number of surfaces present:

$$\frac{1}{1-\epsilon_j} J_{ji} - \sum_{k=1}^{N} F_{j-k}\,\tau_i\,(k-j) J_{ki} =$$

$$\frac{\epsilon_j}{1-\epsilon_j} B_{ji} + \sum_{k=1}^{N} F_{j-k}\,\epsilon_i\,(k-j) B_{gi}\,(k-j) \qquad \textbf{(B6)}$$

where

F_{j-k} = geometric view factor looking from surface j to surface k

$\epsilon_i\,(k-j)$ = gas emissivity as a function of the beam length from surface k to surface j

$\tau_i\,(k-j)$ = gas transmissivity $= 1 - \epsilon_i\,(k-j)$

$B_{gi}\,(k-j)$ = gas Planck blackbody flux per unit area

Further details regarding this model are presented in Reference B.2.

B.3 Convective Heat Transfer

As mentioned in section 2.1, convective models are included for both vertical slab and horizontal pool

surfaces. The model for heat transfer on a vertical plane consists of a Nusselt laminar flow solution for wall liquid layers and either a Couette-type forced turbulent flow model for the air : water-vapor boundary layer or a natural convection turbulent boundary layer correlation.[B.2] The temperature of the liquid-gas interface, TGI, is varied until the sum of the convective plus radiative heat transfer rates through the gas boundary layer is equal to the heat transfer rate through the liquid.

$$\text{Maximum of } (q_C, q_{NC}) + q_{RAD} = q_F \quad . \tag{B7}$$

The subscripts C, NC, RAD, and F indicate forced convection, natural convection, radiation, and liquid. The heat fluxes, q, are the rates of heat transfer per unit area. If there is no liquid layer, the interface temperature is set equal to the wall temperature, and terms related to the transport of mass and its associated enthalpy (the first terms on the right-hand side of Eqs (B9) and (B10)) are dropped in the gas boundary layer correlations.

The correlations used are presented below in dimensional form using SI units (q is in W/m^2).[B.2]

Nusselt Liquid Layer

$$q_F = 0.943\,(TGI - TW) \cdot \left[\frac{\rho_f(\rho_f - \rho_g)h_{fg}K_f^3(9.807)}{\mu_f Lc\,(TGI - TW)}\right]^{1/4} \tag{B8}$$

Forced Convection Gas Boundary Layer

$$q_C = 0.037\rho_b U_b Re^{-0.2} Sc^{-0.4} \ln(1+B)\,(MFVB - MFVI) \cdot \{C_{pv}(TBULK - TGI) + h_{fg}\}/B + 0.037\,K_g\,Re^{0.8}\,Pr^{0.6} \cdot (TBULK - TGI)/L \tag{B9}$$

Natural-Convection Gas Boundary Layer

$$q_{NC} = \frac{0.0188\,\rho_b \tau \mu^{1/4}}{(\rho_b \tau \delta)^{1/4}} \cdot Sc^{-2/3} \ln(1+B)\,(MFVB - MFVI) \cdot \{C_{pv}(TBULK - TGI) + h_{fg}\}/B + 0.0246\,K_g\,Gr^{2/5}\,Pr^{7/15} \cdot [1 + 0.494\,Pr^{2/3}]^{-2/5}\,(TBULK - TGI)/L \tag{B10}$$

where

TGI, TW, TBULK = liquid-gas interface, wall surface, and bulk gas temperatures (K)

ρ_f, ρ_g, ρ_b = liquid, saturated steam, and bulk gas densities (kg/m^3)

h_{fg} = heat of vaporization (J/kg)

K_f = liquid thermal conductivity (W/m-K)

K_g = gas thermal conductivity (W/m-K)

μ_f = liquid viscosity (kg/m-s)

μ = gas viscosity (kg/m-s)

C_{pv} = water vapor specific heat (J/kg-K)

C_p = gas specific heat (J/kg-K)

D = diffusion coefficient of water vapor through gas (m^2/s)

β = coefficient of expansion of gas (K^{-1})

Lc = characteristic vertical length of liquid film (m)

L = characteristic vertical length of gas film (m)

U_b = bulk (free-steam) gas velocity (m/s)

Re = Reynolds number based on length L ($U_b\rho_b L/\mu$)

Pr = Prandtl number ($C_p\mu/K_g$)

Sc = Schmidt number, $\mu/(\rho_b D)$

MFVB = mass fraction of vapor in bulk gas

MFVI = mass fraction of vapor at liquid-gas interface

B = mass transfer driving force (MFVB − MFVI)/(MFVI − 1)

Gr = Grashoff number based on length L, 9.807β (TBULK-TGI)$L^3\rho_b^2/\mu^2$

τ = characteristic velocity in natural-convection boundary layer, $1.185\,(\nu_g/L)Gr^{1/2} \cdot (1 + 0.5Pr^{2/3})^{-1/2}$ (m/s)

ν_g = gas boundary layer kinematic viscosity (m^2/s)

δ = gas boundary layer thickness,
$0.565 LGr^{-0.1}Pr^{-8/15}$
$\cdot[1 + 0.5Pr^{2/3}]^{0.1}$ (m) .

The liquid properties, ρ_f, μ_f, K_f are computed at a temperature

$$T = TW + 0.31(TGI - TW) \quad . \tag{B11}$$

The gas properties μ,C_p,K_g,D, and β in Re, Pr, Sc, and Gr are evaluated at a temperature

$$T = TGI + (TBULK - TGI)/3 \quad . \tag{B12}$$

The model for convective heat transfer to a pool surface is one for laminar flow over a horizontal flat plate.[B.3]

The correlation used is

$$q_{cp} = .664K_g Re^{1/2} Pr^{1/3} (TBULK - TSURF)/L \quad , \tag{B13}$$

where TSURF is the temperature of the pool surface and the other terms have been defined previously. Mass transfer from pools to the gas is approximated by assuming that the thermal conductivity of water in the pools is zero (i.e., all heat is deposited on the surface and results in the evaporation of water). The mass transfer is then

$$\dot{M} = (q_{cp} + q_{RAD})/[C_{PL}(TSURF - TPOOL) + h_{fg} + C_{pV}(TBULK - TSURF)] \quad , \tag{B14}$$

where C_{PL} is the liquid specific heat, TPOOL is the bulk pool temperature, and the other terms were defined previously. Eq (B13) and (B14) are not valid in all regions that may be encountered (e.g., when condensation is occurring). However, they are reasonably valid when the gas is superheated, such as during a burn. We have chosen to ignore the pools whenever the gas in the compartment is not superheated. Since the gas is saturated only at relatively low temperatures, we feel that ignoring the pools then results in negligible errors. Future versions of HECTR will treat the pools in more detail.

B.4 Containment Sprays

The containment spray model can treat a droplet distribution that includes up to ten drop sizes. The drops are assumed to be isothermal, spherical, and travelling at a terminal velocity corresponding to their instantaneous size and mass. The drops are tracked to the bottom of the compartment, with their final mass and temperature determining the heat and mass transfer rates.

It is assumed that the compartment gas is homogeneous and does not change during the fall time of the drops. Therefore, the solutions are quasi-steady state. The correlations presented are valid for both condensation on and evaporation from the drops. The differential equations describing drop behavior are shown below.[B.4]

$$\frac{dm}{dt} = -(1 + .25\,Re^{1/2}\,Sc^{1/3})2\pi D\rho D_c\,1n(1 + B) \quad . \tag{B15}$$

$$\frac{dT_d}{dt} = \frac{dm}{dt}\frac{1}{mC_{PL}}\left(\frac{C_p(T_d - TBULK)}{(1 + B)^{1/Le} - 1} + h_{fg}\right) \quad . \tag{B16}$$

$$\frac{dz}{dt} = \left[\frac{4}{3}\frac{(9.807)D\,(\rho_d - \rho)}{\rho\,C_d}\right]^{1/2} \tag{B17}$$

where

m = droplet mass (kg)
t = time (s)
Re = Reynolds number
Sc = Schmidt number
D = droplet diameter (m)
ρ = gas density (kg/m^3)
D_c = Diffusion Coefficient (m^2/s)
B = Mass Transfer driving force (defined in Section B.3)
T_d = droplet temperature (K)
C_{PL} = droplet specific heat (J/kg − K)
C_p = gas specific heat (J/kg − K)
TBULK = bulk gas temperature (K)
Le = Lewis number
h_{fg} = heat of vaporization (J/kg)
z = fall height (m)
ρ_d = droplet density (kg/m^3)
C_d = drag coefficient

The above equations are solved using a standard Runge-Kutta differential equation solver for each drop size.

The first version of HECTR only allowed sprays to be present in one compartment (usually the dome). However, because we felt that there might be significant errors due to the absence of sprays in the wetwell region for Grand Gulf, an effort was undertaken to modify HECTR to allow spray carryover from one compartment to another. One case (B2′) which reflects this upgrade is presented in Chapter 2.0.

B.5 Wall Conduction

The surfaces in HECTR are treated either as slabs or as lumped masses. In either case, all of the surface properties are assumed to be constant. Walls considered as slabs are assumed to have insulated rear surfaces. A finite-difference formulation is then used to calculate the forward wall surface temperatures given the heat flux to those surfaces. Two different mesh sizes are used inside the slabs: A fine mesh is used near the surface receiving the heat flux to better handle the steep temperature gradients that typically occur there; a coarser mesh is used for the remainder of the wall where the temperature varies more slowly.

The temperature (T) of a surface considered as a lumped mass is given as a function of time by

$$\frac{\partial T}{\partial t} = \frac{qA}{mC_p} \quad , \tag{B18}$$

where

q = incident heat flux (watts/m^2)

m = mass (kg)

C_p = surface material specific heat (J/kg-K)

A = exposed surface area (m^2)

B.5 References

[B.1] D. K. Edwards, "Molecular Gas Band Radiation," *Advances in Heat Transfer*, ed T. F. Irvine, Jr., and J. P. Hartnett, Vol. 12, 115-194, 1976.

[B.2] M. Berman, *Light Water Reactor Safety Research Program Semiannual Report, January-March 1981*, Sandia National Laboratories, NUREG/CR-2163, SAND81-1216, July 1981.

[B.3] J. R. Welty et al, *Fundamentals of Momentum, Heat and Mass Transfer*, John Wiley & Sons, 1969.

[B.4] Internal Communication from M. R. Baer, April 24, 1980.

APPENDIX C

The MARCH Code

The MARCH (Meltdown Accident Response Characteristics) code[C.1] was developed by the Battelle Columbus Laboratories (BCL) for the US Nuclear Regulatory Commission and first used in the WASH 1400 report. The code has been widely used in nuclear reactor safety studies, even though it is known to contain many limitations and some errors.[C.2] The code is fast running and inexpensive, so that many computer runs can be made in a study at reasonable cost. MARCH has models for many phenomena, including core meltdown, core slump, pressure vessel failure, core-concrete interaction, and containment failure. For our study of Grand Gulf, we are mainly concerned with the MARCH subroutines BOIL (which predicts the behavior of the reactor core and coolant system) and MACE (which calculates the containment response).

Both HECTR and CLASIX-3 are essentially containment response codes. The two codes used hydrogen production and steam production rates derived from MARCH calculations. The most widely used reactor-core and coolant-system code that will predict hydrogen production is MARCH.

MARCH has frequently been used for BWR safety studies using a two-compartment model, a drywell and a wetwell. We have been in telephone contact with R. O. Wooton and P. Cybulskis of BCL about using MARCH in this study. R. O. Wooton informed us that they have not checked out MARCH for BWR studies with more than two compartments (our configurations B, C, D, and E). In particular, Wooten was concerned with the treatment of containment sprays in multicompartment models. With considerable effort we developed multicompartment MARCH input of the Grand Gulf containment that appears to give reasonable results, in fair agreement with results obtained from HECTR and CLASIX-3.

C.1 Accident Scenarios Considered

The accident scenarios considered are variations on two types: the TPE accident scenario, and the small-to-medium break LOCA inside the drywell. The TPE accident is initiated by a transient event such as the loss of off-site power. The reactor is shut down and the safety relief valves open when the pressure in the reactor gets too high. Then one or more safety relief valves fail to reseat and there is a failure of emergency core cooling. The water level in the reactor pressure vessel is gradually reduced until MARCH predicts that, at 33 min into the accident, core uncovery begins.

The small-to-medium break LOCA, S_1 to S_2, inside the drywell differs from the TPE accident in that steam and hydrogen are first injected into the drywell and not directly into the suppression pool. As a result, nearly all the air initially in the drywell is forced through the suppression pool and into the wetwell early in the accident, raising the pressure in the wetwell to about 17 psia. A failure of emergency core cooling is again assumed. The history of reactor coolant pressure and temperature, rate of steam and hydrogen generated, and reactor core behavior for this accident is very similar to that for the TPE accident. For both accidents the reactor is at low pressure when the core begins to melt and substantial clad oxidation begins, approximately 60 min into the accident. Accidents in which the reactor coolant pressure is high during core uncovery, such as the TQUV accident sequence, were not considered in this report. We discuss the history and the generation of hydrogen in the next section of this appendix.

C.2 Production of Hydrogen

The rate and total amount of hydrogen produced by the BOIL subroutine of the MARCH computer program can be varied over very wide limits depending on the input parameters selected by the code user. Predictions of hydrogen generation depend on existing code models, experimental data, and engineering judgment. Input parameters are adjusted to provide some "reasonable" hydrogen production rate.

Let us consider the course of the BWR accidents considered. The pressure in the reactor vessel drops rapidly as shown in Figure C.1. At the time core uncovering begins, 33 min into the accident (Figure C.2), the pressure is about 525 psia; by the

time the core is completely uncovered, at 50 min, the pressure is down to about 200 psia. There are slight differences in these figures for different accidents because of the coupling of the reactor coolant system to the containment. During core uncovering the steam generation rate is very high, as shown in Figure C.4, and the core stays cool. MARCH indicates that at the time the core is completely uncovered, there is fission-product release (presumably caused by clad rupture) but the amount of clad oxidation is negligible, far below 1%, and hence there is negligible production of hydrogen.

For our MARCH study we have taken the zirconium inventory of the reactor core as 174 700 lb. This zirconium will be referred to as "clad," even though it includes clad and other zirconium structures in the core.

The rate of steam generation drops greatly after the core is completely uncovered. The clad and reactor core begin to heat up rapidly. MARCH predicts an increasing rate of clad oxidation, limited by the shortage of steam. The beginning of core melting occurs at 60 min into the accident. The amount of clad oxidation at that time is less than 1%. Consequently, the generation of hydrogen caused by clad oxidation is closely tied to core melting for the low-pressure BWR accident.

In MARCH, the user specifies the fraction of zirconium at each reactor core node that will be allowed to oxidize, and the fraction of the core that, when melted, will slump into the lower plenum of the pressure vessel. If one uses 75% core melt for the criterion for slump, then about 20% of the clad will be oxidized at core slump. This corresponds to about 1500 lb of hydrogen produced. Since we are considering accidents with greater amounts of hydrogen produced, we are forced to consider slumped-core behavior.

The model of molten core behavior most frequently used in MARCH assumes that the core is held up until a given fraction melts. At that time the entire core is assumed to drop into the lower plenum and all the remaining zirconium is oxidized in one time step. This gives rise to a large spike in hydrogen production, and usually a very large burn in containment, resulting in containment failure. This difficulty was noted in our earlier work on the Sequoyah ice condenser plant and in the CLASIX-3 analysis of Grand Gulf. If one believes the hydrogen production spike is not realistic, one must try to avoid it by some artifact. However, there is no evidence that the zirconium in the debris cannot indeed oxidize very rapidly and produce a large hydrogen release spike.

MARCH also contains an option which treats the slumped debris as composed of spherical particles with three concentric shells. The initial diameter and composition of the shells are input parameters to the code. We had difficulty using this option and did not get it to work until very late in the study. Some preliminary calculations with this debris bed model resulted in predictions of rapid quenching—the surface temperature of the particles was quickly reduced to a point where zirconium oxidation ceased. A model which results in quenching the melt will clearly provide a lower bound on hydrogen generation subsequent to core slumping.

MARCH contains an option in which each node is assumed to slump into the lower plenum as soon as it melts and then to oxidize in a single time step. Use of this option insures that MARCH will give a series of small hydrogen production spikes instead of one large spike. This behavior (small sections of molten core falling directly into the lower plenum) is probably unrealistic, since experiments have indicated that the molten core will tend to refreeze in the lower, cooler portions of the core. A pool of molten core might form such that gradual dripping into the lower plenum could occur, as in the option considered, but at a later time. Even if such late-time dripping did occur, it could not be modelled in MARCH, which assumes a sudden massive drop of the molten core into the lower plenum.

For our study we delayed core slump in MARCH by requiring complete core melt before slump. As a result, we arbitrarily eliminated the large hydrogen production spike. Various hydrogen production parameters are shown in Figures C.5 through C.10. However, core behavior predicted by this model is unrealistic. The hottest portion of the core is predicted to be at an unphysically high temperature (above the vaporization temperature).

It can be seen from the previous discussion that the hydrogen production rates predicted for the HECTR, CLASIX-3, and MARCH computations are unreliable, especially after about 1500 lb (680 kg) of hydrogen are produced. A more reliable prediction of hydrogen production rate will require a better model of core melting and slumping and experimental data on these phenomena, so that simple programs like MARCH can be adjusted to give desired rates of hydrogen production.

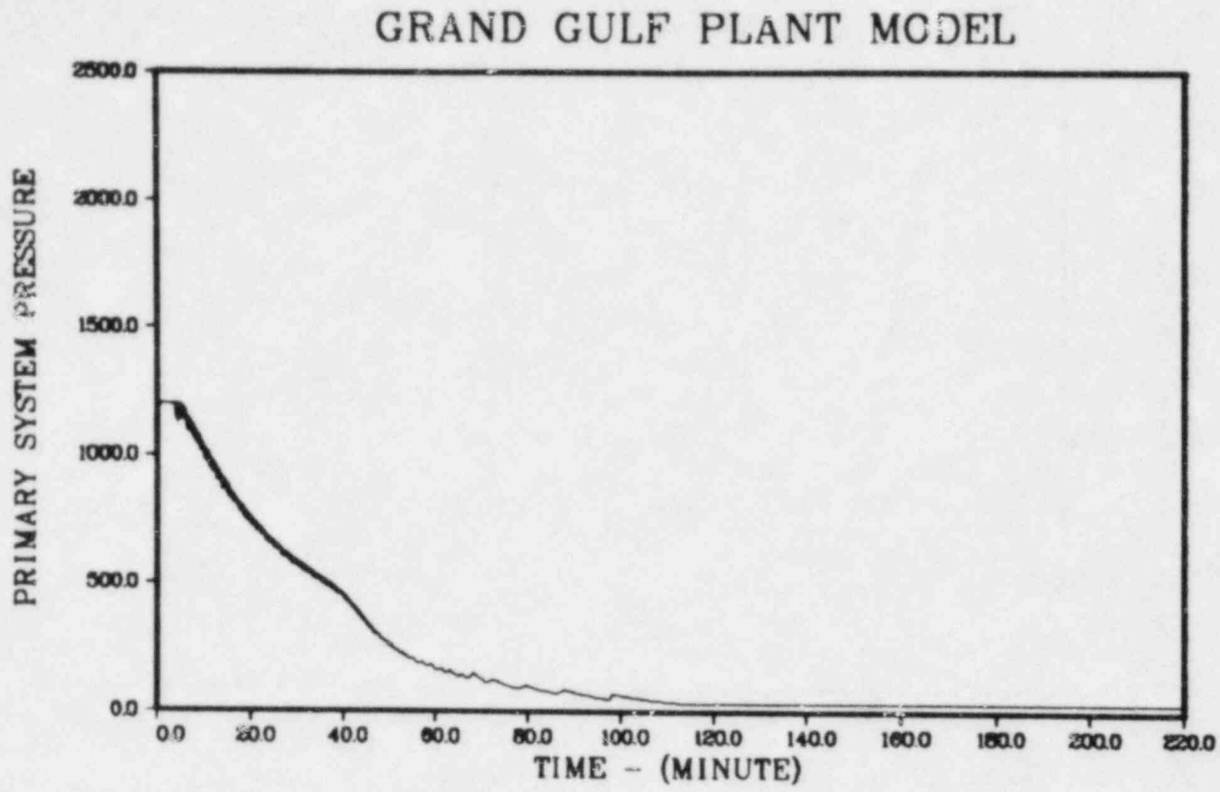

Figure C.1. Case A-1. Reactor coolant pressure, psia.

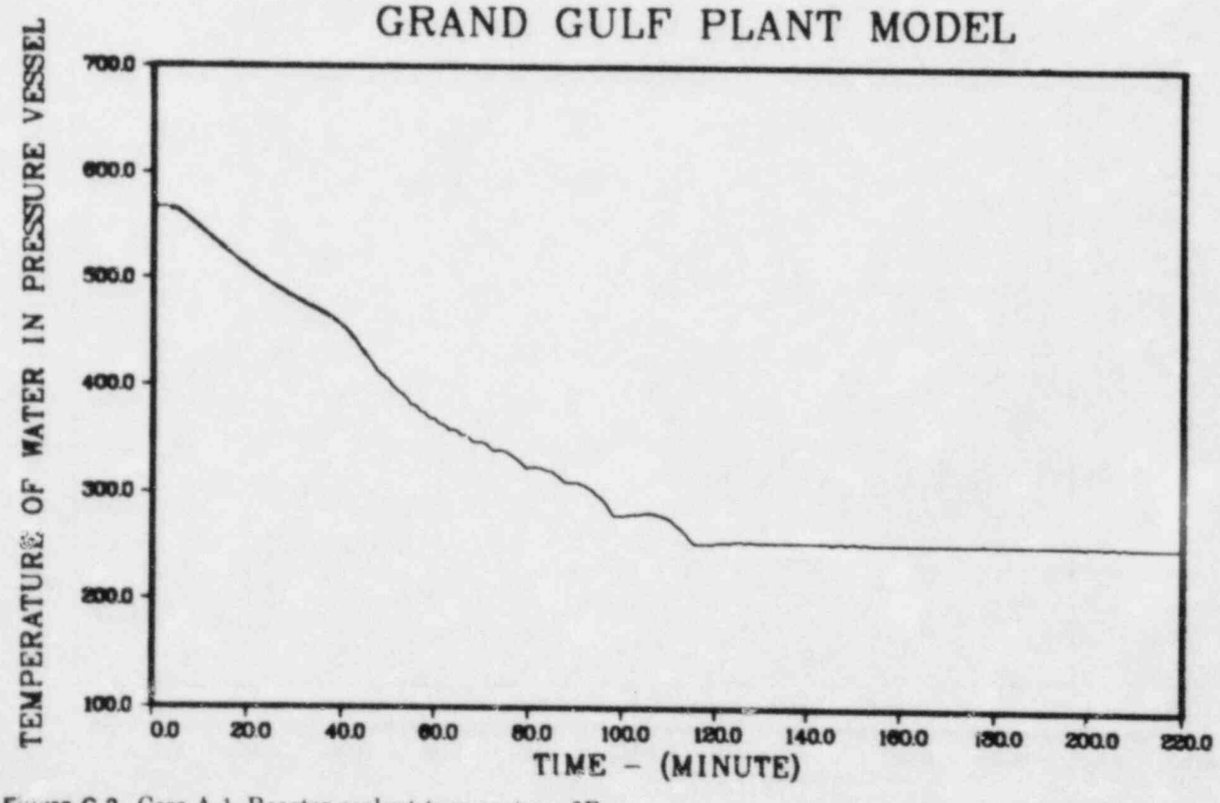

Figure C.2. Case A-1. Reactor coolant temperature, °F.

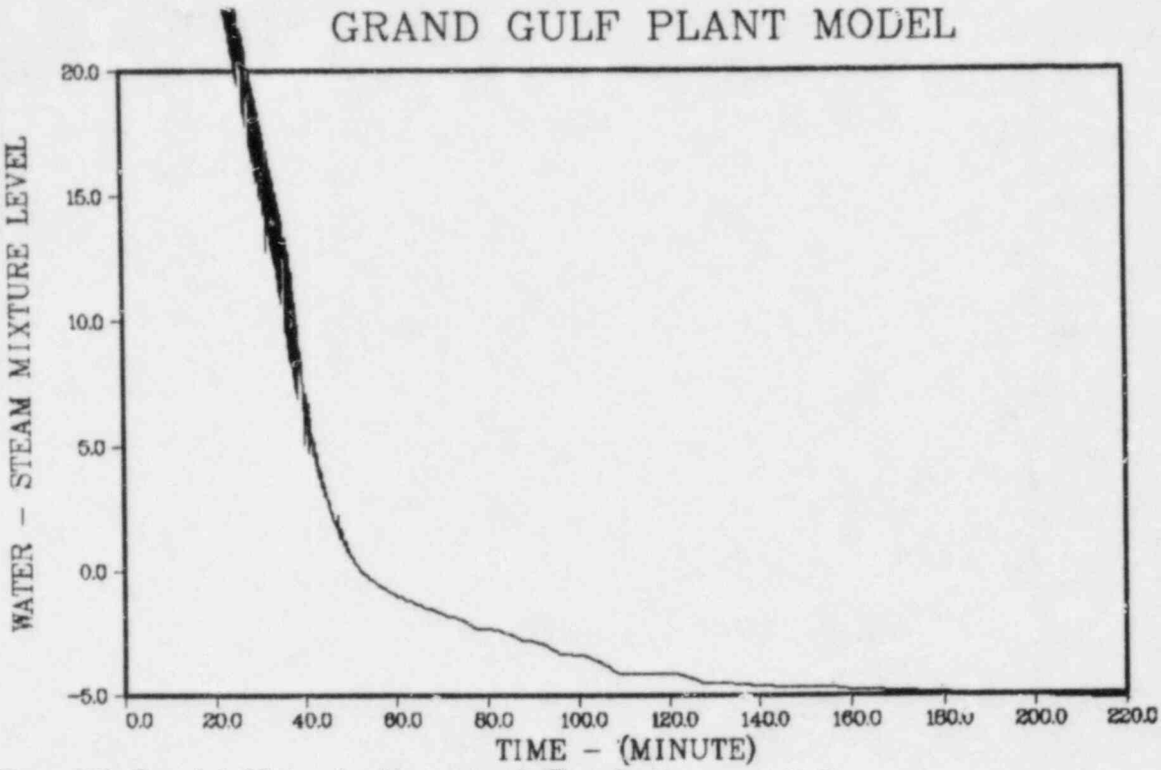

Figure C.3. Case A-1. Mixture level in reactor, ft (Top of active core at 12 ft).

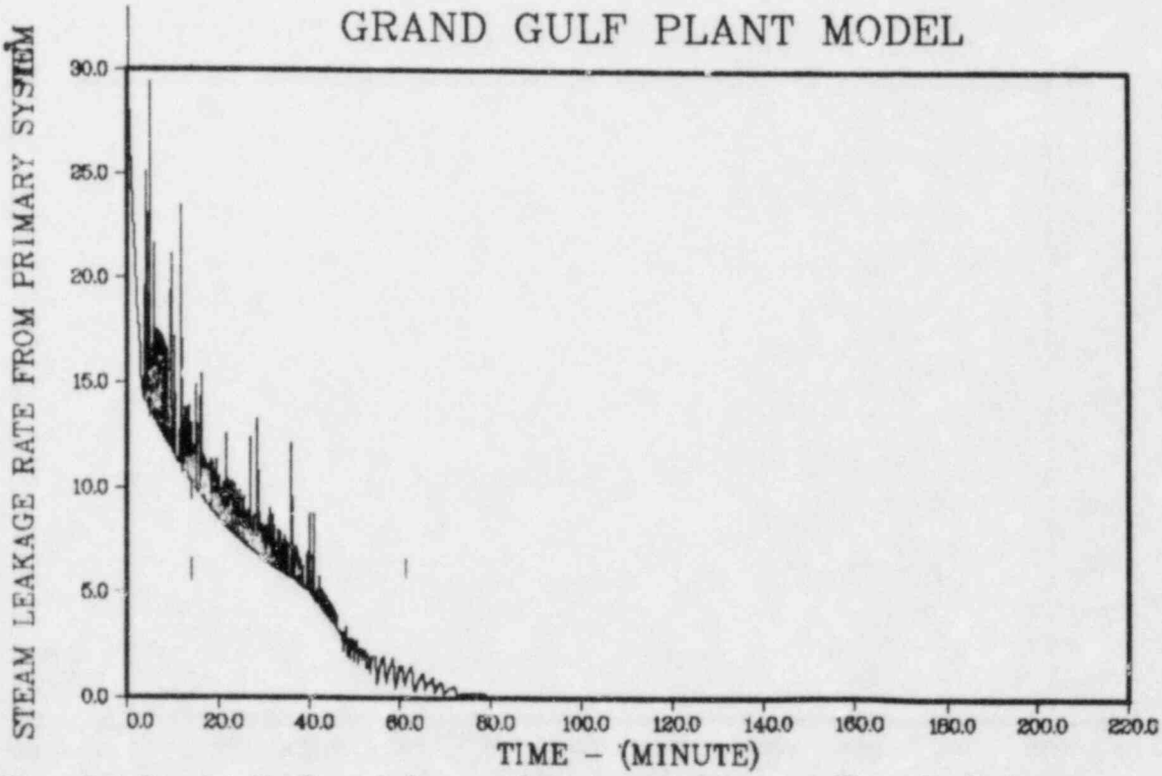

Figure C.4. Case A-1. Net Steam leakage rate from reactor coolant system (Steam Production rate - steam reacted with zirconium), 10^3 lb/min.

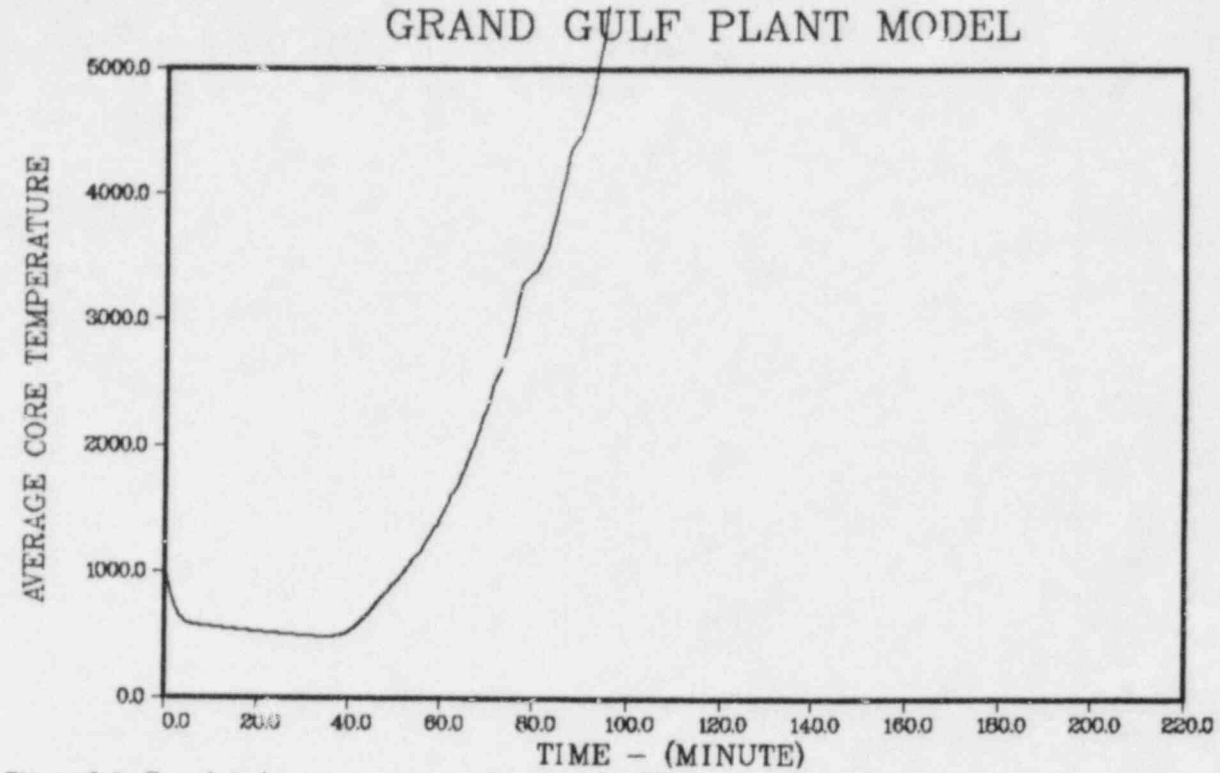

Figure C.5. Case A-1. Average reactor core temperature, °F.

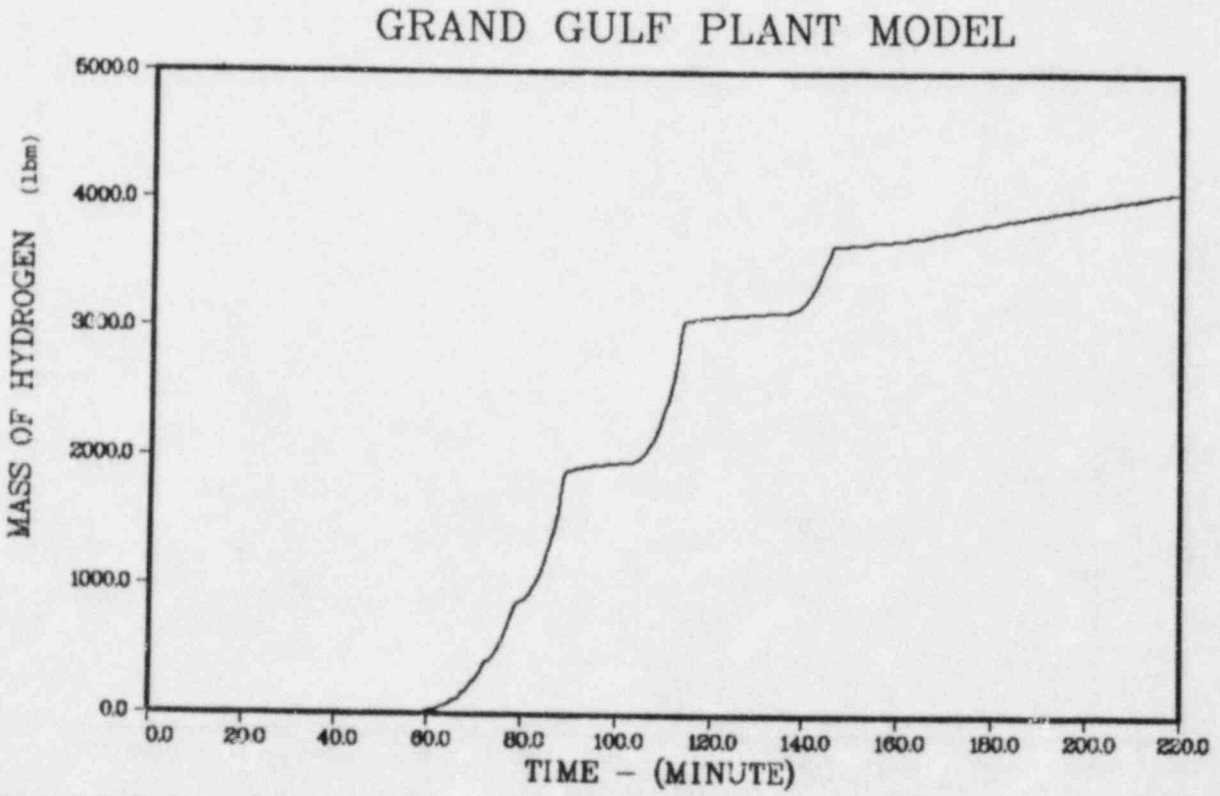

Figure C.6. Hydrogen Release into Containment for Case A-1 without burns. Approximately true for all MARCH cases.

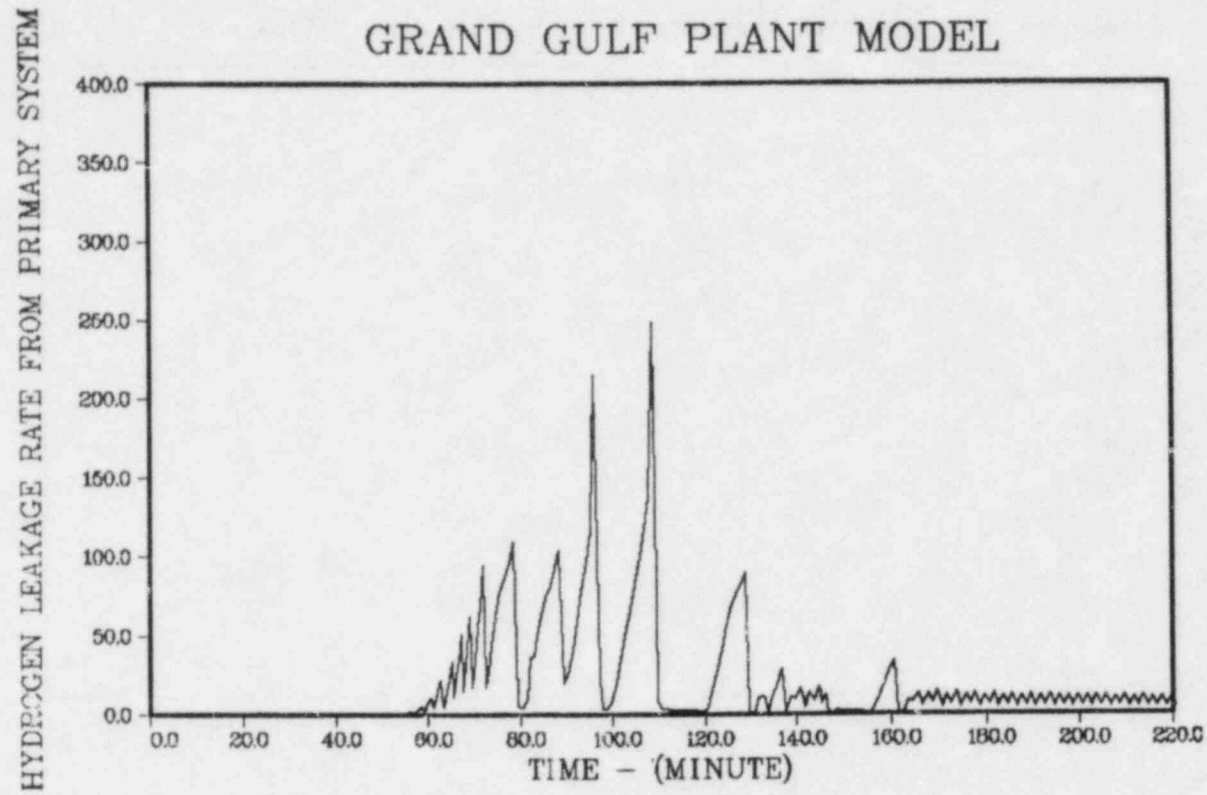

Figure C.7. Case A-1. Hydrogen leakage rate into containment, lb/min.

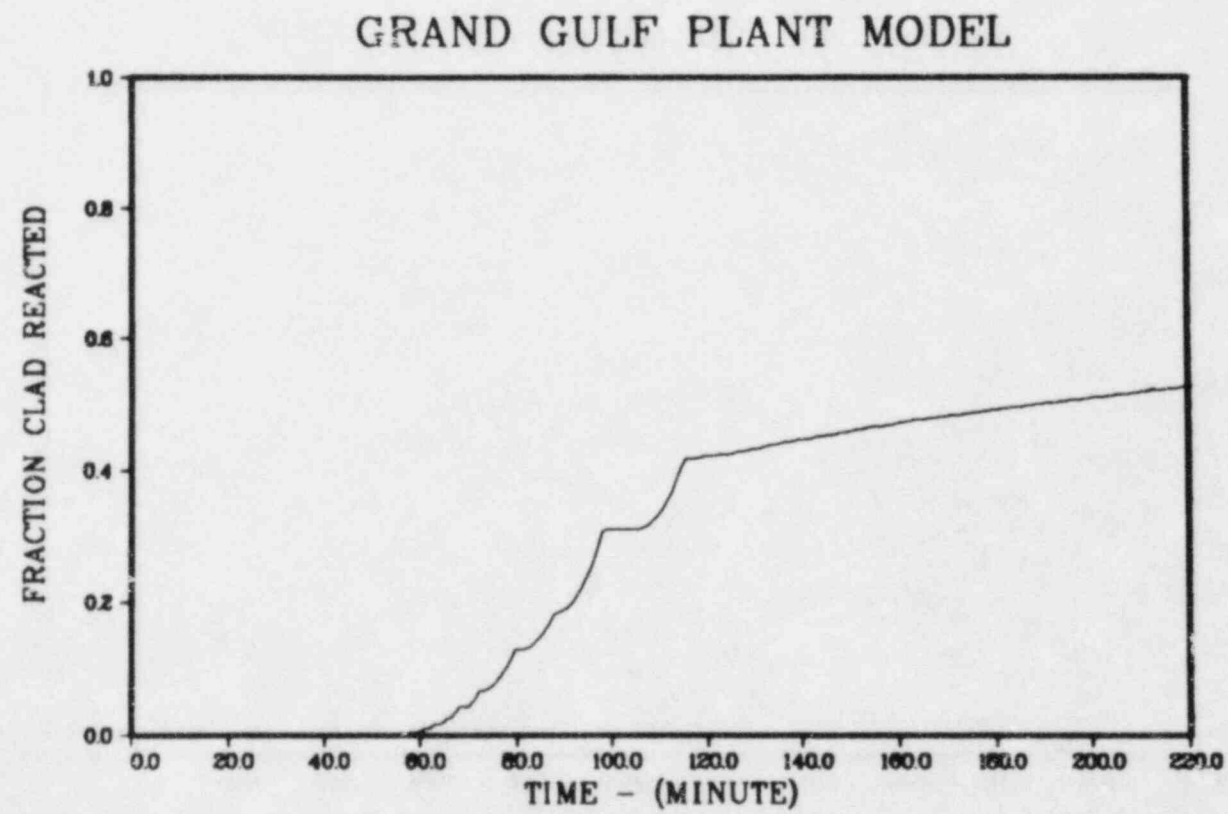

Figure C.8. Case A-1. Fraction of zirconium reacted.

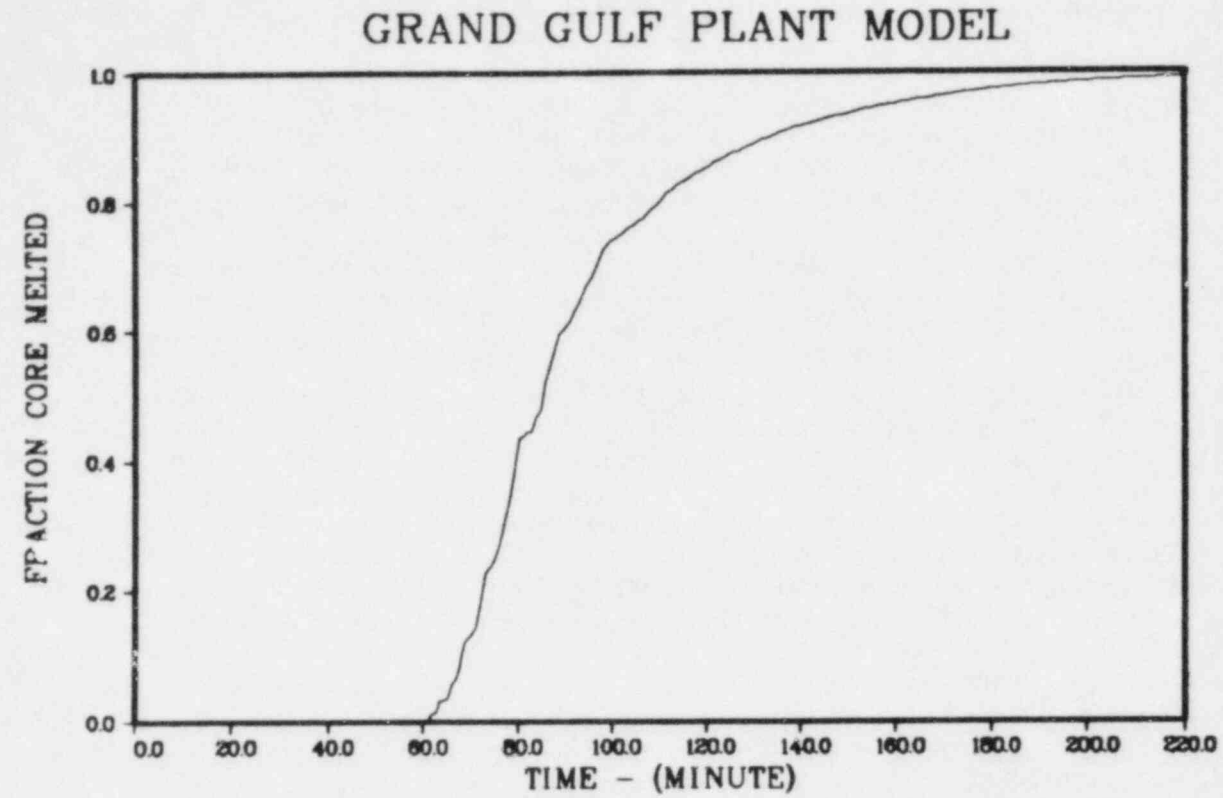

Figure C.9. Case A-1. Fraction of reactor core melted.

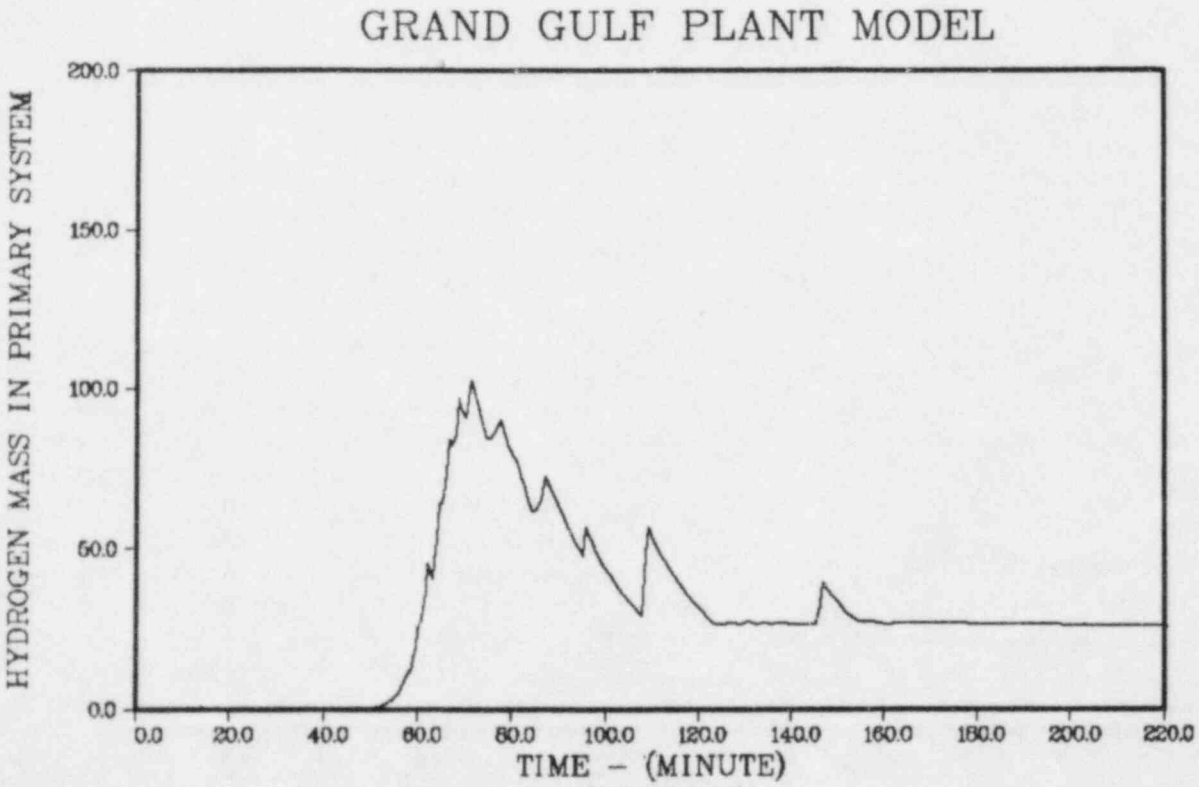

Figure C.10. Case A-1. Hydrogen mass in reactor coolant system, lb.

C.3 Compartment Interconnections

Compartments are interconnected in MARCH by the use of a series of one-way, zero-flow-resistance connections. Usually, the user employs two one-way connections between two compartments, one in each direction. At each time-step MARCH attempts to equalize the pressures of all compartments so interconnected. If the difference in pressure between the compartments is too great, the code requires a few time-steps to equalize pressure. When the drywell was connected to the wetwell by a single one-way connection to the wetwell, MARCH did not equalize pressures between the wetwell and drywell.

Our study using HECTR shows that the MARCH model of equal pressure in all the wetwell/containment compartments is reasonable. Pressure differences between compartments based on realistic estimates of flow resistance were found to be small. However, the drywell presents a problem. In the CLASIX-3 analysis, considerable discussion is given to the vacuum breakers. Some simple calculations made at SNL suggest that the resistance of the vacuum breakers is too great to permit large flows into the drywell after a wetwell/containment burn. However, a large pressure in the wetwell can drive the suppression pool downward and uncover the vents to the drywell. This suggests that most of the flow to the drywell may be from the bottom of the wetwell after a large hydrogen burn.

For most of the calculations discussed in Chapter 3.0 we ignored the presence of the drywell volume by having a connection from the drywell to the wetwell, but no connection back to the drywell. This results in having a constant drywell temperature, pressure and gas content, effectively isolating the drywell. This was done to get a comparison with HECTR computations. HECTR has no drywell model. However, we have a number of calculations in which either the wetwell or upper containment was connected to the drywell. These calculations are considered in section 3.8 of the text.

C.4 Hydrogen Burn Model

In considering the hydrogen burn model, we must discuss the criterion used for the initiation and burning of hydrogen in a single compartment. In addition, for multicompartment models we must also discuss the criterion used for propagation of combustion from one compartment to an adjacent compartment. We will first consider the behavior in a single compartment.

In MARCH, HECTR, and CLASIX-3, one specifies the hydrogen mole fraction at which combustion is assumed to start (ignition). We have used values of 0.10 and 0.08. The completeness of the burns can be specified in each code. In MARCH, one specifies the value of hydrogen mole fraction at which combustion is assumed to be extinguished. For complete combustion, this value would be zero.

A compartment is assumed to be inert if the oxygen mole fraction is too low. The MARCH code uses an oxygen mole fraction of 0.065 for inerting; HECTR and CLASIX-3 use an oxygen mole fraction of 0.050 for inerting. We have altered the MARCH code to use an oxygen mole fraction of 0.050 for inerting, and carried out most of our runs with this value. However, our first runs in the B configuration were made using the 0.065 limit. In section 3.4 we compare the results obtained with the two limits.

We have inserted into the MARCH code a criterion for steam inerting: a steam mole fraction of 0.56 or more. In none of the cases considered did steam inerting occur except in the drywell during portions of the drywell break accident.

A major weakness in MARCH is its lack of more realistic flame propagation options. In all three codes, one may require each compartment to meet the hydrogen ignition criteria in order to have a burn. Several of the cases used this criterion. For most of the cases calculated by HECTR, the flame was assumed to propagate into adjacent compartments after some time delay if the hydrogen mole fractions in the adjacent compartments were above the appropriate flammability criterion (for upward, downward, or horizontal propagation) and the compartments were not otherwise inerted. In MARCH, one has an option that will allow flame propagation between adjacent compartments. Apparently, when the option is used the only thing that will stop such propagation between interconnected compartments is a hydrogen mole fraction in the second compartment that is below the limit considered for extinguishment. If complete compartment combustion is considered, MARCH will cause all the hydrogen in all the interconnected compartments to be burned (if there is sufficient oxygen to combine with the hydrogen). Combustion will begin in an adjacent compartment even if the initial oxygen or hydrogen mole fraction in that compartment is below the inerting or flammability limit.

MARCH prints out the number of moles burned in each compartment and the adiabatic isochoric pressures corresponding to the burning of the hydrogen in each compartment. Given these numbers, one can determine whether a burn is mainly in one compartment, or is truly a multicompartment burn. In

HECTR and CLASIX-3, burns are strictly confined to a single compartment whenever the hydrogen mole fraction in the other compartments is below some specified propagation limit.

In HECTR and CLASIX-3, one can specify for each compartment a burn time which is equal to the ratio of a characteristic compartment length to the flame speed. In MARCH, one specifies a single burn time. We have investigated the effect of burn time on the peak pressure generated by a hydrogen burn for identical initial conditions. Without sprays, heat transfer effects cause a small reduction in peak pressure for increasing burn times. With sprays, the effect of longer burn times on reducing the peak pressure is much greater. This is shown in Figure C.11.

CLASIX-3 uses a flame speed of 6 ft/s (2 m/s), with some runs at 12 ft/s (4 m/s). We have used burn times corresponding to 2 m/s for runs intended to duplicate the CLASIX-3 runs. However, experimental data from tests carried out at Sandia and McGill indicate that the effective speed of the flame front may be much higher. Possible causes of these higher speeds are turbulence and the folding of flame around obstacles in the path. Because of the long distances for flame propagation inside the containment building, and the multitude of obstacles in parts of the flame path, the flame speed is expected to be high, possibly higher than the value (8 m/s) used in most of the MARCH calculations.

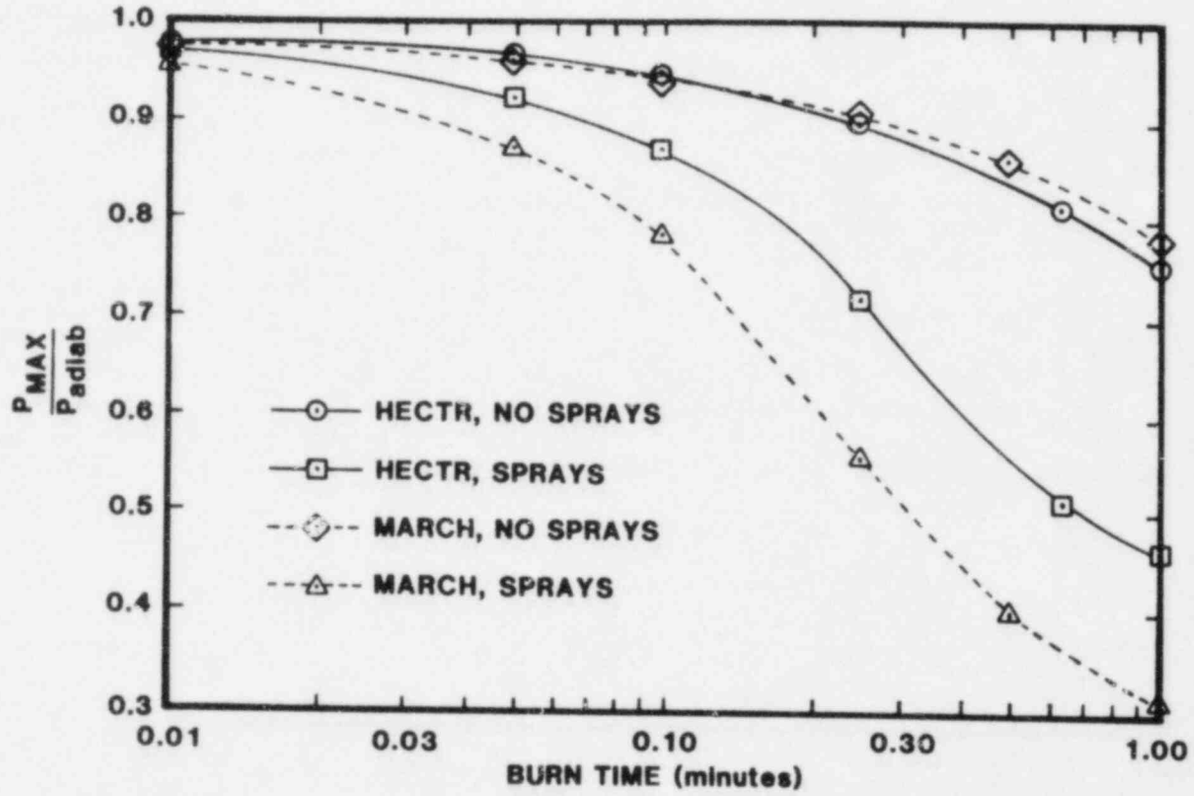

Figure C.11. Effect of Hydrogen Combustion Burn Time on the Predicted Single Compartment Peak Pressure by HECTR and MARCH Codes.

C.5 Natural Convection and Mixing

None of the three codes (MARCH, HECTR, or CLASIX-3) contains provision for natural convection. Considering the large density inversions found after wetwell burns and the results of the RALOC calculations, a large amount of mixing by natural convection is expected. If the mixing in containment is rapid enough, the results of configuration A (in which all the wetwell/containment volume is considered as one compartment with a homogeneous atmosphere) may be more realistic than those of the multicompartment models.

The mixing that does occur in MARCH and the other codes is artificial. It is caused by forcing flows between the compartments and having each inflow immediately mix with the previous contents of the compartment. This means that the degree and speed of mixing is governed by the compartmentalization model used in the code. Consequently, we have carried out studies with both MARCH and HECTR for a variety of compartmentalizations. The results vary greatly with the compartment model used. We discussed this point further in Chapter 3.0.

C.6 Sprays

The MARCH manual[C.1] is not very clear on the proper use of the spray option in the code. Nevertheless, we believe we have correctly carried out the insertion of sprays. When sprays are on, the peak pressure after a given burn is reduced and the temperature and pressure fall much more rapidly than without sprays. In Figure C.11 is shown the effect on peak burn pressure caused by convective heat transfer only (no spray case) and then convective heat transfer with sprays. Note that the reduction of peak pressure predicted by MARCH is greater than that predicted by HECTR for the same burn time.

C.7 Containment Failure

In MARCH one can specify a value of pressure at which containment is assumed to be breached. Depending on the option used, the code continues the computation past containment failure with the pressure in containment assumed to be atmospheric. We used an arbitrary high containment failure pressure, 100 psia (above the NRC estimated value for Grand Gulf, 71 psia), for all of our MARCH calculations. As a result, the code calculated each run as if the containment had not failed, since 100 psia pressure was not reached in any of the cases considered.

C.8 References

[C.1] R. O. Wooton and H. I. Avci, *MARCH (Meltdown Accident Response Characteristics) Code Description and User's Manual*, Battelle Columbus Laboratory, NUREG/CR-1711, BMI-2064 R3, October 1980.

[C.2] J. B. Rivard et al, *Interim Technical Assessment of the MARCH Code*, Sandia National Laboratories, NUREG/CR-2285, SAND81-1672 R3, November 1981.

DISTRIBUTION:

US NRC Distribution Contractor (CDSI) (340)
7300 Pearl Street
Bethesda, MD 20014
315 copies for R3
25 copies for NTIS

US Nuclear Regulatory Commission (13)
Office of Nuclear Regulatory Research
Washington, DC 20555
Attn: R. T. Curtis
J. T. Larkins (10)
P. Worthington (2)

US Nuclear Regulatory Commission (3)
Office of Nuclear Regulatory Research
Washington, DC 20555
Attn: B. S. Burson
M. Silberberg
L. S. Tong

US Nuclear Regulatory Commission (6)
Office of Nuclear Reactor Regulation
Washington, DC 20555
Attn: J. K. Long
J. F. Meyer
R. Palla
K. I. Parczewski
G. Quittschreiber
D. D. Yue

US Nuclear Regulatory Commission (11)
Office of Nuclear Reactor Regulation
Washington, DC 20555
Attn: V. Benaroya
W. R. Butler
G. W. Knighton
T. M. Su
Z. Rosztoczy
C. G. Tinkler (6)

US Department of Energy
Operational Safety Division
Albuquerque Operations Office
PO Box 5400
Albuquerque, NM 87185
Attn: J. R. Roeder, Director

US Bureau of Mines
Pittsburgh Research Center
PO Box 18070
Pittsburgh, PA 15236
Attn: M. Hertzberg

Swedish State Power Board (3)
El-Och Vaermeteknik
Sweden
Attn: Eric Ahlstroem (2)
Wiktor Frid

Berkeley Nuclear Laboratory
Berkeley GL 139PB
Gloucestershire
United Kingdom
Attn: J. E. Antill

Gesellschaft fur Reakforsicherheit (GRS)
Postfach 101650
Glockengasse 2
5000 Koeln 1
Federal Republic of Germany
Attn: Dr. M. V. Banaschik

Battelle Institut E. V.
Am Roemerhof 35
6000 Frankfurt am Main 90
Federal Republic of Germany
Attn: Dr. Werner Baukal

UKAEA Safety & Reliability Director (3)
Wigshaw Lane, Culcheth
Warrington WA34NE
Cheshire
United Kingdom
Attn: J. G. Collier (2)
S. F. Hall

British Nuclear Fuels, Ltd.
Springfield Works
Salwick, Preston
Lancs
United Kingdom
Attn: W. G. Cunliffe, Building 396

AERE Harwell (3)
Didcot
Oxfordshire OX11 ORA
United Kingdom
Attn: J. Gittus, AETB (2)
J. R. Matthews, TPD

DISTRIBUTION (cont):

Kernforschungszentrum Karlsruhe (5)
Postfach 3640
75 Karlsruhe
Federal Republic of Germany
Attn: Dr. S. Hagen (3)
Dr. J. P. Hosemann
Dr. M. Reimann

Simon Engineering Laboratory
University of Manchester
M139PL
United Kingdom
Attn: Prof. W. B. Hall

Kraftwerk Union (3)
Hammerbacher strasse 12 & 14
Postfach 3220
D-8520 Erlangen 2
Federal Republic of Germany
Attn: Dr. K. Hassman (2)
Dr. M. Peehs

Gesellschaft fur Reaktorsickerheit (GRS mbH) (3)
8046 Garching
Federal Republic of Germany
Attn: E. F. Hicken (2)
H. L. Jahn

Technische Universitaet Muenchen
D-8046 Garching
Federal Republic of Germany
Attn: Dr. H. Karwat

McGill University (3)
315 Querbes
Outremont, Quebec
Canada H2V 3W1
Attn: John H. S. Lee

AEC, Ltd.
Whiteshell Nuclear Research Establishment (3)
Pinawa, Manitoba
Canada
Attn: D. Liu (2)
H. Tamm

National Nuclear Corp. Ltd.
Cambridge Road
Whetestone, Leicester, LE83LH
United Kingdom
Attn: R. May

CNEN NUCLIT
Rome, Italy
Attn: A. Morici

CEC
Rue De La Loi 200
1049 Brussels
Belgium
Attn: B. Tolley
Director of Research, Science & Education

Bechtel Power Corporation
15740 Shady Grove Road
Gaithersburg, MD 20877
Attn: D. Ashton

Northwestern University
Chemical Engineering Department
Evanston, IL 60201
Attn: S. G. Bankoff

Brookhaven National Laboratory (3)
Upton, NY 11973
Attn: R. A. Bari (2)
A. Berlad

Westinghouse Hanford Company (5)
PO Box 1970
Richland, WA 99352
Attn: G. R. Bloom (3)
L. Muhlstein
R. D. Peak

UCLA
Nuclear Energy Laboratory
405 Hilgard Ave.
Los Angeles, CA 90024
Attn: I. Catton

Argonne National Laboratory
9700 South Cass Ave.
Argonne, IL 60439
Attn: H. M. Chung

University of Wisconsin
Nuclear Engineering Department
1500 Johnson Dr.
Madison, WI 53706
Attn: M. L. Corradini

DISTRIBUTION (cont):

Los Alamos National Laboratory (7)
PO Box 1663
Los Alamos, NM 87545
Attn: H. S. Cullingford (4)
R. Gido
J. Carson Mark
G. Schott

Battelle Columbus Laboratory (3)
505 King Ave.
Columbus, OH 43201
Attn: P. Cybulskis (2)
R. Denning

Power Authority State of NY (3)
10 Columbus Circle
New York, NY 10019
Attn: R. E. Deem (2)
S. S. Iyer

Massachusetts Inst of Technology
Room 1-276
Cambridge, MA 02139
Attn: M. N. Fardis

Offshore Power System (3)
8000 Arlington Expressway
PO Box 8000
Jacksonville, FL 32211
Attn: G. M. Fuls (2)
D. H. Walker

Electric Power Research Institute (7)
3412 Hillview Ave.
Palo Alto, CA 94303
Attn: J. J. Haugh (4)
K. A. Nilsson
G. Thomas
L. B. Thompson

Fauske & Associates
627 Executive Dr.
Willowbrook, IL 60521
Attn: R. Henry

Mississippi Power & Light (5)
PO Box 1640
Jackson, MS 39205
Attn: S. H. Hobbs

General Electric Co. (2)
175 Curtner Ave.
MC N 1C157
San Jose, CA 95125
Attn: K. W. Holtzclaw

Duke Power Co. (3)
PO Box 33189
Charlotte, NC 28242
Attn: F. G. Hudson (2)
A. L. Sudduth

S. Levy, Inc.
1999 S. Bascom Ave., Suite 725
Campbell, CA 95008
Attn: C. Roy Jones

Westinghouse Corporation (5)
PO Box 355
Pittsburgh, PA 15230
Attn: N. Liparulo (3)
J. Olhoeft
V. Srinivas

General Physics Corporation (5)
1000 Century Plaza
Columbia, MD 21044
Attn: Chester Kupiec

TVA (2)
400 Commerce, W9C157-CD
Knoxville, TN 37902
Attn: Wang Lau

EG&G Idaho
Willow Creek Building, W-3
PO Box 1625
Idaho Falls, ID 83415
Attn: Server Sadik

NUS Corporation
4 Research Place
Rockville, MD 20850
Attn: Richard Sherry

University of Michigan
Dept of Aerospace Engineering
Ann Arbor, MI 47109
Attn: Martin Sichel

DISTRIBUTION (cont):

Roger Strehlow
505 South Pine St.
Champaign, IL 61820

Applied Sciences Association, Inc.
PO Box 2687
Palos Verdes Pen., CA 90274
Attn: D. Swanson

Acurex Corporation
485 Clyde Ave.
Mountain View, CA 94042
Attn: Ray Torok

Bechtel Power Corporation
PO Box 3965
San Francisco, CA 94119
Attn: R. Tosetti

Factory Mutual Research Corp.
PO Box 688
Norwood, MA 02062
Attn: R. Zalosh

Sandia National Laboratories (87)
PO Box 5800
Albuquerque, NM 87185
Attn: 1131 B. Morosin
1131 W. B. Benedick
1131 J. Fisk
1500 W. Herrmann
1513 M. R. Baer
1513 D. W. Larson
2510 D. H. Anderson
2512 V. M. Loyola
2513 J. E. Kennedy
2513 S. F. Roller
2513 J. E. Shepherd
2612 B. V. Burnham
8513 W. J. McClean
8523 W. T. Ashurst
8523 K. D. Marx
8523 B. R. Sanders
9268 D. Tomasko
9400 A. W. Snyder
9410 D. J. McCloskey
9411 V. L. Behr
9411 A. S. Benjamin
9411 F. E. Haskin
9412 J. W. Hickman
9412 A. M. Kolaczkowski
9412 R. G. Spulak
9415 D. C. Aldrich
9420 J. V. Walker
9420A J. B. Rivard
9422 D. A. Powers
9422 A. R. Taig
9424 M. J. Clauser
9425 W. J. Camp
9425 A. J. Wickett
9440 D. A. Dahlgren
9441 M. Berman (25)
9441 A. L. Camp
9441 R. K. Cole, Jr.
9441 J. C. Cummings, Jr.
9441 S. E. Dingman
9441 N. A. Evans
9441 D. P. Kelly
9441 L. S. Nelson
9441 P. G. Prassinos
9441 E. W. Shepherd
9441 M. P. Sherman
9441 S. R. Tieszen
9441 M. J. Wester
9442 W. A. Von Riesemann
9444 L. D. Buxton
9444 R. K. Byers
9444 S. L. Thompson
9444 G. G. Weigand
9445 L. O. Cropp
9445 W. H. McCulloch
8214 S. L. Tyler
3141 L. J. Erickson (5)
3151 W. L. Garner (3)

NRC FORM 335 (11.81)

U.S. NUCLEAR REGULATORY COMMISSION

BIBLIOGRAPHIC DATA SHEET

1. REPORT NUMBER (Assigned by DDC)
NUREG/CR-2530
SAND82-0218

4. TITLE AND SUBTITLE (Add Volume No., if appropriate)
Review of the Grand Gulf Hydrogen Igniter System

2. (Leave blank)

3. RECIPIENT'S ACCESSION NO.

7. AUTHOR(S) J. C. Cummings, A.L.Camp, M. P. Sherman, M.J. Wester, D. Tomasko, R.K. Byers, B.W. Burnham

5. DATE REPORT COMPLETED
MONTH: February | YEAR: 1983

9. PERFORMING ORGANIZATION NAME AND MAILING ADDRESS (Include Zip Code)

Sandia National Laboratories
Albuquerque, NM 87185

DATE REPORT ISSUED
MONTH: March | YEAR: 1983

6. (Leave blank)

8. (Leave blank)

12. SPONSORING ORGANIZATION NAME AND MAILING ADDRESS (Include Zip Code)

Division of Systems Integration
Office of Nuclear Reactor Regulation
U. S .Nuclear Regulatory Commission
Washington, DC 20555

10. PROJECT/TASK/WORK UNIT NO.

11. FIN NO.
A1308 and A1246

13. TYPE OF REPORT
Technical

PERIOD COVERED (Inclusive dates)

15. SUPPLEMENTARY NOTES

14. (Leave blank)

16. ABSTRACT (200 words or less)

The Mississippi Power and Light Company has proposed installation of a Hydrogen Igniter Systems (HIS) at the Grand Gulf Nuclear Station (BWR Mark III) to burn hydrogen generated during accidents more severe than the design-basis accidents. Sandia National Laboratories, under a contract with the U. S. Nuclear Regulatory Commission, has performed a technical evaluation of the adequacy of the proposed HIS to meet the threat posed by hydrogen combustion. Areas considered in this review include HIS design and testing, location and distribution of igniters, containment pressure and temperature response calculations, detonations, containment atmosphere mixing mechanisms, actuation criteria for the HIS, and the spectrum of hydrogen-generating accidents.

17. KEY WORDS AND DOCUMENT ANALYSIS

17a. DESCRIPTORS

17b. IDENTIFIERS/OPEN-ENDED TERMS

18. AVAILABILITY STATEMENT
Unlimited

19. SECURITY CLASS (This report)
Unclassified

21. NO. OF PAGES
230

20. SECURITY CLASS (This page)
Unclassified

22. PRICE
S

NRC FORM 335 (11.81)

UNITED STATES
NUCLEAR REGULATORY COMMISSION
WASHINGTON, D.C. 20555

120555078877 1 N01048
US NRC
ADM DIV OF TIDC
POLICY & PUB MGT BR-PDR NUREG
W-501
WASHINGTON DC 20555